

Water Mist Suppression in Conjunction with Displacement Ventilation

**By
Benjamin Piers Hume**

Supervised by Mike Spearpoint

**Fire Engineering Research Report 03/4
February 2003**

This project report was presented as partial fulfillment
of the M.E. Fire degree at the University of Canterbury

School of Engineering
University of Canterbury
Private Bag 4800
Christchurch, New Zealand

Phone 643 364-2250

Fax 643 364-2758

A man of genius makes no mistakes. His errors are the volition, and are the portals of discovery. – James Joyce

Abstract

This study proposes and investigates a new type of water mist system where by air and water mist are blown into a fire compartment at low level using a displacement ventilation system. The air/water mist mixture enters the compartment and due to thermal stratification spreads out across the floor forming a protective lake. As the lake increases in depth, it creates a protective cool clean environment that protects the occupants and electrical equipment. The water mist has a very fine diameter in the order of $20\mu\text{m}$ that allows it to remain suspended within the air for long periods, providing cooling and radiant protection while not causing significant damage to electrical equipment. The density of the water mist is controlled to create a level where flame suppression occurs. Theoretically occupants and electrical equipment can remain safely within the compartment protected by the air/water mist lake, until the fire is extinguished.

To investigate the feasibility of this concept a test compartment and associated displacement water mist system were designed based in the standard ISO room. A full-scale test compartment was built and tests run for a number of 20 kW fires of different types and in different positions. The proposed displacement water mist system was tested along with comparison tests using a conventional sprinkler. Within the live test compartment, lights and a computer were installed and monitored to determine the effect of the water mist on electrical equipment.

The basic setup and a selection of fires were also simulated using the computational fluid dynamics program Fire Dynamics Simulator (FDS). FDS simulations were run as they provided more information on the species concentrations within the compartment, while allowing a comparison of how FDS simulated the situation compared to the live tests. With the use of computer programs become more wide spread, this comparison provided valuable information on the limits of computer modeling in this situation.

The results from the testing suggested that with the experimental setup used the objectives were not completely met as the fire was not extinguished and mixing created within the compartment resulted in combustion products being present around the occupants. The setup did however result in reduced temperatures and

a better atmosphere than occurred with no suppression, water mist only or conventional sprinklers. The displacement water mist system was the only suppression system tested that did not cause the computer or lights within the room to short-circuit and fail.

The primary reason that the system did not function as intended was that the water mist nozzles used created an extremely high level of entrainment of the surrounding air. Effectively this caused the compartment to become turbulent and mixing of the upper and lower layers to occur. The entrained air also lowered the local density of water mist below that required for suppression. Additionally there is some question as to whether or not the density of water relative to the size of the fire was sufficient in the first place. A density of 200 g/m^3 was used based on past research, but some debate exists that suggests that this value would need to be on the order of 600 g/m^3 for suppression of the 20 kW fires used in this study.

A comparison between the live test and FDS simulations showed that while providing similar results to the live testing, FDS cannot be solely used to test the displacement water mist system. Instead FDS could be used for the initial investigation, but that live testing will be needed for accurate results.

Acknowledgements

I would like to thank the following people for their assistance and support in helping me to complete this project:

- My supervisor, Mike Spearpoint, for his dedication and support.
- The New Zealand Fire Service Commission for their support of the Fire Engineering programme at the University of Canterbury.
- Gary Luff of the New Zealand Fire Service who provided fire-fighting equipment for the live tests and well needed encouragement when the testing did not run as intended.
- Kees Brinkman and Dean Johnston for their support and guidance.
- The Engineering librarians, particularly Christine McKee for her assistance in obtaining obscure information.
- Grant and Russell for building the live test compartment.
- Mum and Dad for their support over the years to which I owe everything.
- And finally to Tanzi my fiancée who has put up with the long nights and smoky clothes.

Contents

ABSTRACT	III
ACKNOWLEDGEMENTS	V
CONTENTS	VII
LIST OF FIGURES	X
LIST OF TABLES	XV
GLOSSARY OF TERMS	XVI
ACRONYMS:	XVI
NOMENCLATURE:	XVI
1. INTRODUCTION	1
1.1 OVERVIEW	1
1.2 RESEARCH OBJECTIVES	2
1.3 REPORT LAYOUT	2
2. BACKGROUND	3
2.1 DEVELOPMENT OF WATER MIST SYSTEMS	3
2.2 EXTINGUISHMENT MECHANISMS	6
2.3 DROPLET SIZE	9
2.4 WATER DENSITY REQUIREMENTS	16
2.5 WATER MIST GENERATION	17
2.6 EXISTING OPERATING SYSTEMS/CONCEPTS	18
2.7 HISTORICAL TESTING	19
2.8 DISPLACEMENT VENTILATION	25
2.9 SUMMARY	31
3. CONCEPT	33
3.1 BASE CONCEPT	33
3.2 THEORETICAL ADVANTAGES	35
3.3 SUMMARY	37

<u>4.</u>	<u>EXPERIMENTAL DESIGN</u>	39
4.1	INVESTIGATION PROCEDURE	39
4.2	SIMULATION RUN SELECTION	39
4.3	BASE COMPARTMENT SPECIFICATIONS	42
4.4	INTERNAL FITTING SELECTION	43
4.5	FIRE SELECTION	44
4.6	AIRFLOW DESIGN UNDER NORMAL CONDITIONS	47
4.7	AIRFLOW DESIGN UNDER FIRE CONDITIONS	48
4.8	WATER SUPPLY UNDER FIRE CONDITIONS	50
4.9	THERMOCOUPLE AND DETECTOR LOCATIONS	52
<u>5.</u>	<u>FULL SCALE TESTING</u>	55
5.1	OBJECTIVE	55
5.2	TEST COMPARTMENT DESIGN	56
5.3	TEST FIRES	63
5.4	NOZZLE SELECTION	64
5.5	FAN SELECTION	68
5.6	CONTROLS SELECTION	70
5.7	DETECTOR MOUNTING	71
5.8	SPRINKLER SELECTION	72
5.9	TRIAL OBSERVATIONS	73
5.10	EXPERIMENTAL TIME LINE	79
5.11	FULL SCALE TEST RESULTS AND DISCUSSIONS	81
5.12	FULL SCALE TEST GENERAL DISCUSSION	142
5.13	CONCLUSION	154
<u>6.</u>	<u>FDS SIMULATIONS</u>	155
6.1	OBJECTIVE	155
6.2	FDS BACKGROUND	155
6.3	MODEL DEVELOPMENT	166
6.4	SIMULATION RESULTS AND DISCUSSIONS	175
6.5	FDS SIMULATION OBSERVATIONS	206
6.6	FDS CONCLUSION	210

<u>7.</u>	<u>COMPARISON RESULTS</u>	<u>211</u>
7.1	BASE CALCULATIONS, FDS AND FULL SCALE TEST COMPARISON	211
7.2	GENERAL CONCLUSION	227
<u>8.</u>	<u>FUTURE WORK</u>	<u>229</u>
<u>9.</u>	<u>CONCLUSION</u>	<u>231</u>
<u>10.</u>	<u>REFERENCES</u>	<u>233</u>
<u>11.</u>	<u>APPENDIX</u>	<u>239</u>
11.1	FULL SCALE COMPARTMENT PLANS	239
11.2	DISPLACEMENT VENTILATION DESIGN FILES	242
11.3	WATER MIST NOZZLES CHARACTERISTICS	243
11.4	NOZZLES LAYOUT	249
11.5	CENTRIFUGAL FAN SPECIFICATIONS	250
11.6	FDS INPUT FILES	251
11.7	FDS THERMOCOUPLE RESULTS	261
11.8	LIVE AND FDS COMPARISON GRAPHS	275

List of Figures

Figure 1 - Heat absorption during heating and phase change of water [10]	6
Figure 2 - Comparison of specific heat capacity and evaporation [11]	7
Figure 3 - Saturation pressure of water vapour in air below the boiling point [14]	8
Figure 4 - Spectrum of Drop Diameters [18]	10
Figure 5 - Classification of water sprays by drop size distribution [49]	11
Figure 6 - Division of different classes of water mist according to NFPA 750	12
Figure 7 - Water drop evaporation [23]	12
Figure 8 - Falling velocities in still air of varying droplet sizes [19]	14
Figure 9 - Trajectories for droplets of different sizes at an airflow of 4m/s [19]	15
Figure 10 - Counterflow non-premixed flame apparatus [24]	16
Figure 11 - Experimental set up in water spray injection orientation [29]	22
Figure 12 - 1/3 ISO room low-level water mist injection set-up [19]	23
Figure 13 - Displacement ventilation at work [31]	25
Figure 14 - Displacement ventilation room stratification [30]	27
Figure 15 - Displacement ventilation airflow pattern [32]	28
Figure 16 - Ventilation system selection [32]	30
Figure 17 - Displacement water mist concept	34
Figure 18 - Basic compartment layout	43
Figure 19 - Airflow mass balance	48
Figure 20 - Required supply airflow rate	49
Figure 21 - Perforated steel supply diffuser	57
Figure 22 - Air-conditioning unit and plenum supply point	58
Figure 23 - Air-conditioning unit and plenum supply from outside the compartment	58
Figure 24 - Electric duct heater installed with fan	59
Figure 25 - Main compartment door	60
Figure 26 - Internal compartment loads operating	61
Figure 27 - The back of the completed compartment	62
Figure 28 - The front of the completed compartment	62
Figure 29 - Pool fire pan	63
Figure 30 - Typical wood crib	64
Figure 31 - QuickMist™ Nozzle	65
Figure 32 - Water mist characteristics from QuickMist™ nozzle	66
Figure 33 - Water mist nozzles installed in test compartment	67
Figure 34 - Water filter, pressure gage and control valve	68
Figure 35 - Fan and electric duct heater controller	71
Figure 36 - Conventional sprinkler system	72
Figure 37 - Vertical plenum mounted nozzle array	75
Figure 38 - Horizontal plenum mounted nozzle array	76
Figure 39 - Pool fire detector results	78

<i>Figure 40 - Wood crib fire detector results</i>	<i>78</i>
<i>Figure 41 - Run 1: Occupant Thermocouple Tree</i>	<i>84</i>
<i>Figure 42 - Run 1: Fire Thermocouple Tree</i>	<i>84</i>
<i>Figure 43 - Run 1: Back Corner Thermocouple Tree</i>	<i>85</i>
<i>Figure 44 - Run 1: Front Corner Thermocouple Tree</i>	<i>85</i>
<i>Figure 45 - Run 1: Supply and Extract Temperatures</i>	<i>86</i>
<i>Figure 46 - Run 2: Occupant Thermocouple Tree</i>	<i>88</i>
<i>Figure 47 - Run 2: Fire Thermocouple Tree</i>	<i>89</i>
<i>Figure 48 - Run 2: Supply and Extract Temperatures</i>	<i>89</i>
<i>Figure 49 - Run 3: Occupant Thermocouple Tree</i>	<i>92</i>
<i>Figure 50 - Run 3: Fire Thermocouple Tree</i>	<i>92</i>
<i>Figure 51 - Run 3: Supply and Extract Temperatures</i>	<i>93</i>
<i>Figure 52 - Run 4: Occupant Thermocouple Tree</i>	<i>95</i>
<i>Figure 53 - Run 4: Fire Thermocouple Tree</i>	<i>95</i>
<i>Figure 54 - Run 4: Supply and Extract Temperatures</i>	<i>96</i>
<i>Figure 55 - Run 5: Occupant Thermocouple Tree</i>	<i>99</i>
<i>Figure 56 - Run 5: Fire Thermocouple Tree</i>	<i>99</i>
<i>Figure 57 - Run 5: Supply and Extract Temperatures</i>	<i>100</i>
<i>Figure 58 - Run 6: Occupant Thermocouple Tree</i>	<i>102</i>
<i>Figure 59 - Run 6: Fire Thermocouple Tree</i>	<i>102</i>
<i>Figure 60 - Run 6: Supply and Extract Temperatures</i>	<i>103</i>
<i>Figure 61 - Run 7: Occupant Thermocouple Tree</i>	<i>105</i>
<i>Figure 62 - Run 7: Fire Thermocouple Tree</i>	<i>106</i>
<i>Figure 63 - Run 7: Supply and Extract Temperatures</i>	<i>106</i>
<i>Figure 64 - Run 8: Occupant Thermocouple Tree</i>	<i>109</i>
<i>Figure 65 - Run 8: Fire Thermocouple Tree</i>	<i>109</i>
<i>Figure 66 - Run 8: Supply and Extract Temperatures</i>	<i>110</i>
<i>Figure 67 - Run 9: Occupant Thermocouple Tree</i>	<i>112</i>
<i>Figure 68 - Run 9: Fire Thermocouple Tree</i>	<i>113</i>
<i>Figure 69 - Run 9: Supply and Extract Temperatures</i>	<i>113</i>
<i>Figure 70 - Run 10: Occupant Thermocouple Tree</i>	<i>116</i>
<i>Figure 71 - Run 10: Fire Thermocouple Tree</i>	<i>116</i>
<i>Figure 72 - Run 10: Supply and Extract Temperatures</i>	<i>117</i>
<i>Figure 73 - Run 11: Occupant Thermocouple Tree</i>	<i>119</i>
<i>Figure 74 - Run 11: Fire Thermocouple Tree</i>	<i>120</i>
<i>Figure 75 - Run 11: Supply and Extract Temperatures</i>	<i>120</i>
<i>Figure 76 - Run 12: Occupant Thermocouple Tree</i>	<i>123</i>
<i>Figure 77 - Run 12: Fire Thermocouple Tree</i>	<i>123</i>
<i>Figure 78 - Run 12: Supply and Extract Temperatures</i>	<i>124</i>
<i>Figure 79 - Run 13: Occupant Thermocouple Tree</i>	<i>127</i>

<i>Figure 80 - Run 13: Fire Thermocouple Tree</i>	127
<i>Figure 81 - Run 13: Supply and Extract Temperatures</i>	128
<i>Figure 82 - Run 14: Occupant Thermocouple Tree</i>	130
<i>Figure 83 - Run 14: Fire Thermocouple Tree</i>	131
<i>Figure 84 - Run 14: Supply and Extract Temperatures</i>	131
<i>Figure 85 - Run 15: Occupant Thermocouple Tree</i>	134
<i>Figure 86 - Run 15: Fire Thermocouple Tree</i>	134
<i>Figure 87 - Run 15: Supply and Extract Temperatures</i>	135
<i>Figure 88 - Run 16: Occupant Thermocouple Tree</i>	138
<i>Figure 89 - Run 16: Fire Thermocouple Tree</i>	138
<i>Figure 90 - Run 16: Supply and Extract Temperatures</i>	139
<i>Figure 91 - Central floor pool fire Tree 1, 1.3m temperature readings</i>	144
<i>Figure 92 - Central floor pool fire Tree 1, 1.8m temperature readings</i>	145
<i>Figure 93 - Central floor pool exhaust temperature readings</i>	146
<i>Figure 94 – Central 1m pool fire Tree 1, 1.3m temperature readings</i>	147
<i>Figure 95 - Central 1m pool fire Tree 1, 1.8m temperature readings</i>	147
<i>Figure 96 - Central 1m pool fire exhaust temperature readings</i>	148
<i>Figure 97 – Corner pool fire Tree 1, 1.3m temperature readings</i>	149
<i>Figure 98 – Corner pool fire Tree 1, 1.8m temperature readings</i>	150
<i>Figure 99 – Corner pool fire exhaust temperature readings</i>	150
<i>Figure 100 – Centre floor crib fire Tree 1, 1.3m temperature readings</i>	151
<i>Figure 101 – Centre floor crib fire Tree 1, 1.8m temperature readings</i>	152
<i>Figure 102 – Centre floor crib fire exhaust temperature readings</i>	152
<i>Figure 103 - State relations for propane [47]</i>	161
<i>Figure 104 - Cumulative Volume Fraction and Cumulative Number Fraction functions of the droplet size distribution from a typical industrial-scale sprinkler.</i>	164
<i>Figure 105 - Base FDS compartment</i>	174
<i>Figure 106 – Simulation 1: Compartment temperature profile under normal operation</i>	176
<i>Figure 107 - Simulation 2: Flame and smoke surfaces</i>	178
<i>Figure 108 - Simulation 2: Occupant Thermocouple Tree</i>	178
<i>Figure 109 - Simulation 2: Occupant temperature at 60 sec</i>	179
<i>Figure 110 - Simulation 2: Occupant temperature at 180 sec</i>	179
<i>Figure 111 - Simulation 2: Occupant temperature at 400 sec</i>	180
<i>Figure 112 - Simulation 2: Roof exhaust duct</i>	180
<i>Figure 113 - Simulation 3: Occupants Thermocouple Tree</i>	183
<i>Figure 114 - Simulation 3: Occupant temperature profile at 60 sec</i>	183
<i>Figure 115 - Simulation 3: Occupant temperature profile at 120 sec</i>	184
<i>Figure 116 - Simulation 3: Airflow effected flame and smoke front</i>	184
<i>Figure 117 - Simulation 3: Velocity within compartment at low flow</i>	185
<i>Figure 118 - Simulation 3: Velocity within compartment at high flow</i>	185

Figure 119 - Simulation 4: Occupant Thermocouple Tree	188
Figure 120 - Simulation 4: Water mist activation	188
Figure 121 - Simulation 4: Compartment velocities during fire mode	189
Figure 122 - Simulation 4: Normal flow visibility	189
Figure 123 - Simulation 4: High flow visibility	190
Figure 124 - Simulation 4: Normal mode oxygen concentration	190
Figure 125 - Simulation 4: Fire mode oxygen concentration	191
Figure 126 - Simulation 5: Occupant Thermocouple Tree	193
Figure 127 - Simulation 5: Visibility at 60 sec	193
Figure 128 - Simulation 5: Visibility at 120 sec	194
Figure 129 - Simulation 5: Velocity at 120 sec	194
Figure 130 - Simulation 6: Fire heat release rate	196
Figure 131 - Simulation 6: Occupant Thermocouple Tree	197
Figure 132 - Simulation 6: Flame and smoke front at 60 sec	197
Figure 133 - Simulation 6: Flame and smoke front at 350 sec	198
Figure 134 - Simulation 6: Compartment temperature at 60 sec	198
Figure 135 - Simulation 6: Compartment temperature at 120 sec	199
Figure 136 - Simulation 7: Occupant Thermocouple Tree	200
Figure 137 - Simulation 7: Water vapour 15 sec after mist activation	201
Figure 138 - Simulation 7: Water vapour at 400 sec	201
Figure 139 - Simulation 8: Occupant Thermocouple Tree	203
Figure 140 - Simulation 8: Visibility after 100 sec	204
Figure 141 - Simulation 8: Flame and smoke front	204
Figure 142 - Simulation 8: Oxygen concentration at 400 sec	205
Figure 143 - Compartment temperature after 400 Sec and under various scenarios	207
Figure 144 - Compartment CO ₂ concentration after 400 Sec and under various scenarios	208
Figure 145 - Compartment soot density after 400 Sec and under various scenarios	209
Figure 146 - Interface height calculated based on a zone model	212
Figure 147 - Simulation 4: Normal flow visibility	212
Figure 148 - Centre floor fire under normal conditions - exhaust temperatures	213
Figure 149 - Centre floor fire under normal conditions – Tree 2, 0.3m temperatures	214
Figure 150 - Centre floor fire under normal conditions – Tree 2, 2.1m temperatures	215
Figure 151 - Centre floor fire under normal conditions – Tree 1, 0.7m temperatures	216
Figure 152 - Centre floor fire under normal conditions – Tree 1, 1.8m temperatures	216
Figure 153 - Centre floor fire with high airflow only – exhaust temperatures	217
Figure 154 - Centre floor fire with high airflow only – Tree 2, 0.3m temperatures	218
Figure 155 - Centre floor fire with high airflow only – Tree 1, 1.8m temperatures	218
Figure 156 - Centre floor fire, high airflow and water mist – exhaust temperatures	220
Figure 157 - Centre floor fire, high airflow and water mist – Tree 1, 0.3m temperatures	221
Figure 158 - Centre floor fire, high airflow and water mist – Tree 1, 1.8m temperatures	221

<i>Figure 159 – Back corner fire, high airflow and water mist – exhaust temperatures</i>	<i>222</i>
<i>Figure 160 – Back corner fire, high airflow and water mist – Back corner 1.3m temperatures</i>	<i>224</i>
<i>Figure 161 – Centre floor fire, low airflow and water mist – exhaust temperatures</i>	<i>225</i>
<i>Figure 162 – Centre floor fire, low airflow and water mist – Tree 1, 0.3m temperatures</i>	<i>225</i>
<i>Figure 163 – Centre floor fire, low airflow and water mist – Tree 1, 1.8m temperatures</i>	<i>226</i>

List of Tables

<i>Table 1 - Mixing and displacement ventilation system comparison</i>	<i>26</i>
<i>Table 2 - Fire simulations</i>	<i>40</i>
<i>Table 3 - Settling time of water drops [41]</i>	<i>51</i>
<i>Table 4 - Initial experimental timeline</i>	<i>79</i>
<i>Table 5 - Experimental timeline for pool fire tests</i>	<i>80</i>
<i>Table 6 - Experimental timeline for wood crib fires</i>	<i>80</i>

Glossary of Terms

Acronyms:

CFD	Computational Fluid Dynamics
DNS	Direct Numerical Simulation
FDS	Fire Dynamic Simulator; the CFD model used in this research
HRR	Heat Release Rate
HRRPUA	Heat Release Rate Per Unit Area
IMD	International Maritime Organization
LES	Large Eddy Simulation
NFPA	National Fire Protection Association
NIST	National Institute of Standards and Technology
SMD	Saunter Mean Diameter

Nomenclature:

A_d	surface area of droplet
A_f	area of fuel
C	empirically derived constant
C_d	drag coefficient
C_p	constant pressure specific heat
D	fire diameter, droplet diameter
D^*	characteristic fire diameter
D_{vx}	X% volume diameter
T_o	centreline plume temperature above ambient
F_d	drag force on droplet
f	external force vector (sprinkler droplet drag)
G	gravitational force on particle
g	acceleration of gravity
H	enclosure height
K	temperature
k	thermal conductivity, turbulent kinetic energy
L	flame height
m_∞	mass loss rate

m_e	mass entrained into plume
m_s	mass of supply air
m_u	mass into upper layer
p	pressure
q_r	radiative heat flux vector
q'''	heat release rate per unit volume
Q^*	dimensionless HRR
Q	total heat release rate, flow rate
Q_c	convective heat release rate
Re	Reynolds number
T	temperature
t	time
$u (u, v, w)$	velocity vector
V_p	wood fuel surface regression rate
χ	combustion efficiency
Y_F	mass fraction of fuel
Y_{Fi}	mass fraction of fuel in the fuel stream
Y_o	mass fraction of oxygen
$Y_{O\ inf}$	mass fraction of oxygen in ambient
z	height above fire base
z_o	virtual origin of fire
Z	mixture fraction
Z_f	mixture fraction at flame surface
$Z_{f,eff}$	effective flame mixture fraction
$\tilde{\rho}$	density
σ	Stefan-Boltzmann constant
τ	viscous stress tensor
Δh_c	heat of combustion
∞	subscript, at ambient conditions

1. Introduction

1.1 Overview

Currently in the fire safety field few fire suppression systems exist that do not pose some form of hazard to occupants or electronics within a room during a fire. In the case of a conventional sprinkler system, the occupants may be protected but the large quantity of water delivered causes major damage to electronic equipment and internal surfaces. This problem has become more relevant in today's age where the presence of computers are becoming common at home and work and where large volumes of data are stored in an electronic form. Conversely gas or conventional water mist systems provide a greater level of safety for electronic equipment but can create an environment that adversely affects occupants. In both types of system the combustion products are contained within the compartment and if the fire is not suppressed then these build up and the interior quickly becomes untenable.

This study aims to overcome these drawbacks by investigating the use of a fine water mist combined with a displacement ventilation system to create an environment where occupants and electrical equipment are protected in a "lake" of clean, water mist filled air.

The displacement water mist system operates by introducing relatively large volumes of air at low level, and combining it with very fine water mist. The air/water mist mixture enters the compartment and due to thermal stratification, spreads out across the floor forming a protective lake. The water mist within the air has such a fine diameter that it can remain suspended for long periods, providing cooling and radiant protection while not causing significant damage to electrical equipment. The density of the water mist is also controlled to create a level where flame suppression occurs.

The entire system is intended to operate in a relatively stable and laminar manner so that the hot upper layer of combustion gases is not mixed with the relatively cool clean lower layer. The upper layer is exhausted through the roof to optimize the heat that is expelled from the compartment while the lower layer provides occupant and electrical protection.

1.2 Research Objectives

The primary objective of this research was to determine if a fine water mist could be used in conjunction with a displacement ventilation system, to create a fire suppression system that allowed occupants and electronics to remain safely within a compartment for the duration of the fire.

To reach this primary objective the research was broken down into three sections as follows:

1. Design and build a full-scale displacement water mist system and compare its effectiveness to other fire suppression systems under a number of different fire scenarios.
2. Model the designed system in the computer simulation program Fire Dynamics Simulator (FDS) and investigate the operation of the system and its effect on the compartment atmosphere.
3. Compare the temperature results from live testing with those generated by the FDS simulations to determine the accuracy of the FDS model.

1.3 Report Layout

This report is broken down into a number of sections with Section one of this report providing general information and the objectives of this research. Section two contains background information on both water mist and displacement ventilation systems, with Section three outlining in detail the theoretical concept of a displacement water mist system. The experimental design of the system is covered in Section four with the full scale testing and FDS simulations presented and reviewed in Sections five and six respectively. Section seven presents a comparison between the live tests and the FDS simulations. A discussion on possible future work is presented along with a summary on the findings of this research in sections eight and nine. Finally the references used throughout this paper are presented along with appendices containing relevant data.

2. Background

This section of the report outlines the history of water mist suppression systems along with the key components and fire suppression modes involved in its use. A brief description of past experiments involving water mist is then presented followed by a review of air conditioning systems and the history and concepts of displacement ventilation. A summary is also given which outlines the major points covered and how they relate to each other.

2.1 *Development Of Water Mist Systems*

The term “water mist” refers to a very fine water spray that remains suspended in air for an extended period of time [1]. Water mist fire protection systems were first researched during the 1950’s and 1960’s [2] but did not gain favour in the fire community due to both economic and technical reasons. Economically there were less expensive systems available such as conventional sprinklers and halon gaseous agents. Technically the mist systems raised concerns due to the high pressures required to produce a fine spray, the potential for blocking of the small orifice nozzles and doubts about the long-term ability to maintain the equipment [3].

In the 1980s though a number of events occurred which revived the international communities interest in water mist system development and use. These were:

- They became more economically viable.
- The International Maritime Organization (IMO) ruled that marine sprinklers must be installed in all existing and new passenger ships carrying more than 35 passengers.
- The 1987 signing of the Montreal Protocol, which required the phasing out and use of ozone depleting substances (halon).

Since the occurrence of these events the rate of research into water mist suppression has increased dramatically with a number of papers being presented at annual world conferences such as INTERFLAM [4] and 'Water Mist Instead of Halons' [5]. While our knowledge of these systems has greatly increased there is still much to be learned about the use of water mist and the calculations involved in designing effective and reliable systems.

Water mist systems operate on the principle of generating very fine droplets of water and delivering them to the fire zone. The advantage of this is that water mist can be very effective at fire suppression due to its high specific heat and heat of vaporization coupled with the increased surface area allowing faster heat absorption [6]. As a comparison, conventional sprinkler systems operate by generating relatively larger drops that fall through the fire zone and provide suppression by cooling and wetting of the surfaces.

Existing water mist systems have both advantages and disadvantages over conventional sprinkler systems. This can make them a better option in some situations, rather than competing directly in all scenarios [7]. Some of these advantages and disadvantages are listed below [8].

Advantages:

- Replacement for halon and CO₂ systems in many applications.
- Safer than CO₂.
- Cools the fire area dramatically.
- Uses less water than conventional sprinklers.
- Prevents reignition.
- Has some smoke scrubbing qualities.
- Can be used to suppress explosions.

Disadvantages:

- More expensive.
- Less effective against small fires.
- Requires greater water pressure than conventional sprinkler systems and can require the use of compressed gas or high-pressure pumps.
- New technology and as such uncertainty exists as to how to evaluate such systems.
- Fire and component testing is required to verify that water mist is effective for the particular hazard.
- Slower to extinguish fires than gas systems [9].

One of the current areas of interest is how to develop analytical methods for the design of new systems. Existing design methods for conventional sprinklers tend to rely on historical test data and some success has been reached in computer modelling using zone and Computational Fluid Dynamic (CFD) models. In the case of water mist systems though, the design process relies more on actual trials due to the lack of historical data and the complex interactions that occur on small scales making analytical calculations extremely difficult. When modelling a conventional sprinkler with CFD the individual water particle is often tracked. With water mist the particles are extremely small and there is a greater order of magnitude required. This causes the processing time to be extremely long and complex. Additional to this, the fundamental reactions that occur on such small levels are not completely understood and as such a high level of error is introduced.

2.2 Extinguishment Mechanisms

There are a number of complex interactions that occur between water mist and fires, which can lead to extinguishment. The three primary mechanisms of extinguishment are heat extraction, oxygen depletion and radiation blocking, with secondary mechanisms involving air dilution and kinetic effects such as reduced flame velocity. As the primary mechanisms are better understood and play a greater relevance in extinguishment these are investigated further below.

Heat extraction:

Water provides an excellent form of heat extraction due to its high specific heat and heat of vaporization. As shown in Figure 1 the majority of the energy absorbed by water in heating occurs during the phase change from liquid to gas.

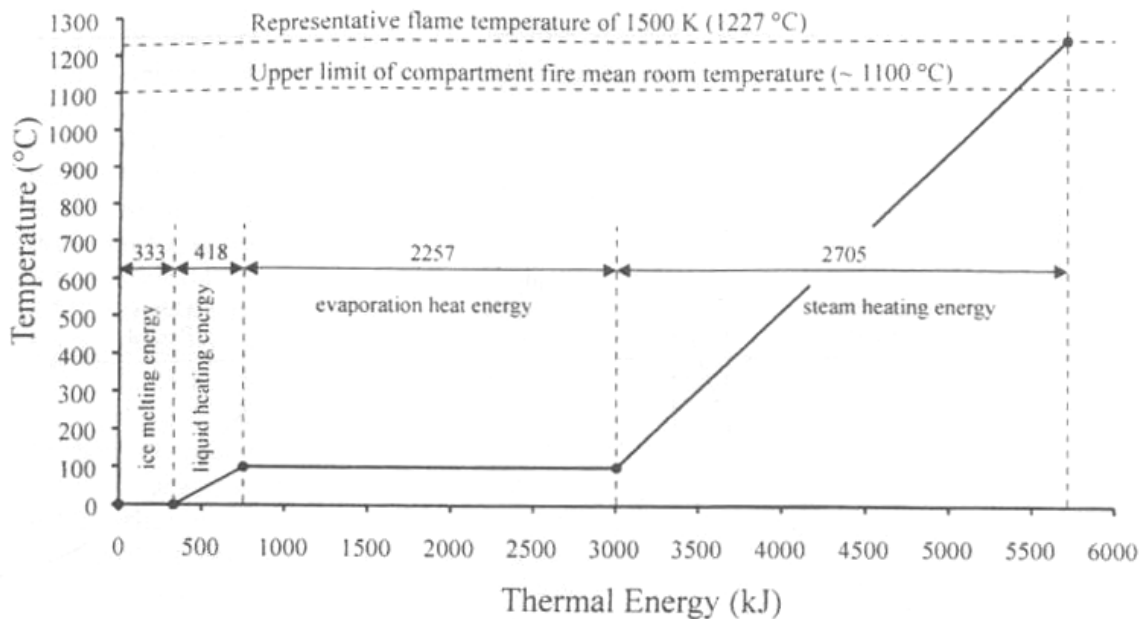


Figure 1 - Heat absorption during heating and phase change of water [10]

In comparison to some other extinguishing agents, this value is extremely high as shown in Figure 2. As can be seen, water is nearly twice as effective at heat absorption as the other extinguishing agents. The two plots on the graph are the heat of vaporization (H_{vap}) and the specific heat of vapour at 20°C (c_p vapour (20C)).

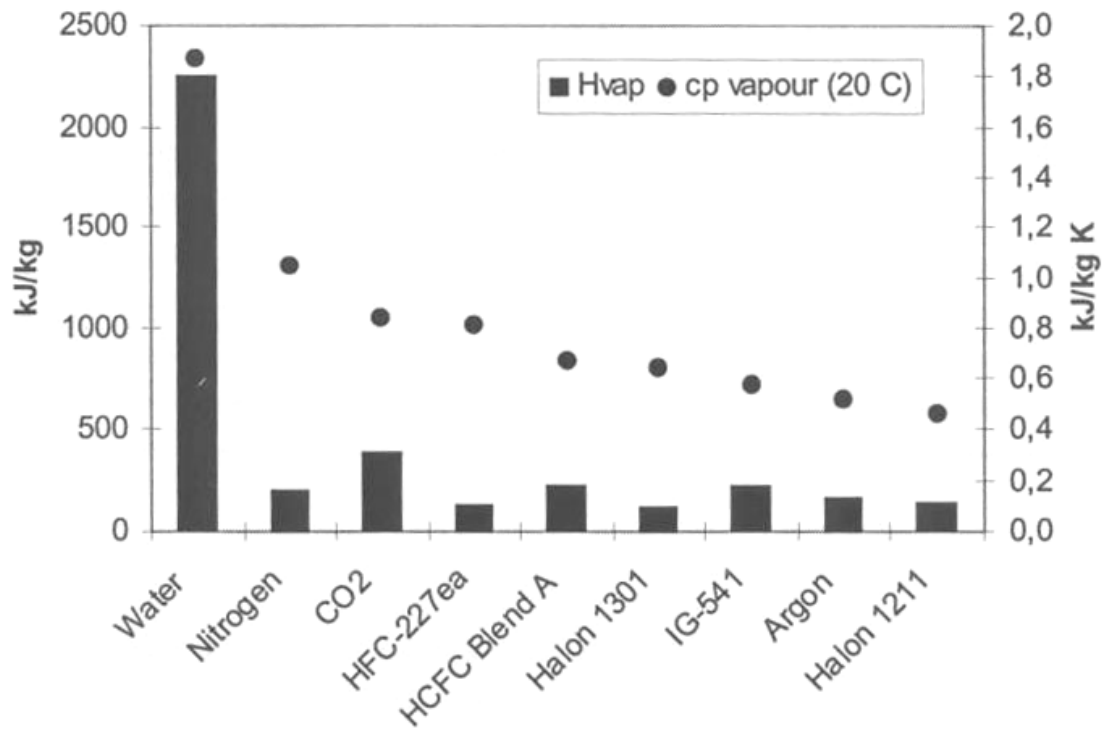


Figure 2 - Comparison of specific heat capacity and evaporation [11]

The water mist particles absorb heat in three areas 1) from the hot gases and flame, 2) from the fuel, and 3) from the surrounding objects and surfaces [1]. Cooling of the fuel and of the surrounding surface can result in lower pyrolysis rates and hence reduced heat release rates along with reduced fire spread. In the case of gas and flame cooling, the water mist particles within the flame zone cool the reaction zone by being converted to steam. The reduction in temperature reduces radiation feedback to the surface and reduces the reaction rate within the flame. Previous studies [12] have suggested that it is not necessary to extract all of the heat from the reaction but that absorption of between 30% and 60% may be enough to cause burning to stop.

Oxygen Displacement:

The second, and arguably more important mechanism for fire suppression by water mist is oxygen displacement. Water droplets expand by approximately 1900 fold when evaporated. When water mist is injected within a hot compartment it results in rapid evaporation, expansion and displacement of the air

in the compartment with steam. If the amount of oxygen within the compartment is sufficiently reduced, typically to 7% – 13%, then the fire will be extinguished [1].

Unfortunately, the dilution of oxygen by water vapour is limited by the temperature. As water mist is injected into the compartment the air is cooled below the temperature at which it can hold enough vapour. The critical inerting limit of water vapour in air is 25% - 30% [13]. From Figure 3 it can be seen that this corresponds to approximately 65-70°C.

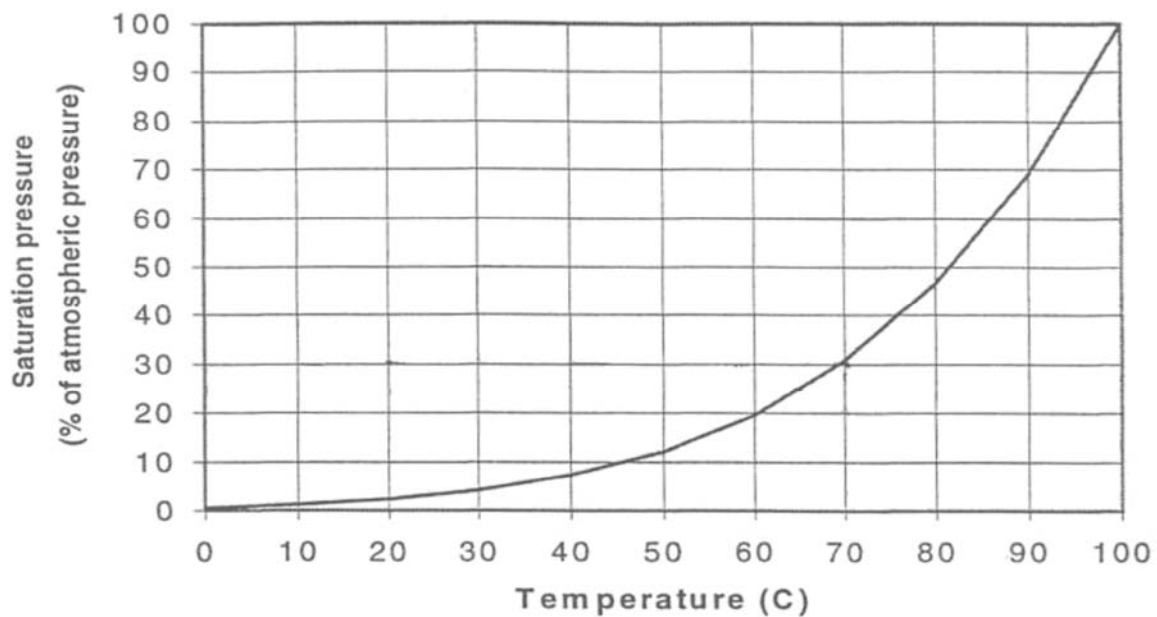


Figure 3 - Saturation pressure of water vapour in air below the boiling point [14]

Below this temperature the water vapour condenses out as particles and the oxygen concentration remains high enough to support combustion. This is to some extent why testing has shown it is easier to extinguish larger fires than smaller fires. In a small fire the temperature is not sufficient to maintain a sufficient water vapour content to suppress the fire. Instead suppression relies primarily on other mechanisms.

Radiation Blocking:

The third primary mechanism by which water mist suppresses a fire is through radiation blocking. The presence of fine water droplets effectively absorb and disperse the radiant heat given off by the fire. This assists in suppressing the fire by reducing the feedback to the fuel surface and hence reducing the pyrolysis rate. Additionally it reduces the spread of the fire to surrounding objects and protects personnel and objects within the compartment from direct thermal radiation.

Theoretical and practical work carried out in the field of radiation blocking has indicated that smaller droplets provide greater radiation attenuation than larger drops [15]. This is due primarily to the optical absorption and scattering characteristics created in smaller diameter drops [16]. Tests have indicated that a spray with 90% of its droplets less than 200 μm in diameter is capable of blocking approximately 60% of radiation at 1m when at a concentration of 100 g/m^3 [17]. Hence the ideal water mist for providing radiant heat blocking is slow moving, densely packed, fine particles [10].

2.3 Droplet Size

When discussing water mist systems, often the immediate interest is in the size of the water particles being produced as this factor greatly effects how the spray will interact with the fire and which of the extinguishment mechanisms listed above will play significant roles. Figure 4 shows the spectrum of drop sizes from 0.1 μm to 1,000 μm in relation to everyday occurrences.

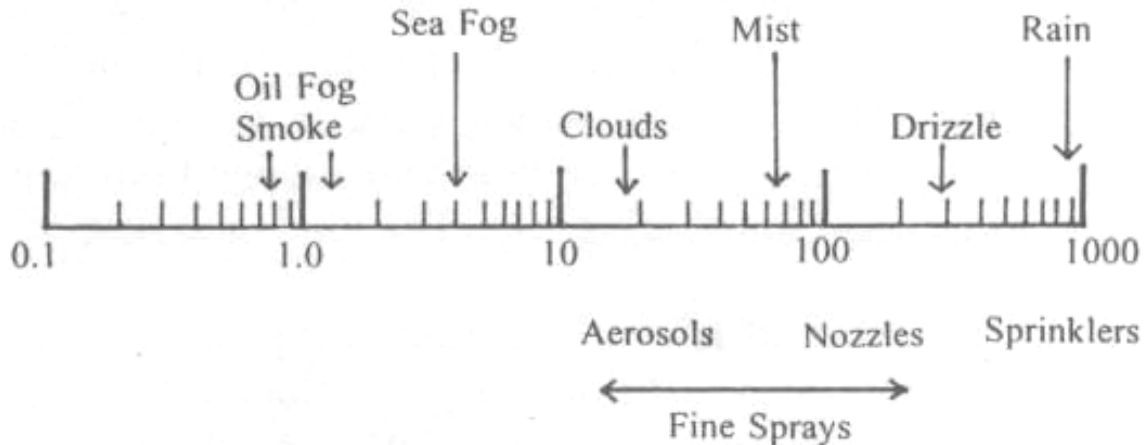


Figure 4 - Spectrum of Drop Diameters [18]

Often a single average value will be given for a drop size produced by a nozzle but this is limited by the type of average used and the fact that the distribution of drop sizes is not clearly indicated. The most common of the single figure identifiers used are as follows [19]:

- *Arithmetic Mean*: A simple weighted average based on the diameters of all individual drops in the spray.
- *Surface Mean*: The diameter of a drop whose surface area, if multiplied by the total number of drops, will equal the total surface of all the drops in the spray sample.
- *Volume Mean*: (D_{v50}) The diameter of a drop whose volume, if multiplied by the total number of drops will be equal to the total volume of the spray.
- *Saunter Mean Diameter*. (SMD) Also known as the Volume Surface Mean it is the diameter of a drop whose ratio of volume to surface area is equal to that of the entire spray sample.

As can be seen with the above identifiers two sprays could have the same mean but have widely varying distribution patterns. As awareness of this factor has increased alternate methods to define a spray have been introduced. Initially NFPA 750 [20] defined a water mist as having a D_{v99} (99% volume diameter) of less than 1,000 μm as measured in the coarsest part of the spray, on a 1m plane

from the nozzle, and at its minimum operating design pressure. As a comparison a conventional sprinkler may have a D_{v99} in the order of 5,000 μm [10]. It had been suggested that this definition is too loose, because it permits drop sizes, which are not dissimilar to that of a conventional sprinkler in their characteristics. As an alternative to this Mawhinney and Solomon [21] proposed a mist classification system based again on the 'cumulative percent volume' distribution plot. The graphical representations of these definitions are shown in Figure 5.

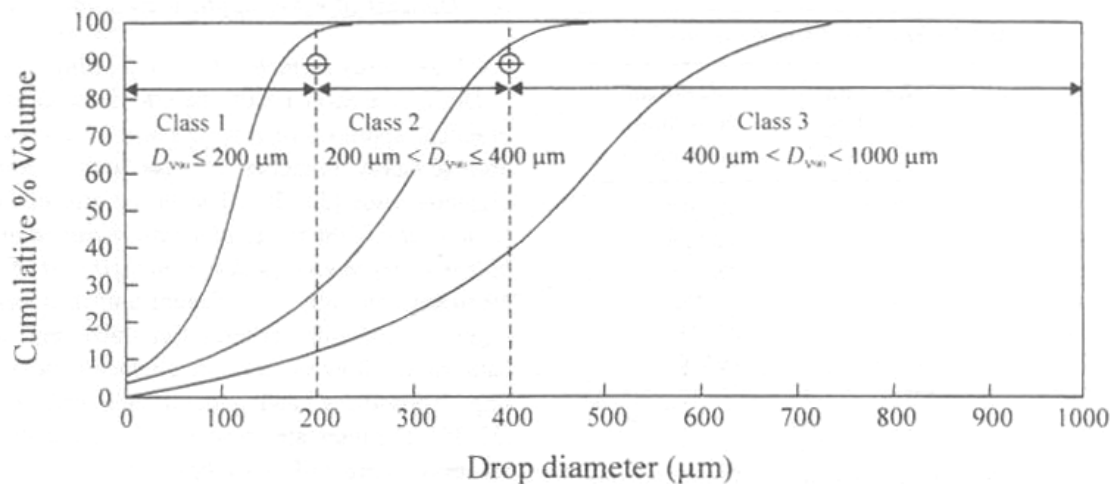


Figure 5 - Classification of water sprays by drop size distribution [49]

As can be seen the three sections differentiate between fine and coarse mists with class 1 representing a fine spray. It should be noted though that there is no scientific basis for the above spray classifications. [22]

Based on their work NFPA 750 1996 accepted a modified version of this graph as standard. The NFPA 750 1996 graph is shown in Figure 6.

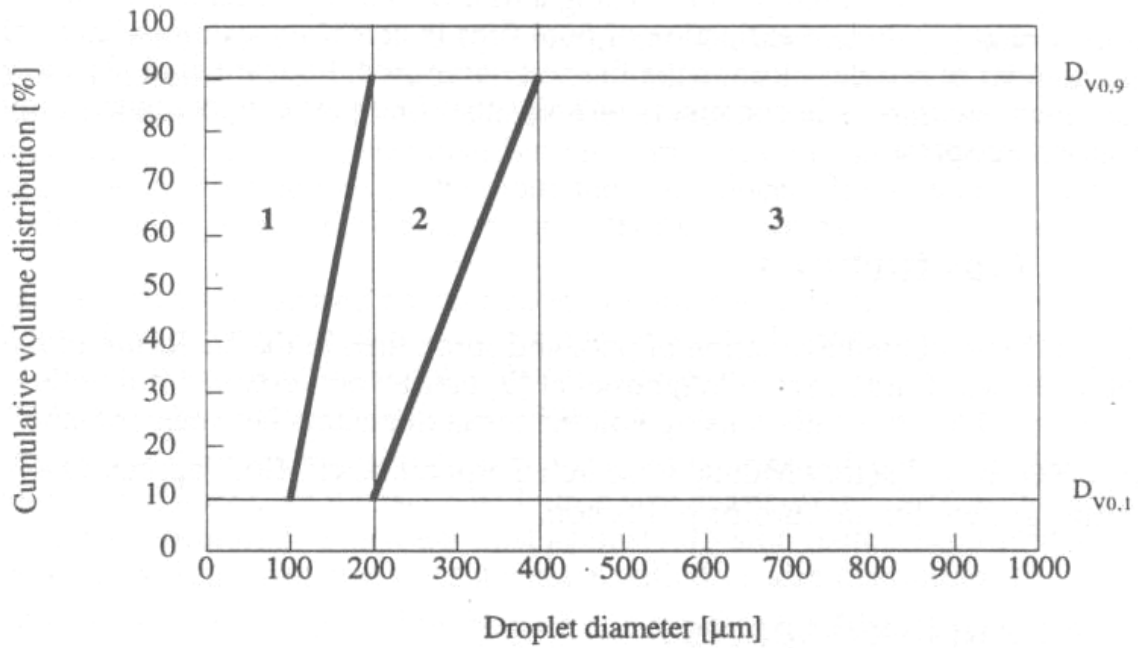


Figure 6 - Division of different classes of water mist according to NFPA 750

The size of water particles plays an important part in the characteristics and interaction with a fire. In the case of heat extraction smaller particles result in a higher surface area and hence faster heat extraction for a given volume. This is shown clearly in Figure 7 which shows the time taken for varying drop sizes to evaporate at a number of temperatures.

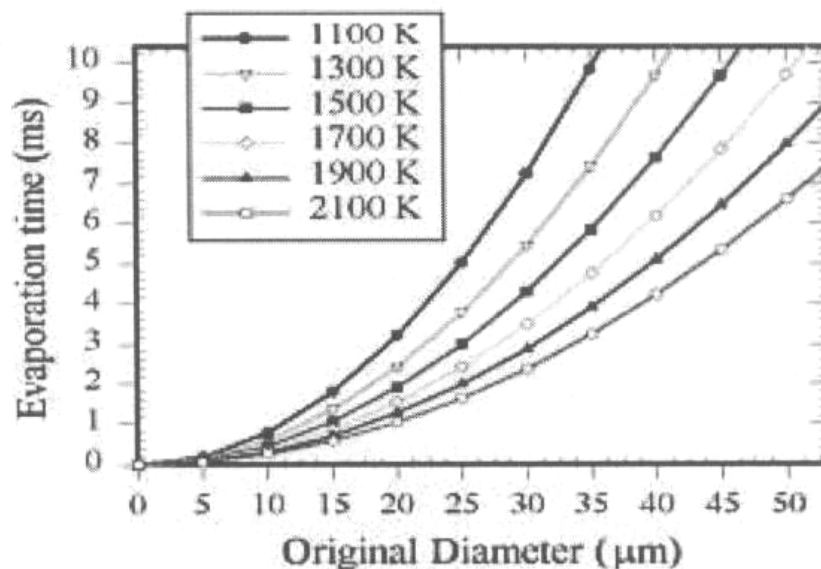


Figure 7 - Water drop evaporation [23]

Testing carried out using a counter flow non-premixed test apparatus, as described in the following section has shown that particles in the region of 20 μm provide the greatest extinguishment capacity [23].

What must be considered though is the required survival time of a droplet injected into a fire. The smaller the droplet diameter the faster the heat extraction, but the shorter the survival time. It may be a requirement of a ceiling injection system that the droplet survives the fire plume to reach the base of the fire and provide wetting of the fuel.

Additional to this is the falling rate of a particle as it passes through the plume. As a particle becomes smaller the drag force created across its surface becomes larger in relation to its mass and hence the gravitational force on it. Hence a large particle will fall quickly to the floor while a small particle will fall at a much slower rate. If this rate is lower than the velocity within the plume then the particle will be lifted within the plume and circulated within the compartment.

The equations involved in this calculation are as follows:

$$G = m \cdot g = g \cdot \rho \cdot \pi \cdot D^3 / 6 \quad \text{Equation 1: Gravitational Force}$$

$$F_d = \frac{1}{2} \rho_g \cdot v^2 \cdot C_d \cdot A_d \quad \text{Equation 2: Drag Force}$$

$$C_d = \frac{24}{\text{Re}} + 0.1935 \cdot \text{Re}^{0.3695} \quad \text{Equation 3: Drag Coefficient}$$

Based on these equations Figure 8 can be generated for the falling velocities of varying size particles [19].

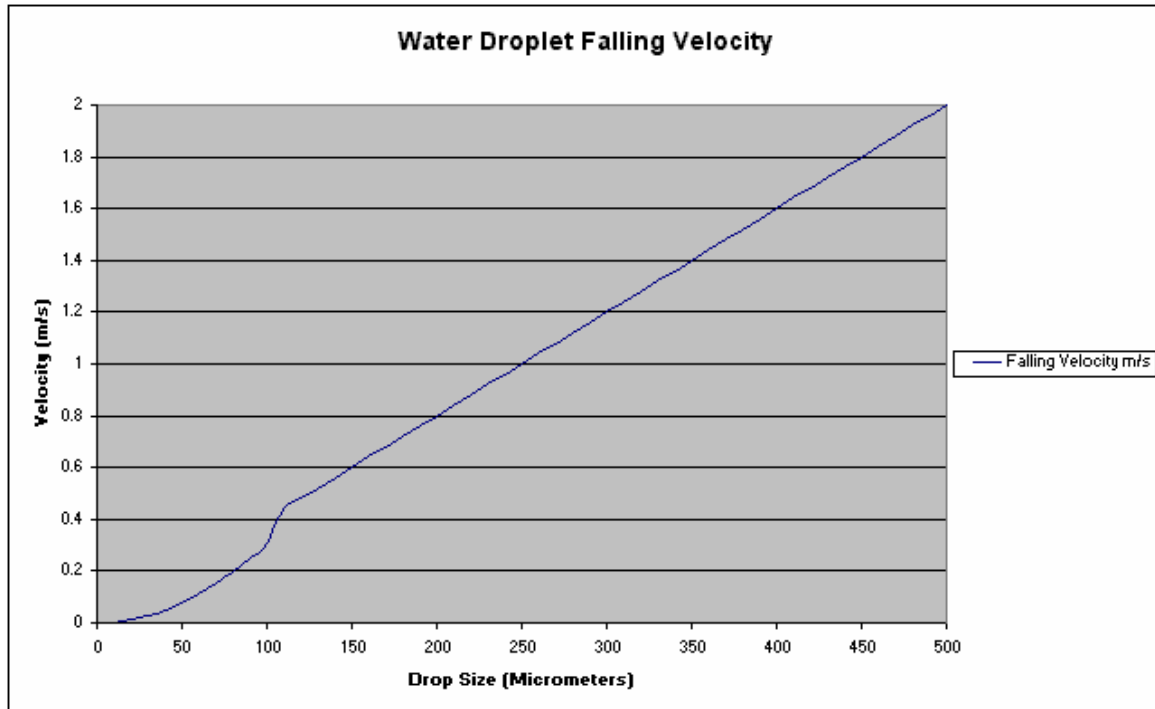


Figure 8 - Falling velocities in still air of varying droplet sizes [19].

In the case of radiation blocking, as has already been discussed, smaller drops provide the greatest attenuation. Radiation suppression also requires that the water particles circulate around the compartment and do not impinge on any objects. Testing by Anderson et al. [19] has shown that particles of the order of 20 μm or less can flow with the airflow relatively well. Figure 9 shows the paths of varying size particles in a 4 m/s airflow. The innermost curve is generated from the 1 μm particles.

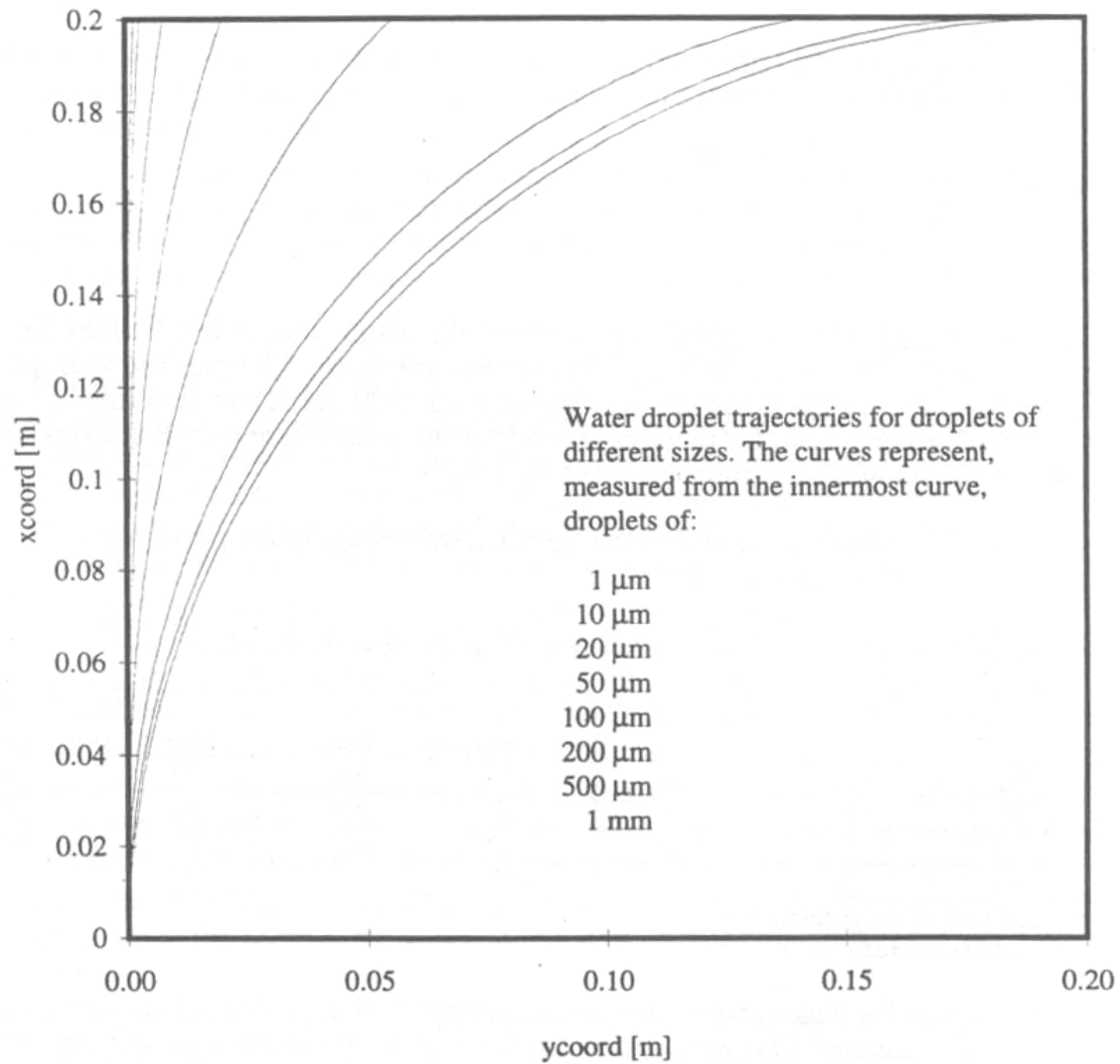


Figure 9 - Trajectories for droplets of different sizes at an airflow of 4m/s [19]

For the reasons listed here, it is often stated in literature that no 'ideal' water mist distribution exists for all situations. The selection of a water mist particle distribution is instead dependent on the particular fire and the suppression characteristics that will play the most significant role.

2.4 Water Density Requirements

Of key importance in any mist system design is the water mist mass density required for extinguishment. This property is commonly tested using a counter flow non-premixed flame apparatus on a small idealized scale or recorded through trial and error in large tests.

In the counter flow non-premixed flame apparatus fuel is injected from one side while air and water mist are injected from the other direction. During the test the quantity of water mist is increased until the flame front is extinguished. Figure 10 depicts this setup.

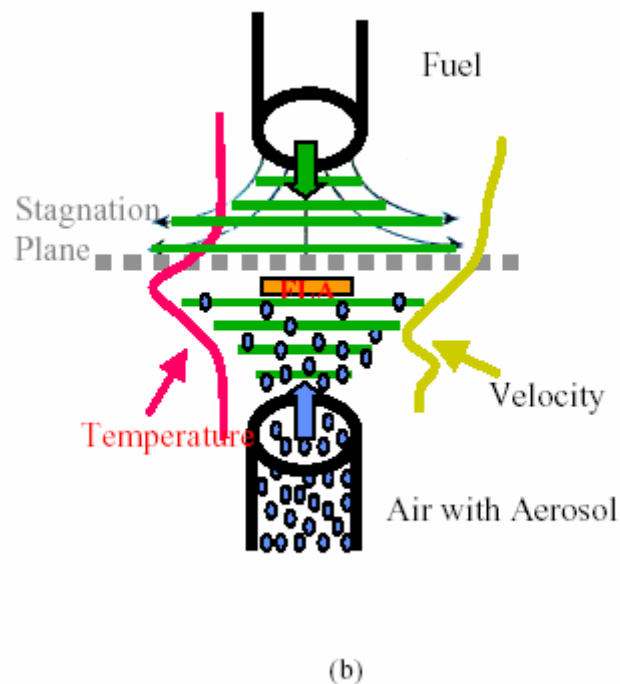


Figure 10 - Counterflow non-premixed flame apparatus [24]

Testing of this nature has indicated that flame extinction will occur at water to air mass values of less than 160 g/kg.

Full scale testing under realistic conditions carried out in the Norwegian Fire Research Laboratory found that a value of 60 – 70 g/kg was required for large fires and 400 – 600 g/kg was required for smaller fires [25]. Lund Institute of

Technology tested propane diffusion fires in a 1/3 scale ISO room. In these tests values in the region of 70 - 140 g/kg were recorded for particles with a $D_{v50} = 30 - 40\mu\text{m}$ [19]. The general conclusion from these tests was that a water mist to air mass ratio of 150 – 200 g/kg would be sufficient to extinguish a fire.

2.5 Water Mist Generation

The generation of water mist has in recent years been investigated almost as thoroughly as the use of water mist. Primarily corporations such as 'Marioff' have increased their development in nozzle types to meet the growing demand from the fire engineering community.

There are a number of water mist generation systems around of which the primary methods used for fire protection are listed below [19].

- **Hydraulic nozzles:** These nozzles use a single fluid passed through a small orifice or swirl chamber to break up the water flow and create fine particles. The size of the particle produced primarily depends on the pressure used. Low pressure nozzles defined as being below 12 bar tend to create larger particles such as in conventional sprinklers. High pressure nozzles operating above 34 bar can create a finer water mist. In the medium pressure range the size continually decreases with pressure. The advantage with this type of nozzle is that it is well understood. The disadvantage is that to create fine sprays such as those used in class 1 mist systems, the pressure must be high and hence the system requires specialized pumping equipment. Also due to the small orifice diameter it can be prone to clogging if a filter is not used.
- **Pneumatic nozzles:** Twin fluid or air atomizing nozzles generally produce the smallest droplets. Air or another gas such as nitrogen is fed into a mixing chamber with the liquid and then ejected through a small orifice. The orifice sizes are not as small as hydraulic nozzles and gas and liquid are typically at pressures in the low range. The advantage with this system is that standard compressed gas bottles can be used in conjunction with

low pressure pumps. The disadvantage is that two sets of pipes must be connected to each nozzle and two systems must be maintained.

- **Impingement nozzles:** Impingement nozzles operate by causing the water stream to impact on another object and hence cause it to breakup. The source of impact can be a fixed plate or the use of an opposing water stream. This type of nozzle tends to create a coarser spray than that of the nozzles listed above but are well tested and very robust. This is the principle that conventional sprinklers operate on.

As well as these core mist generation systems new developments are occurring all of the time to develop new systems. These include silicon wafer nozzles with micro nozzles in the order of 30µm in diameter, Flashing nozzles which heat water under pressure so that when exposed it condenses rapidly to create drops, and ultrasonic misters which create particles using ultrasonic waves.

Each of these methods has advantages and disadvantages that must be weighed up before selection.

2.6 Existing Operating Systems/Concepts

Existing water mist suppression systems tend to operate on the concept of high level ceiling injection either locally or in a total flooding arrangement. Typically if the zone is large then a local activation system is used, while if the zone is small then all nozzles are activated to create a total flooding system.

There are a number of reasons for this with the main basis being that as with conventional sprinkler systems the nozzles cannot be covered or blocked in this position. They can be positioned in such a way that they will cover the majority of the floor area and be able to react to a fire in any position. It also provides direct cooling to the hot upper layer [1], allows easy installation and through basic physics it can be assumed that the majority of water will eventually fall to the floor through the compartment.

When a fire occurs the ventilation systems are typically shut down in the fire zone as past experiments have shown that with ventilation systems operating a mist system is less effective [20]. The reason for this is that when shut down the hot combustion gases and water mist are not extracted and circulated within the compartment. This maintains a higher temperature as required to support the critical water vapour limit for oxygen depletion and also feeds the combustion gases with a previously reduced oxygen concentration back into the fire as well. Once the fire is extinguished the compartment is rapidly cooled by the continued injection of water mist.

The disadvantages with this operating concept are that in re-circulating the combustion gases through the zone the atmosphere becomes uninhabitable for any occupants who remain in the compartment. Additionally as mist systems can be employed to protect electrical equipment it results in combustion gases being drawn down to the electronics and running the risk of causing damage.

2.7 Historical Testing

As has been discussed, with the recent increased interest in water mist systems more research has taken place into different arrangement and uses of water mist nozzles. This section of the report outlines some of the more relevant research tests conducted and attempts to provide a brief overview of the knowledge gained.

Researcher: Civil Aviation Administration of the UK and the Federal Aviation Administration of the U.S. [1]

Test Scenario: Investigation of water mist in passenger aircraft cabins.

Observations and Findings: The objective of the water mist system was not to suppress any pool fire but rather to prevent the spread of the fire through the cabin and cool the interior atmosphere to extend the occupant survival time. The tests achieved and extended survival time by using water mist systems operated in 2.4m zones by a single heat detector. The mechanisms that were used

consisted of radiant heat blocking, gas cooling and wetting of fuels within the cabin. Ultimately though the high cost of the system prevented its installation in all aircraft.

Researcher: Various research organizations [1].

Test Scenario: Marine Machinery Spaces

Observations and Findings: The International Marine Organization requires that all machinery spaces on large passenger ships be fitted with a fire protection system. This has typically been a CO₂ or Halon system but recent research has turned to the use of water mist. Typically in this application the nozzles are arranged in a deluge configuration with water supply being either fresh or salt water. This system has advantages over a typical sprinkler system as the piping and related weight can be minimized. The mechanisms used in this arrangement are radiation blocking, gas cooling, surface wetting and oxygen depletion through re-circulation and evaporation as previously discussed.

Researcher: Wighus et al. [27]

Test Scenario: Gas Turbine Enclosures

Observations and Findings: This research was initially instigated in response to the need for a fire suppression system for diesel turbines on board offshore drilling platforms. The tests carried out by Wighus et al. confirmed that water mist could be used to successfully suppress fires in turbines. Water mist provides a good fire suppression solution for this type of scenario as it can be continually injected (unlike gas systems which have limited operating time), and provide less thermal shock to the turbine blades than standard sprinklers. The mechanisms involved in suppression include cooling and steam displacement and dilution of oxygen.

Researcher: Simpson et al. – Fire and Safety International [28].

Test Scenario: Fire suppression using water mist in Telecommunications and Electronic Cabinets.

Observations and Findings: This set of experiments tested the effects and efficiency of water mist used within telecommunication and electrical cabinets. In each test case the fire within a 2.44m high, by 0.61m wide and 0.46m deep electrical cabinet were all extinguished within less than two seconds using less than 1 litre of water. Of particular relevance in this set of experiments is that while the low current trips on the circuit boards activated, the current was so low that electric shock was not considered a perceivable danger. In addition to these extinguishment characteristics, after a short period of drying out, all of the electrical systems could be switched back on and continued to function.

Researcher: Evans et al. [29].

Test Scenario: Determining the effect of water mist injection angles on a methane flame.

Observations and Findings: This research involved the injection of water mist into a methane flame through nozzles that could be located in different positions. Some of the experimental tests are shown in Figure 11.

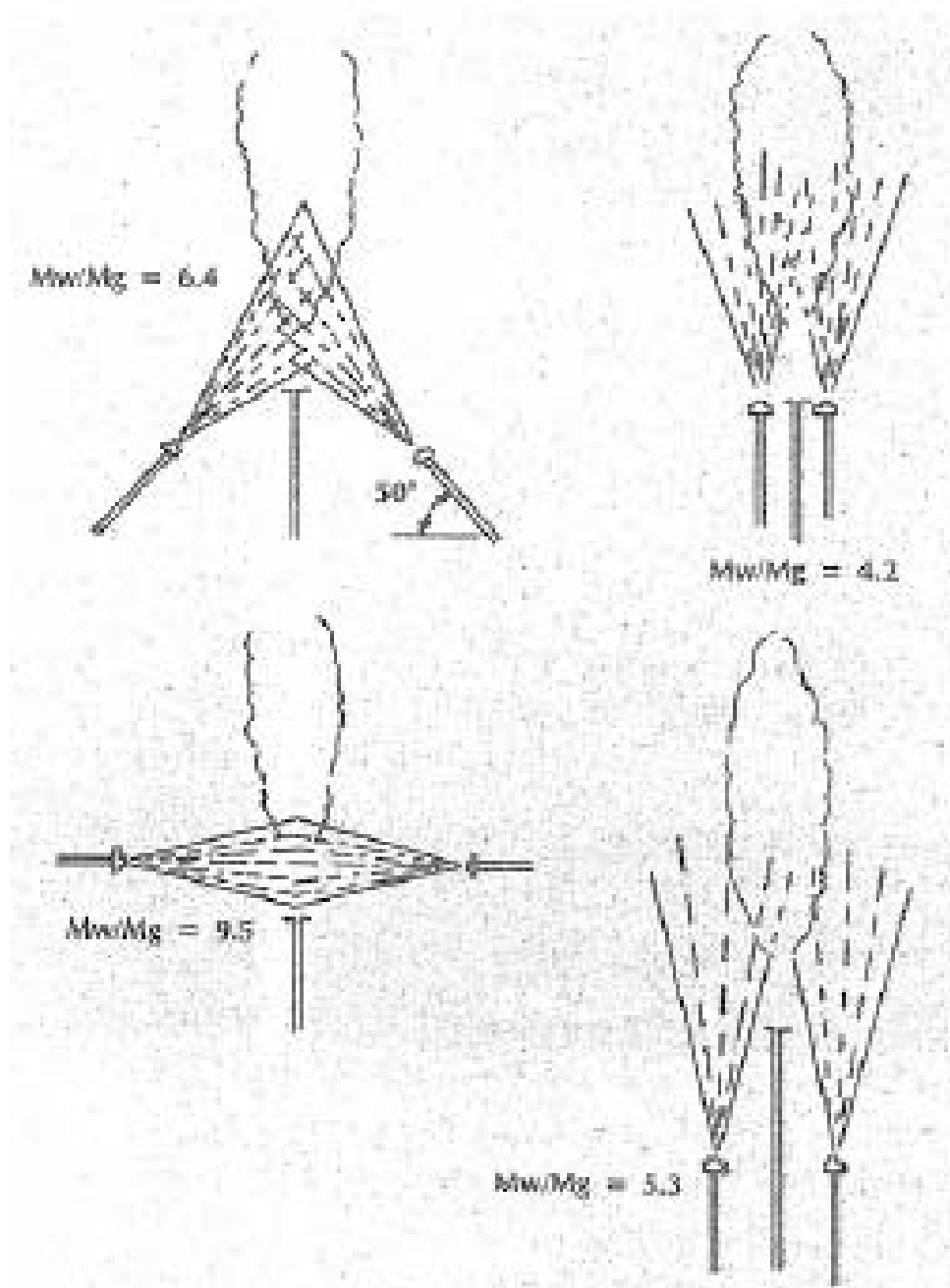


Figure 11 - Experimental set up in water spray injection orientation [29]

The experiments showed that the most effective direction for the water mist to be injected was vertically up, in line with the flame. The required mass rate water to mass rate methane in this scenario was approximately 4 for extinguishment. In comparison horizontal injection resulted in an extinguishment ratio of 9.5 and opposed flow injection resulted in an extinguishment ratio of 20. This indicated that the flow patterns in relation to the reactants were very important to the success of extinguishing the fire.

Researcher: Anderson et al. – Lund University [19]

Test Scenario: Fire suppression using low-level water mist injection within a 1/3 ISO room.

Observations and Findings: The tests carried out at Lund University studied the effectiveness of water mist injection at low level into a 1/3 scale ISO room with an open door. It simulated different fire positions, nozzles positions, water mist densities and water mist droplet sizes in the naturally ventilated room. The research also reviewed how obstacles affected the water mist particles. A layout of the test is shown in Figure 12.

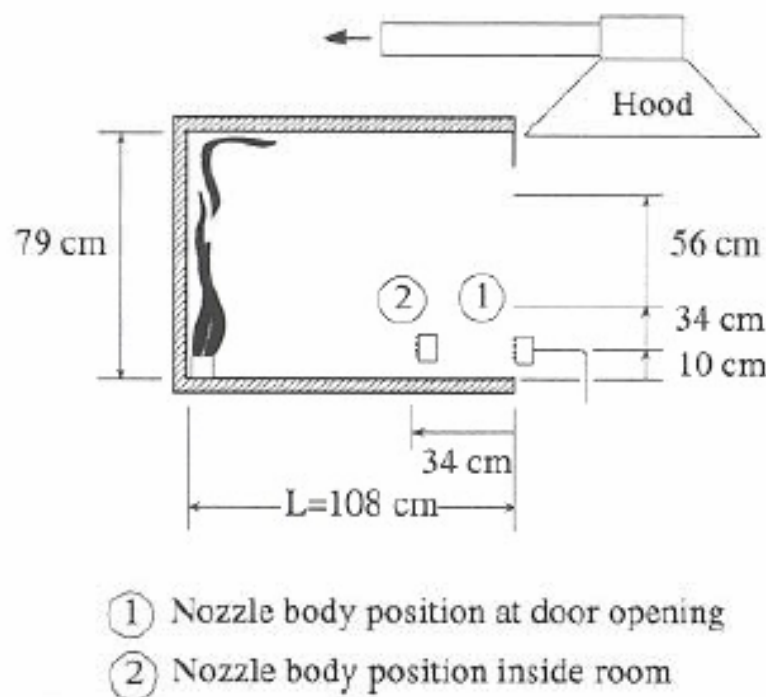


Figure 12 - 1/3 ISO room low-level water mist injection set-up [19]

The results of these tests indicated that a water mist density of between 100 – 200 g/m³ was needed for suppression of a diffusion flame using fine particles. Lower values of water mist density were required as the droplet diameter decreased. Calculations carried out further indicated that for the water particles to follow the airflow around an obstacle the particles needed to be in the region of 1–

20 μ m. Based on these findings they suggest the ideal water droplet size for a low level total flooding system is between 10 – 20 μ m. They also noted, however, that momentum needed to be given to the spray for it to reach all areas of the room, as other distribution modes were very slow.

This test and associated report provides the most relevant information on water mist interaction in relation to the experiments covered in this study and the author recommends them to anyone interested in low-level water mist fire suppression.

2.8 Displacement Ventilation

There are two main types of air movement ventilation system used in air conditioning today. The first is known as a mixing system and has been in wide spread use since the beginning of room ventilation systems. In mixing ventilation systems air is introduced into a room through high speed mixing diffusers located near the ceiling, at hotter or colder temperatures than the room air, to provide heating and cooling as required. The jet of air mixes with the room air providing a relatively constant temperature throughout the zone.

The second type of system is called a displacement ventilation system and is less widely used. Displacement ventilation operates by providing supply air through low velocity diffusers located near the floor. Return grills are located close to the ceiling through which the warm room air is exhausted. The cool supply air spreads over the floor and rises as it is heated by heat sources within the room [30]. This is shown in Figure 13 below.



Figure 13 - Displacement ventilation at work [31]

A comparison of the main differences between mixing ventilation and displacement ventilation is listed in Table 1.

Property	Mixing Ventilation	Displacement Ventilation
Location of supply air diffusers	Near the ceiling	Near the floor
Type of supply air diffuser used	High speed, mixing	Low speed, little mixing
Location of room exhaust air grills	Near the ceiling	Near the ceiling
Supply air temperature in cooling mode	Typically 12°C	Typically 3°C below room temperature (19°C)
Volume of supply air	Dependent on cooling required based on a supply temperature of 12°C	Based on convective flow generated by heat sources in room. Generally greater than a mixing system
Energy efficiency	Relatively good with an economizer operating	Very good dependent on climate. Often better than mixing system

Table 1 - Mixing and displacement ventilation system comparison

While a relatively misunderstood technology in mechanical engineering heating ventilating and air conditioning (HVAC), displacement ventilation had been applied for hundreds of years in a very basic form where it was used to provide fresh air for industrial plants. In the 1940's it began to receive more attention and was investigated for heavy industrial purposes but dropped out of sight. During the 1970's it re-appeared when interest increased in its use for light industry. Then again another surge in interest occurred during the 1980's as its use in commercial premises developed. Throughout this process research, development and implementation has typically been lead from Scandinavian countries, with interest following through to other countries.

Displacement ventilation calculation procedures can be very complex and vast quantities of literature have been written about it. For this reason the objective of this section is to provide the reader with an overview of how displacement ventilation works and the concepts behind it rather than the specific calculations

involved. For a more detailed analysis of the calculations involved in displacement ventilation the author recommends the paper written by Zhivov et al.[30].

The design of displacement ventilation systems is based on similar concepts to those used in fire engineering. A heat source loses heat to the surrounding air through convection and radiation. This in turn heats the air surrounding the object and causes it to rise. As the heated air rises, it mixes with the surrounding air creating a plume, which entrains more air as its height increases. This can be thought of as an inverted cone. Based on the heat source present, the volume of air can be calculated within the plume for a given height.

In designing a displacement system a height is selected, typically just above the occupants, where warm air is allowed to accumulate and be extracted. This is known as the stratification level [30]. Below this layer the air remains relatively cool and clear of pollutants. Based on this height, the volume of air entering the upper layer from plumes within the room is determined. This figure then becomes the volume of supply and exhaust air required within the room to maintain a comfortable condition. A schematic of the room zones and air entrainment is shown in Figure 14.

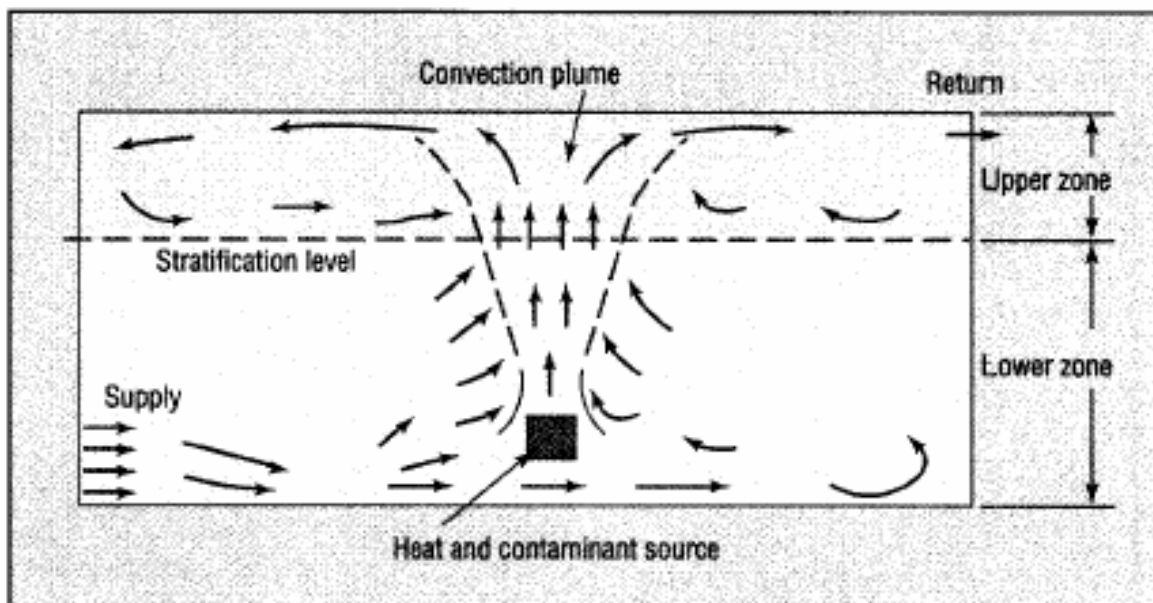


Figure 14 - Displacement ventilation room stratification [30]

In tests carried out by Fitzner, a heated drum was placed within a room operating with a displacement ventilation system. Smoke was added to the room to show the path that was taken for the entrained air, the plume and the stratification layer [32]. A photograph of this test is shown in Figure 15.

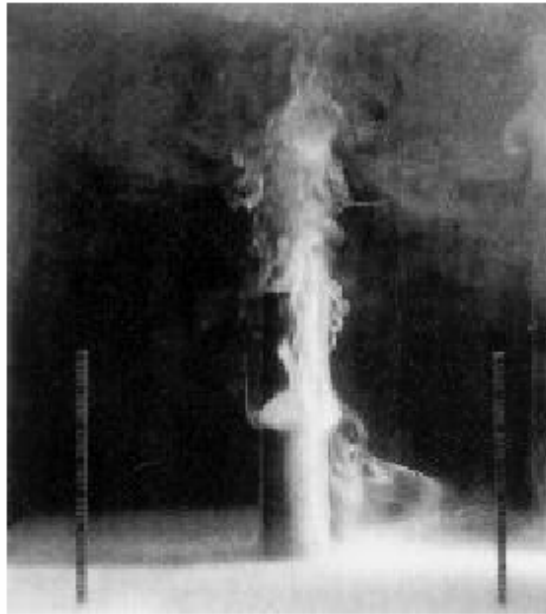


Figure 15 - Displacement ventilation airflow pattern [32]

Heat sources within the room can be made up of any object that creates heat. This may include people, computers, lights or a TV. Through research and testing a number of these heat sources have been analyzed, allowing them to be approximated by a single level cylinder with a certain diameter. As an example, a person sitting in a room is modelled as a 0.3m diameter cylinder 1.3m from the ground and having a heat generation of 70 watts. A person standing is modelled as having a height of 1.8m with a heat release of 105 watts [30].

While seemingly a simple process, this design procedure can be time consuming and complex when performed for multiple heat sources and by hand. This is the case particularly for those who have never dealt with this concept before. Due to this, engineers with no experience in fields with similar concepts often avoid displacement systems. Recently though, computer programs have been developed that analyze the room variables and based on these provide the ventilation rate required for operation. These have greatly increased the use of displacement ventilation system use.

This basic design procedure is vastly different from that of a conventional mixing system which is well understood by HVAC engineers, and where the airflow is calculated based on the volume of cold air required to provide an equal level of cooling to the heat generated by sources within the room. Effectively this concept treats the room as a black body and creates an energy balance on the loads. Due to the vast differences in operation between a mixing system and a displacement system, each system has advantages and disadvantages over the other. In the case of a displacement system these are as follows:

Advantages:

- Maintains a less contaminated environment for occupants.
- Smaller cooling plant is required for large spaces.
- Less design required for rooms with high ceiling where a conventional mixing system would struggle.
- Lower energy use when used with an economizer (based on New Zealand climate).
- Captures pollutants at the source.

Disadvantages:

- May add complexity to the supply air ducting.
- Hot upper layer can cause increased radiation feedback to occupants.
- Can be harder to operate on variable outside air volumes which result in lower energy use.
- More airflow required, so larger fans are needed.
- Difficult to remove high sensible and latent heat gains due to higher air temperatures.

A general guide to selecting which type of system should be used, has been developed. This is shown in Figure 16 [32].

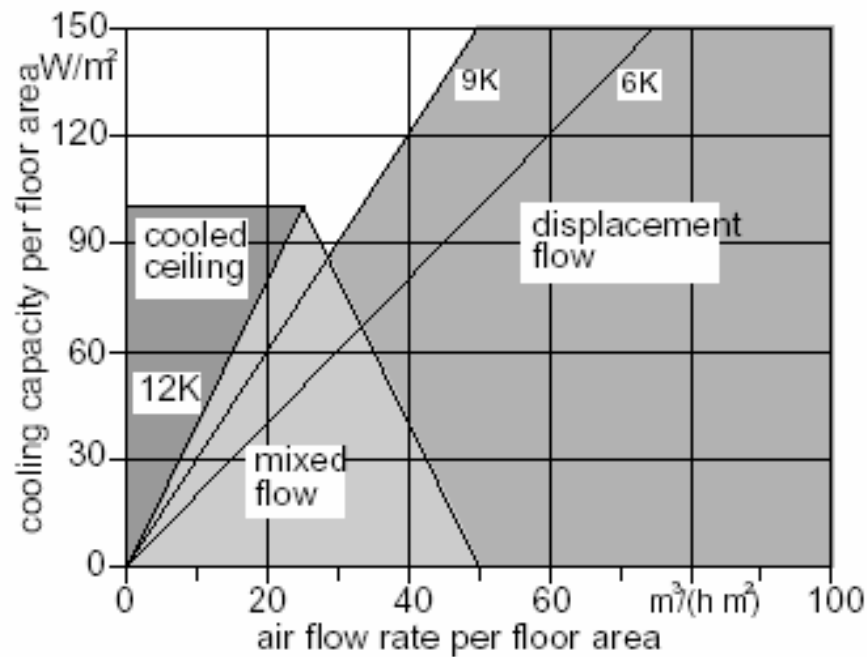


Figure 16 - Ventilation system selection [32]

The lines within Figure 16 represent the design temperature difference between the supply airflow and the room temperature. For example 12K represents a supply air temperature of 10° with a room temperature of $22^\circ C$. As can be seen, displacement ventilation systems tend to operate in the region with low temperature differences.

In simplified terms it states that for high rates of ventilation, displacement ventilation systems provide a better choice, while at lower ventilation rates and high cooling loads, conventional ventilation may operate more effectively. This is by no means an exact selection criteria and the designer must take care to ensure that the required room characteristics are achieved.

2.9 Summary

Recent research and fire testing have shown that fine spray water mist technologies have the potential of either replacing or providing new answers to current fire protection techniques that are no longer deemed environmentally acceptable and where traditional techniques have not been as effective as desired [33]. It is often stated in literature though that no 'ideal' water mist distribution exists for all situations. The selection of a water mist distribution is instead dependent on the particular fire and the suppression characteristics, which will play the most significant role. There is a long way to go before water mist suppression systems can be considered to be well understood, but recent research is promising and provides another avenue for fire engineers to consider.

In terms of displacement ventilation systems it is clear that this type of system can provide benefits over that of a conventional mixing system in certain circumstances. It is also clear that the design and operation of these systems relies on principles that are analogous with fire engineering, namely plume theory and stratification levels. While this is the case, the author was unable to find any literature investigating this type of ventilation system and its interaction with a fire.

3. Concept

This section provides an overview of the proposed water mist fire suppression system investigated in this study. The basic concept behind the system is discussed along with its theoretical advantages over existing systems.

3.1 Base Concept

As has been previously discussed, typical water mist systems operate by injecting a fine water spray into a compartment through a series of nozzles located on the ceiling. During operation the ventilation system is typically shut off and ventilation avoided.

The concept behind the proposed new system is to combine a low level displacement ventilation system with low level water mist injection.

Under normal operation the displacement ventilation system would provide air-conditioning to the compartment using low velocity air. During a fire an early detection system would increase the airflow from the displacement ventilation system and water mist would be injected into the air stream. Using the concepts of a typical displacement system the air/water mixture would flow into the compartment forming a lake of cool clean air and fine water particles that could be expected to flood all areas of the compartment. As the lake builds up the water mist, which is injected in sufficient quantities, would be entrained into any fire plume within the compartment, cooling it and suppressing or controlling its size through cooling, oxygen depletion and radiation blocking.

As a displacement system operates on a laminar flow system, there theoretically should be little mixing between the hot toxic upper layer and the lower layer. This separation would allow the upper layer to be exhausted out of the room in its hottest form resulting in the maximum amount of heat and toxic products being removed from the compartment.

For occupants within the room the air/water mix would provide a layer of cool breathable air that provides protection from the radiation feedback caused by the

hot upper layer and from any hot source such as the fire. This environment allows occupants to remain in the compartment if confined or if necessary. The use of a very fine mist means that in the case of vital operations, occupants can continue to work on basic electronics that must remain manned without causing damage to them and with minimal risk of electrical shock to the user.

A basic concept of the displacement water mist system is shown in Figure 17.

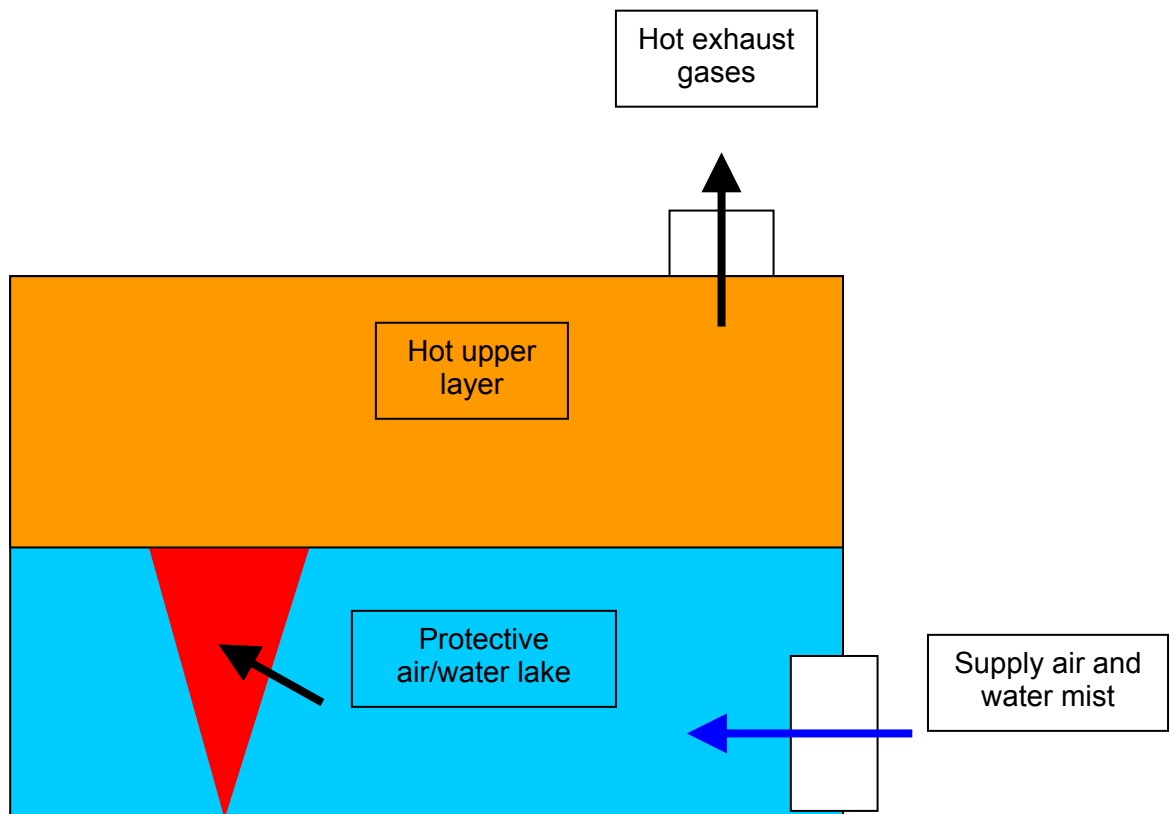


Figure 17 - Displacement water mist concept

3.2 Theoretical Advantages

In relation to existing fire suppressions systems the displacement water mist systems offers theoretical advantages in a number of ways for certain situations.

In the case of a conventional sprinkler system, the quantity of water that is injected into the compartment is much greater than a water mist system and the drops are much bigger. Activation of a conventional sprinkler results in everything within the compartment becoming wet, which in the case of electronics can cause failure and damage. Water mist systems on the other hand inject significantly lower quantities of water into the compartment and in a very fine spray. Tests on this type of water particle injection on electronics have shown that while surge protectors may trip if internal circuits are wet directly, the equipment can typically be dried and restarted within a very short time with no detrimental effects [28].

Another theoretical advantage of the displacement water mist system over that of a conventional sprinkler is that it maintains a protective lower layer for occupants. On activation a conventional sprinkler system cools the hot upper layer causing the temperature difference between the lower and upper layers to become less, which decreases the stratification forces maintaining the layer separation. This combined with the falling water particles can result in mixing of the two layers and a more toxic lower layer environment. Additionally as a conventional sprinkler system does not extract the combustion products these remain in the room and build-up if the fire continues to burn.

A similar build-up of toxic products occurs with a gaseous protection system. When gaseous systems are used to extinguish a fire, ventilation systems in the compartment must be shut down otherwise the fire protection system can be expected to fail [34]. In a study on halon and carbon dioxide fire protection systems, a failure rate of 37% was attributed to leakage from the compartment. Maintaining a sealed environment through, results in hot toxic combustion products being trapped within the compartment and making the area uninhabitable. The base design of the displacement water mist system is that the

ventilation rate is actually increased to remove these gases and allow the zone to be occupied.

One of the drawbacks of ceiling mounted water mist installations is that they typically require that the compartment be hot enough on activation of the water mist to evaporate the water. This evaporation is needed to create a high enough level of oxygen displacement to extinguish the fire. This effectively means that the ventilation must be stopped. The stopping of the ventilation again leads to a build-up of combustion products that, while assisting in extinguishment, pose a threat to occupant safety. Furthermore if an occupant were present and alive the low oxygen concentrations and high temperatures would provide additional hazards.

The low level injection offered by the displacement water mist system can offer advantages in suppression efficiency over high level injection. Tests have shown that for water mist fire suppression, low level injection can be up to two times as effective as high level injection [9]. This is due to the fact that with high level injection the water particles must be large enough and have sufficient momentum to fall through the fire plume and reach the base of the fire. Other studies [28] have agreed with this finding and have found that in some situations low level injection was able to extinguish a fire where high level injection was unable to.

In terms of construction, the displacement water mist system would cost more than a conventional sprinkler system but the same or less than a gas or ceiling water mist system. This is due to less piping being required as all of the water mist nozzles are located in one area in a small installation or in a small number of groups in large installations. In addition to this, as the combustion products are exhausted by a pressurization fan rather than extracted, a standard fan can be used rather than an expensive high temperature smoke extract fan. The displacement air system itself would be practically identical to that used in a standard displacement system and hence poses no additional cost.

One possible drawback to this system is that placement of the water mist nozzles at low level could lead to them being blocked by a foreign object placed in the way. While this is a possibility its occurrence is limited by the fact that as they are

located with the air supply diffuser, any foreign object will also block the air supply and cause the room to quickly become uncomfortable.

3.3 Summary

As has been discussed the suppression system that this study proposes and investigates is a combination between displacement ventilation and low level water mist injection. This design theoretically offers a system that can protect the compartment and its occupants throughout the fire.

It offers a number of possible advantages over existing fire suppression systems when the interior of the room must be protected or if the occupants must remain within the room during the fire.

4. Experimental Design

The objective of this section is to outline the way in which the proposed displacement water mist system was investigated and tested to reach the objectives outlined in section 1.2. A general background of the investigation procedure is presented, followed by a detailed description of the test environment and global factors.

4.1 Investigation Procedure

At the onset of the project it was decided that both a computational and experimental process should be undertaken to investigate the effectiveness of an operational displacement water mist system. In fire engineering it is becoming more frequent for fire safety designs to be tested on a computer using programs such as the NIST computational fluid dynamics program FDS (used in this study). For this reason it becomes advantageous to review how well the computer simulation models the live test. If the model provides relatively high accuracy, then future tests can be carried out at less cost on a computer with relative certainty that the results are accurate. In addition the FDS simulations provide far greater levels of output data than the live tests, allowing the interior atmosphere to be investigated.

4.2 Simulation Run Selection

With the basic concept outlined and modes of testing selected the actual test runs that needed to be carried out had to be determined. Through discussion it was decided that the tests should cover both a liquid pool fire and a cellulose based fire so as to provide information relevant to the different combustion modes. It was also decided that four test points within the compartment should be used to provide data on the compartment conditions and specific comparison information. The first was at ground level in the centre of the compartment at a distance of 0.7m from the outside wall. The second test point was in the same location but at 1m off the ground. The third and fourth test points were again at ground level in the back and front corner respectively. The four test points are shown in Figure

18. The ground level tests were intended to model a low level fire that generated significant volumes of smoke through plume entrainment. The 1m high test point simulated a desk fire in which a smaller volume generation occurred but at a higher temperature. The actual tests carried out are listed in Table 2.

Test run	Fire type	Location	Airflow	Suppression
Live: Run 1	Pool	Centre floor	Normal	No suppression
Live: Run 2	Pool	Centre floor	Normal/High	No suppression
Live: Run 3	Pool	Centre 1 m	Normal	No suppression
Live: Run 4	Pool	Back floor	Normal	No suppression
Live: Run 5	Pool	Centre floor	Normal/High	Water Mist
Live: Run 6	Pool	Centre 1 m	Normal/High	Water Mist
Live: Run 7	Pool	Back floor	Normal/High	Water Mist
Live: Run 8	Pool	Front floor	Normal/High	Water Mist
Live: Run 9	Pool	Centre floor	Normal	Water Mist
Live: Run 10	Wood crib	Centre floor	Normal	No suppression
Live: Run 11	Wood crib	Centre floor	Normal/High	Water Mist
Live: Run 12	Wood crib	Centre 1 m	Normal/High	Water Mist
Live: Run 13	Pool	Centre floor	Normal	Sprinklers
Live: Run 14	Pool	Centre 1 m	Normal	Sprinklers
Live: Run 15	Wood crib	Centre floor	Normal	Sprinklers
Live: Run 16	Pool	Centre floor	Normal/High	Water Mist + Shield
Live: Run 17	Pool	Centre floor	Normal/High	Water Mist + Observers
FDS: Sim 1	No fire	N/A	Normal	No suppression
FDS: Sim 2	Pool	Centre floor	Normal	No suppression
FDS: Sim 3	Pool	Centre floor	Normal/High	No suppression
FDS: Sim 4	Pool	Centre floor	Normal/High	Water Mist
FDS: Sim 5	Pool	Centre 1 m	Normal/High	Water Mist
FDS: Sim 6	Pool	Front floor	Normal/High	Water Mist
FDS: Sim 7	Pool	Back floor	Normal/High	Water Mist
FDS: Sim 8	Pool	Centre floor	Normal	Water Mist

Table 2 - Fire simulations

Tests were performed with no water mist suppression, water mist suppression only, displacement water mist suppression and conventional sprinkler suppression to allow comparison and evaluation of the displacement water mist systems effectiveness.

As can be seen from Table 2 the majority of tests were carried out using pool fires particularly in the case of the FDS simulations. The use of primarily pool fires was based on the fact that pool fires tend to be simpler to repeat accurately over a number of live runs. In the case of the FDS runs, simulation time was the limiting factor and hence pool fires were used to allow the maximum level of comparison with the live tests. For the same reason conventional sprinklers were not simulated using FDS.

In each of the tests the basic structure was to operate the system displacement ventilation system to create a constant environment. The specified fire would be ignited and on detection the suppression system would be activated if required. The actual time line followed is outlined more clearly in the following sections

4.3 Base Compartment Specifications

To carry out the testing procedure for both the computer simulations and the live tests the first design criteria was the test compartment size. The compartment design had to be such that it modelled an office space in which a displacement ventilation system could be used. It also had to be, where possible, in line with international compartment test standards so allow the experiments to be repeated if necessary.

Based on these criteria, it was decided that the compartment should be in line with ISO Standard 9705 [35], which calls for the compartment to be 3.6m in length, 2.4m in width and 2.4m in height. This compartment size is used internationally with both centre and corner fire test.

While the ISO room is the base design for testing, the nature of the displacement water mist system is such that modifications needed to be made to allow for practical use in the computational and live situations. The ISO compartment is typically fitted with only one opening, which is a door in one of the 2.4m by 2.4m end walls. The design of this displacement water mist system called for the compartment to be closed internally other than a low level supply air grill and a ceiling mounted exhaust. Based on these requirements the door was removed from the design and a simple roof vent added the specifics of which are discussed in section 4.6.

The supply of the low level air to the compartment posed an additional problem as the supply air had to be conditioned before entering the compartment. While this is relatively simple in the case of the computer model, it is more difficult in live tests as typically a mixing chamber is required. To remain inside the basic ISO compartment size specifications it was decided that a false wall would be installed at the front end of the compartment creating a 0.6m deep plenum for the supply air to be conditioned in. This placement meant that the set up could, if necessary, be installed in an existing ISO room installation for any future work.

load was present then the compartment would simply be a uniform temperature rather than stratified layers forming. Secondly light bulbs provided an additional source of light to assist in observations within the compartment. Thirdly light bulbs could be monitored to see the effect that water mist of sprinklers had on them and finally light bulbs could be positioned at a repeatable point.

It was decided that a typical office of this size could be expected to have two occupants with an average heat load of 100 watts each [36]. This meant that two 100 watt light bulbs were needed within the compartment. The light bulbs were each mounted on the centre line of the compartment 750 mm from each end and at a height of 1m. The height was selected based on the point source equivalent for a human used in the design of the displacement ventilation system [32].

It was decided that within an office a typical electrical load would be a computer. This also provided a good source of electrical monitoring, as one of the design objectives was to investigate if it could continue operating during the tests. The computer base was located at 0.7m from the floor and in the centre of the compartment. 0.7m was selected as this is the typical height of a workbench within New Zealand.

4.5 Fire Selection

As stated, it was decided that two types of fire needed to be simulated in the study. The first being a liquid pool fire and the second being a cellulose based fire. These fires were selected as they provided basic range for the different burning properties of fuel i.e. charring and evaporation.

The size of the fire was selected at 20 kW based on the fire load that could be expected from a waste paper basket [37]. A waste paper basket was selected as it provides a common point of fuel within an office. The fuel sources themselves were selected as Heptane for the pool fire and wood for the cellulose fire. These fuels were chosen as they were readily available and meet the requirements of different burning characteristics.

The size of the pool fire and the containment pan was calculated in the following manner:

Data and requirements:

Fuel:	Heptane
Required HRR:	20 kW
Approximate burn time:	10 minutes
Heptane density (ρ):	675 kg/m ³
Heat of combustion (Δh_c):	44.6 MJ/kg
Mass loss rate (m_∞):	0.101 kg/m ² .s
$K\beta$:	1.1
Combustion efficiency:	95%

(Data taken from SFPE [37])

Using this data, the pool fire heat release rate can be determined based on the equations proposed by Heskestad [38]. The base calculation of this work is shown below.

$$Q = A_f \chi \Delta h_c \dot{m}_\infty'' (1 - e^{-k\beta D}) \quad \text{Equation 4: Pool fire HRR}$$

Where Q is the heat release rate, χ is the combustion efficiency and D is the effective diameter of the pool surface converted to circular coordinates. As the HRR is known the equation can be rearranged to solve for the diameter. Based on 20 kW the area required is 0.0258 m², or in square coordinates 160 mm by 160 mm. Using the burning rate of the fuel, the required depth can then be determined as 16 mm for a ten-minute fire.

Based on these equations the pan for the pool fire was made to be 160 x 160 x 16 mm deep.

The calculation of the wood crib fire was based on the work presented by Barbrauskas [37] that states that the HRR from a wood crib is the lesser of the fuel surface area HRR and the porosity rate of fuel. The basic calculation of which are shown below in Equation 5 and Equation 6.

$$\dot{m} = \frac{4}{D} m_0 V_p \left(1 - \frac{2V_p t}{D}\right)$$

$$\text{or } \dot{m} = \frac{4}{D} m_0 V_p \left(\frac{m}{m_0}\right)^{\frac{1}{2}} \quad \text{when } m = m_0 - \sum_i^t m_i t_i \Delta t$$

Equation 5: Wood surface HRR

$$\dot{m} = 4.4 \times 10^{-4} \left(\frac{S}{h_c}\right) \left(\frac{m}{D}\right)$$

Equation 6: Porosity HRR

Where D=Thickness of sticks (m)

m_0 = Crib initial mass (kg)

t = time (s)

h_c = Crib height (m)

S = Clear space (m)

V_p = Fuel surface regression rate ($2.2 \times 10^{-6} D^{-0.6}$) (m/s)

The wood properties assumed for the wood crib were as follows:

Fuel:	Wood
Required HRR:	20 kW
wood density (ρ):	550 kg/m ³
Heat of combustion (Δh_c):	12.4 MJ/kg

(Data taken from Fire Engineering Design Guide [39])

Combining and solving these equations leads to a wood crib 100 mm square by 110 mm high, with six 10 mm x 10 mm sticks on each level.

4.6 Airflow Design Under Normal Conditions

The size of the vents providing supply air and exhaust to the compartment were both calculated based on the volume of supply air needed under normal operating conditions. The actual supply airflow needed using displacement ventilation, had to be calculated based on the two lights and the computer positioned within the compartment as these provided the heat sources. The objective of the ventilation system was to provide and maintain the compartment interior at 22°C as would be expected within a typical office.

As has been discussed in section 2.8 on displacement ventilation, the actual calculation to determine the required airflow for a displacement system can be complex and as such is typically carried out by a computer program. For this study the HALTON [40] design program was used to work out the conditions within the compartment and the required airflow. The results were that an airflow of 0.048 m³/s was required at 19°C. A full printout from the program can be seen in appendix 11.2.

Based on this the supply air vent could be determined as the maximum supply air velocity for a displacement system is 0.2 m/s. Using the supply air rate and this speed leads to a vent size of 0.24 m² being required, or an approximately supply vent size of 0.5m x 0.5m. This provides the minimum vent size required, but as the HALTON results in appendix 11.2 show the flow actually accelerates as it spreads across the floor. To account for this the supply vent size needed to be increased. The final size selected was 0.5m high and 0.6m wide, located at floor level in the centre of the front false plenum wall.

The exhaust duct was not limited to the velocity across it, but the pressure drop needed to be minimised during both normal and high flow operations. For this reason a vent of 0.4m by 0.4m was selected as at normal operation the velocity across the vent was 0.3 m/s which, while providing adequate flow for temperature readings, results in a minimal pressure drop. The exhaust vent was located on the compartment centre line, 600 mm from the false wall of the plenum. This can be seen clearly on the plans in appendix 11.1. The selection of this location was

based on positioning the extract away from any direct plume impact from the test fires within the compartment. It was positioned near the front of the compartment rather than then back to provide an exhaust above the supply point and reduce any entrainment back into the supply air.

4.7 Airflow Design Under Fire Conditions

With the airflow under normal conditions calculated the airflow that was to be provided under fire operation needed to be determined.

The airflow in fire mode is primarily based on the level at which the upper layer is required to be stabilised at. That is with a known fire size the plume entrainment and flow characteristics can be determined at any height. Therefore if the lower protection layer is required to be maintained at a height of x , the air entrained into the plume below height x can be calculated, giving the required supply airflow to the lower layer. Effectively a mass flow balance is performed between the lower layer, the plume and the upper layer. Referring to Figure 19 it can be seen that $m_s = m_e = m_u$ at the layer balance point.

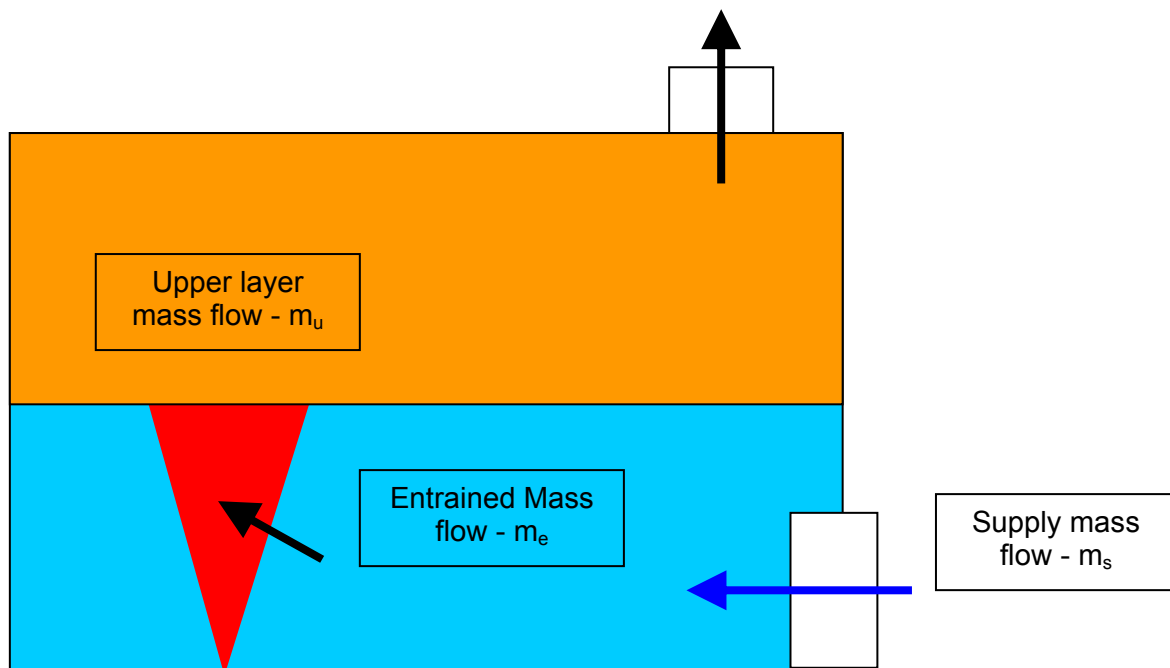


Figure 19 - Airflow mass balance

The plume entrainment was calculated based on the work performed by Heskestad [38]. From his work, the mass flow across a horizontal plane of a plume is given by using Equation 7, Equation 8, Equation 9 and Equation 10.

$$z_o = 0.083Q_c^{\frac{2}{5}} - 1.02D$$

Equation 7: Virtual origin

$$L = 0.235Q_c^{\frac{2}{5}} - 1.02D$$

Equation 8: Flame height

$$\dot{m}_p = 0.071\dot{Q}_c^{\frac{1}{3}} \cdot (z - z_o)^{\frac{5}{3}} + 1.92 \cdot 10^{-3} \cdot \dot{Q}_c$$

Equation 9: Plume entrainment above flame

$$\dot{m}_p = 0.0056Q_c \frac{z}{L}$$

Equation 10: Plume entrainment below flame

Where:

D = the diameter of the fire (m)

Q = the total heat released by the fire (kW)

Q_c = the convective component of heat released (kW)

Z = the height above the fire level (m)

Using these equations, Figure 20 can be generated showing the required lower level supply airflow rate at varying HRR's and layer interface height.

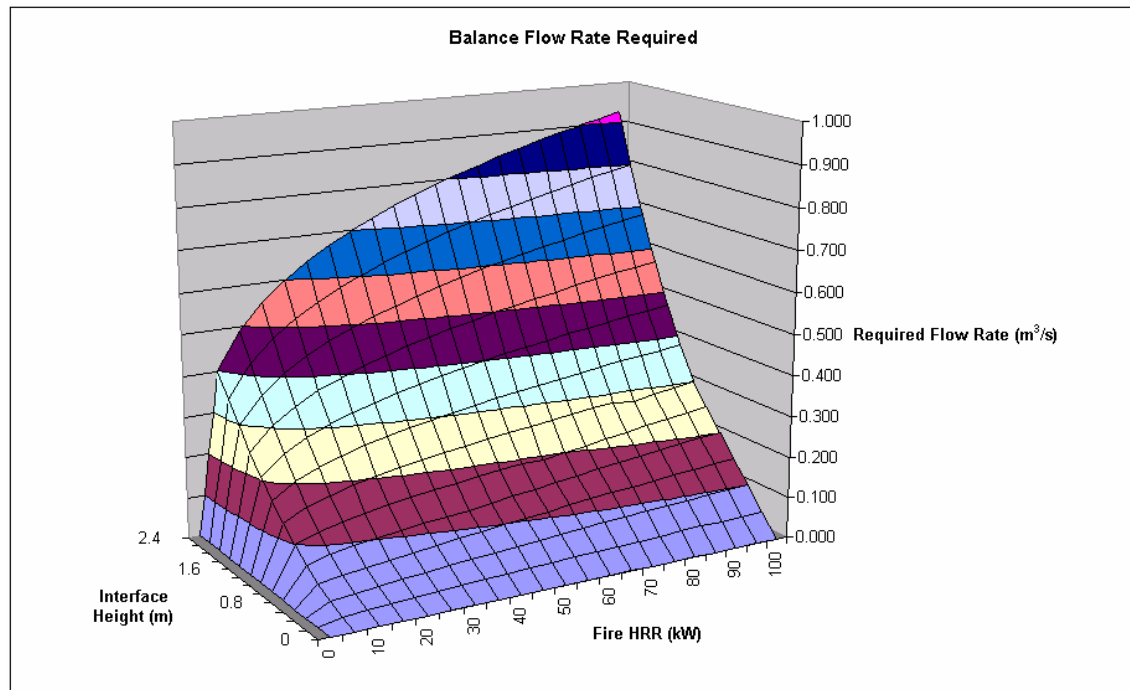


Figure 20 - Required supply airflow rate

As the fire size is known at 20 kW and with the equivalent diameter of the pool fire being 0.181m the only variable required is the layer height. This was selected based on the initial objectives of the system of being able to provide a protective layer for the occupants. The assumption is made that the occupants are sitting at a desk, resulting in their heads being approximately 1.3m high. Allowing a safety factor for mixing and radiation protection a height of 1.5m was selected. Ideally a height of 2m would be better as it would allow a further safety factor and the option for the occupants to move around, but looking at Figure 20 it can be seen that as the high increases the required flow rate becomes exponentially larger based on the equations presented above. The concern was that at these higher flow rates turbulence would be created within the compartment and also the cost of the supply fan would be significantly increased to cope with the larger pressure drops created across the supply diffuser.

Using the height of 1.5m and the 20 kW pool fire, an airflow of 0.275 m³/s is required. Within displacement ventilation systems airflow is typically expressed in air changes per hour. This flow effectively gave an air change rate of 57 air changes per hour. It was decided to increase the safety factor marginally and round the air change rate to 60 air changes per hour, or effectively to replace the air within the compartment every 60 seconds. This resulted in a fire mode air supply rate of 0.288 m³/s.

4.8 Water Supply Under Fire Conditions

The volume of water mist that was to be injected into the compartment and its drop size were primarily based on the work carried out by Anderson et al. at Lund University using a 1/3 scale ISO room. The conclusions from their testing indicated that the ideal droplet size was from 10 – 20 µm as at these diameters the droplets stayed suspended for significant periods of time and were able to follow the airflow path reasonably well. Similarly it is stated that “Small droplets below approximately 20 µm have a residence time sufficiently long to be carried by air currents to all parts of the enclosure” [7].

In specific terms of setting time for particles, Table 3 gives the time for particles of varying sizes to settle 1m.

Drop Diameter (μm)	Time to settle 1m (seconds)
5	1280
10	324
20	81
50	13

Table 3 - Settling time of water drops [41]

As can be seen particles in the range of 10 – 20 μm have long settling times that are well in excess of the 60 second air change rate that will be supplied to the compartment. This would suggest that once injected particles of this size would remain in the compartment atmosphere until exhausted hence maximising their use.

In relation to following the airflow around obstacles to reach all parts of the compartment, the Anderson et al study generated the graph outlined in Figure 9, which as discussed, shows that particles in the region of 20 μm follow the airflow very well. This finding was also confirmed in other studies [18] that found 20 μm droplets follow the air supply very well.

The remaining variable for the water injection is the volume of water that was required. Again the work carried out by Anderson et al. indicated that water densities between 70 – 140 g/m^3 were required in actual tests but they suggest that this be increased to 200 g/m^3 to account for all out and different conditions. This value is generally supported by other studies identified in section 2.8 but some reference is made to smaller fires requiring densities of up to 600 g/m^3 but these are not covered in detail so the general level of 200 g/m^3 was selected.

Based on an airflow of 0.288 m^3/s during fire mode operation, the resulting water mist must be injected at 3.45 L/min with an average water particle size of 20 μm .

4.9 Thermocouple and Detector Locations

To allow analysis of the compartment interior during the tests and to provide common points for comparison between the live test and the FDS simulations internal measurements needed to be taken. It was decided that these readings would be in the form of temperatures from thermocouples as they could be installed easily and provided valuable information. Ideally the atmospheric conditions within the compartment should be tested as well but due to the limited scale of the project it was decided that this was not feasible and that thermocouples alone would provide sufficient information.

Within the compartment the thermocouples were arranged in five sets. The first set consisted of supply and exhaust measurements. One thermocouple was to be located directly in the supply air path to insure that the 19°C called for in the system design, was maintained. The other thermocouple was located in the exhaust air path so that the temperature of the exiting gases could be known.

The second (Tree 1) and third (Tree 2) set of sensors set were arranged into two thermocouple trees with five thermocouples each. They were positioned 1.5m from the back wall and 0.7m from the side walls respectively. These positions provided monitoring directly above the central fire test point and monitoring at a position within the compartment away from the direct effects of the test fires. The later of these two sensor arrays was known as the occupant tree as the results recorded the temperatures that an occupant could be expected to be exposed to. Thermocouples were placed at heights of 0.3m, 0.7m, 1.3m, 1.8m and 2.1m. The 0.3m and 1.3m sensors were located at this height to measure the temperatures directly above the test fires and hopefully provide basic information on the running rate of the fire.

Additionally in Tree 1 the 1.3m sensor was used to measure the temperature that would be felt at head level by a sitting occupant. The 0.7m sensor was located to model the temperatures felt at the height of a standard work desk within an office. Similarly the 1.8m sensor was located to record the temperature that the head of a typical person when standing. The final 2.1m sensor was positioned to record the upper layer level within the compartment, while being at a great enough

distance from the roof to avoid being within any ceiling jets generated. In the case of tree 2 the thermocouples we used to monitor to some extent the path of the fire plume and assess whether it was rising vertically.

Finally the fourth and fifth set of sensors sets were arranged into two thermocouple trees with two thermocouples each. The trees were positioned in the back (Tree 3) and front (Tree 4) corners of the test compartment directly above the corner fire test points. The sensors themselves were positioned at a height of 0.3m and 1.3m consecutively and spaced 100 mm from each wall. These positions were selected as they would be directly above the ground level corner fires, with the 0.3m sensor within the fire flame and the in the fire plume.

A graphical layout of the thermocouple points within the compartment is included in appendix 11.1.

In selecting the type of detectors to be installed in the compartment, the operating principle of the displacement mist system had to be considered. The design called for fast detection to minimise the size of the fire before the system activated. Based on this requirement it was decided to install smoke detectors rather than a heat detector. Smoke detectors were selected as they typically provide detection much sooner than a heat detector [42]. An ionisation and optical sensors were both selected so that a comparison between the detection times could be made while also insuring the earliest detection time using this type of technology. These were to be positioned centrally on the roof of the compartment to be similar in nature to that of a typical installation.

5. Full Scale Testing

This section of the report outlines the full-scale experiments performed to investigate the operation of the displacement water mist system. The objectives of the experiments are outlined below, followed by a review of the test apparatus and selection process for each of the major components. A discussion of the trial runs is presented, followed by the results of the actual tests carried out.

5.1 Objective

The requirements and objectives for carrying out full scale testing were to:

- Build a compartment similar to an actual commercial office.
- Investigate the feasibility and procedure for building an operating displacement water mist system.
- Investigate the operation of the displacement water mist system under live conditions.
- Allow direct observations of internal conditions.
- Allow comparison of this system with a conventional sprinkler system.
- Investigate the effects on electronics within the compartment.
- Provide actual results to compare against the FDS simulation.

5.2 Test compartment design

As outlined in section 4.3, the basic internal compartment dimensions are 3m long, 2.4m wide and 2.4m high.

One of the first design considerations for building the compartment was how to supply air at a constant 19°C. While on the outset this requirement does not appear to be difficult, on a small scale it can be, due to the operating nature of small systems.

The selected design involved using the 0.6m deep plenum chamber on the front of the compartment as a mixing and conditioning area for the incoming air before it entered the compartment through the supply diffuser. The plenum space and supply diffuser are shown on the technical drawings of the compartment in appendix 11.1 along with the overall compartment schematics.

The supply diffuser selected for the compartment was based on the HALTON [40] design and consisted of perforated sheet steel. The holes were each 4 mm in diameter and provided a free area of 30%. This type of diffuser is generally used as it provides a large enough pressure drop that the flow from the bottom of the grill is approximately the same as from the top while still allowing a relatively laminar flow to be formed. A similar perforated steel plate was also installed midway down the plenum chamber to assist in the mixing process and to provide a stable flow above the supply diffuser. The back of the supply diffuser can be seen in Figure 21 and the placement of the perforated steel plates can be seen in appendix 11.1.

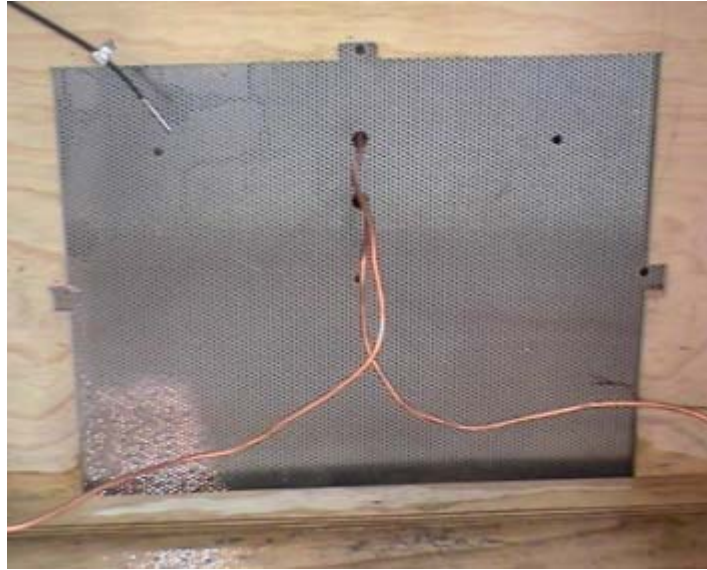


Figure 21 - Perforated steel supply diffuser

To provide the air-conditioning, a stand-alone heat pump provided continuous cooling to the air within the plenum. Air was supplied to the plenum from a fan via flexible aluminium ducting, passing through an electric duct heater along the way. The warm supply air and cool air-conditioned air then mix within the plenum chamber and entered the compartment through the supply diffuser. As stated the supply air temperature needed to be 19°C to maintain the thermal balance within the compartment. For this to occur the air entering the plenum had to be heated via the electric duct heater to a temperature that compensates for the cooling provided by the heat pump.

This arrangement was selected as it provides far more control than the use of a single heat pump that provides cooling and heating. A simple heat pump at the sizes required for this experiment, only has the ability to operate on full cooling or full heating and no variation in between. In a standard compartment this type of operation is sufficient as the compartment is typically large enough that the supplied air mixes with the compartment air to create a relatively constant temperature. In this experimental set-up however the plenum is so small and the airflows so little that this operation would result in the supply of air to the compartment modulating between being significantly lower or higher than the required 19°C. The use of an electric heater allows the inlet air temperature to be controlled very accurately as the heat input can be varied.

Based on this design a standalone 2.5 kW cooling only heat pump was selected as it was the smallest unit available and allowed the system to operate at high outside air temperatures. A 3 kW electric duct heater was selected to counter the 2.5 kW of cooling and provide the required level of heating at low outside air temperatures. Figure 22, Figure 23 and Figure 24 show the installed air-conditioning unit and duct heater in place.



Figure 22 - Air-conditioning unit and plenum supply point



Figure 23 - Air-conditioning unit and plenum supply from outside the compartment

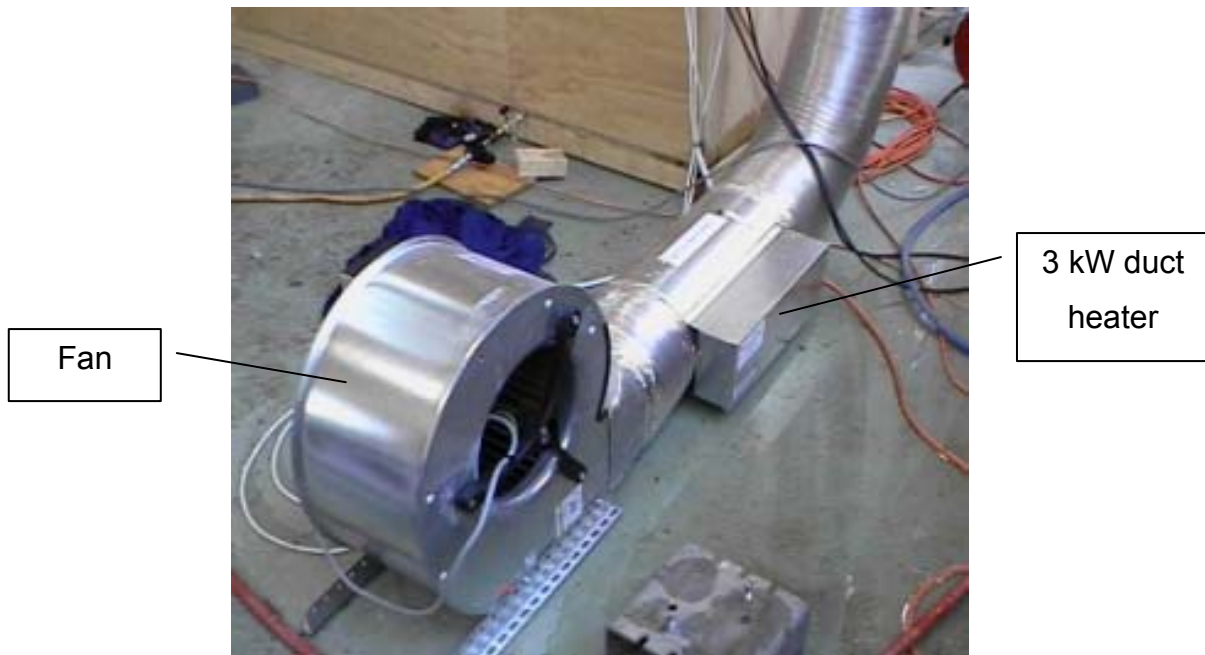


Figure 24 - Electric duct heater installed with fan

It was decided on the outset of the project that as the fires were to be small and the temperatures relatively low and for short duration, that the structure of the compartment would be made from 15 mm plywood. For the same reasons it was also decided that the windows on either side of the compartment would be made from 15 mm transparent thermoplastic acrylic resin (Perspex).

On the roof of the compartment the vent was cut and a 50 mm skirt attached. This allowed the exhaust thermocouple to be mounted directly in the extract air path and not level with the roof where errors may have resulted from radiation, ceiling jets or water spray.

To provide access to the main compartment a full height 2.4m high by 1.2m wide door was fitted to the back. The door was mounted on hinges and fitted with four horizontal braces that could be used to secure the door tightly. Between the mating edges of the door and the compartment a length of fire resistant rope was fitted to insure that the door sealed tightly. The door can be seen in Figure 25. For access to the plenum chamber and the back of the supply grill, a 1.2m by 1.2m panel was cut and fitted so that it could be taken out by the removal of four screws.



Figure 25 - Main compartment door

Within the compartment fire resistant panel was fixed to the walls of the two test corners along with a sheet covering the floor below the central test point. This provided protection to the wooden walls and stopped the fire spreading and becoming larger than could be handled. A small table was constructed within the compartment to support the computer at 0.7m while single lengths of wood were fixed to the floor to position the light bulbs at the required height and position. In each case the electrical feed to the internal loads were feed outside to a multi box and through an RCD. The RCD provided electrical protection and allowed the time at which an electrical short circuit occurred to be recorded. The operating internal heat loads can be seen in Figure 26.



Figure 26 - Internal compartment loads operating

The remaining internal components were the smoke detectors and thermocouples. Bead thermocouples were installed along vertical wires and positioned as specified in section 4.9. Bead thermocouples were selected due to their availability and robustness. They were each connected back to a monitoring computer, which allowed the output from each to be displayed on screen and recorded for later evaluation. Two smoke detectors, discussed in section 5.7, were installed on the roof in the centre of the compartment as would typically be the case in a commercial insulation. They were both connected back to a monitoring computer that again recorded the output levels while providing a real time chart of what the outputs were. The completed compartment can be seen in Figure 27 and Figure 28.



Exhaust vent

Controls

Observation windows

Figure 27 - The back of the completed compartment



Air-conditioner

Fan and heater

Figure 28 - The front of the completed compartment

5.3 Test Fires

As previously discussed the two test fires were a 20 kW Heptane pool fire and a 20 kW wood crib fire.

In the case of the pool fire a stainless steel dish was constructed to the dimensions calculated in section 4.5. The final pan is shown in Figure 29.



Figure 29 - Pool fire pan

The wood crib was manufactured from 10 mm thick plywood cut into strips and lengths as specified by the calculations in section 4.5. The crib was held together with standard PVA wood glue. The final crib can be seen in Figure 30.



Figure 30 - Typical wood crib

The pool fire was ignited by simply using a burning piece of paper, while the wood cribs were ignited by soaking the bottom layer in **methylated spirits** for approximately 5 minutes prior to use. This allowed the fires to be ignited in the same manner as that of the pool fires with the methylated spirits providing a short duration ignition point for the crib.

5.4 Nozzle Selection

The water mist nozzle selection for the experimental set up was primarily based in the water mist requirements rather than the type of nozzle used. As it was purely a research test and reliability was not a major concern, it was felt that a specific fire system nozzle was not needed and that any type of nozzle that produced the mist characteristics required would be adequate.

A number of companies throughout New Zealand and overseas were contacted to provide a nozzle based on the requirements of a Dv_{50} 20 μm and a total water supply of 0.0588 l/s as outlined in section 4.8. Additional to these requirements the suppliers were limited to a maximum operating air pressure of 5.5 bar and a water pressure of 8 bar due to the limitations of the test facility equipment.

Due to the very fine nature of the spray required it quickly became apparent that there were in fact limited options available to produce such a fine drop size. A number of suppliers simply could not provide a nozzle to these specifications or if they did they required extremely high pressures in the region of 150 bar which was not possible with the facilities available.

Spraying Systems Ltd, located in Wellington New Zealand, proved to be the only company that could provide the spray characteristics required, using the available water and air pressures. They suggesting 6 duel flow air atomising nozzle from their QuickMist™ range. A photo of the selected nozzles is shown in Figure 31.



Figure 31 - QuickMist™ Nozzle

These nozzles are a general use nozzle and are not designed for typical fire suppression use as they are made from a polymer based material that has a maximum operating temperature of 93°C. It was however decided that this did not create an issue during the testing phase, as they would be located at low level in a cool fresh air supply.

The basic operating principle of these nozzles is that high pressure air and water combine in a mixing chamber below the nozzle tip and are then expelled through

the nozzle tip at high pressure and velocity. This process creates very small particles in the order of that required for the experiment.

The actual flow and particle size produced at the nozzle is dependant on both the air pressure and water pressure supplied. As a general rule the greater the air pressure the smaller the particles, but the less the water flow. Conversely the greater the water pressure the larger the water particle but the greater water flow. Consequently the result of this is that a balance point must be reached where the particle size and water flow match that required. A full listing of the nozzle specifications is included in appendix 11.3, but for the specific requirements needed for this experiment the graph in Figure 32 has been created.

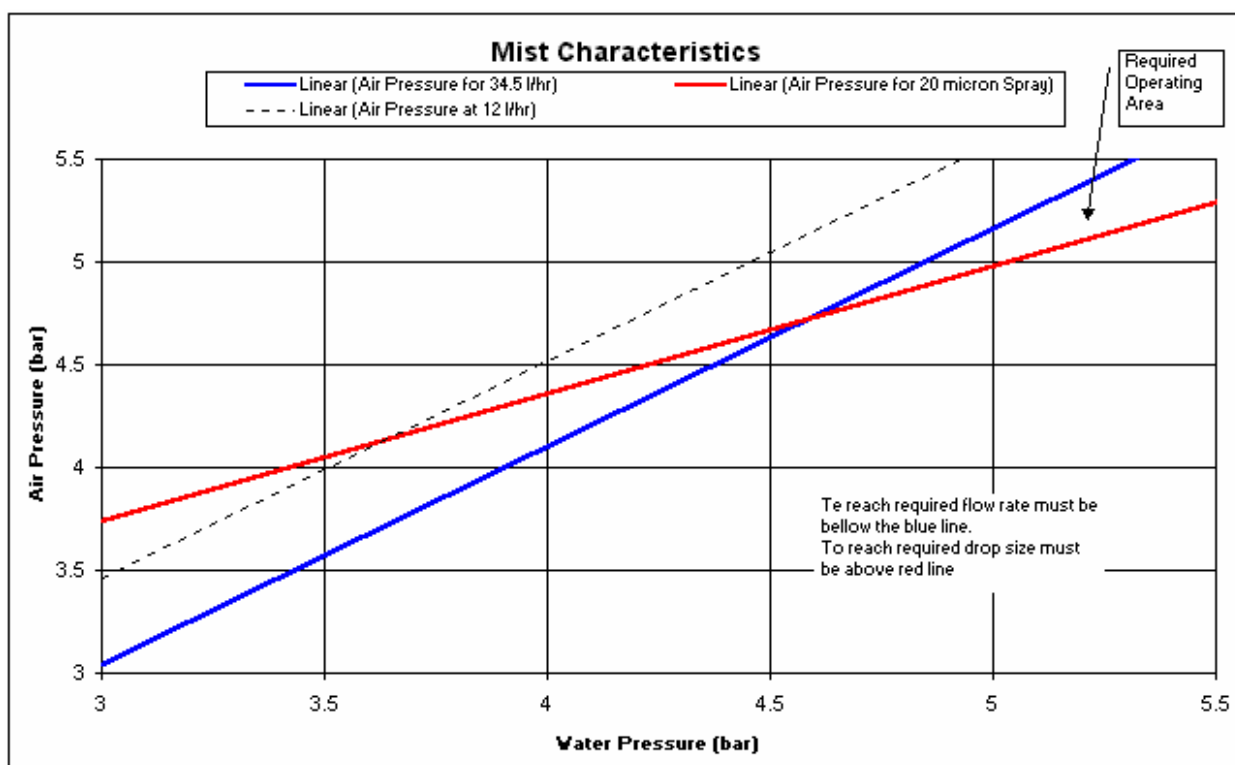


Figure 32 - Water mist characteristics from QuickMist™ nozzle

From Figure 32 it can be seen that to reach the required water flow rate the air and water pressure must be at an operating point below the blue line. For the particles to be in the 20 μm diameter range though, the operating point must be above the red line. The result of this is that the only acceptable operating point for the nozzle is between the two lines in the upper right hand section.

Based on this graph and the air and water pressures available at the experimental site, the selected operating target was 5 bar air and 5 bar water. At this point the six nozzles collectively provided a theoretical water flow rate of 0.66 l/s with a DV_{50} of 20 μm and a combined airflow rate of 0.013 m^3/s . This airflow rate is above that required to reach the 60 air changes per hour but as it is very small compared to the supply airflow it was ignored.

Within the compartment the nozzles needed to be fitted to the supply air diffuser in such a way to provide the majority of water mist into the supply air stream. The chosen layout of the nozzles is shown in appendix 11.4. $\frac{1}{4}$ ' copper tubing was used to attach the nozzles together and to the air and water supplies. This allowed the nozzles to be adjusted in place while still meeting the pressure requirements. The nozzle set up is shown in Figure 33.

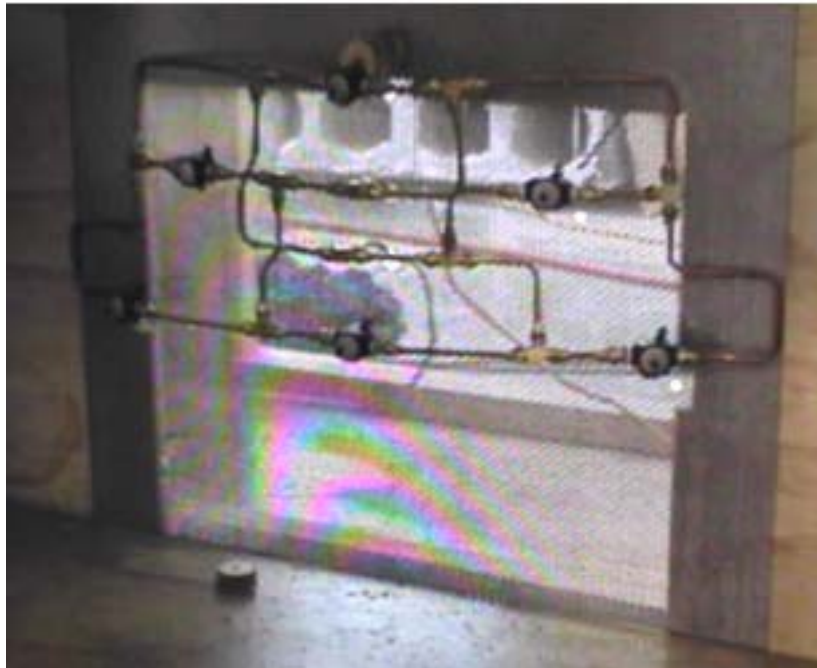


Figure 33 - Water mist nozzles installed in test compartment

On both the water and air feeds a pressure valve, needle valve and control valve were installed to provide control and allow the pressures to be regulated and measured on each line. In addition to this it was also found that on the water supply a very fine filter was required. It quickly became apparent that the filter played a vital role as without it the nozzles quickly became clogged as discussed

further on in section 5.9. Figure 34 shows the water filter and valves installed in place.



Figure 34 - Water filter, pressure gage and control valve

The final component that was added to the main water feed was an ultrasonic flow metre. This allowed for accurate water flow measurements to be taken and confirmed throughout the experimental process. If the nozzles became blocked, the flow level could be seen to drop indicating a problem.

5.5 Fan Selection

The selection of the fan was based on the requirements that it be able to provide the normal operating flow and pressure while being able to be increased to the higher flow and pressure in fire mode as outlined in section 4.6 and 4.7.

This requirement is in itself a relatively complex task as typically fans are designed to operate at a fixed speed. A speed controlled must be wired into the fan to allow the speed to be modulated down. Care must be taken though as

there is a minimum flow that the fan can provide before stalling occurs which is where the fan stops and begins to over heat.

To circumvent these problems the system was designed with an adjustable damper installed in the supply flow allowing the pressure drop associated with operation to be increased. Additionally a variable speed controller discussed in section 5.6, was added to allow modulation of the fan speed. The result of this addition was that as long as the selected fan could provide the fire mode airflow, the system could be adjusted down so as to also provide the normal operation airflow. It also meant that if the fan was oversized and provided too much airflow in fire mode, then the damper could be adjusted so that the pressure drop increased and the flow reduced to the value required.

As stated the fan need to provide the flow and pressure required for the system. The airflows were known from the calculations covered in sections 4.6 and 4.7 but the pressure drop needed to be determined. Typically this would be performed using readily available engineering calculations and constants achieved through experiments of varying airflows through different types of components. Unfortunately there was very little accurate data for pressure drop across a perforated steel plate in the configurations that the experiment called for. For this reason it was decided that, as the system was primary based on a HALTON [40] design, the pressure drop could be determined based on readings generated by their systems. The result of this investigation suggested that the pressure drop for the two layers of perforated steel operating in fire mode and with a face velocity of 0.98 m/s was in the region of 200 Pa.

Based on this pressure drop, required airflow of 0.288 m³/s, experimental set up and the fans available for use from Asset Services, a single entry, 1.2 kW centrifugal fan was selected. At the design flow of 0.288 m³/s this fan could provide 470 Pa, which was well above the 200 Pa estimated to be required. The performance sheet for the selected fan can be seen in appendix 11.5, with a photo of the fan in place and set up shown in Figure 24.

The advantage with using a fan providing such an excess of available pressure was that it allowed changes to be made to the experimental apparatus on site with

remaining confidence that the airflow requirements could still be met. Once installed the airflow was simply adjusted by setting the fan to maximum speed and then adjusting the damper setting until the required flow was reached. The normal airflow was achieved by adjusting the speed controller until the required airflow of $0.048 \text{ m}^3/\text{s}$ was achieved.

In each case the airflow was determined using a vane anemometer with readings taken across the compartment diffuser in accordance with the grid layout specified in ASHRAE [43].

5.6 Controls Selection

As has been previously discussed, the selected fan required a variable speed drive to allow the airflow to be modulated. As the selected fan was single phase 240 V, a standard rheostat controller could be used. The selected controller was the "Woods" msc05 infinitely variable 5 amp speed drive. This controller allowed the fan to be modulated from maximum speed, down to a minimum speed of approximately 20%.

In the case of the electric duct heater the control systems required are much more complex due to the level of control required and the higher currents in use. Through discussions with Siemens Building Technologies a control system was designed consisting of a primary controller that monitored the compartment supply air temperature and provided a modulated 0-10 volt output on two circuits. Each output was then sent to a frequency modulator and passed through to a high current solid-state relay. Each relay directly modulated the power supplied to each of the two 1.5 kW heater banks within the duct heater.

The primary controller was programmed in such a way that the first stage of heating was ramped up from 0 to 1.5 kW as the supply temperature dropped. Once its maximum output was reached the second circuit was then activated as well and ramped up in a similar manner. The result of this programming was that at a supply air temperature of 19°C no heating was applied, while at 17.5°C , 3 kW of heating was applied. As this range of control was extremely tight for this type

of application the possibility existed for the system to “hunt”. When hunting occurs the system modulates from full heating to no heating and back again. This is caused by a response time that is too short. To insure that this did not occur and that the system remained stable, a lag time of two minutes was programmed in. This time allowed the warmer air to enter the plenum, mix and reach the compartment supply diffuser and temperature sensor before the system over compensated.

Both the fan speed and electric duct heater controllers are shown mounted in place in Figure 35.

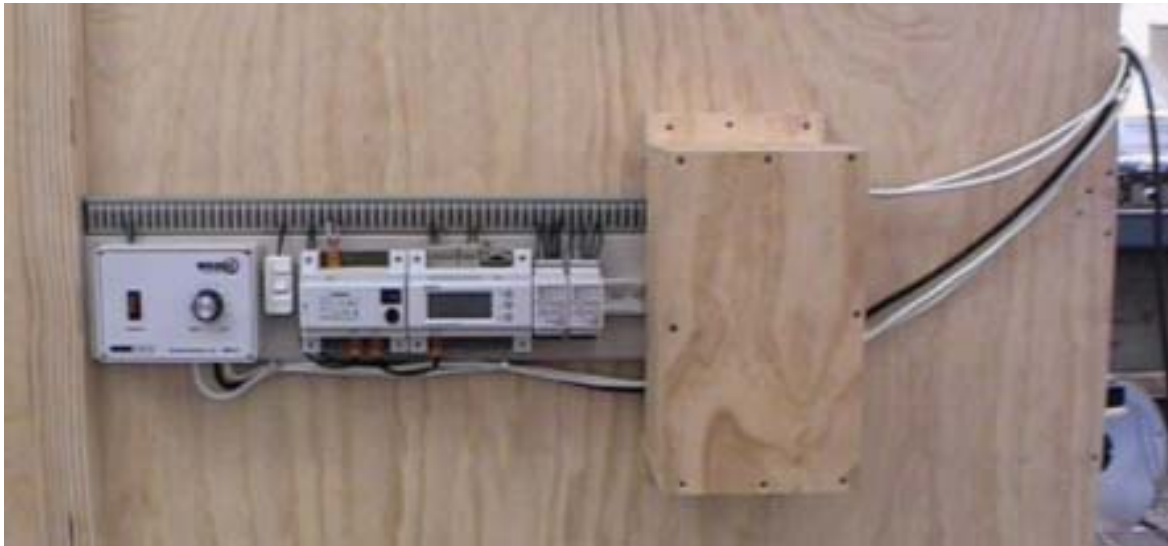


Figure 35 - Fan and electric duct heater controller

5.7 Detector Mounting

Commercially available ionisation and optical sensors were selected so that a comparison between the detection times could be made while insuring the earliest detection time using this type of technology. The selected sensors were analogue addressable from the *Appollo* XP95 range. It was expected that in a flaming pool fire the ionic detector would activate first while in the wood crib fire the optical detector would activate first. Two sensors were selected rather than a dual technology sensor due to cost and existing equipment supplies. As discussed in section 4.9 they were mounted in the centre of the roof and connected back to a data logger which displayed the individual readings on live bases. Activation was

assumed to have occurred when the output signal reached a value of 55 which is the value specified by *Appollo* to for the detectors to meet the ISO standard for detectors.

5.8 Sprinkler Selection

The conventional sprinkler head that was selected was a standard commercial Wormald 15 mm pendant head with a K value of 8.0. The head was installed in the centre of the compartment and was operated at a pressure of 40 kPa. This provided a total flow of 50 l/min or 7 mm/min over the floor area. Control of the sprinkler was performed using a hand operated control valve and pressure gauge. The piping set up to the compartment can be seen in Figure 36.



Figure 36 - Conventional sprinkler system

5.9 Trial Observations

As with any process involving experimentation, initial trials must be carried out to determine that the system is operating correctly and that all of the components involved are operating as required. No specific layout and test procedure was followed during these trials as they were purely used to ensure that the system was operating as designed.

It quickly became apparent that under normal operation the system functioned as anticipated. The fan operated well at low speed and the control system maintained a steady supply temperature of approximately 19°C. Within the compartment the two light bulbs and computer obviously created heat as the temperature profile taken by the thermocouple trees showed an increase in temperature with height as had been anticipated.

Under fire conditions the air supply system and controllers appeared to operate as required, providing the increased flow rate on demand. Unfortunately the water mist system when operating showed a number of characteristics that had not been intended.

The first of these was that the water mist output of the nozzles was observed to rapidly decrease during the first test run. On closer inspection it was found that the nozzles had become blocked with foreign particles from the water supply. The initial assumption had been that the water supply was pre-filtered and as such a secondary fine filter was not necessary right before the nozzle array. This proved to be in error as the supply pipes had obviously contained some foreign material. In addition to this it quickly became apparent that a flow metre would be needed to monitor the nozzles, ensuring that this problem did not arise again and that the water flow required was actually being delivered.

With the flow metre and filter installed a flow rate of 0.086 l/s was recorded at a water and air pressure of 5 bar. This is slightly above the flow rate of 0.066 l/s based on the manufactures data, and as such suggests that either the nozzles were operating slightly differently to the manufacturers data or that one of the

pressure gages in use was in error. If the pressure gages were in error it would suggest that the particles had a Dv_{50} greater than 20 μm .

Unfortunately the experimental set up limitations did not allow the air and water pressures to be adjusted to obtain the correct flow rate as the air pressure was at a maximum and the water pressure had only basic control. When the water pressure was adjusted down the decrease became so great that the flow dropped below that required. If the air pressure was then lowered to increase the flow the particle size could not be maintained. On reviewing this information and the manufactures data shown in appendix 11.3, it was decided that while the particles would be slightly larger than ideally required, the flow water density was of more importance in the experiments, so the air and water pressures were set to provide 0.086 l/s.

The next problem associated with the water mist system and one that had not been expected to the extreme extent to which it occurred, was the entrainment and throw created by the nozzles. It had been expected in the design phase that the nozzles would entrain the surrounding air, but it had been expected that this would be minimal and would primarily involve the supply air from the diffuser. In actual fact with the nozzles located flush with the diffuser grill the entrainment was so great that the water mist created a plug flow that did not spread out. Additionally due to the lack of mixing the throw from the nozzles far exceeded that expected from a single nozzle. In initial tests within the compartment the water mist plug flow moved across the compartment at high speed, missing the fire zone, hit the back wall and was simply diverted up the wall and along the roof to the exhaust grill. Further more, this rapid cycling caused the upper layer to be disrupted and forced into the lower layer, negating one of the primary design objectives of maintaining a clear lower layer.

To investigate this phenomenon further the nozzle array was removed from the compartment and placed in the open. When activated the same plug flow effect occurred and a strong suction could be felt from behind the array. It was evident that the nozzle spray was severely affected by this entrainment and that the water mist was being drawn into the core of the mist flow rather than spreading out. The mist was also observed to travel in excess of 10m across the ground. In

comparison with one nozzle activated the spray travelled only 2m as had been indicated by the manufacturer.

This severely affected the testing procedure as the design called for a relatively slow moving mist that flowed with the displacement air supply. To try and correct for this the nozzle array was curved so that all of the nozzles pointed in an arc. The result of these changes was that spray spread out further and had a shorter throw, but it was still far greater than what was called for in the initial design. The new nozzle array was installed back in the compartment and another test run. While the spread and throw were reduced and a more even flow was created, the water mist still tended to hit the back wall at speed and be deflected up it. While reduced, this again created mixing between the upper and lower layers, which had been intended to be avoided.

To attempt to circumvent this problem and find a solution, the nozzle array was moved into a vertically upright position within the plenum. A diagram of this is shown in Figure 37.

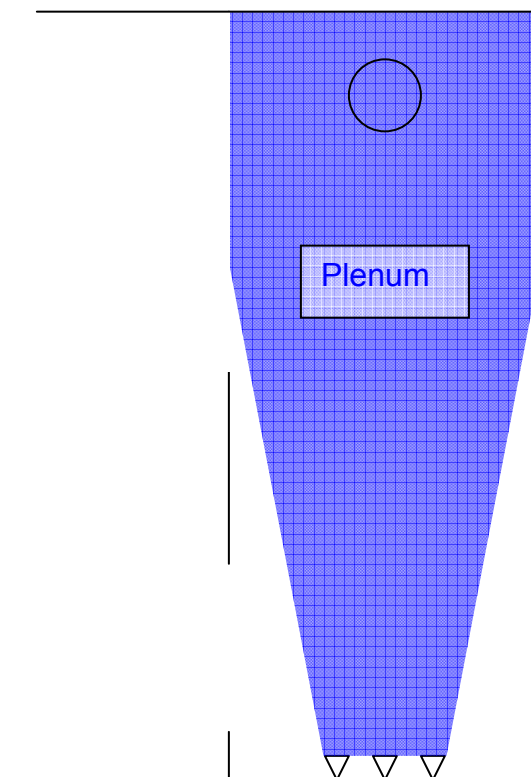


Figure 37 - Vertical plenum mounted nozzle array

This concept relied on the high speed water mist sprays mixing with the supply air within the plenum and then this mixture being supplied to the compartment as a laminar flow. During the initial test it became apparent that with the perforated steel supply grill in place a lot of water was simply being deposited on it as it attempted to pass through. A second test was run where the supply grill was removed leaving a clear opening. This appeared to work more efficiently than previously but the volume of water mist flowing out was still significantly lower than that required as the majority had been deposited on the walls of the plenum chamber. It appeared that within such a confined location the water mist was either impacting the walls at high velocity, or being hit by other particles creating larger particles that simply dropped out of the airflow.

The third set up tested was the installation of the nozzles at the back of the plenum facing toward the open supply hole. This arrangement is shown in Figure 38.

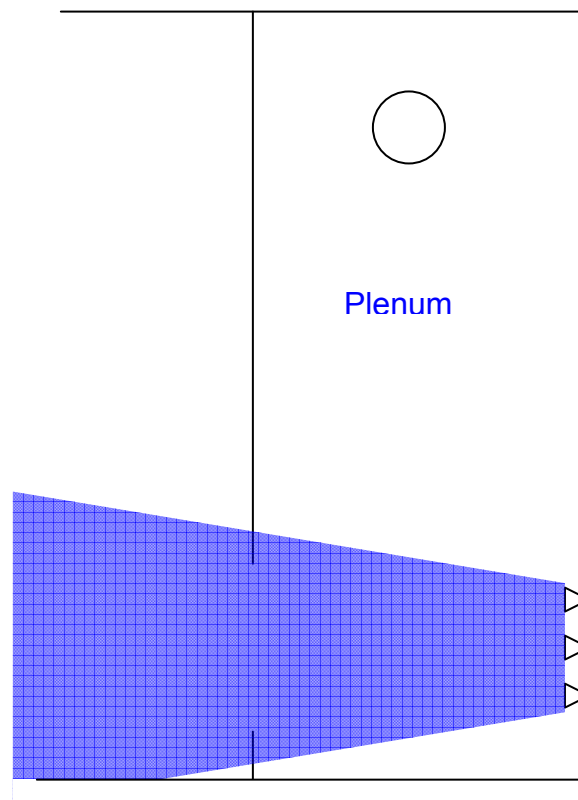


Figure 38 - Horizontal plenum mounted nozzle array

During trials this array proved to give a slower moving mist as had been intended. It appeared that after the initial operation of the nozzles, a negative pressure was

pulled within the compartment that caused the water mist particles to slow significantly. Unfortunately through, due to the location and set up of the nozzles a large majority of the water impacted on the edges of the opening and resulted in a much lower water density than what was required.

Based on the findings of these tests and the limited time frame available it was decided that the experiments should be carried out using the curved nozzle array on the outside of the supply diffuser. This set up, while creating excessive mixing and parameters that were to be avoided under the initial design, allowed the required volume of water to be supplied to the compartment under the best conditions available at the time.

The final observation regarding the initial experimental set up that was made, related to the two smoke detectors. The initial design called for the smoke detectors to be monitored and when an alarm level was reached, for the suppression systems to be activated. In practice though the fires were ignited and detection occurred within a few seconds. In relation to the pool fire, this resulted in no upper layer being formed and hence no clearly observable differences between activation and non-activation. In regard to the wood crib fires, the early detection meant that the fire did not have sufficient time to develop. In one such test case the water mist system was activated within 6 seconds of the crib being ignited. The result was that the fire had not established itself and appeared to be simply blown out.

It was further observed during the trial testing was that the way in which each of the detectors was reacting was not as expected. It had been anticipated that during a pool fire the ionic detector would activate first as this type of sensor tends to provide better detection of flaming fires. In the case of the wood crib fires it had been anticipated that the optical detector would activate first as this type of sensor detects smoky, smouldering fires more quickly than an ionic sensor. In both cases during trial testing though, the ionic detector activated first.

Through observation it appears that the ionic detector was operating first during the wood crib fire due to the presence of the methylated spirits used to ignite the crib and hence somewhat discounting the cellulose fire detection. Graphs of the

detector readings during a pool fire and a crib fire are shown in Figure 39 and Figure 40.

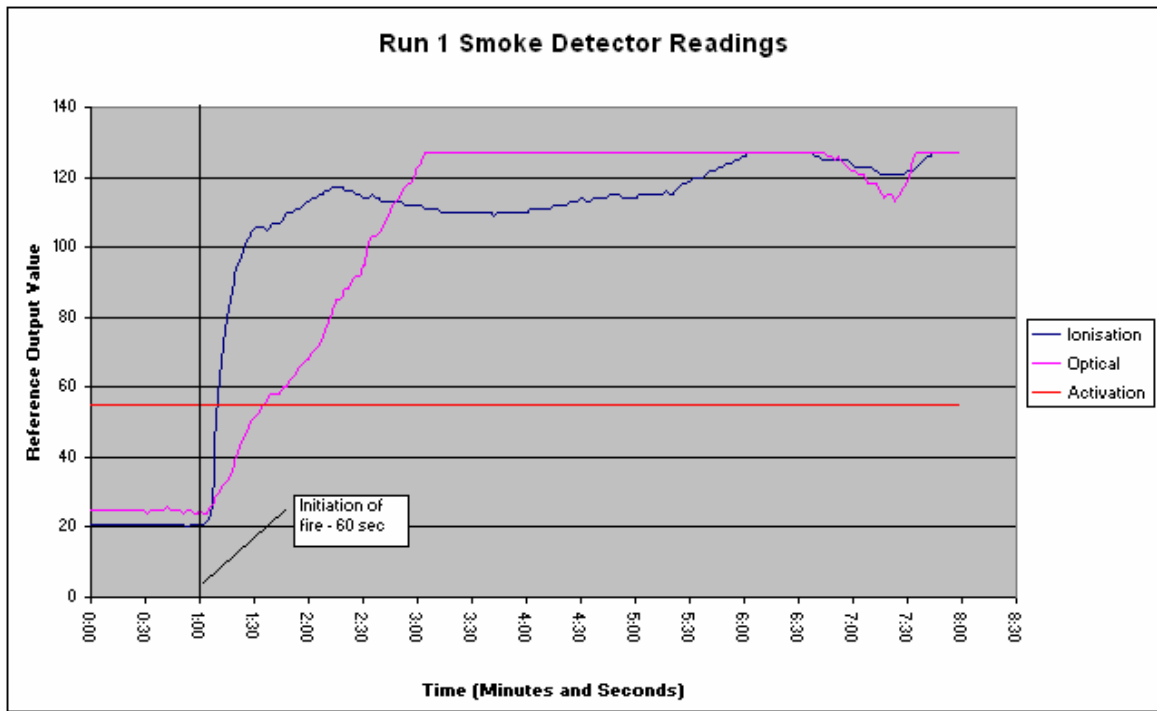


Figure 39 - Pool fire detector results

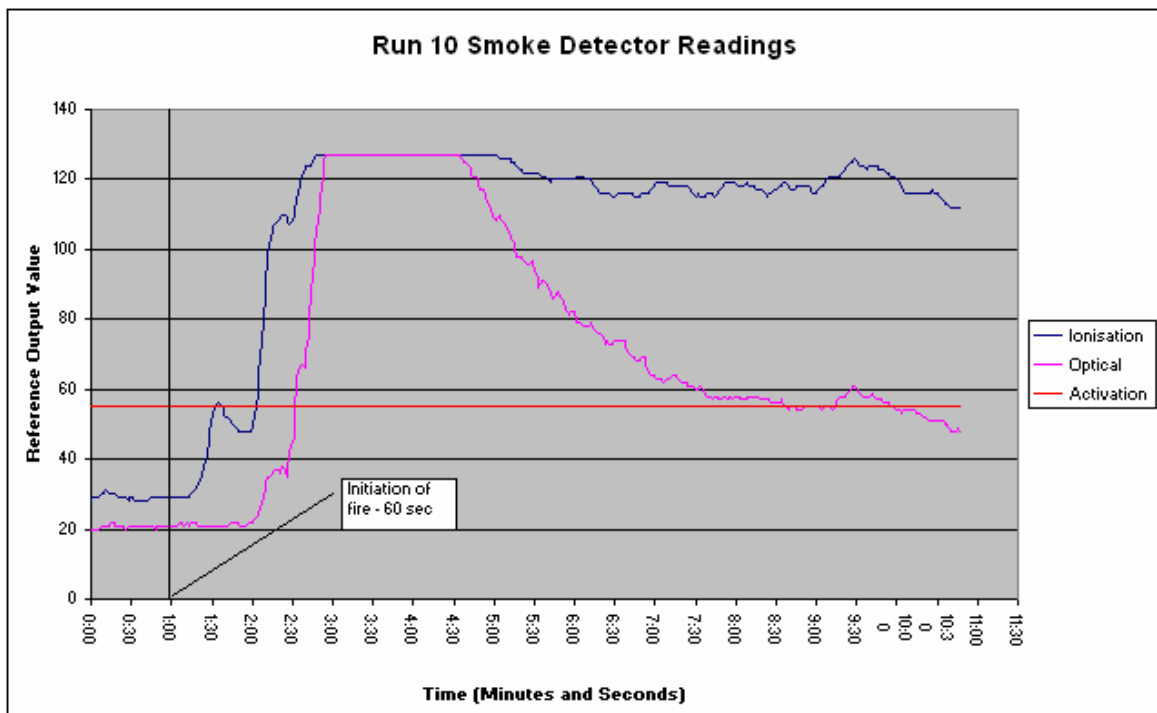


Figure 40 - Wood crib fire detector results

For the reasons discussed above it was decided that the detectors would be ignored for the purpose of activating the suppression system and a simple timed activation used. This allowed an upper layer to be formed and for the wood crib fire to become established.

5.10 *Experimental Time Line*

The initial time frame selected for the experiment was as follows.

Time	Action
0:00	Video, Thermocouple data logger and Smoke detector data logger started
1:00	Fire ignited
Variable	On detector reaching activation point of 55, all suppression systems required for experimental run started. This included increased airflow, water mist or sprinklers as required.
Variable	Shut off of system if; fire extinguished, compartment flooding, danger to compartment.

Table 4 - Initial experimental timeline

Unfortunately as discussed in the trial observation, it became apparent that the detectors activated almost immediately upon the fire being lit. The result being that extinguishment measures began before temperatures had begun to increase and an upper layer had been formed. As also discussed in one case of a wood crib the fire was simply blown out by the water mist system due to its small size.

In response to this the time line for pool fires was modified that that below.

Time	Action
0:00	Video, Thermocouple data logger and Smoke detector data logger started
1:00	Fire ignited
2:00	Suppression systems required for experimental run started. This included increased airflow, water mist or sprinklers as required.
N/A	Shut off of system if; fire extinguished, compartment flooding, danger to compartment.

Table 5 - Experimental timeline for pool fire tests

In the case wood crib fires through, it was observed that the fires often had not taken hold and no significant results would have been obtainable in the 60-second time frame. For this reason the timeline for wood crib fires was modified so that suppression did not begin until an arbitrary time when the fire was considered to have taken hold. The resulting timeline is shown below.

Time	Action
0:00	Video, Thermocouple data logger and Smoke detector data logger started
1:00	Fire ignited
2:00	Suppression systems required for experimental run started. This included increased airflow, water mist or sprinklers as required.
N/A	Shut off of system if; fire extinguished, compartment flooding, danger to compartment.

Table 6 - Experimental timeline for wood crib fires

5.11 Full Scale Test Results and Discussions

This section of the report describes each of the experimental test runs carried out. It presents the graphical results and discusses the observations made during testing. Run 1 presents data from all of the thermocouple trees within the compartment and gives an overview of general operation. In the following runs only the three main thermocouple set results are presented and discussed. These typically include the tree above the fire, the “occupant” tree (Tree 1) and the supply and exhaust sensor readings.

For clarity, the observations referred to within the section were made by a number of observers present at the testing. The primary observers were two New Zealand Fire Service senior training officers, Mike Spearpoint the project supervisor and the author.

5.11.1 Run 1: Centre Floor, Pool Fire, Low Flow, No Mist

<u>Fire Location:</u>	Centre of compartment at ground level.
<u>Fire Type:</u>	Heptane pool fire.
<u>Airflow Characteristics:</u>	Constant low flow operation.
<u>Suppression:</u>	None.
<u>Objectives:</u>	To determine the conditions within the compartment subjected to a pool fire under normal operating conditions with no suppression and normal flow.

Observations:

As stated the primary objective of this test was to provide a base for which all centre pool fires could be compared to. It provided information on the compartment conditions expected if the fire occurred in a normal compartment with no suppression.

The Heptane pool fire ignited readily at 60 seconds. This can be clearly seen in Figure 42 where the temperature of the 0.3m thermocouple on tree 2 immediately jumped to 310 °C. Once ignited it was observed that the flame sloped slightly away from the supply air diffuser. This appeared to be due to the airflow entering

the compartment, spilling across the floor and hitting the base of the fire with a tangential velocity.

Within the compartment a noticeable smoke layer developed quickly. As the test proceeded, the interface between the upper and lower layers dropped to a point that after 4 minutes the light bulbs and computer became obscured. This layer was accompanied with an increase in temperature along the vertical axis of the compartment.

This temperature increase can be clearly seen in Figure 41, which represents the position an occupant would be within the compartment. With the onset of the fire the temperature at all of the thermocouples increase with the upper-most thermocouples increasing at a greater rate. At the peak temperatures within the compartment the three thermocouples above 1.3m exceeded 110°C with the roof 2.1m sensor reaching a peak of 130°C. As discussed in SFPE [44] these temperatures are at the limit of human endurance and would cause significant harm or possibly death. At the 1.8m thermocouple the temperature reached a peak of 90°C that while not causing death could cause significant harm to an occupant. As expected the lowest peak temperature of 40°C was recorded at the thermocouple located at 0.3m. While this temperature is survivable, observations of the compartment suggested that the interface layer at this time was very close to the ground and would have posed a serious threat.

Figure 42 displays the information from the thermocouple tree located directly above the fire. The 0.3m and 0.7m sensors were located closest to the fire and as such show the greatest increase. As expected the 0.3m sensor was located within the flame region of the fire, accounting for the immediate increase and high temperatures. The jagged results from this sensor are most likely due to the unstable nature of the flame. This is amplified to some extent by the slope of the flame causing the flaming region to move off the sensor at periods. The 0.7m sensor was located just above the flame region resulting in a slower increase as the surrounding cool air was drawn into the fire plume, cooling it as it rose. Similarly the three top thermocouples show a slower increase similar to that of Tree 1, but with slightly higher temperatures due to being located within the main

fire plume. The point at which the fire decays can be clearly seen from the rapid decay in temperature by the 0.3m and 0.7m sensors at 5 minutes 30 seconds.

Figure 43 and Figure 44 display the results recorded within the front and back corners of the compartment. As can be seen, in each case the results were similar to each other and to that of the corresponding sensors in Tree 1. This indicates that the temperature at a particular height within the compartment (excluding those within the fire plume) remained similar throughout the compartment, suggesting relatively stable layer development.

The final graph recorded from this test run is Figure 45, which shows the temperatures recorded at the supply diffuser and the rooftop exhaust. As expected the supply temperature remains at approximately 19°C throughout the experiment. The extract thermocouple shows a peak temperature of just under 130°C, which is below that of any of the sensors located at 2.1m within the compartment. This is not what theoretically would be expected, as the hottest temperatures within the compartment are typically located at the ceiling. As such the hottest temperatures would be above the 2.1m sensor and be recorded by the extract thermocouple. The probable for this result is that as the sensors are bead thermocouples, they will be recording some level of thermal radiation from within the compartment. Typically an aspirated thermocouple would be used to check this result as it provides a more accurate air temperature reading, but this type of sensor was not available for this experiment.

One point that can clearly be seen on all of these graphs is the period of time that it takes the compartment to return to what may be considered acceptable temperatures. Once the fire burns out the environment within the compartment takes approximately 2 minutes until all of the sensors display readings below 50°C. Additionally during this period it was observed that the smoke layer took a significant time to clear and in fact the main compartment door had to be opened to assist in this process. This is due to the fact that the displacement system was operating in normal mode where one compartment air change takes ten minutes.

The results of this test suggest that even with a 20 kW fire, this compartment quickly became uninhabitable for occupants due to both temperature and

combustion products. Additionally the compartment remained uninhabitable for a significant time after the fire had gone out.

Graphical Data:

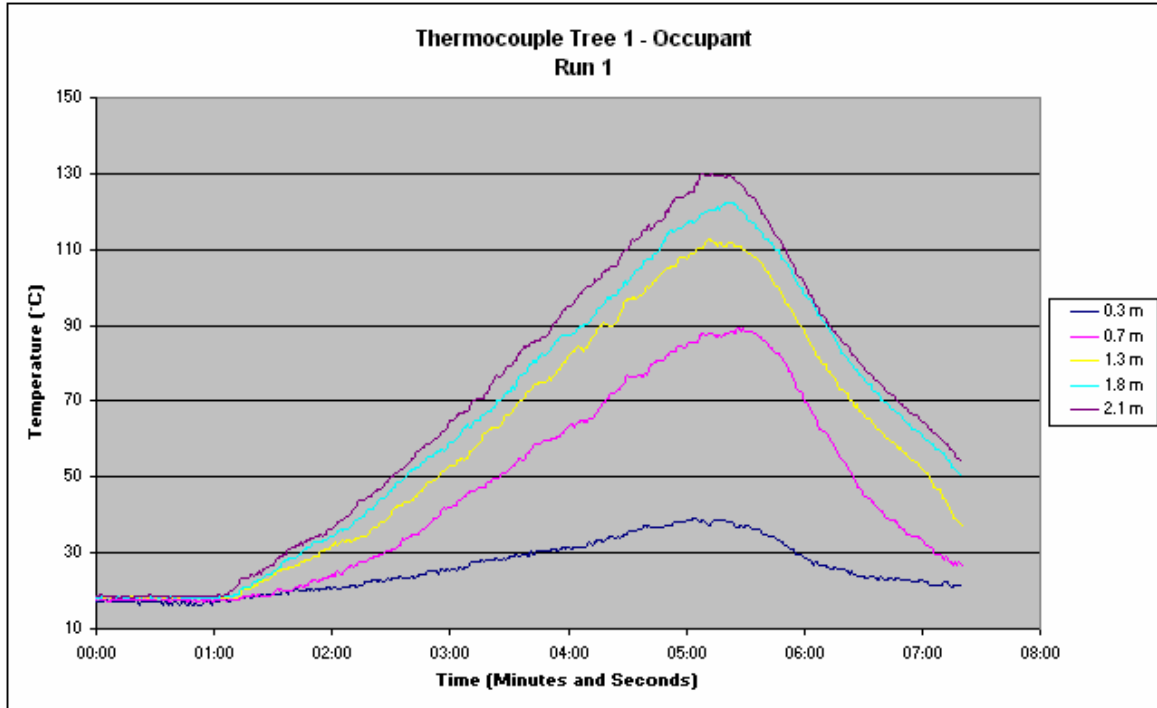


Figure 41 - Run 1: Occupant Thermocouple Tree

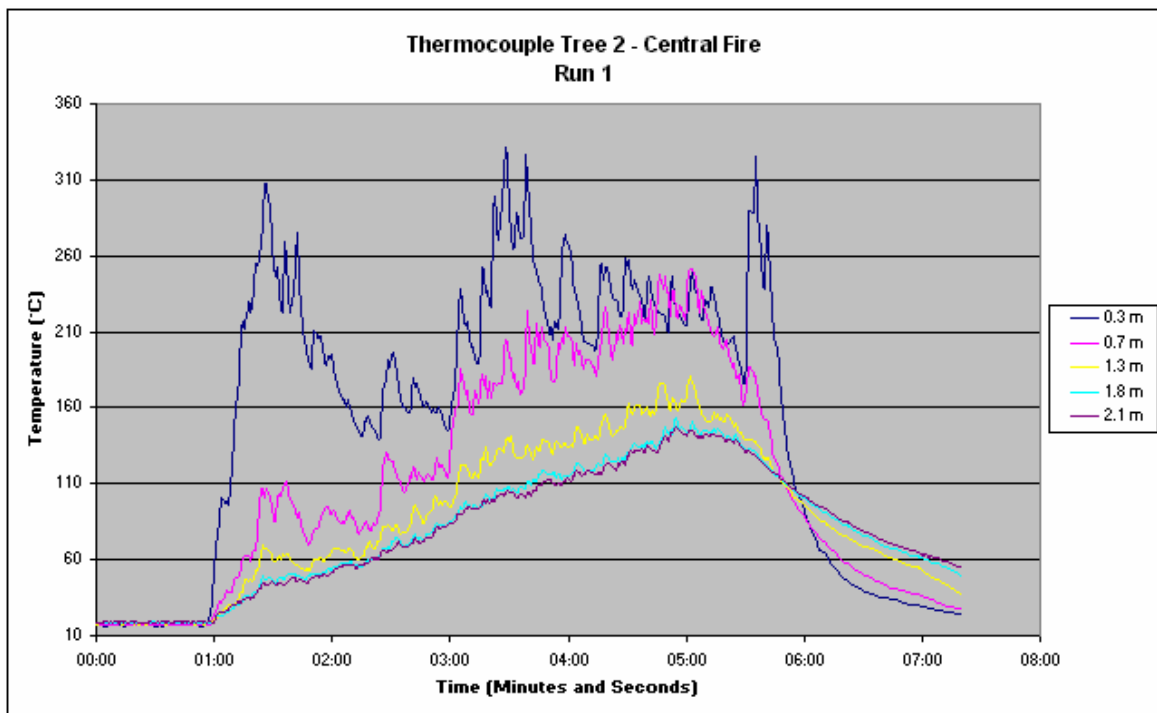


Figure 42 - Run 1: Fire Thermocouple Tree

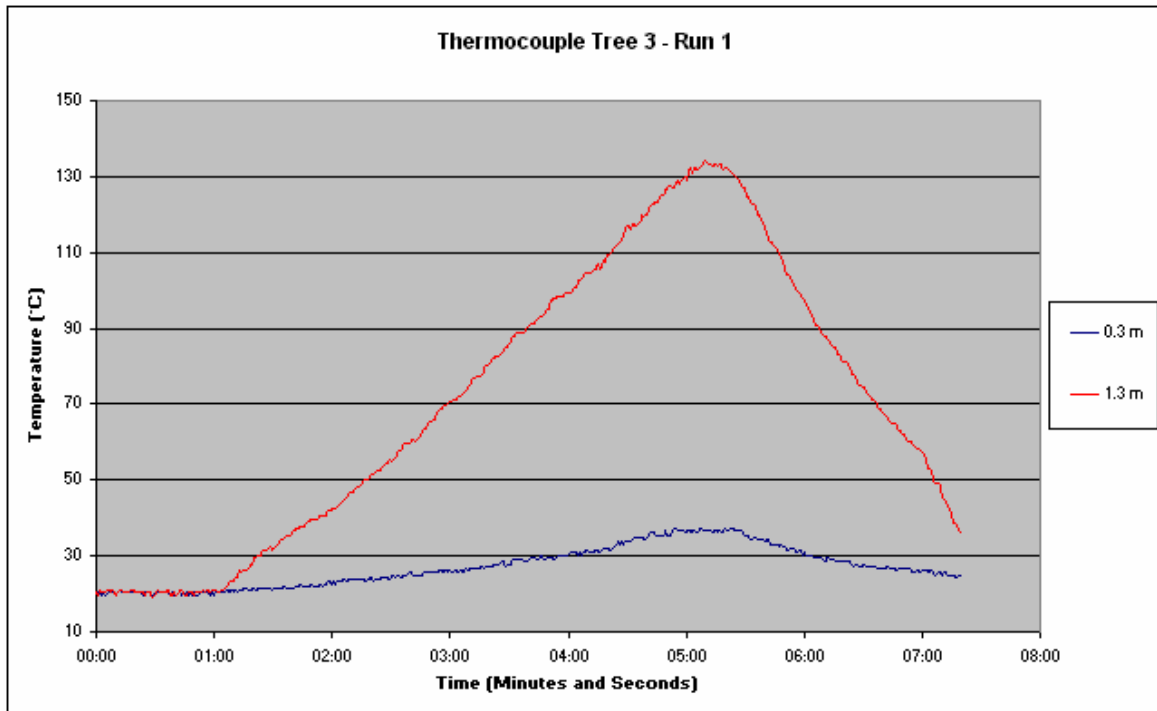


Figure 43 - Run 1: Back Corner Thermocouple Tree

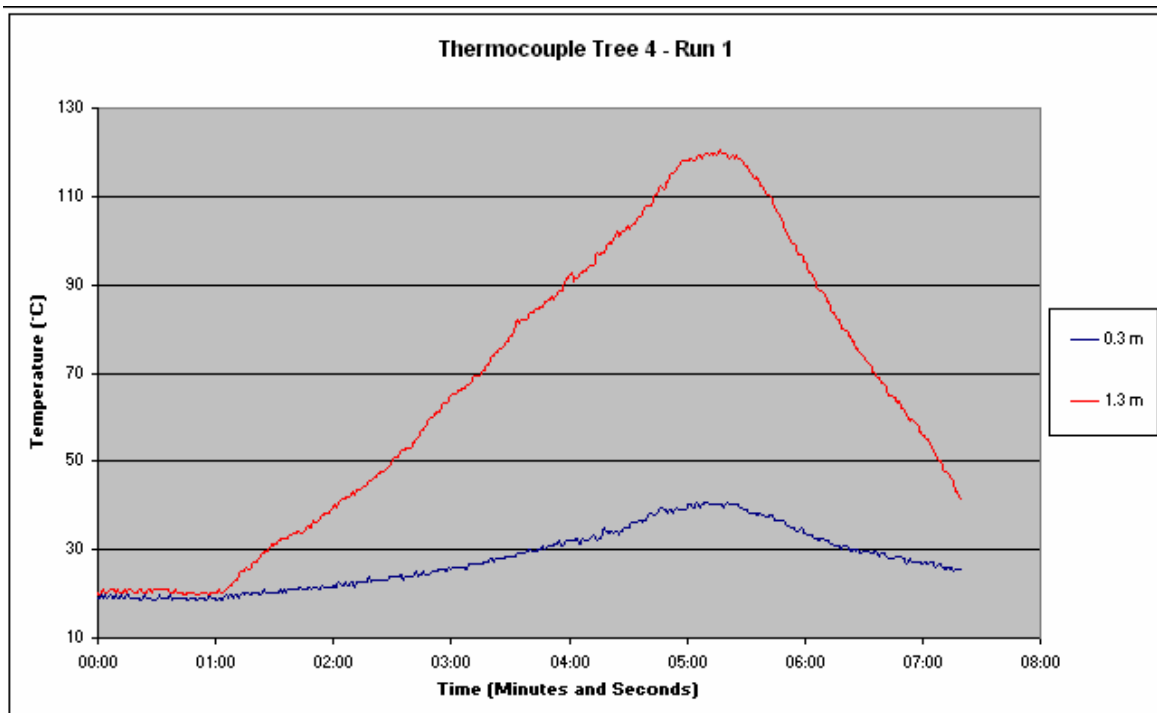


Figure 44 - Run 1: Front Corner Thermocouple Tree

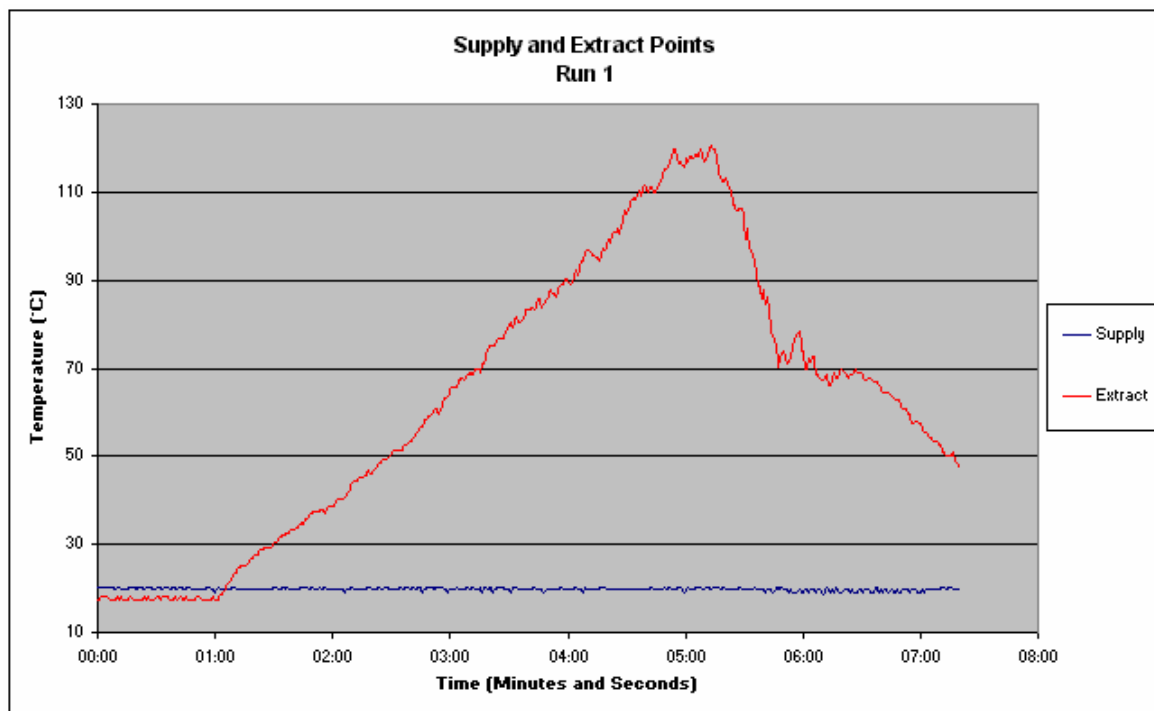


Figure 45 - Run 1: Supply and Extract Temperatures

5.11.2 Run 2: Centre Floor Pool Fire, High Flow, No Mist

- Fire Location: Centre of compartment at ground level.
- Fire Type: Heptane pool fire.
- Airflow Characteristics: Low flow operation for 60 seconds followed by high flow operation.
- Suppression: None.
- Objectives: To determine the conditions within the compartment subjected to a pool fire when the supply airflow is increased but no suppression is added.
- Observations:

Run 2 was similar in nature to Run 1 with the exception that the displacement air supply system set to fire mode after 60 seconds. As stated the primary objective was to provide information on the compartment conditions when only the airflow was increased.

Initially the pool fire reacted the same as had occurred in Run 1 with the flame showing a slight slope away from the supply diffuser and an upper layer forming quickly. When the displacement system was set into fire mode and the airflow

increased, the flame showed an increased slope away from the diffuser and appeared to burn slightly more vigorously. As the fire continued to burn it was observed that the wooden flooring on the down stream side of the pan began to char due to the increased radiation from the sloped flame.

The second noticeable observation when the displacement system was set into fire mode was the increase in height of the interface layer. While not completely exhausting the smoke layer, it appeared that the layer increased in height slightly before descending again in a slower manner than had been occurring under the normal operating condition. The smoke layer that formed was relatively dense in the upper region but was noticeably clearer in lower levels. The interface between the upper layer and lower layer also appeared to become slightly more disturbed with the initiation of the higher airflow possibly resulting in the appearance of the interface layer dropping.

This decrease can be clearly seen in Figure 46 taken from Tree 1. The temperatures increase at a constant rate within the compartment until the airflow is increased. At this point the rate of increase can be seen to stabilise momentarily before again continuing to increase but at a decreased rate. As a result the peak temperatures within the compartment reached 110°C at their maximum.

The increased draft effect on the fire can be clearly seen in the data taken from Tree 2 directly above the fire and shown in Figure 47. As the fire is initiated the temperatures at the 0.3m and 0.7m thermocouples increases dramatically. Once the system moves into fire mode though, the temperatures at these thermocouples drop off quickly, and while remaining elevated, are far below that expected from such close proximity to the fire. An interesting point to note is that all of the readings from Tree 2 are approximately the same after three minutes. This may be due to the fact that while the plume is no longer rising directly through Tree 2, some effect is still felt due to the unstable nature of the flame. Additionally the radiation to the low level sensors increases as the flame is forced on an angle to one side and exposes a greater area to the sensors, increasing the view factor.

Figure 48 displays the supply and exhaust temperatures from the compartment. As expected the supply temperature remains constant while the exhaust temperatures show a similar characteristic to that of the two graphs discussed above with a second gradient after the initiation of increased flow. The maximum temperature at the extract point is below that recorded at the 2.1m sensors throughout the compartment.

The results from this graph show that the increased flow reduced the rate of temperature increase and the density of smoke at low levels, and extended the length of time before the compartment became uninhabitable.

Graphical Data:

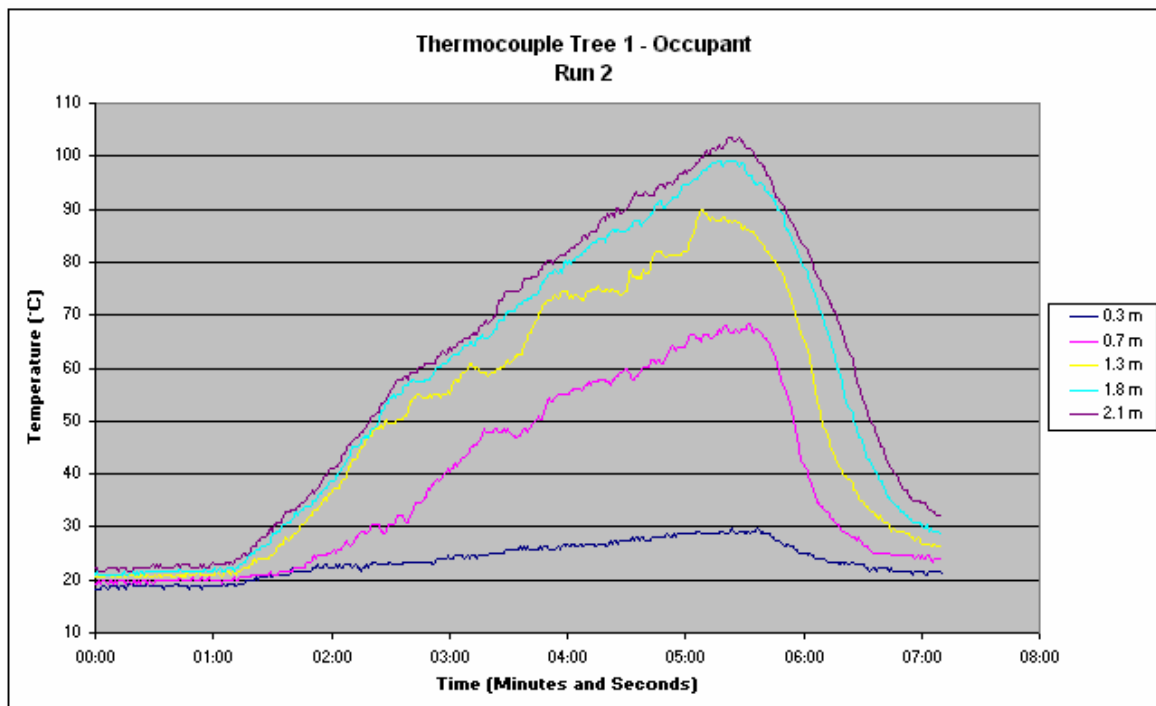


Figure 46 - Run 2: Occupant Thermocouple Tree

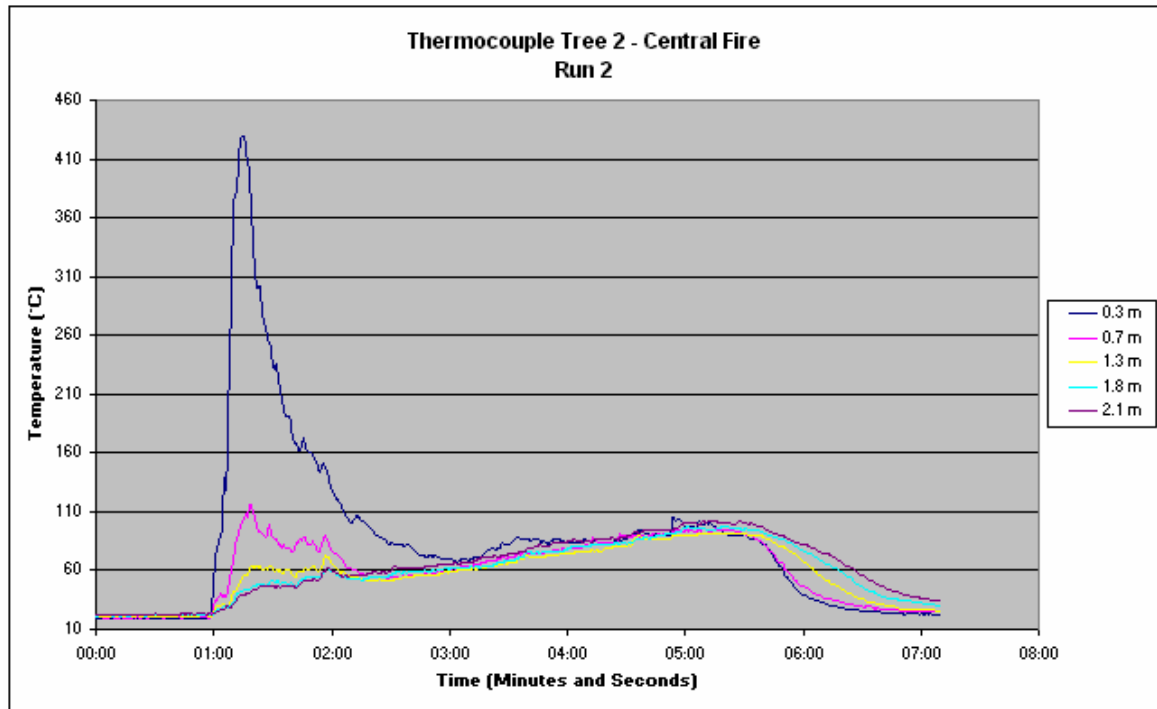


Figure 47 - Run 2: Fire Thermocouple Tree

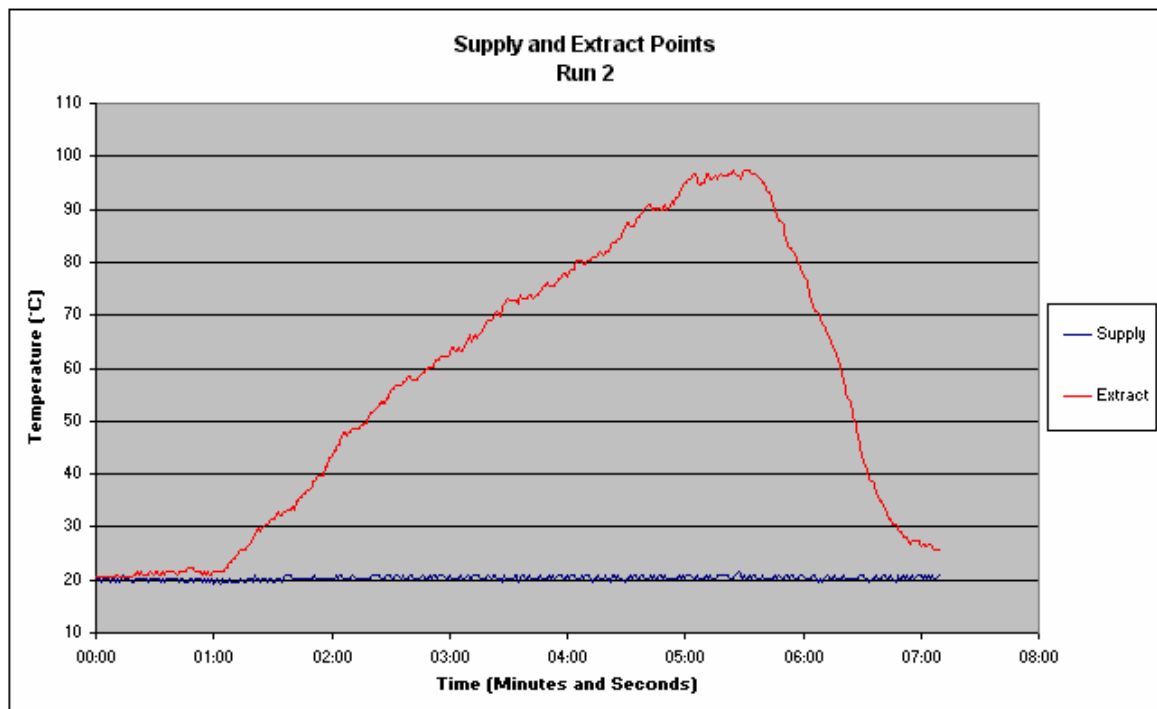


Figure 48 - Run 2: Supply and Extract Temperatures

5.11.3 Run 3: Centre High, Pool Fire, Low Flow, No Mist

<u>Fire Location:</u>	Centre of compartment at 1 metres.
<u>Fire Type:</u>	Heptane pool fire.
<u>Airflow Characteristics:</u>	Constant low flow operation.
<u>Suppression:</u>	None.
<u>Objectives:</u>	To determine the conditions within the compartment subjected to a pool fire at desk height under normal operating conditions with no suppression and normal flow.

Observations:

Run 3 simulated the effect of a pool fire that occurred on a desk at 1m in height. The immediate observation of this fire was that the airflow from the supply diffuser did not affect its burning characteristics. That is the fire did not slope away from the diffuser and tended to burn as if in a still environment.

A smoke layer quickly formed and dropped to the level of the fire at approximately 2.5 minutes. The upper layer then slowed in its descent and became denser. This was particularly relevant to the smoke build-up above the 1.8m sensor where the smoke appeared to be very dense. At no point during the test did the area beneath the fire appear to have significant smoke build up. The lighter smoke density during the test allowed the supply airflow to be seen spreading across the floor.

These same characteristics can be seen in the recorded data. Figure 49 clearly show the rise in temperature of the three sensors above 1m. The temperatures recorded at the 1.8m and 2.1m sensors show the increased build-up observed in this region. The 1.3m sensor had a similar trend to the top sensors but to a much lesser extent, while the 0.3m and 0.7m sensors showed little increase in temperature.

Figure 50 show the temperatures taken directly above and below the fire. As expected the readings from 0.3m and 0.7m sensors have little increase, while the three sensors above the fire show a rapid increase as expected. This is due to the plume rising vertically and means that the sensors above the fire are in the

high temperature core of the fire plume. This graph also shows an increase in temperature at the three top sensors after four minutes. This may have been due to the formation and temperature increase in the upper layer resulting in increased radiation and evaporation of the fuel.

Figure 51 shows a similar trend to that to the two thermocouple trees but again the exhaust temperature peaks at a lower temperature than the sensors within the compartment possibly due to less radiation effect.

This build-up of an upper layer above the fire is typically what would be expected in a high level fire due to the entrainment of air into the plume occurring only above the level of the fire. The result is that as the layer drops to the level of the fire, the entrainment into the plume from the lower layer decreases until the entrainment occurs primarily within the upper layer. This causes the upper layer to become denser as the combustion products accumulate in this area, while leaving the lower layer below the fire level relatively clear of smoke.

The results of this test suggest that while this fire scenario generates a relatively cool, clear zone below the fire level, the compartment would still be dangerous for occupants.

Graphical Data:

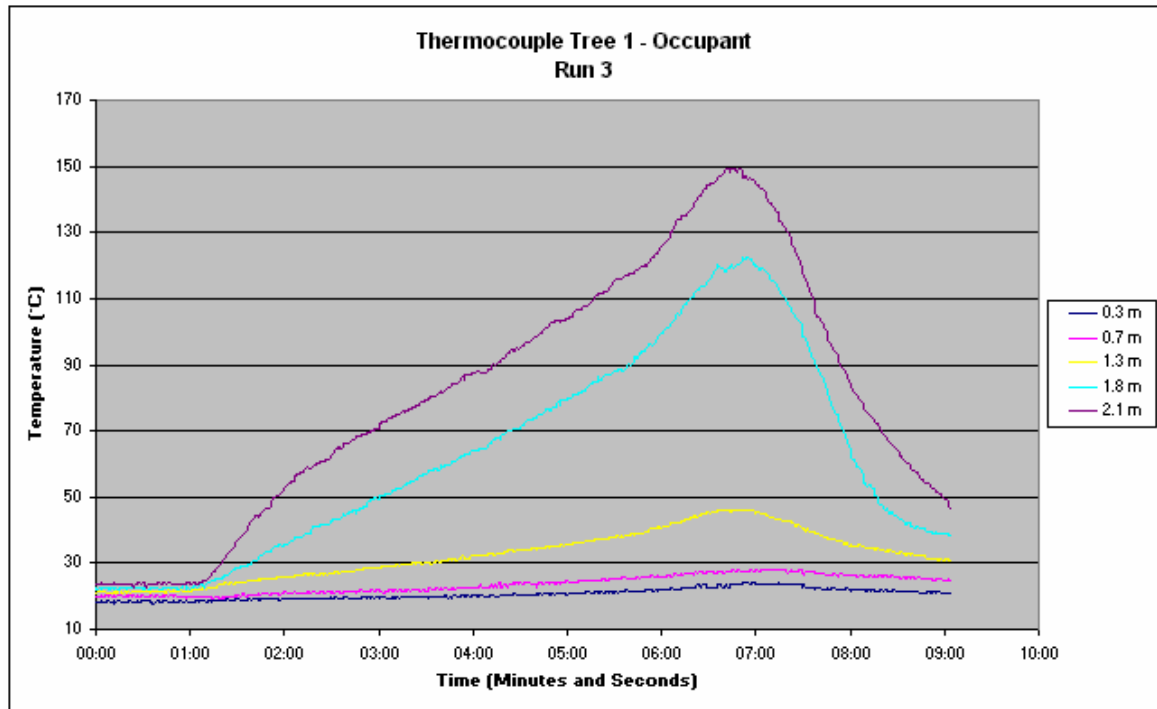


Figure 49 – Run 3: Occupant Thermocouple Tree

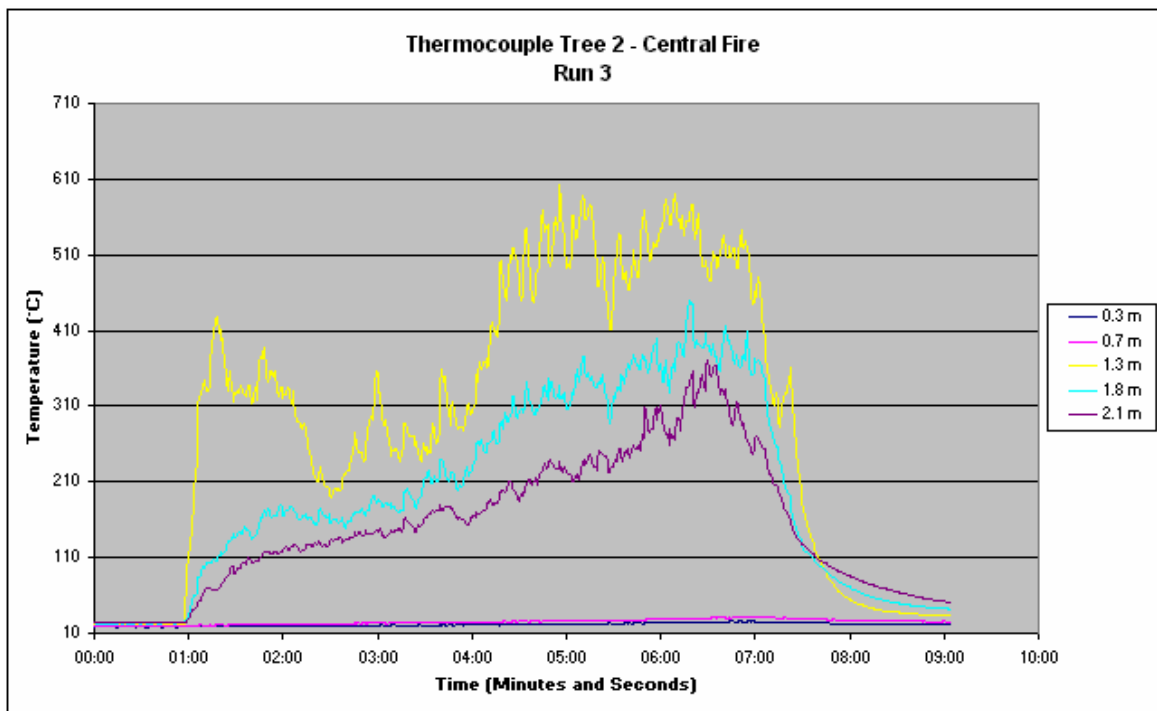


Figure 50 - Run 3: Fire Thermocouple Tree

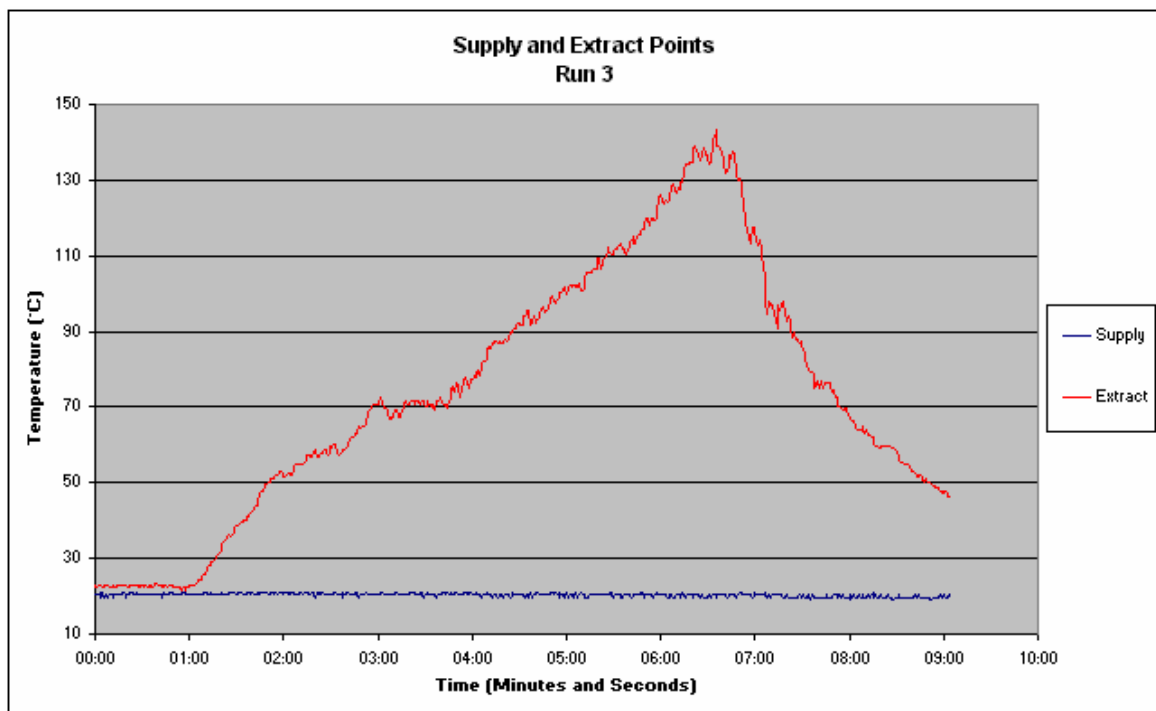


Figure 51 - Run 3: Supply and Extract Temperatures

5.11.4 Run 4: Back Floor, Pool Fire, Low Flow, No Mist

<u>Fire Location:</u>	Back Corner of compartment at ground level.
<u>Fire Type:</u>	Heptane pool fire.
<u>Airflow Characteristics:</u>	Constant low flow operation.
<u>Suppression:</u>	None.
<u>Objectives:</u>	To determine the conditions within the compartment subjected to a pool fire under normal operating conditions with no suppression and normal flow when a fire is located in the back corner of the compartment.

Observations:

Run four was similar to the initial three runs in that it provides a base to which the following experiments can be compared.

In this run the pool fire was ignited in the back corner of the compartment. As expected the flame tended to flow up the corner of the two walls. The flame appeared to be very stable. It was unclear if the flame was following the corner

due simply to natural convection, or whether the supply airflow from the diffuser was providing a tangential velocity and assisting in causing the flame flow along the corner. It was most likely a combination of the two effects.

The most apparent characteristic of this run was the extended height that the flame front reached. During the test the flame tip often touched the top of the fire protection panel at 1.8m in height. This is far in excess of that seen when the fire was located in the centre of the compartment, but is as expected, as less air is entrained by the plume per unity height and hence the fuel mass must travel a greater distance to become fully combusted.

A smoke layer quickly formed on the roof and dropped within the compartment but at a slower rate than that experienced in the central fires. This was due to less entrainment occurring between the fire base and the roof and hence a lower volume of combustion products being injected into the upper layer.

The results shown in Figure 52, Figure 53 and Figure 54 all show the steady increase in the temperature within the compartment consistent with the stable flame. This is also evident from the sensors located directly above the fire. While still giving a jagged curve, the overall readings are significantly more stable than that recorded from the central fires. As with the previous test runs, the maximum exhaust temperature, is below that of the 2.1m sensors within the compartment.

While the layer did not drop as significantly during this run, the environment created below 1.3m was still at a point that could be considered life threatening.

Graphical Data:

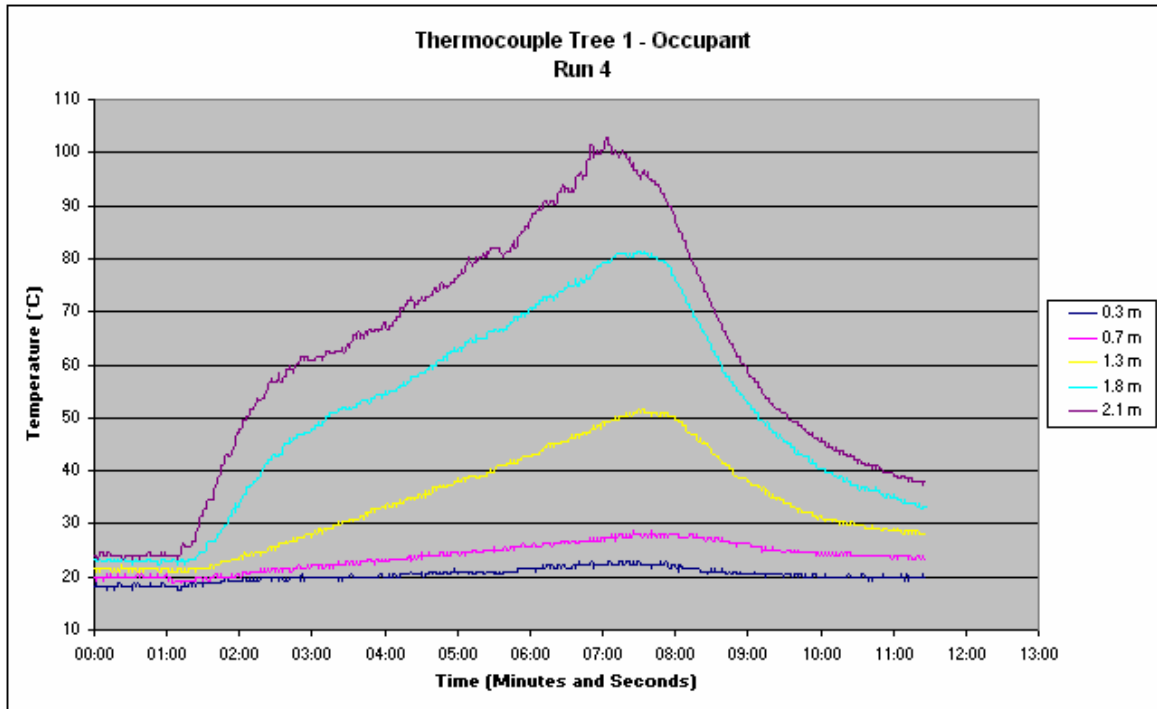


Figure 52 - Run 4: Occupant Thermocouple Tree

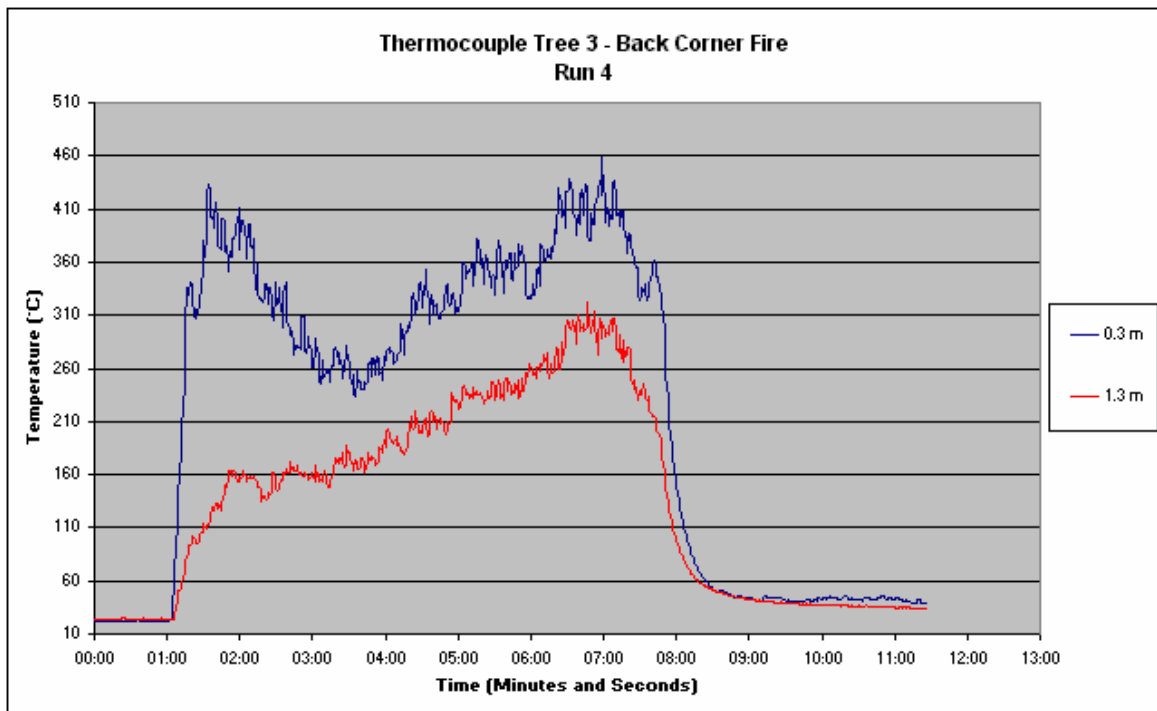


Figure 53 - Run 4: Fire Thermocouple Tree

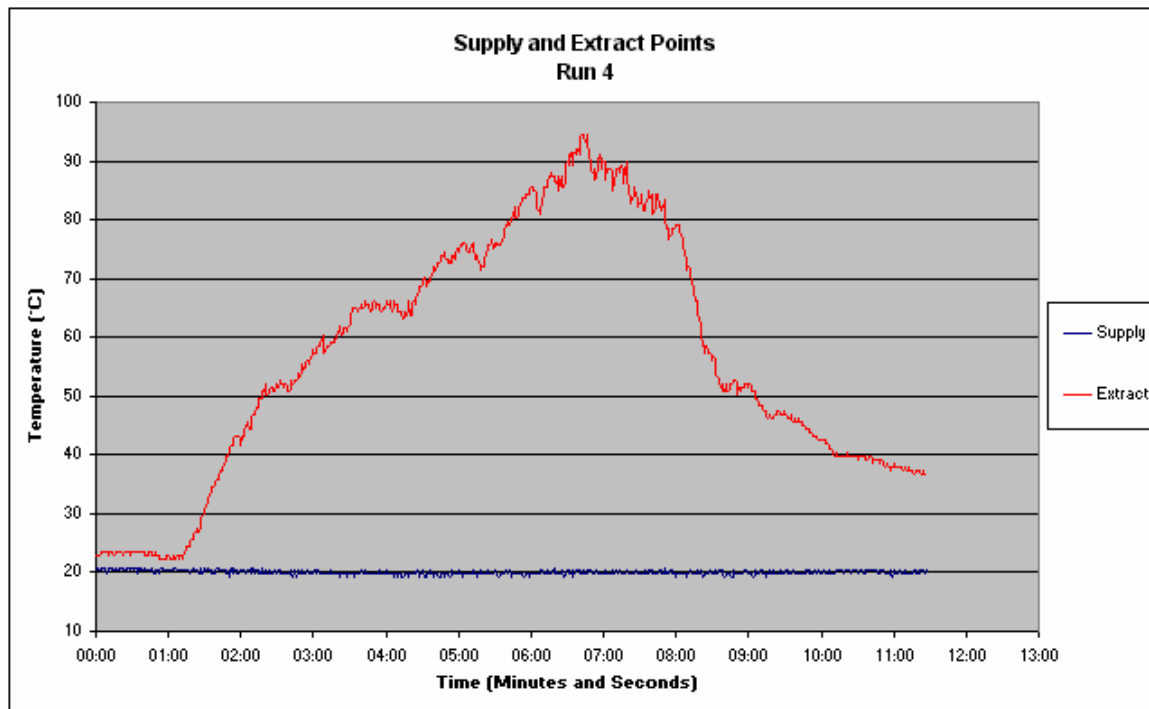


Figure 54 - Run 4: Supply and Extract Temperatures

5.11.5 Run 5: Centre Floor, Pool Fire, High Flow, With Mist

- Fire Location: Centre of compartment at ground level.
- Fire Type: Heptane pool fire.
- Airflow Characteristics: Low flow operation for 60 seconds followed by high flow operation.
- Suppression: Water mist at 60 seconds.
- Objectives: To determine the conditions within the compartment subjected to a ground level pool fire, under the operation of the displacement water mist system.
- Observations:

This run provided information of the characteristic within the compartment when a central pool fire was ignited, but the displacement water mist system was operation. As discussed in section 5.9 and section 5.10, the experiment was arranged so that the displacement water mist system was activated after two minutes (one minute after ignition).

On ignition the fire began to burn similarly to the normal operation tests with a slight slope away from the supply diffuser, but in a relatively stable manner. A smoke layer began to form in the compartment and drop.

At two minutes the system was set to fire mode with the airflow increased and water mist nozzles activated. The effect on the pool fire was immediate with the flame being pushed away from the supply diffuser. The flame also initially appeared to flare-up as the increased airflow and high velocity water mist hit it. After a second the intensity appeared to decrease from what had been occurring during normal operation but the flame became less stable and vigorous. The flame continued to effectively burn at a 30° angle from the floor throughout the test run and with the same vigorous nature.

On instigation of the displacement water mist system the volume of smoke exiting from the roof exhaust increased dramatically. Within the compartment it was observed that the water mist moved across the floor, hit the back wall, and moved up and across the roof. This was the same result as had occurred during the trial runs and was an undesirable effect. As the system was activated the upper layer first rapidly decreased in depth, before increasing slightly as the water mist flow entered from the back wall of the compartment. This then stabilised during the test and the upper layer appeared to thin out.

On initiation it could also be seen that the upper layer near the water mist nozzles was drawn, to some extent, into the water mist flow forcing it into the lower layer. Effectively a slight circulation effect appeared to be occurring within the compartment. During the test though, the lower layer appeared to remain relatively clear except for water mist.

The build-up of water mist within the compartment could be seen very clearly with the computer and lights becoming obscured. At approximately two minutes a noticeable build-up of water formed on the observation windows. At no time during the test did the RCD protection on the lights and computer activate and all of the loads continued to operate through out the test and also after the test was complete.

When the fire burnt out and the water mist was stopped, the compartment cleared very quickly of all remaining suspended particles.

Within the compartment the build-up of water on the ground was minimal and ranged from 0 mm to 3 mm deep in parts. A char mark could be observed directly behind the pool fire pan, where the flame had been pushed over.

The thermocouple results from this test show that a similar rapid effect occurred with the temperatures within the compartment. Figure 55 shows the temperatures taken at Tree 1. The point of system initiation is accompanied by a rapid drop in temperatures throughout the compartment. While it was observed that some level of mixing occurred between the upper and lower layer, an observation backed up by the rapid increase in temperature of the 0.3m sensor, Figure 55 clearly shows that there was a noticeable temperature difference between the top and bottom of the compartment suggesting that some form of stratification was still occurring.

Figure 56 gives the temperatures taken directly above the Fire. This graph shows a large drop in temperature. This is primarily due to the vigorous nature of the water mist jets disrupting the fire plume and tending to push the heat generated away from the thermocouple tree.

The exhaust air temperature shown in Figure 57 displays the same effect whereby the temperature exiting the compartment decreases rapidly after initiation of the system. In this case the decrease occurs just slightly after the decrease recorded within the compartment as it would have taken a longer time for the water mist to mix and cool the upper layer. What is interesting to notice in this graph is that the supply air temperature taken directly behind the supply air diffuser increases slightly after the displacement water mist system is set into fire mode. This is most likely due to the air temperature control system being over whelmed by the increased flow and not being able to provide the necessary cooling to the outside air.

In regard to life safety within the compartment, the temperatures are all below 34°C and as such clearly pose no threat to occupants. The actual air quality is somewhat less obvious but is investigated and discussed further in run 17.

Graphical Data:

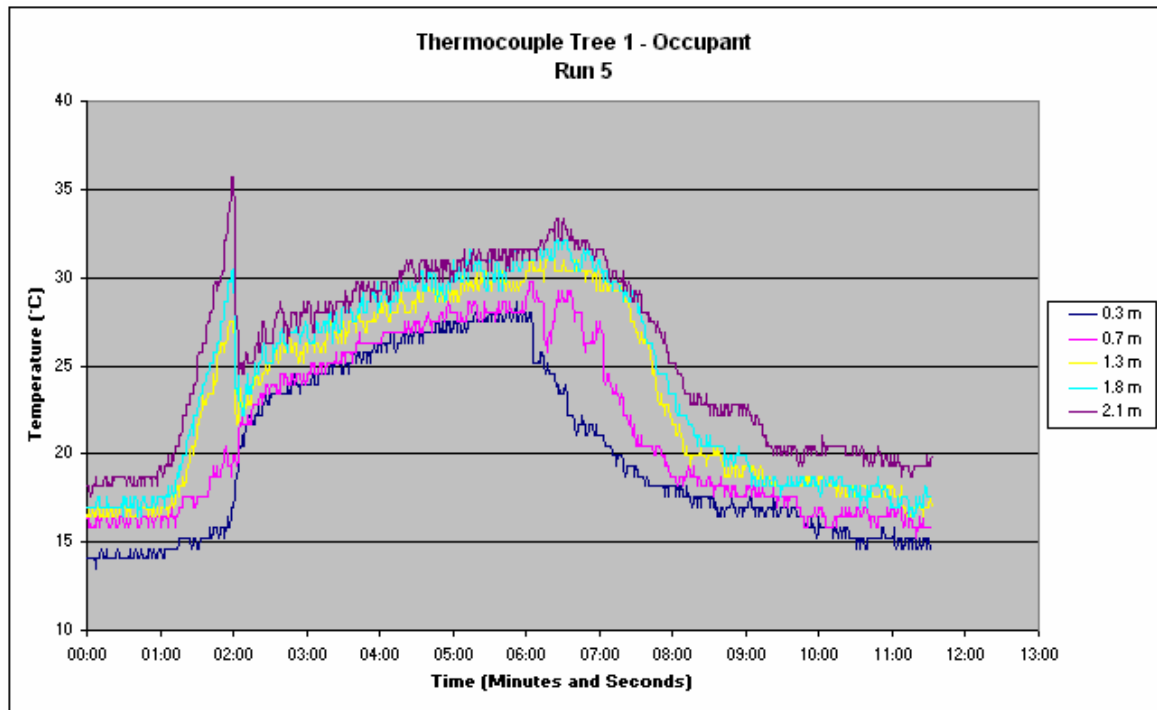


Figure 55 - Run 5: Occupant Thermocouple Tree

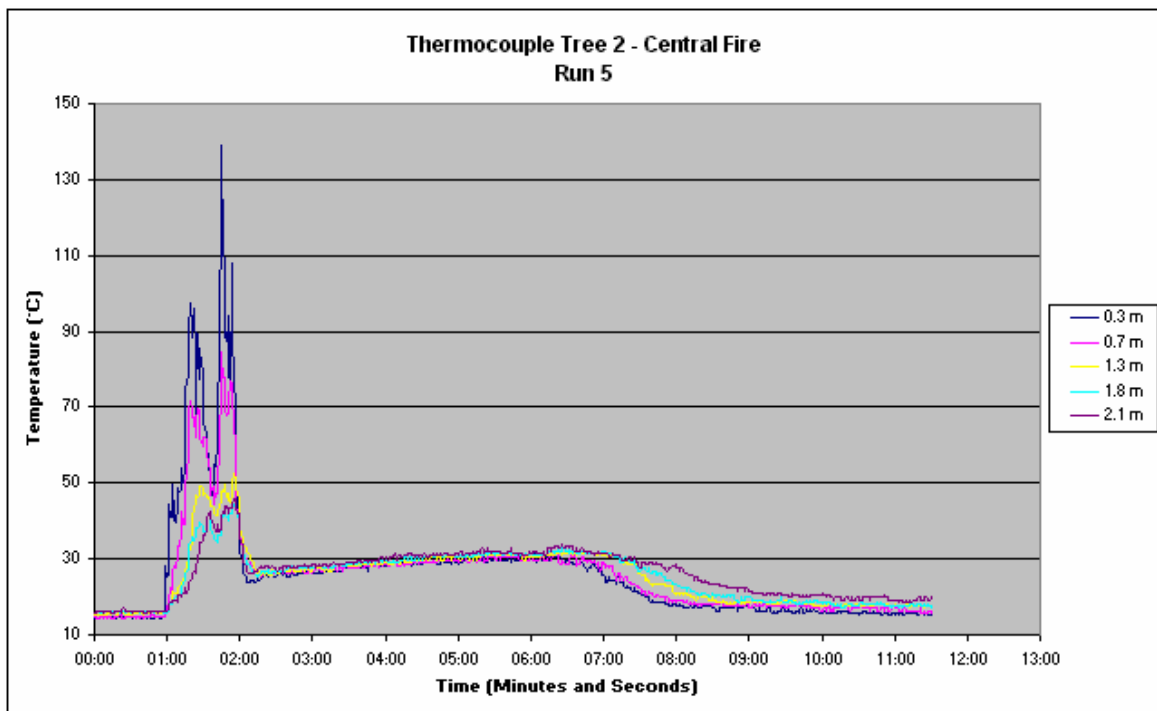


Figure 56 - Run 5: Fire Thermocouple Tree

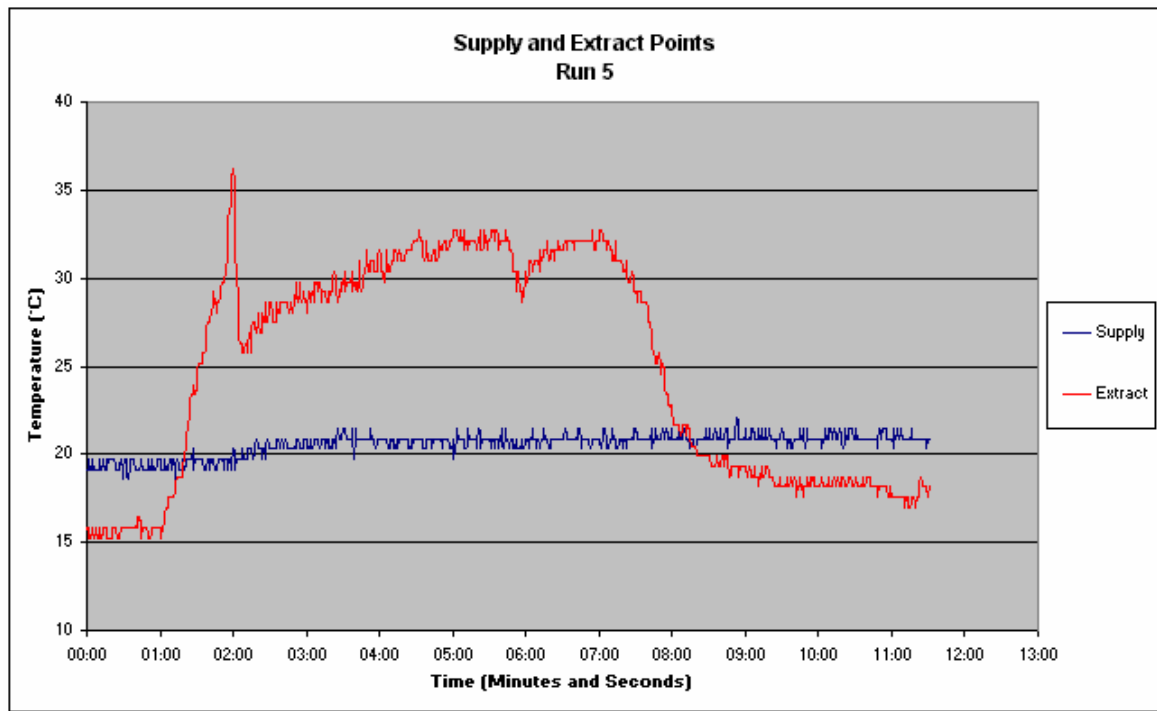


Figure 57 -Run 5: Supply and Extract Temperatures

5.11.6 Run 6: Centre High, Pool Fire, High Flow, With Mist

Fire Location: Centre of compartment at 1 metre.

Fire Type: Heptane pool fire.

Airflow Characteristics: Low flow operation for 60 seconds followed by high flow operation.

Suppression: Water mist at 60 seconds.

Objectives: To determine the conditions within the compartment subjected to a 1m pool fire, under the operation of the displacement water mist system.

Observations:

This run was similar in nature to run 5, but with the pool fire located at a height of 1m.

At the initiation of this fire the flame burnt in a stable manner and was not affected by the supply air as seen in run 3. Once the displacement water mist system was set to fire mode and initiated the same flow characteristics that were observed in

run 5 occurred. The effect of the fire was different though, in that the water mist could be seen to affect the flame in a relatively slow manner from the back of the compartment. This forced the flame to be pushed towards the supply air diffuser.

Initially the flame appeared to be significantly reduced by the presence of the water mist, but after approximately 10 seconds showed signs of increasing again slightly. During this time the flame began to burn in a more disrupted form, possibly due to the water mist expansion that was occurring within the flame front. The airflow during this run did not appear to effect the flame as had been seen in run 1, but the location of the fire resulted in the density of water mist being observably lower. This may have been due to the circulation effect that the water mist nozzles created, causing less water to be present in the centre of the compartment.

On activation of the system, the upper layer initially decreased in depth before increasing slightly, stabilising and thinning out. The lower layer appeared slightly clearer than that seen in run 5.

Again the RCD did not trip and the electrical loads within the compartment continued to operate throughout the run and after.

Figure 58, Figure 59 and Figure 60 show the temperatures within the compartment at Tree 1, above the fire at Tree 2 and at the exhaust and supply points. As can be seen in Figure 58 the temperatures throughout the compartment rapidly decreases after initiation of the displacement water mist system and remain relatively constant until four minutes when the upper layer temperatures begin to increase. This phenomenon occurs on all of the graphs and in particular can be seen in Figure 60 where the exhaust temperature dramatically increases to 90°C, which is well above that recorded at any of the other temperature sensors. This was due to the water mist being shut off early and not being restarted until 5 minutes. One point to note from Figure 59 is that the temperatures remain high during the fire indicating that the flame and plume remained relatively vertical above the fire. This corroborates the events that were observed within the compartment.

Again the temperatures, other than during the spike, remained low within the compartment and would not have posed a danger to occupants.

Graphical Data:

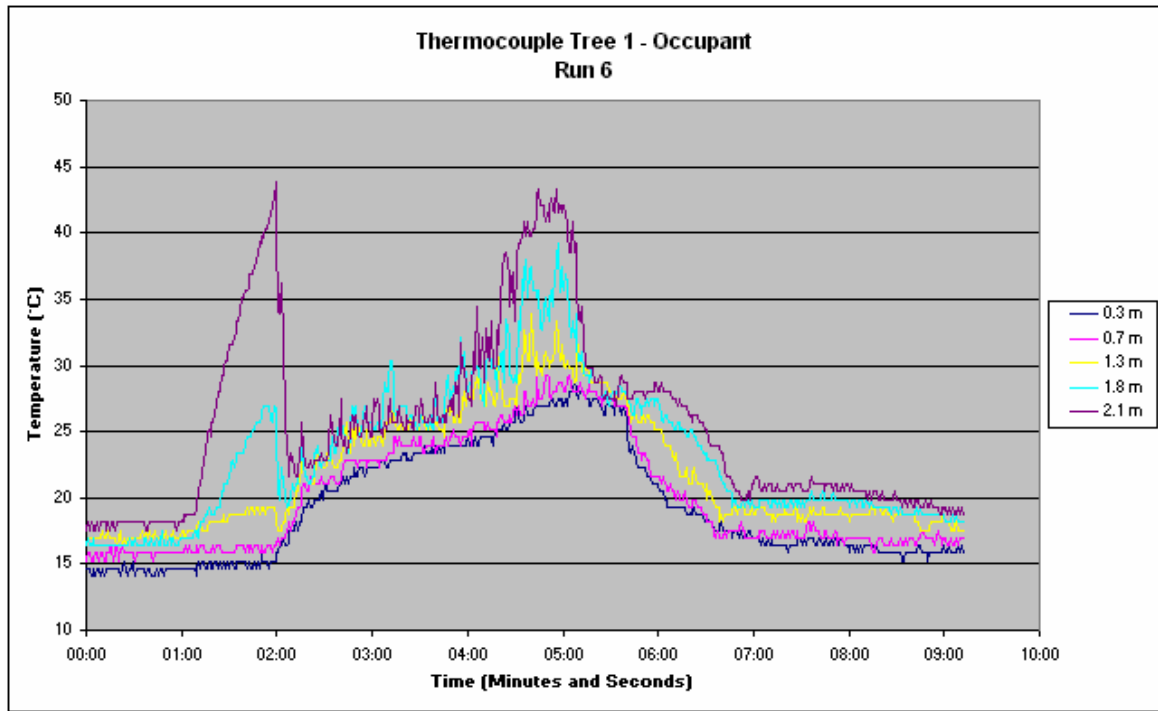


Figure 58 - Run 6: Occupant Thermocouple Tree

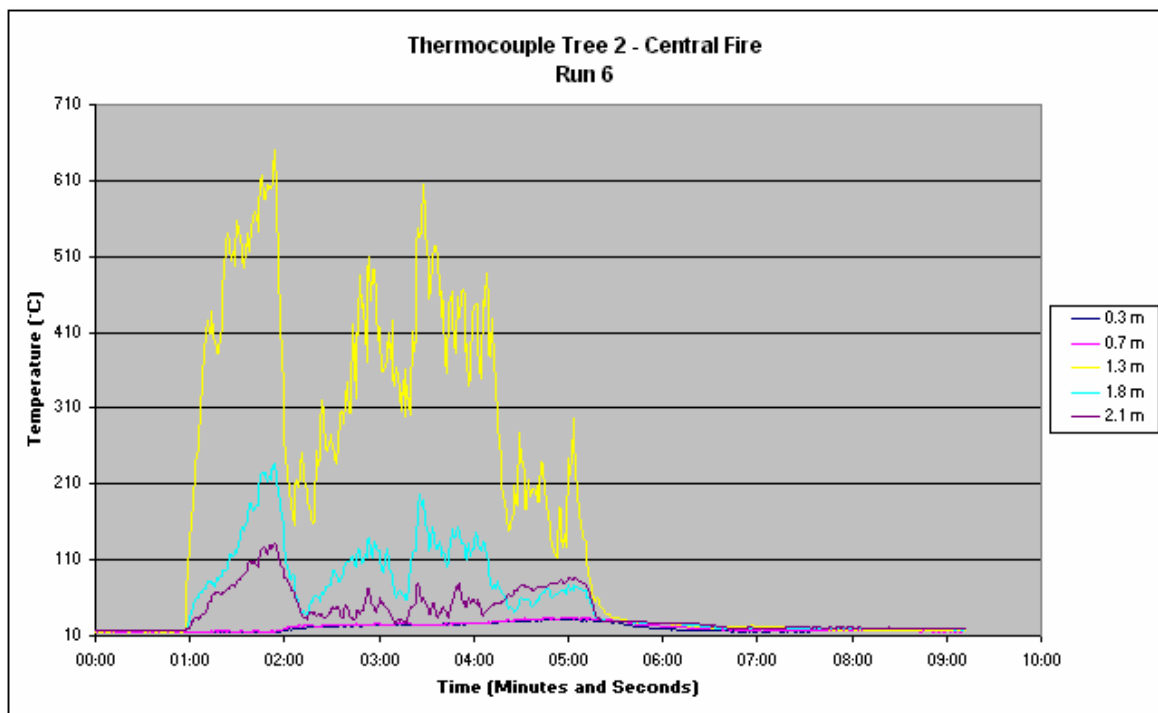


Figure 59 - Run 6: Fire Thermocouple Tree

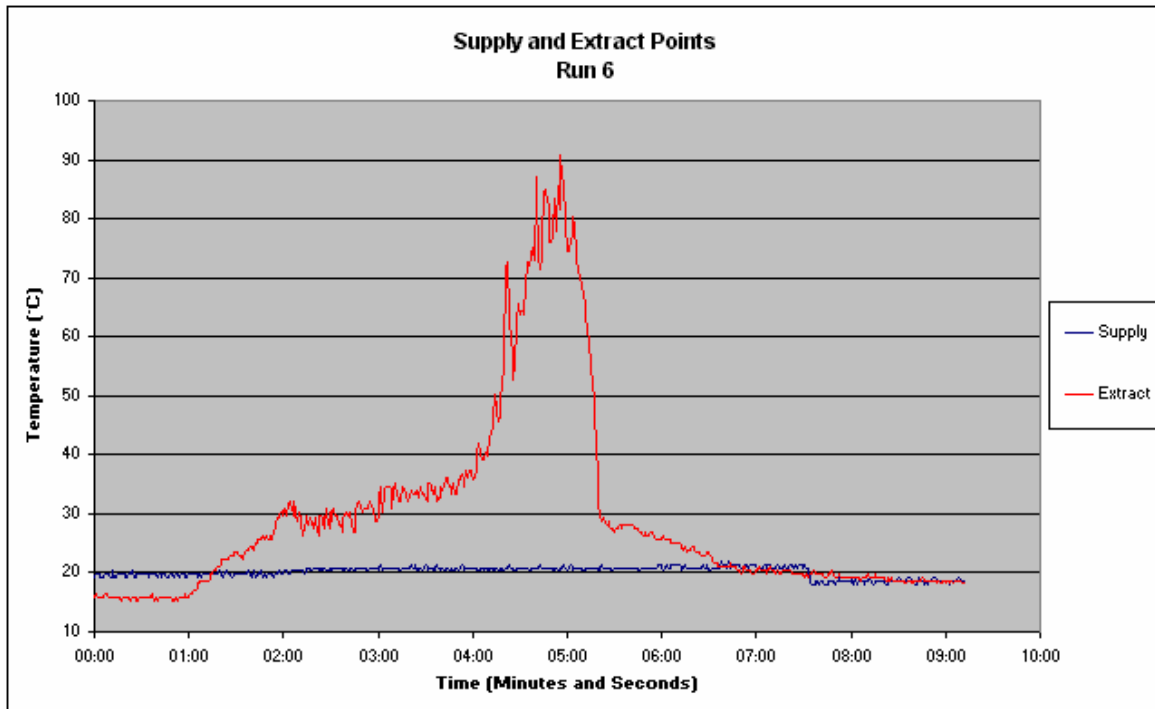


Figure 60 - Run 6: Supply and Extract Temperatures

5.11.7 Run 7: Back Floor, Pool Fire, High Flow, With Mist

<u>Fire Location:</u>	Back corner of compartment at ground level.
<u>Fire Type:</u>	Heptane pool fire.
<u>Airflow Characteristics:</u>	Low flow operation for 60 seconds followed by high flow operation.
<u>Suppression:</u>	Water mist at 60 seconds.
<u>Objectives:</u>	To determine the conditions within the compartment subjected to a ground level, back corner, pool fire under the operation of the displacement water mist system.

Observations:

As had occurred in the normal operation mode, the fire burnt up the corner of the wall and began to create a smoke layer.

On activation of the system into fire mode, the water mist could be seen to spread across the floor and hit the fire. As it hit, the fire appeared to increase in size

momentarily. It then decreased in size and burn in a turbulent manner. It continued to burn in this state for the remainder of the run. Within the compartment the smoke layer decreased in depth before increasing with the addition of the airflow generated by the water mist, finally stabilising after a short time.

It was observed during this test that after 1 minute the computer and light bulbs became hard to see. After 3 minutes water drops began to form on the windows of the compartment. The water mist was stopped after six minutes to reduce the water build-up within the compartment.

The RCD did not trip and the electrical loads within the compartment continued to operate throughout the run and after.

Figure 61 shows the temperatures recorded at Tree 1. At two minutes when the system was put into fire mode the temperature within the compartment dropped dramatically. An interesting point to observe in this run is that the lower level sensors actually recorded a decrease in compartment temperature from the set point of 19°C. That may have been due to the water temperature was approximately 12°C, resulting in cooling of the air and possibly of the sensors through direct contact. The point at which the water mist being shut off can be seen by an increase in the temperatures recorded in the upper levels, and a decrease in temperature at the lower levels. This indicates that with the water mist nozzles shut off, less mixing occurs within the compartment and stratification quickly returns.

Figure 62 shows the temperatures recorded above the corner fire. In this case, on activation of the system the sensor at 1.3m above the fire shows the temperature dropped rapidly as occurred in the rest of the compartment. The sensor just above the fire at 0.3m however did not show an appreciable decrease but became very unstable indicating the extremely turbulent nature of the flame.

The final graph of the supply and exhaust temperatures shown in Figure 63, again displays the rapid decrease in temperature on activation of the system. As the fire continues to burn the exhaust temperature increases. This may be due to heat

build-up within the compartment as not all of the hot combustion gases are exhausted.

Overall the temperatures within the compartment remained at a safe level for occupants.

Graphical Data:

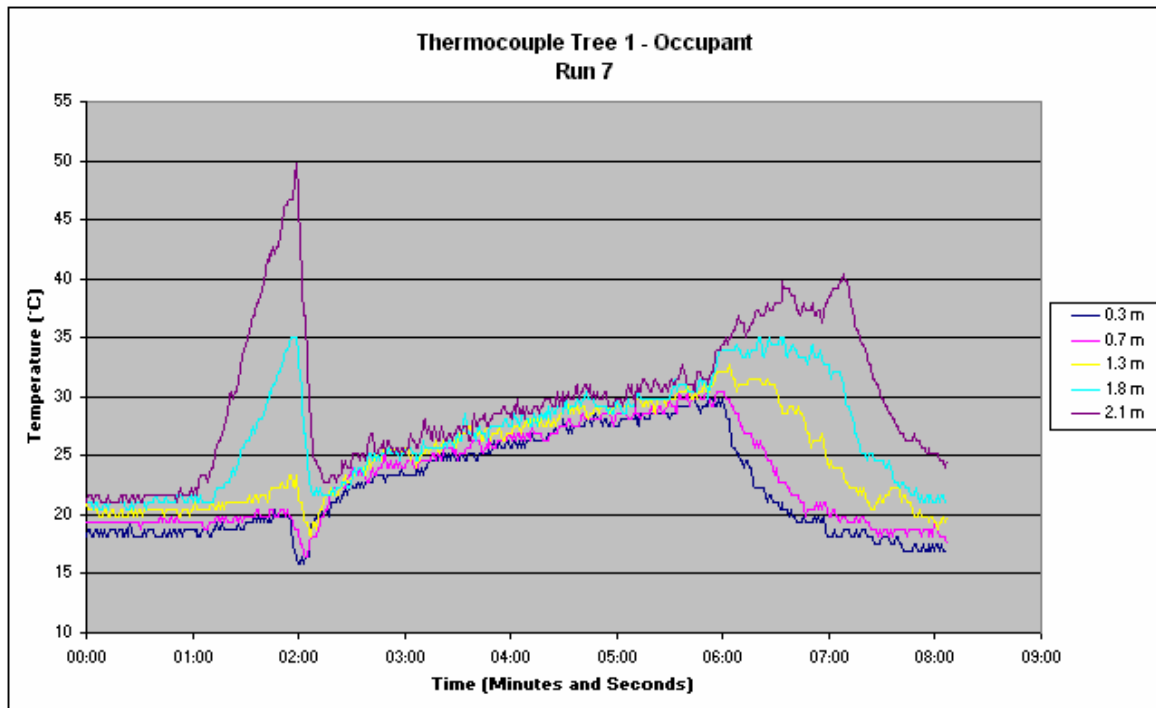


Figure 61 - Run 7: Occupant Thermocouple Tree

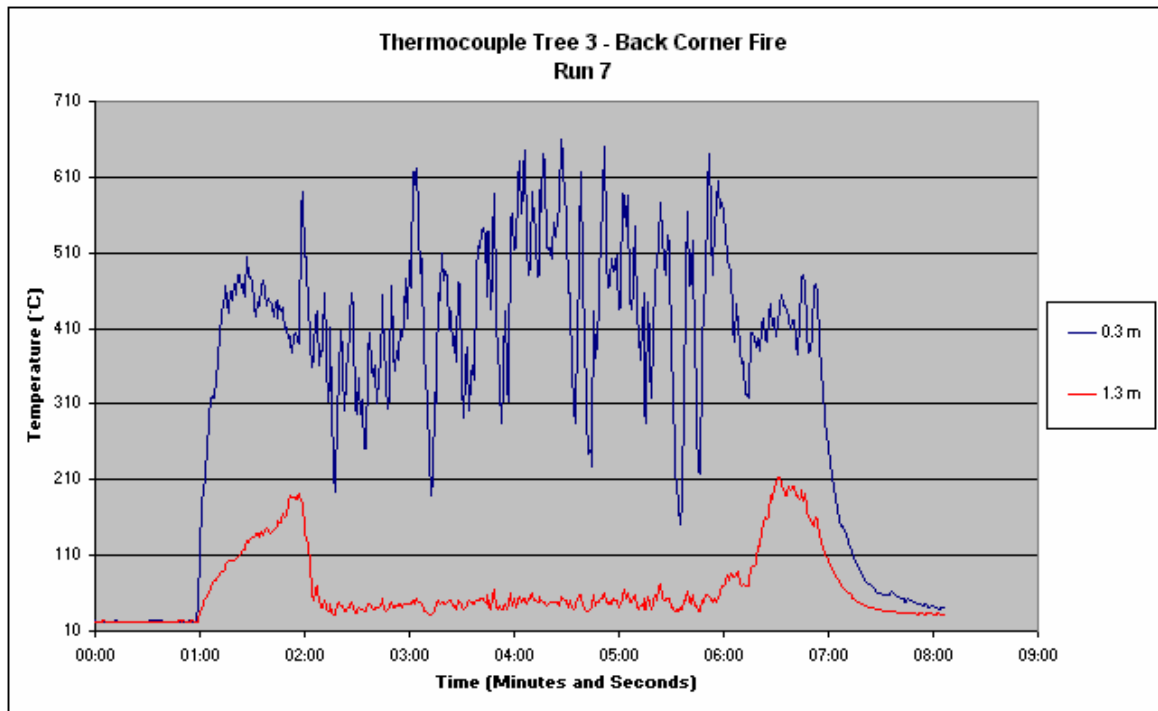


Figure 62 - Run 7: Fire Thermocouple Tree

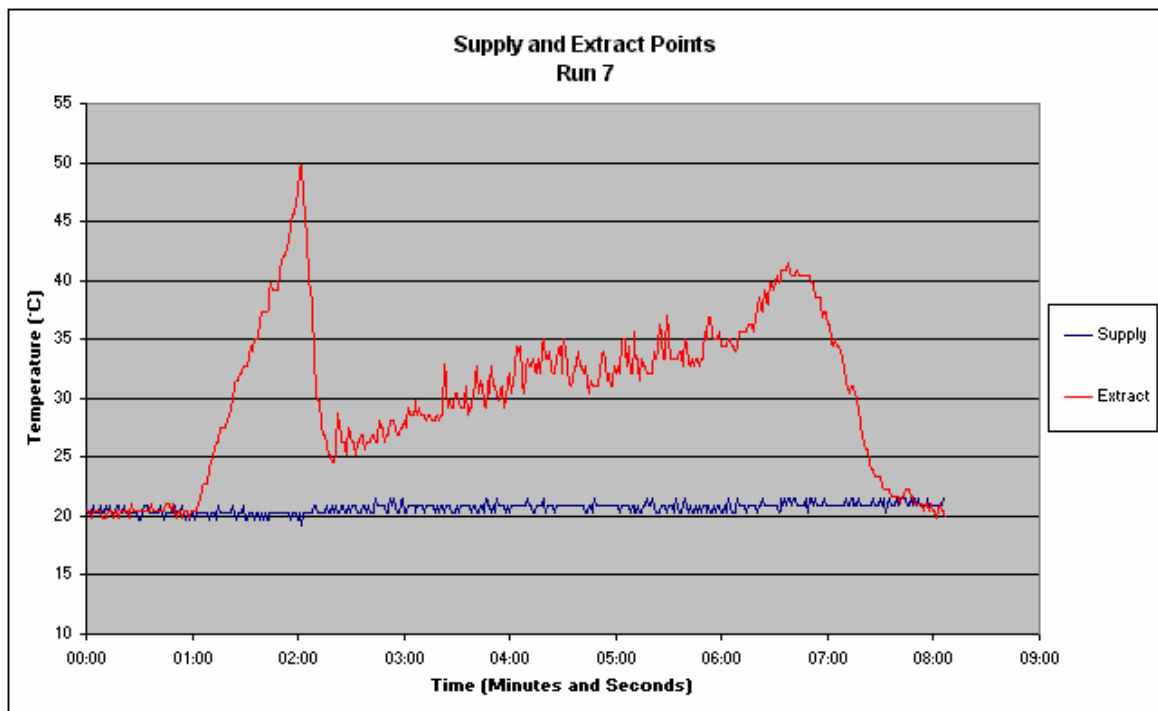


Figure 63 - Run 7: Supply and Extract Temperatures

5.11.8 Run 8: Front Floor, Pool Fire, High Flow, With Mist

<u>Fire Location:</u>	Front corner of compartment at ground level.
<u>Fire Type:</u>	Heptane pool fire.
<u>Airflow Characteristics:</u>	Low flow operation for 60 seconds followed by high flow operation.
<u>Suppression:</u>	Water mist at 60 seconds.
<u>Objectives:</u>	To determine the conditions within the compartment subjected to a ground level, front corner pool fire under the operation of the displacement water mist system.

Observations:

While a specific base case with no suppression was run for this fire arrangement, this test was intended to provide comparison with the back corner test to assess the effect location had on the compartment characteristics.

On ignition the fire appeared to burn in a similar manner to that of the back corner pool fire. When the system was set into fire mode the flame immediately came away from the wall and curved towards the water mist nozzles. It appeared that the entrainment created by the nozzle operation drew air past the fire causing it to become more turbulent and be drawn toward the nozzles.

The water mist itself, moved across the floor as usual, hitting the back wall and moving up. It then circulated through the compartment until coming into contact with the front corner fire. As it contacted with the flame, the flame flared up before appearing to decrease slightly and burn even more turbulently than it had been previously. It continued to burn in this manner until the water mist nozzles were shut off. The water mist nozzles were shut off just before seven minutes to avoid excess wetting of the compartment. At this time the flame reverted back to a more stable form, burning into the corner.

Within the compartment the smoke layer decreased in depth before increasing with the water mist addition and then stabilising. It was also observed at the front of the compartment that the upper layer was partially drawn into the water mist nozzles.

The RCD did not trip and the electrical loads within the compartment continued to operate throughout the run and after.

The data recorded from this run shows the same characteristic rapid drop in temperature when the system is set into fire mode. Figure 64 clearly shows an extremely rapid drop on the upper layer sensors and a corresponding increase in temperature in the lower sensors. After the initiation of the system, all of the temperatures within the compartment increase slightly as the heat builds up.

Figure 65 shows a decrease in the 0.3m and 1.3m sensors above the fire, as the system activates and the plume and flame are drawn away from the corner and into the water mist nozzles. The 0.3m sensor provides unstable readings as while the flame is drawn away from the sensor, the turbulent nature results in it occasionally passing over it.

Finally Figure 66 shows the extract and supply temperatures. As has previously been seen the supply temperature increases slightly on initiation of the system while the exhaust temperature decreases rapidly.

In all three graphs there is a marked increase in the temperatures and stratification when the water mist nozzles are shut off.

Again the temperatures within the compartment remain acceptable for an occupant.

Graphical Data:

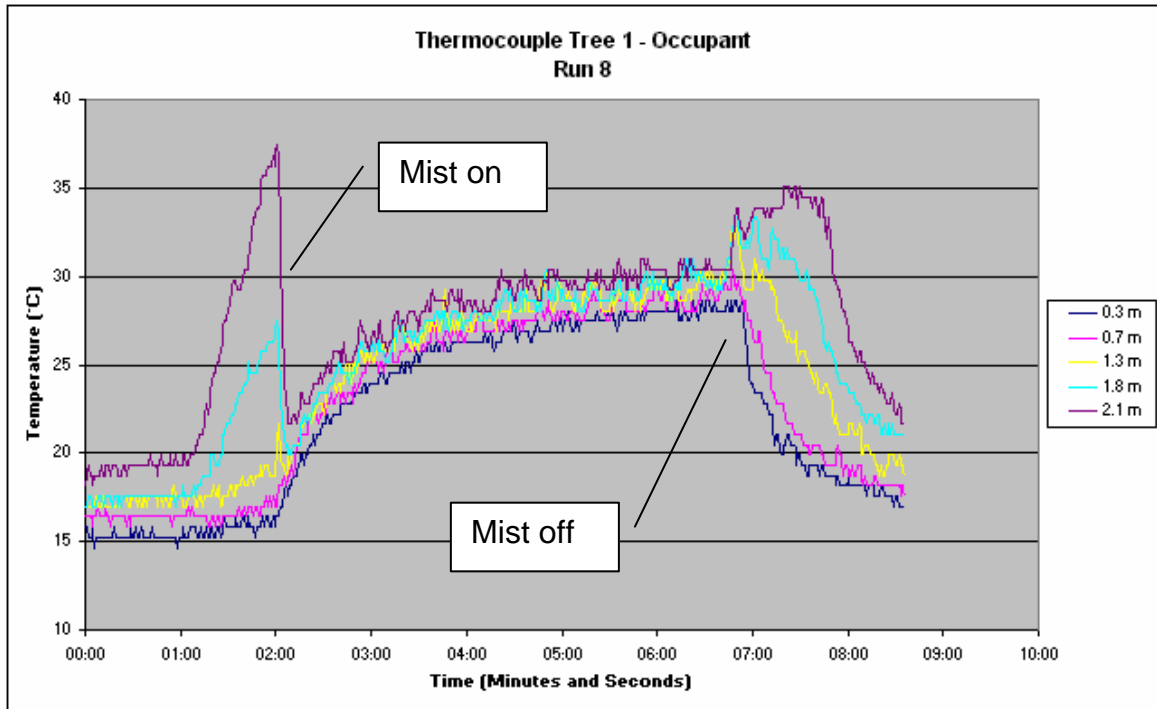


Figure 64 - Run 8: Occupant Thermocouple Tree

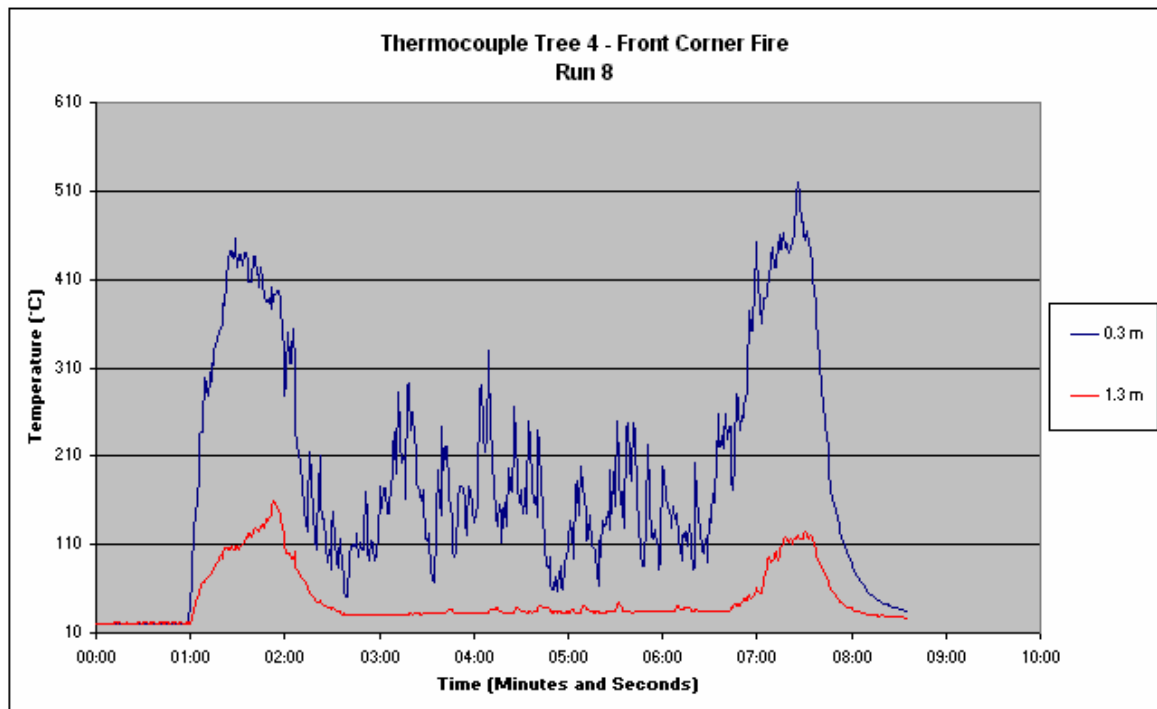


Figure 65 - Run 8: Fire Thermocouple Tree

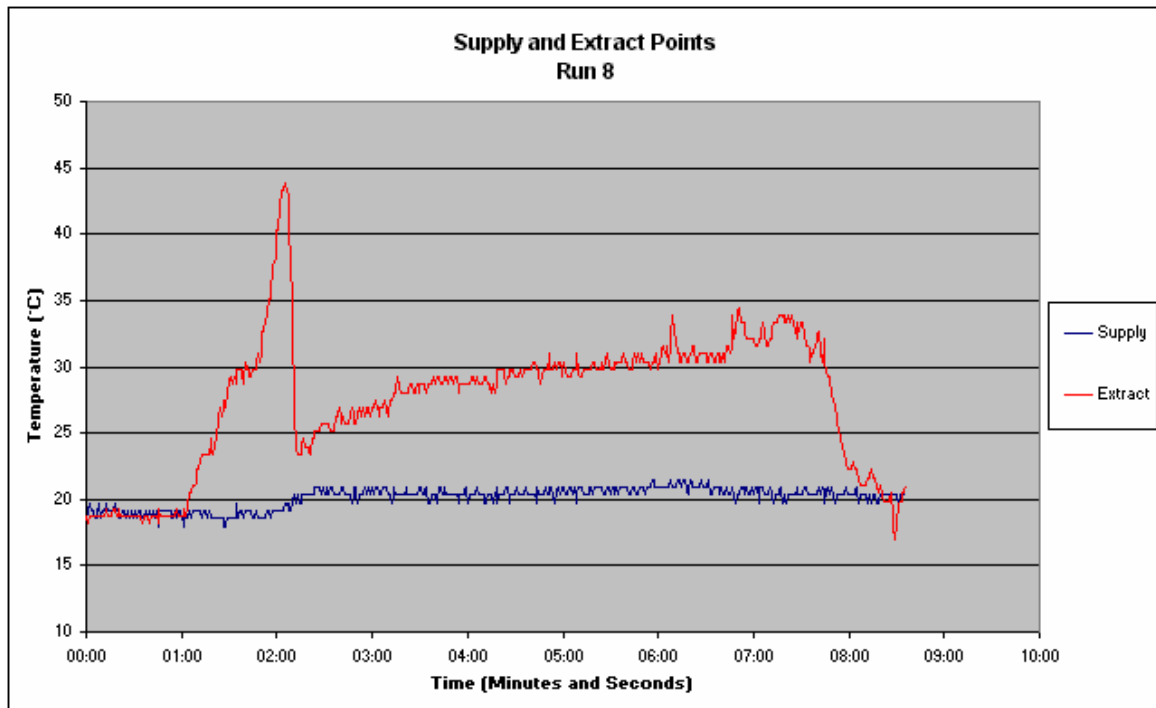


Figure 66 - Run 8: Supply and Extract Temperatures

5.11.9 Run 9: Centre Floor, Pool Fire, Low Flow, With Mist

<u>Fire Location:</u>	Centre of compartment at ground level.
<u>Fire Type:</u>	Heptane pool fire.
<u>Airflow Characteristics:</u>	Constant low flow operation.
<u>Suppression:</u>	Water mist at 60 seconds.
<u>Objectives:</u>	To determine the conditions within the compartment subjected to a pool fire under normal low flow conditions but with water mist injection.

Observations:

The objective of this run was to see the effects on the compartment if the airflow was not increased and only the water mist nozzles were activated.

Once burning the fire began to form a smoke layer in the same way that occurred under the normal conditions. When the water mist nozzles were activated fire burnt in a similar manner to that of run 5, with the fire laying over at an angle of

approximately 30° and burning turbulently. It continued to burn in this manner until the water mist nozzles were shut off after 6 minutes 30.

The main observation of this test run was that there was no increase in the volume of smoke venting from the exhaust duct during the test. Within the compartment a circulation and mixing effect appeared to take place with the upper layer mixing with the lower layer. The appearance of the compartment suggested that the interior of the compartment was simply being circulated.

This circulation and lack of exhausting from the compartment resulted in an increase in both the density of combustion products, water mist and obscuration levels. After approximately 2 minutes of testing the RCD protection on the light bulbs and computer tripped indicating that there was sufficient water present to create a short circuit.

At the completion of the experiment when the fire had burnt out and the water mist nozzles shut off, the compartment took a long time to become clear, with the airflow needing to be turned up to clear the compartment.

The data recorded from this test run also supports the observed occurrence of mixing within the compartment. The results taken from Tree 1 and shown in Figure 67 show a rapid decrease in upper layer temperature and corresponding increase in lower layer temperatures. These values all converge to within 3°C of each other. The temperature within the compartment continues to increase as the fire supplies additional heat to the environment.

Figure 68 of the temperatures directly above the fire, show the same characteristic decrease in temperatures. In this case though, the temperatures would be expected to stay somewhat elevated as the flame continued to burn. They decrease though due to the flame and plume being pushed away by the water mist toward the back of the compartment. An interesting point to note from this test is that the initial temperatures taken above the fire are not in the 400°C range that had been recorded in other tests. This is most likely due to the pan not being placed directly under the sensors. With the flame being pushed slightly away from the supply diffuser, the sensors would only have been exposed to the outer region of the plume rather than centre line.

Figure 69 shows the supply and exhaust temperatures from the compartment. In this case the supply air temperature remains relatively constant. The exhaust air temperature shows the same effect as the previous graphs whereby the temperature drops when the water mist is activated and increases again when it is stopped.

While the temperatures within the compartment are elevated, they are still not significant enough to pose a threat to an occupant. Of more concern in this simulation is the build-up of combustion products within the compartment. It is unclear the exact levels that existed but observations made on site would suggest that the levels present would pose a threat to an occupant.

Graphical Data:

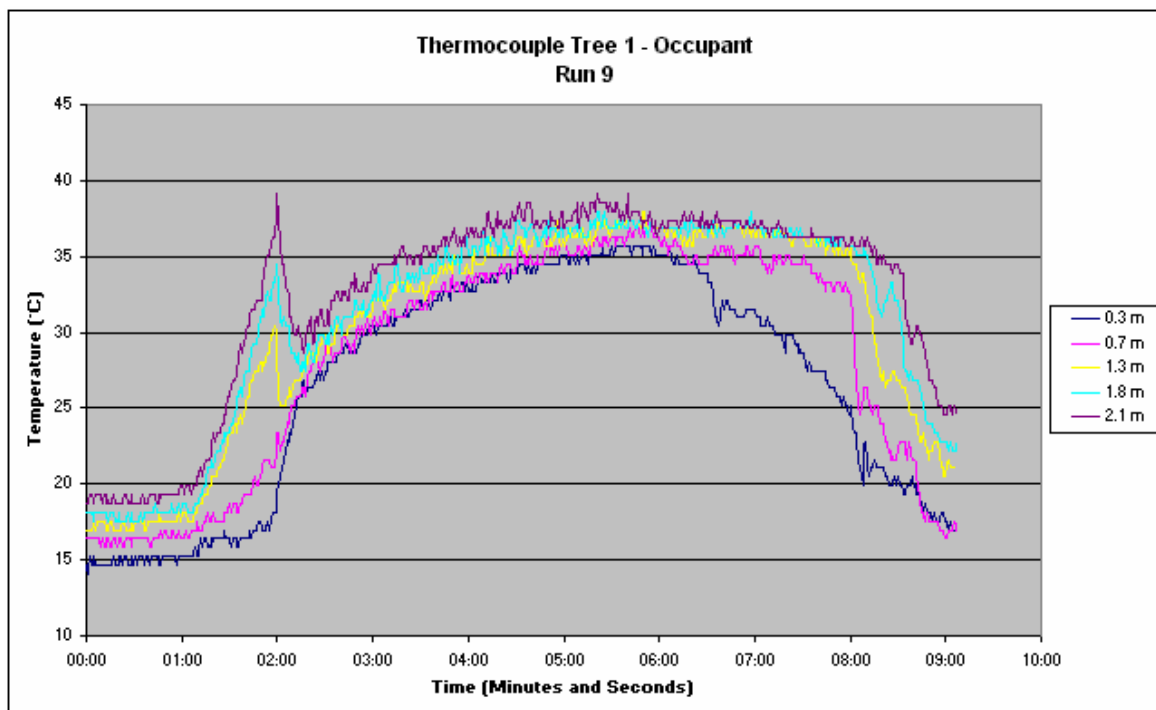


Figure 67 - Run 9: Occupant Thermocouple Tree

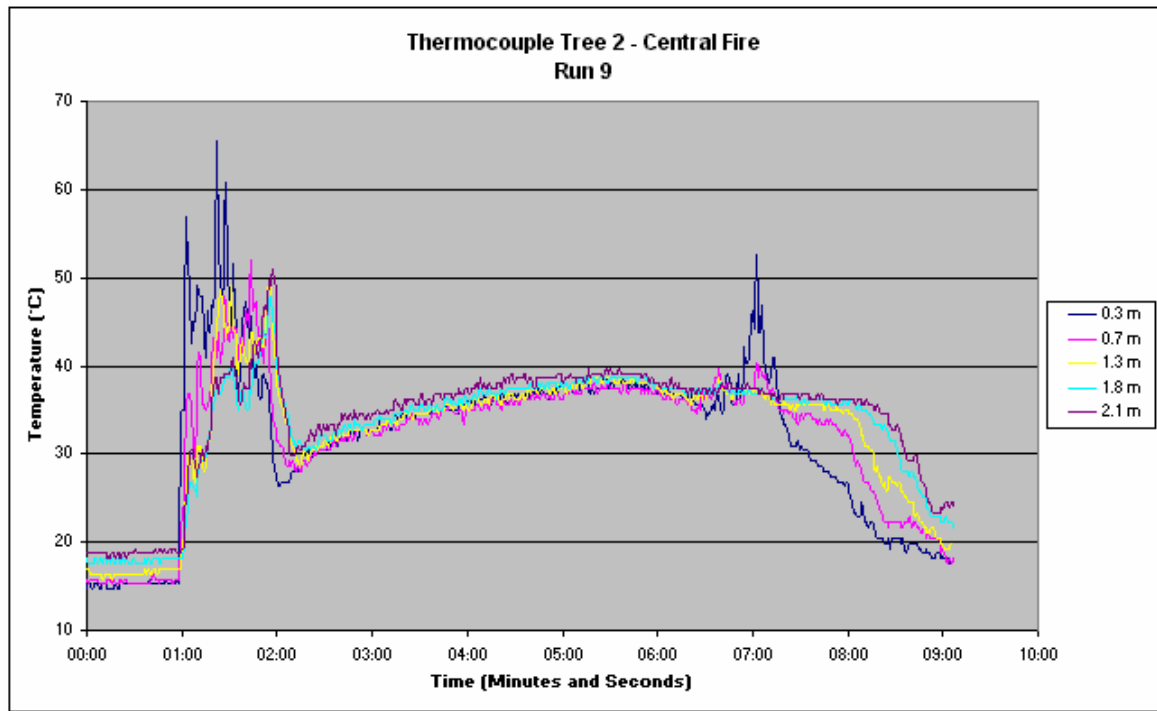


Figure 68 - Run 9: Fire Thermocouple Tree

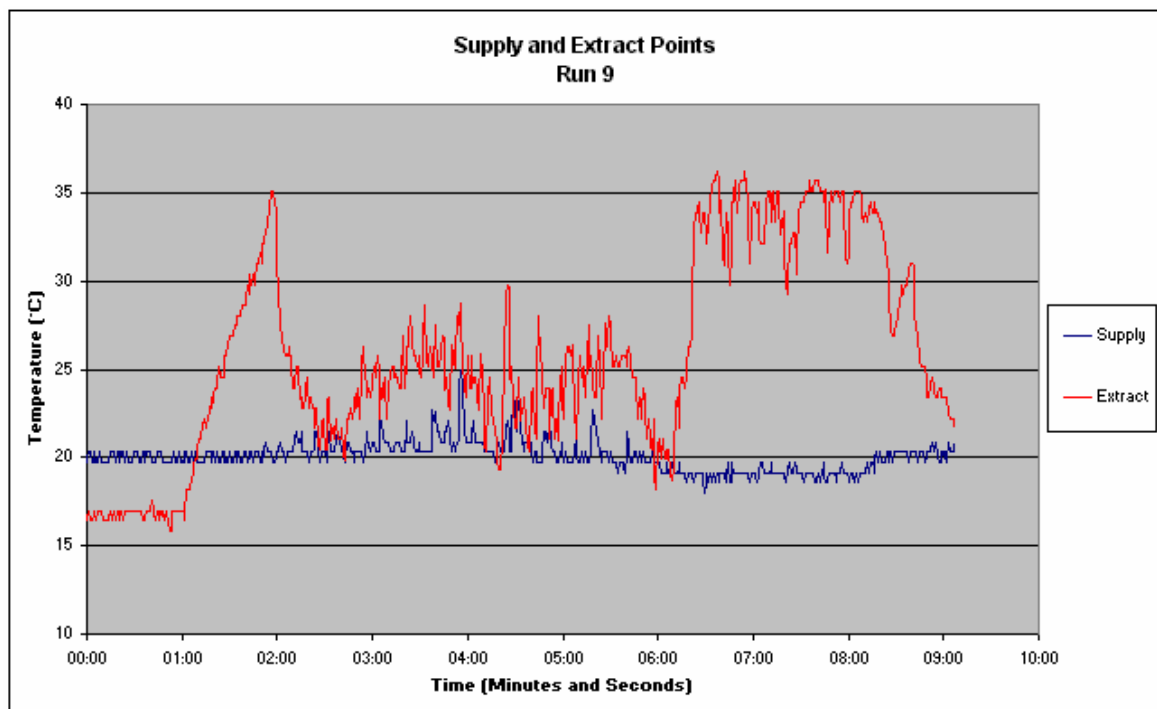


Figure 69 - Run 9: Supply and Extract Temperatures

5.11.10 Run 10: Centre Floor, Crib Fire, Low Flow, No Mist

<u>Fire Location:</u>	Centre of compartment at ground level
<u>Fire Type:</u>	Wood crib fire.
<u>Airflow Characteristics:</u>	Constant low flow operation
<u>Suppression:</u>	None
<u>Objectives:</u>	To determine the conditions within the compartment subjected to a cellulose based fire under normal operating conditions with no suppression and normal flow.

Observations:

As with the initial pool fire test runs, this run was designed to provide a measure of the compartment environment that could be expected under normal operation conditions.

The main problem encountered with the crib fire test was the length of time taken for the fire to take hold. After ignition the fire in the crib did not begin to grow until after two minutes. At this time the flames began to move up the side of the crib and the fire became larger.

As had been in the pool fires the flames that developed tended to slope away from the supply air diffuser as the airflow affected the fire. While this was the case for the actual flame the smoke rising from the crib tended to rise vertically. This appeared to be due to the low depth of moving air created by the displacement system.

As the fire grew the smoke production increased and an upper smoke layer formed. This layer increased in depth and density as the fire continued, until the light bulbs appeared only as a glowing source. Throughout the test the environment remained in a relatively stable form with little mixing between the upper and lower layers.

The fire continued to burn for a significant time and was finally suppressed after eleven minutes as it was about to collapse and cause possible damage to the compartment.

As can be seen in Figure 70 the temperatures within the compartment did not increase significantly until after three minutes. At this time the upper layer temperature climbed rapidly, with the lower level sensors recording a rise as the layer dropped and became denser. The maximum temperature reached at the roof of the compartment was 60 °C.

Figure 71 shows the temperatures recorded directly above the wood crib. Again the temperature can be seen to rapidly increase after three minutes, with the 0.3m sensor increasing to a peak temperature within the flame of 710 °C. The sensors above this level also recorded an increase but as they were located within the plume and not the flame the temperature increase was less significant.

Finally Figure 72 displays the temperatures recorded at the supply and exhaust grill. Again the exhaust air sensor shows the same profile as that recorded within the compartment, but has a peak temperature of 55 °C. This is 5°C below that recorded on the 2.1m sensor within the compartment and as previously discussed is most likely due to the increased radiation feedback within the compartment.

In terms of life safety, the temperatures within the compartment remain below 60°C even at the roof. This indicates that while uncomfortable, the compartment would not pose a threat to occupants in terms of temperature. In terms of combustion products it is unclear the effects on an occupant but on entering the compartment at the completion of the run, the environment was toxic and could not be occupied for any length of time.

Graphical Data:

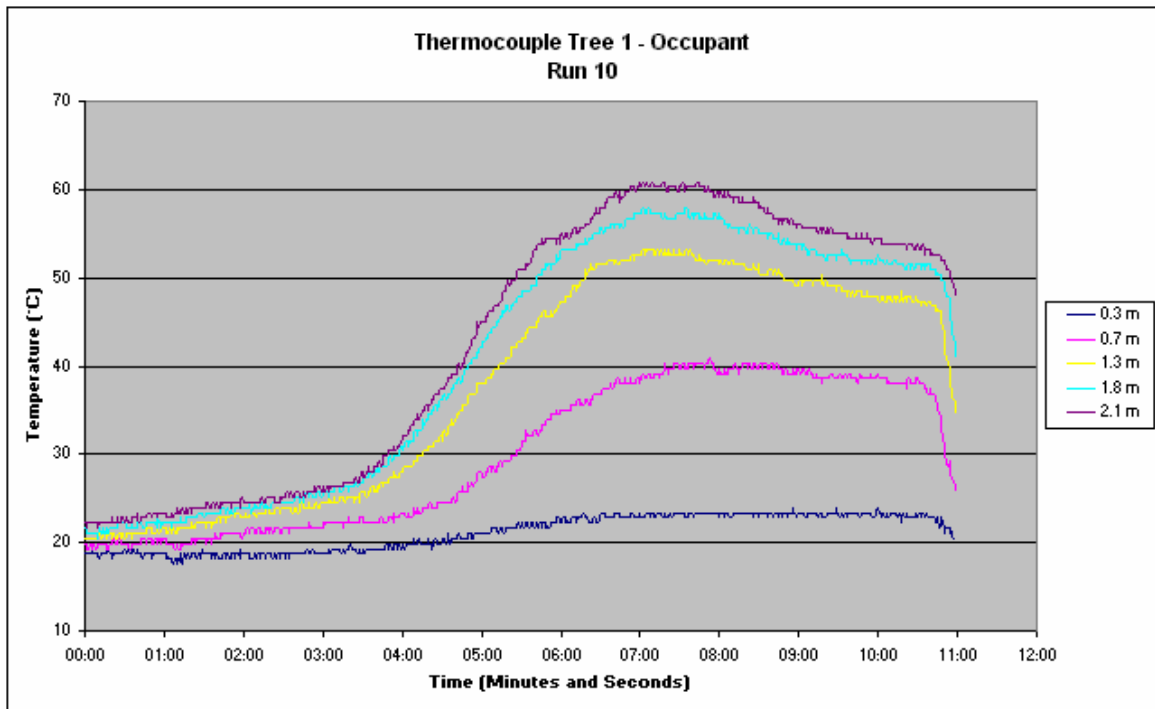


Figure 70 – Run 10: Occupant Thermocouple Tree

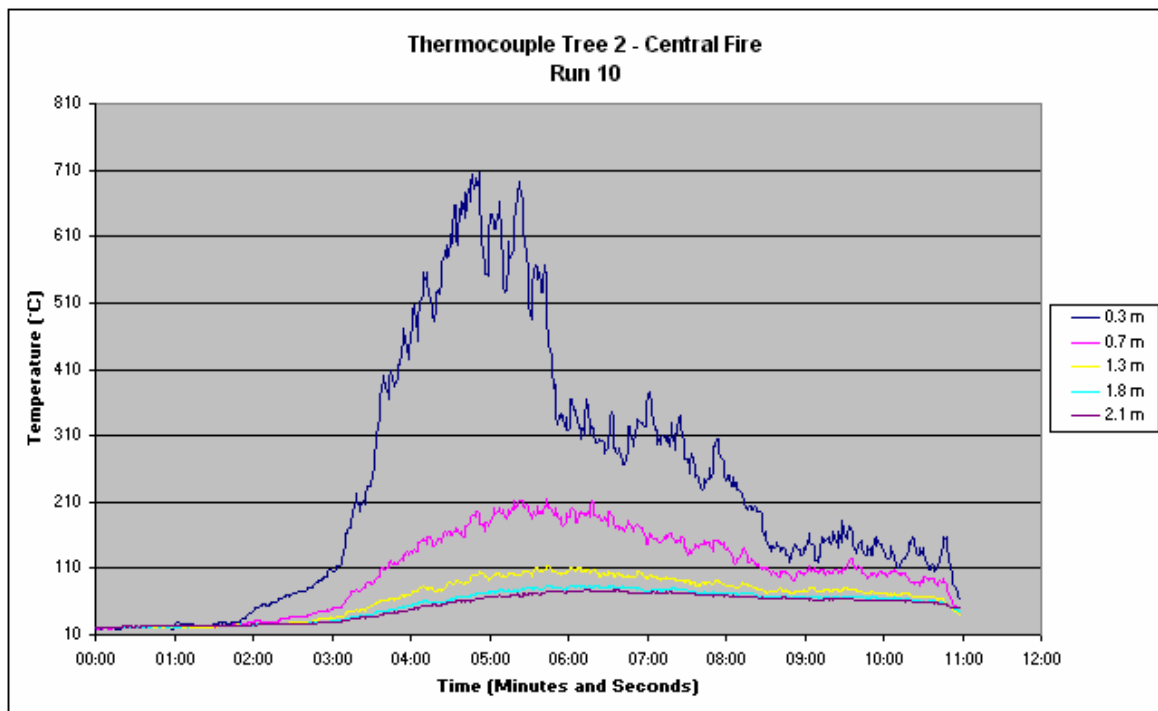


Figure 71 - Run 10: Fire Thermocouple Tree

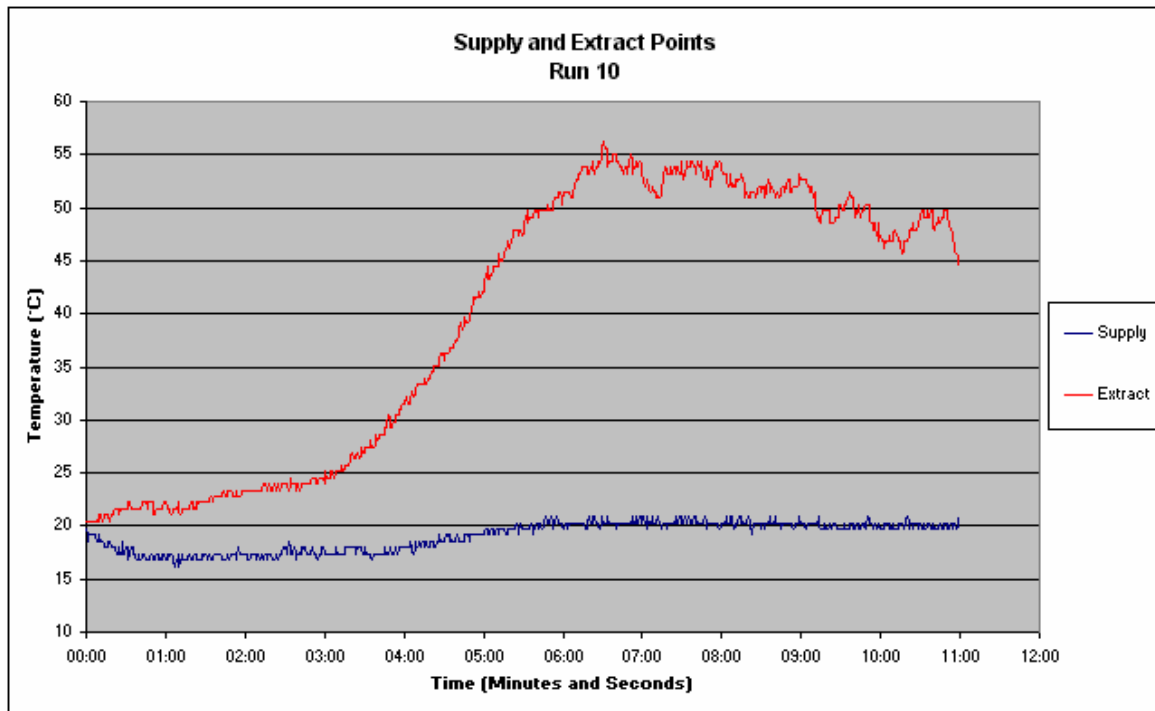


Figure 72 - Run 10: Supply and Extract Temperatures

5.11.11 Run 11: Centre Floor, Crib Fire, High Flow, With Mist

<u>Fire Location:</u>	Centre of compartment at ground level.
<u>Fire Type:</u>	Wood crib fire.
<u>Airflow Characteristics:</u>	Low flow operation for 6 minutes followed by high flow operation.
<u>Suppression:</u>	Water mist at 6 minutes.
<u>Objectives:</u>	To determine the conditions within the compartment subjected to a ground level cellulose based fire under the operation of the displacement water mist system.
<u>Observations:</u>	

As has been discussed, crib fires took a longer time to burn to what may be considered an appreciable level. As such the crib fire in this run was observed and it was decided that the fire had sufficiently developed and taken hold at seven minutes.

As previously seen the fire accelerated after an initial incipient phase. Smoke was generated at a much higher rate and an upper layer formed. In the case of this test run the fire tended to develop on the front side of the crib rather than uniformly.

On activation of the system into fire mode, the fire appeared to be extinguished on the front face of the crib but was forced through the crib behind it by the high airflow. This caused the flame to spread through the crib and effectively become more established and generally larger in size. With the increased airflow and water mist the volume of smoke that appeared to be generated was less.

Within the compartment the smoke layer initially appeared to lift, followed by stabilisation and a decrease in density as the water mist airflow combined with it.

At no time during the test did the RCD protection on the lights and computer activate and all of the loads continued to operate through out the test and after the test was complete.

Figure 73 clearly shows the effect within the compartment with the rapid decrease in upper layer temperature and increase in lower layer temperature. As the run continued the temperatures can be seen to increase to a peak at 8.5 minutes. This is most likely caused by the increased fire size created by the high velocity airflows spreading the fire and increasing the thermal output within the compartment.

Figure 74 shows an even more significant effect directly above the fire but this is primarily due to the fire being blown through the crib and the flame and plume rising on an angle away from the sensors. Once the fire mode was initiated, this sensor tree effectively provided information on the compartment conditions rather than the plume conditions.

Finally Figure 75 shows the supply and exhaust temperatures from the compartment. The same effect that is seen in Figure 73 is seen here with a sudden decrease in temperature followed by a slight increase and peak.

Once activated the temperatures within the compartment remained below 25 °C, indicating it posed no threat to life safety. Additionally as the majority of smoke appeared to be ventilated from the compartment, the air may have remained breathable. This is discussed further in run 17.

Graphical Data:

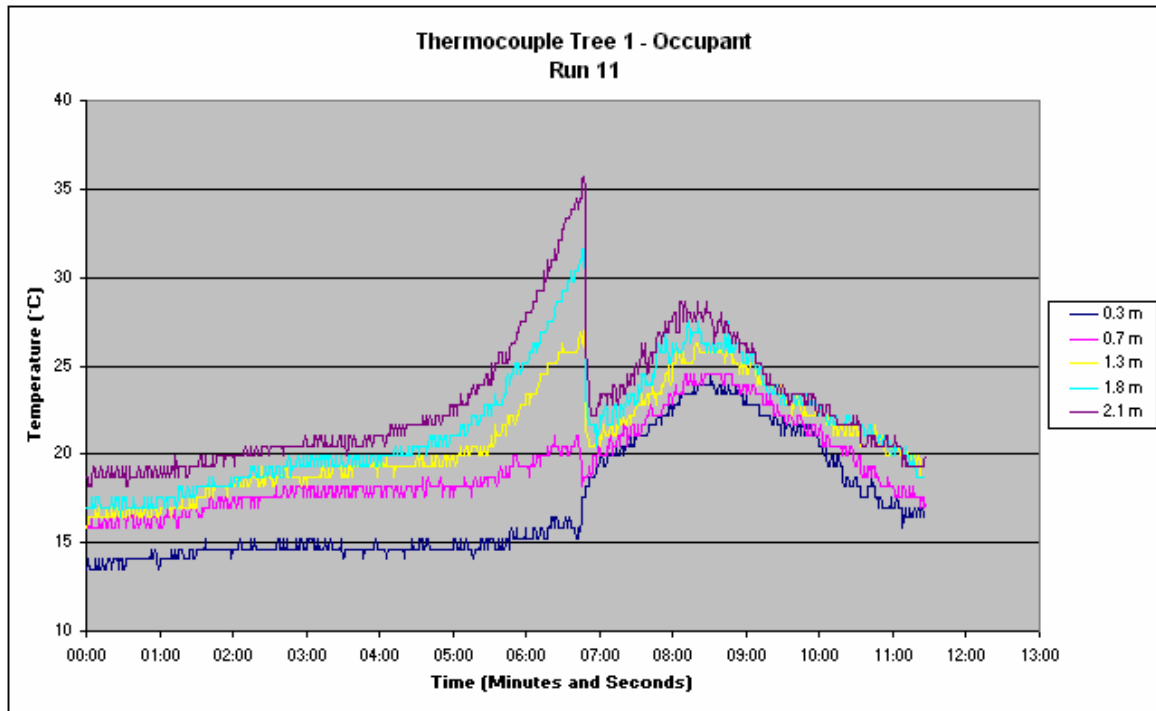


Figure 73 - Run 11: Occupant Thermocouple Tree

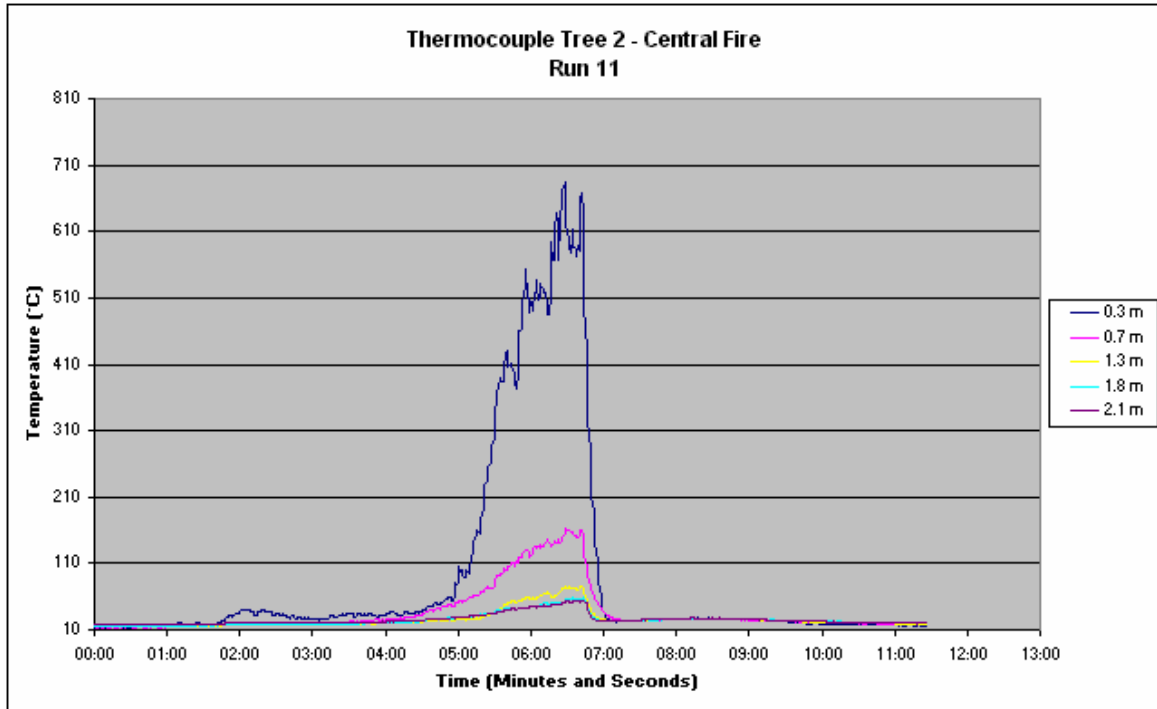


Figure 74 - Run 11: Fire Thermocouple Tree

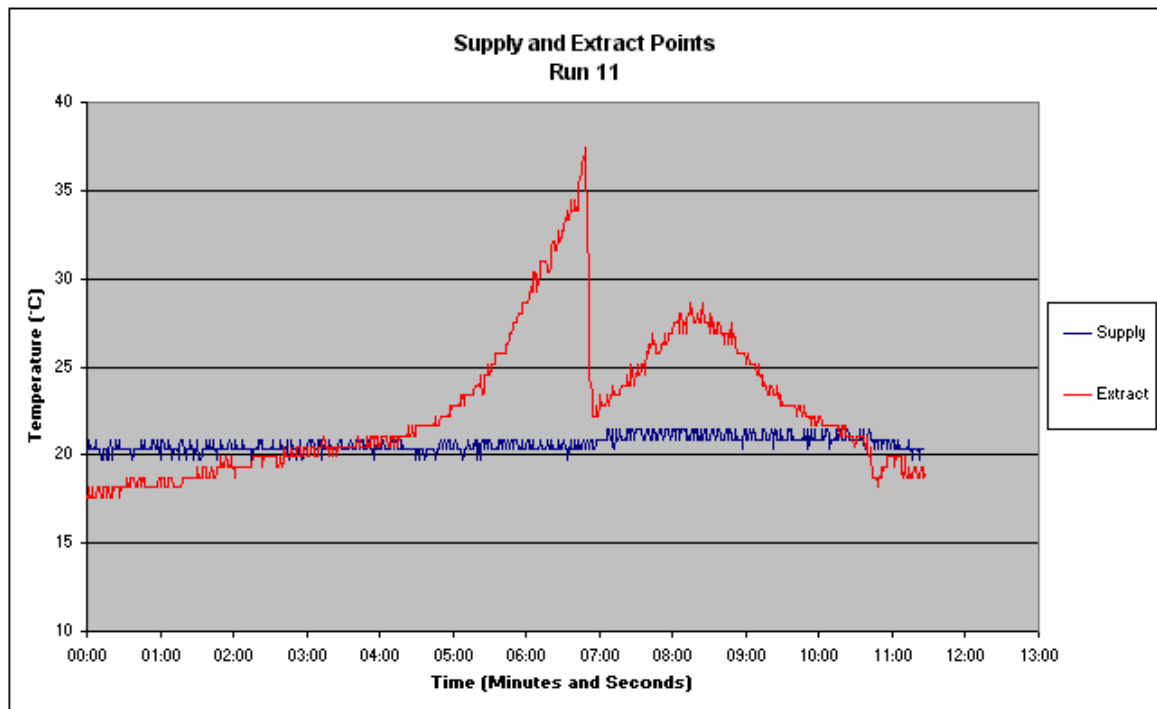


Figure 75 - Run 11: Supply and Extract Temperatures

5.11.12 Run 12: Centre High, Crib Fire, High Flow, With Mist

<u>Fire Location:</u>	Centre of compartment at 1 metre.
<u>Fire Type:</u>	Wood crib fire.
<u>Airflow Characteristics:</u>	Low flow operation for 4 minutes followed by high flow operation.
<u>Suppression:</u>	Water mist at 4 minutes.
<u>Objectives:</u>	To determine the conditions within the compartment subjected to a 1m high cellulose based fire under the operation of the displacement water mist system.

Observations:

This test run was similar in nature to that of run 6 with a high level fire but with the use of a crib fire in this case. As had been previously performed the system was set to fire mode after the fire appeared to have developed sufficiently to be established. This occurred at five minutes on the time line.

As had occurred in run 6 the crib fire began by burning in a very stable manner, not affected by the supply air and with a plume that rose vertically. On activation of the system into fire mode the fire showed effects of being affected by airflow from the rear of the compartment that caused the fire to flare up and the flame and plume to move towards the front of the compartment slightly. This was much less noticeable than which had occurred at ground level and resulted in the flame remaining in contact with the 1.3m sensor.

As the water mist was activated it moved across the floor and up the back wall, circulating forward as it was deflected. The result was water mist suspended in the forward moving airflow that had affected the fire. As the suspended water mist came into contact with the fire, the fire was observed to become slightly more turbulent but decrease in size. The fire continued to burn in this decreased manner for the remainder of the test, but it was observed that the fire appeared to be on the verge of being extinguished at times during this period. The fire was finally extinguished by operator intervention after 11 minutes as it was assessed to be in danger of falling from the mounting platform.

As occurred in run 11 the smoke layer initially appeared to lift, followed by stabilisation and a decrease in density as the water mist airflow combined with it. At no time during the test did the RCD protection on the lights and computer activate and the loads continued to operate throughout and after the test.

The graphical data recorded throughout the experiment supports the observations made during testing that the fire decreased in size. Looking at Figure 76 the point of initiation can be seen by a rapid drop in temperature throughout the compartment, followed by a relatively constant temperature profile until the water mist nozzles were shut off after 9 minutes. During this time the temperatures remained around 20 °C which could be considered normal. It can also be seen that the temperature difference between the sensors was only 3°C suggesting that there was mixing within the compartment or not enough heat generation to create significant stratification. As the temperatures are in the range of ambient conditions it would suggest the latter of these two possibilities.

Figure 77 shows that the sensors located at 1.8m and 2.1m above the fire initially picked up the plume temperature, but on activation of the system began to pick up the compartment temperature. This may have been due to the airflow from the back of the compartment causing the plume to not rise vertically or it may have been due to the mixing that was occurring within the compartment. The readings taken directly above the fire at 1.3m show the high temperatures associated with the flame front. This graph shows a decrease in temperature as the water mist interacts with the flame, followed by a more turbulent period that tends to suggest an overall decreasing temperature trend.

Figure 78 showing the exhaust air temperature, has a similar profile to these two graphs in that a rapid decrease in temperature is followed by a relatively stable period where the exhaust air is only slightly above that of ambient. The exhaust temperature did not increase until the water mist was shut off.

In terms of life safety, the temperatures within the compartment were the same as that which would be expected for normal habitation. It appeared that the significant portion of smoke and associated combustion products had been exhausted leaving a relatively inhabitable environment.

Graphical Data:

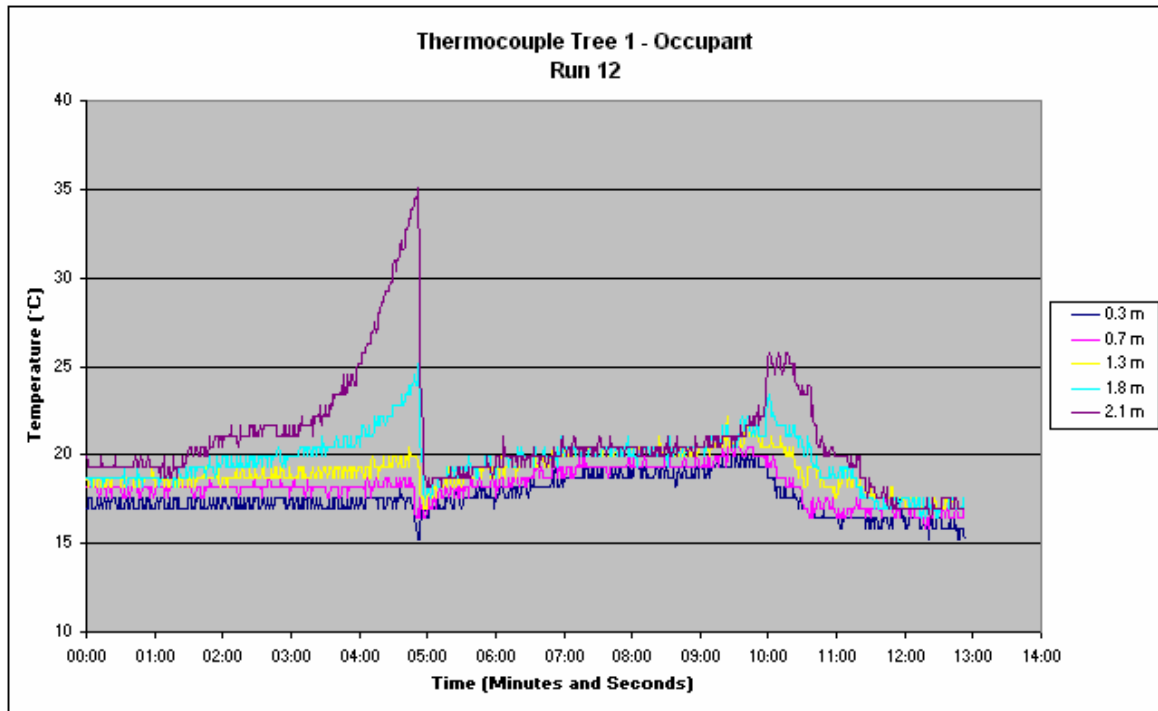


Figure 76 - Run 12: Occupant Thermocouple Tree

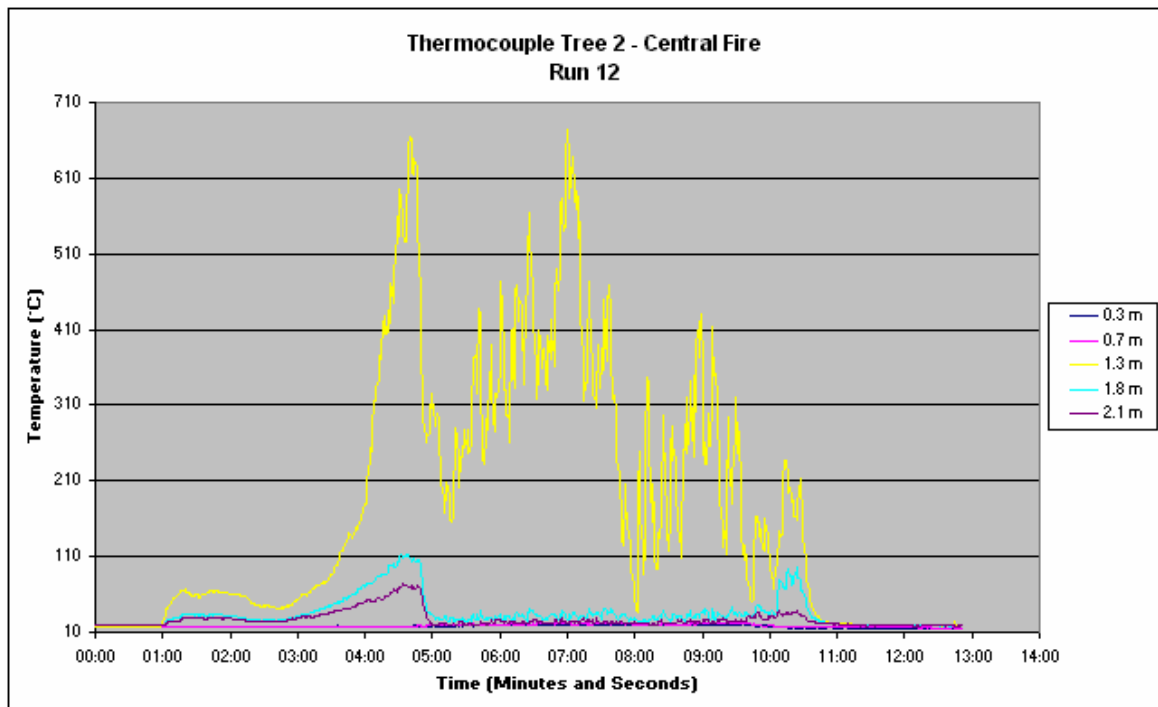


Figure 77 - Run 12: Fire Thermocouple Tree

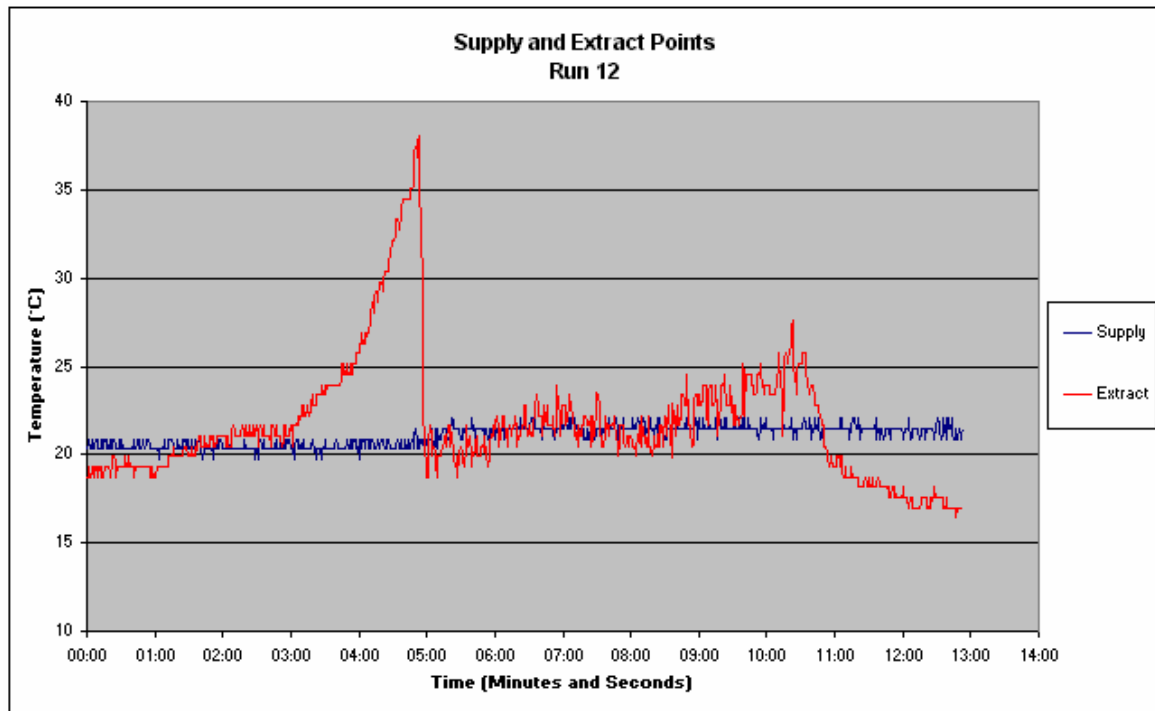


Figure 78 - Run 12: Supply and Extract Temperatures

5.11.13 Run 13: Centre Floor, Pool Fire, Low Flow, With Sprinkler

<u>Fire Location:</u>	Centre of compartment at ground level.
<u>Fire Type:</u>	Heptane pool fire.
<u>Airflow Characteristics:</u>	Constant low flow operation.
<u>Suppression:</u>	Standard sprinkler at 60 seconds.
<u>Objectives:</u>	To determine the conditions within the compartment subjected to a ground level pool fire under normal operation with a standard sprinkler

Observations:

The aim of this test run was to determine the conditions within the compartment when exposed to a pool fire and protected with a conventional sprinkler.

This test run was operated to the same timeframe as that of the other pool fire tests, with the conventional sprinkler activated after 60 seconds.

After ignition the fire grew and reacted as was discussed in run 1 under normal operating conditions, forming a smoke layer at the roof that began to drop within the compartment.

At the initiation of the sprinkler the water drops could be seen to impact into the pool fire resulting in the fuel being splashed out of the pan. This fuel then ignited causing the fire to become larger than the pan size allowed. Throughout the test run this continued with fuel continuing to be splashed out until the fire burnt out.

Within the compartment the upper layer was seen to be disrupted by the sprinkler and mixed with the lower layer to some extent. As the fire continued to burn throughout the run, smoke continued to be generated and while some appeared to be scrubbed out by the water droplets, the overall density increased.

In regard to the internal loads, both bulbs were seen to crack and break after approximately seven seconds of activation and the computer and RCD tripped shortly after indicating a short circuit. At the completion of the fire the circuits were checked again and the RCD continued to trip. The light bulbs were replaced and checked to ensure their safe operation. Again the computer was checked and found to continually trip the RCD indicating that a significant short circuit had occurred. When checked it was found that the computer was full of water with the keyboard and screen needing to be drained to remove the majority of it. This build-up of water was common within the compartment with the floor having between 2 and 5 cm of water. This did not include the additional water that leaked out of the compartment during testing.

Figure 79 shows the temperatures recorded within the compartment. As can be seen when the sprinkler was activated the temperature within the upper layer dropped dramatically. The temperature reading from the 1.3 m, 1.8m and 2.1m sensors then became very similar suggesting that this section of the compartment was relatively well mixed. Following the initial rapid decrease in temperature the thermocouples at Tree 1 all showed a continual increase in temperature until the fire burnt out.

The temperatures recorded above the pool fire in Figure 80, are initially not as high as expected. This was due to the fact that again the pool fire was set slightly

too far back on the test point resulting in the sensor not being located within the flame front or centre line of the plume. The interesting point to note about this graph though, is that at two minutes when the sprinkler is activated the temperature at these probes increases. This is caused by the spilt fuel igniting beneath the sensors and causing the sensors to be located within a new plume.

The final graph shows the supply and extract temperatures during the test run. These can be seen in Figure 81. On the supply air side, the temperature can be seen to drop as the sprinkler activates, suggesting that water was passing through the supply diffuser, wetting the sensor and cooling it down. The exhaust air sensor shows the temperature increasing as the fire begins and the upper layer increases. When the sprinkler activates the temperature momentarily decreases before continuing to increase at a slower rate until the fire burns out. An important point to note about this result is that the maximum temperature recorded at this point is 60°C while within the compartment the maximum temperature was recorded as 35 °C. This is unusual as in past test runs the external temperature had been lower than the internal temperature. One explanation for this result is that the water from the sprinkler is impacting on the thermocouple sensors within the compartment, causing them to be cooled and show temperatures below that of the actual environment. This leads to the possibility that the temperature within the compartment may not actually decrease rapidly as seen, but may simply stabilise.

With this in mind it is hard to establish the actual temperature within the compartment, but it must be assumed to be at least 60 °C.

While the temperature within the compartment appears to be below levels that could cause harm to occupants, it is again unclear what the atmosphere inside the compartment would be like as the combustion products are not exhausted and simply build up.

Graphical Data:

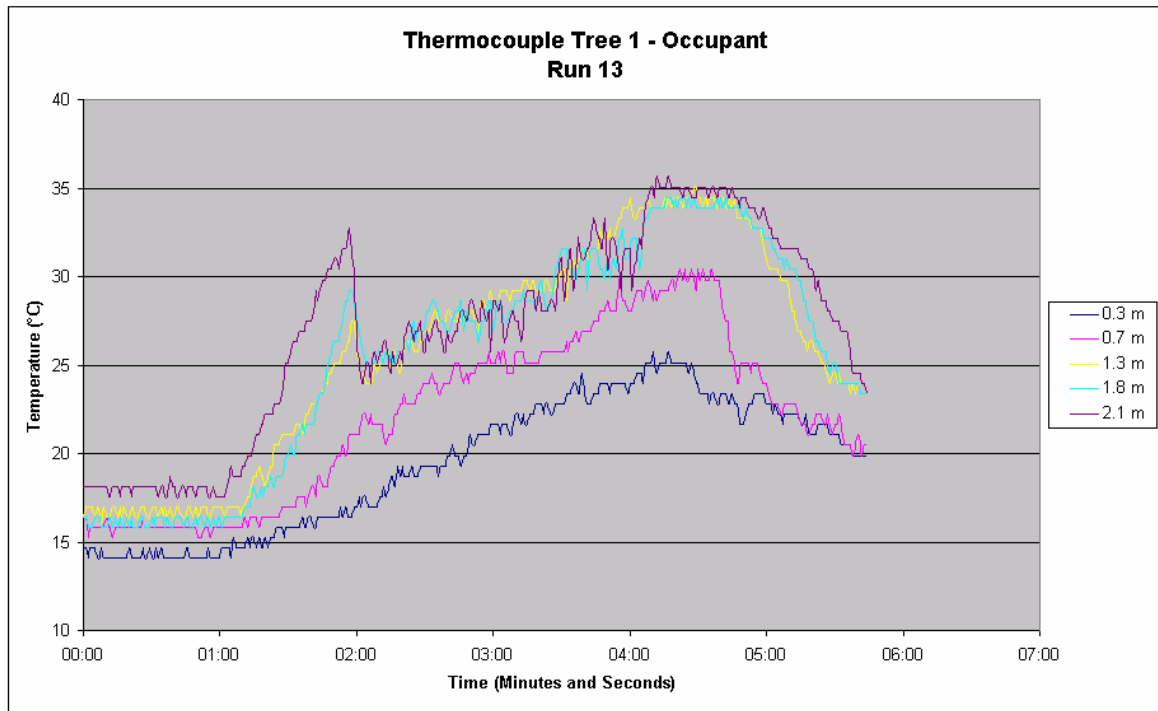


Figure 79 - Run 13: Occupant Thermocouple Tree

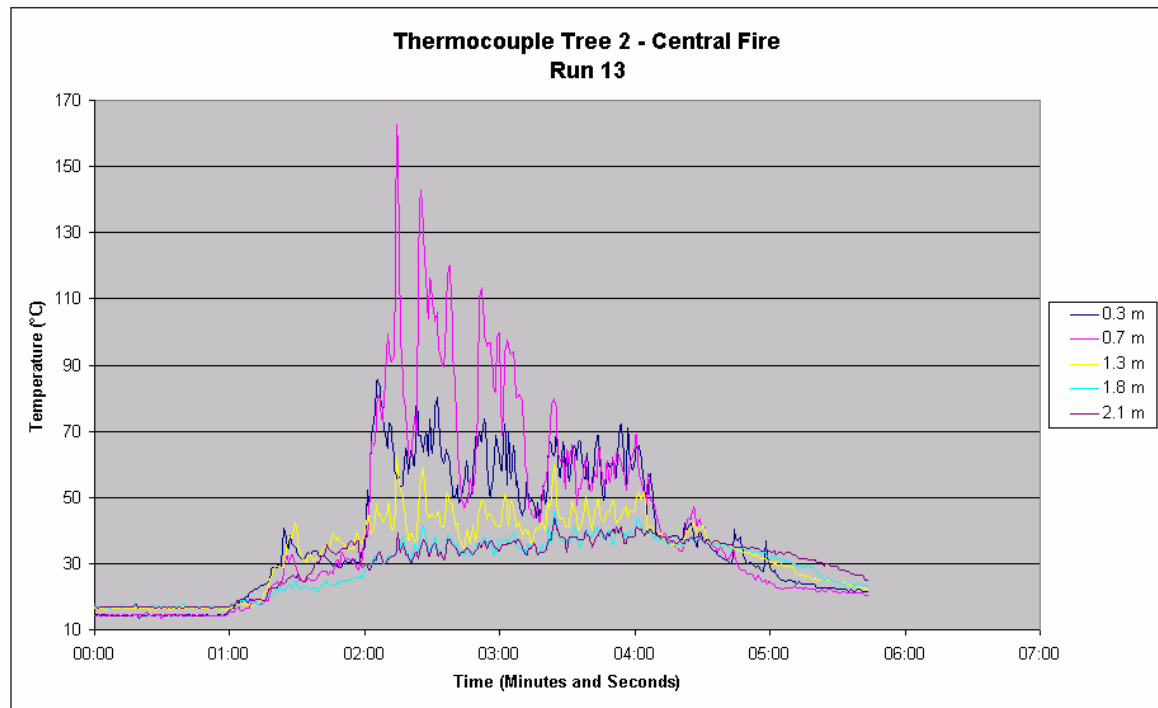


Figure 80 - Run 13: Fire Thermocouple Tree

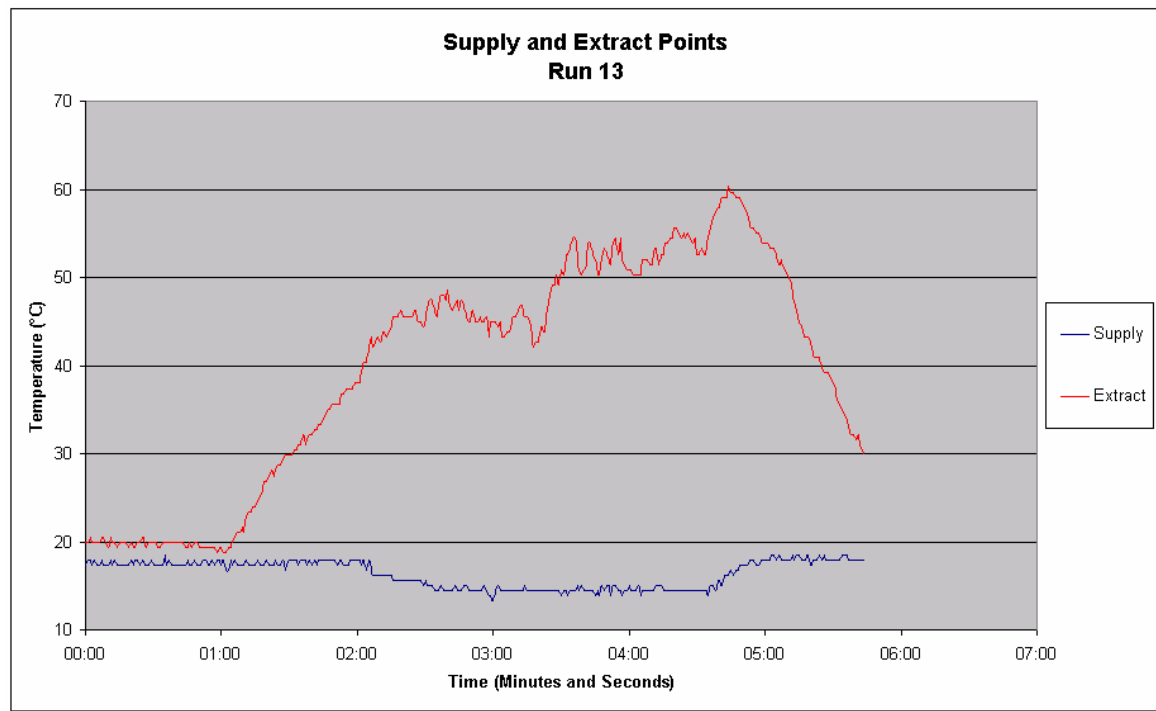


Figure 81 - Run 13: Supply and Extract Temperatures

5.11.14 Run 14: Centre High, Pool Fire, Low Flow, With Sprinkler

Fire Location: Centre of compartment at 0.7 metres.

Fire Type: Heptane pool fire.

Airflow Characteristics: Constant low flow operation.

Suppression: Standard sprinkler at 60 seconds.

Objectives: To determine the conditions within the compartment subjected to a 1m high pool fire under normal operation with a standard sprinkler

Observations:

This test run was similar to that carried out in run 13, but with the pool fire located at 1m high.

The fire initially burnt in a very stable manner and formed a relatively dense upper layer. The reaction to the application of the sprinkler was similar to that observed in run 13, where by the fire flared up and fuel was splashed out of the pan,

burning on the surrounding platform and ground. Again this continued through to burn out.

Within the compartment the upper layer was seen to collapse to some extent and mix with the lower layer. As the fire continued the density of smoke within the compartment was observed to increase as very little was vented through the exhaust. When the fire had reached burnout, the sprinkler was shut off and the compartment left to clear. It became obvious that the compartment was going to take a long time to ventilate completely so the supply air fan had to be turned up and the door opened.

Unfortunately the computer was still unusable from the previous sprinkler test but the light bulbs were installed and operating. In that case though, they had not been operating long and as such had not become hot. The result was that when the sprinkler activated the bulbs did not break and the RCD did not trip until after approximately six minutes. On investigation it was found that this was caused by water seeping into the base of the bulb elements. As with run 13 a large volume of water was collected within the compartment, which required draining.

The temperatures within the compartment at Tree 1 are shown in Figure 82. As the sprinkler is activated the 1.8m and 2.1m sensors reduce in temperature significantly, while lower sensors begin to increase in temperature. Again the 1.8m and 2.1m sensors tend to display the same temperature while the lower sensors suggest a more stratified temperature profile. As the run continues, the temperatures at all of the sensors increase slowly before decreasing.

Figure 83 shows the temperatures recorded directly above the pool fire. In this case the 1.3m sensor is located within the flame and shows a high temperature. The 1.8m and 2.1m sensors also show elevated temperatures due to being located within the fire plume. On activation of the sprinkler the 1.3m sensor shows a slight increase in output while the top two sensors show a drop in temperature. As the run continued the temperature at the 1.3m sensor became erratic and shows a slight decreasing trend.

Figure 84 again shows a decrease on the supply air temperature as the water passes through the diffuser and cools the sensor. The exhaust air sensor shows

a similar profile to that recorded within the compartment, but indicates that there is no reduction in temperature, but more of a stabilisation followed by slower increase rate. The maximum temperature recorded at the extract is 60°C while within the compartment the maximum is 35 °C. As discussed this may be due to the internal sensors becoming wet.

As with run 13, the temperatures within the compartment appear to be below levels that could cause harm to occupants. It is unclear what the atmosphere inside the compartment would be like but when the compartment was entered directly after the test, the atmosphere was noticeably toxic and could not be remained in for any length of time.

Graphical Data:

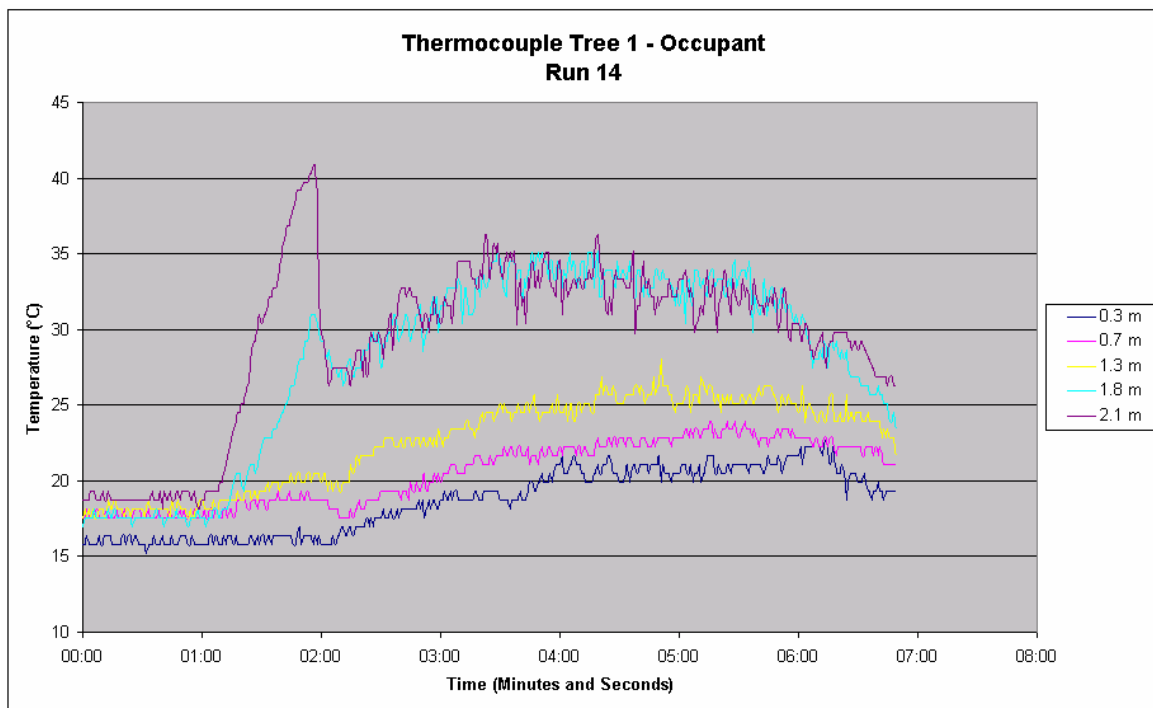


Figure 82 - Run 14: Occupant Thermocouple Tree

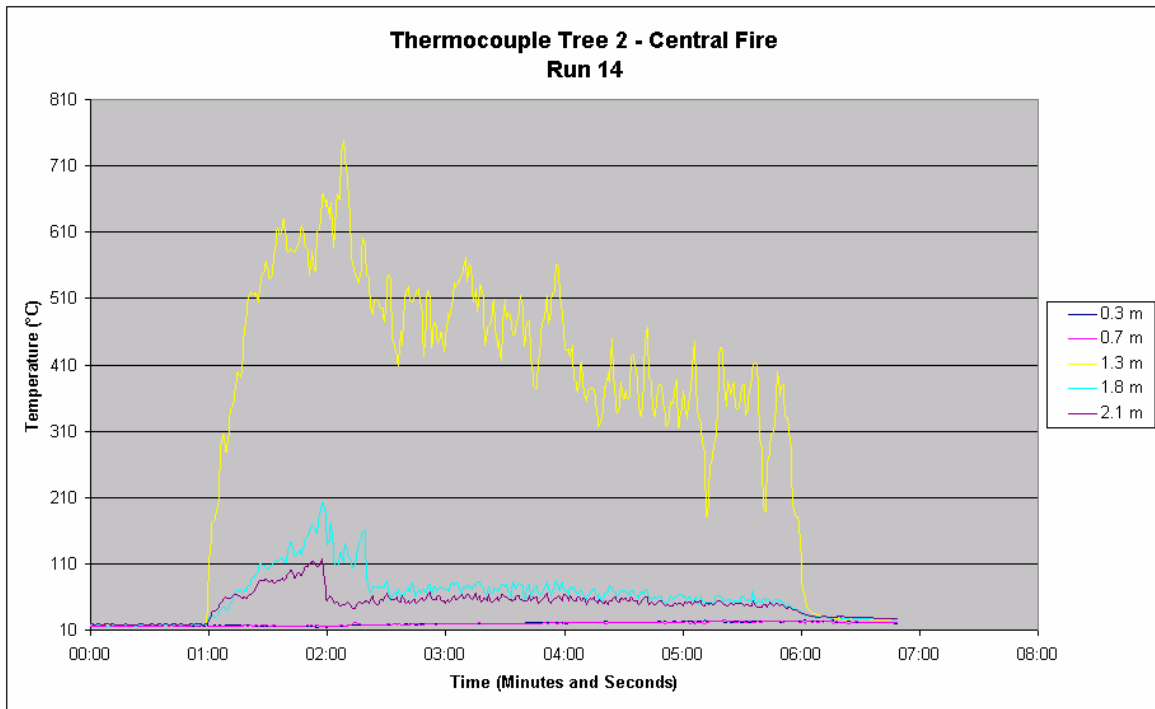


Figure 83 - Run 14: Fire Thermocouple Tree

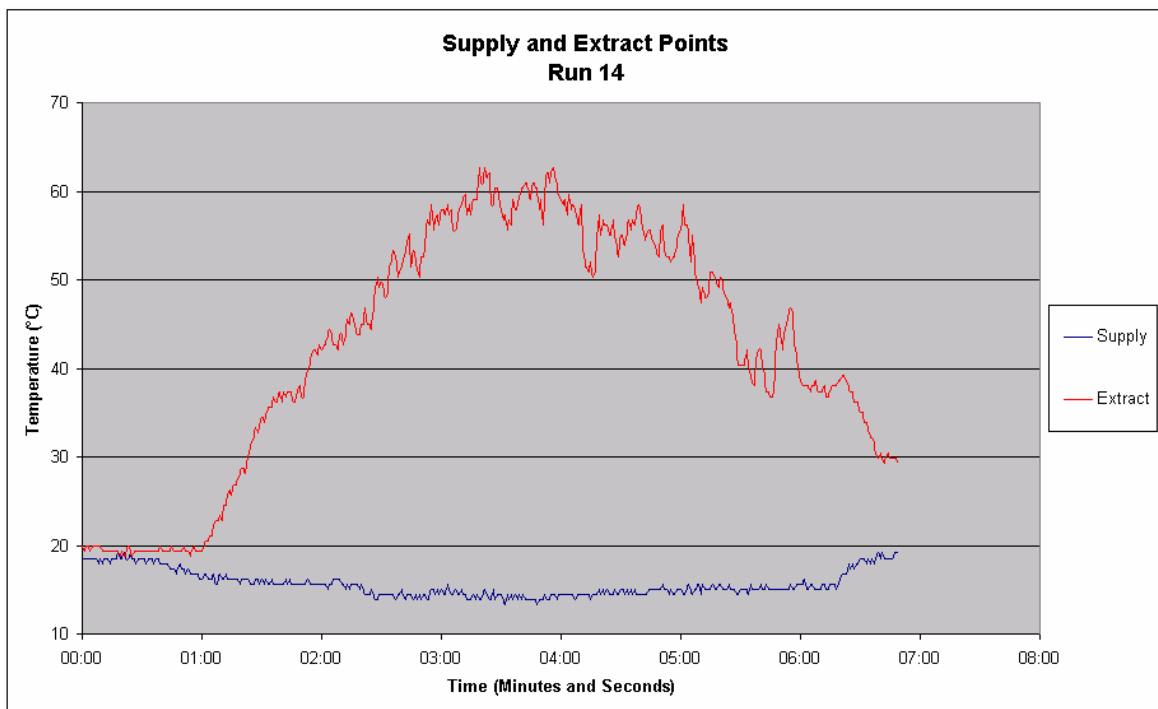


Figure 84 - Run 14: Supply and Extract Temperatures

5.11.15 Run 15: Centre Floor, Crib Fire, Low Flow, With Sprinkler

<u>Fire Location:</u>	Centre of compartment at ground level
<u>Fire Type:</u>	Wood crib fire.
<u>Airflow Characteristics:</u>	Constant low flow operation.
<u>Suppression:</u>	Standard sprinkler at 4 minutes.
<u>Objectives:</u>	To determine the conditions within the compartment subjected to a cellulose based fire at ground level under normal operation with a standard sprinkler

Observations:

The objective of this test run was to determine the compartment characteristics caused by a wood crib fire using conventional sprinkler suppression.

As with the previous tests, the wood crib was allowed to burn until the fire had developed to a point that it could be considered to have taken hold and was stable. This occurred at five minutes. During this build up, the crib fire grew creating a clearly visible upper layer that began to descend and become denser.

On activation of the sprinkler the crib began to sizzle and large quantities of steam were produced causing visibility within the compartment to decrease dramatically. After 10 seconds of operation, no further glowing could be observed from the exterior windows, the sprinkler system was shut off and the compartment left to clear. This appeared to be taking an excessive period of time so at 6 minutes 30 seconds the air supply system was set to fire mode flow. Within one minute of the airflow being increased the crib showed signs of flaming ignition and smoke began to rise from the wood crib again. As this was not part of the test run, the airflow was decreased and shortly later entry into the compartment was made to extinguish the fire.

The computer was still unusable from the previous sprinkler tests but the light bulbs were again installed and operating. As they had just been wet by the previous test they had not become hot. The result was that when the sprinkler activated the bulbs did not break and the RCD did not trip. It appeared on investigation that due to the short duration water had not seeped into the base of

the bulbs. Additionally the short duration resulted in less water accumulating than had occurred in runs 13 and 14.

The temperature data within the compartment corroborates that observed during testing. Figure 85 shows the temperatures recorded at Tree 1. As expected the temperatures, particularly in the upper levels, increase as the fire grows and the upper layer forms and descends. At initiation of the sprinkler the temperatures all decrease rapidly before stabilising when the sprinklers are shut off and the fire is initially assumed to be out. The point at which the airflow is increased is accompanied by a decrease in temperature as the warm compartment air is ventilated with ambient air. Shortly after the temperatures can be seen to increase as the fire begins to take hold and grow. As the airflow is cut and the fire decays the temperature decreases until entry is made and the fire suppressed.

The temperatures above the crib fire are shown in Figure 86. As before the temperatures initially increase as the fire grows, then drop rapidly with the application of the sprinkler. They then stabilise until increasing again when the airflow is increased and the fire begins to grow.

Figure 87 shows the same trend as Figure 85 and Figure 86 but as before the temperatures recorded are above those measured within the compartment. In this case though, the temperature difference is less, possible due to the short operating time of the sprinklers resulting in less wetting of the surface.

The temperatures within the compartment appear to be below levels that could cause harm to occupants. When entry was made to the compartment to extinguish the fire it was observed to be noticeably toxic and could not be remained in for any length of time.

Graphical Data:

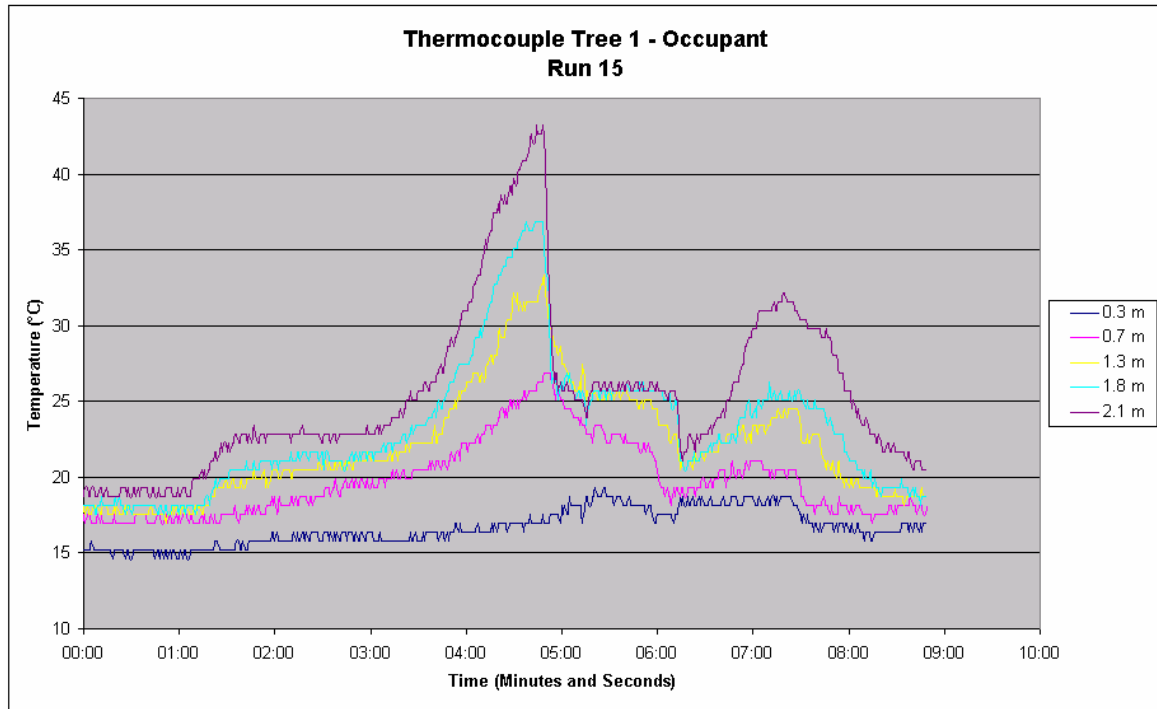


Figure 85 - Run 15: Occupant Thermocouple Tree

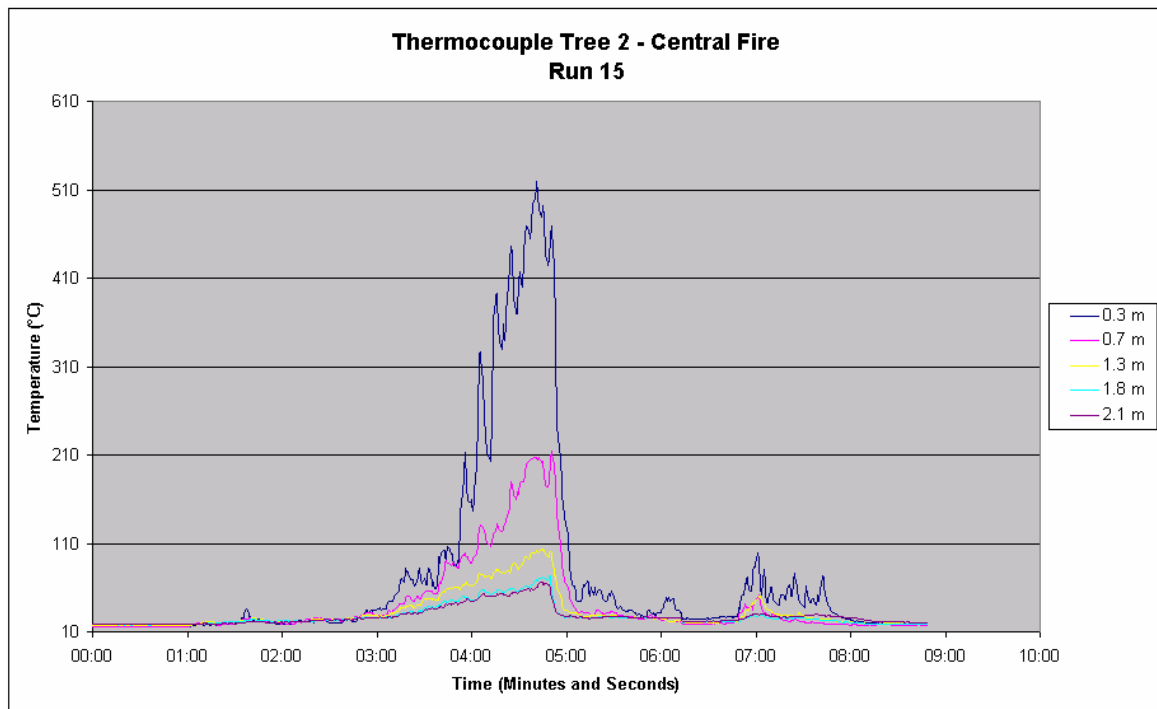


Figure 86 - Run 15: Fire Thermocouple Tree

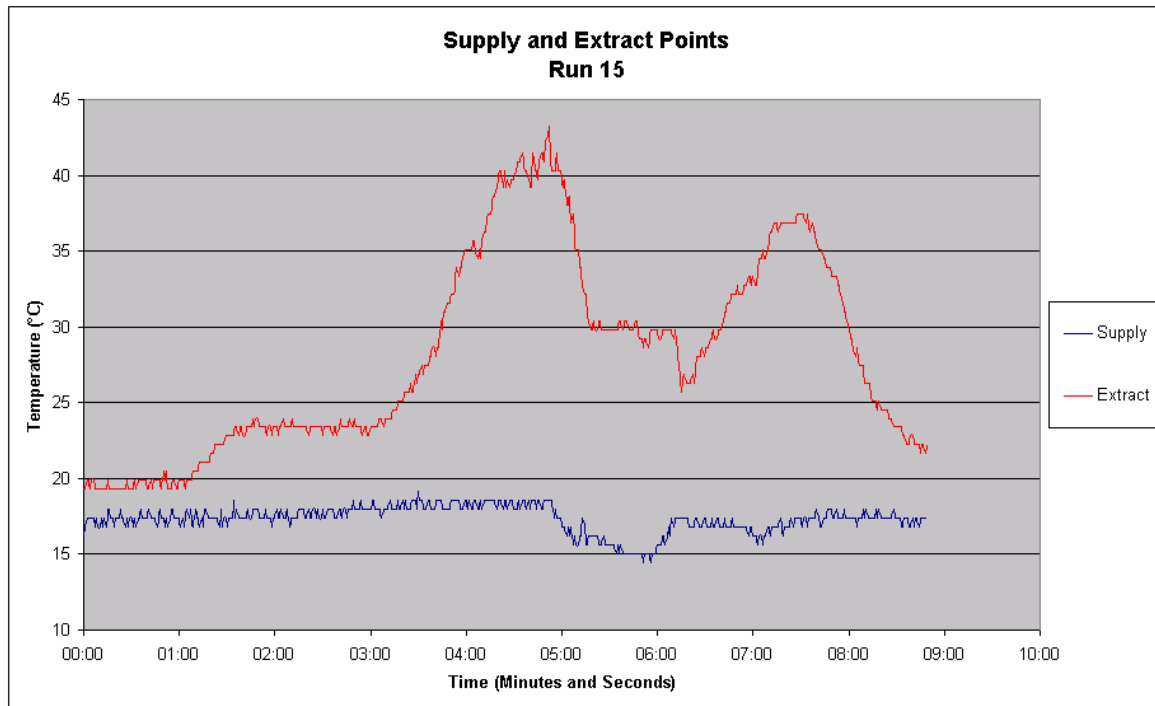


Figure 87 - Run 15: Supply and Extract Temperatures

5.11.16 Run 16: Centre Floor, Pool Fire, High Flow, With Mist and Shield

<u>Fire Location:</u>	Centre of compartment at ground level
<u>Fire Type:</u>	Heptane pool fire
<u>Airflow Characteristics:</u>	Low flow operation for 60 seconds followed by high flow operation.
<u>Suppression:</u>	Water mist at 60 seconds.
<u>Objectives:</u>	To determine the conditions within the compartment subjected to a pool fire shielded from direct water mist and airflow by a wooden board.
<u>Observations:</u>	

The objective behind this test run was to determine the compartment characteristics if the fire was shielded from the direct airflow and water mist. The shield was made of a wooden panel that was 400 mm in height and 600 mm in length. This was placed 100 mm in front of the central fire and mounted parallel to the front wall

Once the fire was ignited it grew in a relatively stable manner, with a slight slope towards the wooden shield. On activation of the displacement water mist system into fire mode, the fire immediately became turbulent and began to burn vigorously. The flame appeared to be pushed down and towards the shield possibly due to the high velocity airflow created by the nozzles, circulating around the edges of the wooden panel. This burn pattern was observed throughout the test phase.

Within the compartment the upper layer that had formed, initially decreased in depth as it was ventilated from the compartment, but then increased slightly as the water mist circulated through the compartment and mixed with it. Again the upper layer appeared to be drawn into the water mist jets directly above the inlet. As the run continued the upper layer became less dense and some mixing was observed to occur between the upper and lower layers.

In this run both light bulbs and the computer were installed and continued to operate throughout the test run without tripping the RCD. At the completion of the compartment a small quantity of water had built up on the floor. On inspection of the wooden shield, the side closest to the fire had char marks from where the fire had circulated forward.

Internally the temperatures within the compartment showed an initial increase as the fire developed. When the system was set to fire mode the upper sensors rapidly decreased, while the lower sensors recorded an increase in temperature. After the initial reaction to the water mist addition, all of the compartment sensors showed a gradual increase in temperature within the compartment, followed by a relatively quick decrease when the fire burnt out. This can be seen in Figure 88. An interesting point to note about this graph is that the temperature difference between all of the sensors is minimal suggesting that a lot of mixing was occurring within the compartment.

Figure 89 displays the temperatures recorded directly above the fire. As can be seen the 0.3m sensor recorded an initially very high temperature due to it being located within the fire plume. Interestingly the sensors above this do not show as large an increase as what may be expected. This is possibly due to the plume

being pushed forward by the supply airflow and moving forward of the sensor tree. On activation there is again an immediate drop in the temperatures. In the case of the 0.3m sensor the drop remains throughout the run and the readings become erratic. This is likely due to the airflow circulating across the top edge of the shield creating a circular eddy behind it that effectively acts as a down draft. This down draft would have provided cool air near the sensor while causing the fire to become turbulent as observed.

Finally Figure 90 shows the supply and exhaust temperatures recorded from the compartment. The supply air temperature can be seen to remain relatively constant throughout the run. The exhaust air sensor shows a steady rise after the fire is ignited followed by a slightly slower temperature increase after the water mist is activated. This is similar to that recorded within the compartment.

The temperatures within the compartment remain below 35°C throughout the run suggesting that there would be little thermal danger to occupants. The atmosphere within the compartment appeared to clear with the activation of the system suggesting that it may be able to be occupied. This is discussed further in run 17.

Graphical Data:

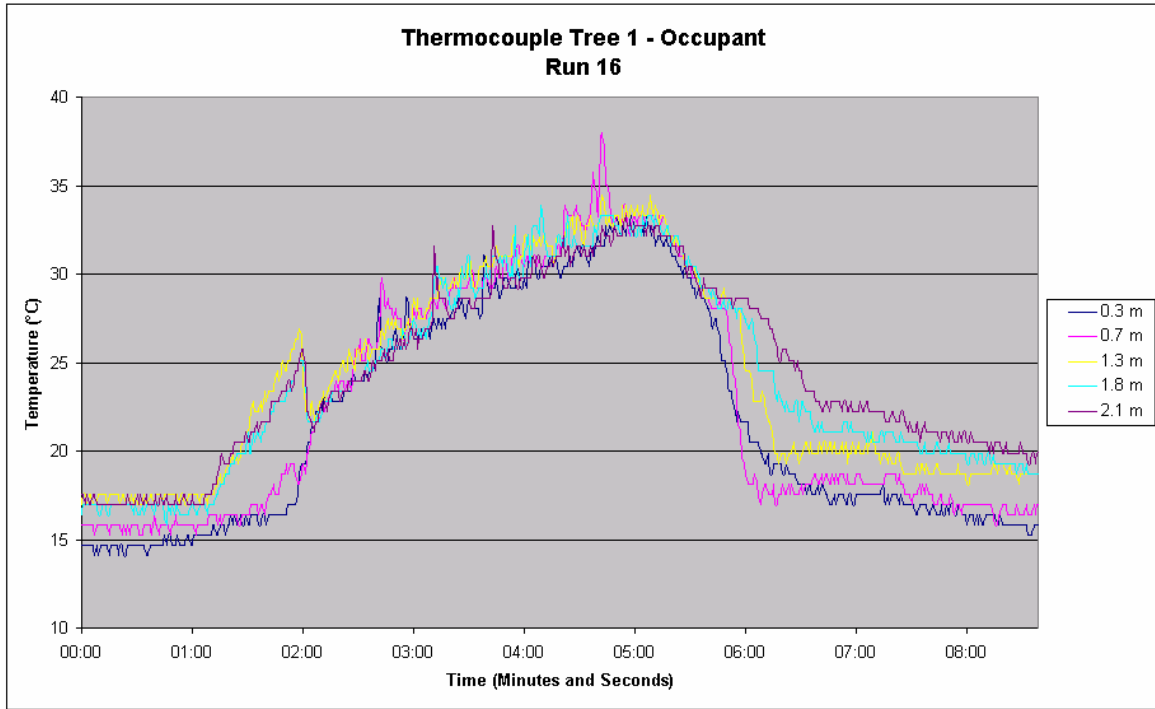


Figure 88 - Run 16: Occupant Thermocouple Tree

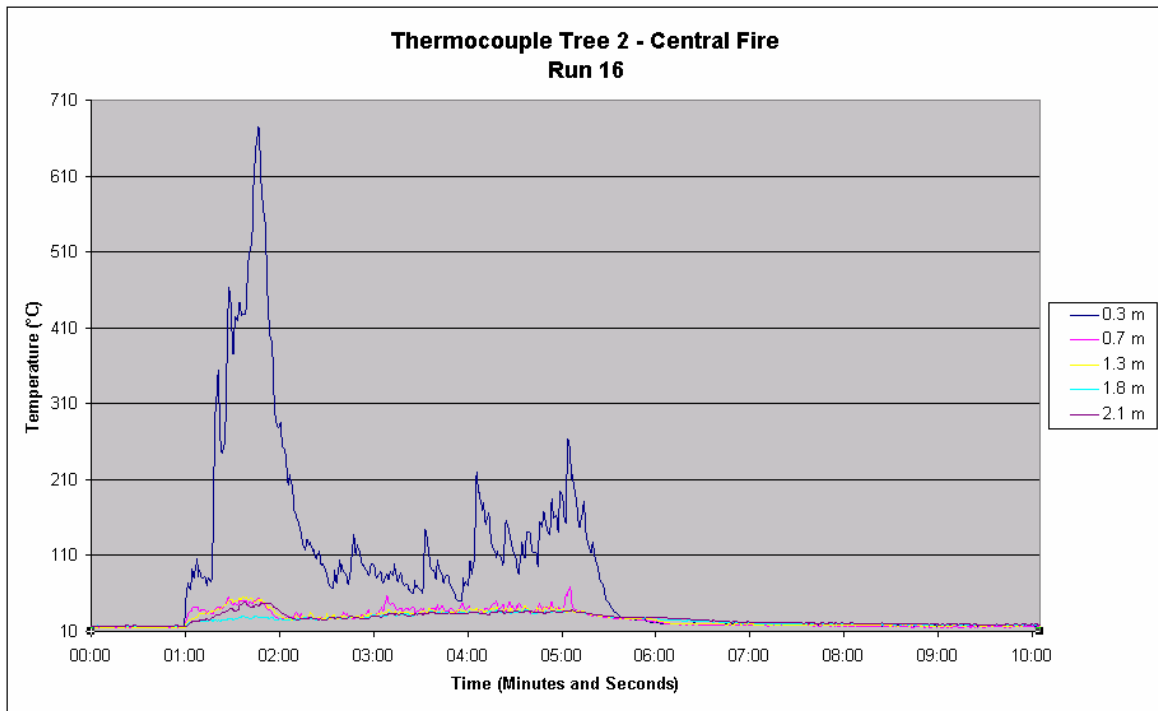


Figure 89 - Run 16: Fire Thermocouple Tree

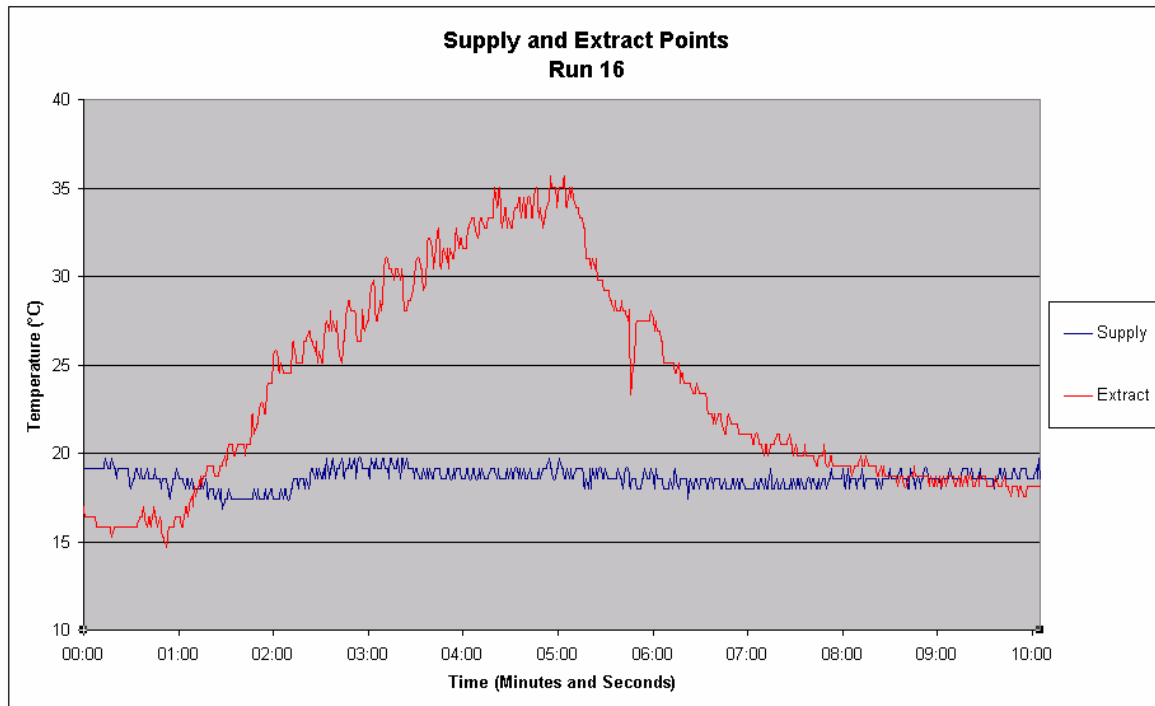


Figure 90 - Run 16: Supply and Extract Temperatures

5.11.17 Run 17: Centre Floor, Pool Fire, High Flow, With Mist and Observers

<u>Fire Location:</u>	Centre of compartment at ground level
<u>Fire Type:</u>	Heptane pool fire
<u>Airflow Characteristics:</u>	Low flow operation for 60 seconds followed by high flow operation.
<u>Suppression:</u>	Water mist.
<u>Objectives:</u>	To observe the fluid mechanics within the compartment during a live test and determine through observation the relative survivability for occupants.
<u>Observations:</u>	

The final test run carried out during full scale testing was again a pool fire located at ground level within the compartment with the activation of the displacement water mist system. In this run though, two occupants were present in the compartment to observe the internal characteristics and the environment. Both occupants were wearing full fire fighting protective clothing and breathing

apparatus. One of the occupants, Gary Luff, was a senior training officer with the New Zealand Fire Service and the other was the author.

As had been seen in previous experiments, once ignited the fire began to burn in a steady manner with the same slight slope way from the supply air diffuser. In this test run the occupant's ignited the fire and due to the restricted clothing the pan had to be placed further away from the thermocouple tree than normal to allow access. The result of this was the plume rose on the back side of the sensor array.

As the fire proceeded an upper layer was seen to form and the temperature was felt to rise within the compartment. In the early stages of the fire the upper and lower layers remained separated, resulting in a relatively clear lower layer.

On activation of the system into fire mode, the fire immediately began to burn in a turbulent manner. The mist was observed to cross the floor, hit and move up the back wall, before being reflected into the rest of the compartment.

A definite airflow could be felt being drawn into the water mist nozzles from the front section of the compartment. As the system stabilised, the airflow appeared to form a circulation effect within the compartment. A down draught could easily be felt on the front wall.

Approximately three seconds after the water mist was activated the temperature within the compartment was felt to drop. By ten seconds after initiation, the majority of combustion products and smoke appeared to have cleared the compartment. At this time it was decided to remove the breathing apparatus.

On removal of the breathing apparatus the atmosphere was found to be warm and humid but could easily be breathed with no irritation. Movement around the compartment was unrestricted with the only point of irritation being found to be directly in line with the fire plume. Vertically the lower level air was found to be clearer than the high level air but the upper level air remained acceptable. An increase in pollutants was felt at approximately 1.6m but not in significant quantities to cause problems.

The occupants remained within the compartment until burnout had occurred. During this time no major irritation was experienced by either occupant, though both became relatively damp. If standard clothing had been worn it most likely would have become damp as well.

For safety reason the internal loads were not operated during this test run but previous results would suggest that it would not have short circuited.

The temperature readings recorded within the compartment during this test run were similar in nature to those recorded in run 5 with the same situation but with no occupants present. For this reason they are not presented in this report.

5.12 Full Scale Test General Discussion

The most significant observation from the live testing was that the fire was not extinguished by the displacement water mist system. In fact the only case in which the fire was extinguished was with a wood crib and conventional sprinkler. The primary reason for not extinguishing the fire appeared to be due to the large air entrainment created by the water mist nozzles.

As discussed previously the creation of the water mist and the layout of the nozzles caused large volumes of air to be entrained into the water mist flow and for it to have a very high velocity. Two effects resulted from the entrainment and caused the system to act in a different manner than intended. The first was that the volume of water injected into the compartment was based on the supply airflow. As more air was entrained than that supplied, the density of the water mist decreased to below that required for extinguishment. In fact it was noted that with the nozzles activated the fire appeared to burn more vigorously and in the case of the wood crib, spread. This was also shown clearly when the nozzles were taken from the compartment and pointed directly at the pool fire. Even under this scenario the fire was not extinguished.

The second was that the system had been designed based on the concept that little mixing would occur between the upper and lower zones within the compartment. In the live test though the high entrainment and velocity of the water mist caused circulation and cooling of the upper layer that resulted in it mixing with the lower layer to some extent. This was clearly seen in Run 7 where the water mist was shut off and the compartment immediately began to stratify. In addition the injection of the water mist into the upper layer and exhaust effectively lowered the density of water throughout the compartment.

On a positive note two fires did appear to be controlled and suppressed to some extent, these being the pool and crib fires at 1m. Under these scenarios the fires were out of the direct impingement of the nozzles and the airflow was relatively slow. This was due to the fact that the water mist tended to circulate around the outside leaving the centre of the compartment relatively undisturbed. The water

mist in this section of the compartment tended to move slowly with the airflow as had been intended in the entire compartment. While this caused the fires to show signs of suppression the water density in this region was observed in Run 17 to be substantially lower than in other sections of the compartment. The most likely cause of this is that the majority of water mist was circulated around the outside of the compartment with the high velocity airflow. This does tend to indicate though, that the concept of a dense water mist following a slow air stream is feasible for providing some form of suppression.

One other possible reason that the fires were not suppressed was simply that the density of 200 g/m^3 was not high enough. This figure had been based on the work performed at Lund [19] but other research has indicated that for small fires, densities in the region of $400 - 600 \text{ g/m}^3$ may be required. Unfortunately the option to increase the water density was not available and the limited time frame meant that larger fires could not be investigated.

In regard to the computer and light bulbs within the compartment the tests, though crude, showed that these could be operated in a displacement water mist environment without shorting out or failing. In no run where the displacement water mist system was activated, did the RCD trip and indicate an electrical short. In fact even after repeated tests without drying the computer continued to operate. The only time that the computer and light bulbs failed was when only the water mist was activated and when the sprinkler activated. The damage caused by the sprinkler was the most significant with the computer not being able to be operated and the light bulbs breaking after the first test run with the sprinkler. This indicates a significant point for real life tests whereby it is quite possible that if a sprinkler activated in a previously lit environment, the light bulbs could break, reducing the light levels.

Finally while the system did not operate as intended the environment created within the compartment by the displacement water mist system was significantly better than under any other scenario. This is discussed and referred to in the following figures, as well as being physically observed during Run 17 with occupants present within the compartment. During Run 17 both occupants were able to move about the compartment breathing easily with a pool fire burning.

The remainder of this discussion presents a comparison between the live tests carried out. Four separate scenarios are looked at and in each case the temperatures at the 1.3m, 1.8m and exhaust are compared. These temperatures were used as the two internal temperatures relate to the head height of an occupant sitting and standing. The exhaust air temperature is used because, as discussed previously, it appears that the water mist, sprinkler droplets and compartment radiation were affecting the readings from the thermocouples.

The first comparison looks at a central floor level ground fire and compared normal (Norm-No Mist), high airflow (High-No Mist), displacement water mist (High-Mist), water mist only (Norm-Mist) and sprinkler operation (Norm-Spk). Figure 91 and Figure 92 show the internal temperatures at 1.3m and 1.8m. The greatest temperature is recorded under normal conditions followed by the high airflow test run. This was expected as under these conditions no water cooling or suppression is occurring. The remaining three scenarios result in similar temperatures with the displacement water mist system resulting in the lowest temperature. In each of these three cases the point of activation is immediately followed by a rapid decrease in temperature.

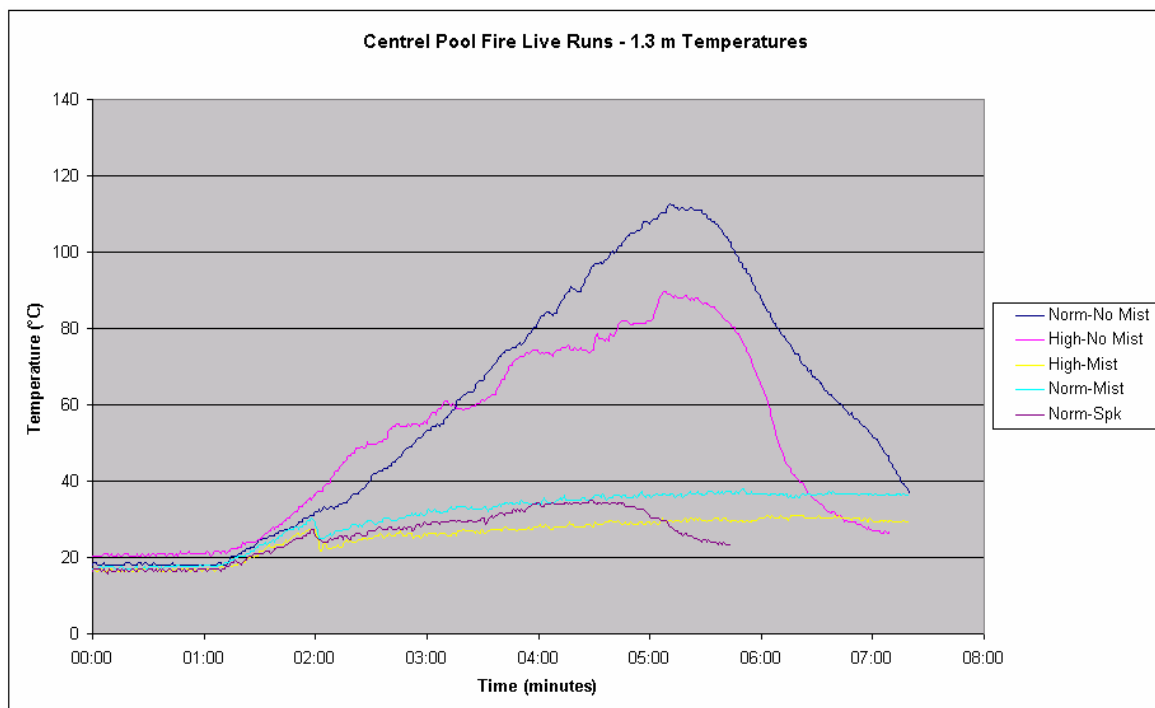


Figure 91 - Central floor pool fire Tree 1, 1.3m temperature readings

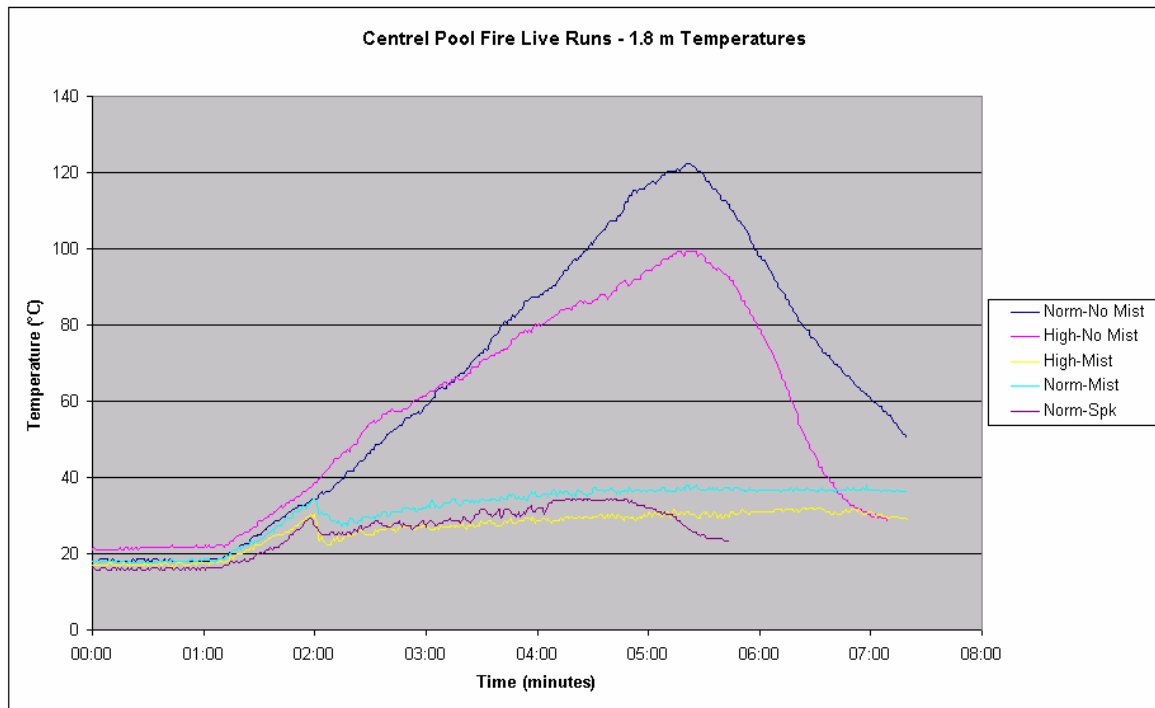


Figure 92 - Central floor pool fire Tree 1, 1.8m temperature readings

Looking at Figure 93 we see a similar result except that the temperatures from the conventional sprinkler system are much higher than the water mist system and that the displacement water mist system is slightly higher now than the water mist only (Norm-Mist). In regard to the conventional sprinkler this would suggest that the internal thermocouple readings are affected as the water drops wet them. It is unclear why the temperature from the displacement water mist system is higher than that recorded from the water mist only, but it may be due to the low exhaust volume under the water mist only condition. The placement of this sensor may have resulted in the compartment air mixing with the outside air to create a lower temperature.

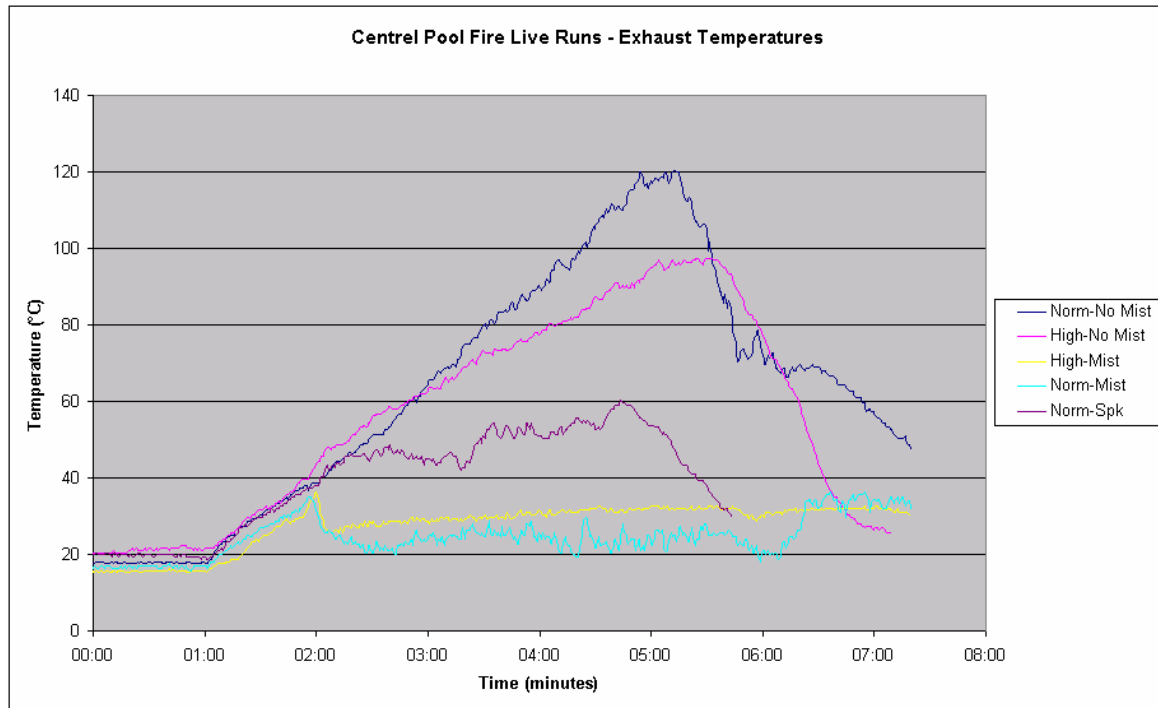


Figure 93 - Central floor pool exhaust temperature readings

The next set of figures compares the same three points for a central pool fire at ground level low airflow (Norm-No Mist), at 1m low airflow (Norm 1m-No Mist), at 1m displacement water mist (High 1m-Mist) and at 1m with conventional sprinkler (Norm 1m-Spk).

The first observation from Figure 94, Figure 95 and Figure 96 is that, as expected at low levels the temperature is higher from the ground level fire, while at high level it is greater for the 1m fire. This is due to more entrainment occurring within the plume of the floor level fire so the upper layer increases in size more rapidly. Conversely the 1m fire has less entrainment so the layer builds more slowly but at a higher temperature.

Figure 94 and Figure 95 show a similar result as seen in the first comparison whereby the temperatures within the compartment are lowest when the displacement water mist system is activated followed by the sprinkler.

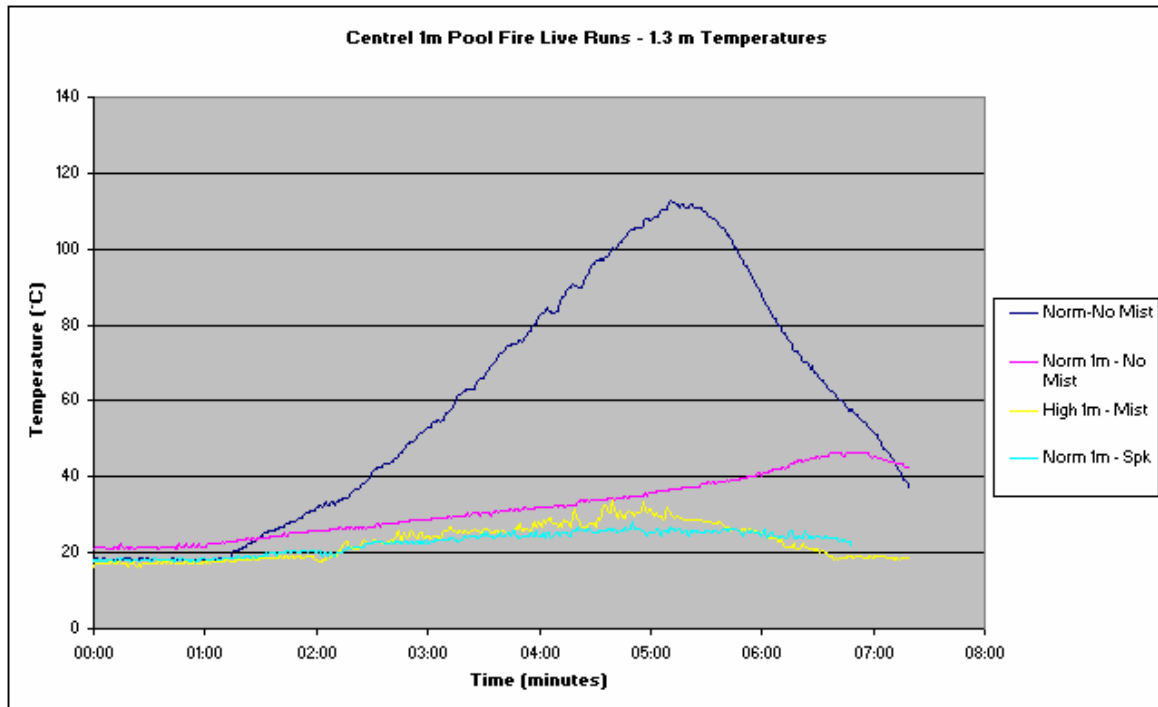


Figure 94 – Central 1m pool fire Tree 1, 1.3m temperature readings

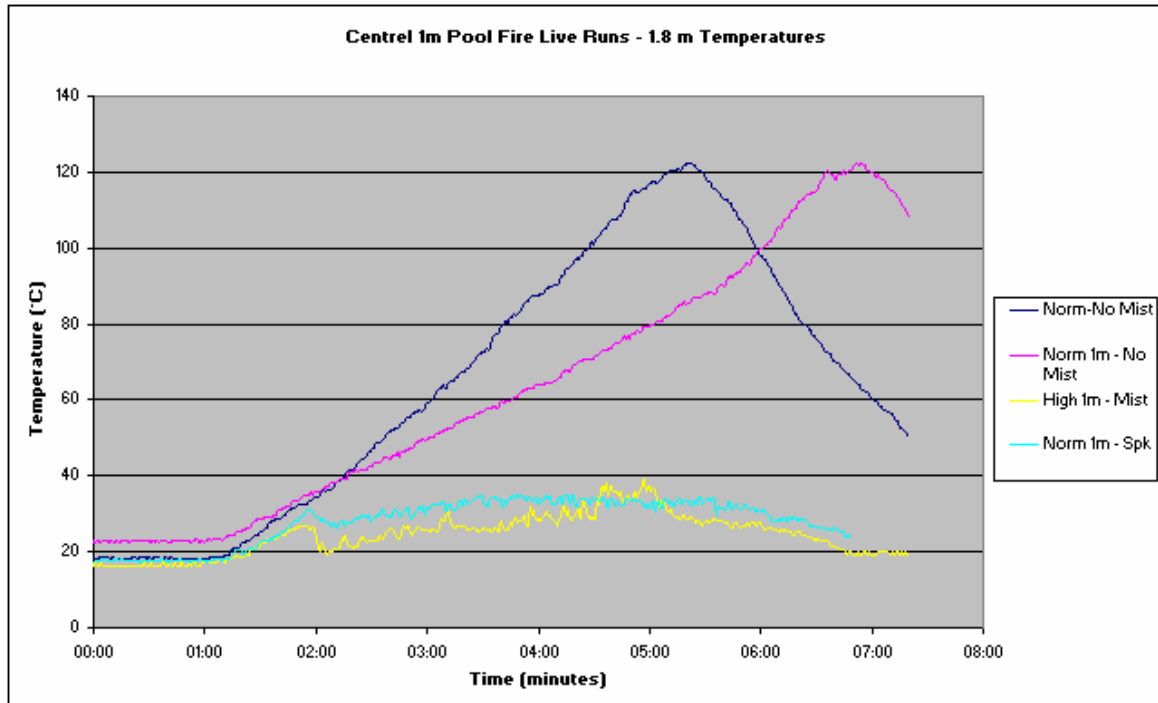


Figure 95 - Central 1m pool fire Tree 1, 1.8m temperature readings

Figure 96 also shows the same results in that the sprinkler temperatures are much greater than that of the displacement water mist system. Again the most likely cause is simply that the thermocouples within the compartment are being wetted by the sprinkler water droplets. The increase in temperature from the displacement water mist system resulted from the water mist being shut off and the ceiling jet exiting the exhaust vent.

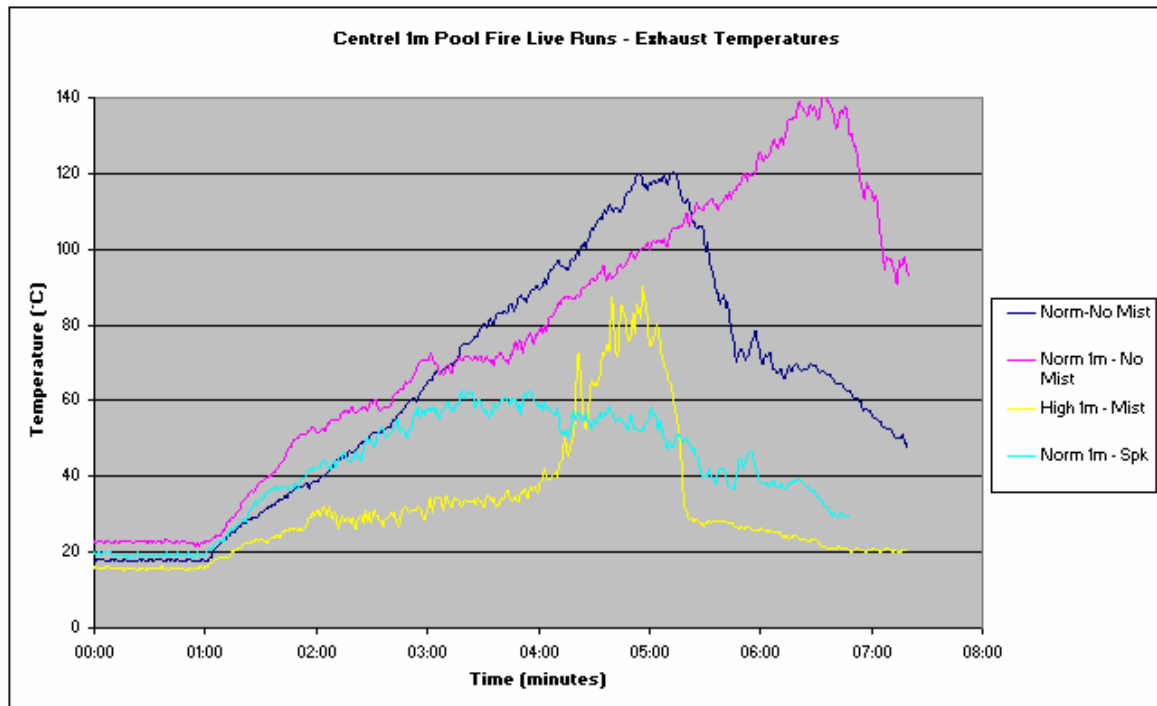


Figure 96 - Central 1m pool fire exhaust temperature readings

The third comparison investigated a corner pool fire located at the central floor with low airflow (Norm-No Mist), back corner with low airflow (Norm-No Mist Back), back corner displacement water mist (High-Mist Back) and front corner displacement water mist (High-Mist Front).

The first observation from Figure 97, Figure 98 and Figure 99 is that in all positions the temperature of the central fire is greater than that of the corner fire. These results are interesting in that as the corner entrains less air the upper level and exhaust temperatures could be expected to be high. It is possible that in the case of the internal sensors that at 1.8m the sensor is below the upper layer formed causing it to be lower than the central fire scenario where the upper layer has dropped more quickly. In the case of the exhaust sensor though, it would be

expected that the temperature from the corner test would be higher. One possible cause for this is that the close proximity of the walls and increased travel distance across the roof are cooling the plume and ceiling jet.

Looking at the displacement water mist stems it is clear that the temperatures are decreased significantly at all points. Additionally the results from the front and back corner are almost identical. In both cases a rapid temperature drop can be observed to occur on activation.

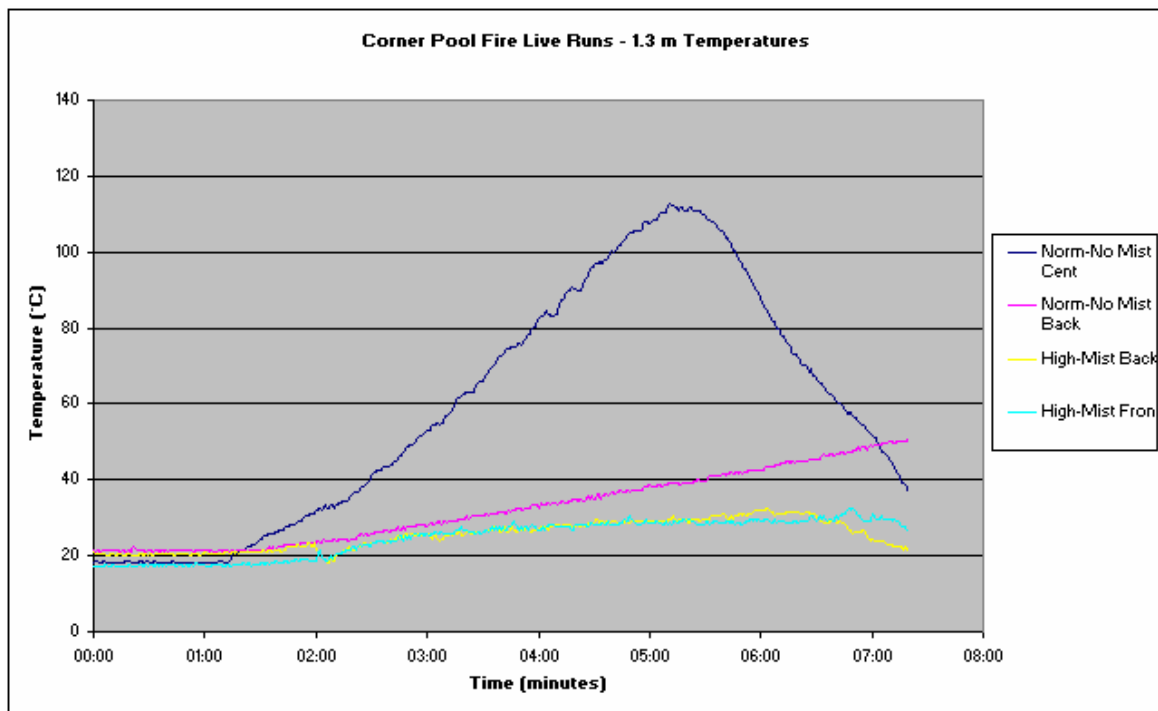


Figure 97 – Corner pool fire Tree 1, 1.3m temperature readings

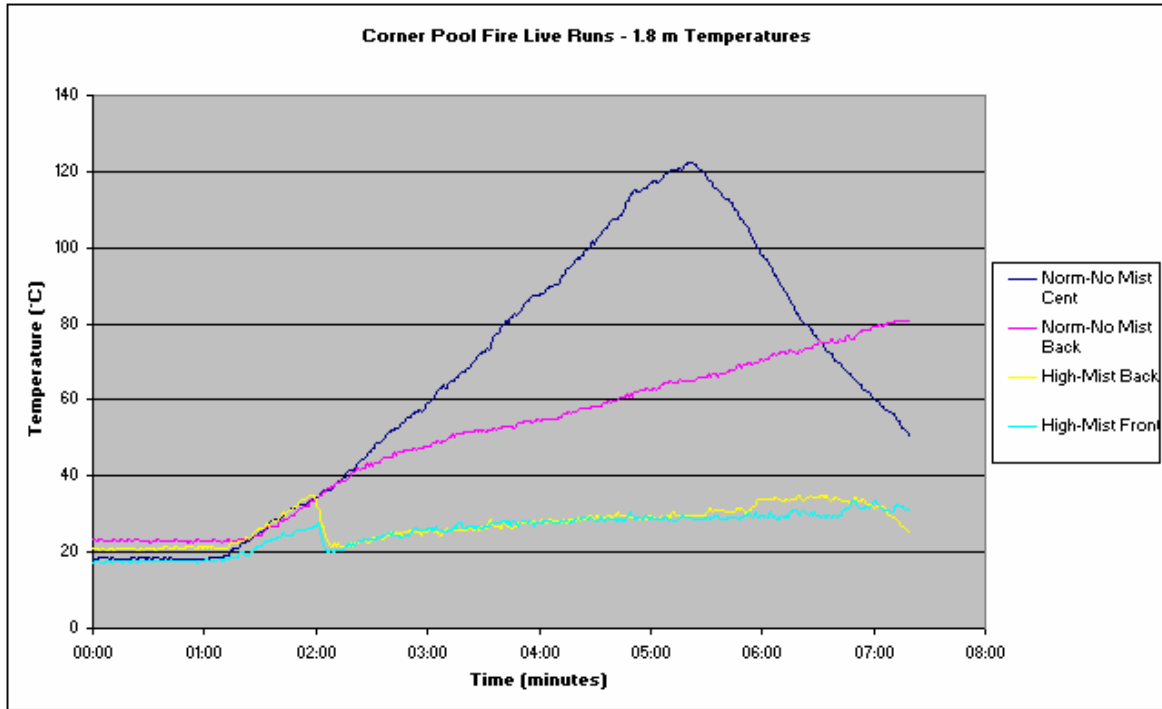


Figure 98 – Corner pool fire Tree 1, 1.8m temperature readings

An important point to note in Figure 99 is that the exhaust temperatures drop rapidly as well, backing up the previous statement that the water mist is mixing and cooling the upper layer. This was not intended to occur with the initial design.

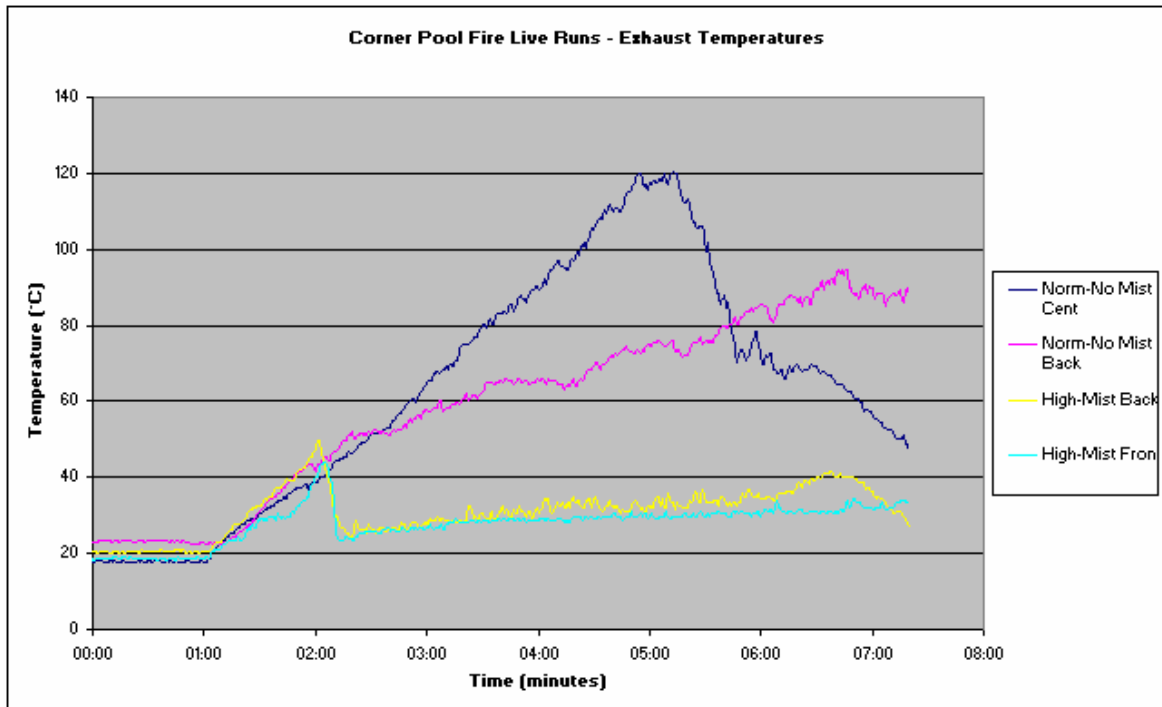


Figure 99 – Corner pool fire exhaust temperature readings

The final comparison performed related to the wood crib. The four fires modelled were a central floor pool fire low airflow (Norm-No Mist Pool), central floor crib fire low flow (Norm-No Mist Crib), central floor crib fire with displacement ventilation (High-Mist Crib) and a central floor with a sprinkler (Norm-Spk Crib).

Figure 100, Figure 101 and Figure 102 show the comparison between these test runs. The first observation is that the temperatures reached during a crib fire were much less than those recorded for a pool fire. The growth phase and duration of the crib fire was much longer as well.

In relation to the comparison between the crib runs, the results were similar to those observed with a pool fire. The displacement water mist and sprinkler both generated a rapid decrease in temperature within the compartment. One point that must be noted in this comparison though is that shortly after activation of the conventional sprinkler the fire was extinguished. This is not clearly shown in the temperature data which tends to suggest that the temperature remains constant. This is most likely due to the low airflow in the sprinkler test run. The low flow results in the warm atmosphere being exhausted slowly over a long period of time so the temperature data shows an elevated temperature for an extended period.

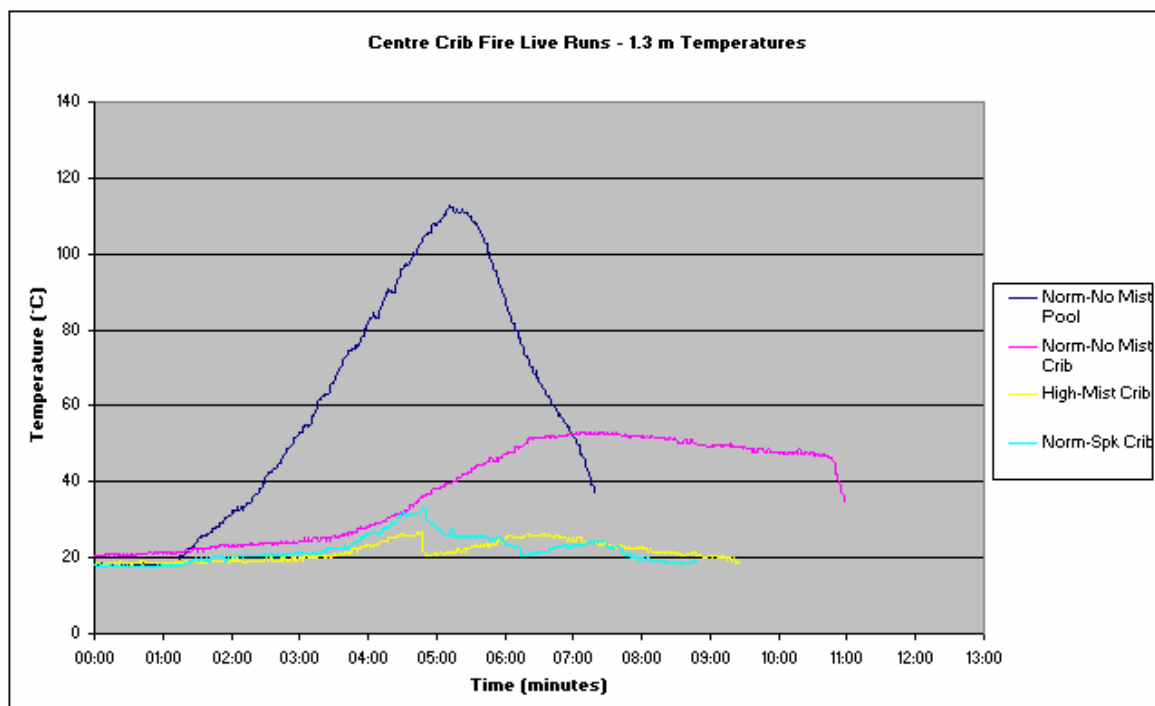


Figure 100 – Centre floor crib fire Tree 1, 1.3m temperature readings

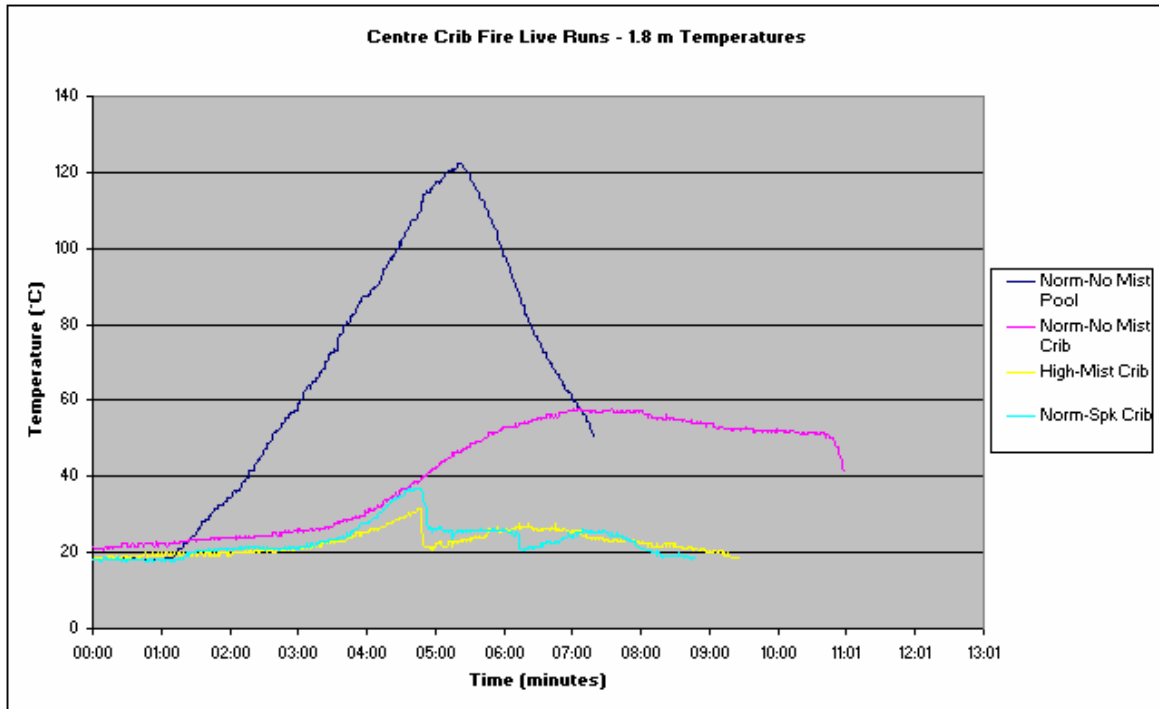


Figure 101 – Centre floor crib fire Tree 1, 1.8m temperature readings

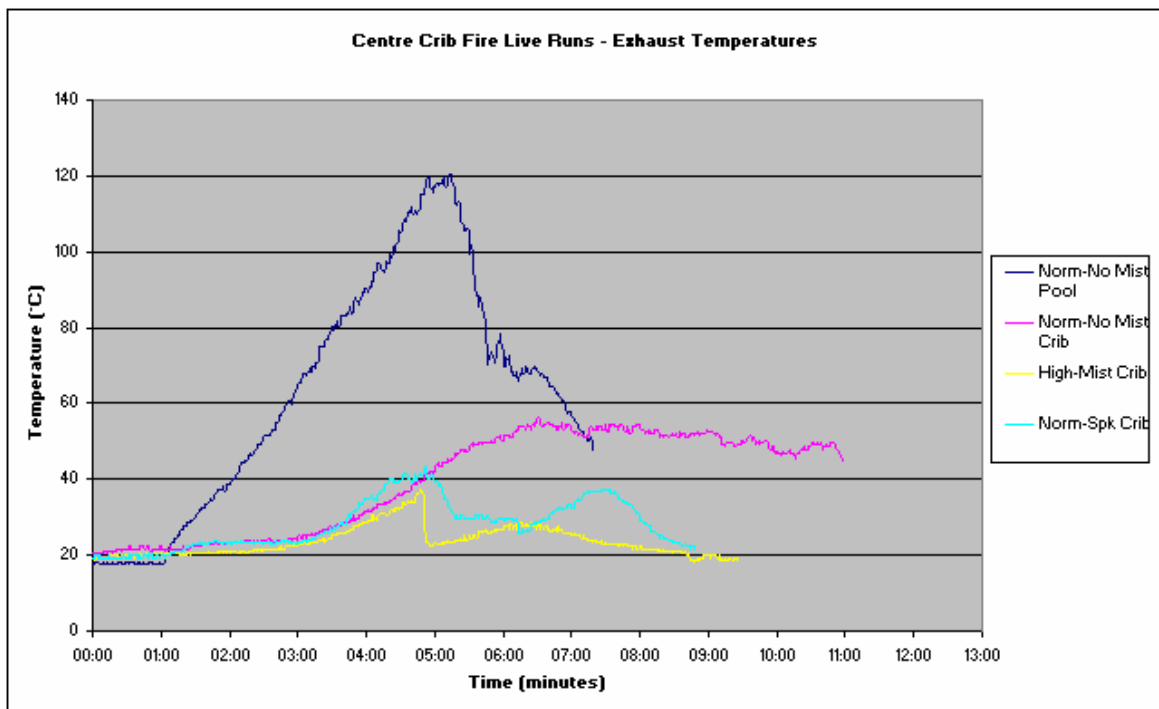


Figure 102 – Centre floor crib fire exhaust temperature readings

Looking at the temperature results in a global sense there is little difference between the water mist only and the displacement water mist. Furthermore the increase in temperature recorded at the sprinkler is only marginally above that of

the mist systems. What must be considered though is that only the displacement water mist system increases the airflow, removing a significant portion of the combustion gases from the compartment and making it far safer to inhabit as found in Run 17.

5.13 Conclusion

While the displacement water mist system did not appear to operate exactly as intended, the temperature readings and direct observations made during the tests suggest that the concept is valid but needs to be refined.

The type of water mist nozzles used in the experiment caused a high level of entrainment, which in turn caused mixing to occur between the upper and lower layers within the compartment. The high entrainment rate also affected the density of water within the air as it passed over the fires. Effectively the density of water was too low for suppression, and the increased airflow and turbulence increased the fire ferocity in some cases. There is also some debate as to whether the density of 200 g/m^3 was sufficient to cause suppression in the first place and that with such small fires a higher density of up to 600 g/m^3 would have been needed. Unfortunately this could not be investigated and will need to be studied in future work.

While not operating as intended the temperatures within the compartment were seen to drop rapidly when the displacement water mist system was activated. On all counts the temperatures recorded by the displacement water mist system were lower than that recorded by just the use of water mist or by the use of a conventional sprinkler.

Additionally the atmosphere within the compartment became breathable at all levels once the system was activated. In comparison, while not tested by the occupants, the atmosphere within the compartment using just water mist or a conventional sprinkler appeared to be far less tenable.

In relation to the effects on the computer and light bulbs within the compartment the conventional sprinkler and water mist only systems both caused the RCD to register an electrical short circuit and trip. The displacement water mist system did not cause the RCD to trip even after repeated operation.

6. FDS Simulations

This section of the report covers the investigation carried out on the proposed displacement water mist system using the computer simulation program FDS. The objectives of the simulations are outlined, followed by a general background on the various concepts and equations behind the FDS model. Finally the results of the test simulations outlined in section 4.2 are presented along with a discussion on these results.

6.1 Objective

The primary objectives of carrying out FDS computer simulations were to;

- Review the operation of the displacement ventilation system under normal conditions.
- Provide additional information on the internal characteristics of the compartment during displacement water mist operation.
- Provide results to compare against the live test runs.

6.2 FDS Background

As stated, this section of the report outlines the various concepts and equations behind the FDS model. It is only designed to give a brief overview and broad understanding of the mathematics behind the field model, the aim being to develop a familiarity with FDS. It is primarily based on a report presented by Nathaniel Petterson while attending the University of Canterbury [45]

Three main researchers performed the majority of work relevant to the FDS model. Hinze [46] describes the equations and theory behind turbulence, McGrattan et al [47] provided the actual equations used in FDS and Cox [48] who

provided the derivations and basic concepts for the conservation equations and turbulence modelling.

6.2.1 Hydrodynamic model

The general fluid dynamic equations used by FDS describing the transport of mass, momentum and energy can be used to describe a large array of physical processes, many of which have nothing to do with fire engineering. The base equations involved in the modelling process were modified to a simplified form that uses an approximate form of the Navier-Stokes equations for flow in a thermally expandable multi-component fluid [47].

This simplified form is achieved by filtering out acoustic waves to obtain “low Mach number” equations. They describe the low speed movement of gases driven by a chemical heat release and buoyancy forces. These equations allow for large variations in density and temperature but only small changes in pressure which are common in fire scenarios as they are carried out in open environments [49].

Four equations of conservation are central to the simplified form of the Navier-Stokes equations and are therefore outlined and discussed below. These equations cover conservation of mass, momentum, energy and species. In order to numerically solve the equations in FDS they are discretised in space using a 2nd order central difference method and in time using a 2nd order predictor-corrector scheme [47] [50].

Conservation of Mass

Conservation of mass simply states that the rate of mass storage in a control volume due to density changes is balanced by the rate of inflow of mass by convection [51]. If the density is constant then the equation simply states that what flows in must flow out [48]. The equation is written as:

$$\frac{\partial \rho}{\partial t} + \nabla \cdot \rho \mathbf{u} = 0$$

Equation 11: Conservation of mass

The first term describes the density changes with time and the second defines the mass convection where \mathbf{u} is the vector describing the velocity in the u , v and w directions.

Conservation of Momentum

The conservation of momentum equation is derived by applying Newton's second law of motion. Put simply this states that the rate of change of momentum of a fluid element is equal to the sum of the forces acting on it [48]:

$$\rho \left(\frac{\partial \mathbf{u}}{\partial t} + (\mathbf{u} \cdot \nabla) \mathbf{u} \right) + \nabla p = \rho \mathbf{g} + \mathbf{f} + \nabla \cdot \boldsymbol{\tau} \quad \text{Equation 12: Conservation of momentum}$$

The left hand side of this equation expresses the rate of change of momentum of a volume of fluid. The right hand side comprises the forces acting on it. These forces include gravity (\mathbf{g}), an external force vector (\mathbf{f}) (which represents the drag associated with sprinkler droplets that penetrate the control volume in this case) and a measure of the viscous stress ($\boldsymbol{\tau}$) acting on the fluid within the control volume. Typically gravity is the most important of these three forces as it represents the influence of buoyancy on the flow. The viscous stress ($\boldsymbol{\tau}$) is given by the product between the viscosity of the fluid and a measure of the velocities that the fluid volume is subjected to in a turbulent environment. This velocity term is derived from a deformation factor, which accounts for turbulence in the control volume. The viscosity term is calculated depending on the mode of simulation in FDS, which in turn depends on the user requirements or the grid resolution. Two modes are available in the FDS program being Large Eddy Simulation (LES) and Direct Numerical Simulation (DNS).

The LES mode is typically used where the grid resolution is not fine enough to capture all the relevant mixing processes. For these types of simulation the sub-grid analysis developed by Smagorinsky is used to model the viscosity [47]. This utilises the deformation factor mentioned above to arrive at a value for the local turbulent viscosity based on the fluid density, an empirical constant and a characteristic length which is in the order of the grid size used in the model. This turbulent viscosity is then used to calculate thermal conductivity and diffusivity for

the LES model [47]. In the case of the DNS mode the FDS model uses a set of different equations to directly model the diffusion. These equations are more complex than are to be covered in this report but these are outlined in detail in McGrattan et al, [47].

The equation for the conservation of momentum is simplified by utilizing various substitutions as well as assumptions concerning the sources of vorticity in the force terms to obtain a linear algebraic equation that can be solved quickly and directly in the model calculations using fast Fourier transforms [47].

Conservation of Energy

The equation for the conservation of energy can come in many forms and contain a large number of variables. In general this equation describes the balance of energy within a control volume [51]. In terms of fire simulations it accounts for the energy accumulation due to internal heat and kinetic energy as well as the energy fluxes associated with convection, conduction, radiation, the interdiffusion of species and the work done on the fluid by viscous stresses and body forces [48]. The form used in the FDS model is:

$$\frac{\partial}{\partial t}(\rho h) + \nabla \cdot \rho h \mathbf{u} - \frac{\partial p}{\partial t} + \mathbf{u} \cdot \nabla p = q''' - \nabla \cdot q_r + \nabla \cdot k \nabla T + \nabla \cdot \sum_I h_I (\rho D)_I \nabla Y_I$$

**Equation 13:
Conservation
of energy**

The left side of the equation describes the net rate of energy accumulation while the right side comprises the various energy gain or loss terms that contribute to this accumulation. These include the energy driving the system represented as the HRR (q'''), the radiative flux (q_r) and the convective term ($\nabla \cdot k \nabla T$). The last term represents the energy change associated with species interdiffusion.

Conservation of Species

Within a control volume the species must also be preserved. Equation 14 outlines the equation used in FDS to met this requirement:

$$\frac{\partial}{\partial t}(\rho Y_i) + \nabla \cdot \rho Y_i \mathbf{u} = \nabla \cdot (\rho D)_i \nabla Y_i + W_i^{\text{net}}$$

Equation 14: conservation of species

The first term on the left side represents the accumulation of species due to a change in density with the second term accounting for the general inflow and outflow of species. The right side gives the terms for the inflow or outflow of species from the control volume due to diffusion and the production rate of the particular species.

6.2.2 Combustion model

There are two types of combustion model used in the FDS program. The choice of model is dependent on the grid resolution used. DNS is used when the diffusion of fuel and oxygen can be modelled directly [47]. This applies when, as previously discussed, the grid size is very fine. For larger grid sizes a LES calculation is performed.

In terms of combustion LES assumes turbulent mixing of combustion gases with the surrounding atmosphere [47]. It therefore assumes that the mixing controls combustion and all species of interest can be represented by a single variable known as the mixture fraction (Z).

The mixture fraction is a quantity representing the fraction of material at a given location that originated as fuel [47], and is defined as:

$$Z = \frac{s Y_F - (Y_O - Y_O^{\text{inf}})}{s Y_F^f + Y_O^{\text{inf}}} \quad ; \quad s = \frac{v_O M_O}{v_F M_F}$$

Equation 15: Combustion

In this equation the value Z varies from 1 in a region containing only fuel, to 0 in a region where the oxygen mass fraction is equal to the ambient value, Y_O^{inf} .

This mixture fraction combustion model approximates the combustion process in both space and time so that the fire can be simulated more efficiently [49]. It assumes that large-scale convection and radiative transport can be modelled

directly while small scale mixing can be ignored [47]. An infinite reaction rate is assumed because the combustion processes are on a much shorter time scale than the convection processes. Put basically the reaction occurs so rapidly that both fuel and oxygen cannot coexist [52]. Consequently at the combustion mixture fraction both species instantaneously vanish, their mass fractions (Y_i) dropping to zero. Equation 15 can therefore be simplified to obtain the combustion mixture fraction (Z_f) at which this occurs:

$$Z_f = \frac{Y_o^{\text{inf}}}{sY_F^{\text{fi}} + Y_o^{\text{inf}}} \quad \text{Equation 16: Flame mixture fraction}$$

The value (Z_f) defines combustion and hence the flame location by prescribing a two-dimensional surface in the three-dimensional computational domain [49]. This is known as the flame sheet.

The assumption that fuel and oxygen cannot coexist can also be used to define the state relation between the oxygen mass fraction (Y_o) and the mixture fraction (Z):

$$Y_o(Z) = \begin{cases} Y_o^{\text{inf}} \left(1 - \frac{Z}{Z_f} \right) & Z < Z_f \\ 0 & Z > Z_f \end{cases} \quad \text{Equation 17: Mixture fraction}$$

The mass fractions of all other species of interest can also be described by individual state relations based on the mixture fraction. These state relations are determined by analysis of the stoichiometric reaction of the particular fuel in question. This is explained in more detail in Floyd et al [49]. Figure 103 represents the relations between the mixture fraction and the mass fraction (state relations) of various species for propane.

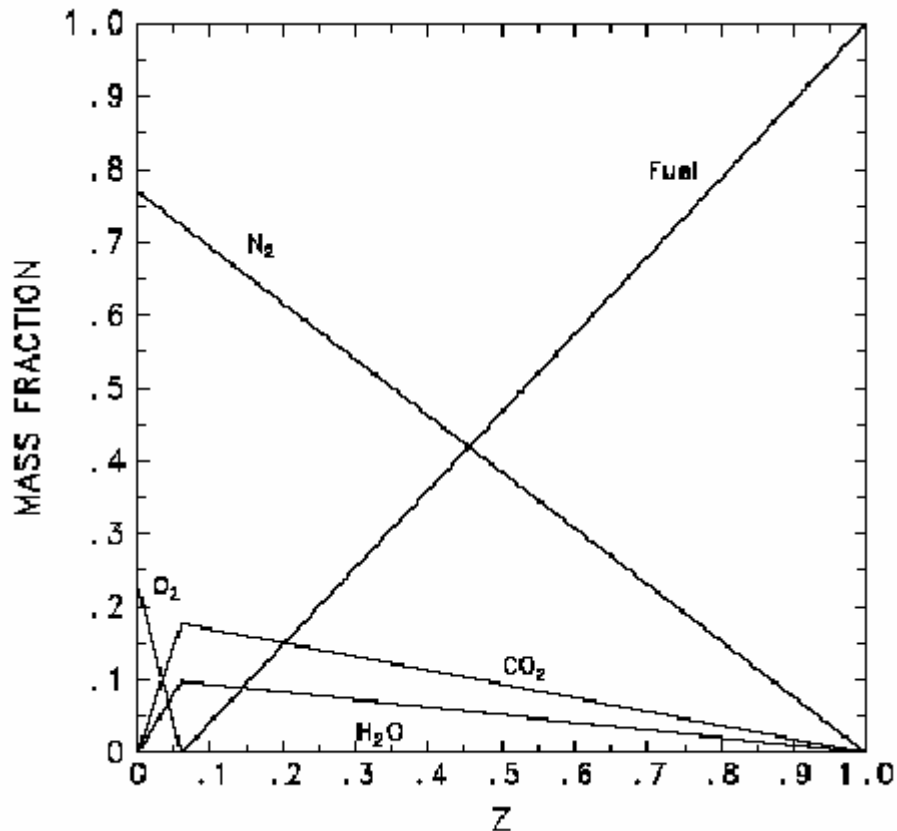


Figure 103 - State relations for propane [47]

With the local oxygen mass fraction known using Equation 17, its derivative with time can be used as a means of determining the oxygen consumption rate (\dot{m}''). This is then used to calculate the local HRR by multiplying it with the HRR per unit mass of oxygen (\dot{H}_o) [47]. They are not reproduced here, as only a general understanding of the FDS calculations is required in order to grasp the overall method of the model.

One problem that occurs due to the local HRR calculation procedure outlined above is that if the fire is not adequately resolved the flame surface defined by the mixture fraction $Z = Z_f$ will tend to underestimate the observed flame height. An indication of whether the fire is adequately resolved is given by the ratio $D^*/\delta x$. Where D^* is the characteristic fire diameter defined as:

$$D^* = \left(\frac{Q}{\rho_\infty C_p T_\infty \sqrt{g}} \right)^{\frac{2}{5}}$$

Equation 18: Characteristic fire diameter

It has been found that a better estimate of the flame height can be provided by using a different value for the mixture fraction (Z). The expression that is used to calculate this new mixture fraction ($Z_{f,eff}$) is:

$$\frac{Z_{f,eff}}{Z_f} = \min\left(1, C \frac{D^*}{\delta_x}\right) \quad \text{Equation 19: Effective mixture fraction}$$

Where C is an empirical constant that is independent of the scenario being simulated [47].

6.2.3 Thermal radiation model

Radiative fluxes within the control volume are computed with the modified finite volume method which is derived from the Radiative Transport Equation (RTE) for a non-scattering grey gas [49]. This equation relates radiation intensity to wavelength. A method similar to the finite volume method used in fluid flow is then used to solve this initial equation. [47]

One important change to the standard equations for the radiation intensity (I_b) needs to be made for the cells through which the flame sheet cuts. This is because in FDS the temperatures are averaged out across the cell and are therefore considerably lower than would be expected for a particular point in a diffusion flame. Because radiation is dependent on the fourth power of temperature this can have a significant impact on the calculated radiation from those particular grids. Elsewhere the temperature is calculated with greater confidence so the source term can assume its ideal value [47]. The radiation relations become:

$$\begin{array}{ll} \kappa I_b = \kappa \sigma T^4 / \pi & \text{Outside flame zone} \\ \chi_r q''' / 4\pi & \text{Inside flame zone} \end{array} \quad \text{Equation 20: Radiation relations}$$

Where q''' is the HRR per unit volume and χ_r is the local fraction of that HRR emitted as thermal radiation. This is not necessarily the same as the global radiative fraction due to re-absorption by smoke released from the fire. This is particularly the case for larger fires. κ is the local absorption coefficient and is

dependent on the mixture fraction and temperature. It is determined by a sub-model implemented in FDS called RADCAL [47].

6.2.4 Sprinkler interactions

The interaction of water droplets within the computational space is very complex as it involves cooling, radiation blocking, particle tracking and viscosity changes. This increases the processing time required significantly for a simulation. The actual calculation for water droplets involve a number of parts that are outlined below.

Sprinkler Droplet Size Distribution

At the initiation of a sprinkler, a sampled set of spherical water droplets is tracked from the sprinkler. In order to compute the droplet trajectories, the initial size and velocity of each droplet must be prescribed. This is done in terms of random distributions which must be defined for the sprinkler. Work by Factory Mutual [47] suggests that the distribution for an industrial sprinkler may be represented by a combination of log-normal and Rosin-Rammler distributions. The resulting general form of which is outlined in Equation 21 outlines.

$$F(d) = \begin{cases} \frac{1}{\sqrt{2\pi}} \int_0^d \frac{1}{\sigma d'} e^{-\frac{[\ln(d'/d_m)]^2}{2\sigma^2}} dd' & (d \leq d_m) \\ 1 - e^{-0.693(\frac{d}{d_m})^\gamma} & (d_m < d) \end{cases} \quad \text{Equation 21: Water droplet size}$$

Where d_m is the median droplet diameter and γ and σ are empirical constants defined for the relevant distribution. A full discussion of the generation of the droplet sets can be found in McGrattan et al [47]. Figure 104 shows a typical distribution that could be generated a commercial sprinkler.

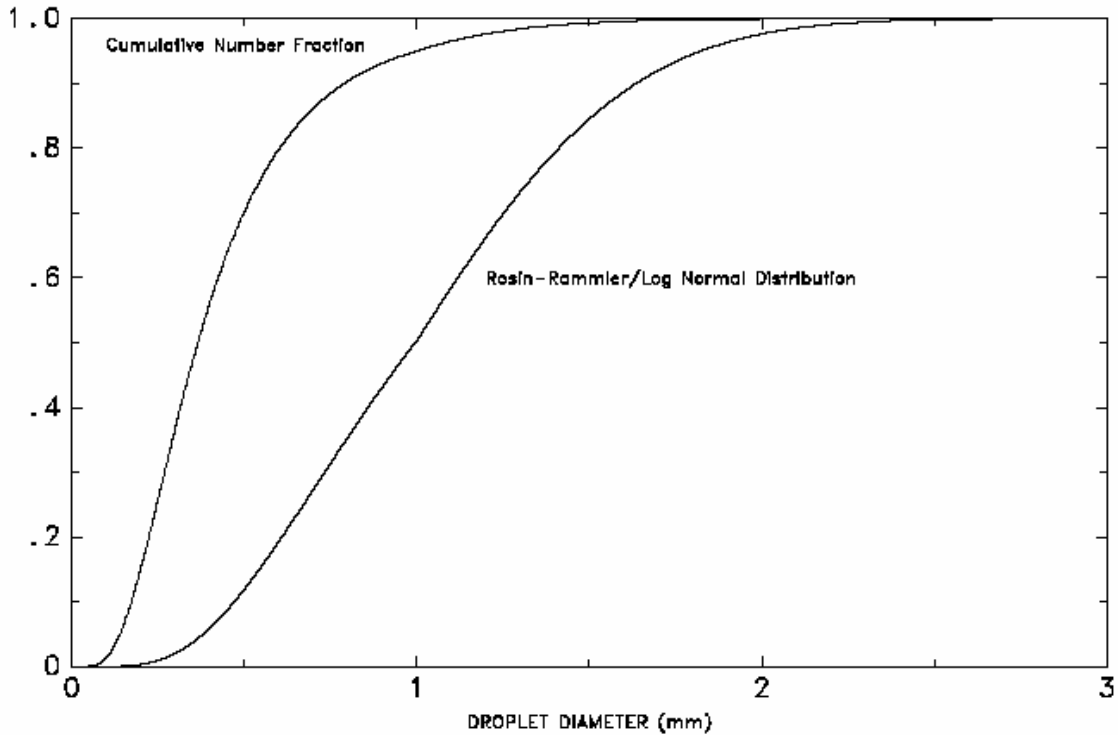


Figure 104 - Cumulative Volume Fraction and Cumulative Number Fraction functions of the droplet size distribution from a typical industrial-scale sprinkler.

Sprinkler Droplet Trajectory in Air

For a sprinkler spray, the force term \mathbf{f} in Equation 12 represents the momentum transferred from the water droplets to the gas. This is obtained by summing the force transferred from each droplet in a grid cell and dividing by the cell volume. The actual trajectory of an individual droplet is calculated based on its initial velocity and direction leaving the nozzle along with the forces that result as it passes through the control zone. These forces are given by:

$$\frac{d}{dt}(m_d \mathbf{u}_d) = m_d \mathbf{g} - \frac{1}{2} \rho C_D \pi r_d^2 (\mathbf{u}_d - \mathbf{u}) |\mathbf{u}_d - \mathbf{u}| \quad \text{Equation 22: drop trajectory}$$

Where m_d is the mass of the droplet and the drag coefficient (C_D) is a function of the local Reynolds number. The right hand term comprises of the force on the droplet due to gravity along with the drag force felt by the droplet. The left hand term gives the acceleration of the droplet caused by these forces. The drag coefficient changes in time and is calculated using Equation 23:

$$C_D = \begin{cases} 24/Re & Re < 1 \\ 24(1 + 0.15 Re^{0.687})/Re & 1 < Re < 1000 \\ 0.44 & 1000 < Re \end{cases} \quad \text{Equation 23: Particle drag}$$

$$Re = \frac{\rho |\mathbf{u}_d - \mathbf{u}| 2r_d}{\mu}$$

Mass and Energy Transfer from Droplets

The evaporation of droplet plays an important part in the simulation as effects the droplet path and available cooling. A water droplet suspended in air will evaporate as a function of the droplet equilibrium vapour mass fraction, the local gas phase vapour mass fraction, the heat transfer to the droplet, and the droplet's motion relative to the gas. Based on these parameters the following mass loss equation can be defined [47]:

$$\frac{dm_d}{dt} = -2\pi r_d Sh \rho D (Y_d - Y_g) \quad \text{Equation 24: Mass loss}$$

Where the term on the left gives the change in mass of the droplet based on the parameters listed above. In addition to calculating the mass transfer due to evaporation, the transfer of energy must also be calculated to determine the cooling effect that is occurring. The droplet heats up due to the convective heat transfer across the surface of the droplet minus the energy required to evaporate the water in the droplet. This energy balance is given in Equation 25:

$$m_d c_{p,w} \frac{dT_d}{dt} = A_d h_d (T_g - T_d) - \frac{dm_d}{dt} h_v \quad \text{Equation 25: Energy balance}$$

where the left hand term expresses the temperature increase within the droplet and the right hand terms give the convective heat gain and the evaporative heat loss respectively.

Interaction of Droplets and Radiation

The blocking of thermal radiation by water droplets is an important consideration, especially for water mist systems as discussed in section 2.8. As water droplets block thermal radiation through a combination of scattering and absorption the radiation-droplet interaction must be solved for both the radiation field and the droplet energy balance. If the gas phase absorption and emission are temporarily neglected for simplicity, the radiative transport equation becomes:

$$\mathbf{s} \cdot \nabla I_{\lambda}(\mathbf{x}, \mathbf{s}) = -[\kappa_d(\mathbf{x}, \lambda) + \sigma_d(\mathbf{x}, \lambda)]I(\mathbf{x}, \mathbf{s}) + \kappa_d(\mathbf{x}, \lambda) I_{b,d}(\mathbf{x}, \lambda) + \frac{\sigma_d(\mathbf{x}, \lambda)}{4\pi} \int_{4\pi} \Phi(\mathbf{s}, \mathbf{s}') I_{\lambda}(\mathbf{x}, \mathbf{s}') d\Omega' \quad (81)$$

Equation 26: Radiation transport

The exact variables in this equation result in the solving of the absorption and scattering of radiation over the range of wave lengths using the local droplet diameter and Mie theory. A full discussion of the radiation attenuation can be found in McGrattan et al [47].

6.3 Model Development

The first stage in simulating the compartment using FDS was the generation of an input file. This was carried out in two stages with a low resolution (large grid) run being performed first so that any errors in the input files could be altered before a high resolution (fine grid) simulation was run. The low resolution simulations, while giving relatively inaccurate answers, could be run in under 15 minutes in comparison to the 56 hours taken for a high resolution runs.

Rather than discuss all of the input files used in the FDS simulations, this section of the report outlines only the input files that were developed for a pool fire positioned at ground level, with the displacement water mist system operated after 60 seconds. The remainder of the simulations input files are very similar to this, but with relevant input calls removed or altered. All of the input files can be found in appendix 11.6.

The first line of the input file simply defines the make of the simulation and the name of the files in which output data will be placed. In this case the output data will be saved under the file 'Cent-Spkh' where the meaning of the name simply represents a sprinkler (water mist) run with a centre ground level fire with a high grid resolution. The writing to the right is not part of the input but is simply a description of the file.

```
&HEAD CHID='Cent-Spkh',TITLE='Cent-Spkh' /Centre fire G - low flow 60 sec then high  
flow + sprinklers activate
```

The following two lines outline the number of cells in the compartment and the size of the compartment. In this case GRID says that there will be 60 cells in the x direction, 48 in the y direction and 54 in the z direction. PDIM indicates that the compartment is 3m in length, 2.4m in width and 2.8m in height. Effectively this results in a cell size of 50 mm square. As can be seen the compartment is defined as higher than the 2.4m called for in the initial design. The height was extended so that a ceiling could be put in place allowing an opening to be formed and the exhaust gases observed. The ceiling is discussed further on.

```
&GRID IBAR=60,JBAR=48,KBAR=54 /  
&PDIM XBAR=3,YBAR=2.4,ZBAR=2.8 /
```

The next input simply outlined the length of time over which the simulation would be run. In this case the time was 400 seconds or 6.5 minutes based on the results of pool fires seen in the live tests.

```
&TIME TWFIN=400. / simulation time = 6.5 MIN,
```

Following the time the next input variables outlined the basic characteristics of the compartment. SURF_DEFAULT='PINE' simply states that the interior walls of the compartment will be made of and react like pine. The second line states that the reaction coming from the burner, discussed further on, is that of a Heptane flame. The third line tells the FDS simulation engine that the definitions of pine and Heptane can be found in the file called "database3" under the appropriate directory. The following two lines define the compartments initial temperature and the temperature of the temperature outside the computational domain.

```
&MISC SURF_DEFAULT='PINE',  
  
    REACTION='HEPTANE'  
  
    DATABASE_DIRECTORY='c:\nist\fds\database3\  
  
    TMPA=22./  
  
    TMPO=22./
```

The last general input call relates to the water mist injection and how it will be viewed in the computational domain. The first of the two lines states simply that the colour of the droplets will be related to their diameter. This was selected as it allowed the droplets to be viewed evaporating within the space. The DTSPAR=3 call sign specifies that viewable droplets will be injected at intervals of 3 seconds. 3 seconds was selected as it was found with the low resolution runs that high injection rates created a significantly more complex calculation and caused the processing time to increase. Additionally with a greater rate of injection the number of particles became very large and it became hard to distinguish the flow patterns within the compartment.

```
&PART QUANTITY='DROPLET_DIAMETER',  
  
    DTSPAR=3./
```

The first set of surface ID's related to the pool fire in the centre of the compartment. There are two methods of placing a fire within a compartment. The first is simply defining a HRR which FDS will generate and combust if possible. The second is by defining the heat of vaporisation of a fuel and allowing it to burn based on radiation feedback and convective heat gain. This second method is far more unstable as the grid resolutions used tend to create large errors. For this reason it was decided to use the first method of simply defining a HRR. The pool fire as defined as a burner having a heat release per unit area of 520 kW/m². This value was selected based on the size of the burner and the required heat release rate of 20 kW. As a 50 mm grid resolution was defined the burner had to be filled to this grid size and could not be specified as 160 mm as required in the live tests. It was decided for symmetry to increase the size to 200 mm square maintaining the heat output at 20 kW. Based on this size a HRRPU value of 500 is

theoretically required to generate 20 kW. During tests though it was found that with this value the resulting HRR was actually less than 20 kW due to FDS not being able to resolve the flame to a high enough accuracy. To account for this it was found that a value of 520 was required. This value, while theoretically giving 20.8 kW output actually generated 20 kW as required.

```
&SURF ID='BURNER',HRRPUA=520. /
```

The next surface ID related to the heat output of the occupant/light bulbs and the computer. For simplicity a standard heat release rate was specified of 1 kW/m² and the size of the obstacles adjusted for it.

```
&SURF ID='HOT',HEAT_FLUX=1./
```

The final surface ID related to the volume of air exiting from the displacement vent. As the flow increased after 60 seconds the flow had to be defined as a ramp, where by the volume of flow is defined by a percentage of maximum with time. As can be seen below the first line outlines that the variable is volume and that the maximum volume flow is 0.288 m³/s at a temperature of 19°C. The following lines simply outline the ramp where by at 0 seconds the flow is 0% of 0.288 m³/s. After 1 second it is increased to the normal operating flow of 16.6% of 0.288 m³/s or 0.048 m³/s. It continues at this rate to 60 seconds when over a period of 2 seconds it increases to the maximum flow of 0.288 m³/s.

```
&SURF ID='BLOW',VOLUME_FLUX=-0.288,TMPWAL=19.,RAMP_V='BLOW RAMP',/
```

```
&RAMP ID='BLOW RAMP',T= 0.0,F=0.0/
```

```
&RAMP ID='BLOW RAMP',T= 1.0,F=0.0/
```

```
&RAMP ID='BLOW RAMP',T= 2.0,F=0.166/
```

```
&RAMP ID='BLOW RAMP',T= 60.0,F=0.166/
```

```
&RAMP ID='BLOW RAMP',T= 62.0,F=1.0/
```

```
&RAMP ID='BLOW RAMP',T= 400.0,F=1.0/
```

With the surface ID's outlined the vents within the space had to be defined. The first of these vents was the supply air diffuser. This was defined using three

dimensional coordinates in the form of xx, yy and zz. In this case the vent lay on the 0 x-axis with edges at 0.9m and 1.5m on the y-axis and 0m and 0.5m on the z-axis. The supply from the vent was defined as BLOW and referenced the air supply defined above.

```
&VENT XB=0,0,0.9,1.5,0,0.5,SURF_ID='BLOW',T_ACTIVATE=1.
```

The second set of vents related to the roof space between 2.4m and the 2.8m defined as the computational space height. Effectively these vents removed the containment above 2.4m and allow the exhaust gases to escape.

```
&VENT XB=0,3,0,2.4,2.8,2.8,SURF_ID='OPEN'/ Roof
```

```
&VENT XB=0,3,0,0,2.45,2.8,SURF_ID='OPEN'/ Roof walls
```

```
&VENT XB=0,3,2.4,2.4,2.45,2.8,SURF_ID='OPEN'/ Roof walls
```

```
&VENT XB=0,0,0,2.4,2.45,2.8,SURF_ID='OPEN'/ Roof walls
```

```
&VENT XB=3,3,0,2.4,2.45,2.8,SURF_ID='OPEN'/ Roof walls
```

The final vent related to the burner and was defined as an obstacle with the burner “vent” on the top. The burner is placed in the middle of the compartment and coloured red.

```
&OBST XB=1.4,1.6,0.6,0.8,0,0.05,
BLOCK_COLOR='RED',SURF_IDS='BURNER','INERT','INERT'
```

The rest set of inputs relates to obstacles within the compartment. In this case the first set of obstacles relate to the ceiling within the space at 2.4. As the exhaust vent is present in the ceiling the compartment cannot be defined as one block, but must be made up of four leaving the vent space free. The finished effect can be seen in Figure 105.

```
&OBST XB=0,3,0,1,2.4,2.45,BLOCK_COLOR='YELLOW',/ Roof1
```

```
&OBST XB=0,3,1.4,2.4,2.4,2.45,BLOCK_COLOR='YELLOW',/ Roof2
```

```
&OBST XB=0,.6,1,1.4,2.4,2.45,BLOCK_COLOR='YELLOW',/ Roof3
```

```
&OBST XB=1,3,1,1.4,2.4,2.45,BLOCK_COLOR='YELLOW',/ Roof4
```

The second set of obstacles related to the two occupants and the computer. These were positioned within the compartment in the same positions as in the live tests and as outlined in section 4.4. The size of the objects was determined by the required area to give the output of the load based on surface with a 1 kW/m² output. In the case of the occupants this was 100 W or 0.1m² each, with the computer being 150 W or 0.15m².

```
&OBST      XB=1,1.1,1.15,1.25,0.8,1,BLOCK_COLOR='MAGENTA',SURF_ID='HOT'/
Person 1
```

```
&OBST      XB=2,2.1,1.15,1.25,0.8,1,BLOCK_COLOR='MAGENTA',SURF_ID='HOT'/
Person 2
```

```
&OBST      XB=1.45,1.6,1.15,1.3,1.05,1.2,BLOCK_COLOR='CYAN',SURF_ID='HOT'/
Computer
```

The final set of inputs required for the simulation was that of the water mist nozzles. These were specified in the same location as that outlined in section 5.8 using the XYZ definition. They were then positioned so that the water was expelled in a horizontal direction by defining the ORIENTATION as positive x. The activation time of the nozzles was defined at 60 seconds rather than based on temperature so that they operated in sequence with the increase in airflow from the supply diffuser and the results corresponded to the live tests were a fixed timeline was used.

```
&SPRK      XYZ=0.05,1.0,0.4,MAKE='mist',ORIENTATION=1,0,0,T_ACTIVATE=60.  /
Sprinkler 1
```

```
&SPRK      XYZ=0.05,1.2,0.5,MAKE='mist',ORIENTATION=1,0,0,T_ACTIVATE=60.  /
Sprinkler 2
```

```
&SPRK      XYZ=0.05,1.4,0.4,MAKE='mist',ORIENTATION=1,0,0,T_ACTIVATE=60.  /
Sprinkler 3
```

```
&SPRK      XYZ=0.05,0.9,0.25,MAKE='mist',ORIENTATION=1,0,0,T_ACTIVATE=60.  /
Sprinkler 4
```

```
&SPRK      XYZ=0.05,1.2,0.25,MAKE='mist',ORIENTATION=1,0,0,T_ACTIVATE=60.  /
Sprinkler 5
```

```
&SPRK XYZ=0.05,1.5,0.25,MAKE='mist',ORIENTATION=1,0,0,T_ACTIVATE=60. /
Sprinkler 6
```

This positioned the water mist nozzles but did not define the water spray generation characteristics. Within FDS sprinklers characteristics such as droplet size and flow rate must be defined. This is carried out in a separate file that the FDS simulation engine refers to. In this case the name of the file was 'mist'. The file used is outlined below.

```
MANUFACTURER
QuickMist
MODEL
mist
OPERATING_PRESSURE
5
K-FACTOR
0.268
OFFSET_DISTANCE
0.05
SIZE_DISTRIBUTION
1
20 4
VELOCITY
1
0. 50. 8.0
```

The initial inputs simply refer to the manufacturer and model of the nozzle. The next definition is the operating pressure defined at 5 Bar to be the same as those used in the live tests. The K-factor is next defined, and is in this case calculated based on the flow that was required. The formula used is shown in Equation 27.

$$Q = K \cdot \sqrt{\text{pressure}} \quad \text{Equation 27: Nozzle water flow}$$

Where Q is l/min. Based on 6 nozzles, a total flow rate of 3.435 l/min and an operating pressure of 5 bar the resulting K value is 0.268.

After the K factor, the offset distance is defined as the point where the droplets have all initialised and broken up. As the nozzle was high pressure it was assumed that the water droplets had already broken up.

The size distribution relates to the size of the water droplets formed by the sprinkler. 20 represents the median value of 20 μm , while 4 refers to the distribution discussed in section 6.2.4. The larger the number the less the distribution spread of droplet sizes. As an example a standard sprinkler has a value of 2.4. As the water mist nozzles create less of a spread than this due to the limited fine size, it was decided that this should be increased to 4. It should be noted that this is an estimated figure as no actual data is available for the spread actually created by the quick mist nozzles. The final sprinkler definition relates to the spray angle and speed at which the water droplets are expelled. The 1 tells the FDS simulation engine to read the following line in a particular order. In this case the first two numbers 0 and 50 represent the angle through which the spray is distributed. Effectively these numbers define the spray in a solid cone with a 50° angle from the normal vector. The final figure refers to the speed of the leaving droplet. Again in this case no actual data was available so an estimate of 8 m/s was used.

In relation to the main file this concluded the general inputs and operation of the compartment. All that remained was to define the outputs that were required. Of primary interest was the thermocouple positions. These we defined as specified in section 4.9 and located using the xyz coordinates. The sample time for these thermocouple points was defined as 1 second using the DTSAM call. A typical thermocouple point is shown below. This represents the point for the 0.3m high sensor located in the front corner.

```
&THCP QUANTITY='TEMPERATURE', XYZ=0.1,0.1,0.3,LABEL='Corner 1 Temp - 300',  
DTSAM=1. /
```

A number of other outputs were generated from each simulation including slice files of temperature, oxygen concentration and water vapour. The FDS calls used for these can be seen in the input files included in appendix 11.6.

This completed the basic FDS input file and only slight modifications were made for each simulation. A picture of the final result can be seen in Figure 105. The ceiling obstacles are seen in yellow, the burner in red, supply diffuser brown and with the water mist nozzles and thermocouple points as red and yellow dots respectively.

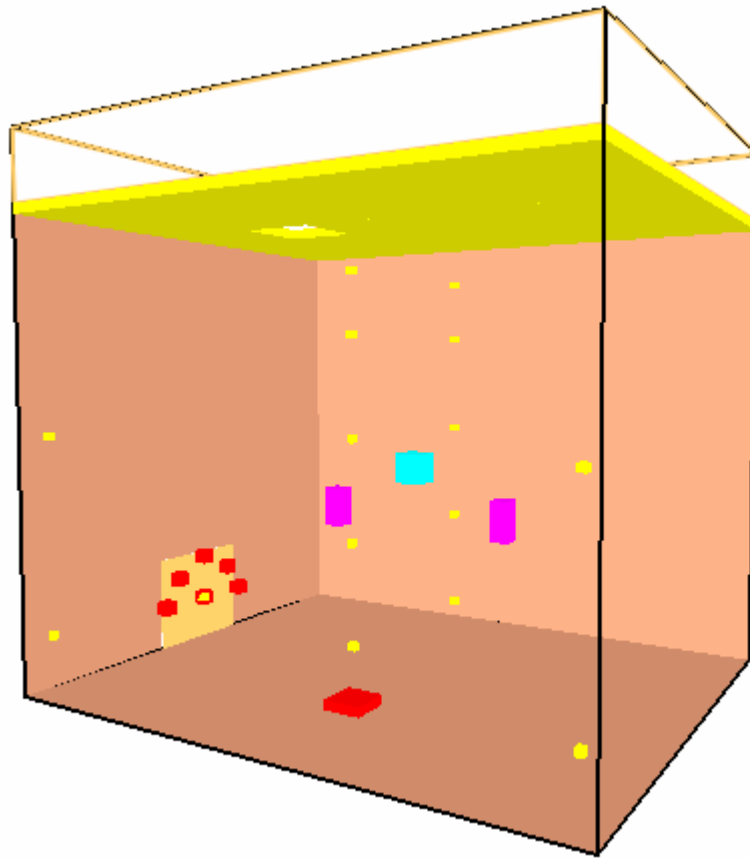


Figure 105 - Base FDS compartment

6.4 Simulation Results and Discussions

This section of the report describes each of the FDS simulation runs carried out for this study. It presents the results and gives a general overview of particular characteristics observed from the simulations. It does not delve into the specifics of the results as the base concepts and results are similar to those found under live testing.

6.4.1 Test 1: Normal Operation

<u>Fire Location:</u>	No Fire
<u>Fire Type:</u>	N/A
<u>Airflow Characteristics:</u>	Constant low flow operation.
<u>Suppression:</u>	None.
<u>Objectives:</u>	To determine the conditions within the compartment under normal operating conditions.

Observations:

The objective behind this simulation was simply to review the operation of the displacement ventilation system and allow a better understanding of the internal compartment airflows. This was carried out by simulating the compartment under normal conditions with no fire and constant low airflow. The results were as expected with the cool supply air spreading across the bottom of the compartment and the internal heat loads heating the air within the compartment to create thermal stratification. A view of the temperatures within the compartment is shown in Figure 106.

Graphical Data:

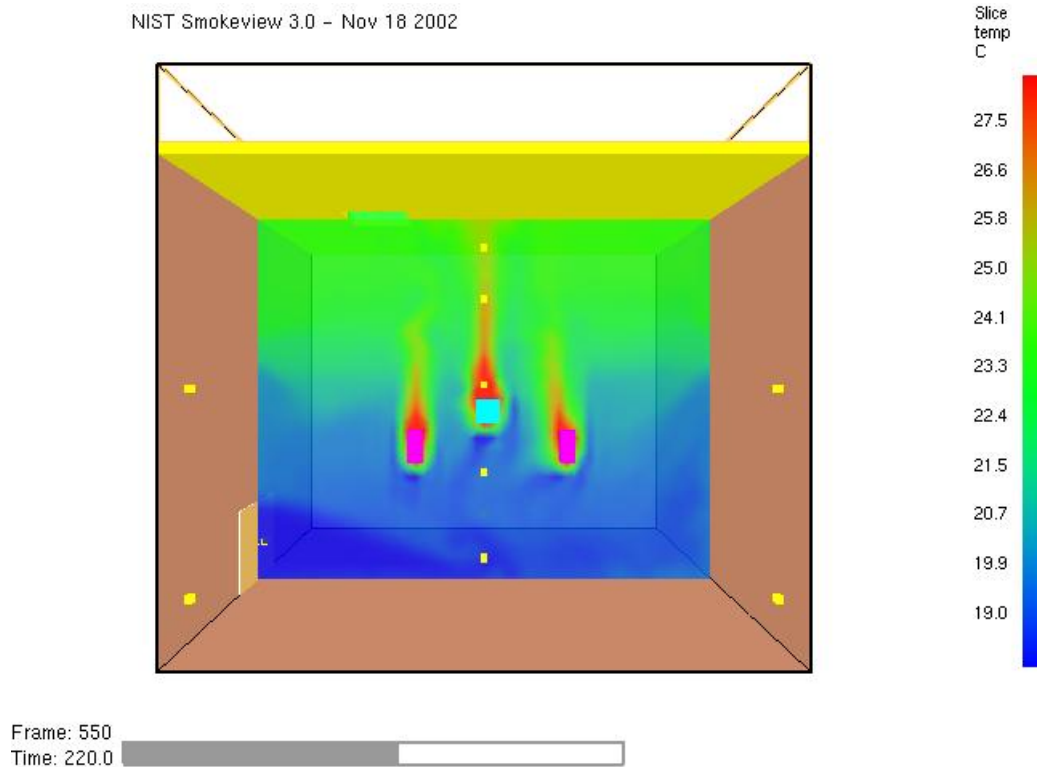


Figure 106 – Simulation 1: Compartment temperature profile under normal operation

6.4.2 Test 2: Ground Central Fire Under Normal Operation

<u>Fire Location:</u>	Centre of compartment at ground level.
<u>Fire Type:</u>	Heptane pool fire.
<u>Airflow Characteristics:</u>	Constant low flow operation.
<u>Suppression:</u>	None.
<u>Objectives:</u>	To determine the conditions within the compartment subjected to a pool fire under normal operating conditions with no suppression and normal flow.
<u>Observations:</u>	

The simulation was used to generate the conditions within the compartment under normal conditions with a central ground level pool fire.

Above the fire, the temperatures recorded were very high as expected and suggested that the fire plume was rising vertically and not being effected by the

supply airflow. They remained relatively constant throughout the simulation. The results recorded at the thermocouples tree above the fire can be seen in appendix 11.7 along with all of the thermocouple results from the simulations. Figure 107 shows the same information but in the form of a snap shot taken from the FDS simulation. It shows the fire at 30 seconds with, as discussed, a near vertical rise on the plume and flame. The white surface represents the theoretical smoke layer and the red surface shows the position of the flame front. As can be seen by this time the smoke layer within the compartment is predicted to have dropped significantly.

As seen in the live tests the temperatures recorded during the simulation at Tree 1 increased as the fire proceeded. The upper level sensor increased first as the warm combustion gases accumulated at the roof. As the upper layer became larger the layer height dropped and the sensors lower in the compartment began to increase in temperature. These results can be seen in Figure 108.

This same increase in temperature associated with the upper layer dropping can be seen in Figure 109, Figure 110 and Figure 111. These show the temperature profile within the compartment at Tree 1 or the occupant position. As can be seen the upper layer quickly forms and heat builds up in the upper layer. As the layer drops warm air is entrained into the plume and hence the effective plume temperature increases. This in turn increases the temperature within the upper layer. Another observation from these graphs is that the boundary between the upper and lower layers is relatively clear.

While it was observed that the airflow within the compartment was relatively stable, it could be seen that the exhaust air leaving the roof vent did not rise vertically. This is seen in Figure 112. As can be seen the flow from the roof vent tends to be pushed towards the front of the compartment. It is most likely due to the position of the fire creating a tangential velocity across the roof combined with the general airflow path within the compartment created by the position of the supply air diffuser.

Graphical Data:

NIST Smokeview 3.0 - Nov 18 2002

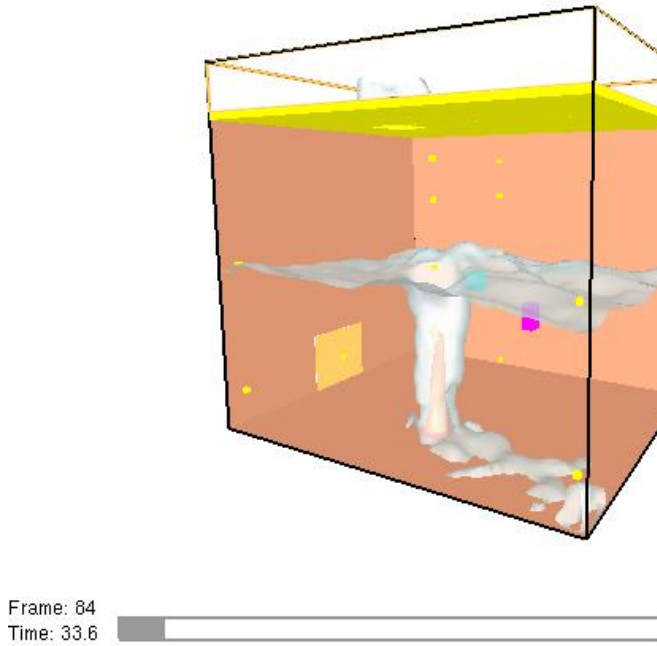


Figure 107 - Simulation 2: Flame and smoke surfaces

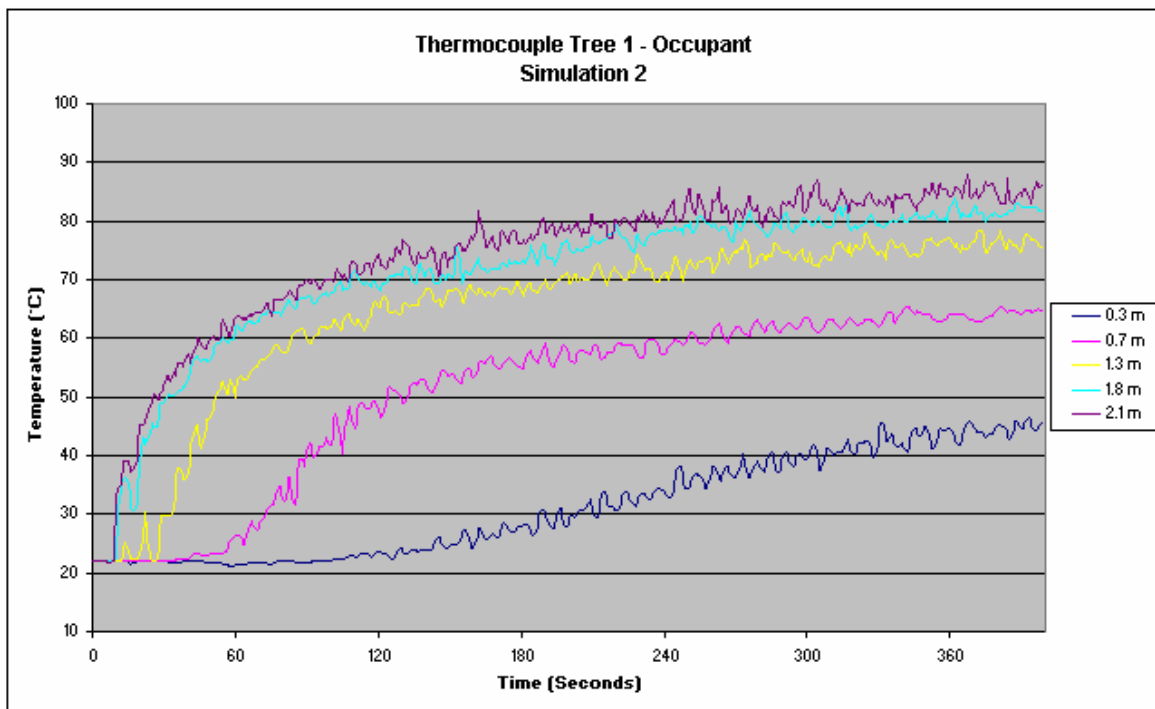


Figure 108 - Simulation 2: Occupant Thermocouple Tree

NIST Smokeview 3.0 - Nov 18 2002

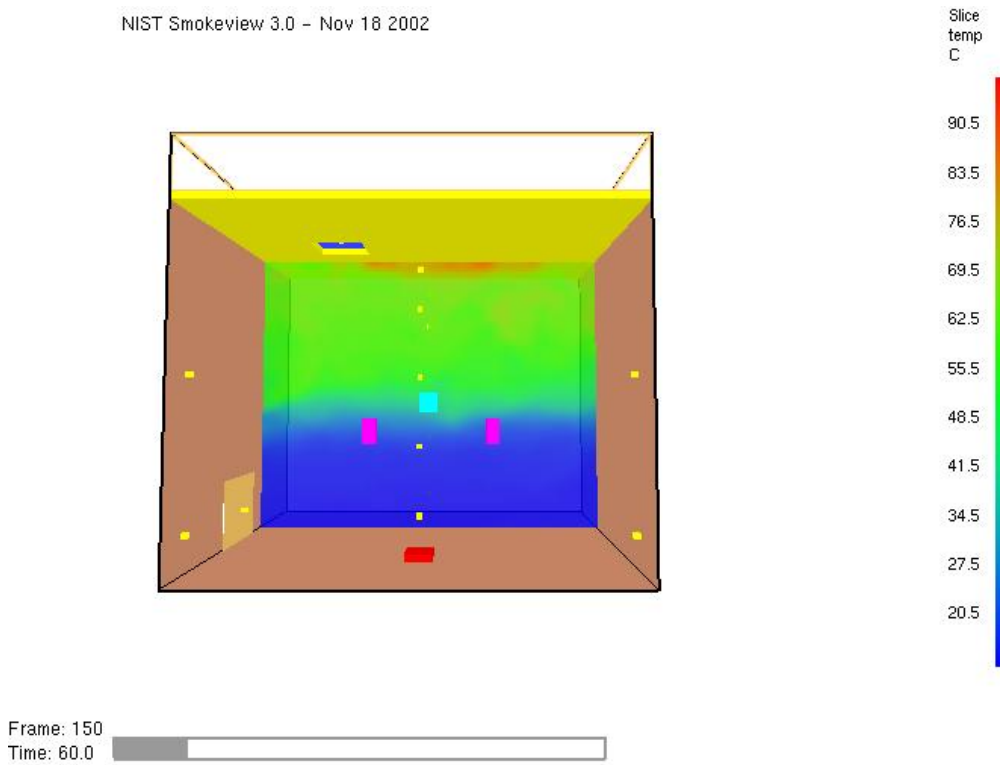


Figure 109 - Simulation 2: Occupant temperature at 60 sec

NIST Smokeview 3.0 - Nov 18 2002

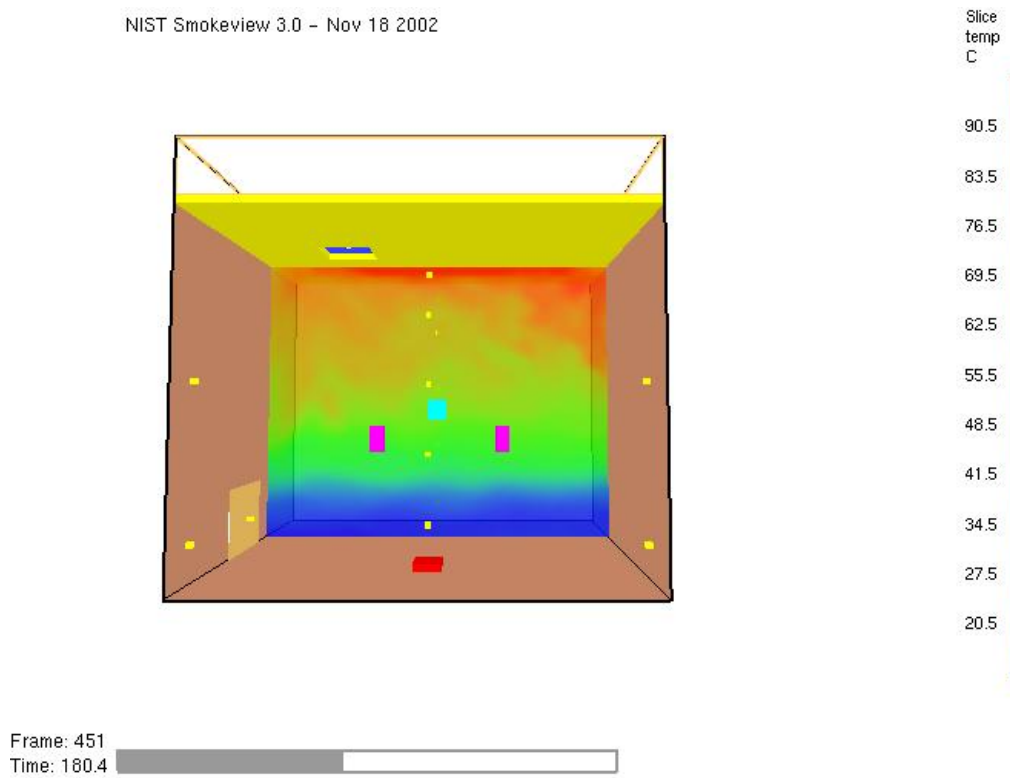


Figure 110 - Simulation 2: Occupant temperature at 180 sec

NIST Smokeview 3.0 - Nov 18 2002

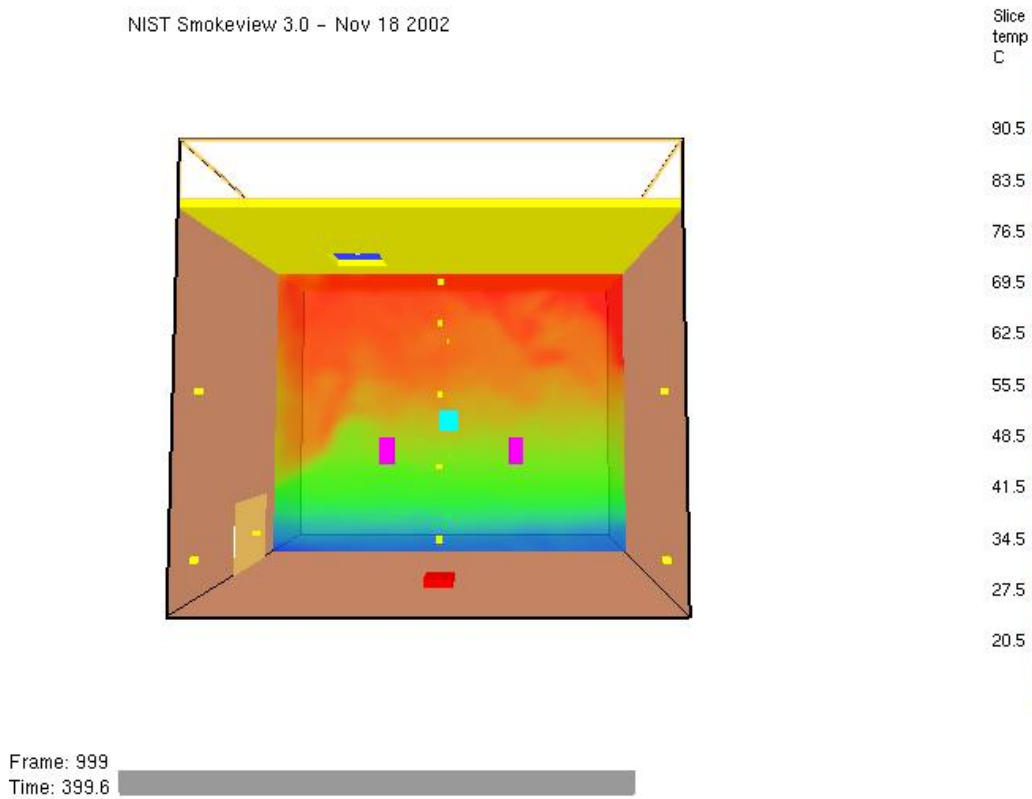


Figure 111 - Simulation 2: Occupant temperature at 400 sec

NIST Smokeview 3.0 - . Norm-Fireh 0180 01.a

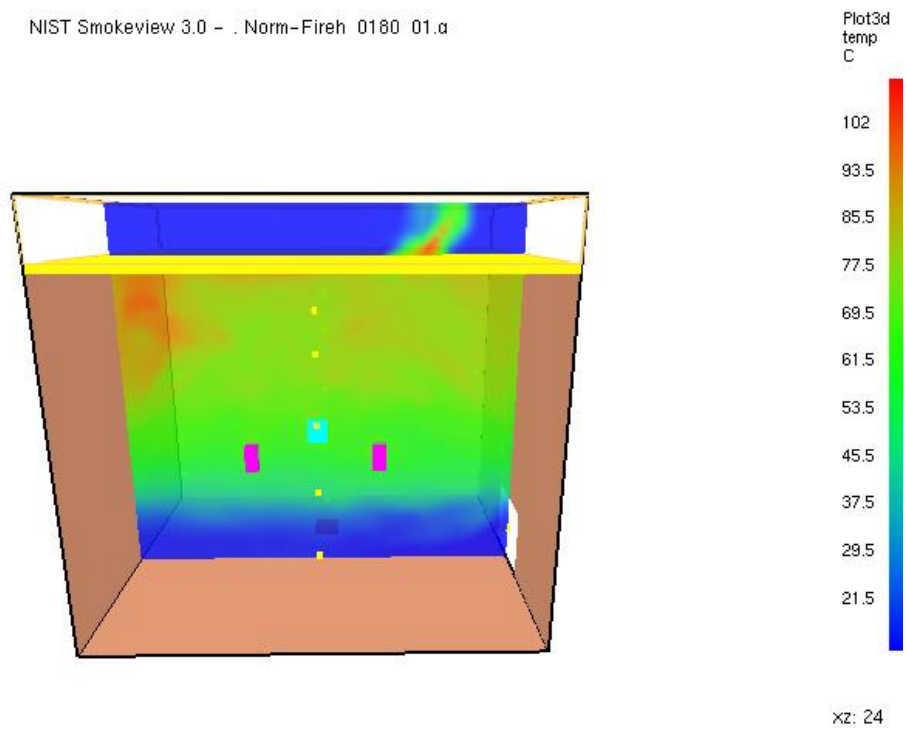


Figure 112 - Simulation 2: Roof exhaust duct

6.4.3 Test 3: Ground Central Fire with High Airflow Only

<u>Fire Location:</u>	Centre of compartment at ground level.
<u>Fire Type:</u>	Heptane pool fire.
<u>Airflow Characteristics:</u>	Low flow operation for 60 seconds followed by high flow operation.
<u>Suppression:</u>	None.
<u>Objectives:</u>	To determine the conditions within the compartment subjected to a pool fire when the supply airflow is increased but no suppression is added.

Observations:

As the airflow was increased the temperatures within the compartment rapidly dropped as the hot upper layer was exhausted at a greater rate. This drop can be clearly seen in Figure 113 which shows the temperatures taken at thermocouple Tree 1. An interesting point to note from this graph is that when the airflow is increased the temperatures recorded by the upper level sensors decreases significantly while the lower level sensors show little change. In fact the 0.7m sensor begins to rise at this point suggesting that a certain level of mixing is occurring at the interface. This can be more clearly seen in Figure 114 and Figure 115 which show a cross section of the temperature within the compartment at 60 seconds and 120 seconds consecutively. These times correspond to just before the airflow is increased and 60 seconds after the airflow is increased. As can be seen in Figure 114 the upper layer is relatively well defined, while in Figure 115 the layer appears to have dropped slightly and the interface layer is less well defined. This is most likely due to turbulence introduced into the compartment from the increased airflow. Comparison between these two figures also shows that the temperature drops markedly in the upper layer 60 seconds after the airflow is increased.

In relation to the increased turbulence within the compartment, Figure 116 shows the flame and smoke front after the high airflow has been initiated. As can be seen the flame is pushed over and the smoke plume is rising more turbulently and on an angle. The smoke interface can also be seen to be less stable and is fluctuating more across the compartment. This also explains why the temperature

readings taken from the sensors above the fire show a rapid drop as the airflow is increased. Effectively the increased airflow pushes the fire plume away from the thermocouple tree causing the sensors to record the compartment temperature rather than the plume temperature. The graph of data recorded from Tree 2 can be seen in appendix 11.7.

The velocities created within the compartment are important as one of the primary objectives of the system is to maintain a clear lower layer environment for the occupants. If the mixing becomes too large then the combustion products contained in the upper layer will mix with the clear lower layer. Figure 117 shows a cross section of the velocity profile within the compartment with a low airflow. As can be seen with a low airflow the centre of the compartment is relatively stable. Air movement is most prominent near the roof due to the presence of the upper layer and ceiling jet created by the fire. In relation to the velocities created by the fire, the inlet air supply velocity is relatively minimal. It can be seen flowing from the supply diffuser and spreading across the floor.

Figure 118 show the same cross section within the compartment but at high airflow. As can be seen the turbulence within the compartment is much greater. In particular the increased airflow from the supply diffuser can clearly be seen affecting almost the entire width of the compartment at low level. An increased velocity is also appreciable on the back wall and the ceiling, as it appears that a circular flow pattern was created within the compartment. An interesting point to note though is that while some circulation appears to be occurring, the velocities at the front of the compartment and centre are not high, suggesting that the upper layer is not being drawn down and mixing with the lower layer.

Graphical Data:

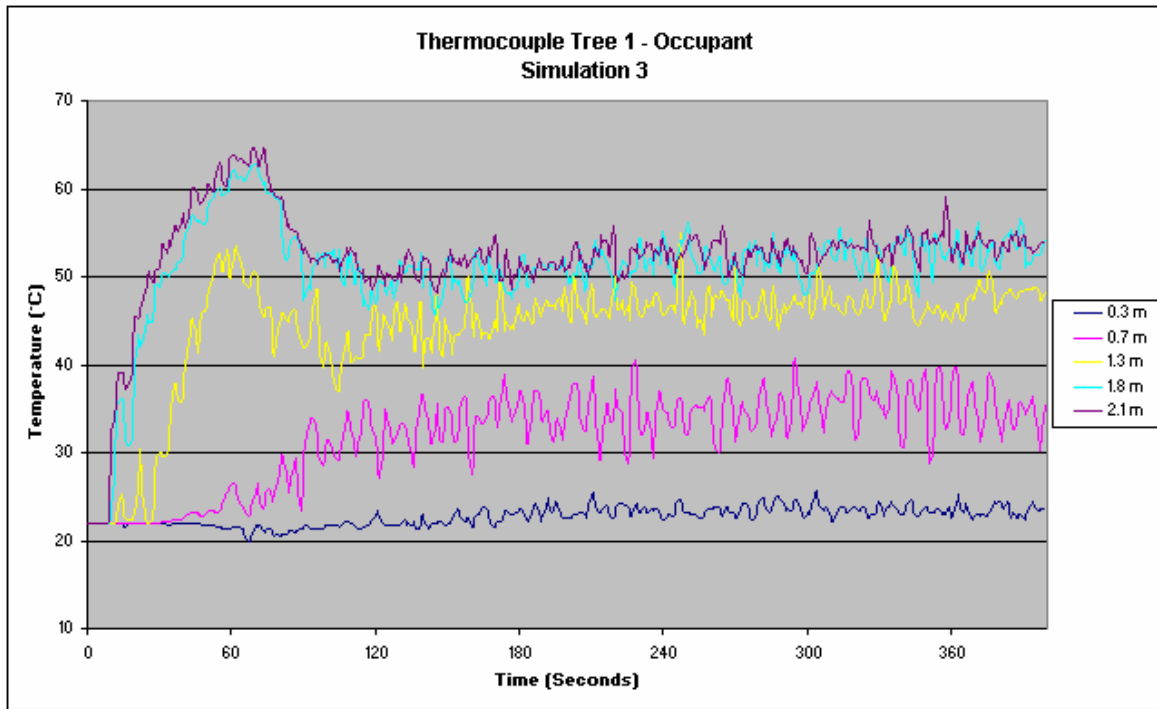


Figure 113 - Simulation 3: Occupants Thermocouple Tree

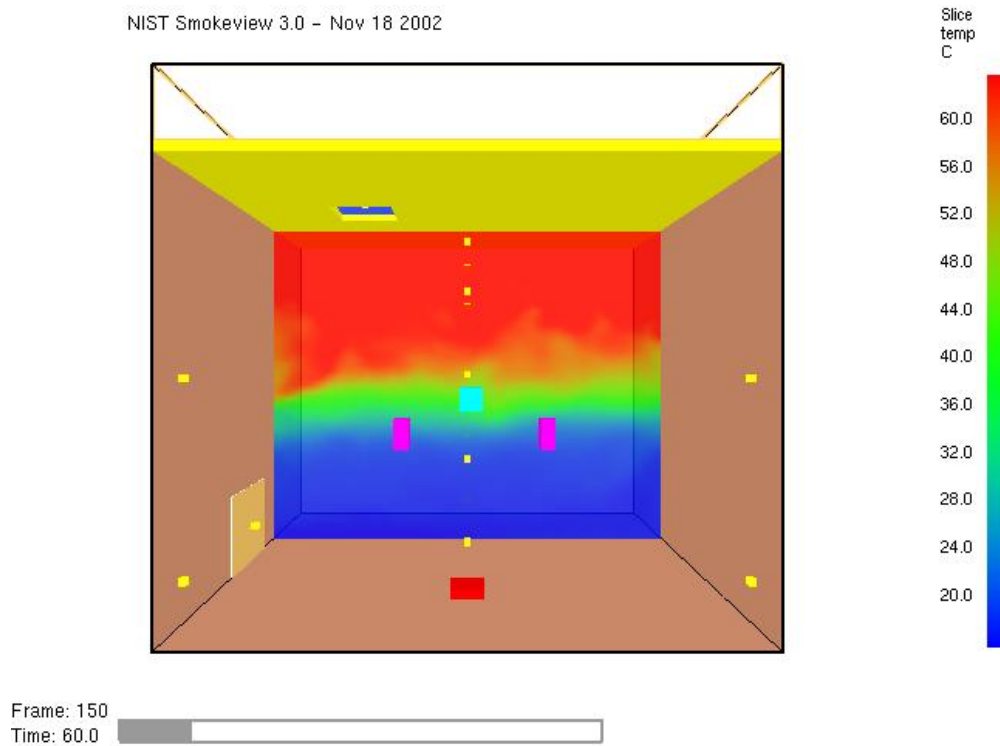
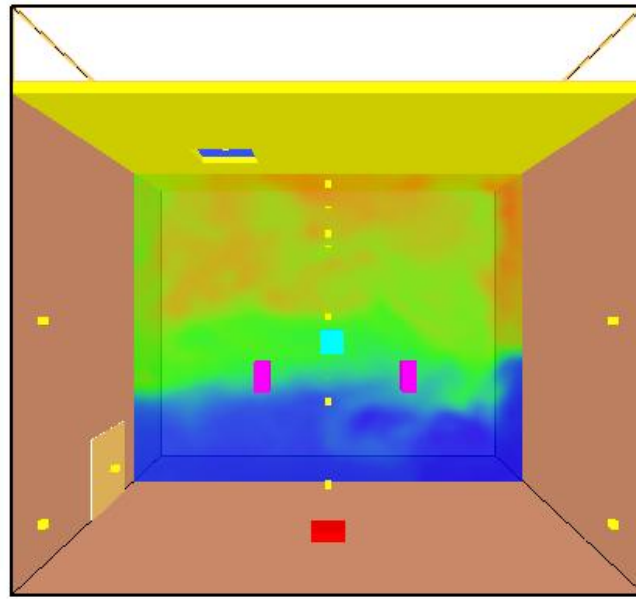


Figure 114 - Simulation 3: Occupant temperature profile at 60 sec

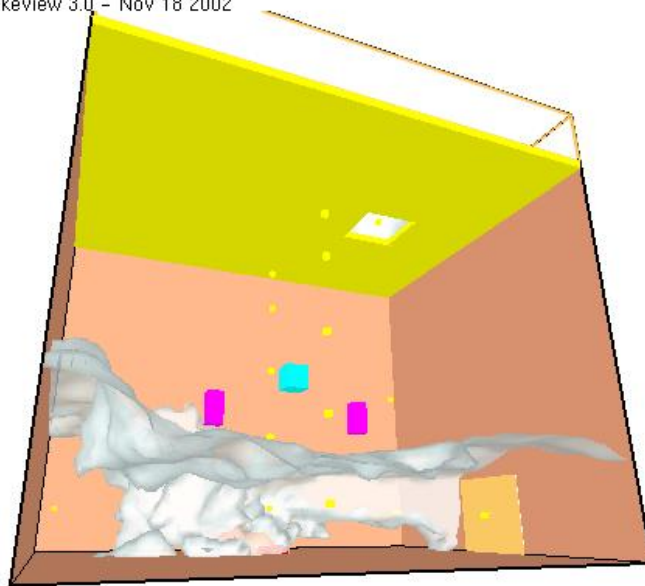
NIST Smokeview 3.0 - Nov 18 2002



Frame: 300
Time: 120.0

Figure 115 - Simulation 3: Occupant temperature profile at 120 sec

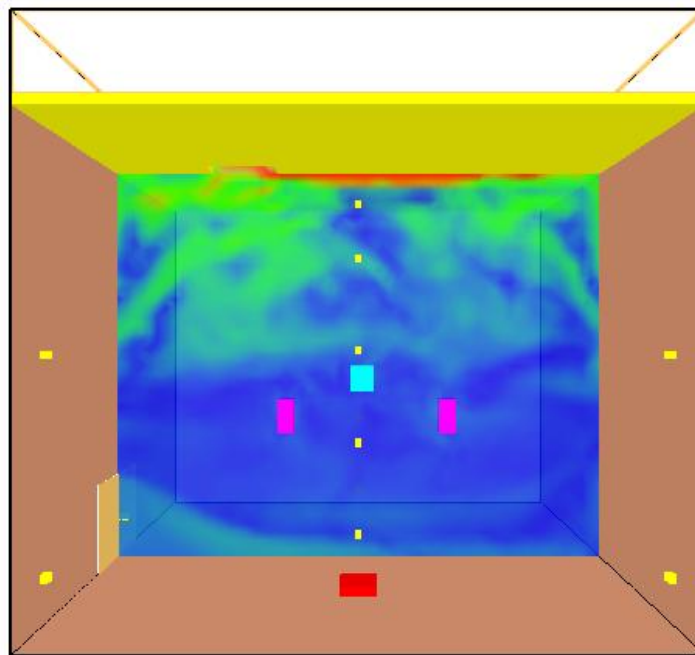
NIST Smokeview 3.0 - Nov 18 2002



Frame: 777
Time: 310.8

Figure 116 - Simulation 3: Airflow effected flame and smoke front

NIST Smokeview 3.0 - . High-Fireh 0060 00.a



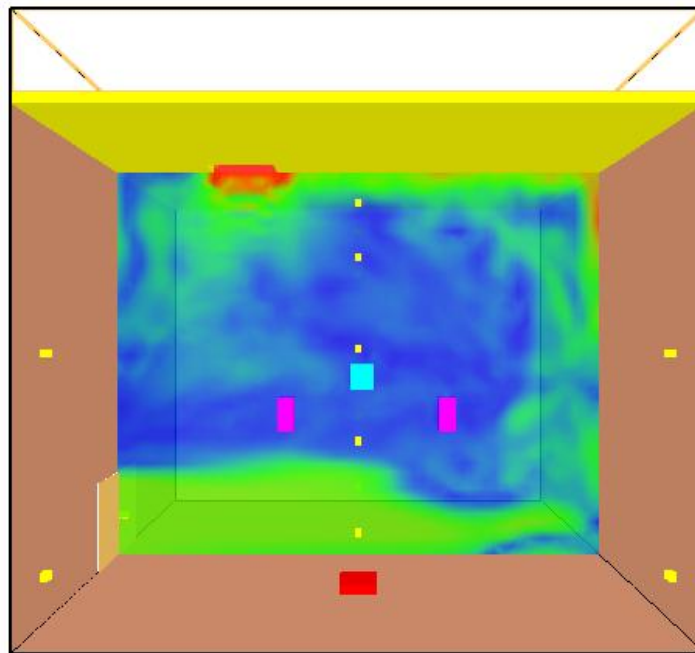
Plot3d
Speed
m/s



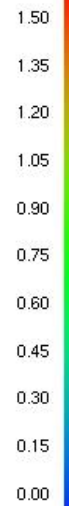
xz: 24

Figure 117 - Simulation 3: Velocity within compartment at low flow

NIST Smokeview 3.0 - . High-Fireh 0120 00.a



Plot3d
Speed
m/s



xz: 24

Figure 118 - Simulation 3: Velocity within compartment at high flow

6.4.4 Test 4: Ground Central Fire with High Airflow and Water Mist

<u>Fire Location:</u>	Centre of compartment at ground level.
<u>Fire Type:</u>	Heptane pool fire.
<u>Airflow Characteristics:</u>	Low flow operation for 60 seconds followed by high flow operation.
<u>Suppression:</u>	Water mist at 60 seconds.
<u>Objectives:</u>	To determine the conditions within the compartment subjected to a ground level pool fire, under the operation of the displacement water mist system.

Observations:

As was seen in the live testing, the temperatures within the compartment rapidly dropped with the initiation of the water mist and high airflow. This can be clearly seen in Figure 119, which shows the temperatures recorded by thermocouple Tree 1. When the system is set to fire mode all of the sensors show a rapid decrease in temperature. This includes the 0.3m sensor which had not displayed a temperature increase yet. The cause for this is most likely the cold water mist. As the cold water interacts with the air at this level it cools it down resulting in the temperature decrease recorded at the 0.3m sensor.

Figure 120 shows a slice file taken just after the system has been set into fire mode. The particles are the water mist droplets that have been injected into the computational space, while the coloured cross section represents the volume of water vapour. As can be seen by the position of the droplets and the green colouring of the water vapour cross section, the water mist radiates out from the nozzles with the majority travelling in a horizontal direction, but with a significant component travelling with a vertical velocity. This would indicate that this could cause significant mixing between the upper and lower layers.

The mixing that is caused can be seen to be significant by looking at Figure 121 which shows a velocity vector cross section of the compartment with the mist nozzles activated. As can be seen there is significant velocity throughout the compartment suggesting a very turbulent environment that may cause mixing between the upper and lower layers.

An indication of the environment within the compartment can be gained by viewing the visibility within the compartment before and after the system is set to fire mode. The visibility cross-sections of the compartment at these times are shown in Figure 122 and Figure 123. As can be seen in normal mode the upper layer has very low visibility while the lower layer remains clear. After the system is set to fire mode the interface between the two layers drops, the upper layer clears slightly and the lower layer remains clear. This would suggest that while mixing is occurring, it is occurring near the interface layer leaving the lower layer relatively clear. One point that must be noted from this is that the lower layer visibility does not decrease with the presence of water mist, suggesting that FDS does not account for the drop in visibility due to water mist.

The final set of cross-sections relating to this simulation show the concentration of oxygen within the compartment in normal mode and fire mode. As can be seen in Figure 124, under normal mode operation the oxygen concentration in the upper layer is a lot lower than the lower layer which is at ambient conditions. This is as expected due to the upper layer being formed by combustion gases which have had a portion of the oxygen removed the burning process. The interface between the two layers can clearly be seen in this cross section as the relatively small transition from the upper layer to the lower layer. Figure 125 shows a similar split between the upper and lower layers but in all areas the level of oxygen is decreased. This is of particular relevance to the lower layer where the oxygen concentration is no longer that of ambient conditions. This may be due to the presence of water vapour, which acts to dilute oxygen concentration. In any case the interface layer is clearly more turbulent suggesting some level of mixing again.

Graphical Data:

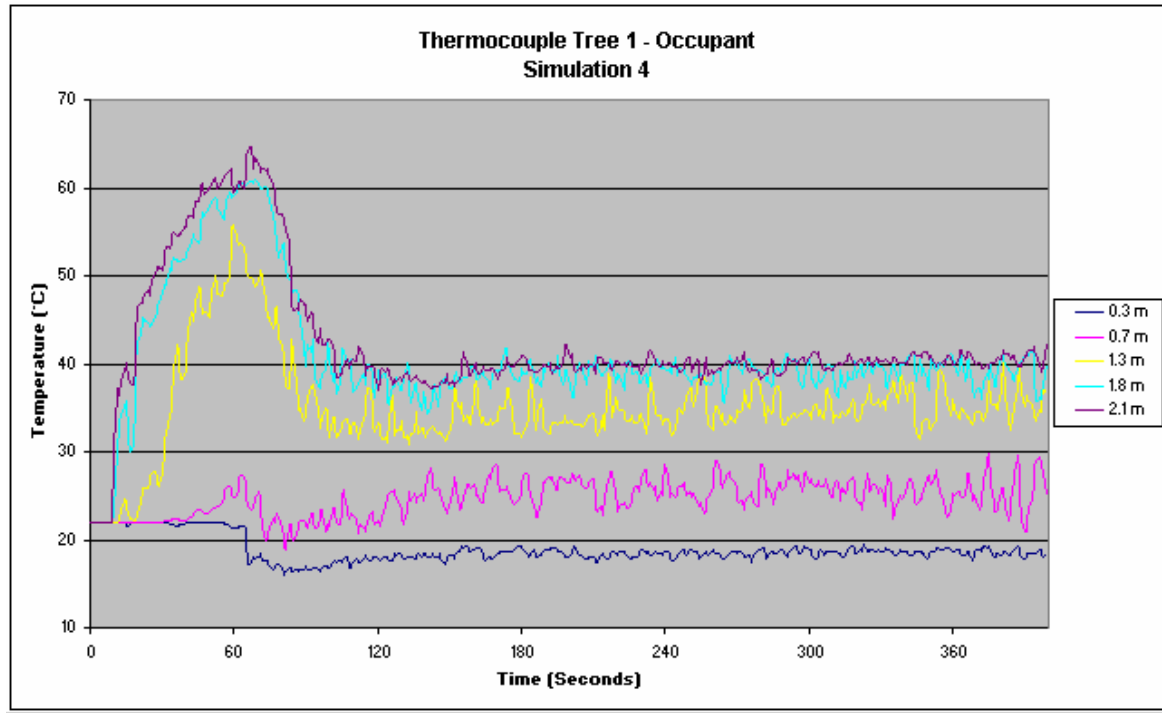


Figure 119 - Simulation 4: Occupant Thermocouple Tree

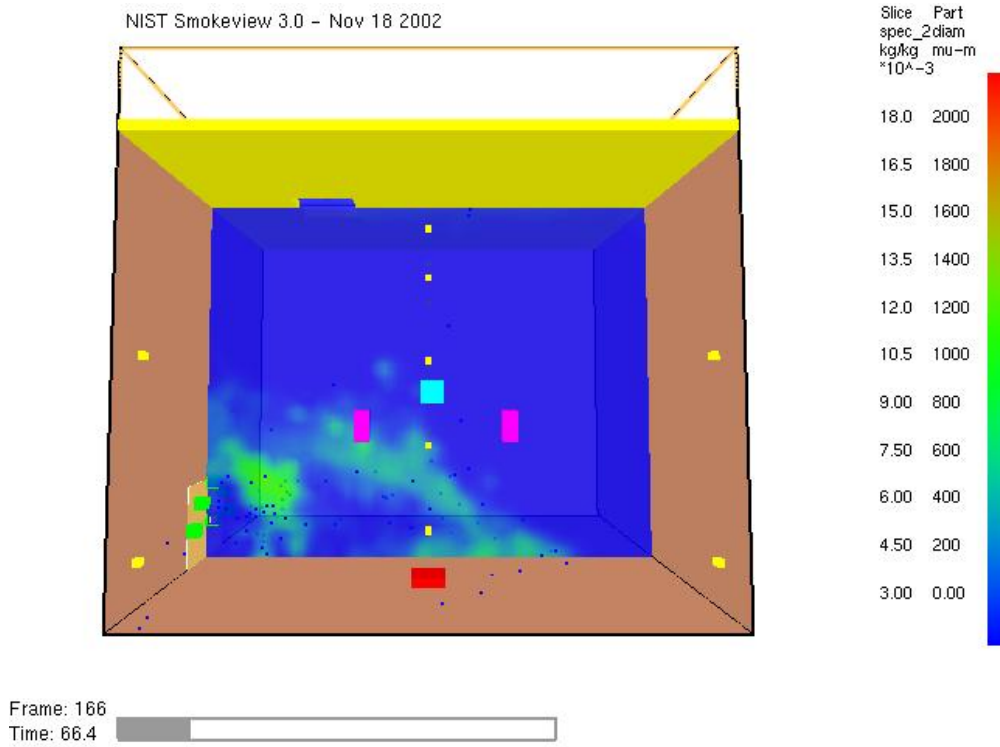


Figure 120 - Simulation 4: Water mist activation

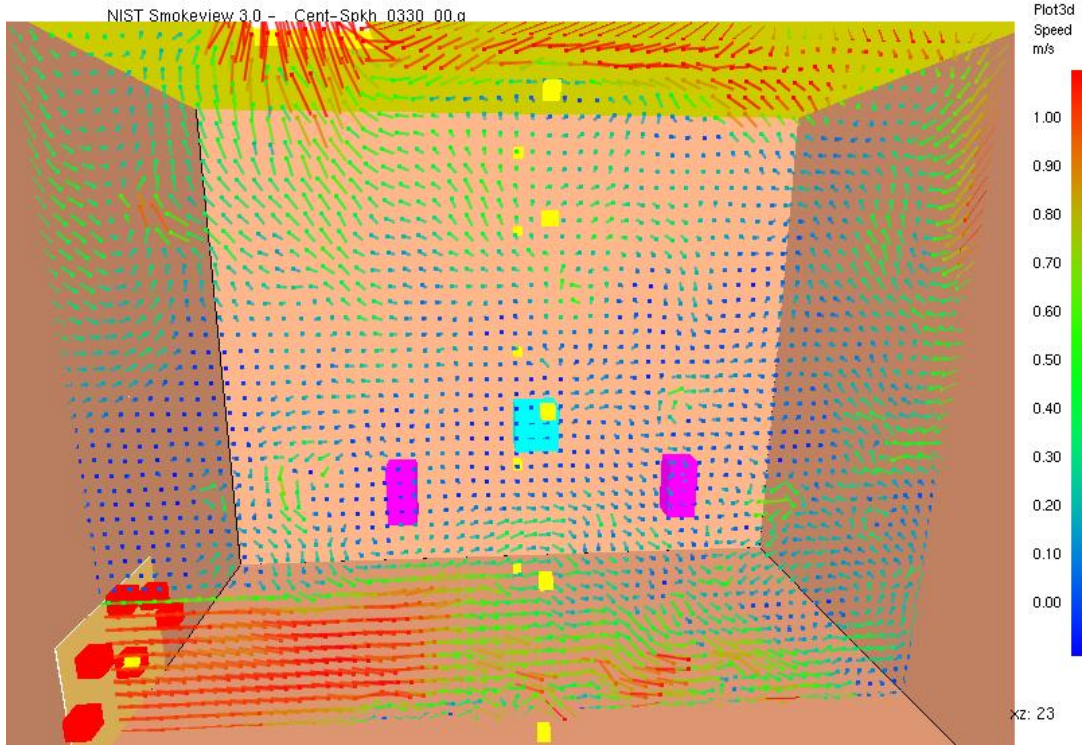


Figure 121 - Simulation 4: Compartment velocities during fire mode

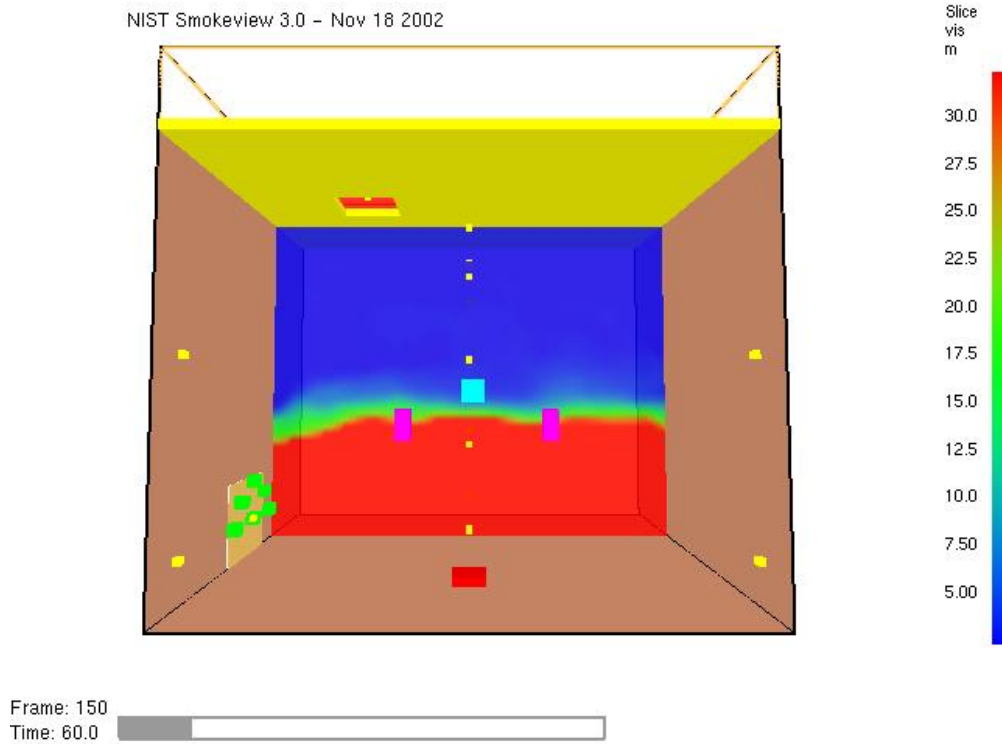
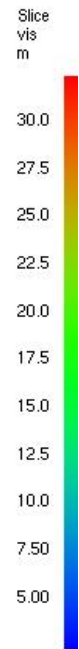
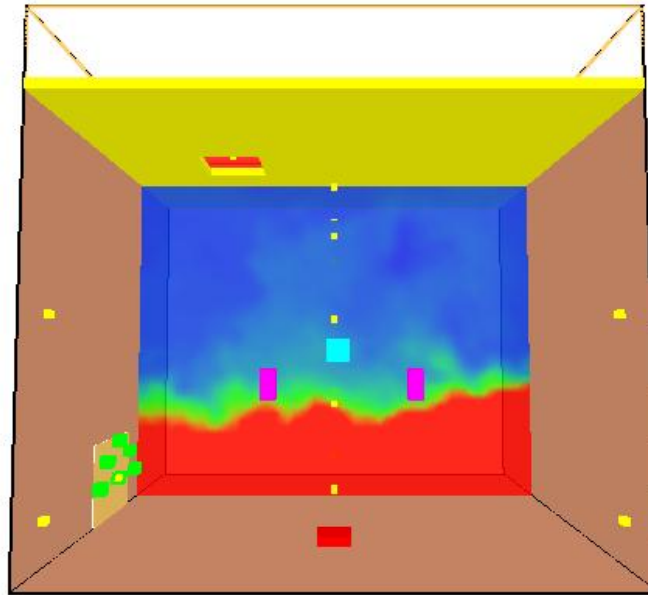


Figure 122 - Simulation 4: Normal flow visibility

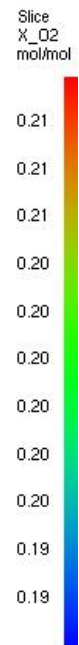
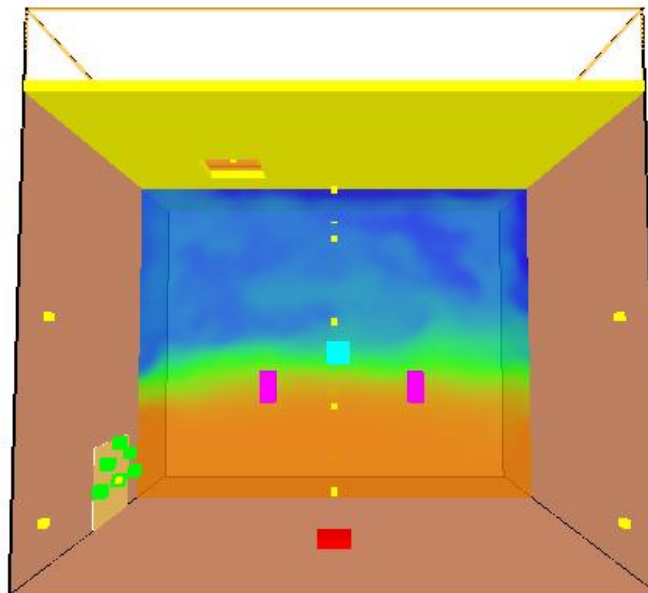
NIST Smokeview 3.0 - Nov 18 2002



Frame: 992
Time: 396.8

Figure 123 - Simulation 4: High flow visibility

NIST Smokeview 3.0 - Nov 18 2002



Frame: 153
Time: 61.2

Figure 124 - Simulation 4: Normal mode oxygen concentration

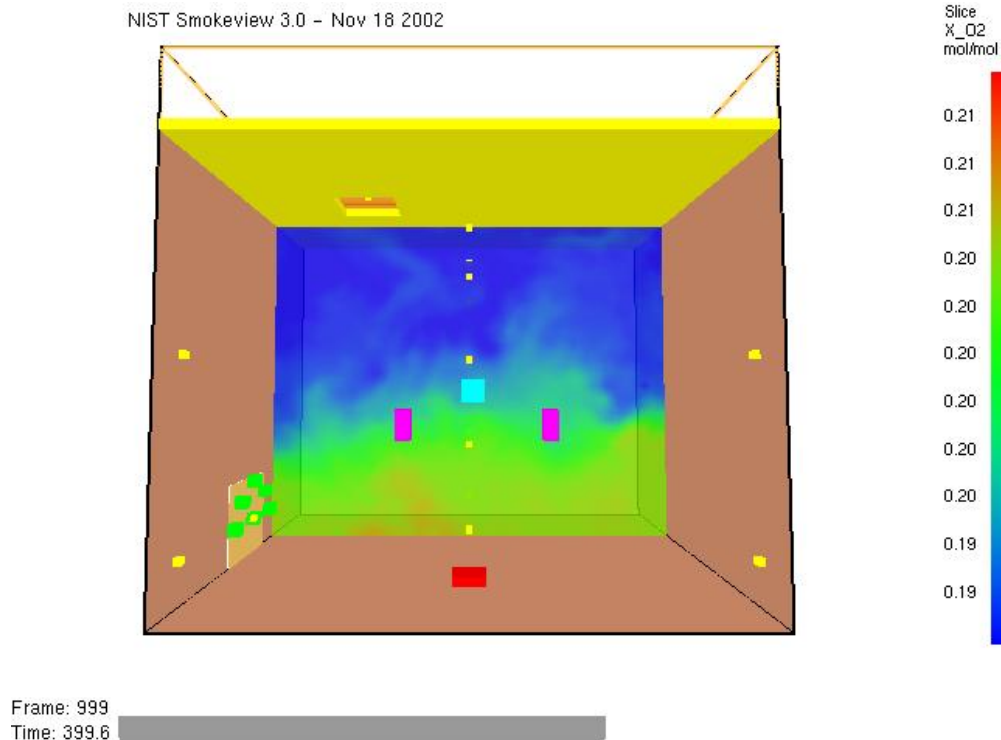


Figure 125 - Simulation 4: Fire mode oxygen concentration

6.4.5 Test 5: 1m Central Fire with High Airflow and Water Mist

<u>Fire Location:</u>	Centre of compartment at 1 Metre.
<u>Fire Type:</u>	Heptane pool fire.
<u>Airflow Characteristics:</u>	Low flow operation for 60 seconds followed by high flow operation.
<u>Suppression:</u>	Water mist at 60 seconds.
<u>Objectives:</u>	To determine the conditions within the compartment subjected to a 1m pool fire, under the operation of the displacement water mist system.

Observations:

As was observed during live testing, the temperatures in the upper layer of the compartment quickly increased as the fire progressed. Below the 1m height of the fire the temperatures remained close to ambient. This can be seen in Figure 126 which shows the temperatures recorded at thermocouple Tree 1. At the

activation of the system into fire mode the temperatures immediately dropped. This indicates that the upper layer is exhausted and cooled.

The lifting of the upper layer can be seen in Figure 127 and Figure 128, which show the visibility cross-sections within the compartment at 60 and 120 seconds respectively. As can be seen, once the system is activated the upper layer is quickly exhausted from the compartment. It must be remembered though that the visibility recorded by FDS appears to only take account of combustion products and not water mist. Bearing this in mind though, it suggests that little mixing is occurring between the upper and lower layers. An interesting point to note from these two figures is the shape of the exhaust plume. When the airflow is low the exhaust gases exit with a tangential velocity, while when the airflow is increased the exhaust gases exit primarily on a vertical path. This would indicate that the compartment is being pressurised causing the gases to be expelled at pressure as expected.

Finally Figure 129 shows a cross section of the velocity within the compartment with the system in fire mode. Again it can be seen that a semi circular airflow is formed within the compartment, with the supply air flowing across the floor and up the back wall. The uneven nature observable in the centre of the compartment suggests the environment is turbulent.

Graphical Data:

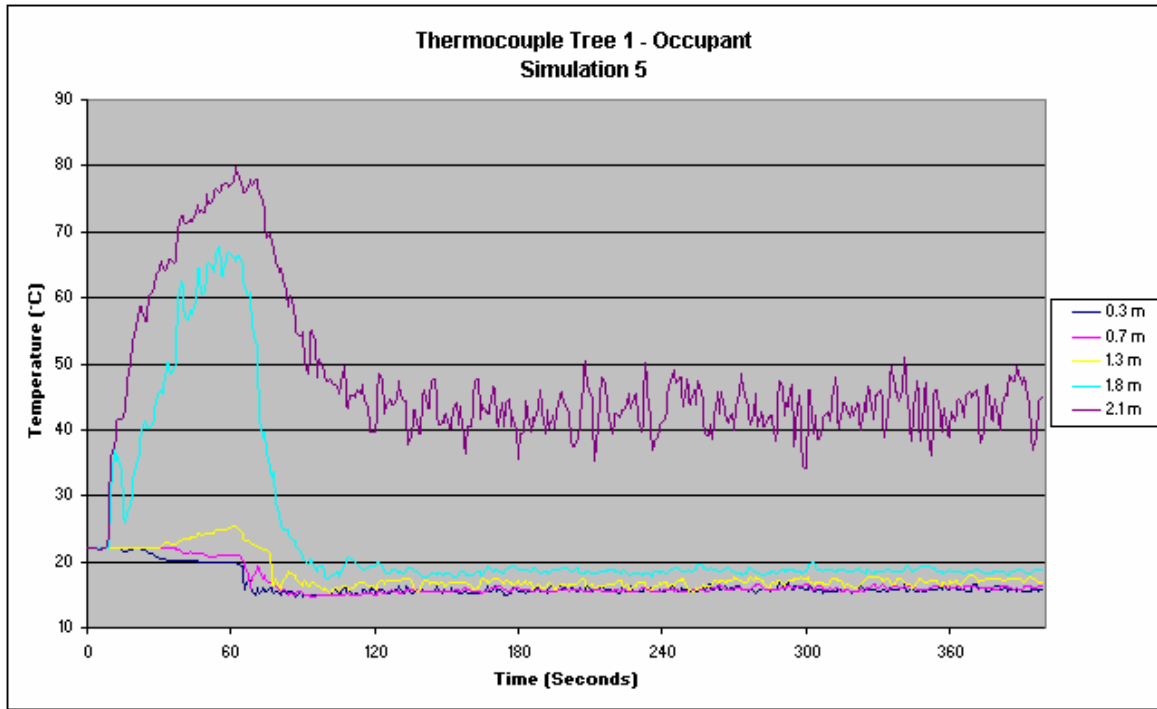


Figure 126 - Simulation 5: Occupant Thermocouple Tree

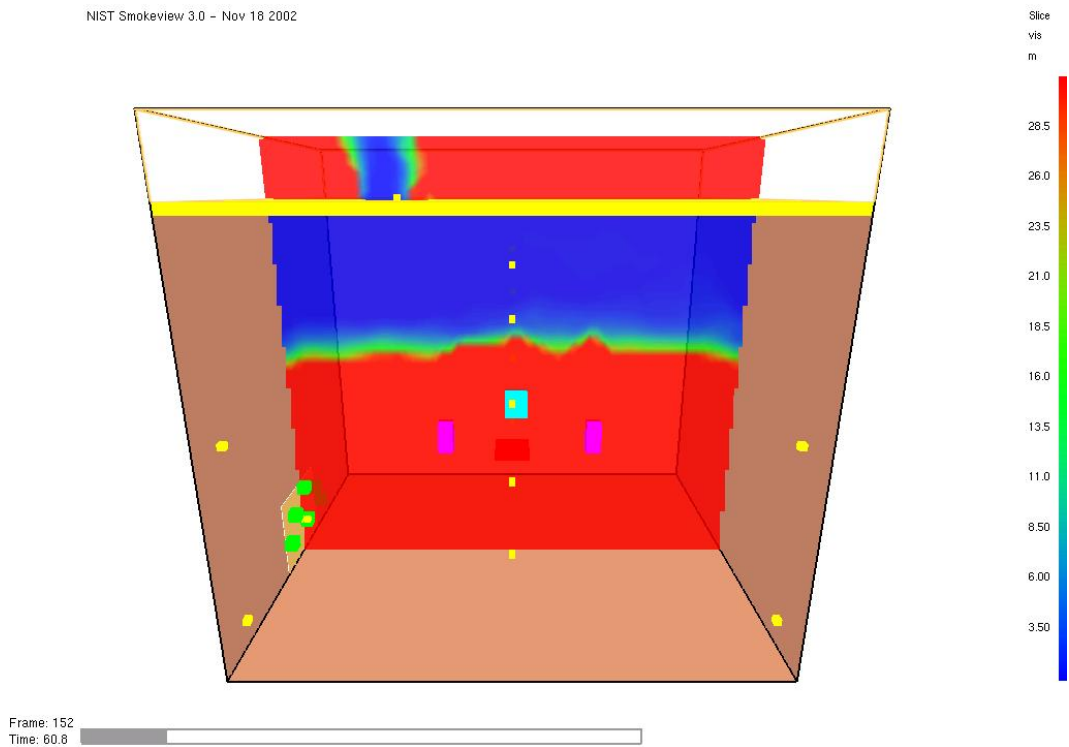


Figure 127 - Simulation 5: Visibility at 60 sec

NIST Smokeview 3.0 - Nov 18 2002

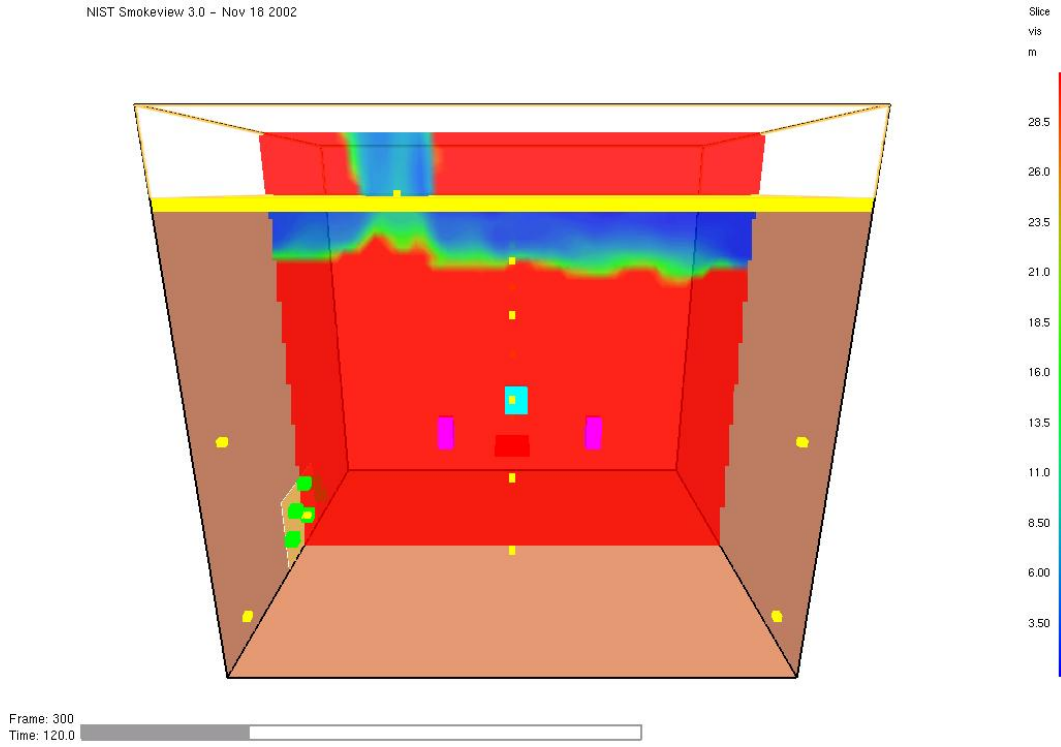


Figure 128 - Simulation 5: Visibility at 120 sec

NIST Smokeview 3.0 - .CentH-Sokh 0180 00.a

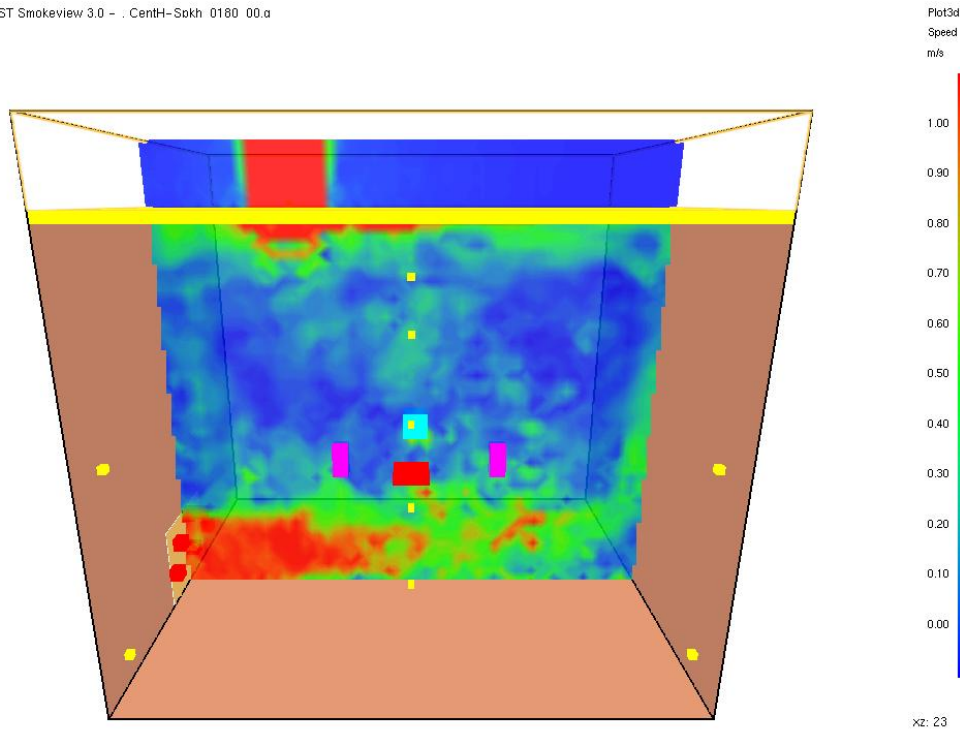


Figure 129 - Simulation 5: Velocity at 120 sec

6.4.6 Test 6: Ground Front Fire with High Airflow and Water Mist

<u>Fire Location:</u>	Front corner of compartment at ground level.
<u>Fire Type:</u>	Heptane pool fire.
<u>Airflow Characteristics:</u>	Low flow operation for 60 seconds followed by high flow operation.
<u>Suppression:</u>	Water mist at 60 seconds.
<u>Objectives:</u>	To determine the conditions within the compartment subjected to a ground level, front corner pool fire under the operation of the displacement water mist system.

Observations:

An interesting development from this simulation was the increase in HRR observed in the results. The HRR output within the compartment is shown in Figure 130. As can be seen the HRR initially stabilises at 20 kW before beginning to gradually increase over the length of the experiment up to 27 kW. This was caused by the flame spreading up the wooden wall within the compartment as unlike the live experiment the simulation had no fire protection in the corners. Initially it was decided to redo the test run but this was revised, as the simulation provided valuable information that suggests that even in fire mode and with water mist the fire would still spread. Additionally it was decided that the increase in HRR was not to such a large extent that it would affect the results and that they could still be compared to that of the live tests.

The same effect was observed in this simulation as had been observed in others where by on activation of the system, the temperatures within the compartment rapidly decreased. Figure 131 shows the temperatures at thermocouple Tree 1. As can be seen sensors 1.8 and 2.1 show a significant increase as the fire grows followed by a rapid decrease on activation. The lower three sensors show different results though as there initially is little temperature rise. The reason for this is more clearly understood by observing the flame and smoke fronts presented in Figure 132 and Figure 133. After 60 seconds the smoke front is still midway up the compartment and has not reached the lower sensors yet and increased the temperature at that point. Once the system is activated the upper layer is quickly exhausted from the compartment and the smoke layer increases in

height. It is also interesting to note that the flame front periodically reaches the roof of the compartment.

Figure 134 and Figure 135 showing the compartment temperature cross-sections suggest that this is correct and that the layer had simply not had sufficient time to reach the lower sensors when the system activated into fire mode. One observation from these results is that the interface appears to remain more stable between the upper and lower layer suggesting that less mixing is occurring. This may be due to the fact that the system activated in fire mode while the upper layer was relatively high, resulting in less mixing at a lower level.

Graphical Data:

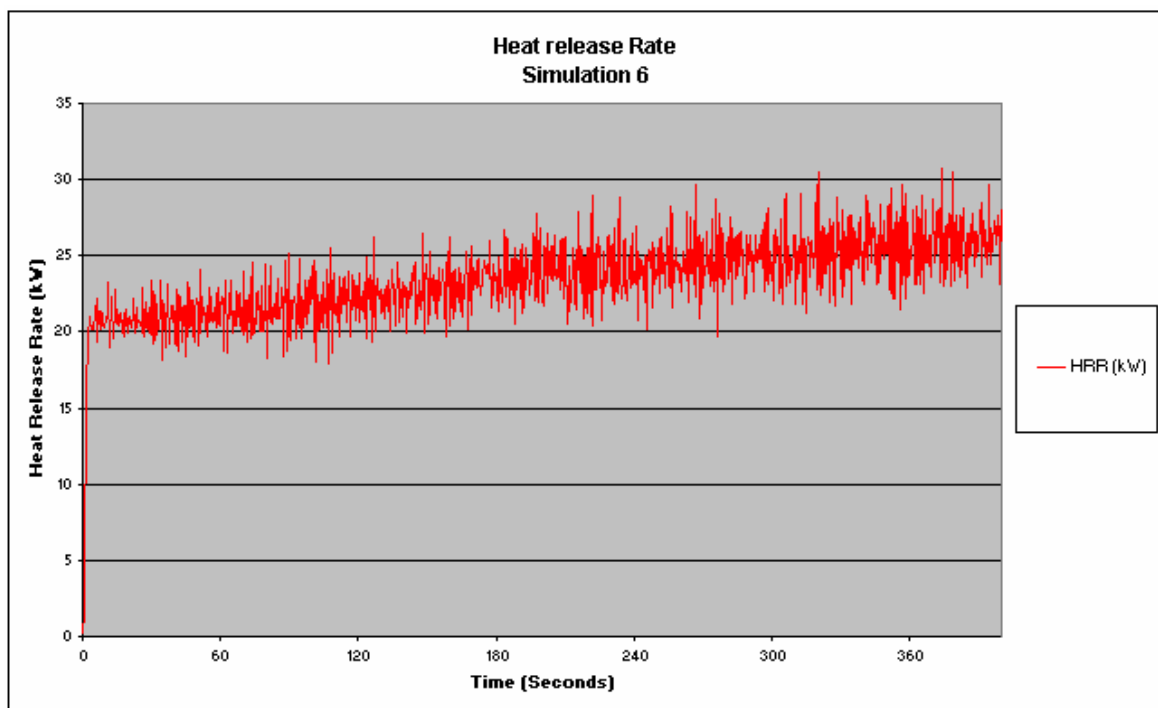


Figure 130 - Simulation 6: Fire heat release rate

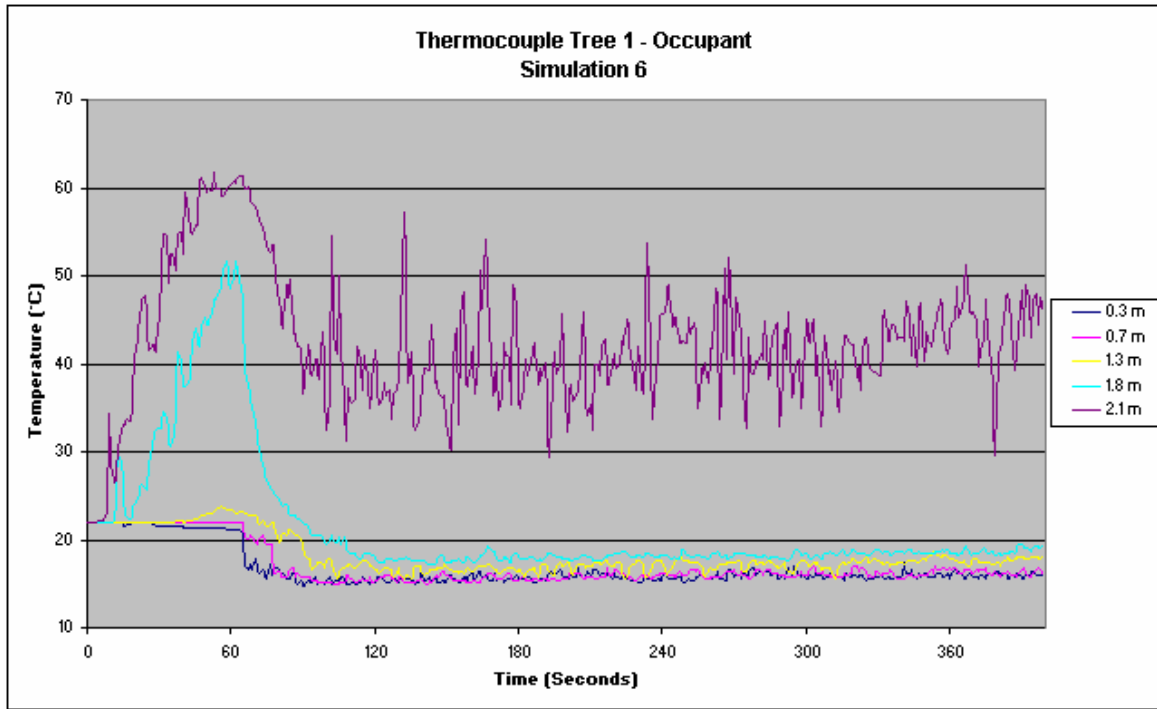
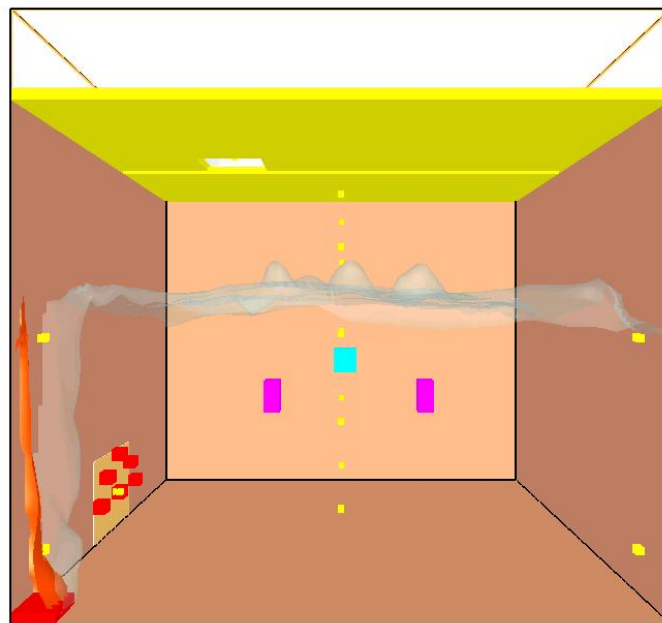


Figure 131 - Simulation 6: Occupant Thermocouple Tree

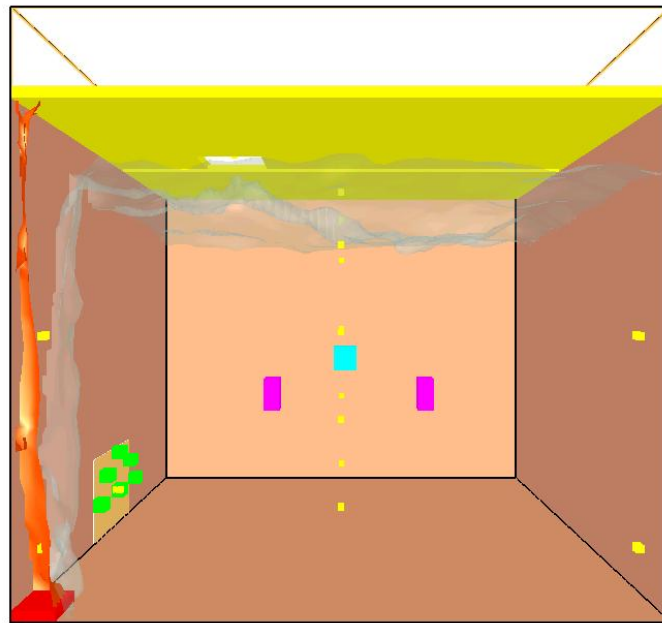
NIST Smokeview 3.0 - Nov 18 2002



Frame: 148
Time: 59.2

Figure 132 - Simulation 6: Flame and smoke front at 60 sec

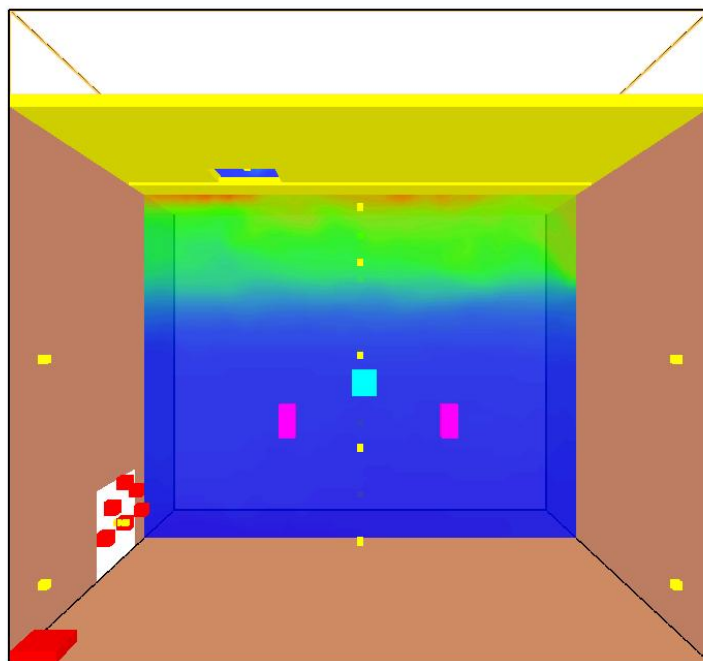
NIST Smokeview 3.0 - Nov 18 2002



Frame: 870
Time: 348.0

Figure 133 - Simulation 6: Flame and smoke front at 350 sec

NIST Smokeview 3.0 - Back-Sokh 0060 00.o



Plot3d
temp
C
99.5
91.5
83.5
75.5
67.5
59.5
51.5
43.5
35.5
27.5
19.5
xz: 33

Figure 134 - Simulation 6: Compartment temperature at 60 sec

NIST Smokeview 3.0 - . Back-Sokh 0180 00.a

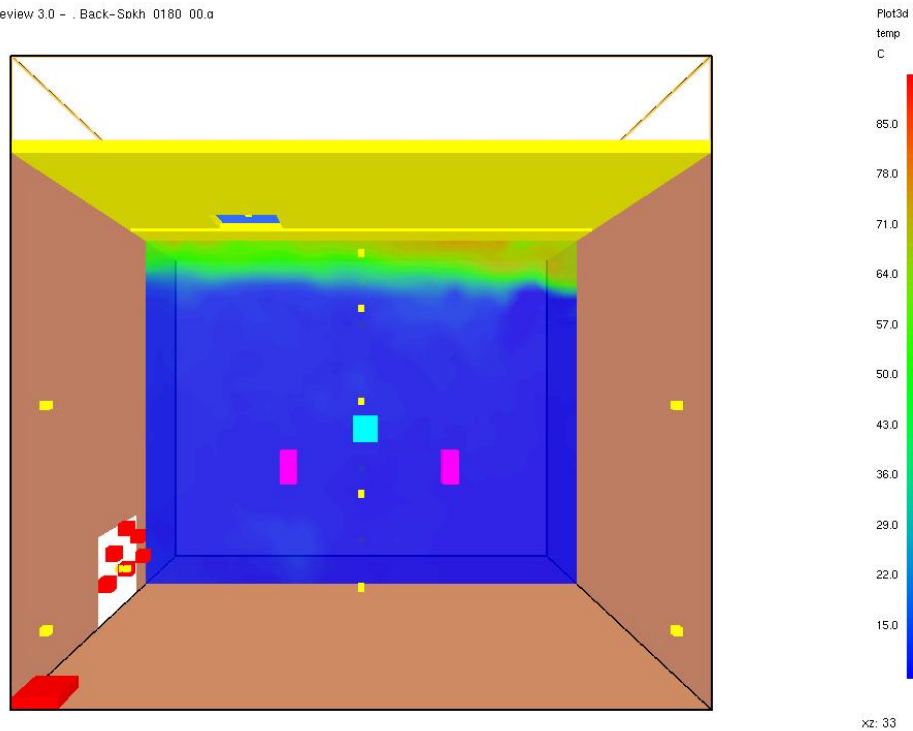


Figure 135 - Simulation 6: Compartment temperature at 120 sec

6.4.7 Test 7: Ground Back Fire with High Airflow and Water Mist

<u>Fire Location:</u>	Back corner of compartment at ground level.
<u>Fire Type:</u>	Heptane pool fire.
<u>Airflow Characteristics:</u>	Low flow operation for 60 seconds followed by high flow operation.
<u>Suppression:</u>	Water mist at 60 seconds.
<u>Objectives:</u>	To determine the conditions within the compartment subjected to a ground level, back corner, pool fire under the operation of the displacement water mist system.

Observations:

The results from the back corner fire simulation were very similar to those recorded for the front corner simulation. That is the upper layer formed and caused a temperature increase in the top two sensors on thermocouple Tree 1. As the system activated in fire mode the temperatures at these two points rapidly

dropped due to the upper layer being exhausted, causing the interface layer to increase and also through cooling by the water mist. The temperatures recorded at thermocouple Tree 1 are shown in Figure 136.

In relation to the mixing that the increased airflow and water mist sprays caused, Figure 137 and Figure 138 show the water vapour content over a cross-section of the compartment. As can be seen in Figure 137 the water mist moves rapidly across the floor of the compartment before moving up the back wall and into the centre of the compartment. This would explain why less mixing appears to occur when the interface layer is at a higher level within the compartment. When the layer is high the water mist and airflow can re-circulate back into the centre of the compartment without causing major disruption to the upper layer. When the interface is low, this re-circulation causes increased mixing of the two layers.

Figure 138 shows the entrainment that is occurring near the nozzle. Gases above the supply diffuser and water mist nozzles appears to be mixing in with the supply air in an eddy effect.

Graphical Data:

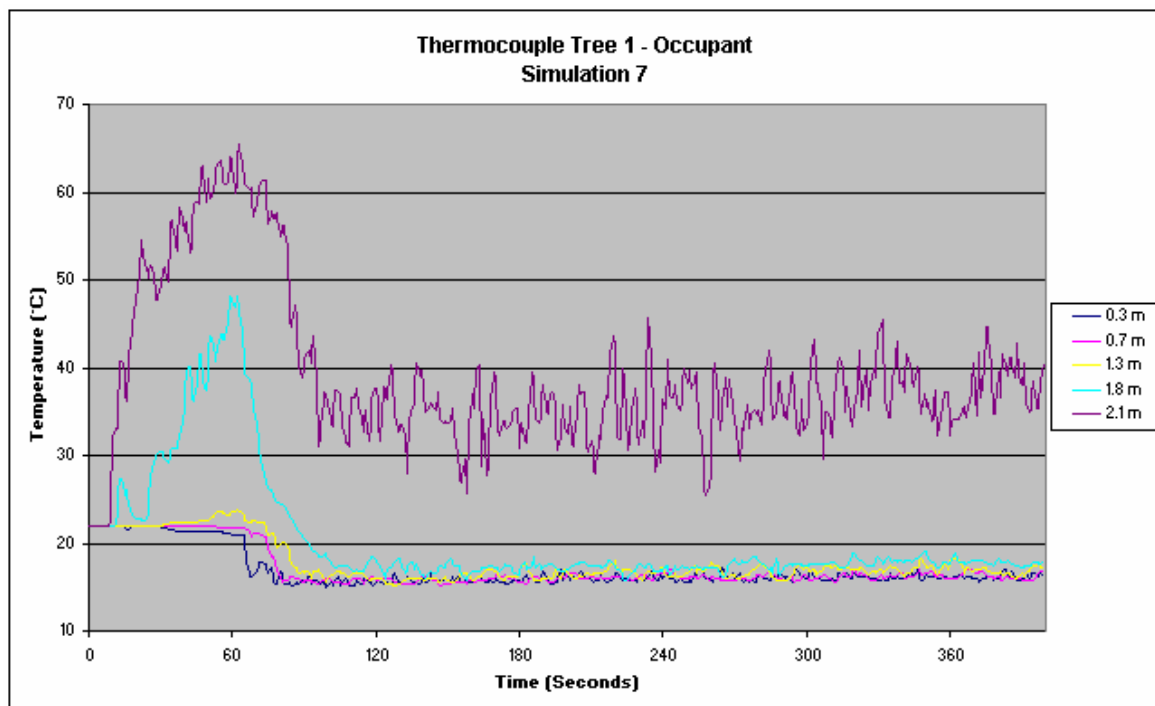


Figure 136 - Simulation 7: Occupant Thermocouple Tree

NIST Smokeview 3.0 - Nov 18 2002

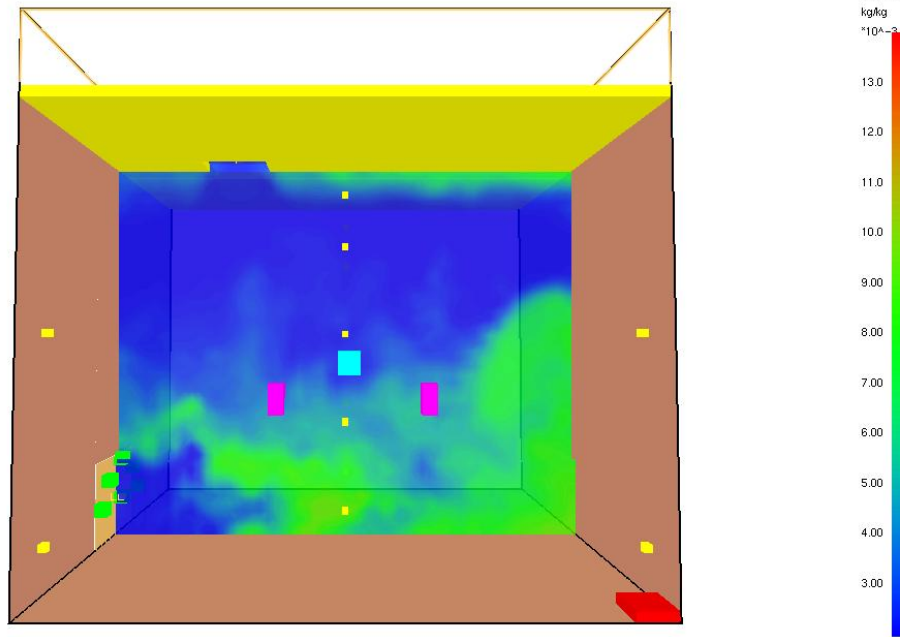


Figure 137 - Simulation 7: Water vapour 15 sec after mist activation

NIST Smokeview 3.0 - Nov 18 2002

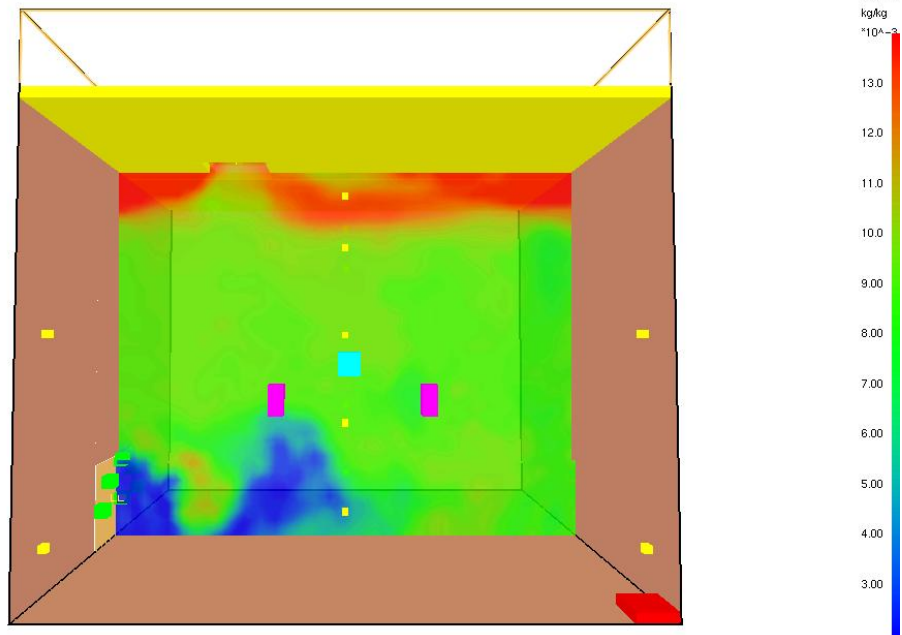


Figure 138 - Simulation 7: Water vapour at 400 sec

6.4.8 Test 8: Ground Central Fire with Normal Airflow and Water Mist

<u>Fire Location:</u>	Centre of compartment at ground level.
<u>Fire Type:</u>	Heptane pool fire.
<u>Airflow Characteristics:</u>	Constant low flow operation.
<u>Suppression:</u>	Water mist at 60 seconds.
<u>Objectives:</u>	To determine the conditions within the compartment subjected to a pool fire under normal low flow conditions but with water mist injection.

Observations:

The final simulation run simulated the scenario where the water mist was injected and the flow remained low. Theoretically the base concept behind this scenario is similar to a standard water mist system in that the percentage of water within the compartment increases and the combustion products are recycled back into the combustion zone.

The results from this simulation showed no decrease in the HRR of the fire as the water built up. Within the compartment the temperatures did not decrease significantly, appearing to only stabilise before continuing to increase at a slower rate. The results actually indicated that when the system was activated temperature in the lower region actually began to increase suggesting that mixing was occurring. The temperatures recorded at thermocouple Tree 1 are shown in Figure 139.

This mixing can be more clearly seen by viewing the visibility within the compartment. As can be seen in Figure 140, shortly after the initiation of the water mist nozzles, the upper layer combustion gases became entrained into the water mist nozzles and spread through the lower layer. Again the visibility in this case represents that due to the presence of combustion products rather than water mist. This mixing continues to occur until the visibility throughout the entire compartment is below 2m. It can also be seen that just above the nozzles the visibility actually increases initially. This may be due to the water mist cooling the upper layer at this point, causing it to collapse and the combustion products to be drawn into the lower layer.

This spread of the smoke front can also be seen in Figure 141 which shows the smoke and flame fronts shortly after water mist initiation. As can be seen the low level mixing occurred on the opposite side of the fire first and then moved to the back fire side corner. This may have been due to the fire plume entraining the mixed lower layer and reducing the overall rate of spread to this corner.

The final graph in this series, Figure 142, shows the oxygen concentration throughout the compartment at 400 seconds. In this simulation less ambient supply air is being added to the compartment so the combustion gases are recycled and the oxygen concentration decreases. The upper layer reached a concentration of 17% while the lower layer had a reduced oxygen concentration of 19%. Again this indicates that mixing is occurring throughout the compartment.

Graphical Data:

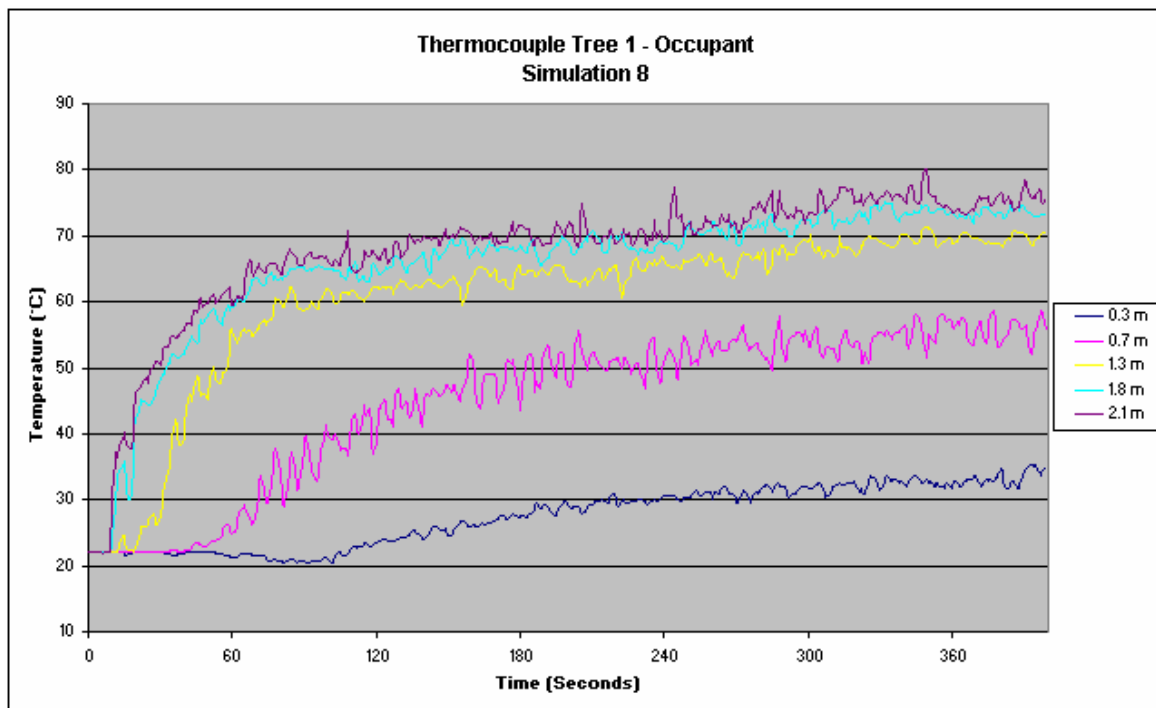


Figure 139 - Simulation 8: Occupant Thermocouple Tree

NIST Smokeview 3.0 - Nov 18 2002

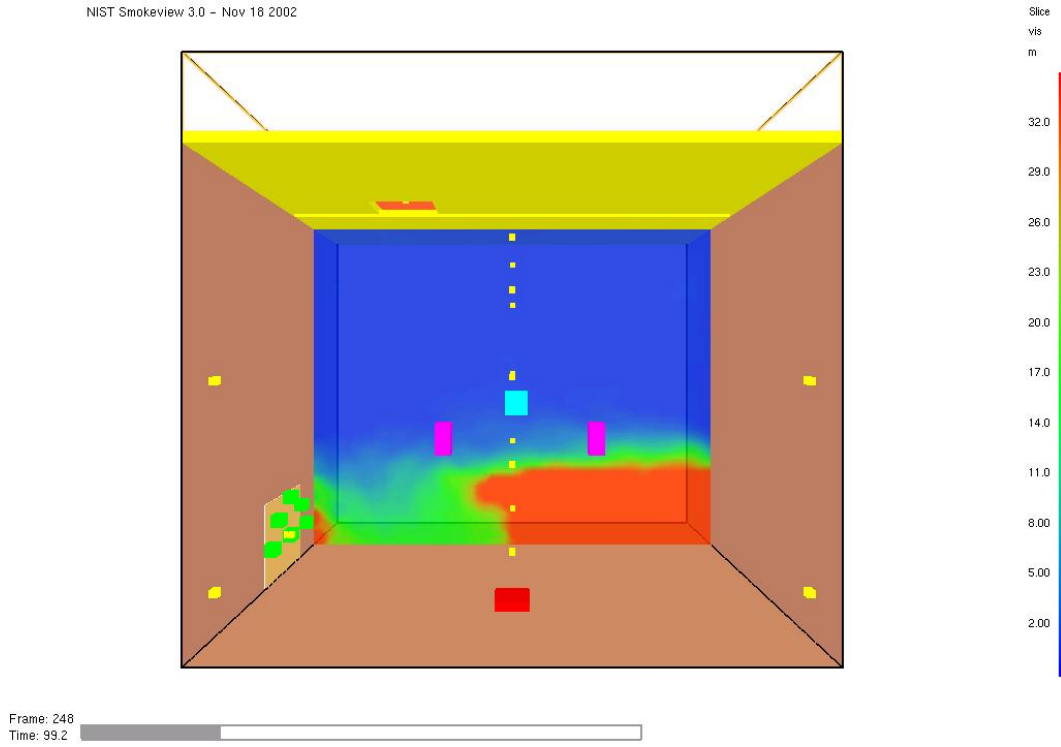


Figure 140 - Simulation 8: Visibility after 100 sec

NIST Smokeview 3.0 - Nov 18 2002

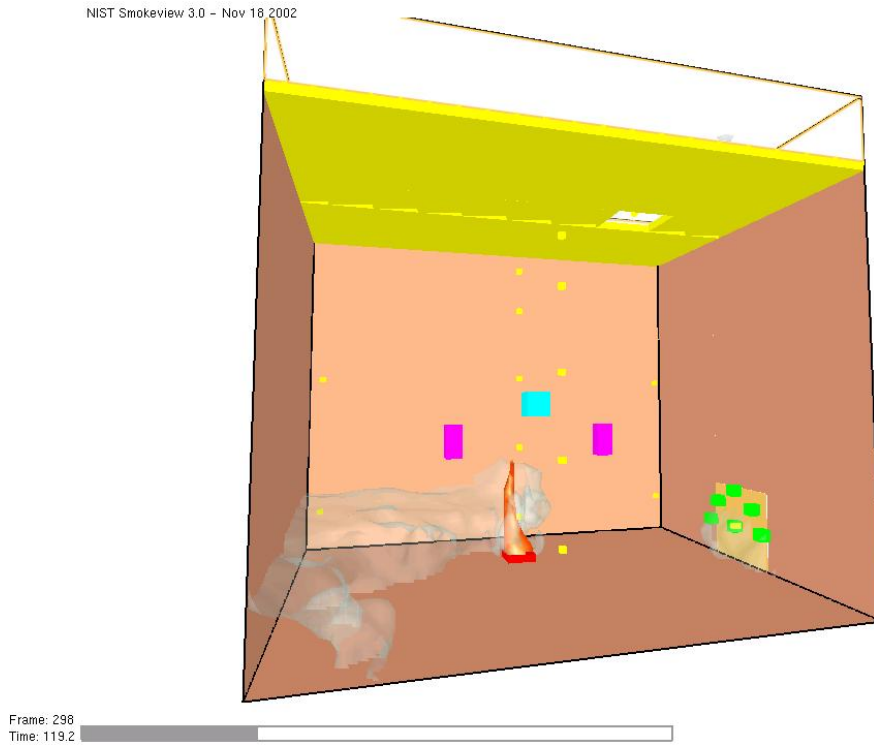


Figure 141 - Simulation 8: Flame and smoke front

6.5 FDS Simulation Observations

As the effectiveness of the system has been established in section 5.12, the aim of this section is to discuss the additional information on the compartment interior not measured in the live tests.

On the surface the FDS simulations appear to give similar results to the live fire tests. In each case the fire did not go out but the temperatures were rapidly decreased. The simulations showed an increased level of mixing within the compartment when the water mist nozzles were activated over that of just the airflow. This would suggest that the simulations can at a minimum be compared to provide general information and comparison between the compartment interior under different conditions. A full comparison of the test results recorded at the thermocouple points is covered in section 7.

The first set of information that can be compared is the temperature profile across the compartment at the completion of the simulation. Four runs were investigated including normal operation with a fire, high airflow with a fire, water mist and high airflow with a fire and finally only water mist with a fire. The temperature cross sections from each of these are shown in Figure 143. As can be seen the temperature is greatest when the system is operating normally. This is followed by the water mist only, then high airflow and finally a combination of the two. This is as could be expected as the increased airflow causes the hot upper layer to be exhausted through the compartment vent. In the case of the two simulations with normal airflow the heat from the fire is contained within the compartment. The addition of water mist in both cases reduces the temperatures further as heat is absorbed by the water droplets.

As would be expected, the two simulations with an increased airflow result in an interface layer height above that of the other two simulations. This is again simply due to more of the upper layer being exhausted as more air is introduced in to the compartment.

An interesting point to note is the patchy upper layer temperature recorded by the two simulations where the water mist is activated. This would suggest that the

water mist is the dominant factor in causing turbulence within the compartment and not the increased airflow.

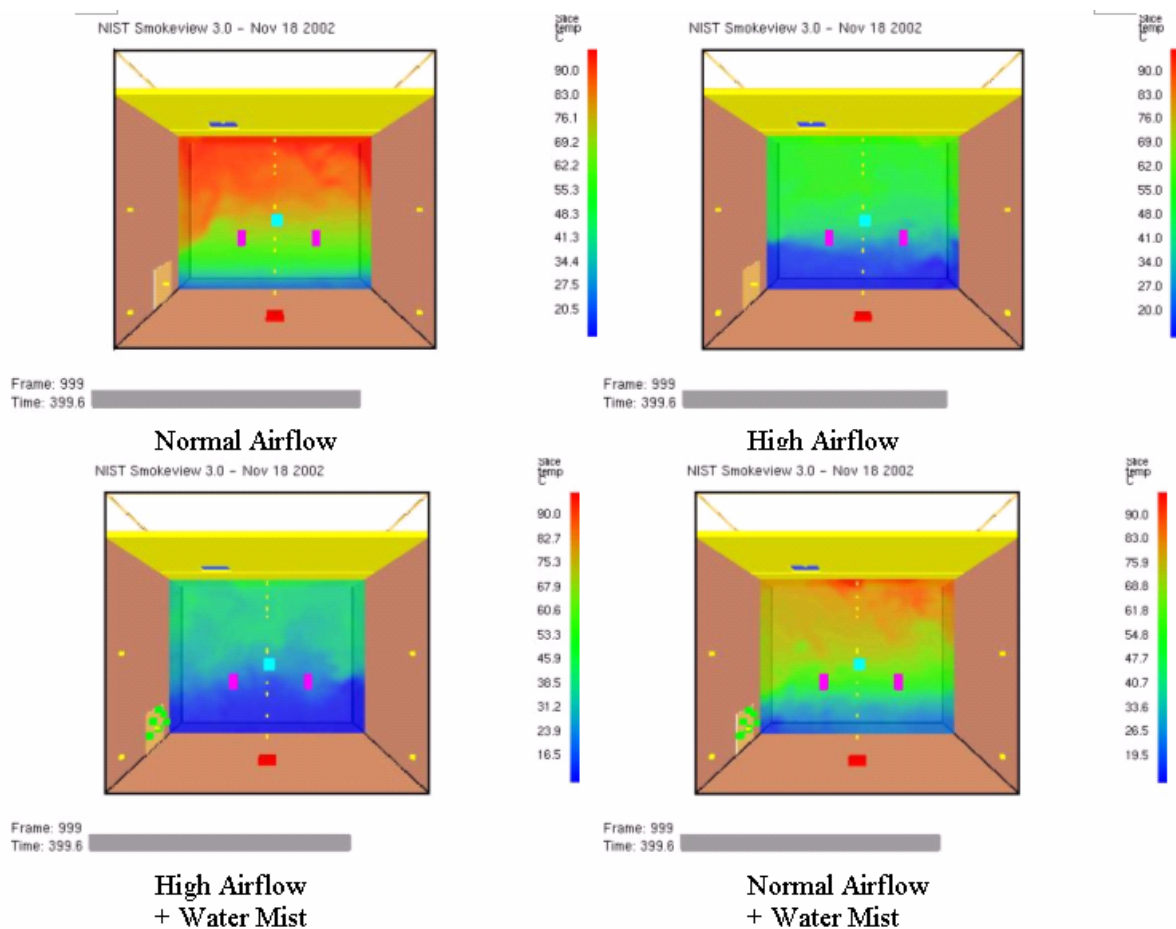


Figure 143 – Compartment temperature after 400 Sec and under various scenarios

One of the objectives and advantages in running the FDS simulations is that they allows more complex variables to be measured within the compartment. One of these variables is the CO₂ concentration shown in Figure 144. This provides information on the mixing within the compartment and its ability to support occupants safely.

Again the two simulations with an increased airflow had a much lower CO₂ mole fraction that that seen in the simulations with low flow. This is primarily due to the fact that more air is being introduced into the compartment while larger quantities of combustion gases are being removed resulting in a lower build-up of combustion gases.

Interestingly with low airflow only a relatively clear layer formed at floor level, while with low flow and water mist this layer mixed with the upper layer causing the CO₂ levels to increase. This would indicate that the water mist only is actually causing the upper layer to collapse to some extent and mix with the lower layer.

As seen in Figure 143, the interface layer is far less clear in the water mist plus high airflow than in just the high airflow indicating increased turbulence within the compartment.

From a life safety point of view the increased airflow simulations result in a far lower CO₂ concentrations and hence less threat to life safety.

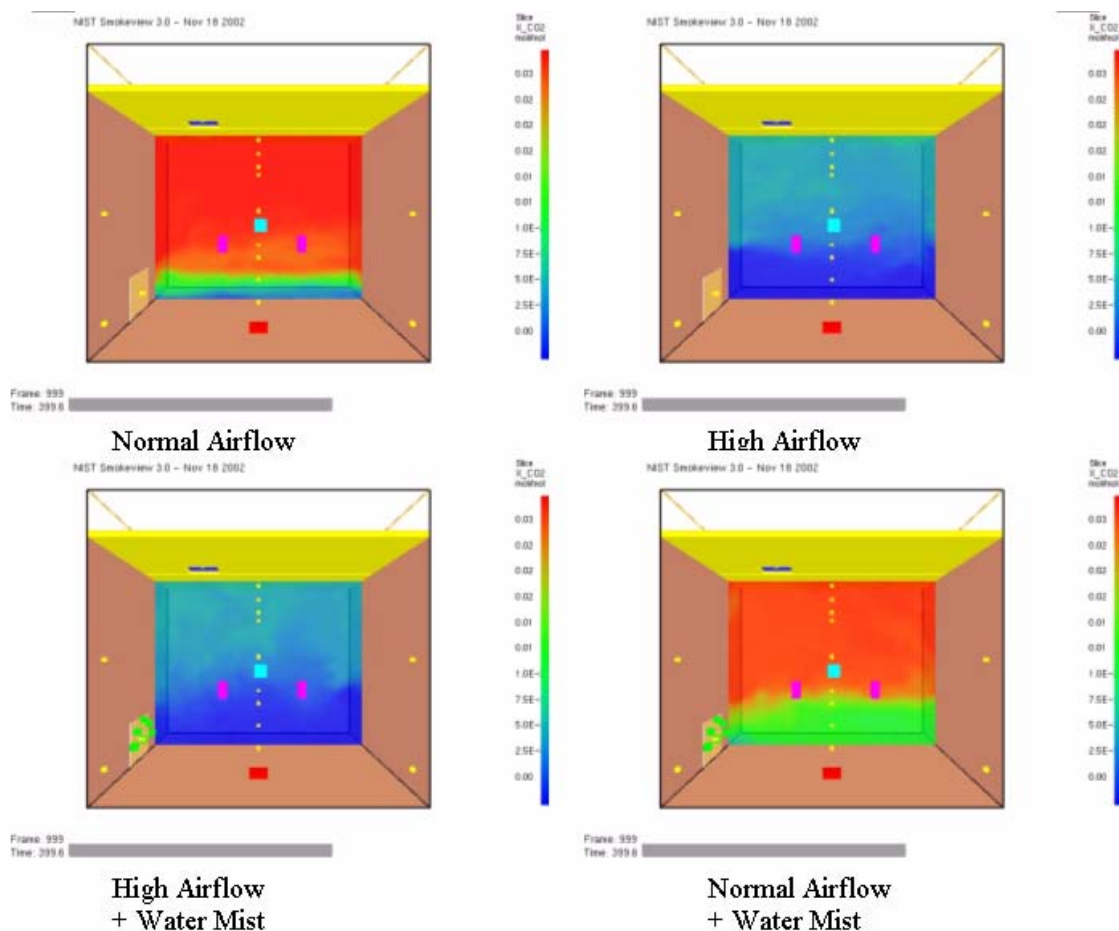


Figure 144 - Compartment CO₂ concentration after 400 Sec and under various scenarios

The final sequence of simulations results shown in Figure 145, display the soot concentration within the compartment. The soot concentration is compared as it

gives a good indication of the mixing that is occurring within the compartment and the distribution of combustion products throughout the space.

As can be seen then the results are similar to the figures above in that the increased airflow results in a lower soot concentration throughout the compartment. In both cases of the water mist being injected into the compartment, mixing within the compartment increases and the soot levels at lower levels are slightly higher than that occurring when no mist is injected.

Again in terms of life safety the results would suggest that the increased airflow within the compartment results in lower levels of combustion products throughout the compartment and hence a greater level of safety.

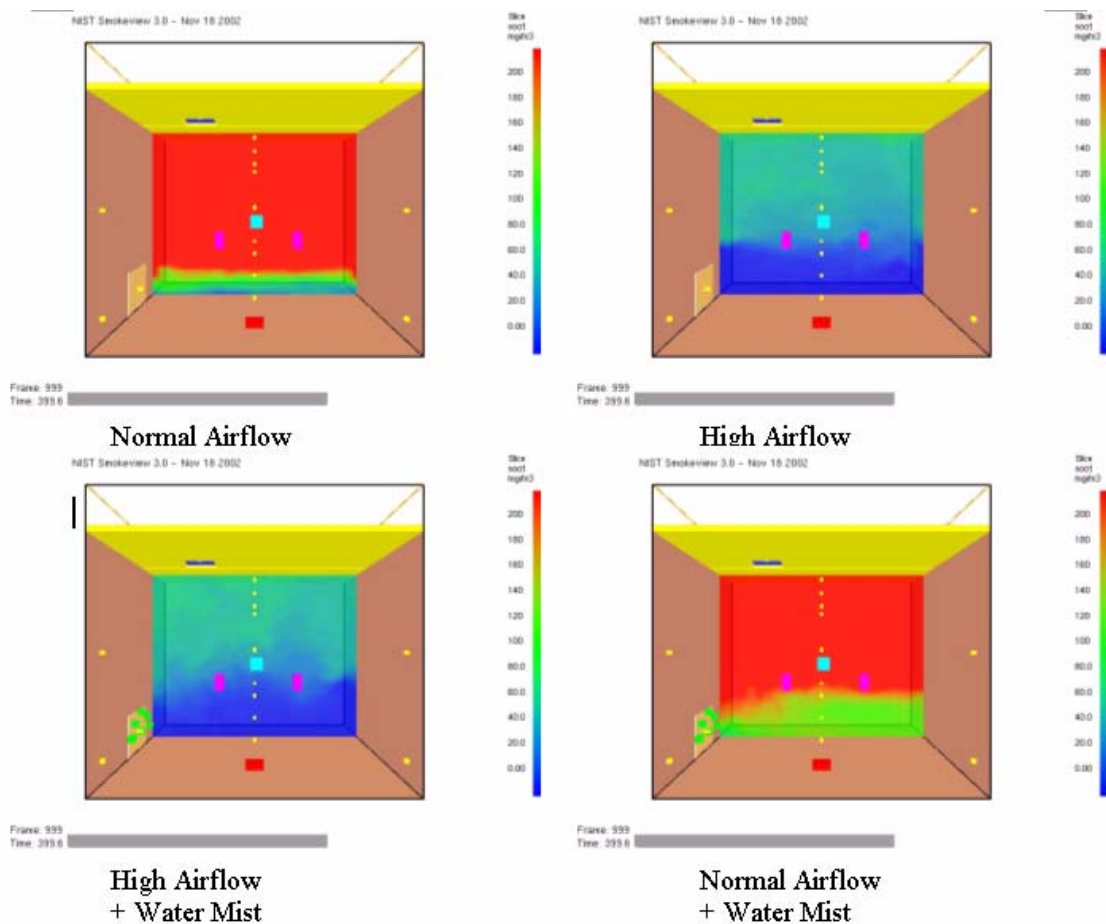


Figure 145 - Compartment soot density after 400 Sec and under various scenarios

6.6 FDS Conclusion

The results from the FDS simulations provided valuable information on the operation of the displacement water mist system. As was required by the first objective the results from the normal operating mode show just how the displacement ventilation system functions under normal conditions. The temperatures within the compartment stabilise around 21°C suggesting that based on the internal loads the system is sized correctly.

In relation to the compartments interior conditions under different fire scenarios and suppression scenarios, the simulations provided valuable information on the flows, temperature and combustion gas concentrations. While in no simulation was the fire extinguished, from the comparisons of the data it appears that the water mist and increased displacement airflow work together to provide the most survivable atmosphere. The increased airflow results in lower concentrations of combustion gases within the compartment, while the water mist assists in decreasing the temperature.

One point that did become apparent from the simulation results is that mixing within the compartment was far greater than had been ideally wanted. Under normal displacement water mist operation a circulation effect appeared to occur within the compartment. This affected the interface layers stability when it was at low levels but not as significantly at high levels as resulted from corner or high level fires.

Interestingly it appeared that the water mist created the most significant mixing effect at both high and normal airflows. As has been previously discussed in section X at low airflows the water mist cooled and collapsed the upper layer causing the combustion gases to be recycled back into the lower layer. Under high airflow conditions the same cooling and increased mixing occurred but the increased airflow resulted in the lower layer remaining clear.

7. Comparison Results

This section of the report compares the results obtained from live testing with those generated through FDS simulation. A number of comparison graphs are presented along with a discussion of the differences and possible reasons for the differences. Only those comparison graphs that provide pertinent and specific data are presented in this section, all of the comparison graphs can be found in appendix 11.8.

7.1 *Base Calculations, FDS and Full Scale Test Comparison*

The first comparison that can be made is between the basic excel spreadsheet that was developed (see section 4.7) and the FDS simulation for a central pool fire under high airflow conditions. As has been previously discussed a spreadsheet was developed based on a two zone model and using Heskestad's plume correlations. The fire size and position are entered and based on this the position of the upper layer is calculated with time. Figure 146 shows the layer height expected for a 20 kW located in the centre of the compartment. As can be seen with the airflow increased the theoretical layer interface height is 1.5m.

This result can be compared to the FDS simulation of the same scenario. Figure 147 shows the layer height shown by the visibility within the compartment after 400 seconds. As can be seen FDS simulation suggests a layer height of approximately 1m rather than 1.5m calculated using the excel spreadsheet. The variation between these two levels is most likely due to the turbulence that actually occurred within the compartment and affected the upper layer volume. The spreadsheet models an ideal situation where the two layers remain stable and separated, hence no turbulence is accounted for. In the FDS case a more lifelike scenario was modelled where there was turbulence within the compartment due to the increased airflow. As discussed in the previous section this turbulence created instability within the compartment and more air was injected into the upper layer as the airflow moved up the back wall.

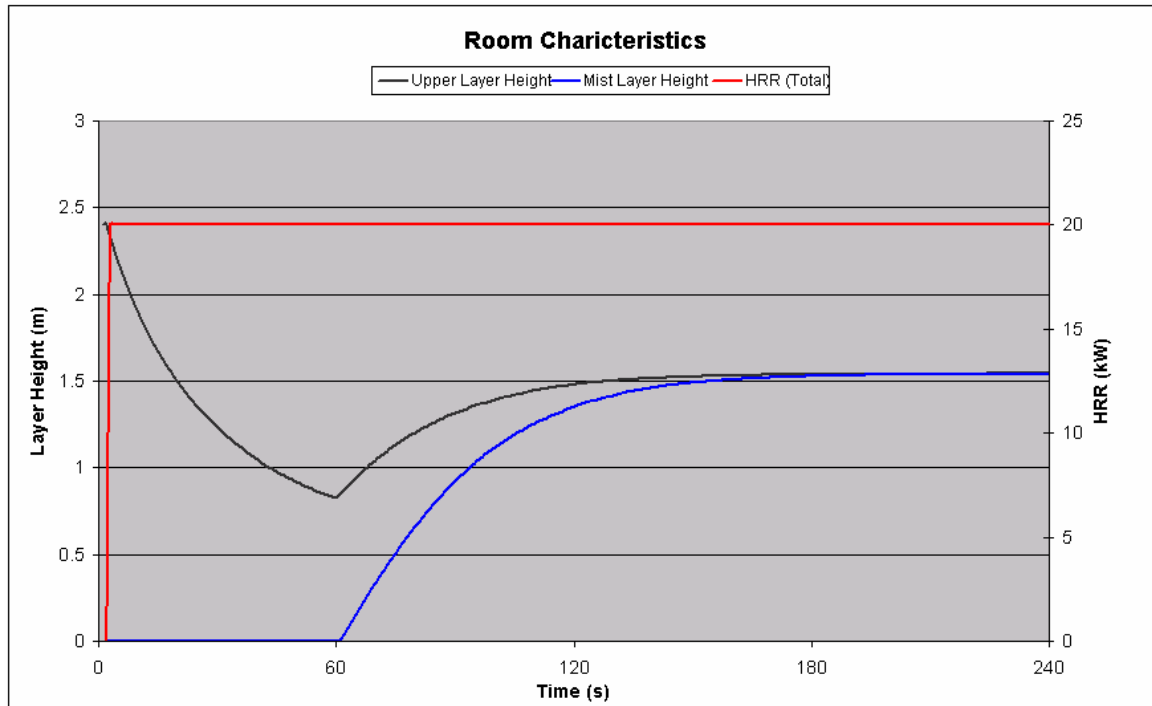


Figure 146 - Interface height calculated based on a zone model

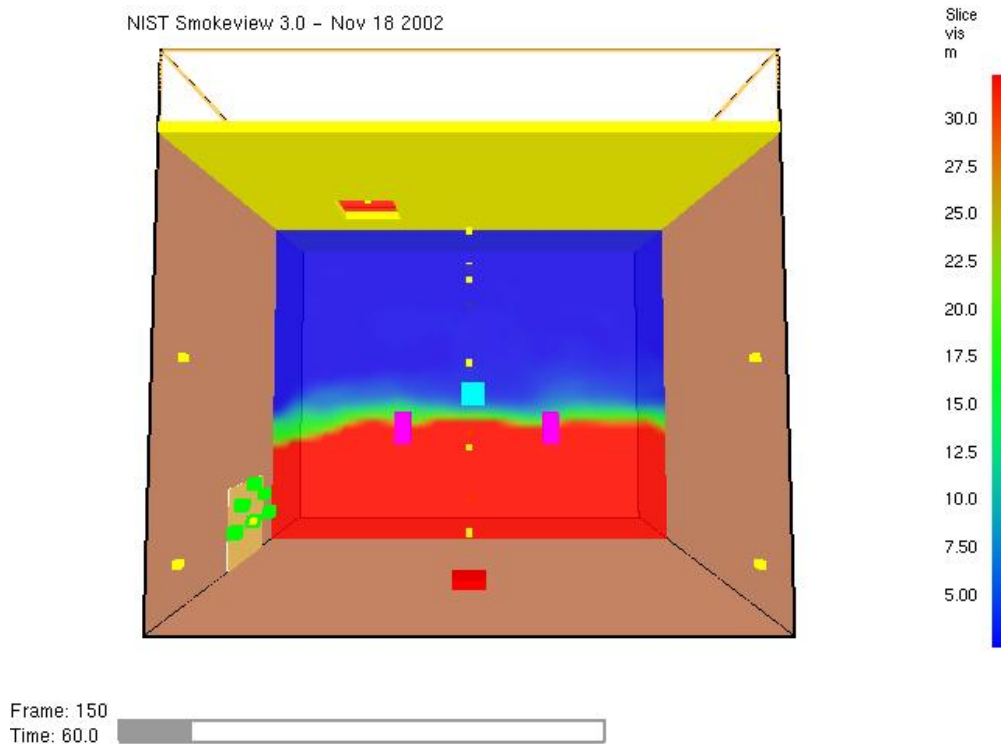


Figure 147 - Simulation 4: Normal flow visibility

These graphs give an indication of the comparison between the excel spreadsheet and the FDS simulations, but the use of the layer height cannot be

used to compare the results from the FDS and live tests. This is simply because under a live test and even the FDS results, it is not always clear where the interface height is within the compartment. In many of the live tests, the interface was not distinguishable or the water mist obscured the view. Additionally even if the layer height could be seen the estimation of the height would lead to larger errors. Instead the thermocouples within the compartment are used as the reference point and the temperatures between them are compared.

The first case that must be compared is that of the base case consisting of a central floor level fire operating under normal operation with low airflow. Figure 148 shows the first temperature comparison between the exhaust air temperatures. As can be seen the results from live test and FDS simulation are quite different with the FDS simulation increasing faster but then stabilising at a lower temperature. On the other hand the live simulation increases at a slower steadier rate and peaks at a much higher temperature. Other than modelling errors, one possible reason for this difference is the HRR from the pool fire in the live test. It was calculated that the HRR was 20 kW from this fire but this was not confirmed by actual testing. It is possible that the actual HRR in the live tests was above 20 kW which would have increased the temperature.

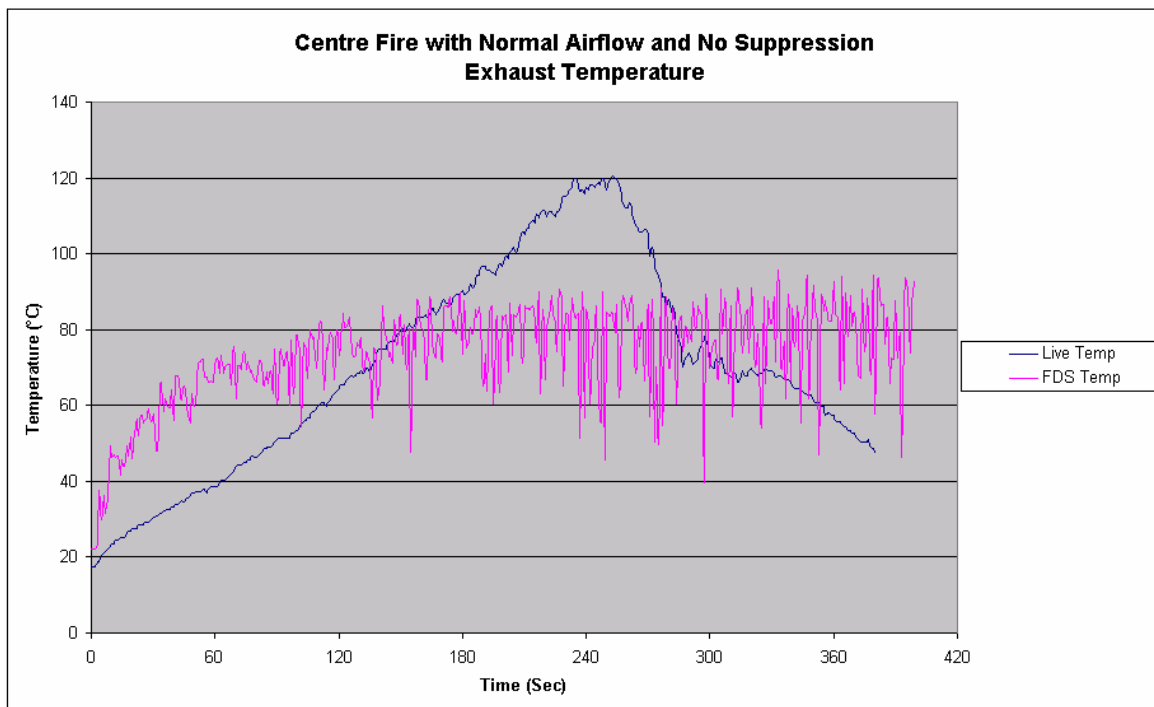


Figure 148 - Centre floor fire under normal conditions - exhaust temperatures

The second sets of analysis points were directly above the fire source at 0.3m and 2.1m. These are shown in Figure 149 and Figure 150. As can be seen, directly above the fire at 0.3m the temperatures from the FDS simulation and the live test are very similar. The peak temperatures are approximately the same with the only major difference being that the live test resulted in slightly more unstable data. This is most likely due to the turbulence within the live compartment and the live flame. The scale of the FDS grid is still relatively large at 50 mm, which results in the flame front appearing to be more stable than it actually is.

Figure 150 shows a different comparison, which is more in line with that of the exhaust air temperatures. The FDS results immediately increase to a high temperature that remains relatively constant throughout the simulation. The live test on the other hand increases constantly to a temperature just above that of the FDS simulation. One possible reason for this is that in the FDS simulation the plume was observed to rise vertically, passing through the thermocouples. This would have resulted in the high relatively constant temperature recorded. In the live test though the placement of the pan and plume path was slightly off line with the thermocouples, leading to the temperature being taken at the edge of the plume and being more in line with the compartment temperature.

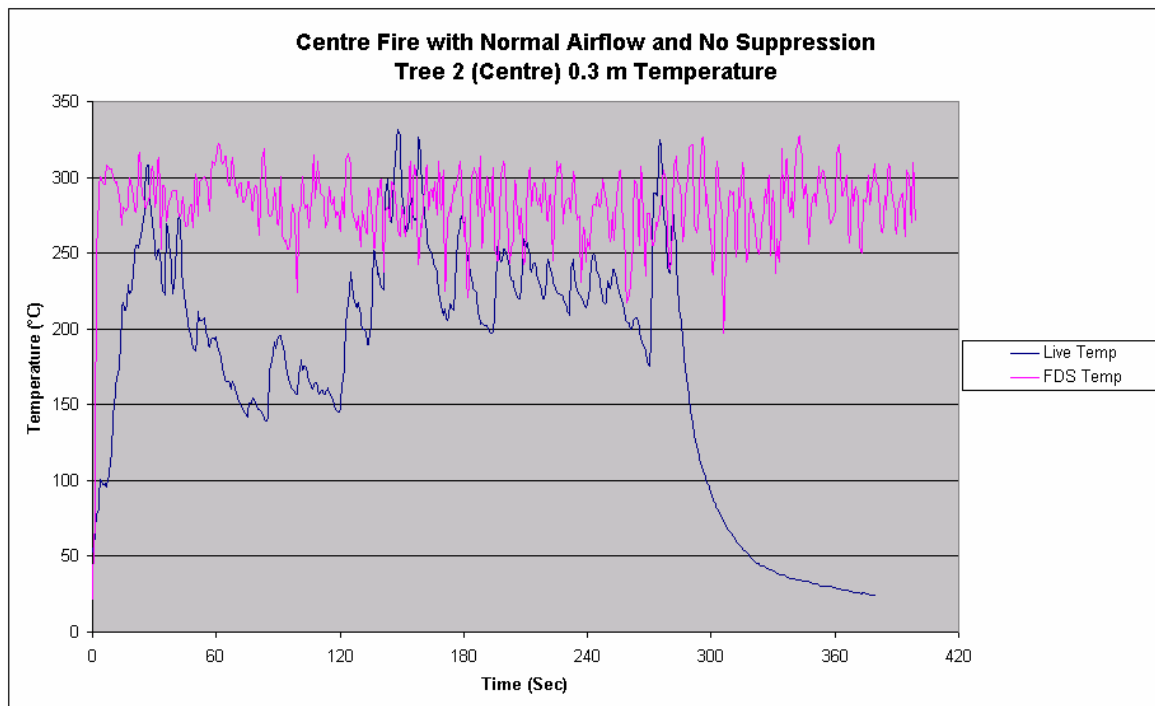


Figure 149 - Centre floor fire under normal conditions – Tree 2, 0.3m temperatures

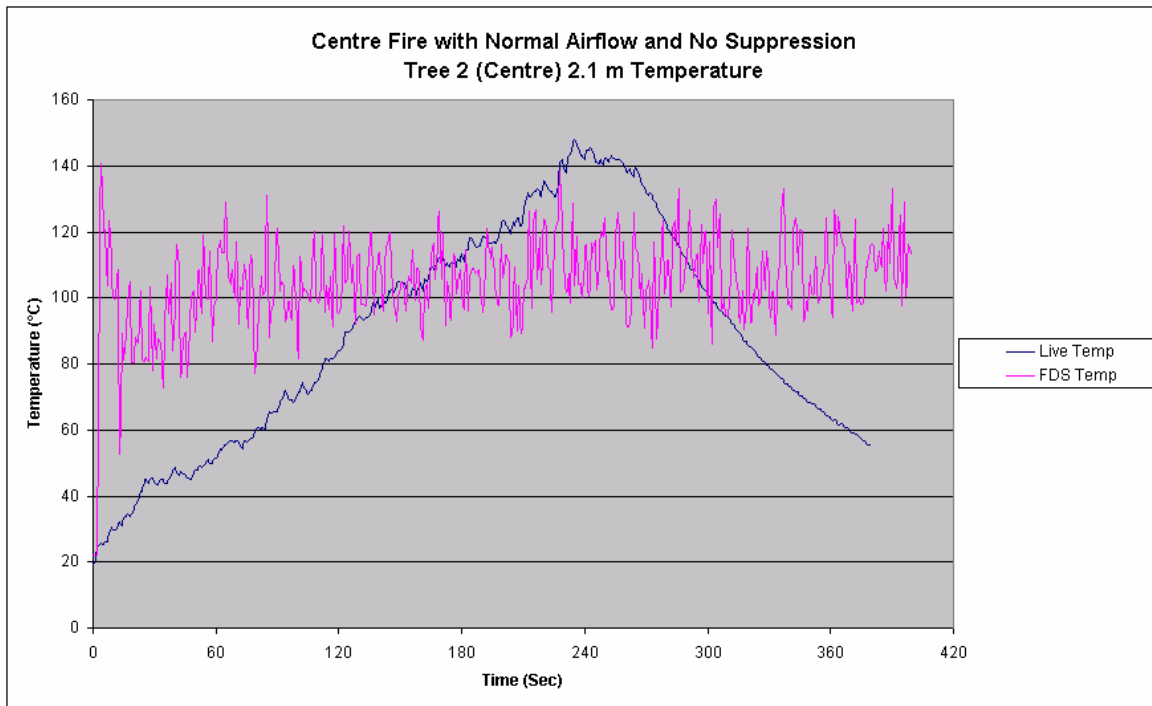


Figure 150 - Centre floor fire under normal conditions – Tree 2, 2.1m temperatures

The final sets of thermocouple readings compared for this scenario are those at 0.7m and 1.8m on Tree 1 (occupancy). These results are shown in Figure 151 and Figure 152 and correspond to the head height of an occupant when sitting at a desk and standing. In both cases the temperature comparisons are similar in that the FDS simulation reaches a relatively more stable but maximum temperature than that recorded in the live test. This is more obvious in the high level reading at 1.8m. Figure 151 shows an interesting trend in that both the live test and FDS simulation both begin to increase at the same time and rate. This would suggest that the layer height is being modelled relatively well by the FDS model at this height within the compartment. Again though the temperature of the live test is significantly higher than that calculated by FDS.

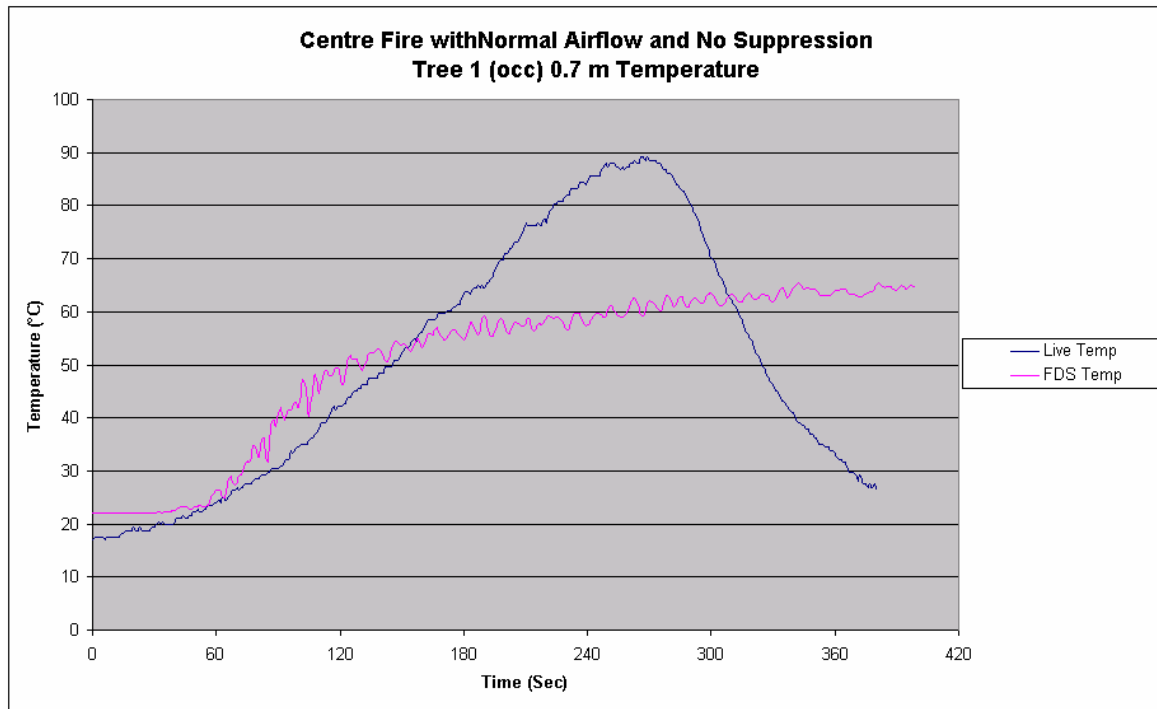


Figure 151 - Centre floor fire under normal conditions – Tree 1, 0.7m temperatures

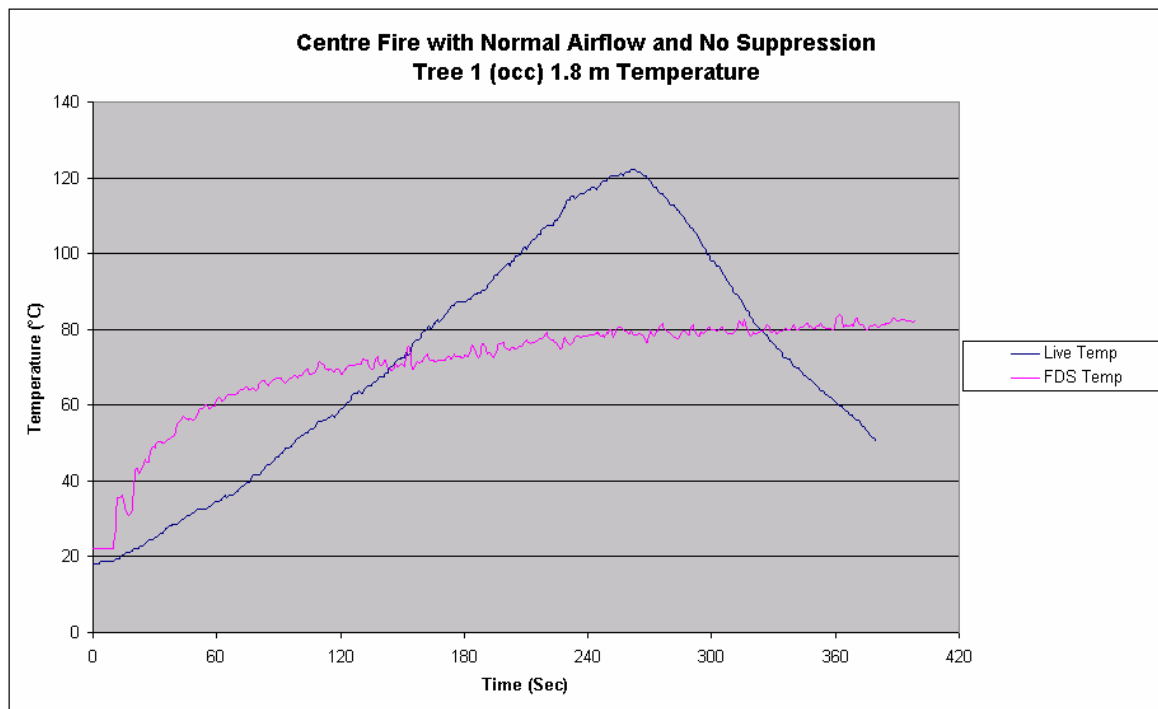


Figure 152 - Centre floor fire under normal conditions – Tree 1, 1.8m temperatures

The results from this test and simulation suggest that at all points the FDS model reaches a relatively stable situation at a lower temperature before the live test. It

is possible that the live test fire was slightly larger than 20 kW leading to the higher temperatures or that the FDS simulation has an error.

The second scenario used to compare the FDS and live test was a central pool fire with the supply airflow increased to the fire mode volume after 60 seconds. Figure 153 shows the exhaust air temperatures from the simulation and the live test. As can be seen there is a big difference between the two in that while the live test continued to increase the FDS test showed a decrease followed by stabilisation. One possible reason for this is that under these conditions the live fire appeared to burn more vigorously, possibly resulting in an increased HRR. In the FDS simulation the fire was limited in size to 20 kW so could not have had a HRR increase. Compounding this would have been the results discussed above where the FDS simulation stabilizes sooner and at a lower temperature than the live test.

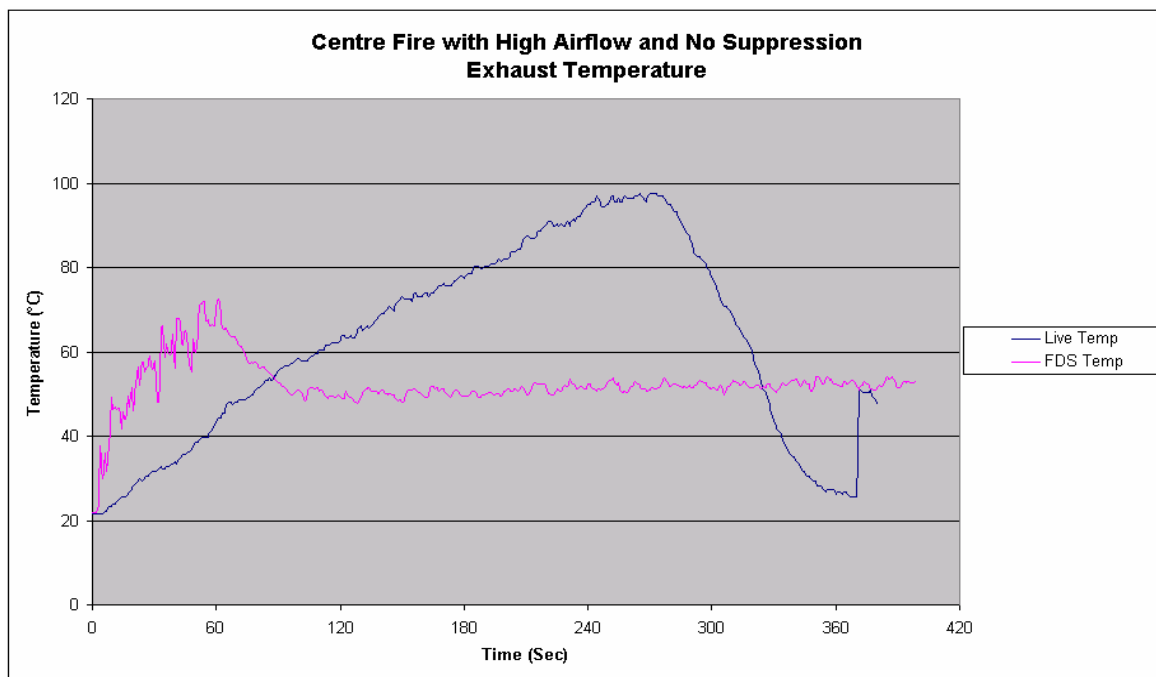


Figure 153 - Centre floor fire with high airflow only – exhaust temperatures

The next comparison for this scenario is shown in Figure 154 and displays the temperature directly above the fire. While not exactly the same, both results tend to show the same trend whereby upon the increase in airflow the temperature drops. This is caused in both cases by the flame and plume being effect by the

airflow and being deflected toward the back wall.

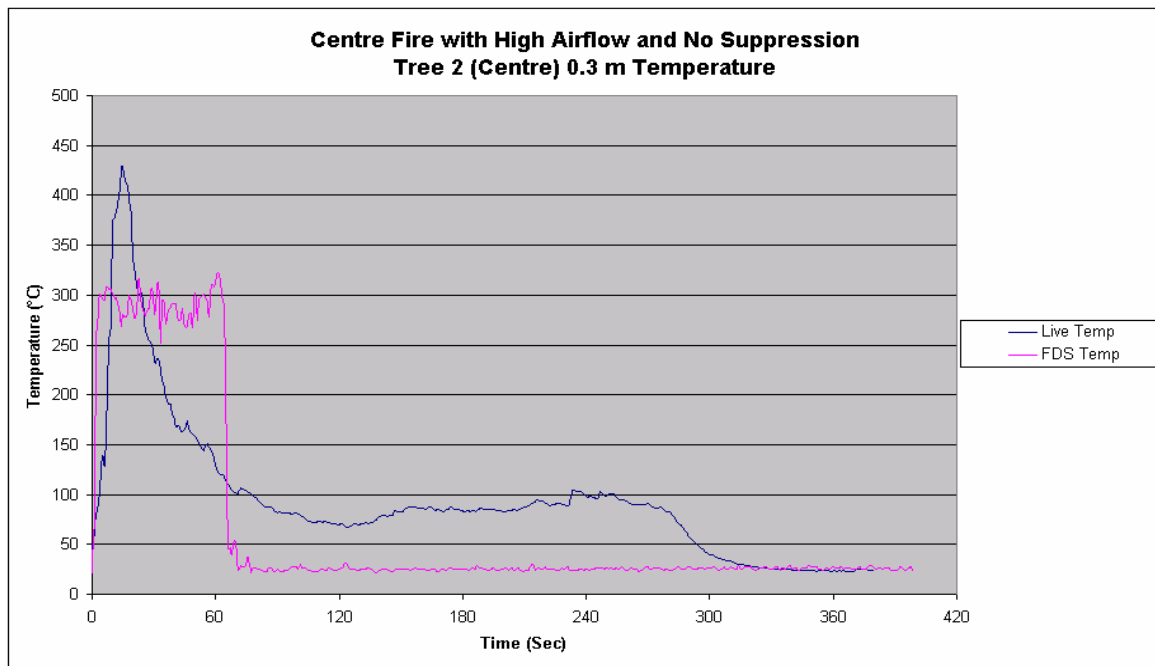


Figure 154 - Centre floor fire with high airflow only – Tree 2, 0.3m temperatures

The final comparison in this scenario looked at the temperatures within the compartment at 1.8m on thermocouple Tree 1. Again the same general trend that was observed and discussed for the exhaust gases occurs here.

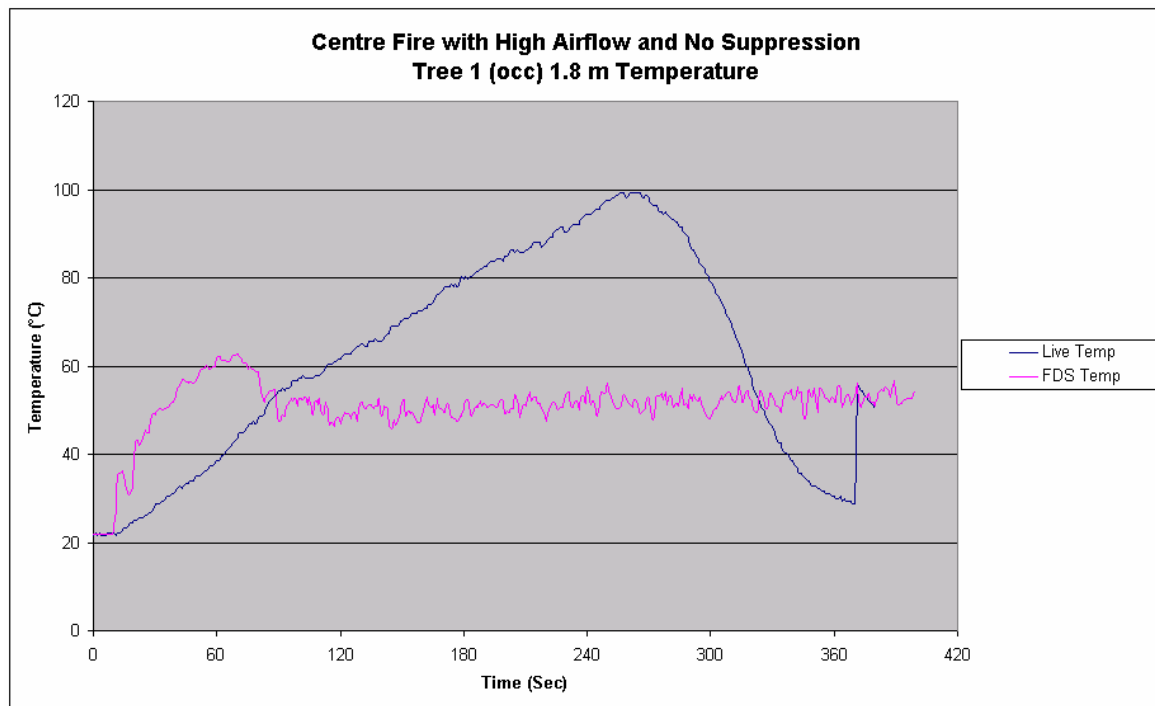


Figure 155 - Centre floor fire with high airflow only – Tree 1, 1.8m temperatures

The first comparison between suppression system activation in the live tests and the FDS simulations relates to a central pool fire with the displacement water mist system. The results obtained and displayed in Figure 156, Figure 157 and Figure 158 need to all be viewed together to obtain an indication of the internal compartment behaviour.

Figure 156 displays the exhaust temperatures and as has been seen previously, the temperature of the FDS simulation remains higher initially than the live tests. In this case though, the simulation temperature remains higher than that of the live test, which has not been the case under the previous conditions. In both the FDS simulation and the live test the activation of the displacement water mist system resulted in a rapid decrease in the temperature.

The same general trend can be seen in Figure 158, which displays the internal compartment temperature at 1.8m. Again the temperature within the simulation remains higher than the live test throughout the run and shows a rapid drop when the displacement water mist system is activated. In contrast to these two plots though, Figure 157 shows the simulation temperature at 0.3m decreasing, while in the live simulation the temperature increases to be above the simulation temperature.

The cause for these general trends and a change in trend at the 0.3m level is possibly due to the level of turbulence within the compartment. In the live test turbulence within the compartment was observed to be very high due to the water mist nozzles entraining large volumes of air. In contrast the level of turbulence that appeared to be present in the FDS simulation was less resulting in a lower level of mixing within the compartment. If this were the case, in the live situation the increased turbulence would have mixed the upper and lower layers more creating a smaller temperature gradient. In the FDS simulation though, with less mixing occurring the temperature gradient would have been larger resulting in lower temperatures at low levels and higher temperatures at high levels hence explaining the results that were recorded.

Another point that must be acknowledged is that the volume of water injected into the room was slightly less in the FDS simulation than recorded by the flow metre

in the live test. The FDS simulation was not modified to account for that as it was assumed that the increased water flow in the live test created a number of larger particles which dropped out of the atmosphere faster creating effectively similar conditions to that intended.

Unfortunately the HRR rates could not be monitored in the live test so we were unable to investigate the direct suppression effect on the flame.

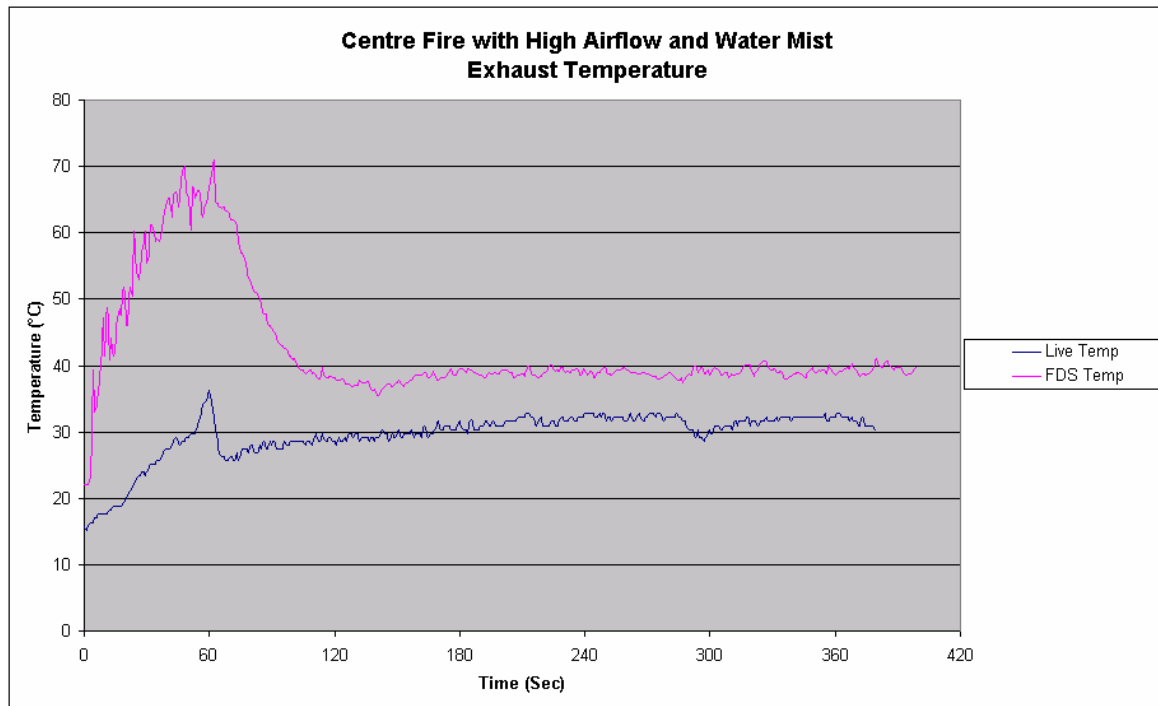


Figure 156 - Centre floor fire, high airflow and water mist – exhaust temperatures

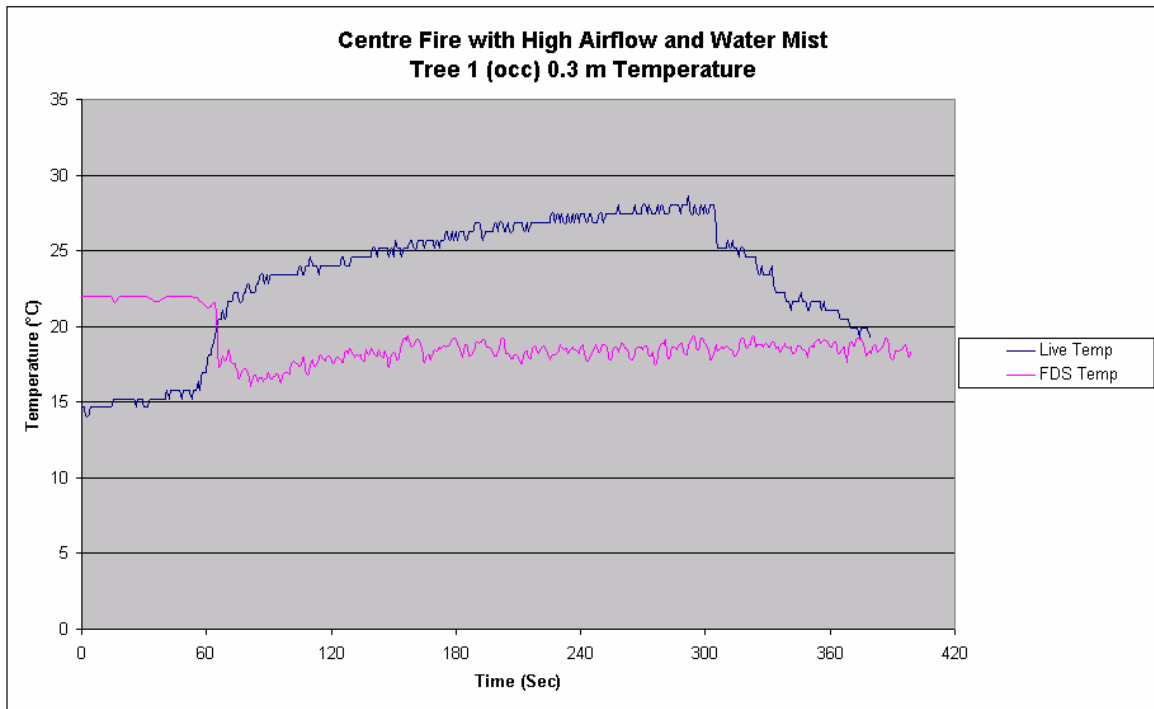


Figure 157 - Centre floor fire, high airflow and water mist – Tree 1, 0.3m temperatures

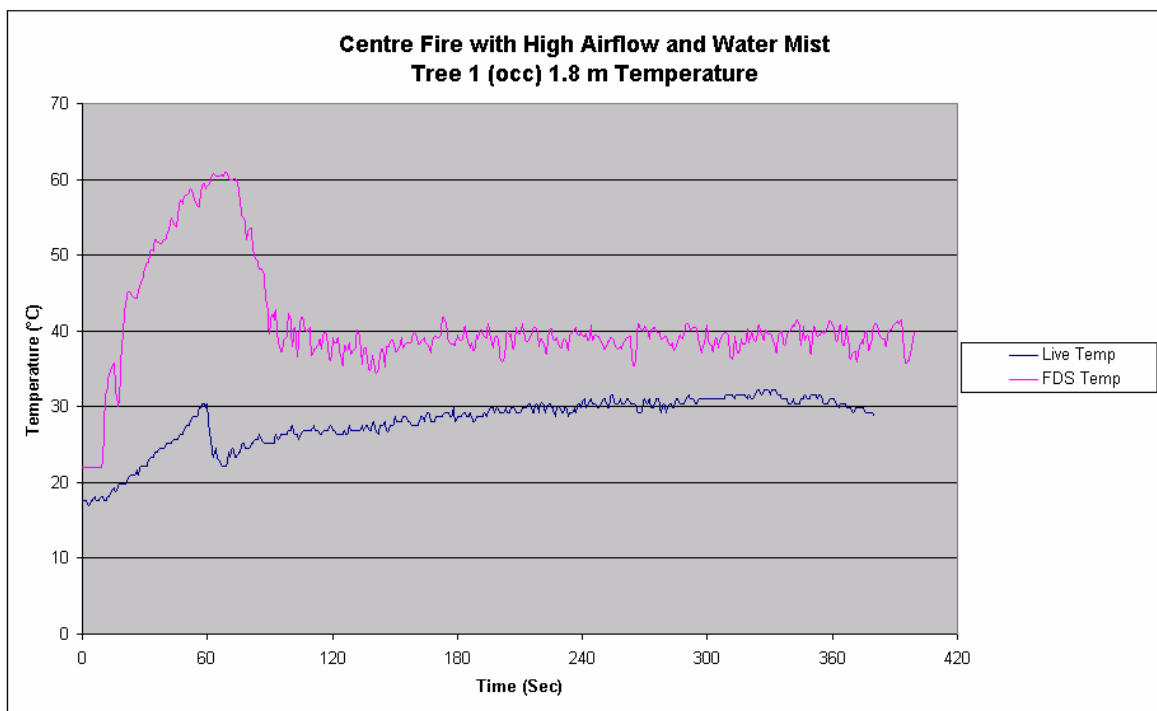


Figure 158 - Centre floor fire, high airflow and water mist – Tree 1, 1.8m temperatures

The results for the comparison of the 1m high pool fire showed a similar trend to that of the floor level pool fire discussed above. The only variation between them was that the transition between the FDS simulation being hotter or colder than the live test occurred at 1.8m instead of 0.7m. This would suggest that the mixing is occurring around the layer interface. In the case of the floor level fire the interface layer was lower than that for the 1 m fire so the transition between over and under results moved with it. Plots for the 1m comparison are shown in appendix 11.8.

The corner fire comparisons also gave similar results to this in that a transition occurs where the FDS simulation over estimated the temperature and then under estimated the temperature. In both the front and back corner comparisons the results were similar and the transition occurred at approximately 1.5m. This can be related to the height of the interface layer within the compartment and the fact that a corner fire results in less entrainment and hence a higher interface layer.

Interestingly other than the initial fire growth, the temperatures at the exhaust vent shown in Figure 159 compared well and gave approximately the same result in the FDS simulation and live test. It is unclear why this was the case when the above theory is considered, but it is possible that again the live fire was larger than 20 kW resulting in the increased temperatures.

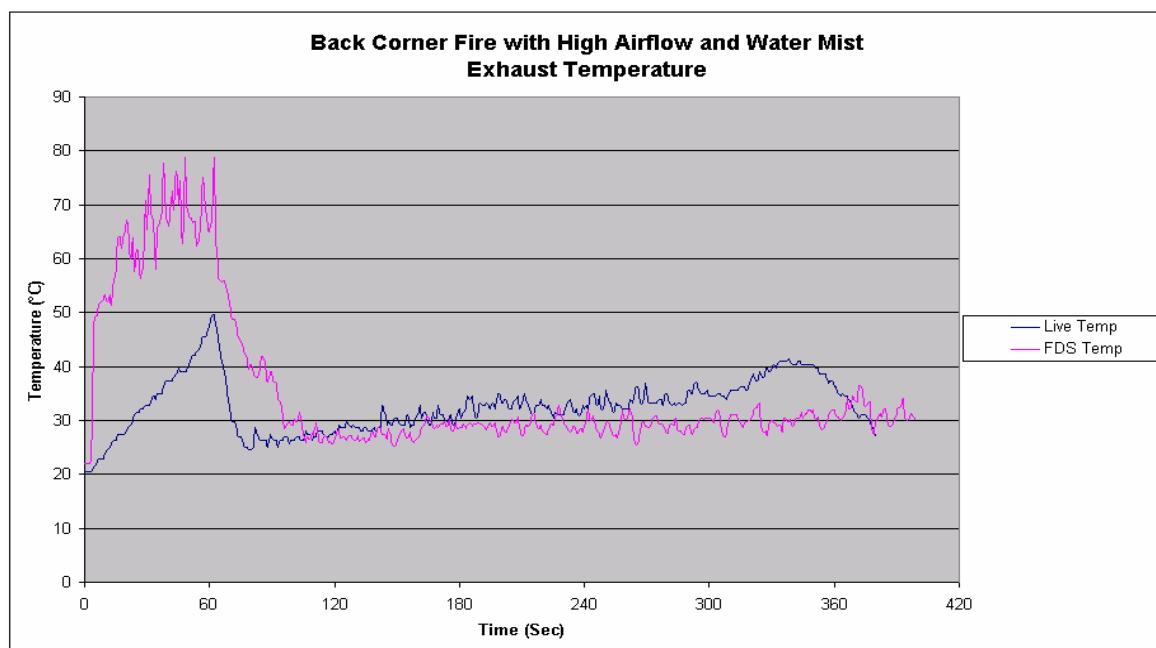


Figure 159 – Back corner fire, high airflow and water mist – exhaust temperatures

One point of interest regarding the corner fire is the temperature readings recorded at 1.3m above the fire. In Figure 160 the FDS temperature can be seen to grow steadily throughout the simulation while the live fire test showed a rapid decrease when the displacement water mist system was activated, followed by an increase when it was deactivated. In regard to the FDS simulation the increase is caused by the fire spreading up the wall as discussed in section 6.4.6. As the fire grows the temperature also increases. As for the large variation between the FDS simulation and live test during water mist activation, the results may be again due to the turbulence. In the FDS simulation the turbulence was not as great so the flame stayed in the corner. In contrast in the live test the turbulence may have forced the flame to move away from the wall and for cool air and water mist to impact on the sensor resulting in lower temperatures.

The other possibility is that FDS is not fully calculating the cooling that is occurring within the flame. This is discussed further in McGrattan et al [47] where it states that with the mixture fraction model, only the dilution effect and not cooling is accounted for in determining the flame front. This is because it is assumed that fuel and oxygen burn regardless of the temperature. A simple suppression algorithm is used in FDS that attempts to gauge whether or not a flame is viable near the stoichiometric mixture fraction surface but this is limited.

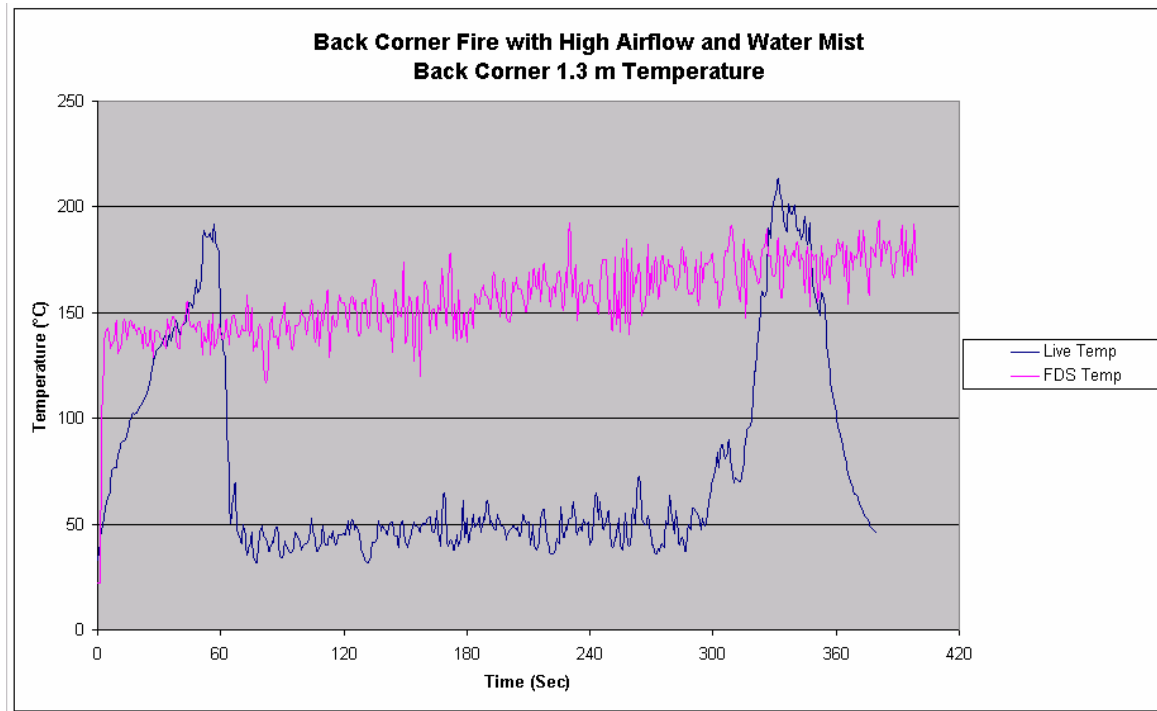


Figure 160 – Back corner fire, high airflow and water mist – Back corner 1.3m temperatures

The final comparison that was performed was for a central floor level pool fire with low airflow but with water mist injection. Figure 161 shows the temperatures recorded at the exhaust vent sensor. As can be seen the difference between the temperatures generated in the FDS simulation are much higher than those recorded in the live tests. Comparing the results inside the compartment at 0.3m and 1.8m shown in Figure 162 and Figure 163, the same FDS over and under estimation trend as discussed above can be seen. Further more by looking at the live test the temperature is almost constant throughout the compartment suggesting a very large degree of mixing. In contrast the FDS simulation results show a large temperature gradient within the compartment suggesting little mixing is occurring.

In addition to this it is possible that the build-up of water mist in the live test caused the thermocouples to become wet and the temperature readings to be lower than the actual air temperature.

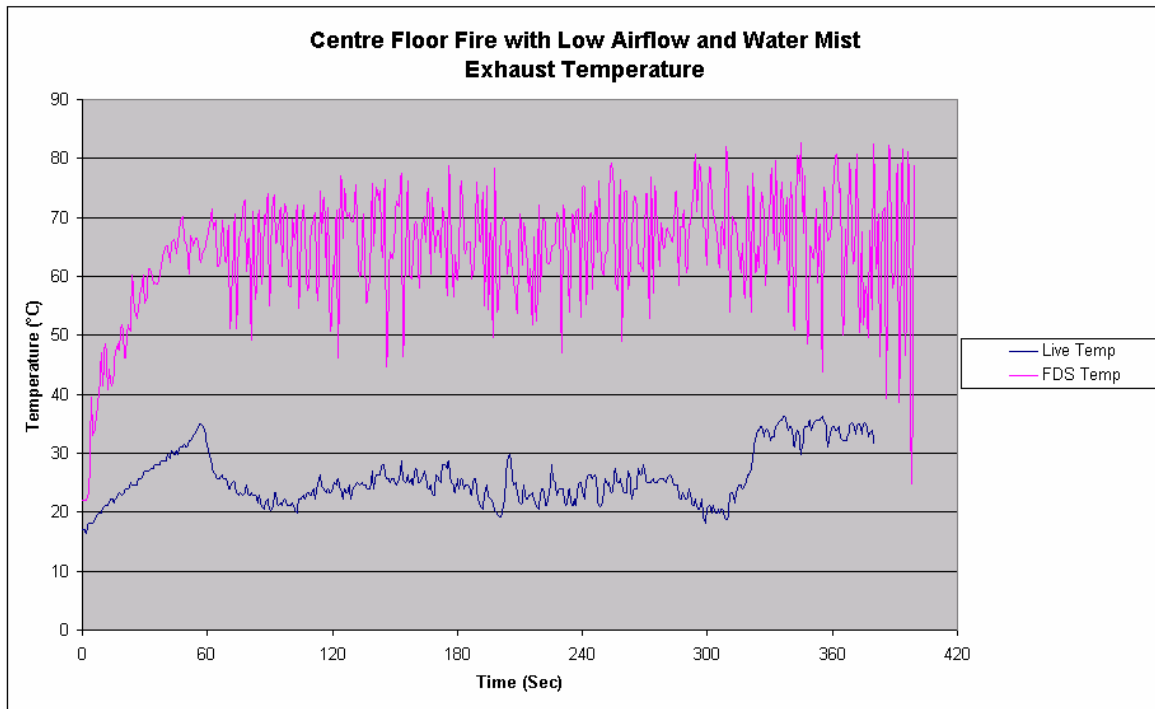


Figure 161 – Centre floor fire, low airflow and water mist – exhaust temperatures

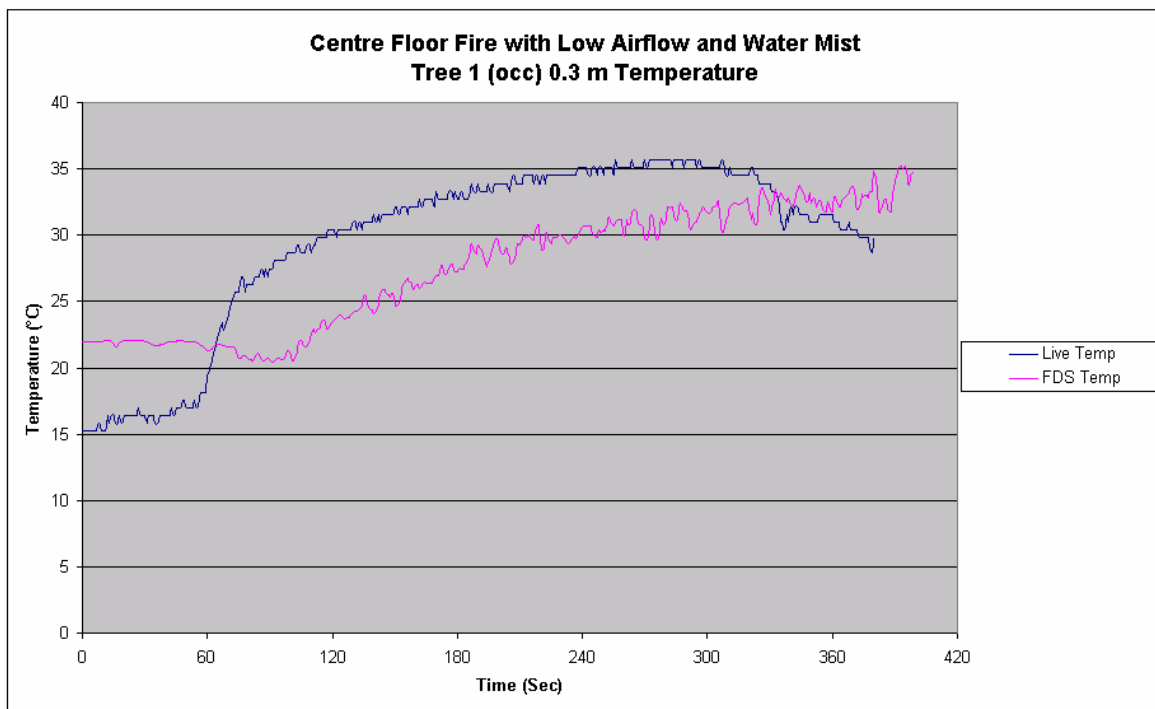


Figure 162 – Centre floor fire, low airflow and water mist – Tree 1, 0.3m temperatures

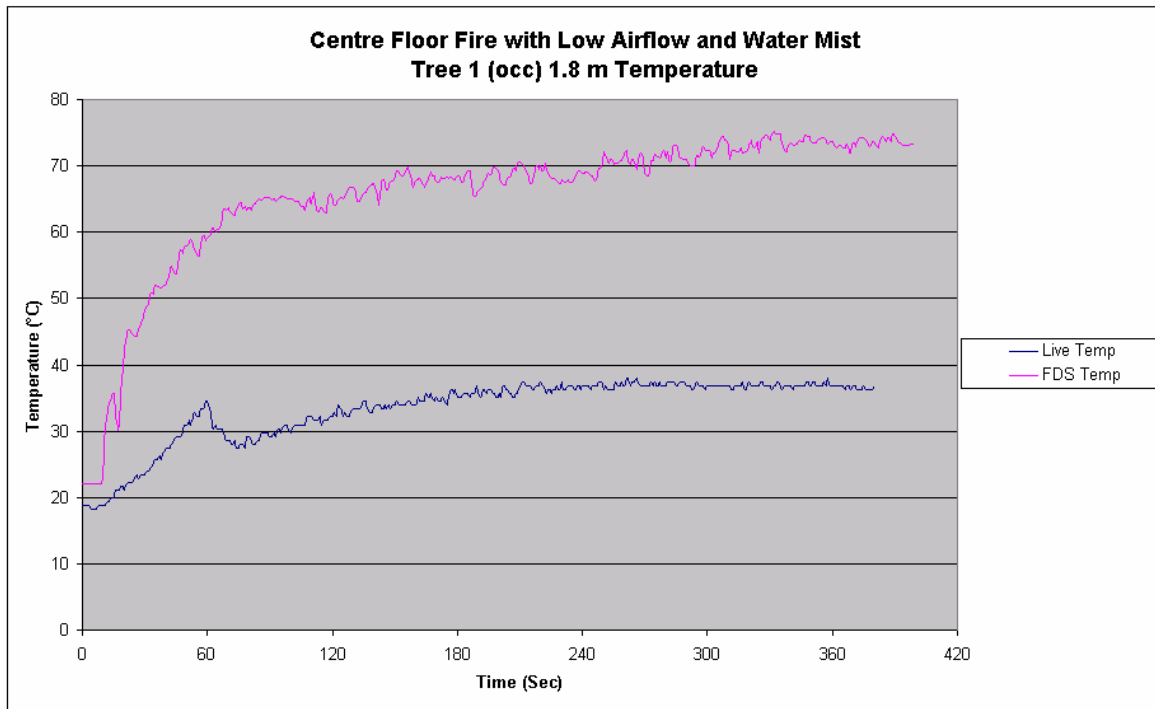


Figure 163 – Centre floor fire, low airflow and water mist – Tree 1, 1.8m temperatures

7.2 General Conclusion

The comparison of the results suggests that the FDS simulation is generating temperature results in relatively the same region as those experienced in the live testing. The FDS results though tended to show a more stable and fast acting environment than the live tests with a faster increase, but lower peak, in temperature. The FDS simulation also appears to generate far less mixing within the compartment than that observed during live testing.

There are a number of possible errors between the FDS and live results, but it appears that the primary one is in the turbulence introduced into the compartment from the water mist nozzles. The FDS simulations tended to under predict the mixing and entrainment that occurred from the injection of the water mist. This may have been due to the way in which the nozzles were described in FDS or simply that due to the small scale of the water mist droplets the drag and entrainment were beyond the computational limits of the program.

Other sources of error related to the live testing itself and the inherent errors that occur in live tests. The HRR from the pool fire was not exactly known and the temperatures generated under identical scenarios, particularly in the first 60 seconds, were not accurately repeatable. A further point of error was the exact characteristics of the water mist generated. The exact size distribution of the water mist was unknown and as previously discussed the flow metre in the live test showed a slightly higher water flow than in the FDS simulations. It is unclear exactly the effect this would have on the two sets of results.

One drawback of this testing is that the HRR from the live fire could not be compared with that of the FDS simulation. The FDS simulations indicated no perceivable drop in the HRR of the fire, resulting in relatively constant temperatures above the fire. This was most likely due to FDS using a mixture fraction model where only the dilution effect and not cooling is accounted for in determining the flame front as it is assumed that fuel and oxygen burn regardless of the temperature. In contrast the live test results showed a noticeable drop in temperature above the fire but it was unclear if this was due to a decrease in HRR

or simply cooling and turbulence within the flame front that could not be modelled in FDS.

In summary while the FDS simulation provided valuable information on the compartment atmosphere and generated temperatures in the region of those recorded under live testing, it is unclear if the water mist fire suppression can accurately be modelled at this stage. Future work would need to be carried out to confirm if the FDS simulation is accurate and the HRR within the compartment remains constant, or if FDS needs to be modified to handle a fine water mist. At this stage FDS could be used for the initial optimization and investigation, but live testing will be needed for accurate results.

8. Future Work

As this research was only the initial concept design and basic testing of a displacement water mist system, there are a number of opportunities for future work. In particular the water density required and the injection method needed to suppress the fire while not mixing the internal atmosphere is the primary concern.

Specifically areas that require further investigation include:

- The method of water mist injection. A number of possible options exist and may include the use of ultrasonic mist generators or a new nozzle arrangement. In regard to the nozzle arrangement, one option that was theorized during this write up was the suspension of nozzles within individual single ended cylinders possibly with a small number of holes at one end. As the nozzles are activated the entrainment causes a negative pressure to be formed within the cylinder. This pressure slows the water droplets down while the required volume of air is drawn in through the holes without the need for an increased supply fan size. This option could substantially decrease the cost of the system while increasing its effectiveness and ease of installation.
- The density of water mist injected. In this study a density of 200g/m^3 was used based on the work performed at Lund [19], but other studies [25] have indicated that for small fires densities of up to 600g/m^3 are required. As the system is designed to operate as soon as possible the fires are small and so the density of water mist used may need to be higher. Testing will need to be carried out to determine the density is required.
- The effect of increased or decreased airflows. The airflow rate of one air change per minute used in this study was primarily based on the fire size of 20 kW. If this airflow were increased though, the layer interface height would increase providing more protection for occupants. On the negative side the increased airflow would require a greater volume of water to be injected and could create more turbulent mixing. The optimum airflow would need to be investigated based on compartment size.

- The effect on different sized fires. In these tests the fire size was maintained at approximately 20 kW. This is not the limiting size in compartment fires though, and the effectiveness of the system on larger fires will need to be investigated.
- Accurate measurements of the fire HRR outputs under live conditions for comparison with FDS results. As discussed in this report, the FDS simulations indicated that there was no decrease in the HRR of the fires. It is unclear if this is actually what happened, or whether FDS simply cannot model the small-scale interaction of the water mist on the fire. Measurements of the HRR during live testing would allow the FDS results to be compared and the actual effect on the flame investigated.

9. Conclusion

As stated the primary objective of this study was to determine if a fine water mist could be used in conjunction with a displacement ventilation system to create a fire suppression system that allowed occupants and electronics to remain safely within a compartment throughout a fire. The results from the testing carried out on the experimental setup used in this study, did not completely meet this objective as the fire was not extinguished and mixing created within the compartment resulted in combustion products being present around the occupants. The setup did however result in vastly reduced temperatures and a better atmosphere than occurred with no suppression, water mist only or conventional sprinklers. Additionally the displacement water mist system was the only suppression system tested that did not cause the computer or lights within the room to short-circuit and fail.

In terms of the live testing, the type of water mist nozzles used in the experiment appeared to generate a much higher level of entrainment than intended. The large volumes of entrained air resulted in two negative effects. Firstly the high velocity flow caused mixing to occur between the upper and lower layers within the compartment hence introducing combustion products into the occupied lower zone. Secondly the high entrainment rate reduced the density of water within the air as it passed over the fire. Effectively the density of water was too low for suppression, and in some cases the high airflow and turbulence resulted in an increase in the fire ferocity. As well as the decreased water density caused by entrainment, there is also some debate as to whether the density of 200 g/m^3 initially designed for was sufficient to cause suppression in the first place and that with such small fires a higher density of up to 600 g/m^3 would have been needed.

The computer simulations carried out with FDS showed a similar result to that seen in the live testing. Under increased airflow the upper and lower layer interface increased in height and remained relatively stable as intended. On activation of the water mist nozzles though, the interface between the layers became disturbed and mixing occurred. This became even more obvious when

the airflow remained low while the water mist nozzles were activated. The upper layer appeared to collapse and large amounts of mixing occurred.

In regard to the tenability within the compartment, both the live testing and FDS simulations suggest that the displacement water mist system used, while not operating specifically as intended, provided the most tenable environment. The observers present in the compartment during the live tests found no difficulty within the compartment during the fire. The FDS results indicated a similar result in that a cross section of the compartments CO₂ and soot levels showed that these combustion products accumulated at the ceiling and were much less dense when the displacement water mist system was operating.

A comparison between the results recorded from the live testing and those generated from the FDS simulations showed that the FDS simulations tended to indicate a faster increase in compartment temperature, but a lower peak temperature. Additionally with the activation of the displacement water mist system the results indicated that more mixing was occurring in the live testing than in the FDS simulations. This resulted in the temperatures between the two methods being different, as the increased mixing tended to reduce the temperature difference between the bottom and top of the compartment. There is also some uncertainty as to how well FDS simulates flame suppression by the water mist. The results from the FDS simulations showed almost no effect on the HRR from the water mist while in the live tests it was observed that in some cases the fire decreased in size suggesting that the HRR was also decreased. Unfortunately this was unable to be investigated thoroughly in this study and is left for future work. The conclusion from the comparison is that while providing similar results to the live testing, FDS cannot be solely used to test the displacement water mist system. Instead FDS could be used for the initial optimization and investigation, but that live testing will be needed for accurate results.

In summary, while the displacement water mist system did not operate exactly as intended, the observations made during this study suggest that the concept is valid but that refinement such as water mist delivery and density need to be investigated further.

10. References

- [1] Mawhinney, J.R. and Solomon R. (1997) *Water mist fire suppression systems*, Fire protection handbook, 18th ed. National Fire Protection Association, Quincy, MA.
- [2] Milke, J. A. (1996) *Comparison of the Performance of water Mist System Designs For Library Stack Areas*, University of Maryland, College Park, Baywood Publishing Co., Inc.
- [3] Mawhinney, J.R. and Back, G. G. (2002) *Water Mist Fire Suppression Systems*, The SFPE Handbook of Fire Protection Engineering, 3ed Ed, National Fire Protection Association, Quincy, MA.
- [4] Hadjisophocleous, G. V. Mawhinney, J.R. (1996) *The Role of Fire dynamics in Design of Water Mist Fire Suppression Systems*, Presented at INTERFLAM '96.
- [5] Cousin, C. S. *The Potential of Fine Water Sprays As Halon Replacements for Fire in Enclosures*, Proceedings of the International Water Mist Conference, Swedish Testing Institute, Boras, Sweden, Nov. 5-7.
- [6] Mawhinney, J.R. and Eng P. *Characteristics of Water Mist For Fire Suppression in Enclosures*. National Research Council, Institute for research in construction, National Fire Laboratory, Canada.
- [7] Holmstedt, G. *Extinguishment Mechanisms of Water Mist*, Lund University, LUND, Sweden.
- [8] Factory Mutual (2000) *The Facts About Water Mist Systems*, Approved Product News, Volume 16, Number 2.
- [9] Ananth, R., Ndubizu, C.C. and Tatem, P. A. (2000) *The Effects of Droplet Size and Injection Orientation on Water Mist Suppression of Low and High Boiling Point Liquid Pool Fires*, Combustion Science and Technology, Vol. 157, Gordon and Breach Science Publishers Imprint, Malaysia, pp 63-86.

- [10] Brenton, J., Drysdale, D. and Grant, G. (2000) *Fire Suppression By Water Sprays*, Progress in Energy and Combustion Science, Vol. 26, Pergamon Press. Oxford. New York. pp 79-130.
- [11] Wighus, R. (2001) *Water mist fire suppression technology – status and gaps in knowledge*. Norwegian Fire Research Laboratory (SINTEF), Presented at International Water Mist Conference, Vienna, Austria, 4-6 April 2001.
- [12] Wighus, R. (1991) *Extinguishment of Enclosed Gas Fires With Water Spray*, Proceedings of the Third International Symposium on Fire Safety Science, The University of Edinburgh, Edinburgh, Scotland.
- [13] Drysdale, D. (1998) *An Introduction to Fire Dynamics. Steady Burning of Liquids and Solids*, 2nd Ed, John Wiley & Son's Ltd, England.
- [14] Wighus, R. (1998) *An Empirical Model for Extinguishment of Enclosed Fires with Water Mist*, Norwegian Fire Research Laboratory, Halon Options Technical Working Conference, 12-14 May, pp 482-489.
- [15] Roberts, G. V., (2001) *An Experimental Investigation of The Thermal Absorption by Water Sprays*, Fire Research Development Group, Home Office, London.
- [16] Boudouvis, A. G., Karayannis, A. N., Keramida, E. P. and Markatos, N. C. (2000) *Numerical Modeling of Radiant Heat Attenuation Through Water Mist*, Combustion Science and Technology, Vol. 159, Gordon and Breach Science Publishers Imprint, Malaysia, pp 351-371.
- [17] Mawhinney, J.R., Dlugogorski, B.Z. and Kim, A. K. (1994) *A Closer Look at the Fire Extinguishing Properties of Water Mist*, Proceedings 4th IAFSS Symp on Fire Safety Science, Ottawa, Canada, pp 47-60.
- [18] Jones, A. and Nolan, P. F. (1995) *Discussions On The Use Of Fine Water Sprays or Mist for Fire Suppression*, Journal Loss Prev. Process Ind., Volume 8, Butterworth-Heinemann Ltd, pp 17-21

- [19] Aderson, P. Arvidson, M. and Holinstedt, G. (1996) *Small Scale Experiments And Theoretical Aspects Of Flame Extinguishment With Water Mist*. Lunds tekniska hogskola, Lunds universitet.
- [20] National Fire Protection Association (1997) *NFPA 750*, Vol. 7, National Fire Protection Association, Quincy, MA.
- [21] Mawhinney, J.R. and Richardson, J. K. (1996) *A Review of Water Mist Fire Suppression Research and Development*. Technical Note, Fire Technology First Quarter 1997, pp 54-89.
- [22] Boyer, J. C., Grosshandler, W. L. and Yang, J. C. (1996) *Minimum Mass Flux Requirements to Suppress Burning Surfaces with Water Sprays*, NIST, Gaithersburg.
- [23] Fleming, J. W., Sheinson, R. S. and Williams, B. A. (2002) *Suppression Effectiveness of Aerosols: The Effect of Size and Flame Type*, Navel Research Laboratory, Washington, DC.
- [24] Presser, C., Widmann, J. and Papadopoulos, J, (2002) *Liquid Agent Transport Around Solid Obstacles*, NIST, Gaithersburg, MD.
- [25] Aune, P., Drangshot, G., Stensaas, J. P. and Wigus, R. (1993) *Full Scale Water Mist Experiments*, Proceedings of the International Water Mist Conference, Swedish Testing Institute, Boras, Sweden, Nov. 5-7.
- [26] Mawhinney, J.R. and Eng P. (193) *Design of Water Mist Fire Suppression Systems for shipboard Enclosures*, Proceedings of the International Water Mist Conference, Swedish Testing Institute, Boras, Sweden, Nov. 5-7.
- [27] Aune, P., Drangshot, G., Stensaas, J. P. and Wigus, R. (1993) *Fine Water Spray System – Extinguishing Tests in Medium and Full Scale Turbine Hood*, Proceedings of the International Water Mist Conference, Swedish Testing Institute, Boras, Sweden, Nov. 5-7.

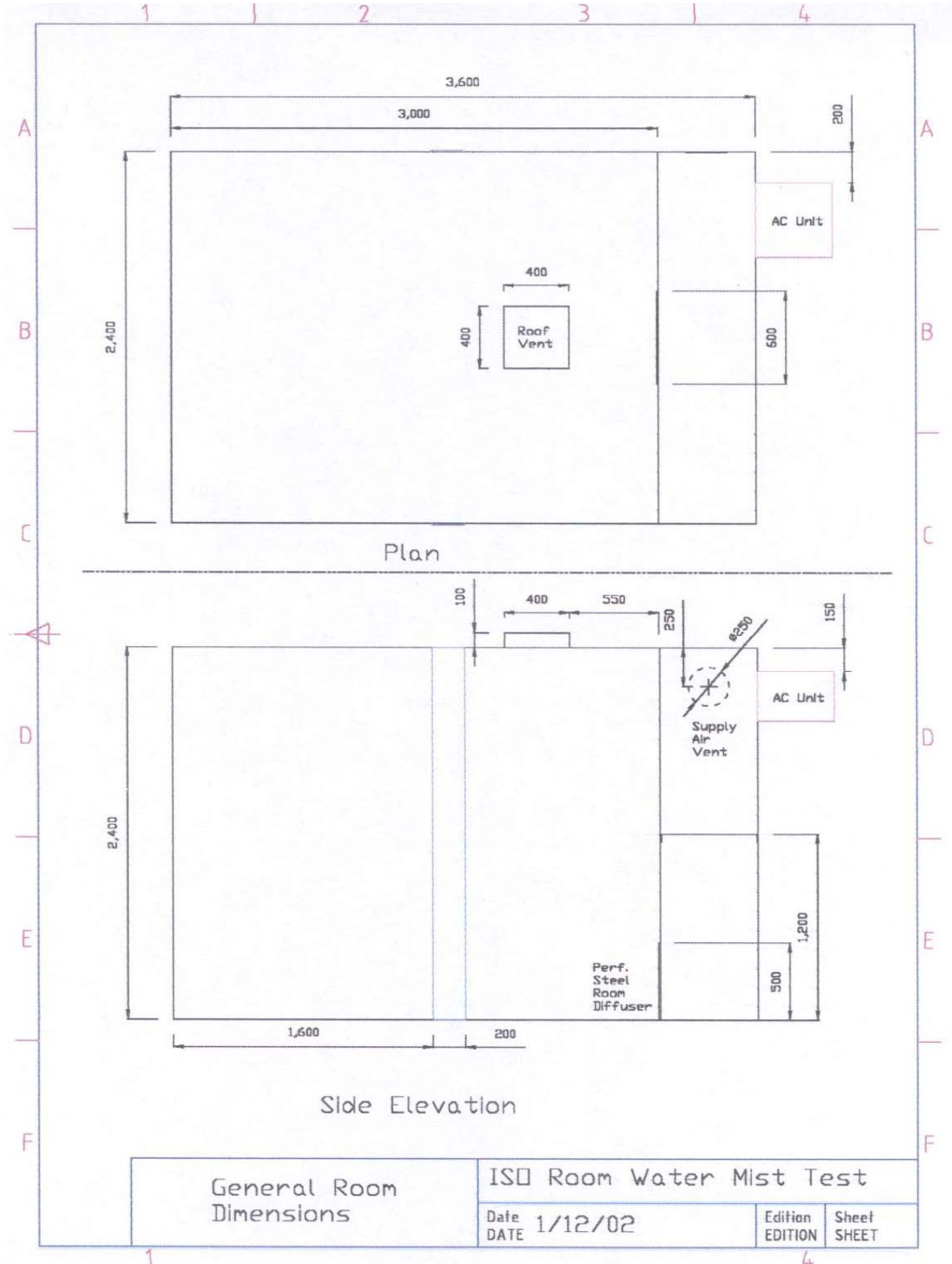
- [28] Simpson, T. and Smith, D.P. (1993) A Fully Integrated Water Mist Fire Suppression System for Telecommunications and Other Electronics Cabinets. Fire and Safety International, Colnbrook, UK.
- [29] Evans, D. and Pfenning, D. (1985) *Water Sprays Suppress Gas-Well Blowout Fires*. Oil and Gas Journal, April 29.
- [30] Nielsen, P. V., Riskowski, G., Shilkrot, E. and Zhivov, A. M. (2000) A Design Procedure For Displacement Ventilation - Part 1 of 2, HPAC Journal, November, pp. 39-49.
- [31] REHVA Project. *Displacement Ventilation in non-industrial premises*. www.rehva.com.
- [32] Fitzner, K. (1996) Displacement Ventilation And Cooled Ceilings, Results Of Laboratory Tests And Practical Installations, Indoor Air '96, Nagoya.
- [33] Bill, R. G. and Croce, P. A. (1993) *Perspectives on Fine Water Spray (Water Mist) Technology at Factory Mutual Research Corporation*. Presented at the International Conference on Water Mist Fire Suppression Systems, Swedish Testing Institute, Boras, Sweden, Nov. 5-7.
- [34] Kim, A. K., Liu, Z. and Su, J. Z. (2001) *Examination of Performance of Water Mist Fire Suppression Systems Under Ventilation Conditions*, Journal of Fire Protection Engineering, Vol. 11, SFPE, August 2001.
- [35] International Organisation for Standardization. (1993) *Fire Tests – Full Scale Room Test For Surface Products*, ISO 9705, Geneva.
- [36] The Institute of Refrigeration, Heating, Air Conditioning Engineers, (2000) *IRHACE Handbook – Millennium Edition*, IRHACE, Aust.
- [37] Babrauskas, V. (1995) *Burning Rates*, The SFPE Handbook of Fire Protection Engineering, 2nd Ed, National Fire Protection Association, Quincy, MA.
- [38] Karlsson, B. & Quintiere, J. G. (2000) *Enclosure Fire Dynamics*, CRC Press LLC, Florida, USA.

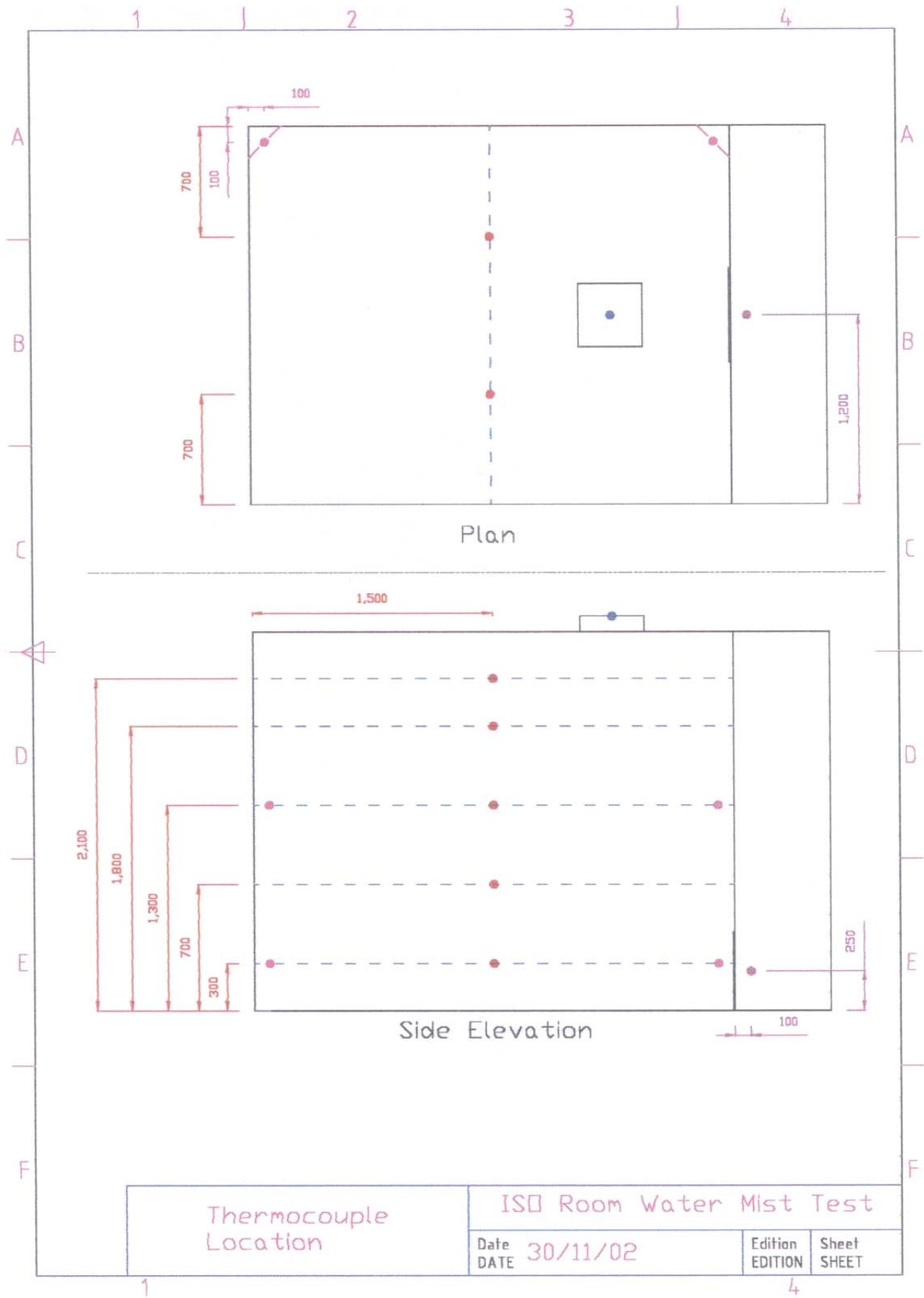
- [39] Buchanan, A. (2001) *Fire Engineering Design Guide*, 2nd Ed, University of Canterbury, Centre for Advanced Engineering, Christchurch, New Zealand.
- [40] Halton, (1995) Halton H.E.L.P. 5.1, Halton.
- [41] NFPA (1995) *Basics of Fire and Fire Science*, The SFPE Handbook of Fire Protection Engineering, 2nd Ed, National Fire Protection Association, Quincy, MA.
- [42] Meacham, B. J., Richard, L. P. and Schifiliti, R. P., (1995) *Design of Detection Systems*, The SFPE Handbook of Fire Protection Engineering, 2nd Ed, National Fire Protection Association, Quincy, MA.
- [43] American Society of Heating, Refrigerating and Air-conditioning Engineers (2000) *ASHRAE handbook - Fundamentals (SI edition)*, Atlanta, Ga.
- [44] Proulx, G. (2000) *Movement of people*, The SFPE Handbook of Fire Protection Engineering, 3rd Ed, National Fire Protection Association, Quincy, MA.
- [45] Petterson, N. (2002) *Assessing the Feasibility of Reducing the Grid Resolution in FDS Field Modelling*, Fire Engineering Research Report, University of Canterbury, Christchurch, NZ.
- [46] Hinze, J.O. (1975) *Turbulence*. 2nd Edition. McGraw-Hill, New York
- [47] McGrattan, K.B., Baum, H.R., Rehm, R.G., Hamins, A., Forney, G.P., Floyd, J.E., Hostikka, S. (2001) *Fire Dynamics Simulator (Version 2) – Technical Reference Guide*, NISTIR 6783 (Draft), National Institute of Standards and Technology, Gaithersburg, Maryland, USA.
- [48] Cox, G. (1995) *Basic Considerations*, Combustion Fundamentals of Fire. Ed. G. Cox. Academic Press, London.
- [49] Floyd, J.E., Baum, H.R., McGrattan, K.B. (2001) *A mixture fraction combustion model for fire simulation using CFD*. The International Conference on Engineered Fire Protection Design (San Francisco), June 11-15. pp 279-290

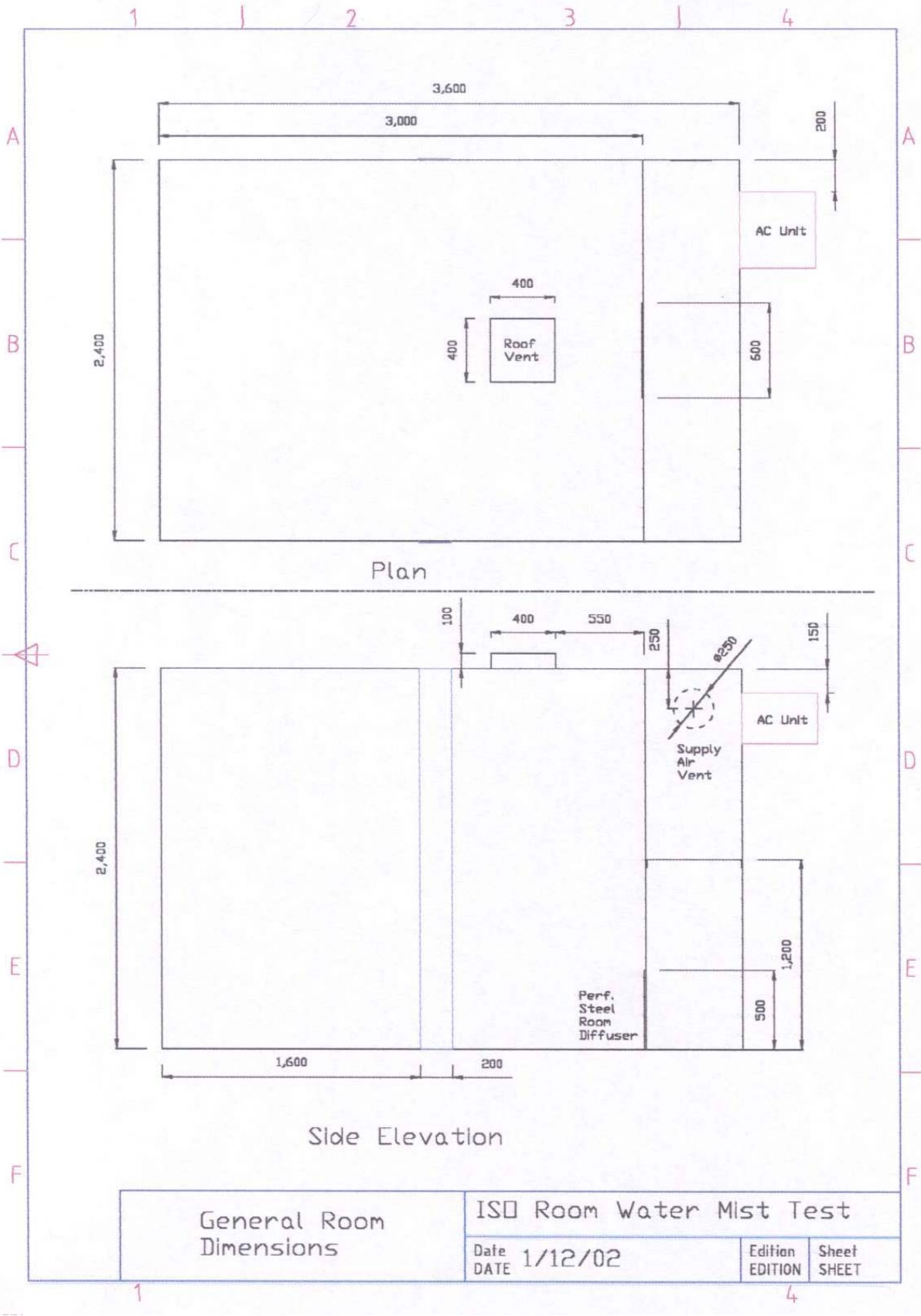
- [50] Kreyszig, E. (1993), *Advanced Engineering Mathematics*. 7th Edition. John Wiley and Sons Inc., New York.
- [51] Lovatt, A. (1998) *Comparison studies of zone and CFD fire simulations*. Fire Engineering Research Report, University of Canterbury.
- [52] Ma, T. and Quintiere, J. (2001) *Accuracy of 3D LES model with combustion for axisymmetric fire plume*. The International Conference on Engineered Fire Protection Design (San Francisco), June 11-15. pp 291-303.

11. Appendix

11.1 Full scale compartment plans







11.2 Displacement ventilation design files

Halton H.E.L.P. 5.1 DISPLACE C:\MYDOCU~1\BEN\FIREEN~1\THESIS\ROOM.DSP
 Project Dimensioning data Calculation Prints Help

SPACE DATA
 Previous Next List New Delete Typical loads

SPACE DIMENSIONS				DEFAULT VALUES FOR SPACE			
Name of space	:	Room		Lp(A)max(N=1)	[dB(A)]:	50.00	
Length (L)	[m]:	3.00		(qv/A)min	[l/sm ²]:	0.00	
Width (B)	[m]:	2.40		Tr	[°C]:	22.00	
height (H)	[m]:	2.40					

Space A Office Hr<3m

nr	name	P[W]	Pt[%]	Pc[%]	H[m]	Tf[°C]	qmi[mg/s]
1	1 100w Light bulb	100.0	96	96	1.2	35.0	0.00
2	1 100w light bulb	100.0	96	96	1.2	35.0	0.00
3	1 PC	100.0	100	80	1.2	40.0	0.00
4	1	0.0	0	0	0.0	0.0	0.00
5	1	0.0	0	0	0.0	0.0	0.00
6	1	0.0	100	100	0.0	0.0	0.00
7	1	0.0	100	100	0.0	0.0	0.00
8	1	0.0	100	100	0.0	0.0	0.00
9	1	0.0	100	100	0.0	0.0	0.00
10	1	0.0	100	100	0.0	0.0	0.00

Ok Cancel

Picture

Space nr : 1 (1)

Choose function.
Edit space data.

Halton H.E.L.P. 5.1 DISPLACE C:\MYDOCU~1\BEN\FIREEN~1\THESIS\ROOM.DSP
 Project Dimensioning data Calculation Prints Help

SPACE DATA :
 Name : Room
 L [m]: 3.0
 B [m]: 2.4
 H [m]: 2.4
 Tr [°C]: 22.0
 Dr [dB]: 4.0
 Lp(A)m [dB]: 50.0
 qvmin [l/s]: 0

DIMENSIONING DATA:
 DM: TEMPERATURE
 P [kW]: 0.3
 Pt [kW]: 0.3
 Pc [kW]: 0.3
 Tf [°C]: 36.5
 H1 [m]: 1.2
 qmi [mg/s]: 0.0

RESULTS:
 qv [l/s]: 48
 Te-Ts [°C]: 5.1

DEVICE DATA:
 Type: AFA 200
 Nr : 1
 qvtot [l/s]: 48
 dpst [Pa]: 5.5
 Ts [°C]: 19.0

DIMENSIONING VALUES

If Ts is not Tr-3 °C
 Tr might change in oz

Qv tot. [l/s]: 48.5
 Tr [°C]: 22.0
 Ts [°C]: 19.0
 v(lim) [m/s]: 0.20

Ok Cancel

Picture




Space nr : 1 (1)

Calculations
Choose function.

11.3 Water mist nozzles characteristics

AIR ATOMIZING NOZZLES

Air Atomizing Nozzles • QuickMist™ Series

QMJ	QMJML	QMJAU
		
1/4" NPT or BSPT (F) air and liquid inlets	1/4" NPT or BSPT (F) air and liquid inlets with mounting lugs	1/4" NPT or BSPT (F) air and liquid inlets. For use with siphon or external mix set-ups.
Patent No. 5385304		

DESIGN FEATURES

KYNAR® QuickMist nozzles offer all the advantages of conventional air atomizing spray nozzles, but use up to 50 percent less air to provide the same degree of atomization. They are manufactured of chemically resistant KYNAR and feature a quick-connect spray set-up for reduced maintenance time.

Automatic aligning of flat sprays in 45° increments eliminates

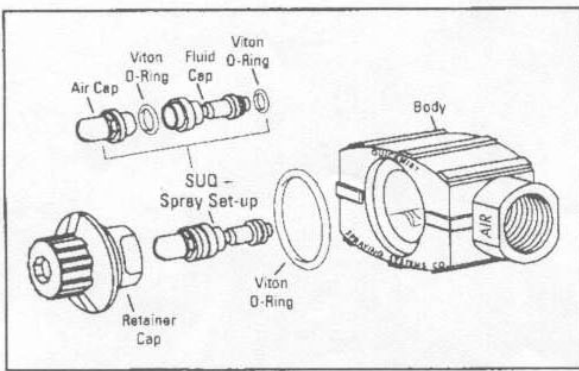
time-consuming manual spray pattern alignment.


- A PVDF chemical-resistant fluoropolymer construction – able to withstand temperatures up to 200°F (93°C) – is particularly well suited to chemical, food processing, and electronics applications which require a variety of temperature ranges and resistance to acids, bases, and oxidizing agents.

- Pressure spray set-ups include round, wide angle round, and flat spray patterns. Siphon-fed set-ups are available in round and external mix flat spray.
- KYNAR QuickMist nozzles are easy for retrofit with 1/4J nozzle assemblies. 1/4" NPT or BSPT (F) air and liquid inlets.

Request Data Sheet Series 38860.

The **Model QMJAU** QuickMist nozzle features an internal air cylinder for controlled on/off operation.





Spraying Systems Co.®

Phone 1-800-95-SPRAY, Fax 1-888-95-SPRAY
 Outside the U.S., Phone 1(630) 665-5000, Fax 1(630) 260-0842
 Visit our Web Site: <http://www.spray.com>

308

Air Atomizing Nozzles • QuickMist™ Series



AIR ATOMIZING NOZZLES

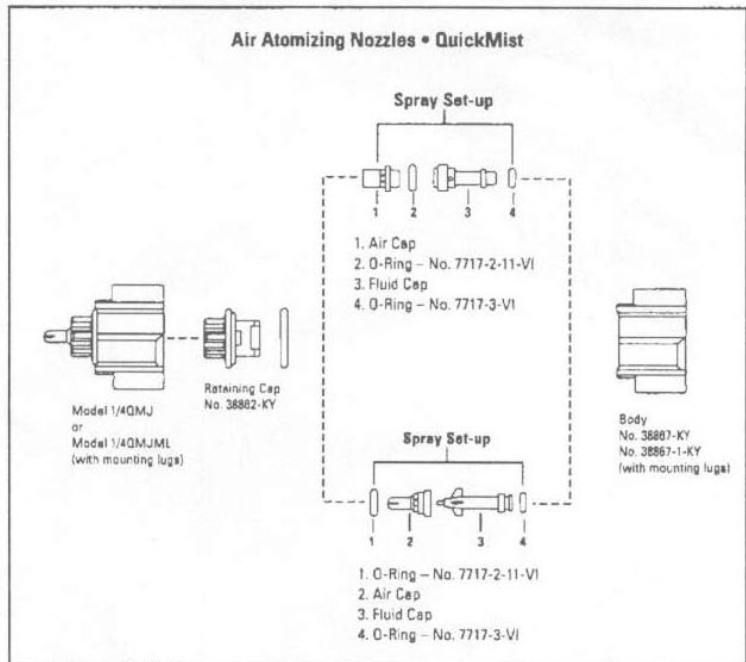
ORDERING INFO

COMPLETE SPRAY NOZZLE STANDARD BODY		
[NOZZLE BODY]	[SPRAY SET-UP]	
1/4 QMJ + SUQR-220B		
Air and Liquid Inlet Conn.	Body Type	Spray Pattern Type
MOUNTING LUG BODY		
[NOZZLE BODY]	[SPRAY SET-UP]	
1/4 QMJML + SUQF-230B		
Air and Liquid Inlet Conn.	Body Type	Spray Pattern Type

SPRAY SET-UP ONLY	
[SPRAY SET-UP]	
SUQR - 220B	
Spray Set-up No.	Material Code

To order spray set-up (includes air cap, VITON® O-rings, and fluid cap) use set-up number: SUQR-220B

* Includes retainer and gasket.
To order fluid cap only, use fluid cap number (shown in performance data charts): PFQ40
To order air cap only, use air cap number (shown in performance data charts): PAQR95
To order spray nozzle without set-up, use inlet connection and nozzle body: 1/4QMJ



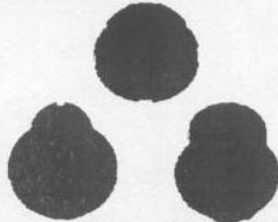
Spraying Systems Co.®

Phone 1-800-95-SPRAY, Fax 1-888-95-SPRAY
Outside the U.S., Phone 1(630) 665-5000, Fax 1(630) 260-0842
Visit our Web Site: <http://www.spray.com>

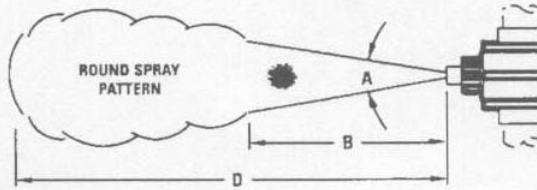
Air Atomizing Nozzles • QuickMist™ Pressure Spray Set-ups Internal Mix

AIR ATOMIZING NOZZLES

AIR CAPS



Round, Wide Angle Round, and Flat Spray Air Caps
Air Caps used in these spray set-ups produce a hollow cone type, round, wide angle round spray, and flat spray patterns.



DESIGN FEATURES

For the wide angle round and flat sprays, dimensions "A", "B", and "C" are the pattern widths at distances from the nozzle as shown. The total distance of spray projection from the nozzle to the maximum dispersal point is represented by "D".

When using a Pressure-Fed Liquid System, the liquid is supplied to the nozzle under pressure. The liquid and compressed air or gas are mixed internally to produce a completely atomized spray.

PERFORMANCE DATA

ROUND SPRAY

Spray Set-up No.	Spray Set-up Consists of Fluid and Air Cap Combination	Spray Pattern	Liquid Capacity (liters per hour) and Air Capacity (liters per minute)															Spray Dimensions				
			Liquid Pressure															Air bar	Liquid bar	Spray Angle A	B (cm)	D (m)
			0.7 bar			1.5 bar			2 bar			3 bar			4 bar							
Air Press. bar	Air l/h	Air l/min	Air Press. bar	Air l/h	Air l/min	Air Press. bar	Air l/h	Air l/min	Air Press. bar	Air l/h	Air l/min	Air Press. bar	Air l/h	Air l/min	Air Press. bar	Air l/h	Air l/min					
SUQR220B	Fluid Cap PFQ40 + Air Cap PAQR95	Round	0.8	18.9	33.5	1.1	35.2	34.7	1.4	40.4	38.4	1.9	50.6	43.2	2.6	56.0	53.3	1.1	0.7	12°	51	4.3
			1.0	14.1	38.8	1.4	29.1	42.7	1.8	33.2	49.1	2.3	44.3	53.9	3.0	50.5	64.0					
			1.1	11.9	41.5	1.7	23.8	50.7	2.2	26.7	59.8	2.8	37.1	67.2	3.4	45.4	74.7					
			1.2	9.8	44.2	1.9	20.2	56.0	2.6	20.9	70.5	3.2	31.9	77.9	3.9	39.5	88.1					
			1.4	5.8	49.5	2.1	16.9	61.4	3.0	15.4	81.1	3.6	26.9	88.8	4.3	35.0	98.7					
			1.5	3.9	52.2	2.3	13.9	66.7	3.4	10.3	91.8	4.0	22.3	99.3	4.7	30.7	109.4					
			—	—	—	2.6	9.5	74.7	3.9	4.4	105.2	4.6	15.7	115.3	5.1	28.5	120.1					
			—	—	—	2.9	5.4	82.8	4.3	0.5	115.9	5.0	11.5	126.0	5.5	22.6	130.8					
			—	—	—	—	—	—	—	—	—	5.4	7.5	136.7	—	—	—					
			2.8	4	14°	38	5.2															



Spraying Systems Co.®

Phone 1-800-95-SPRAY, Fax 1-888-95-SPRAY
Outside the U.S., Phone 1(630) 665-5000, Fax 1(630) 260-0842
Visit our Web Site: <http://www.spray.com>

310

Air Atomizing Nozzles • QuickMist™ Pressure Spray Set-ups Internal Mix



AIR ATOMIZING NOZZLES

PERFORMANCE DATA

WIDE ANGLE ROUND SPRAY

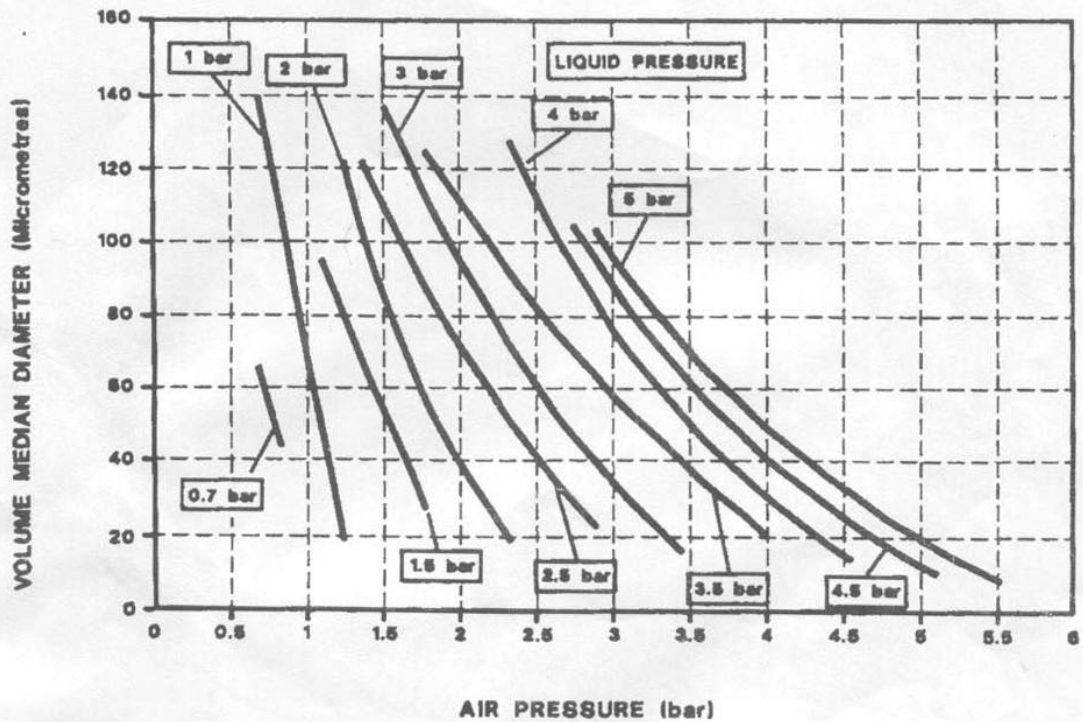
Spray Set-up No.	Spray Set-up Consists of Fluid and Air Cap Combination	Spray Pattern	Liquid Capacity (liters per hour) and Air Capacity (liters per minute)															Spray Dimensions					
			Liquid Pressure																				
			0.7 bar			1.5 bar			2 bar			3 bar			4 bar			Air bar	Liquid bar	A (cm)	B (cm)	C (cm)	D (m)
			Air Press. bar	l/h	l/min	Air Press. bar	l/h	l/min	Air Press. bar	l/h	l/min	Air Press. bar	l/h	l/min	Air Press. bar	l/h	l/min						
SUQW260B	Fluid Cap PFO30 + Air Cap PAQW37	Wide Angle Round	1.1	10.1	45.7	1.1	23.0	40.5	1.5	24.7	48.3	1.9	31.3	53.2	2.2	37.5	55.8	1.1	0.7	15	18	20	2.1
			1.2	8.9	48.4	1.4	19.5	48.7	1.9	20.7	59.2	2.3	27.7	64.2	2.6	34.1	66.7						
			1.4	6.6	53.9	1.7	16.4	58.9	2.3	17.2	70.2	2.8	23.6	77.9	3.0	31.0	77.7						
			—	—	—	1.8	15.4	59.7	2.8	13.1	83.9	3.2	20.6	88.8	3.4	28.1	88.7						
			—	—	—	2.1	12.6	67.9	3.0	11.6	89.4	3.6	17.8	99.8	3.9	24.7	102.3						
			—	—	—	2.3	10.9	73.4	3.3	9.4	97.6	4.0	15.2	110.8	4.3	22.2	113.3						
			—	—	—	2.6	8.4	81.6	3.6	7.3	105.8	4.4	12.6	121.7	4.7	19.7	124.3						
			—	—	—	—	—	—	3.9	5.3	114.0	4.7	10.8	129.9	5.1	17.4	135.2						
			—	—	—	—	—	—	—	—	—	5.0	9.1	138.1	5.5	15.1	146.2						
SUQW280	Fluid Cap PFO60 + Air Cap PAQW37	Wide Angle Round	0.7	21.4	40.1	0.8	83.3	17.7	1.4	69.9	29.7	1.7	108.3	19.6	2.5	111.4	25.7	0.7	0.7	20	30	41	2.1
			0.8	11.8	49.2	1.0	65.8	25.7	1.5	63.0	34.3	1.9	95.9	25.5	2.8	96	35.5						
			—	—	—	1.1	57.5	30.5	1.7	49.8	45.3	2.2	78.4	36.9	3.0	86.2	43.6						
			—	—	—	1.2	49.7	35.9	1.8	43.5	51.7	2.3	72.8	41.4	3.4	67.5	64.6						
			—	—	—	1.4	35.0	48.8	1.9	37.3	58.8	2.5	62.0	52.0	3.7	54.2	85.4						
			—	—	—	1.5	28.1	56.5	2.1	25.5	75.4	2.8	46.6	71.8	4.0	41.4	111.6						
			—	—	—	—	—	—	2.2	19.8	85.0	2.9	41.7	79.6	4.3	29.1	144.5						
			—	—	—	—	—	—	2.3	14.2	95.5	3.2	27.3	107.6	4.6	17.2	185.5						
			—	—	—	—	—	—	—	—	—	—	—	—	4.7	13.3	201.2						
SUQW290	Fluid Cap PFO60 + Air Cap PAQW52	Wide Angle Round	1.0	21.8	88.7	1.2	53.8	74.0	2.1	49.2	121.2	2.5	81.1	114.7	3.4	95.1	142.5	1.1	0.7	18	23	33	2.7
			1.1	18.7	96.2	1.5	44.5	96.1	2.3	43.1	135.3	2.8	71.9	135.1	3.7	85.9	161.9						
			1.2	15.8	103.6	1.8	35.3	117.9	2.6	33.8	155.9	3.0	65.7	148.6	4.0	76.6	181.0						
			1.4	9.5	118.4	2.1	26.0	139.3	2.9	24.5	176.3	3.3	56.5	168.4	4.3	67.3	199.8						
			—	—	—	2.3	19.8	153.3	3.2	15.3	198.2	3.6	47.2	187.9	4.4	64.3	208.0						
			—	—	—	—	—	—	3.4	9.1	209.3	3.9	38.0	207.1	4.7	55.0	224.4						
			—	—	—	—	—	—	3.7	5.0	228.7	4.1	31.8	219.7	5.0	45.8	242.6						
			—	—	—	—	—	—	—	—	—	—	—	—	5.2	39.6	254.6						
			—	—	—	—	—	—	—	—	—	—	—	—	5.5	30.3	272.4						



Spraying Systems Co.*

Phone 1-800-95-SPRAY, Fax 1-888-95-SPRAY
Outside the U.S., Phone 1(630) 665-5000, Fax 1(630) 260-0842
Visit our Web Site: <http://www.spray.com>

1/4QMJ+SUQW260 QuickMist™
AIR ATOMIZING SPRAY
NOZZLE
(METRIC)



SPRAYING WATER AT 21° C.

DESCRIPTION
VOLUME MEDIAN DIAMETER (VMD)
VERSUS AIR PRESSURE
AT CONSTANT LIQUID PRESSURES

Data is based on spraying water under laboratory conditions using the Malvern Particle Analyzer.

All values are computed utilizing the procedures for determining spray characteristics as outlined by ASTM (Standard E799)



Spraying Systems Co.

Spray Nozzles and Accessories
North Avenue at Schmale Rd. • P.O. Box 7900
Wheaton, IL 60189-7900

Ref:
Revision No.

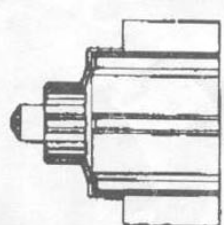
Data Sheet No.
36892-9M

© Spraying Systems Co. 1996

AIR PRESSURE IN bar	LIQUID PRESSURE IN bar									
	0.7	1	1.5	2	2.5	3	3.5	4	4.5	5
0.7	22.3	51.5	18.2							
0.8	9.1	41.2	27.1							
1.0	54.7	30.9	53.8							
1.1		18.7	58.0	81.8						
1.2		53.2	26.1	76.1						
1.4		71.7	41.9	70.4						
1.5		34.4	20.5	63.3	92.5					
1.7		28.8	32.2	55.2	87.7					
1.8		56.0	38.7	59.7	82.2	101.4				
1.9		77.2	46.3	48.3	75.6	91.4				
2.1		84.0	37.0	59.9	51.8	91.9	110.5			
2.2		27.5	73.1	27.5	61.1	86.9	21.6			
2.3		18.4	88.9	18.4	45.2	81.3	25.3			
2.5		10.3	108.0	10.3	53.8	80.1	29.4	118.2		
2.6		3.9	130.9	3.9	64.0	73.3	34.0	27.0		
2.8		18.4		18.4	75.5	66.0	39.3	108.6		
2.9		107.3		107.3	78.1	50.3	44.7	30.9	119.7	
3.0		11.3		11.3	83.4	38.4	51.1	35.2	115.5	130.8
3.2		127.3		127.3	89.3	77.2	58.9	40.7	117.1	28.9
3.3		8.4		8.4	92.3	64.3	64.3	45.0	119.5	30.1
3.4		151.0		151.0	94.2	57.3	66.1	40.7	123.5	115.8
3.6					107.8	66.0	74.0	45.7	101.7	119.5
3.7					118.9	75.5	80.0	47.1	108.6	115.5
3.9					125.2	83.4	87.1	48.5	115.5	115.5
4.0					122.2	90.4	92.1	49.8	117.1	115.5
4.1					142.3	98.8	108.8	51.1	118.2	115.5
4.3					6.6	109.5	118.2	52.4	123.5	115.5
4.4					169.0	108.8	122.2	53.8	127.3	115.5
4.6						124.9	130.9	55.2	130.9	115.5
4.7						142.4	142.4	56.6	136.0	115.5
4.8						151.0	151.0	58.0	142.4	115.5
5.0						172.3	172.3	60.0	151.0	115.5
5.1						187.5	187.5	61.1	161.1	115.5
5.2								62.4	172.3	115.5
5.4								64.3	187.5	115.5
5.5								66.0	208.2	115.5

IN EACH BOX
 FIGURES ABOVE INDICATE WATER ATOMIZED
 IN l/h AT bar WATER PRESSURE
 FIGURES BELOW INDICATE ATOMIZING AIR
 IN l/min AT bar AIR PRESSURE


RECOMMENDED WORKING RANGE
 IS INSIDE HEAVY LINES



DESCRIPTION

1/4QMJ+SUQW-260
 QUICKMIST™
 AIR ATOMIZING NOZZLE

FLUID CAP PFO60
 AIR CAP PAQW37-60
 WIDE ANGLE ROUND SPRAY
 (METRIC)

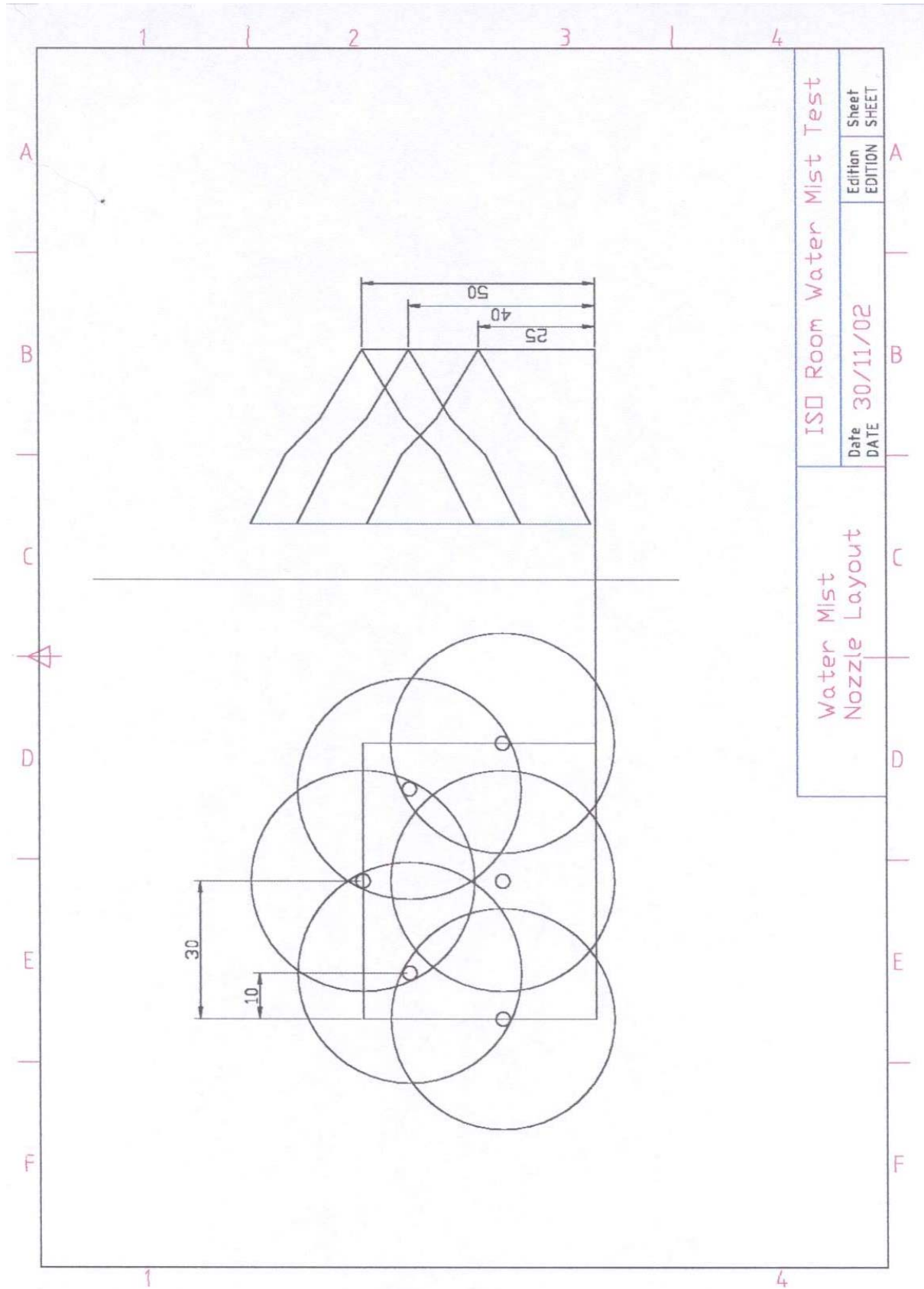
 **Spraying Systems Co.**
 Spray Nozzles and Accessories
 North Avenue et Schmale Rd. • P.O. Box 7800
 Wheaton, IL 60188-7800

Ref: _____ Data Sheet No. **38860M-260**

Revision No. _____

© Spraying Systems Co. 1996

11.4 Nozzles layout



ISD Room Water Mist Test		Sheet SHEET
Date 30/11/02		Edition EDITION
Water Mist Nozzle Layout		A
		B
		C
		D
		E
		F

11.5 Centrifugal fan specifications

Type: CE = Single Inlet

CE 790/E 352- 4 [230V 1N~ 50 Hz]

MP Capacitor 25 μF - 400 VDB

① Free Air relating to fan discharge area 0,0469 m². Max. permissible ambient temperature 60° C

② Velocity (dynamic) pressure For Static Pressure Regain see example

Inlet Ø243

External dimension of discharge

Please state inlet side For installation see examples

GS Geprüfte Sicherheit

The Silent One

Performance/Dimensions

FISCHBACH COMPACT FAN

Air Volume \dot{V}_L [m³/h] @ $\rho = 1,2 \text{ kg/m}^3$ and current [A] (bold figures)

Voltage [V]	Free Air	Total Pressure Δp_t [Pa]						
		60	120	180	240	300	360	420
80	1005 2,30	875 2,22	640 2,10					
100	1330 2,83	1250 2,79	1100 2,67	920 2,48	700 2,23			
125	1765 3,44		1630 3,32	1460 3,14	1260 2,88	1030 2,57	730 2,19	
150	2230 4,00		2190 3,95	2040 3,77	1860 3,53	1630 3,22	1300 2,78	670 2,09
170	2545 4,30			2440 4,16	2280 3,95	2080 3,69	1790 3,32	1200 2,62
190	2850 4,53			2830 4,50	2660 4,31	2450 4,05	2180 3,73	1750 3,22
230	3375 5,08				3350 5,05	3140 4,80	2880 4,50	2520 4,11

Save power and even more silent FISCHBACH SPEED CONTROLLERS Manual and Automatic

Voltage Control	Type*	Order Nr.*
Stepless 0 - 100% and 100% - 0	FDR 70	6164
Stepwise 7 Steps	FDR 750	6202
FISCHBACH AUTOMATIC CONTROL **	FRA 70	6253

* For further details see Publication "Controllers"
** For details of sensors ect. - see Publication "Automatic Controllers"

Sound Pressure Level Lp in dB (A)

Voltage [V]

Volts	80	100	125	150	170	190	230
Inlet*	44	48	55	64	67	69	73
Discharge**	31	35	42	54	56	59	63

* Sound Pressure 'A': 4 m from inlet. Room absorption 8 dB
** Sound Pressure 'A' - free field 4 m from discharge

Please note !
Sound Pressure Lp in dB [A]
Sound Power Lw in dB

Sound Power Lw in dB (Linear)
Mid Frequency [Hz]

Volts	63	125	250	500	1000	2000	4000	8000	Total 45-11200
Inlet									
80	48	50	53	52	45	37	32	32	58
100	55	56	60	52	50	44	39	34	63
125	62	63	67	59	57	51	46	41	70
150	70	71	75	67	67	64	61	56	78
170	75	75	77	69	69	67	65	64	81
190	78	78	80	72	72	70	68	67	84
230	79	83	82	76	75	72	74	72	88
Discharge									
80	49	50	50	51	43	37	34	34	56
100	52	52	55	54	49	42	41	39	60
125	59	60	62	61	56	49	48	46	68
150	70	71	71	73	66	64	63	61	78
170	74	75	75	74	70	68	68	66	81
190	77	78	78	77	73	71	71	69	84
230	80	81	82	79	77	75	75	75	88

11.6 FDS input files

11.6.1 FDS Input File 1: Water mist nozzles

```

MANUFACTURER
QuickMist
MODEL
mist
OPERATING_PRESSURE
5
K-FACTOR
0.268
OFFSET_DISTANCE
0.05
SIZE_DISTRIBUTION
1
20 4
VELOCITY
1
0.50.8.0

```

11.6.2 FDS Input File 2: Normal operation with no fire

```

&HEAD CHID='Norm-Highh',TITLE='Norm-Highh' /no fire 400sec low flow
&GRID IBAR=60,JBAR=48,KBAR=54 /
&PDIM XBAR=3,YBAR=2.4,ZBAR=2.8 /
&TIME TWFIN=400. /simulation time = 6.5 MIN, DT=0.05,
&MISC SURF_DEFAULT='PINE',
  DATABASE_DIRECTORY='c:\nist\fds\database3',
  REACTION='HEPTANE',
  TMPA=22 /
  TMPO=22 /

&PART QUANTITY=TEMPERATURE',
  DTPAR=5 /

/*****SURFACE IDS*****/

&SURF ID=BLOW,VOLUME_FLUX=-0.288,TMPWAL=19,PARTICLES=.TRUE.,RAMP_V=BLOW RAMP /
&RAMP ID=BLOW RAMP,T= 0.0,F=0.0 /
&RAMP ID=BLOW RAMP,T= 1.0,F=0.0 /
&RAMP ID=BLOW RAMP,T= 2.0,F=0.166 /
&RAMP ID=BLOW RAMP,T= 400.0,F=0.166 /

&SURF ID=HOT,HEAT_FLUX=1/TMPWAL=40.

/*****VENTS*****/

&VENT XB=0,0,0.9,1.5,0,0.5,SURF_ID=BLOW,T_ACTIVATE=1./VENT_COLOR=BLUE,T_DEACTIVATE=10.

&VENT XB=0,3,0,2.4,2.8,2.8,SURF_ID=OPEN/Roof
&VENT XB=0,3,0,2.45,2.8,SURF_ID=OPEN/Roof walls
&VENT XB=0,3,2.4,2.4,2.45,2.8,SURF_ID=OPEN/Roof walls
&VENT XB=0,0,0,2.4,2.45,2.8,SURF_ID=OPEN/Roof walls
&VENT XB=3,3,0,2.4,2.45,2.8,SURF_ID=OPEN/Roof walls

/*****OBSTICLES*****/

```

```
&OBST XB=0,3,0,1,2,4,2,45,BLOCK_COLOR=YELLOW,/Roof1
&OBST XB=0,3,1,4,2,4,2,45,BLOCK_COLOR=YELLOW,/Roof2
&OBST XB=0,6,1,1,4,2,4,2,45,BLOCK_COLOR=YELLOW,/Roof3
&OBST XB=1,3,1,1,4,2,4,2,45,BLOCK_COLOR=YELLOW,/Roof4
```

```
&OBST XB=1,1,1,1,15,1,25,0,8,1,BLOCK_COLOR=MAGENTA,SURF_ID=HOT/Person 1
&OBST XB=2,2,1,1,15,1,25,0,8,1,BLOCK_COLOR=MAGENTA,SURF_ID=HOT/Person 2
&OBST XB=1,45,1,6,1,15,1,3,1,05,1,2,BLOCK_COLOR=CYAN,SURF_ID=HOT/Computer
```

```
/*****OUTPUT FILES*****/
```

```
&THCP XB=0,0,0,9,1,5,0,0,5,QUANTITY=MASS FLOW,LABEL='Vent mass Flow in', DTSAM=1./
&THCP QUANTITY=VELOCITY, XYZ=0.05,1,2,0,25,LABEL='Inlet Velocity'/
&THCP QUANTITY=TEMPERATURE, XYZ=0.05,1,2,0,25,LABEL='Inlet Temp'/'
```

```
&THCP XB=0,6,1,1,1,4,2,45,2,45,QUANTITY=MASS FLOW,LABEL='Roof Vent mass Flow out'/
&THCP QUANTITY=VELOCITY, XYZ=0,8,1,2,2,45,LABEL='Outlet velocity'/
&THCP QUANTITY=TEMPERATURE, XYZ=0,8,1,2,2,45,LABEL='Outlet Temp'/'
```

```
&THCP QUANTITY=TEMPERATURE, XYZ=0,1,0,1,0,3,LABEL='Comer 1 Temp - 300', DTSAM=1. /
&THCP QUANTITY=TEMPERATURE, XYZ=0,1,0,1,1,3,LABEL='Comer 1 Temp - 1300'/
&THCP QUANTITY=TEMPERATURE, XYZ=2,9,0,1,0,3,LABEL='Comer 2 Temp - 300'/
&THCP QUANTITY=TEMPERATURE, XYZ=2,9,0,1,1,3,LABEL='Comer 2 Temp - 1300'/
&THCP QUANTITY=TEMPERATURE, XYZ=1,5,0,7,0,3,LABEL='Centre 1 Temp - 300'/
&THCP QUANTITY=TEMPERATURE, XYZ=1,5,0,7,0,7,LABEL='Centre 1 Temp - 800'/
&THCP QUANTITY=TEMPERATURE, XYZ=1,5,0,7,1,3,LABEL='Centre 1 Temp - 1300'/
&THCP QUANTITY=TEMPERATURE, XYZ=1,5,0,7,1,8,LABEL='Centre 1 Temp - 1800'/
&THCP QUANTITY=TEMPERATURE, XYZ=1,5,0,7,2,1,LABEL='Centre 1 Temp - 2100'/
&THCP QUANTITY=TEMPERATURE, XYZ=1,5,1,7,0,3,LABEL='Centre 2 Temp - 300'/
&THCP QUANTITY=TEMPERATURE, XYZ=1,5,1,7,0,7,LABEL='Centre 2 Temp - 800'/
&THCP QUANTITY=TEMPERATURE, XYZ=1,5,1,7,1,3,LABEL='Centre 2 Temp - 1300'/
&THCP QUANTITY=TEMPERATURE, XYZ=1,5,1,7,1,8,LABEL='Centre 2 Temp - 1800'/
&THCP QUANTITY=TEMPERATURE, XYZ=1,5,1,7,2,1,LABEL='Centre 2 Temp - 2100'/'
```

```
&THCP QUANTITY='oxygen', XYZ=0,1,0,1,0,3,LABEL='Comer 1 Oxy by vol - 300'/
&THCP QUANTITY='oxygen', XYZ=0,1,0,1,1,3,LABEL='Comer 1 Oxy by vol - 1300'/
&THCP QUANTITY='oxygen', XYZ=2,9,0,1,0,3,LABEL='Comer 2 Oxy by vol - 300'/
&THCP QUANTITY='oxygen', XYZ=2,9,0,1,1,3,LABEL='Comer 2 Oxy by vol - 1300'/
&THCP QUANTITY='oxygen', XYZ=1,5,0,7,0,3,LABEL='Centre 1 Oxy by vol - 300'/
&THCP QUANTITY='oxygen', XYZ=1,5,0,7,0,7,LABEL='Centre 1 Oxy by vol - 800'/
&THCP QUANTITY='oxygen', XYZ=1,5,0,7,1,3,LABEL='Centre 1 Oxy by vol - 1300'/
&THCP QUANTITY='oxygen', XYZ=1,5,0,7,1,8,LABEL='Centre 1 Oxy by vol - 1800'/
&THCP QUANTITY='oxygen', XYZ=1,5,0,7,2,1,LABEL='Centre 1 Oxy by vol - 2100'/
&THCP QUANTITY='oxygen', XYZ=1,5,1,7,0,3,LABEL='Centre 2 Oxy by vol - 300'/
&THCP QUANTITY='oxygen', XYZ=1,5,1,7,0,7,LABEL='Centre 2 Oxy by vol - 800'/
&THCP QUANTITY='oxygen', XYZ=1,5,1,7,1,3,LABEL='Centre 2 Oxy by vol - 1300'/
&THCP QUANTITY='oxygen', XYZ=1,5,1,7,1,8,LABEL='Centre 2 Oxy by vol - 1800'/
&THCP QUANTITY='oxygen', XYZ=1,5,1,7,2,1,LABEL='Centre 2 Oxy by vol - 2100'/'
```

```
&SLCF XB=0,0,3,0,7,0,7,0,00,2,8,QUANTITY=TEMPERATURE/Slice long centre tree 1 of Room
&SLCF XB=0,0,3,1,2,1,2,0,00,2,8,QUANTITY=TEMPERATURE/Slice along centre of Room
&SLCF XB=0,0,3,1,7,1,7,0,00,2,8,QUANTITY=TEMPERATURE/Slice along centre tree 2 of Room
&SLCF XB=0,0,3,0,1,0,1,0,00,2,8,QUANTITY=TEMPERATURE/Slice along corner trees
```

```
&SLCF XB=0,0,3,1,7,1,7,0,00,2,8,QUANTITY=WATER VAPOR'/Slice along centre tree 2 of Room
&SLCF XB=0,0,3,1,7,1,7,0,00,2,8,QUANTITY='oxygen'/Slice along centre tree 2 of Room
&SLCF XB=0,0,3,1,7,1,7,0,00,2,8,QUANTITY='visibility'/Slice along centre tree 2 of Room
&SLCF XB=0,0,3,1,7,1,7,0,00,2,8,QUANTITY='soot density'/Slice along centre tree 2 of Room
&SLCF XB=0,0,3,1,7,1,7,0,00,2,8,QUANTITY='carbon dioxide'/Slice along centre tree 2 of Room
```

```

&SLCF XB=0,0,3,0,7,0,7,0,0,2,8,QUANTITY=visibility/Slice along centre tree 1 of Room
&SLCF XB=0,0,3,1,2,1,2,0,0,2,8,QUANTITY=visibility/Slice along centre of Room

&SLCF XB=0,0,3,1,2,1,2,0,0,2,8,QUANTITY=WATER VAPOR/Slice along centre of Room

&SLCF XB=1,5,1,5,0,2,4,0,0,2,8,QUANTITY=TEMPERATURE/Slice accross centre of Room
&SLCF XB=1,5,1,5,0,2,4,0,0,2,8,QUANTITY=visibility/Slice accross centre of Room

&SLCF XB=1,5,1,5,0,2,4,0,0,2,8,QUANTITY='soot density'/Slice accross centre of Room

&ISOF QUANTITY=TEMPERATURE,VALUE(1)=50,VALUE(2)=120/
&ISOF QUANTITY=MIXTURE_FRACTION,VALUE(1)=0.05,VALUE(2)=0.001/

&PL3D DTSAM=30,QUANTITIES(5)=oxygen,TSTART=1.,TSTOP=391/

```

11.6.3 FDS Input File 3: Normal operation with a central floor fire

```

&HEAD CHID=Norm-Fireh,TITLE=Norm-Fireh/normal flow but with fire
&GRID IBAR=60,JBAR=48,KBAR=54/
&PDIM XBAR=3,YBAR=2.4,ZBAR=2.8/
&TIME TWFIN=400./simulation time = 6.5 MIN,DT=0.05,
&MISC SURF_DEFAULT=PINE,
  DATABASE_DIRECTORY=c:\nist\fds\database3',
  REACTION=HEPTANE,
  TMPA=22/
  TMPO=22/

&PART QUANTITY=TEMPERATURE,
  DTPAR=5/

/*****SURFACE IDS*****/

&SURF ID=BURNER,HRRPUA=520./

&SURF ID=BLOW,VOLUME_FLUX=-0.288,TMPWAL=19,PARTICLES=.TRUE.,RAMP_V=BLOW RAMP/
&RAMP ID=BLOW RAMP,T=0.0,F=0.0/
&RAMP ID=BLOW RAMP,T= 1.0,F=0.0/
&RAMP ID=BLOW RAMP,T= 2.0,F=0.166/
&RAMP ID=BLOW RAMP,T= 400.0,F=0.166/

&SURF ID=HOT,HEAT_FLUX=1/TMPWAL=40.

/*****VENTS*****/

&VENT XB=0,0,0,9,1,5,0,0,5,SURF_ID=BLOW,T_ACTIVATE=1./

&VENT XB=0,3,0,2,4,2,8,2,8,SURF_ID=OPEN/Roof
&VENT XB=0,3,0,0,2,4,5,2,8,SURF_ID=OPEN/Roof walls
&VENT XB=0,3,2,4,2,4,2,4,5,2,8,SURF_ID=OPEN/Roof walls
&VENT XB=0,0,0,2,4,2,4,5,2,8,SURF_ID=OPEN/Roof walls
&VENT XB=3,3,0,2,4,2,4,5,2,8,SURF_ID=OPEN/Roof walls

&OBST XB=1,4,1,6,0,6,0,8,0,0,0,05,BLOCK_COLOR=RED,SURF_IDS=BURNER,'INERT','INERT'/

/*****OBSTICLES*****/

```

```

&OBST XB=0,3,0,1,2,4,2,45,BLOCK_COLOR=YELLOW,/Roof1
&OBST XB=0,3,1,4,2,4,2,4,2,45,BLOCK_COLOR=YELLOW,/Roof2
&OBST XB=0,6,1,1,4,2,4,2,45,BLOCK_COLOR=YELLOW,/Roof3
&OBST XB=1,3,1,1,4,2,4,2,45,BLOCK_COLOR=YELLOW,/Roof4

&OBST XB=1,1,1,1,15,1,25,0,8,1,BLOCK_COLOR=MAGENTA,SURF_ID=HOT/Person 1
&OBST XB=2,2,1,1,15,1,25,0,8,1,BLOCK_COLOR=MAGENTA,SURF_ID=HOT/Person 2
&OBST XB=1,45,1,6,1,15,1,3,1,05,1,2,BLOCK_COLOR=CYAN,SURF_ID=HOT/Computer

```

```

/*****OUTPUT FILES*****/

```

See: FDS Input File 2: Normal operation with no fire

11.6.4 FDS Input File 4: High airflow operation with a central floor fire

```

&HEAD CHID=Norm-Fireh,TITLE=Norm-Fireh/normal flow but with fire
&GRID IBAR=60,JBAR=48,KBAR=54/
&PDIM XBAR=3,YBAR=2,4,ZBAR=2,8/
&TIME TWFIN=400./simulation time = 6.5 MIN, DT=0.05,
&MISC SURF_DEFAULT=PINE',
  DATABASE_DIRECTORY=c:\nist\fds\database3',
  REACTION=HEPTANE',
  TMPA=22/
  TMPO=22/

&PART QUANTITY=TEMPERATURE',
  DTPAR=5/

/*****SURFACE IDS*****/

&SURF ID=BURNER,HRRPUA=520./

&SURF ID=BLOW,VOLUME_FLUX=0.288,TMPWAL=19,PARTICLES=.TRUE.,RAMP_V=BLOW RAMP'/
&RAMP ID=BLOW RAMP,T= 0.0,F=0.0/
&RAMP ID=BLOW RAMP,T= 1.0,F=0.0/
&RAMP ID=BLOW RAMP,T= 2.0,F=0.166/
&RAMP ID=BLOW RAMP,T= 400.0,F=0.166/

&SURF ID=HOT,HEAT_FLUX=1/TMPWAL=40.

/*****VENTS*****/

&VENT XB=0,0,0,9,1,5,0,0,5,SURF_ID=BLOW,T_ACTIVATE=1./

&VENT XB=0,3,0,2,4,2,8,2,8,SURF_ID=OPEN/Roof
&VENT XB=0,3,0,0,2,45,2,8,SURF_ID=OPEN/Roof walls
&VENT XB=0,3,2,4,2,4,2,45,2,8,SURF_ID=OPEN/Roof walls
&VENT XB=0,0,0,2,4,2,45,2,8,SURF_ID=OPEN/Roof walls
&VENT XB=3,3,0,2,4,2,45,2,8,SURF_ID=OPEN/Roof walls

&OBST XB=1,4,1,6,0,6,0,8,0,0,05,BLOCK_COLOR=RED,SURF_IDS=BURNER,'INERT','INERT'/

/*****OBSTICLES*****/

&OBST XB=0,3,0,1,2,4,2,45,BLOCK_COLOR=YELLOW,/Roof1
&OBST XB=0,3,1,4,2,4,2,4,2,45,BLOCK_COLOR=YELLOW,/Roof2

```

```
&OBST XB=0,6,1,1,4,2,4,2,4,5,BLOCK_COLOR=YELLOW,/Roof3
&OBST XB=1,3,1,1,4,2,4,2,4,5,BLOCK_COLOR=YELLOW,/Roof4

&OBST XB=1,1,1,1,15,1,25,0,8,1,BLOCK_COLOR=MAGENTA,SURF_ID=HOT/Person 1
&OBST XB=2,2,1,1,15,1,25,0,8,1,BLOCK_COLOR=MAGENTA,SURF_ID=HOT/Person 2
&OBST XB=1,45,1,6,1,15,1,3,1,05,1,2,BLOCK_COLOR=CYAN,SURF_ID=HOT/Computer

/*****OUTPUT FILES*****/
```

See: FDS Input File 2: Normal operation with no fire

11.6.5 FDS Input File 5: Displacement water mist operation with a central floor fire

```
&HEAD CHID='Cent-Spkh',TITLE='Cent-Spkh'/Centre fire G - low flow 60 sec then high flow + sprinklers activate
&GRID IBAR=60,JBAR=48,KBAR=54/
&PDIM XBAR=3,YBAR=2,4,ZBAR=2,8/
&TIME TWFIN=400./simulation time = 6.5 MIN, DT=0.05,
&MISC SURF_DEFAULT=PINE,
  DATABASE_DIRECTORY=c:\nist\fds\database3\,
  REACTION=HEPTANE,
  TMPA=22/
  TMPO=22/
```

```
&PART QUANTITY=DROPLET_DIAMETER,
  DTSPAR=3/
```

```
/*****SURFACE IDs*****/
```

```
&SURF ID=BURNER,HRRPUA=520./
```

```
&SURF ID=BLOW,VOLUME_FLUX=-0.288,TMPWAL=19.,RAMP_V=BLOW RAMP/
&RAMP ID=BLOW RAMP,T=0.0,F=0.0/
&RAMP ID=BLOW RAMP,T= 1.0,F=0.0/
&RAMP ID=BLOW RAMP,T= 2.0,F=0.166/
&RAMP ID=BLOW RAMP,T= 60.0,F=0.166/
&RAMP ID=BLOW RAMP,T= 62.0,F=1.0/
&RAMP ID=BLOW RAMP,T= 400.0,F=1.0/
```

```
&SURF ID=HOT,HEAT_FLUX=1/TMPWAL=40.
```

```
/*****VENTS*****/
```

```
&VENT XB=0,0,0,9,1,5,0,0,5,SURF_ID=BLOW,T_ACTIVATE=1./
```

```
&VENT XB=0,3,0,2,4,2,8,2,8,SURF_ID=OPEN/Roof
&VENT XB=0,3,0,0,2,45,2,8,SURF_ID=OPEN/Roof walls
&VENT XB=0,3,2,4,2,4,2,45,2,8,SURF_ID=OPEN/Roof walls
&VENT XB=0,0,0,2,4,2,45,2,8,SURF_ID=OPEN/Roof walls
&VENT XB=3,3,0,2,4,2,45,2,8,SURF_ID=OPEN/Roof walls
```

```
&OBST XB=1,4,1,6,0,6,0,8,0,0,05,BLOCK_COLOR=RED,SURF_IDS=BURNER,'INERT','INERT'/
```

```
/*****OBSTICLES*****/
```

```
&OBST XB=0,3,0,1,2,4,2,45,BLOCK_COLOR=YELLOW,/Roof1
&OBST XB=0,3,1,4,2,4,2,4,2,45,BLOCK_COLOR=YELLOW,/Roof2
```

```
&OBST XB=0,6,1,1,4,2,4,2,45,BLOCK_COLOR=YELLOW,/Roof3
&OBST XB=1,3,1,1,4,2,4,2,45,BLOCK_COLOR=YELLOW,/Roof4
```

```
&OBST XB=1,1,1,1,15,1,25,0,8,1,BLOCK_COLOR=MAGENTA,SURF_ID=HOT/ Person 1
&OBST XB=2,2,1,1,15,1,25,0,8,1,BLOCK_COLOR=MAGENTA,SURF_ID=HOT/ Person 2
&OBST XB=1,45,1,6,1,15,1,3,1,05,1,2,BLOCK_COLOR=CYAN,SURF_ID=HOT/ Computer
```

```
/*****SPRINKLERS*****/
```

```
&SPRK XYZ=0,05,1,0,0,4,MAKE='mist',ORIENTATION=1,0,0,T_ACTIVATE=60./ Sprinkler 1
&SPRK XYZ=0,05,1,2,0,5,MAKE='mist',ORIENTATION=1,0,0,T_ACTIVATE=60./ Sprinkler 2
&SPRK XYZ=0,05,1,4,0,4,MAKE='mist',ORIENTATION=1,0,0,T_ACTIVATE=60./ Sprinkler 3
&SPRK XYZ=0,05,0,9,0,25,MAKE='mist',ORIENTATION=1,0,0,T_ACTIVATE=60./ Sprinkler 4
&SPRK XYZ=0,05,1,2,0,25,MAKE='mist',ORIENTATION=1,0,0,T_ACTIVATE=60./ Sprinkler 5
&SPRK XYZ=0,05,1,5,0,25,MAKE='mist',ORIENTATION=1,0,0,T_ACTIVATE=60./ Sprinkler 6
```

```
/*****OUTPUT FILES*****/
```

See: FDS Input File 2: Normal operation with no fire

11.6.6 FDS Input File 6: Displacement water mist operation with a central 1m fire

```
&HEAD CHID='CentH-Spkh',TITLE='CentH-Spkh' /Centre fire at high level - low flow 60 sec then high flow + sprinklers activate
```

```
&GRID IBAR=60,JBAR=48,KBAR=54/
&PDIM XBAR=3,YBAR=2.4,ZBAR=2.8/
&TIME TWFN=400. / simulation time = 6.5 MIN, DT=0.05,
&MISC SURF_DEFAULT=PINE,
  DATABASE_DIRECTORY='c:\nist\fds\database3',
  REACTION=HEPTANE,
  TMPA=22/
  TMPO=22/
```

```
&PART QUANTITY=DROPLET_DIAMETER,
  DTSPAR=3/
```

```
/*****SURFACE IDs*****/
```

```
&SURF ID=BURNER,HRRPUA=520./
```

```
&SURF ID=BLOW,VOLUME_FLUX=-0.288,TMPWAL=19.,RAMP_V=BLOW RAMP/
&RAMP ID=BLOW RAMP,T=0.0,F=0.0/
&RAMP ID=BLOW RAMP,T=1.0,F=0.0/
&RAMP ID=BLOW RAMP,T=2.0,F=0.166/
&RAMP ID=BLOW RAMP,T=60.0,F=0.166/
&RAMP ID=BLOW RAMP,T=62.0,F=1.0/
&RAMP ID=BLOW RAMP,T=400.0,F=1.0/
```

```
&SURF ID=HOT,HEAT_FLUX=1./TMPWAL=40.
```

```
/*****VENTS*****/
```

```
&VENT XB=0,0,0,9,1,5,0,0,5,SURF_ID=BLOW,T_ACTIVATE=1./
```

```
&VENT XB=0,3,0,2,4,2,8,2,8,SURF_ID=OPEN/Roof
&VENT XB=0,3,0,0,2,45,2,8,SURF_ID=OPEN/Roof walls
```



```

&VENT XB=0,3,2,4,2,4,2,4,5,2,8,SURF_ID=OPEN/Roof walls
&VENT XB=0,0,0,2,4,2,4,5,2,8,SURF_ID=OPEN/Roof walls
&VENT XB=3,3,0,2,4,2,4,5,2,8,SURF_ID=OPEN/Roof walls

&OBST XB=1,4,1,6,0,6,0,8,1,1,0,5,BLOCK_COLOR=RED,SURF_IDS=BURNER,'INERT','INERT'/

/*****OBSTICLES*****/

&OBST XB=0,3,0,1,2,4,2,4,5,BLOCK_COLOR=YELLOW/Roof1
&OBST XB=0,3,1,4,2,4,2,4,2,4,5,BLOCK_COLOR=YELLOW/Roof2
&OBST XB=0,6,1,1,4,2,4,2,4,5,BLOCK_COLOR=YELLOW/Roof3
&OBST XB=1,3,1,1,4,2,4,2,4,5,BLOCK_COLOR=YELLOW/Roof4

&OBST XB=1,1,1,1,1,5,1,2,5,0,8,1,BLOCK_COLOR=MAGENTA,SURF_ID=HOT/Person 1
&OBST XB=2,2,1,1,1,5,1,2,5,0,8,1,BLOCK_COLOR=MAGENTA,SURF_ID=HOT/Person 2
&OBST XB=1,4,5,1,6,1,1,5,1,3,1,0,5,1,2,BLOCK_COLOR=CYAN,SURF_ID=HOT/Computer

/*****SPRINKLERS*****/

&SPRK XYZ=0,0,5,1,0,0,4,MAKE='mist',ORIENTATION=1,0,0,T_ACTIVATE=60./ Sprinkler 1
&SPRK XYZ=0,0,5,1,2,0,5,MAKE='mist',ORIENTATION=1,0,0,T_ACTIVATE=60./ Sprinkler 2
&SPRK XYZ=0,0,5,1,4,0,4,MAKE='mist',ORIENTATION=1,0,0,T_ACTIVATE=60./ Sprinkler 3
&SPRK XYZ=0,0,5,0,9,0,2,5,MAKE='mist',ORIENTATION=1,0,0,T_ACTIVATE=60./ Sprinkler 4
&SPRK XYZ=0,0,5,1,2,0,2,5,MAKE='mist',ORIENTATION=1,0,0,T_ACTIVATE=60./ Sprinkler 5
&SPRK XYZ=0,0,5,1,5,0,2,5,MAKE='mist',ORIENTATION=1,0,0,T_ACTIVATE=60./ Sprinkler 6

/*****OUTPUT FILES*****/

See: FDS Input File 2: Normal operation with no fire

```

11.6.7 FDS Input File 7: Displacement water mist operation with a front corner floor fire

```

&HEAD CHID='Front-Spkh',TITLE='Front-Spkh' /Front corner fire G - low flow 60 sec then high flow + sprinklers activate
&GRID IBAR=60,JBAR=48,KBAR=54/
&PDIM XBAR=3,YBAR=2,4,ZBAR=2,8/
&TIME TWFIN=400./simulation time = 6.5 MIN, DT=0.05,
&MISC SURF_DEFAULT='PINE',
  DATABASE_DIRECTORY='c:\nist\fds\database3',
  REACTION='HEPTANE',
  TMPA=22/
  TMPO=22/

&PART QUANTITY='DROPLET_DIAMETER',
  DTSPAR=3/

/*****SURFACE IDS*****/

&SURF ID=BURNER,HRRPUA=520./

&SURF ID=BLOW,VOLUME_FLUX=0.288,TMPWAL=19,RAMP_V=BLOW RAMP/
&RAMP ID=BLOW RAMP,T= 0.0,F=0.0/
&RAMP ID=BLOW RAMP,T= 1.0,F=0.0/
&RAMP ID=BLOW RAMP,T= 2.0,F=0.166/
&RAMP ID=BLOW RAMP,T= 60.0,F=0.166/
&RAMP ID=BLOW RAMP,T= 62.0,F=1.0/

```

```
&RAMP ID=BLOW RAMP,T= 400.0,F=1.0/
```

```
&SURF ID=HOT,HEAT_FLUX=1/TMPWAL=40.
```

```
/******VENTS*****
```

```
&VENT XB=0,0,0.9,1.5,0,0.5,SURF_ID=BLOW,T_ACTIVATE=1./
```

```
&VENT XB=0,3,0,2.4,2.8,2.8,SURF_ID=OPEN/Roof
```

```
&VENT XB=0,3,0,0,2.45,2.8,SURF_ID=OPEN/Roof walls
```

```
&VENT XB=0,3,2.4,2.4,2.45,2.8,SURF_ID=OPEN/Roof walls
```

```
&VENT XB=0,0,0,2.4,2.45,2.8,SURF_ID=OPEN/Roof walls
```

```
&VENT XB=3,3,0,2.4,2.45,2.8,SURF_ID=OPEN/Roof walls
```

```
&OBST XB=2.8,3,0,0,2,0,0.05,BLOCK_COLOR=RED',SURF_IDS=BURNER,'INERT','INERT'/
```

```
/******OBSTICLES*****
```

```
&OBST XB=0,3,0,1,2.4,2.45,BLOCK_COLOR=YELLOW,/Roof1
```

```
&OBST XB=0,3,1,4,2.4,2.4,2.45,BLOCK_COLOR=YELLOW,/Roof2
```

```
&OBST XB=0.6,1,1,4,2.4,2.45,BLOCK_COLOR=YELLOW,/Roof3
```

```
&OBST XB=1,3,1,1,4,2.4,2.45,BLOCK_COLOR=YELLOW,/Roof4
```

```
&OBST XB=1,1,1,1.15,1.25,0.8,1,BLOCK_COLOR=MAGENTA',SURF_ID=HOT/ Person 1
```

```
&OBST XB=2,2,1,1.15,1.25,0.8,1,BLOCK_COLOR=MAGENTA',SURF_ID=HOT/ Person 2
```

```
&OBST XB=1.45,1.6,1.15,1.3,1.05,1.2,BLOCK_COLOR=CYAN',SURF_ID=HOT/ Computer
```

```
/******SPRINKLERS*****
```

```
&SPRK XYZ=0.05,1.0,0.4,MAKE='mist',ORIENTATION=1,0,0,T_ACTIVATE=60./ Sprinkler 1
```

```
&SPRK XYZ=0.05,1.2,0.5,MAKE='mist',ORIENTATION=1,0,0,T_ACTIVATE=60./ Sprinkler 2
```

```
&SPRK XYZ=0.05,1.4,0.4,MAKE='mist',ORIENTATION=1,0,0,T_ACTIVATE=60./ Sprinkler 3
```

```
&SPRK XYZ=0.05,0.9,0.25,MAKE='mist',ORIENTATION=1,0,0,T_ACTIVATE=60./ Sprinkler 4
```

```
&SPRK XYZ=0.05,1.2,0.25,MAKE='mist',ORIENTATION=1,0,0,T_ACTIVATE=60./ Sprinkler 5
```

```
&SPRK XYZ=0.05,1.5,0.25,MAKE='mist',ORIENTATION=1,0,0,T_ACTIVATE=60./ Sprinkler 6
```

```
/******OUTPUT FILES*****
```

```
See: FDS Input File 2: Normal operation with no fire
```

11.6.8 FDS Input File 8: Displacement water mist operation with a back corner floor fire

```
&HEAD CHID=Back-Spkh',TTITLE=Back-Spkh'/Back Corner fire G - low flow 60 sec then high flow + sprinklers activate
```

```
&GRID IBAR=60,JBAR=48,KBAR=54/
```

```
&PDIM XBAR=3,YBAR=2.4,ZBAR=2.8/
```

```
&TIME TWFIN=400./simulation time=6.5 MIN,DT=0.05,
```

```
&MISC SURF_DEFAULT=PINE',
```

```
  DATABASE_DIRECTORY='c:\nist\fds\database3',
```

```
  REACTION=HEPTANE',
```

```
  TMPA=22/
```

```
  TMPO=22/
```

```
&PART QUANTITY=DROPLET_DIAMETER',
```

```
  DTSPAR=3/
```

```

/*****SURFACE IDS*****/

&SURF ID=BURNER,HRRPUA=520./

&SURF ID=BLOW,VOLUME_FLUX=-0.288,TMPWAL=19,RAMP_V=BLOW RAMP/
&RAMP ID=BLOW RAMP,T= 0.0,F=0.0/
&RAMP ID=BLOW RAMP,T= 1.0,F=0.0/
&RAMP ID=BLOW RAMP,T= 2.0,F=0.166/
&RAMP ID=BLOW RAMP,T= 60.0,F=0.166/
&RAMP ID=BLOW RAMP,T= 62.0,F=1.0/
&RAMP ID=BLOW RAMP,T= 400.0,F=1.0/

&SURF ID=HOT,HEAT_FLUX=1/TMPWAL=40.

/*****VENTS*****/

&VENT XB=0,0,0,9,1,5,0,0,5,SURF_ID=BLOW,T_ACTIVATE=1./

&VENT XB=0,3,0,2,4,2,8,2,8,SURF_ID=OPEN/Roof
&VENT XB=0,3,0,0,2,4,5,2,8,SURF_ID=OPEN/Roof walls
&VENT XB=0,3,2,4,2,4,2,4,5,2,8,SURF_ID=OPEN/Roof walls
&VENT XB=0,0,0,2,4,2,4,5,2,8,SURF_ID=OPEN/Roof walls
&VENT XB=3,3,0,2,4,2,4,5,2,8,SURF_ID=OPEN/Roof walls

&OBST XB=0,0,2,0,0,2,0,0,0,05,BLOCK_COLOR=RED,SURF_IDS=BURNER,'INERT','INERT'/

/*****OBSTICLES*****/

&OBST XB=0,3,0,1,2,4,2,4,5,BLOCK_COLOR=YELLOW/Roof1
&OBST XB=0,3,1,4,2,4,2,4,2,4,5,BLOCK_COLOR=YELLOW/Roof2
&OBST XB=0,6,1,1,4,2,4,2,4,5,BLOCK_COLOR=YELLOW/Roof3
&OBST XB=1,3,1,1,4,2,4,2,4,5,BLOCK_COLOR=YELLOW/Roof4

&OBST XB=1,1,1,1,1,1,5,1,2,5,0,8,1,BLOCK_COLOR=MAGENTA,SURF_ID=HOT/Person 1
&OBST XB=2,2,1,1,1,5,1,2,5,0,8,1,BLOCK_COLOR=MAGENTA,SURF_ID=HOT/Person 2
&OBST XB=1,4,5,1,6,1,1,5,1,3,1,0,5,1,2,BLOCK_COLOR=CYAN,SURF_ID=HOT/Computer

/*****SPRINKLERS*****/

&SPRK XYZ=0,05,1,0,0,4,MAKE='mist',ORIENTATION=1,0,0,T_ACTIVATE=60./ Sprinkler 1
&SPRK XYZ=0,05,1,2,0,5,MAKE='mist',ORIENTATION=1,0,0,T_ACTIVATE=60./ Sprinkler 2
&SPRK XYZ=0,05,1,4,0,4,MAKE='mist',ORIENTATION=1,0,0,T_ACTIVATE=60./ Sprinkler 3
&SPRK XYZ=0,05,0,9,0,25,MAKE='mist',ORIENTATION=1,0,0,T_ACTIVATE=60./ Sprinkler 4
&SPRK XYZ=0,05,1,2,0,25,MAKE='mist',ORIENTATION=1,0,0,T_ACTIVATE=60./ Sprinkler 5
&SPRK XYZ=0,05,1,5,0,25,MAKE='mist',ORIENTATION=1,0,0,T_ACTIVATE=60./ Sprinkler 6

/*****OUTPUT FILES*****/

See: FDS Input File 2: Normal operation with no fire

```

11.6.9 FDS Input File 9: Low airflow and water mist operation with a central floor fire

```

&HEAD CHID=CSpkonlyh',TTITLE=CSpkonlyh' /Centre fire G - low flow and sprinklers only
&GRID IBAR=60,JBAR=48,KBAR=54/
&PDIM XBAR=3,YBAR=2,4,ZBAR=2,8/

```

```

&TIME TWFIN=400./simulation time = 6.5 MIN, DT=0.05,
&MISC SURF_DEFAULT='PINE',
  DATABASE_DIRECTORY='c:\nist\fds\database3',
  REACTION='HEPTANE',
  TMPA=22/
  TMPO=22/

&PART QUANTITY='DROPLET_DIAMETER',
  DTSPAR=3/

/*****SURFACE IDS*****/

&SURF ID=BURNER,HRRPUA=520./

&SURF ID=BLOW,VOLUME_FLUX=0.288,TMPWAL=19.,RAMP_V=BLOW RAMP/
&RAMP ID=BLOW RAMP,T= 0.0,F=0.0/
&RAMP ID=BLOW RAMP,T= 1.0,F=0.0/
&RAMP ID=BLOW RAMP,T= 2.0,F=0.166/
&RAMP ID=BLOW RAMP,T= 400,F=0.166/

&SURF ID=HOT,HEAT_FLUX=1./TMPWAL=40.

/*****VENTS*****/

&VENT XB=0,0,0,9,1,5,0,0,5,SURF_ID=BLOW,T_ACTIVATE=1./

&VENT XB=0,3,0,24,2,8,2,8,SURF_ID=OPEN/Roof
&VENT XB=0,3,0,0,2,45,2,8,SURF_ID=OPEN/Roof walls
&VENT XB=0,3,2,4,2,4,2,45,2,8,SURF_ID=OPEN/Roof walls
&VENT XB=0,0,0,2,4,2,45,2,8,SURF_ID=OPEN/Roof walls
&VENT XB=3,3,0,2,4,2,45,2,8,SURF_ID=OPEN/Roof walls

&OBST XB=1,4,1,6,0,6,0,8,0,0,05,BLOCK_COLOR='RED',SURF_IDS='BURNER','INERT','INERT'/

/*****OBSTICLES*****/

&OBST XB=0,3,0,1,2,4,2,45,BLOCK_COLOR=YELLOW/Roof1
&OBST XB=0,3,1,4,2,4,2,4,2,45,BLOCK_COLOR=YELLOW/Roof2
&OBST XB=0,6,1,1,4,2,4,2,45,BLOCK_COLOR=YELLOW/Roof3
&OBST XB=1,3,1,1,4,2,4,2,45,BLOCK_COLOR=YELLOW/Roof4

&OBST XB=1,1,1,1,1.15,1,25,0,8,1,BLOCK_COLOR=MAGENTA',SURF_ID=HOT/Person 1
&OBST XB=2,2,1,1,1.15,1,25,0,8,1,BLOCK_COLOR=MAGENTA',SURF_ID=HOT/Person 2
&OBST XB=1,45,1,6,1,15,1,3,1,05,1,2,BLOCK_COLOR=CYAN',SURF_ID=HOT/Computer

/*****SPRINKLERS*****/

&SPRK XYZ=0.05,1,0,0,4,MAKE='mist',ORIENTATION=1,0,0,T_ACTIVATE=60./ Sprinkler 1
&SPRK XYZ=0.05,1,2,0,5,MAKE='mist',ORIENTATION=1,0,0,T_ACTIVATE=60./ Sprinkler 2
&SPRK XYZ=0.05,1,4,0,4,MAKE='mist',ORIENTATION=1,0,0,T_ACTIVATE=60./ Sprinkler 3
&SPRK XYZ=0.05,0,9,0,25,MAKE='mist',ORIENTATION=1,0,0,T_ACTIVATE=60./ Sprinkler 4
&SPRK XYZ=0.05,1,2,0,25,MAKE='mist',ORIENTATION=1,0,0,T_ACTIVATE=60./ Sprinkler 5
&SPRK XYZ=0.05,1,5,0,25,MAKE='mist',ORIENTATION=1,0,0,T_ACTIVATE=60./ Sprinkler 6

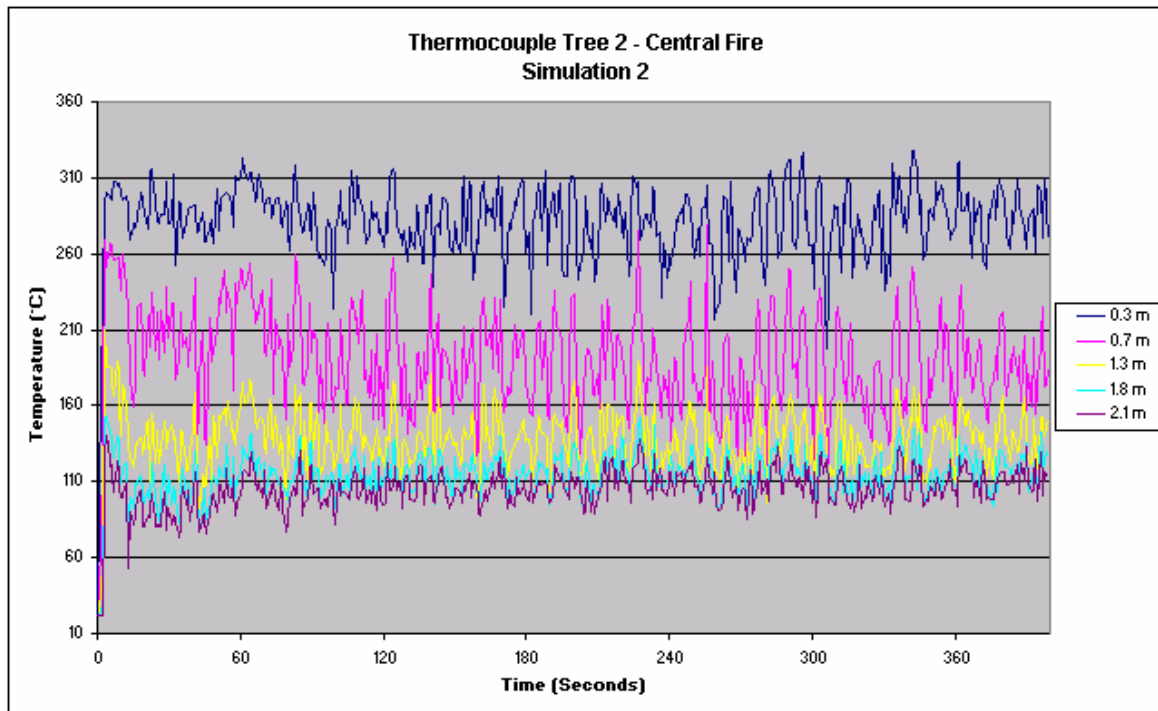
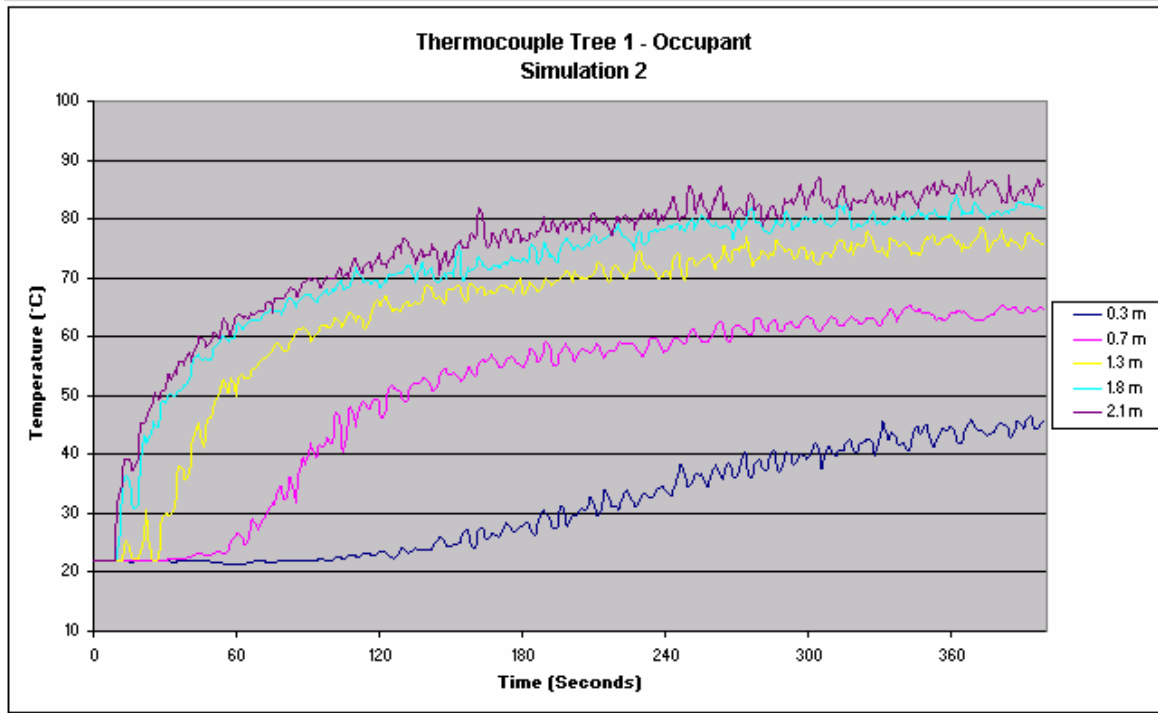
/*****OUTPUT FILES*****/

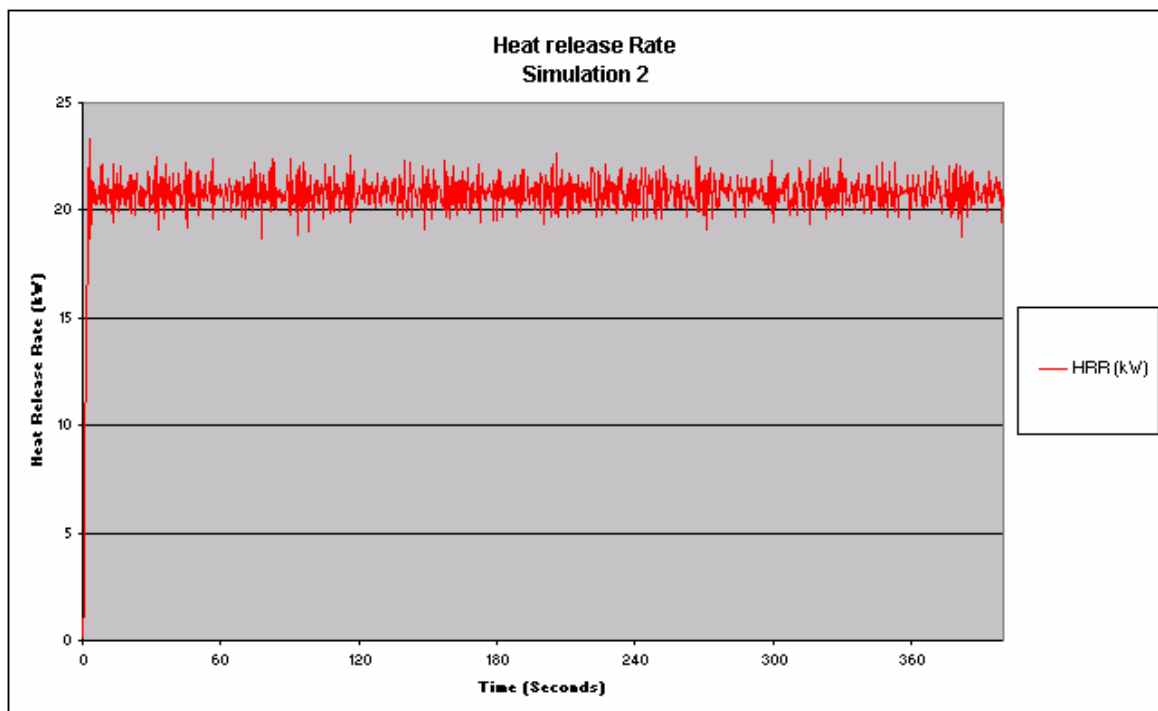
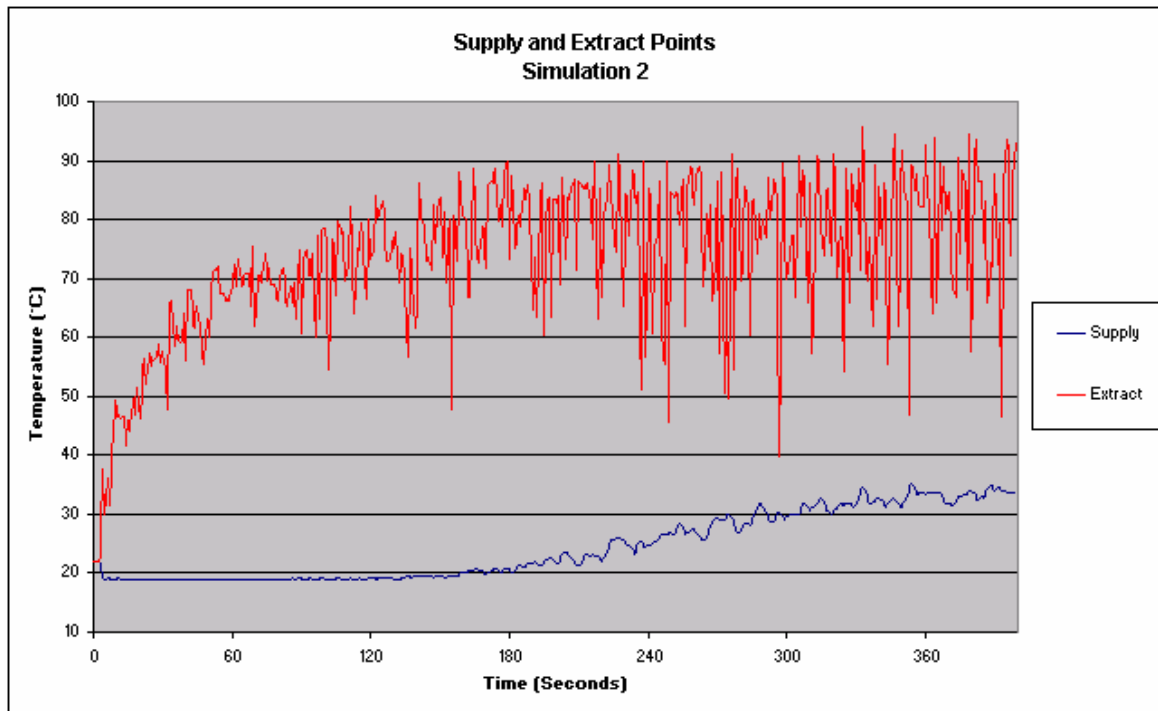
```

See: FDS Input File 2: Normal operation with no fire

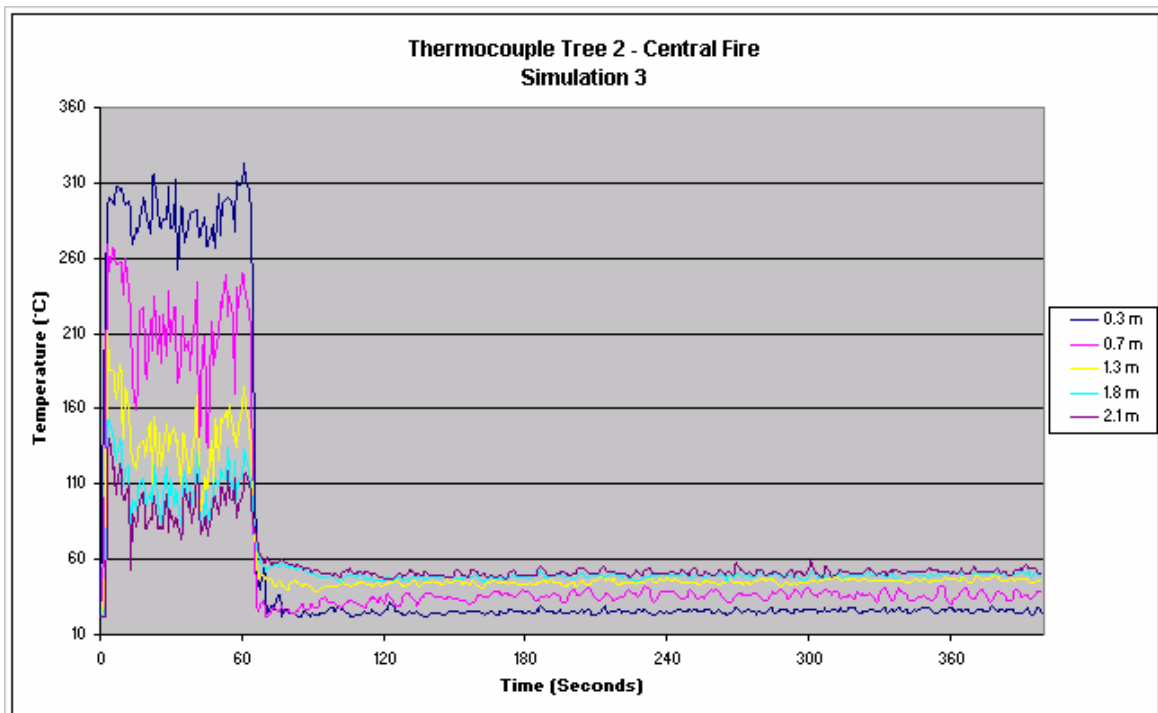
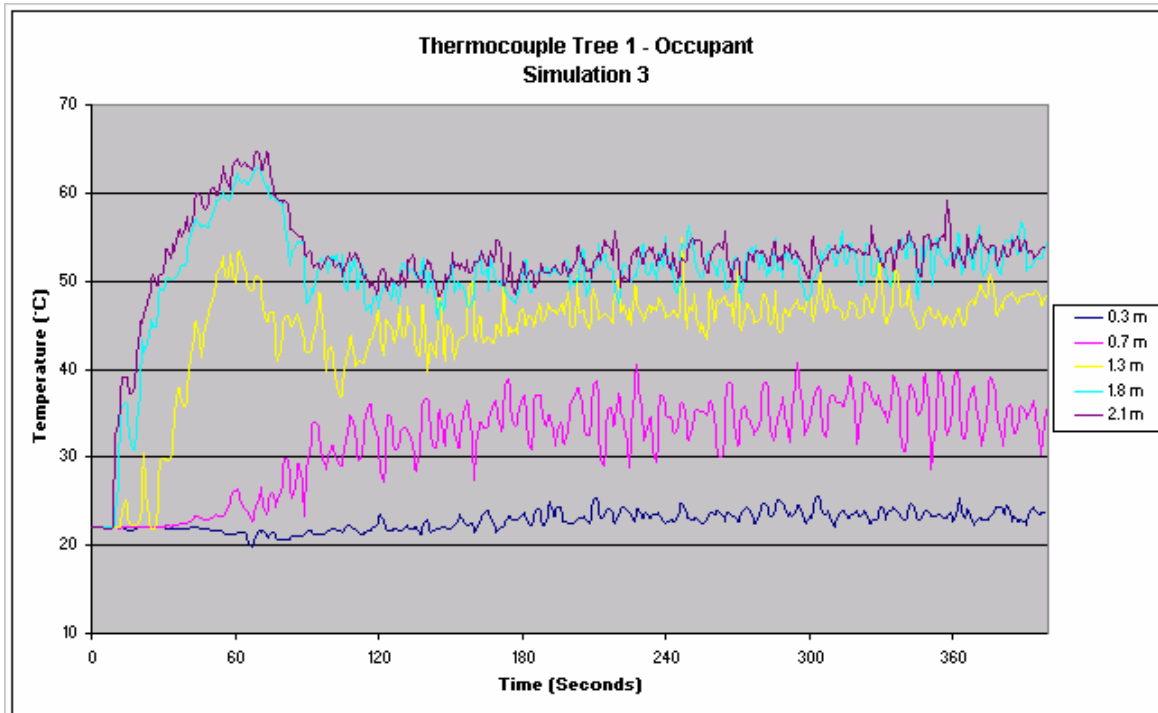
11.7 FDS thermocouple results

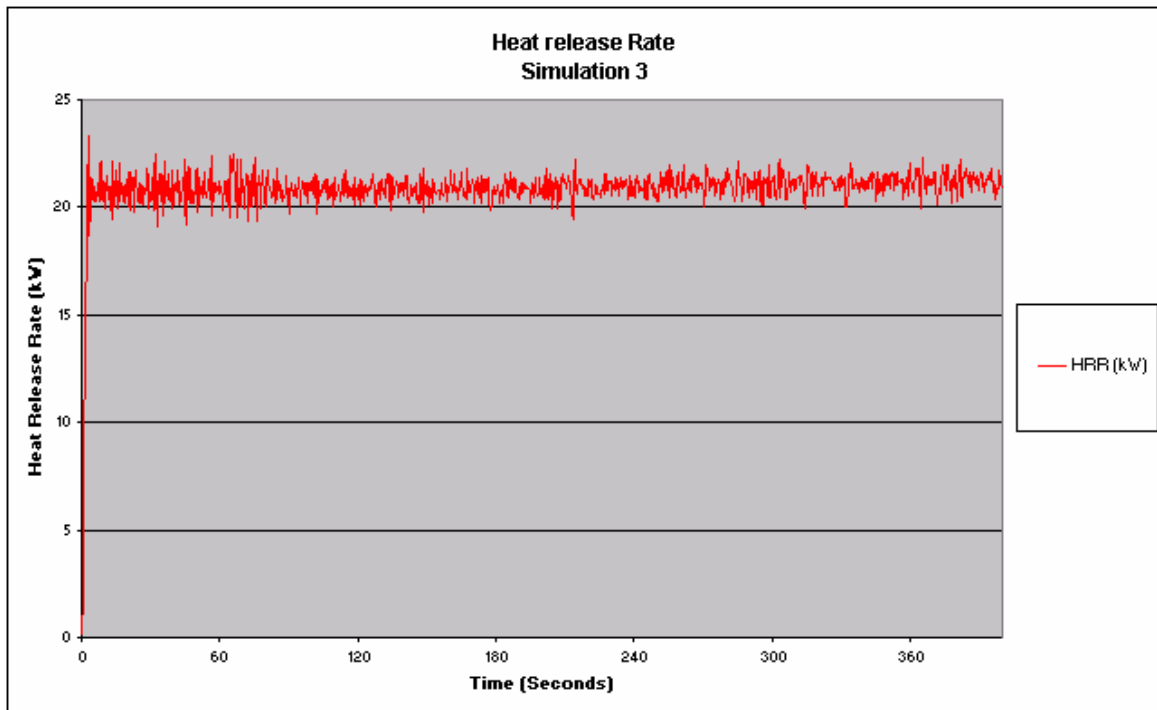
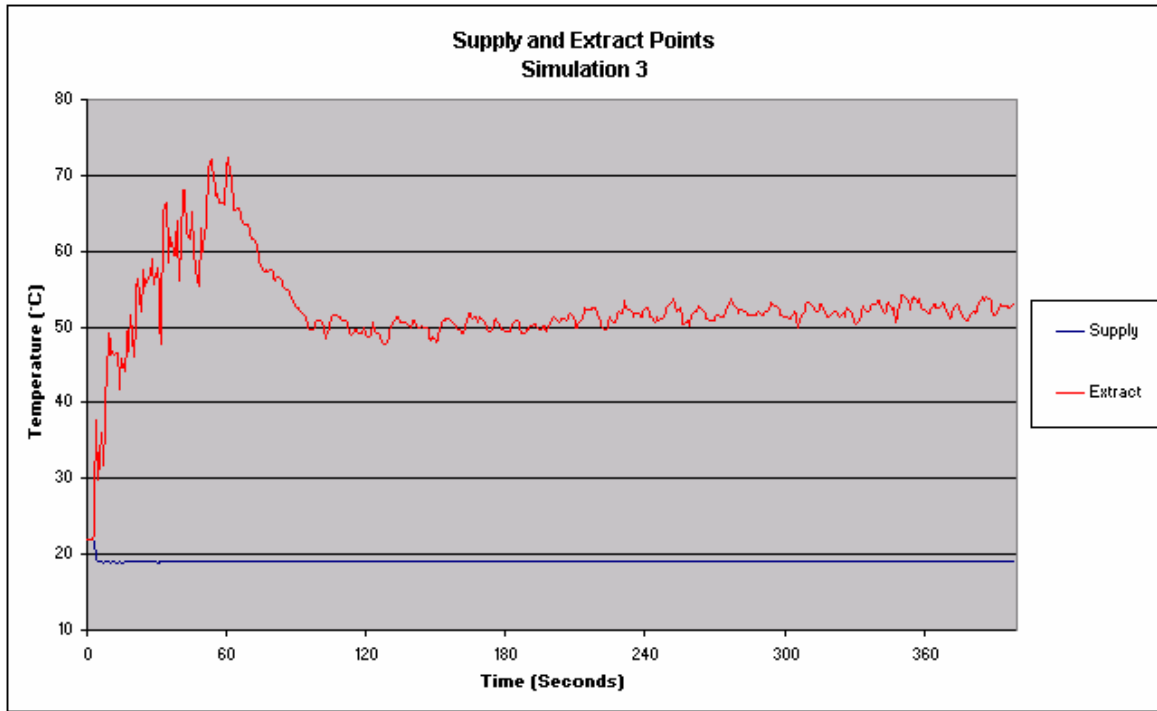
11.7.1 Normal operation with a central floor fire



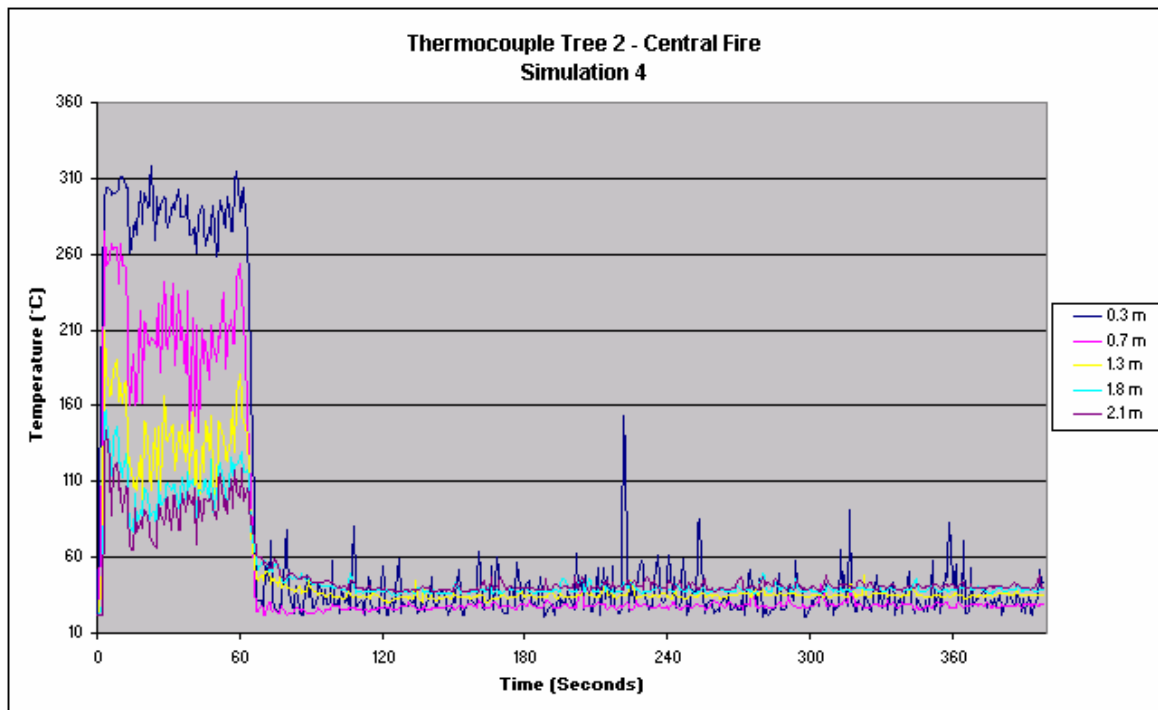
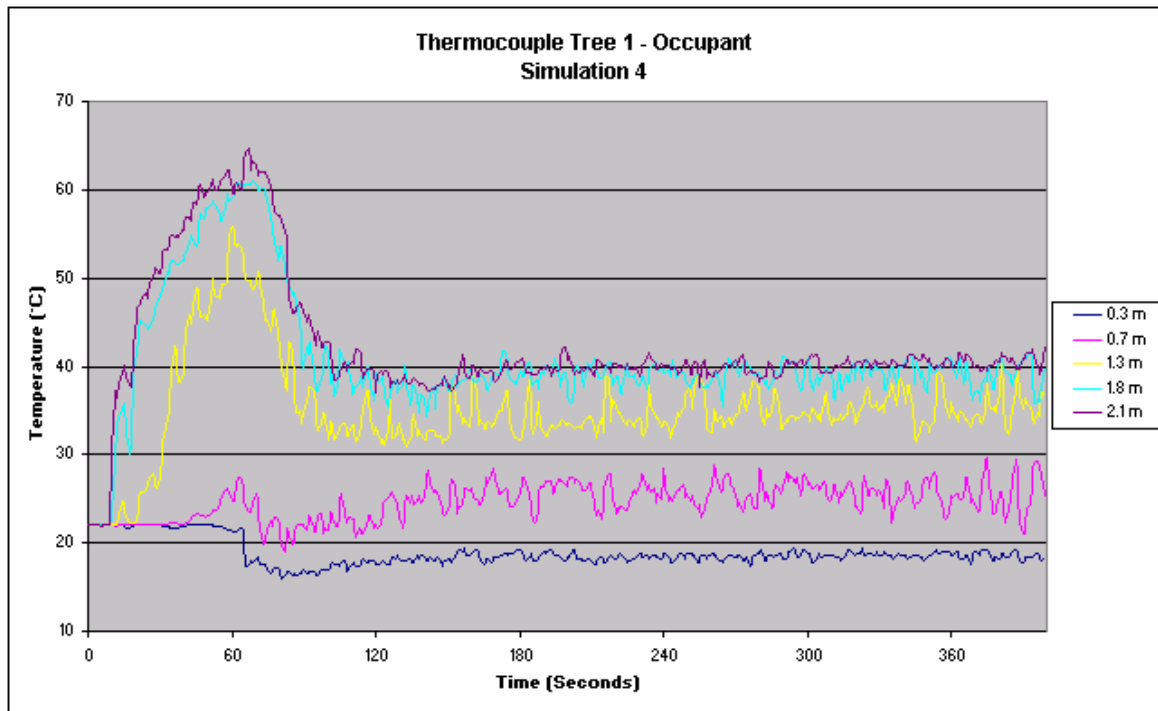


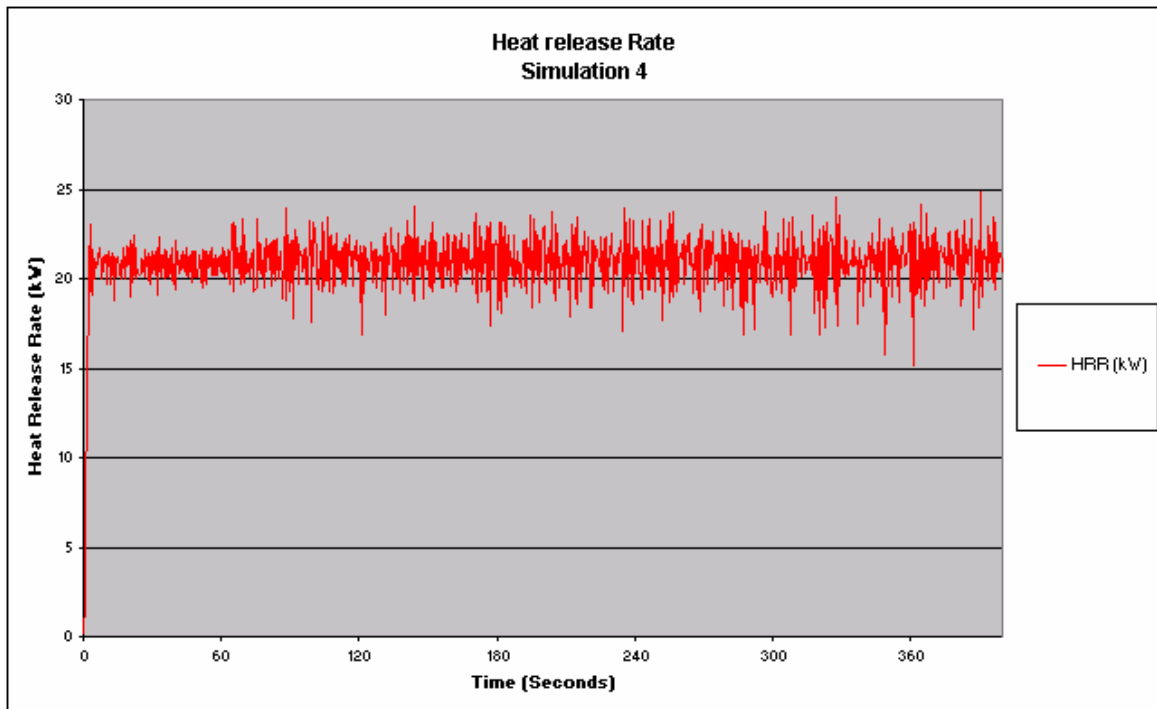
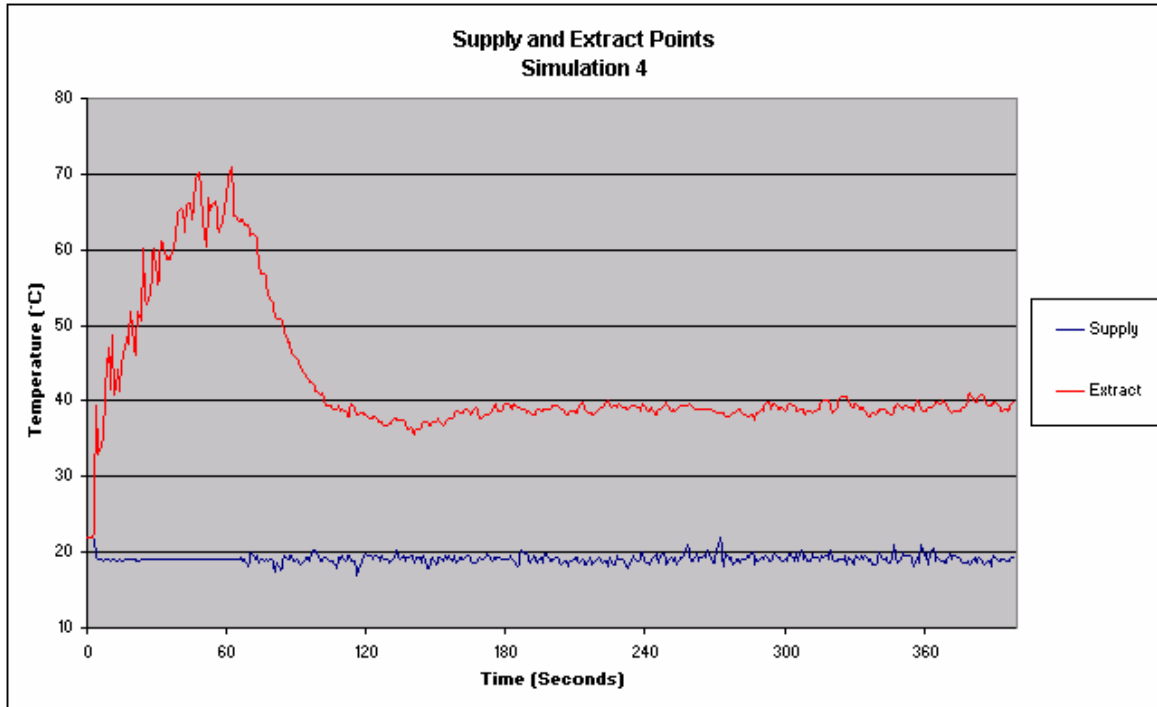
11.7.2 High airflow operation with a central floor fire



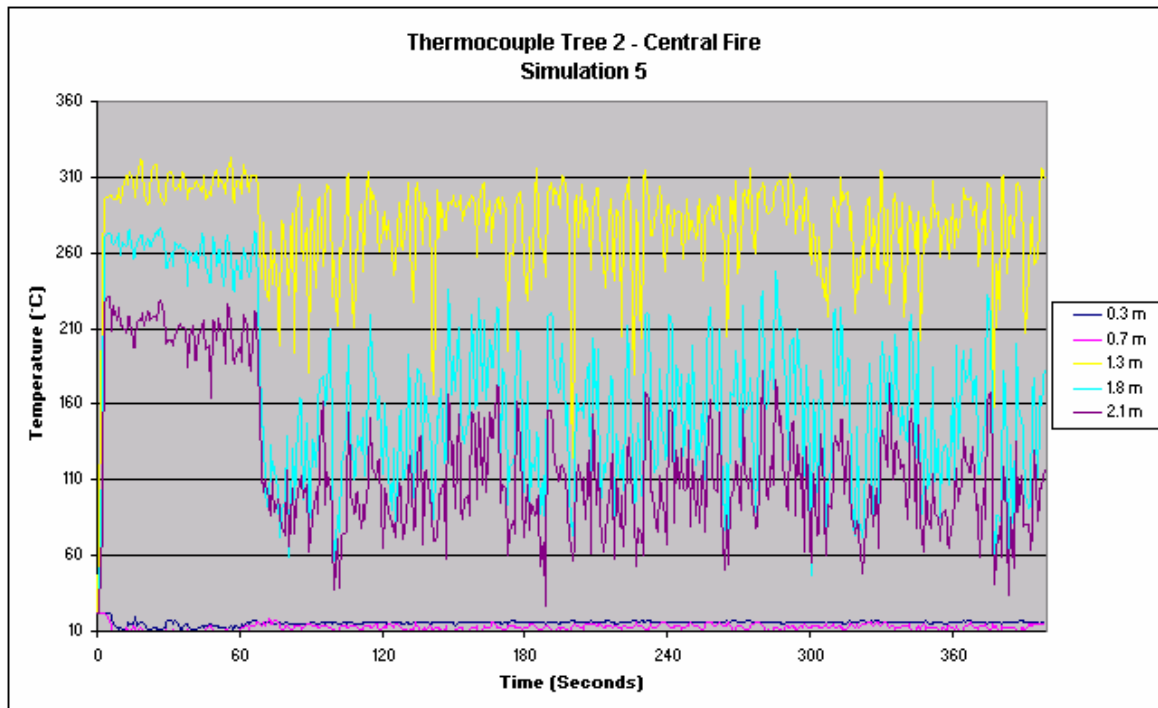
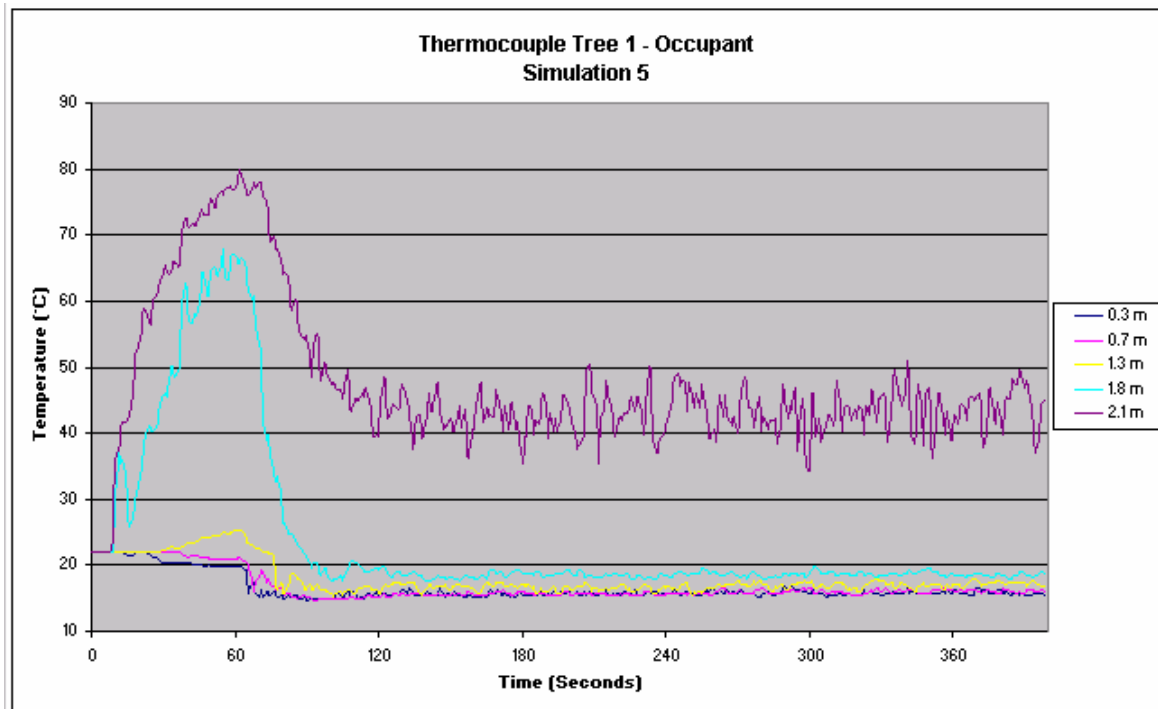


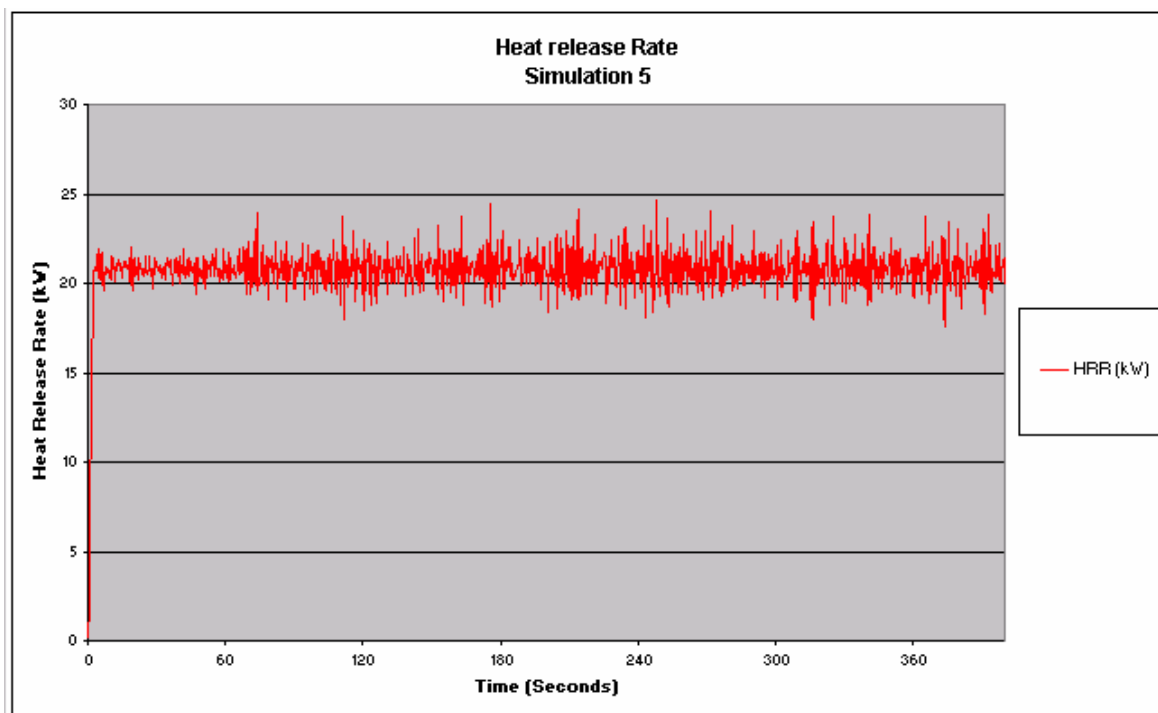
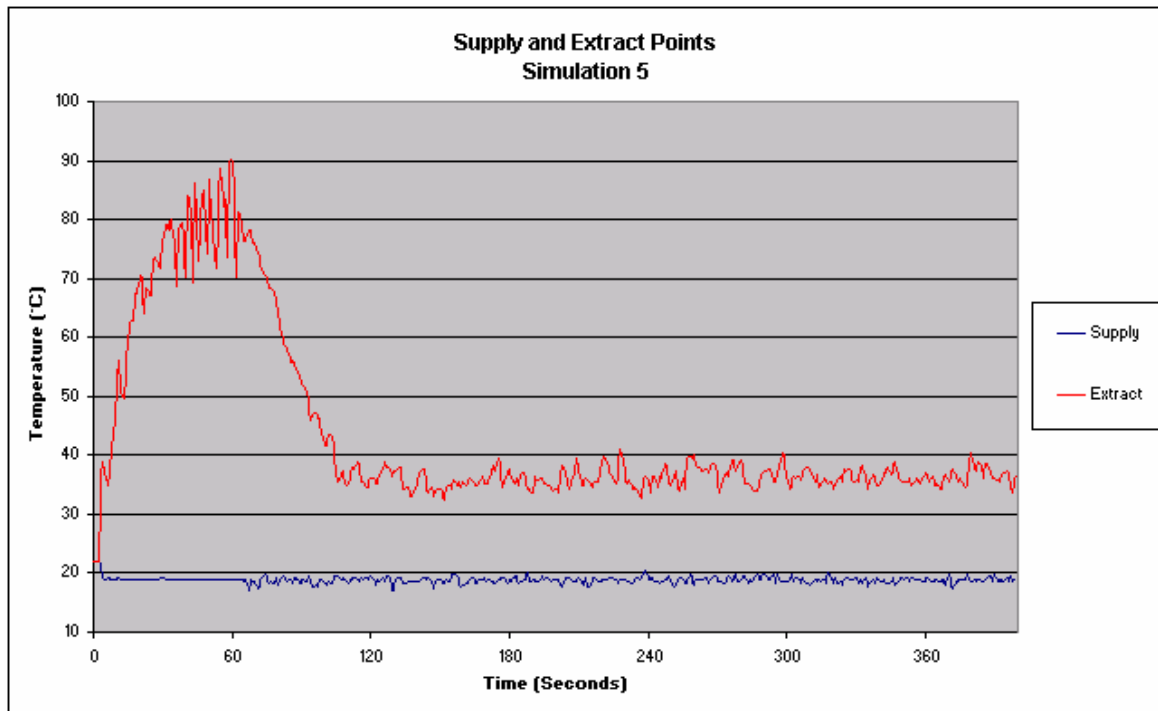
11.7.3 Displacement water mist operation with a central floor fire



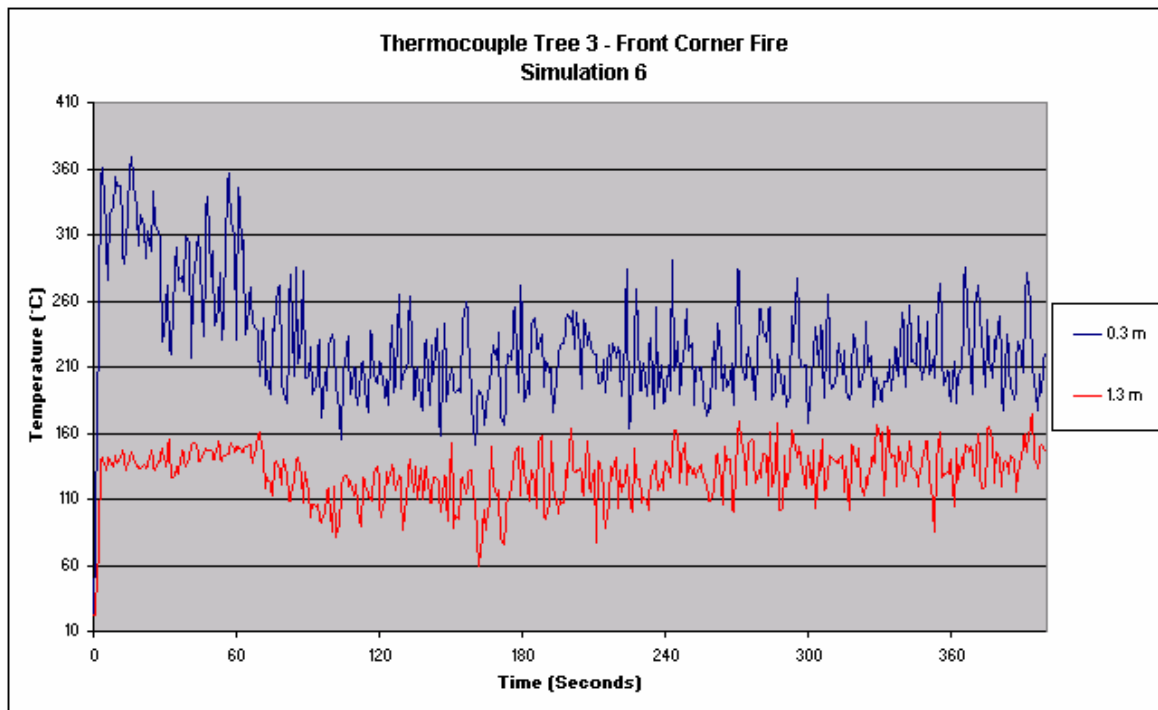
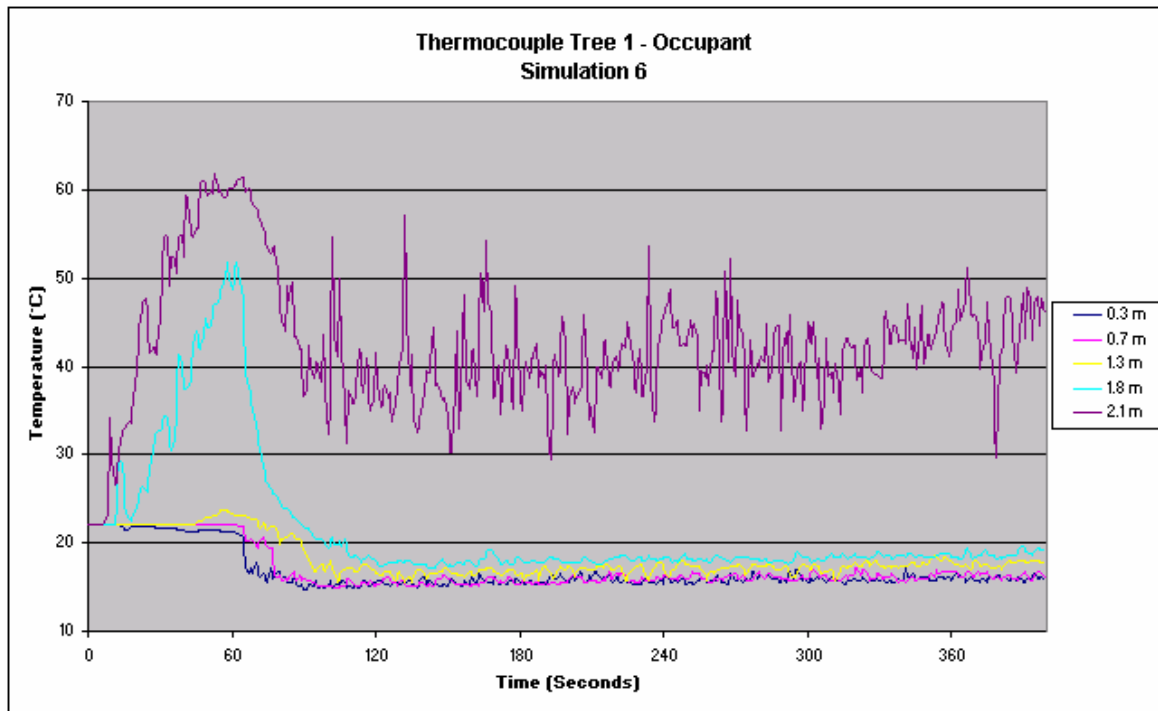


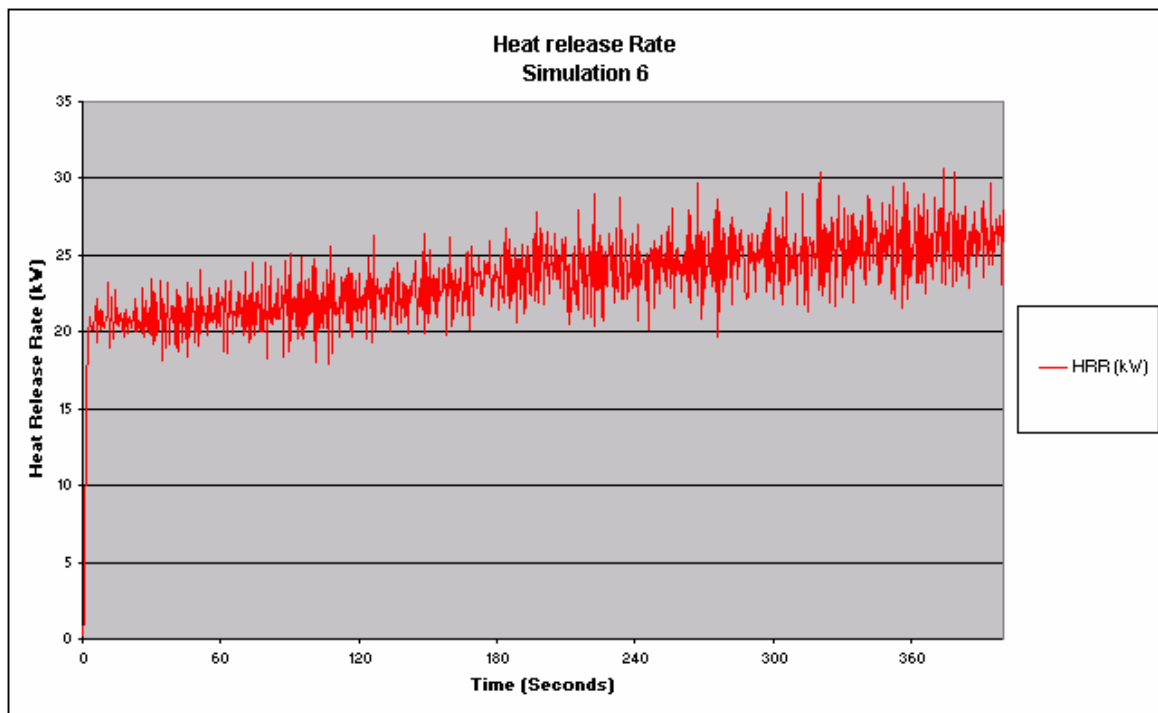
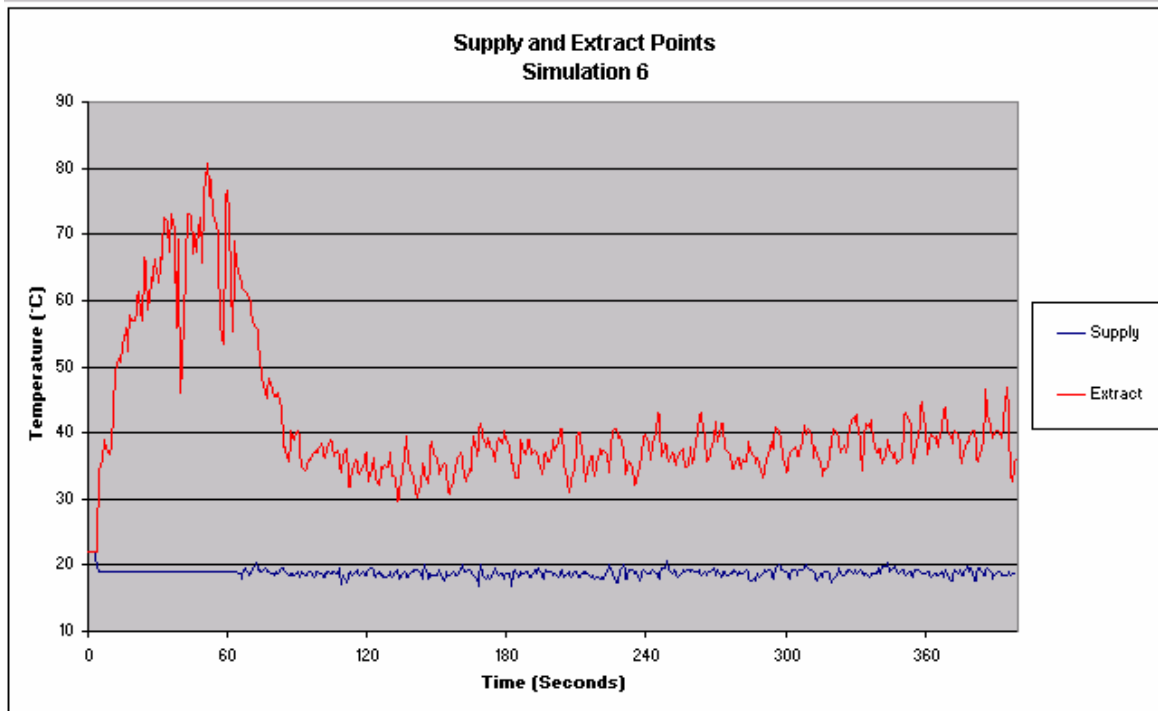
11.7.4 Displacement water mist operation with a central 1m fire



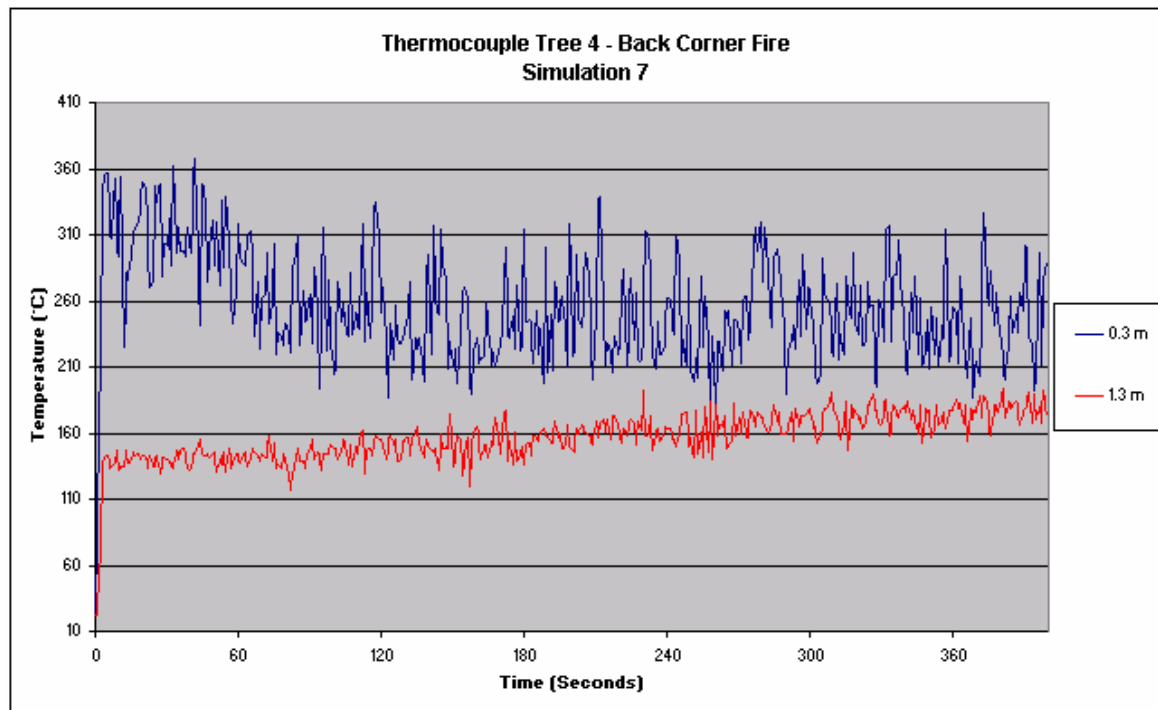
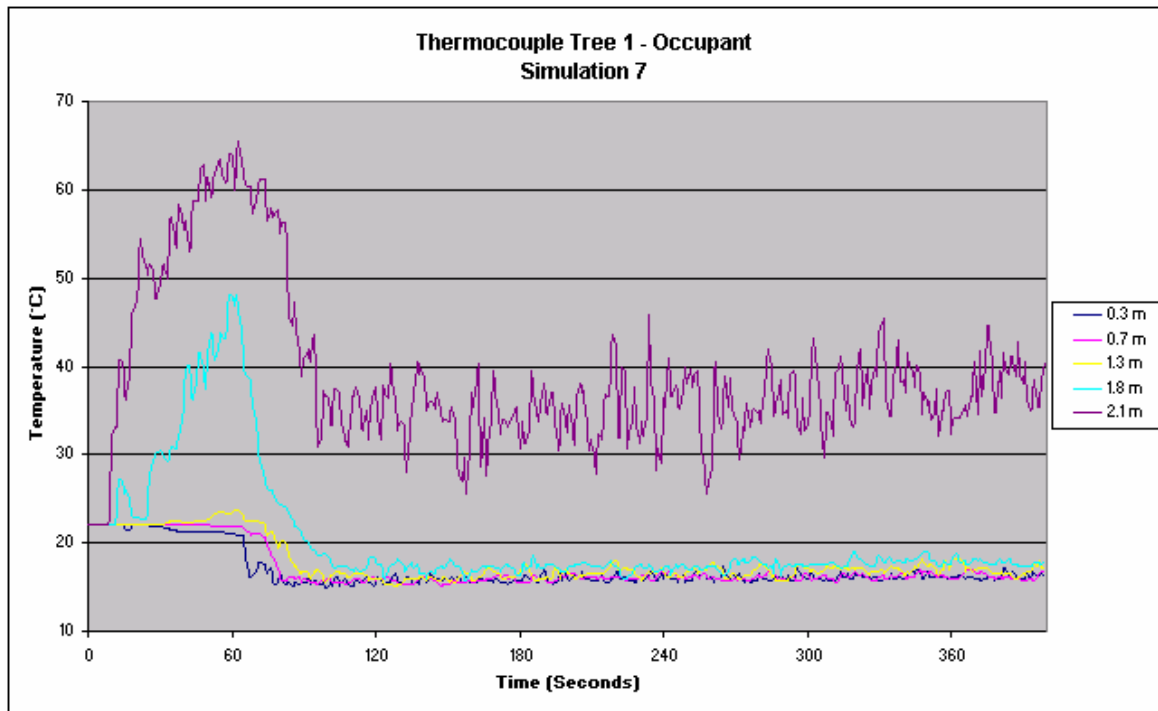


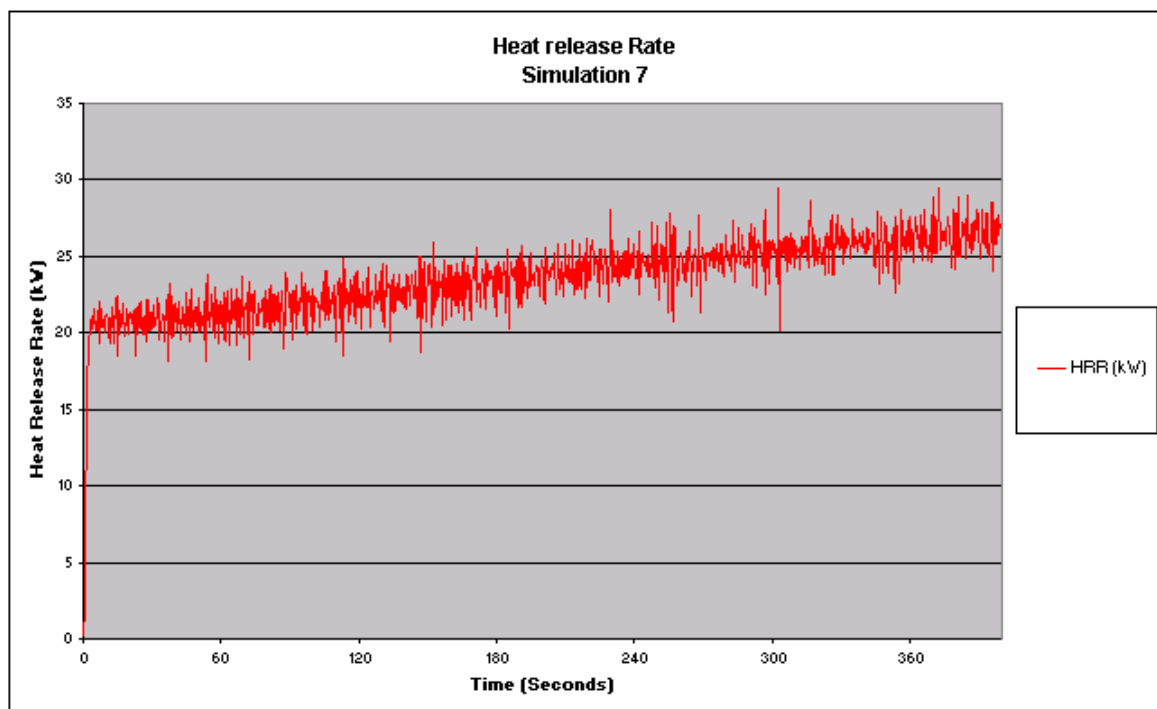
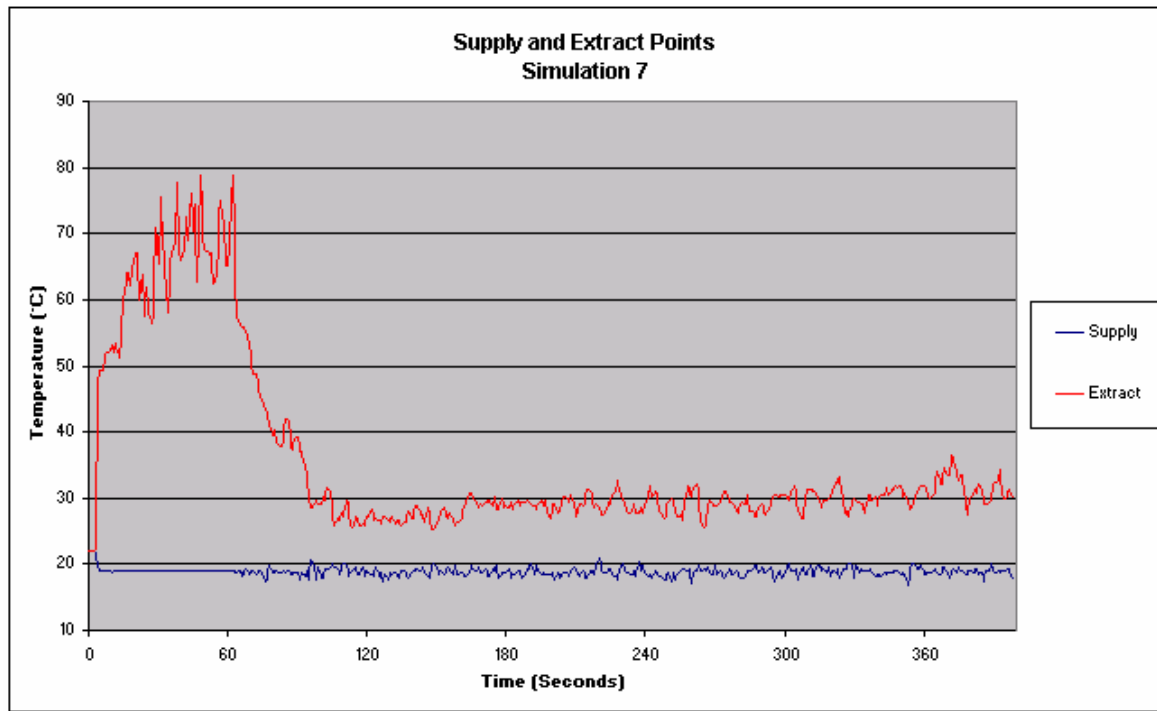
11.7.5 Displacement water mist operation with a front corner fire



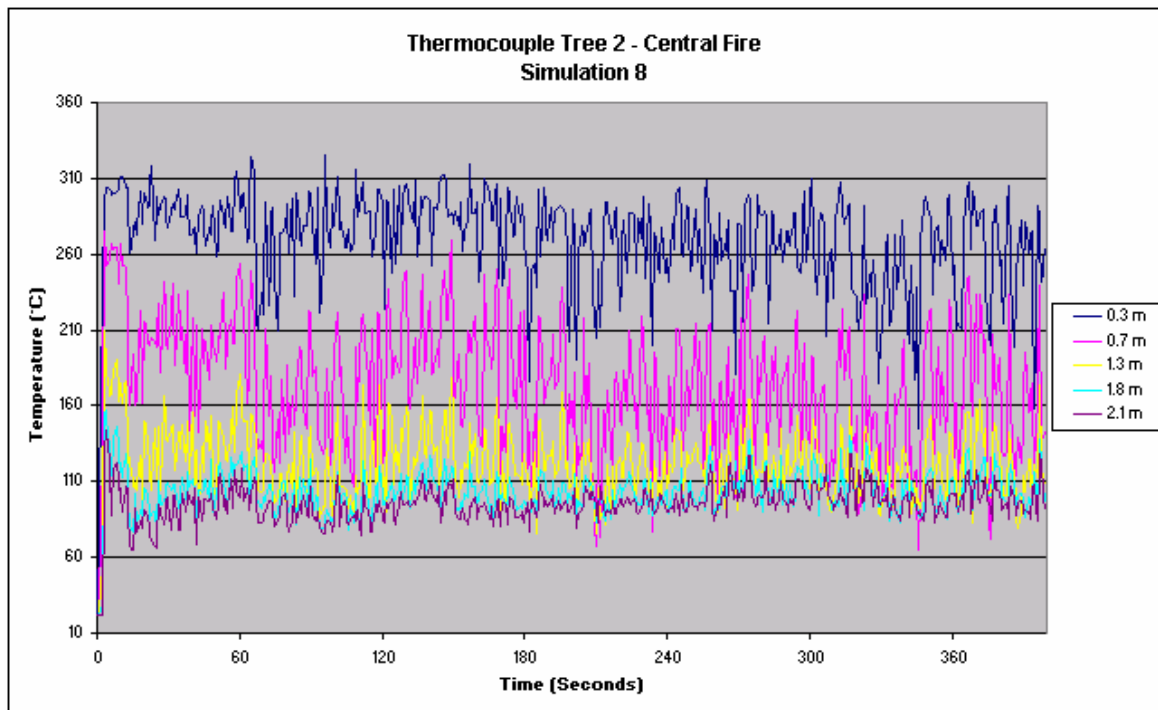
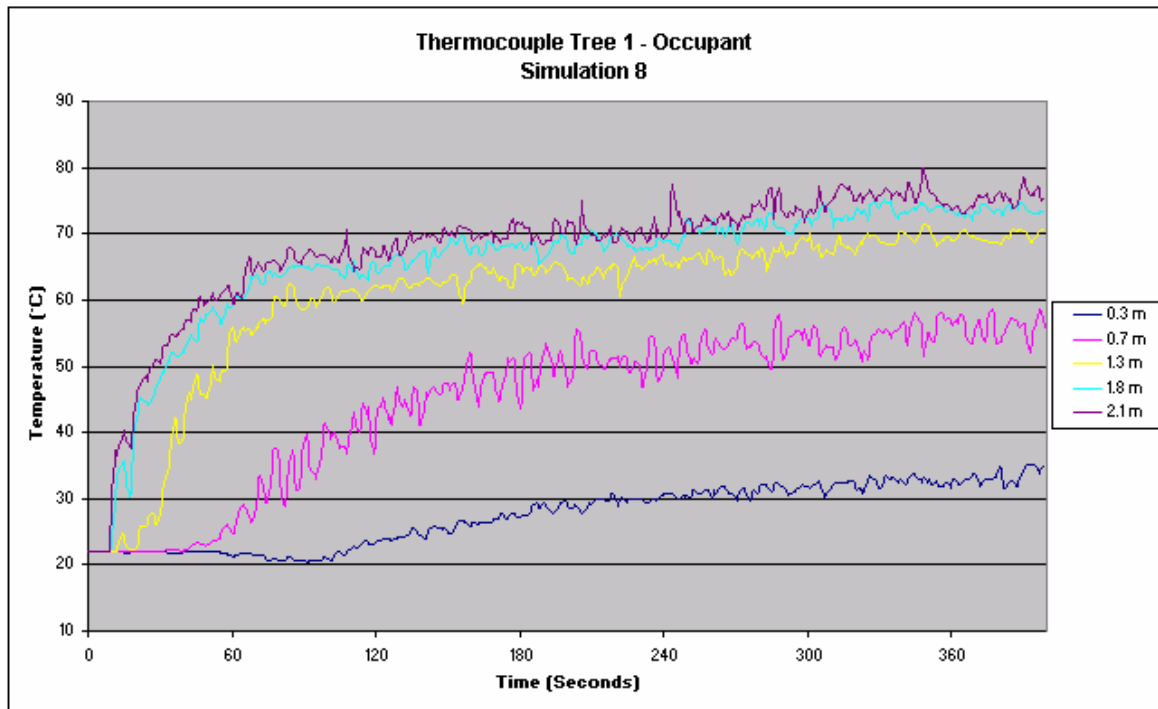


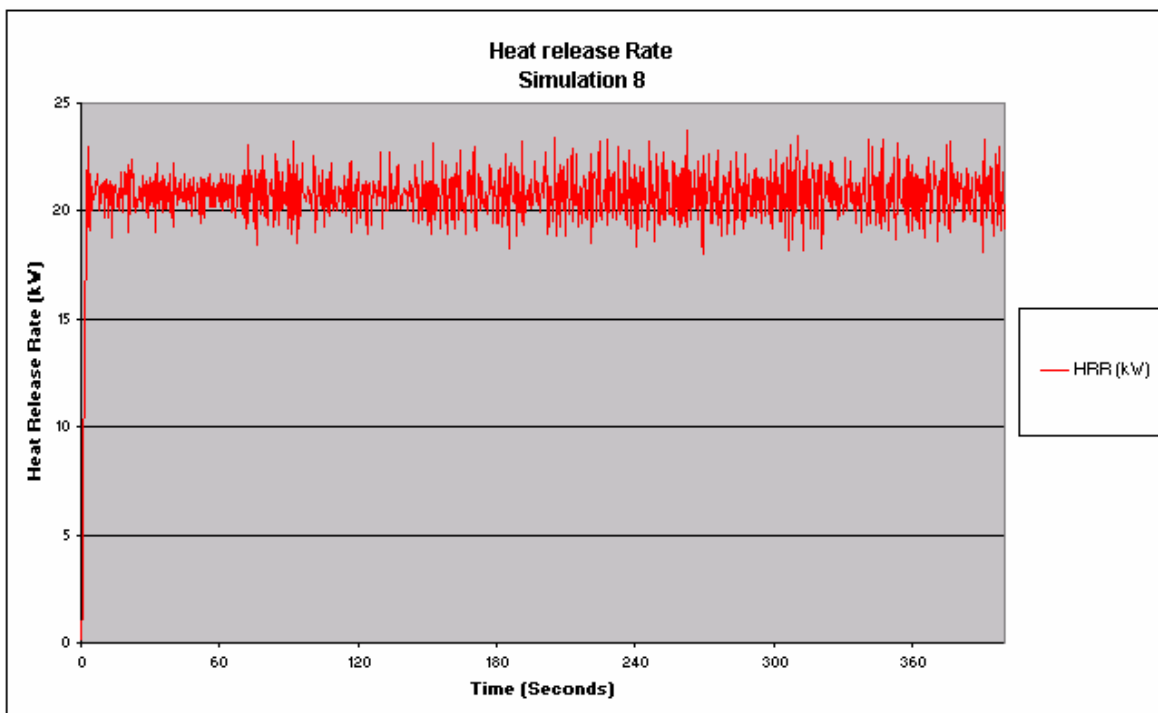
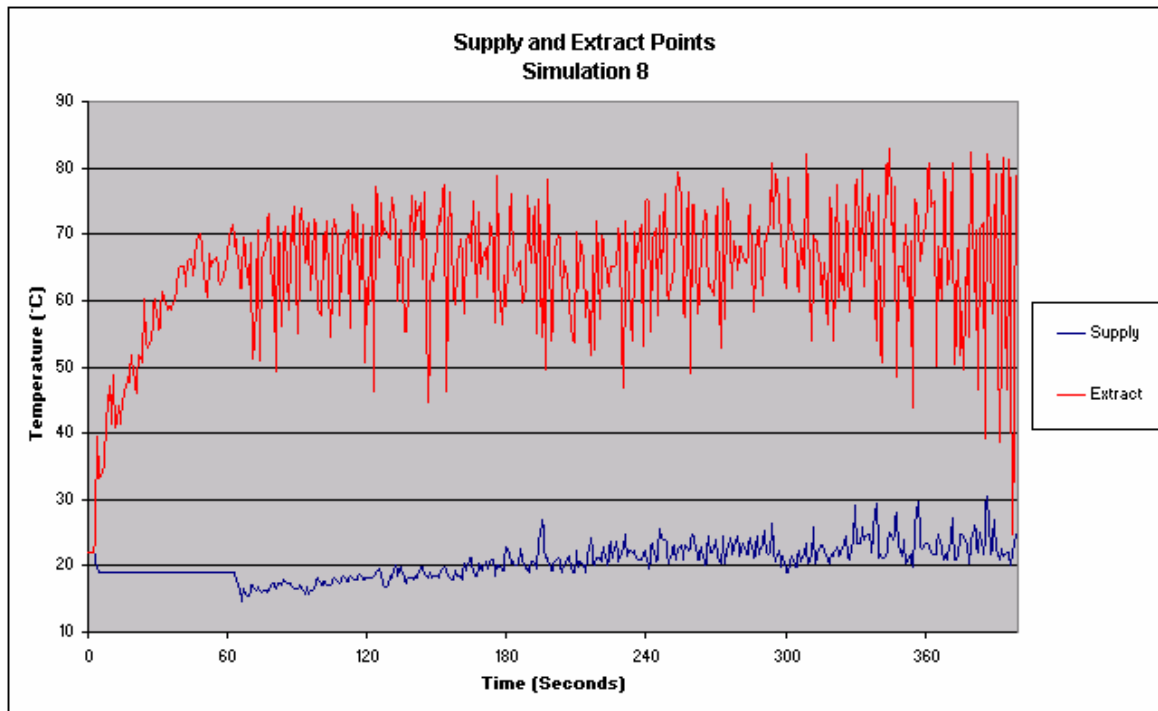
11.7.6 Displacement water mist operation with a back corner fire





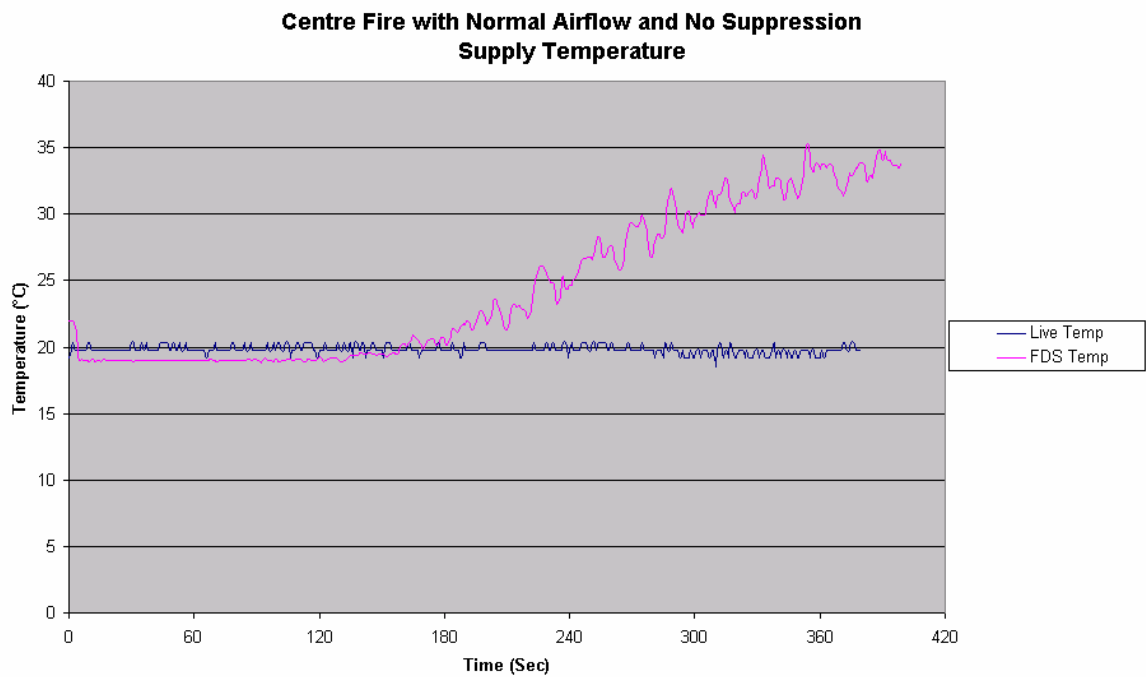
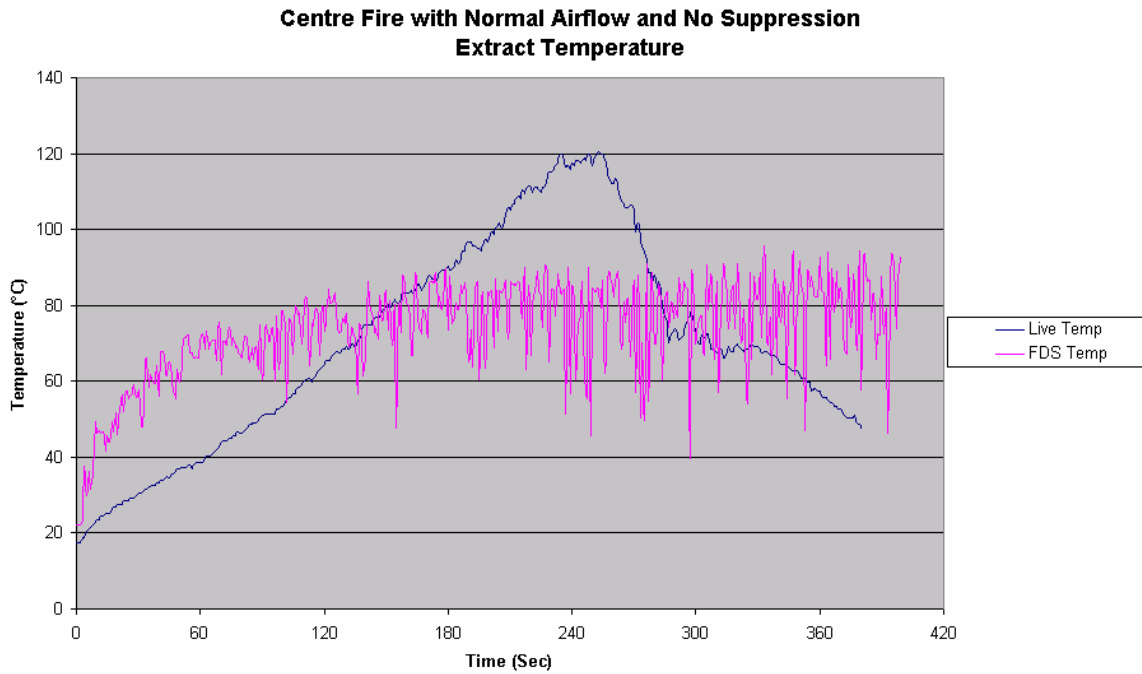
11.7.7 Low airflow and water mist operation with a central floor fire



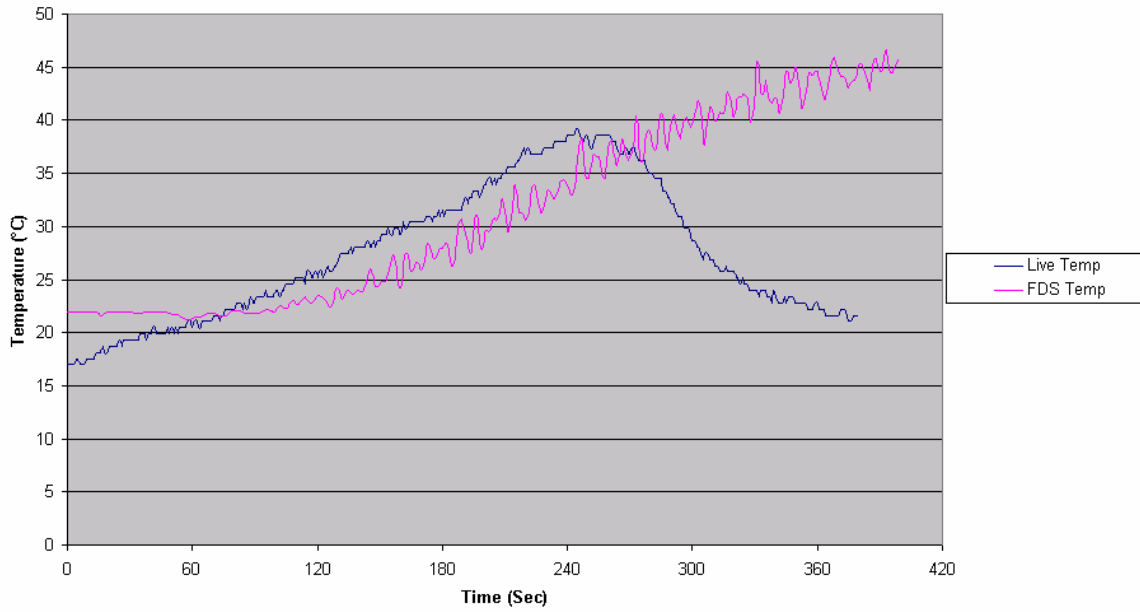


11.8 Live and FDS comparison graphs

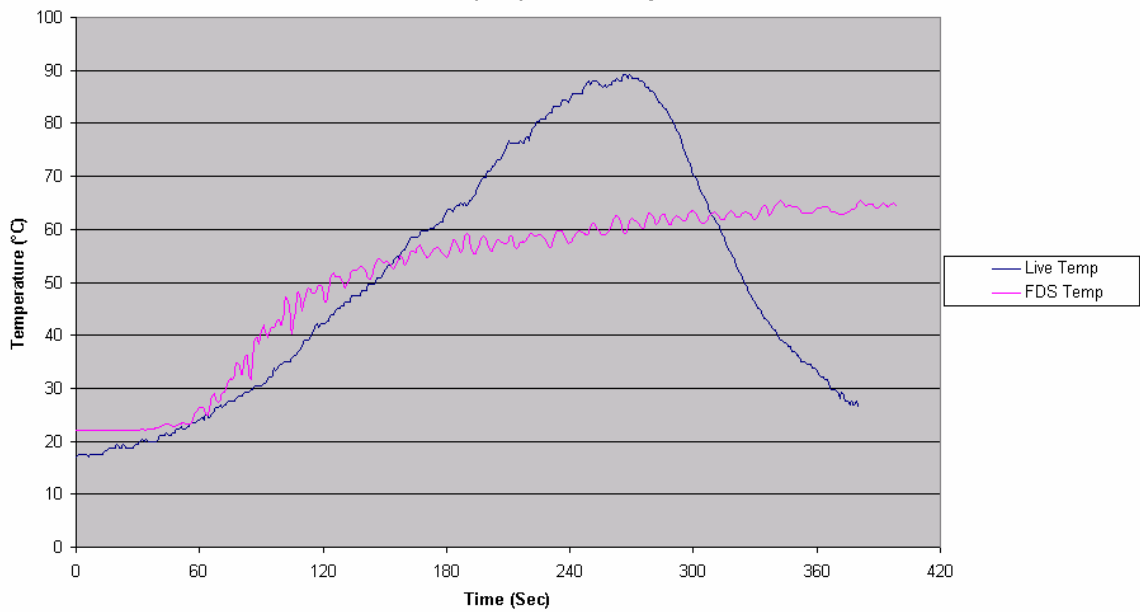
11.8.1 Normal operation with a central floor fire



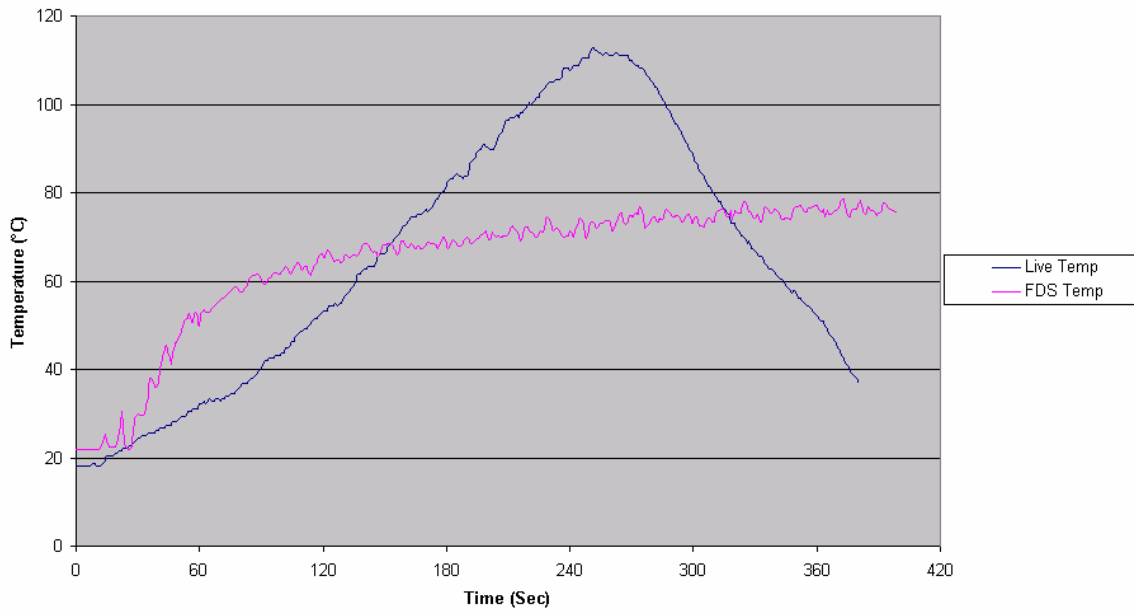
**Centre Fire with Normal Airflow and No Suppression
Tree 1 (occ) 0.3 m Temperature**



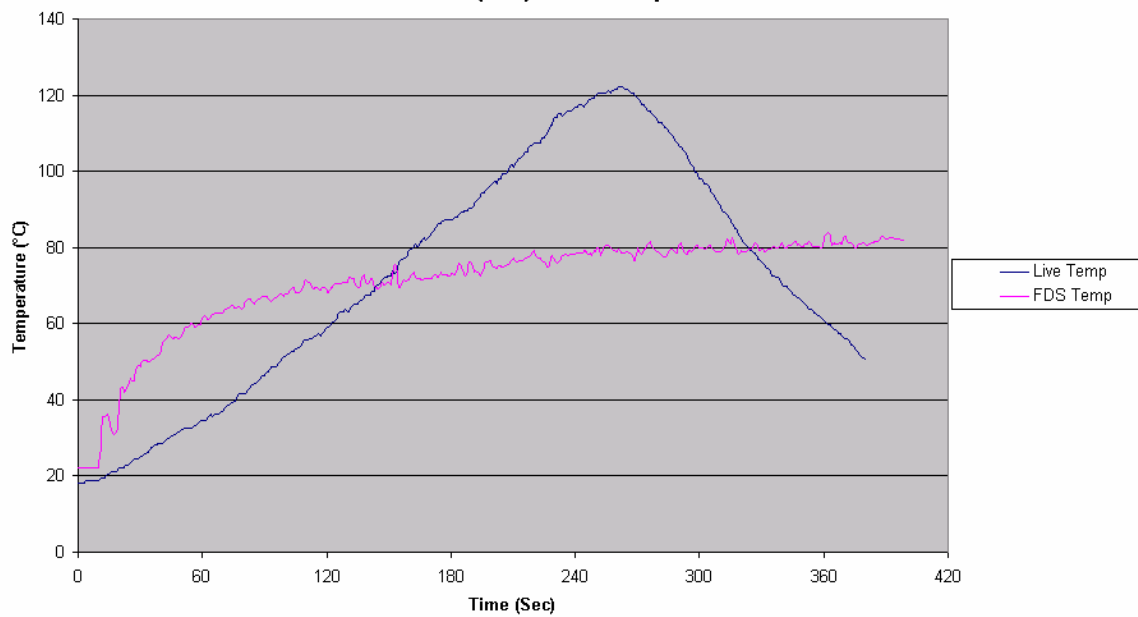
**Centre Fire with Normal Airflow and No Suppression
Tree 1 (occ) 0.7 m Temperature**



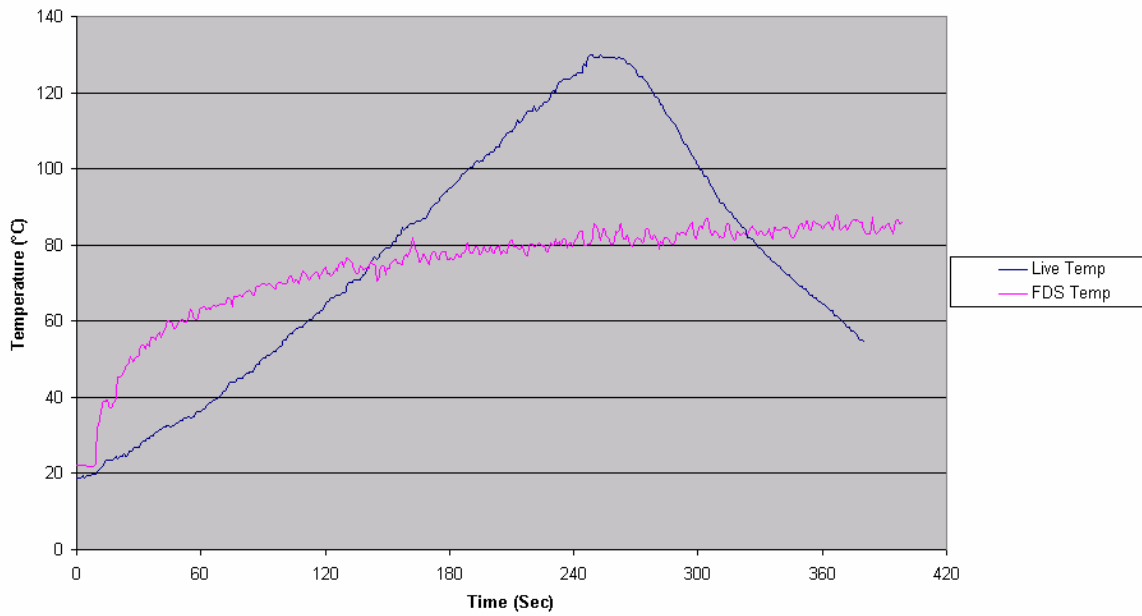
**Centre Fire with Normal Airflow and No Suppression
Tree 1 (occ) 1.3 m Temperature**



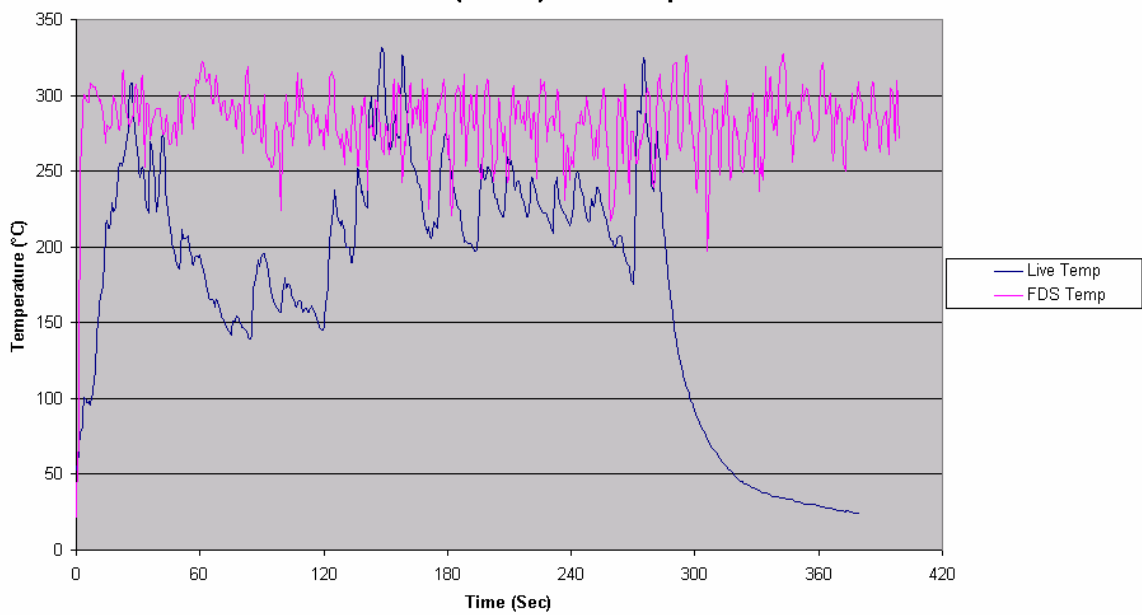
**Centre Fire with Normal Airflow and No Suppression
Tree 1 (occ) 1.8 m Temperature**



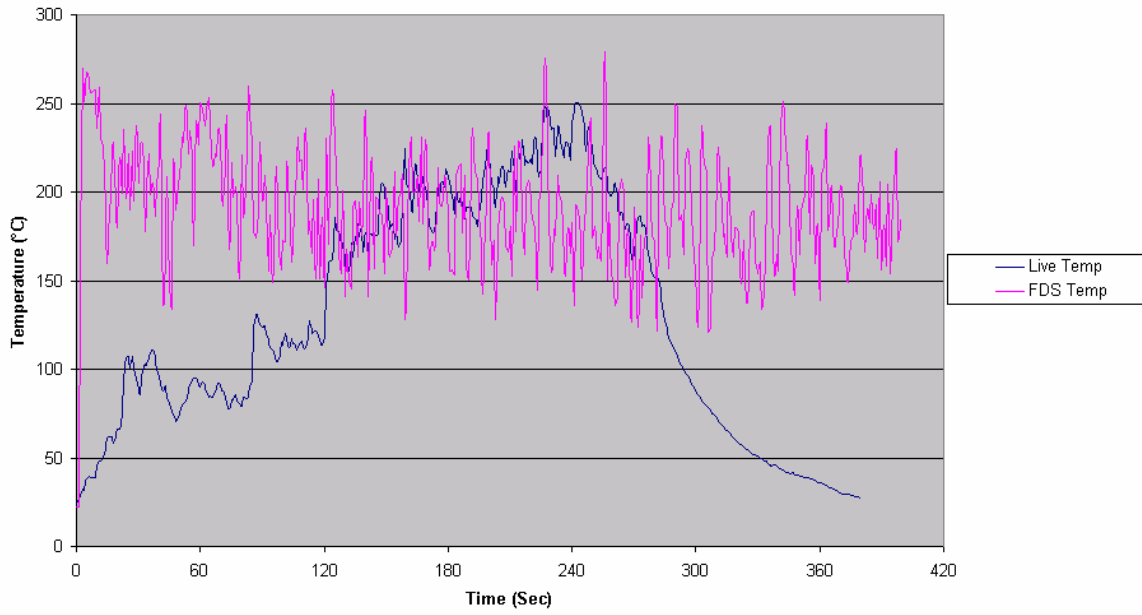
**Centre Fire with Normal Airflow and No Suppression
Tree 1 (occ) 2.1 m Temperature**



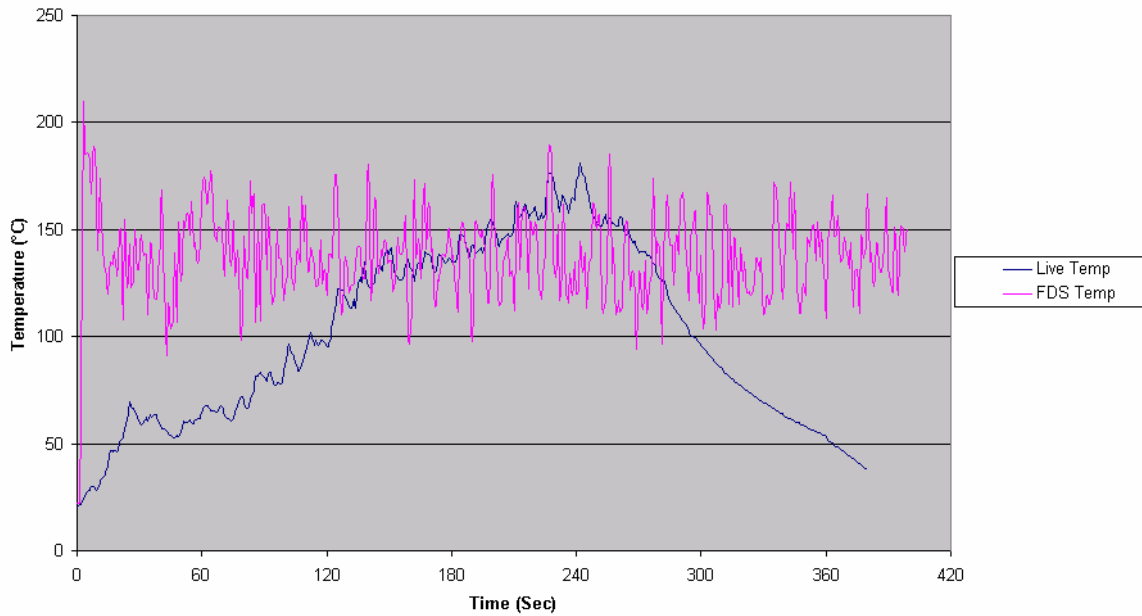
**Centre Fire with Normal Airflow and No Suppression
Tree 2 (Centre) 0.3 m Temperature**



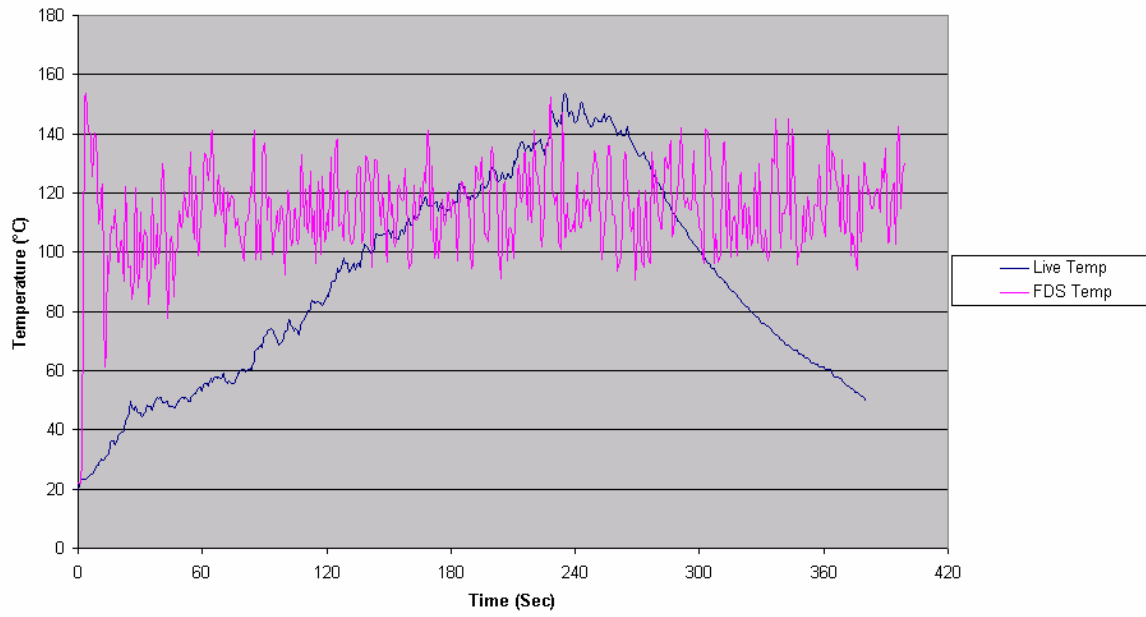
**Centre Fire with Normal Airflow and No Suppression
Tree 2 (Centre) 0.7 m Temperature**



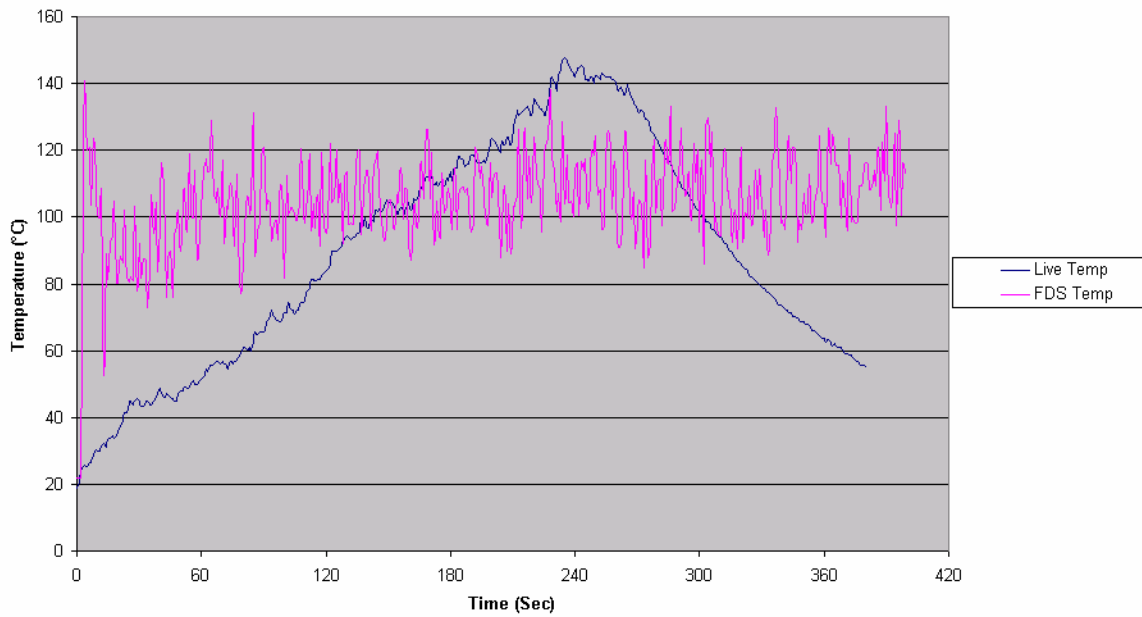
**Centre Fire with Normal Airflow and No Suppression
Tree 2 (Centre) 1.3 m Temperature**



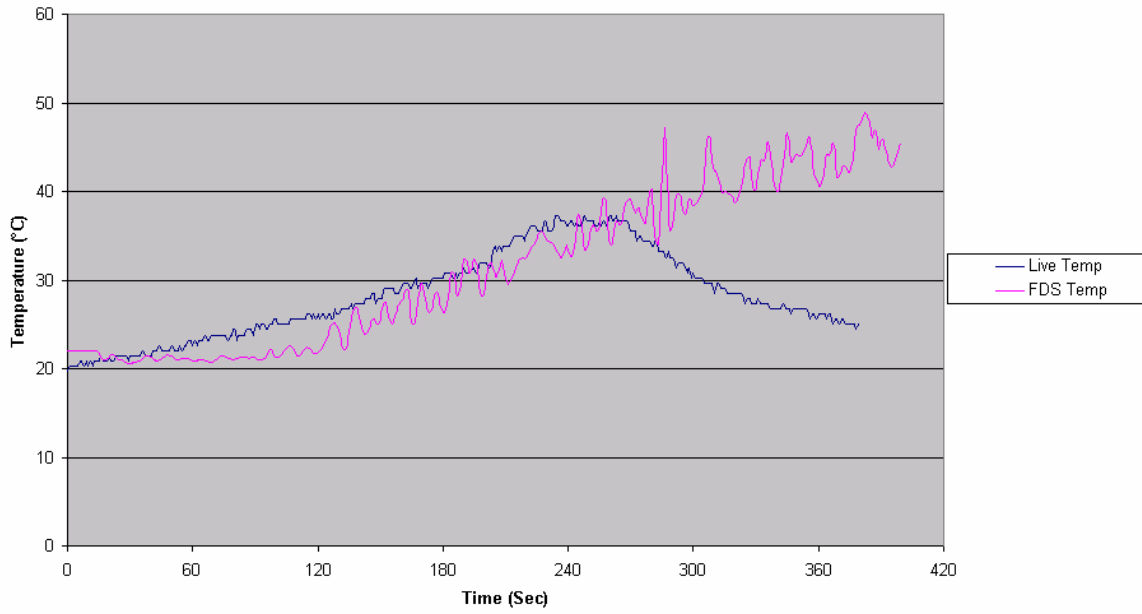
**Centre Fire with Normal Airflow and No Suppression
Tree 2 (Centre) 1.8 m Temperature**



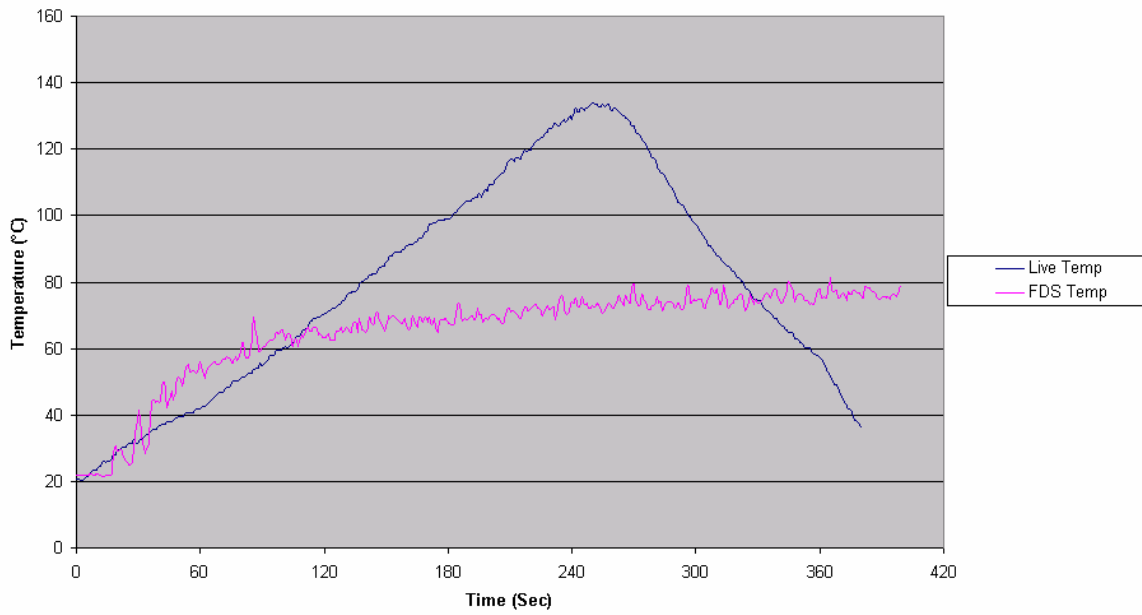
**Centre Fire with Normal Airflow and No Suppression
Tree 2 (Centre) 2.1 m Temperature**



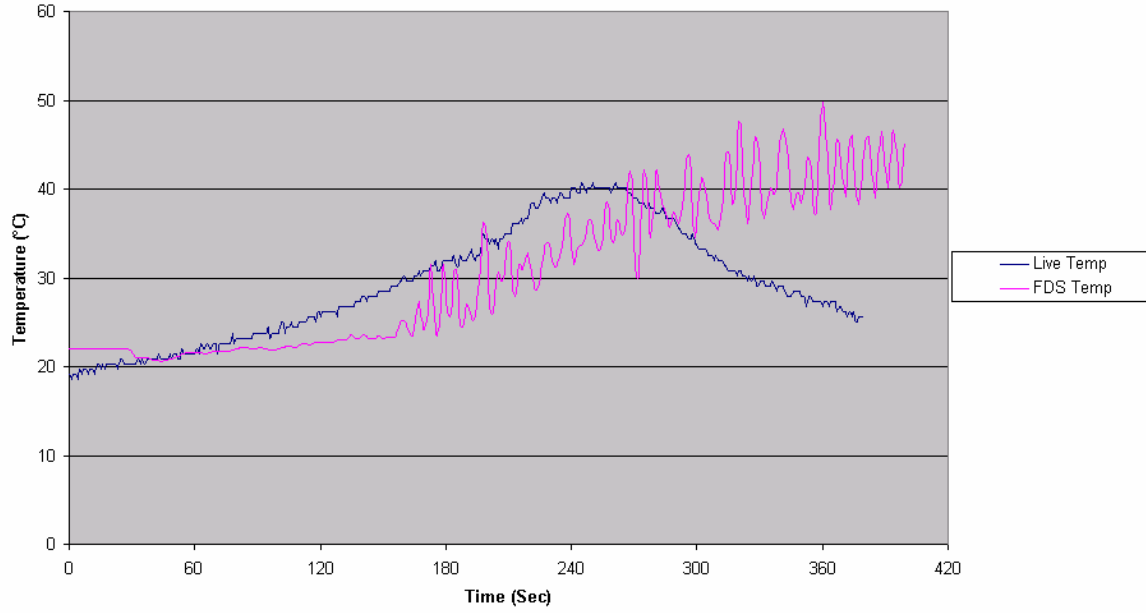
**Centre Fire with Normal Airflow and No Suppression
Back Corner 0.3 m Temperature**



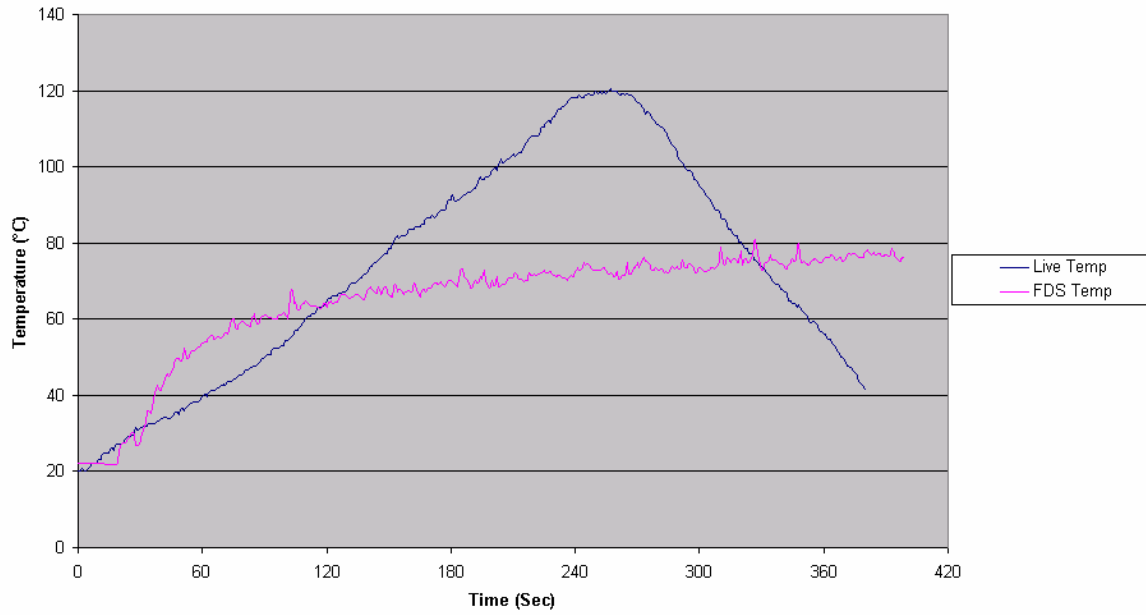
**Centre Fire with Normal Airflow and No Suppression
Back Corner 1.3 m Temperature**



**Centre Fire with Normal Airflow and No Suppression
Front Corner 0.3 m Temperature**

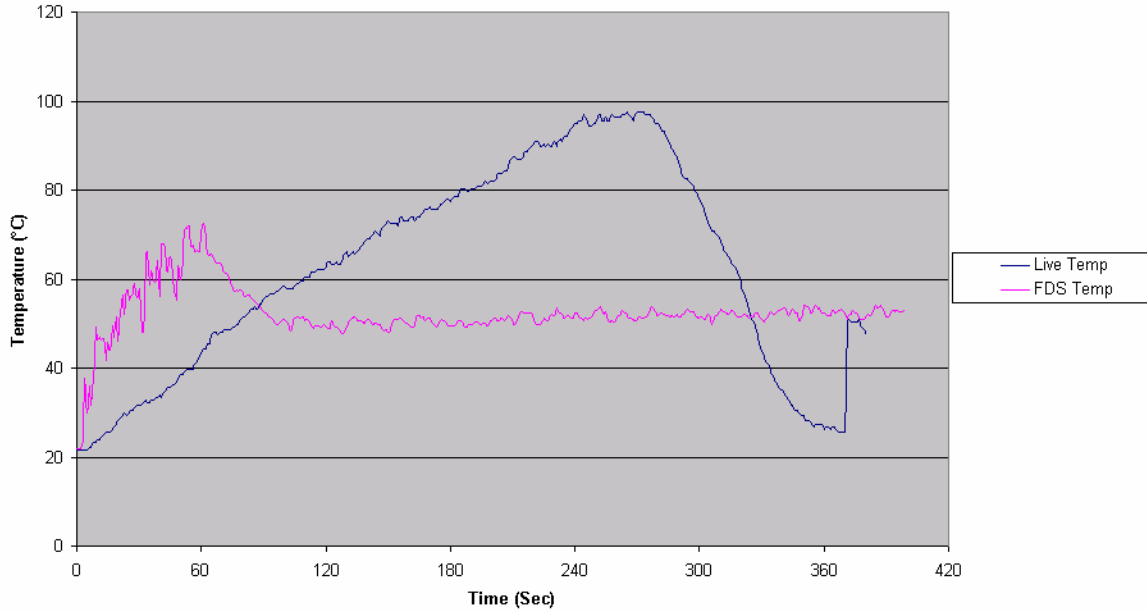


**Centre Fire with Normal Airflow and No Suppression
Front Corner 1.3 m Temperature**

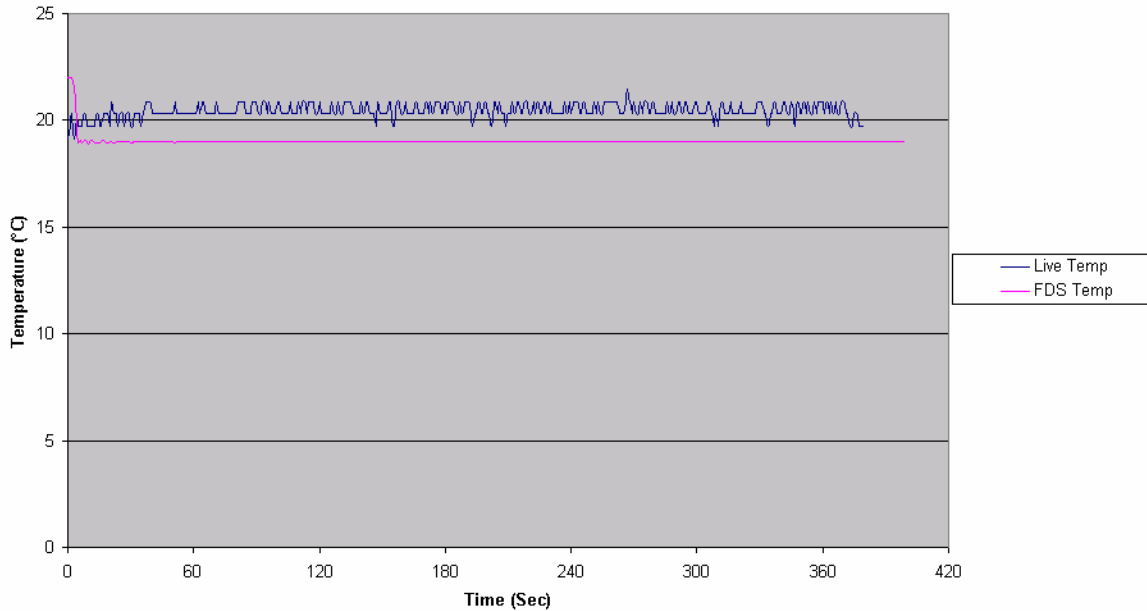


11.8.2 High airflow operation with a central floor fire

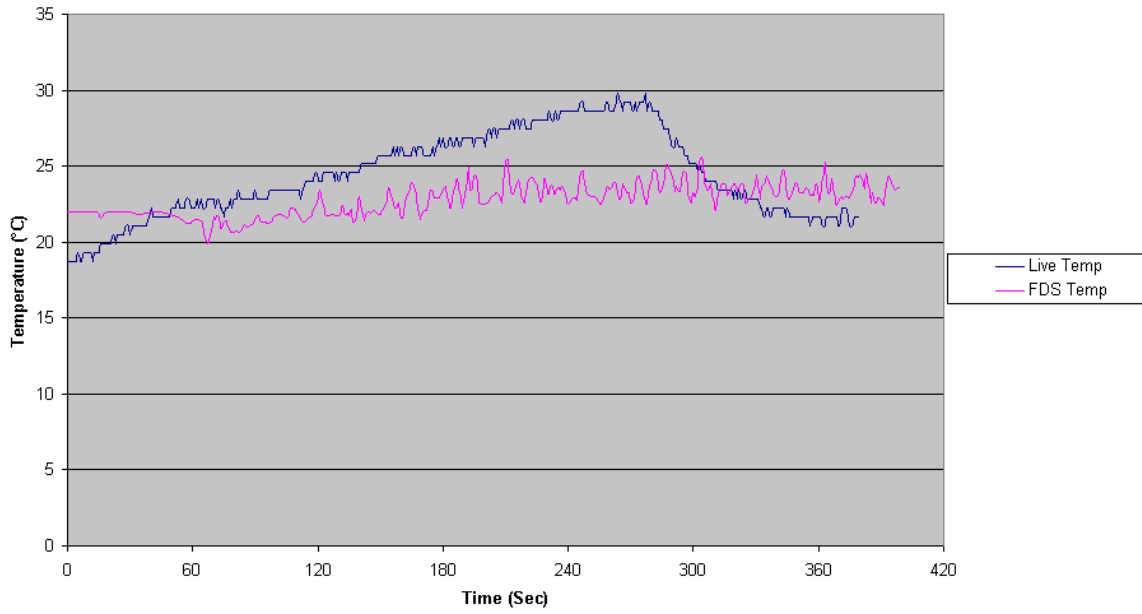
**Centre Fire with High Airflow and No Suppression
Extract Temperature**



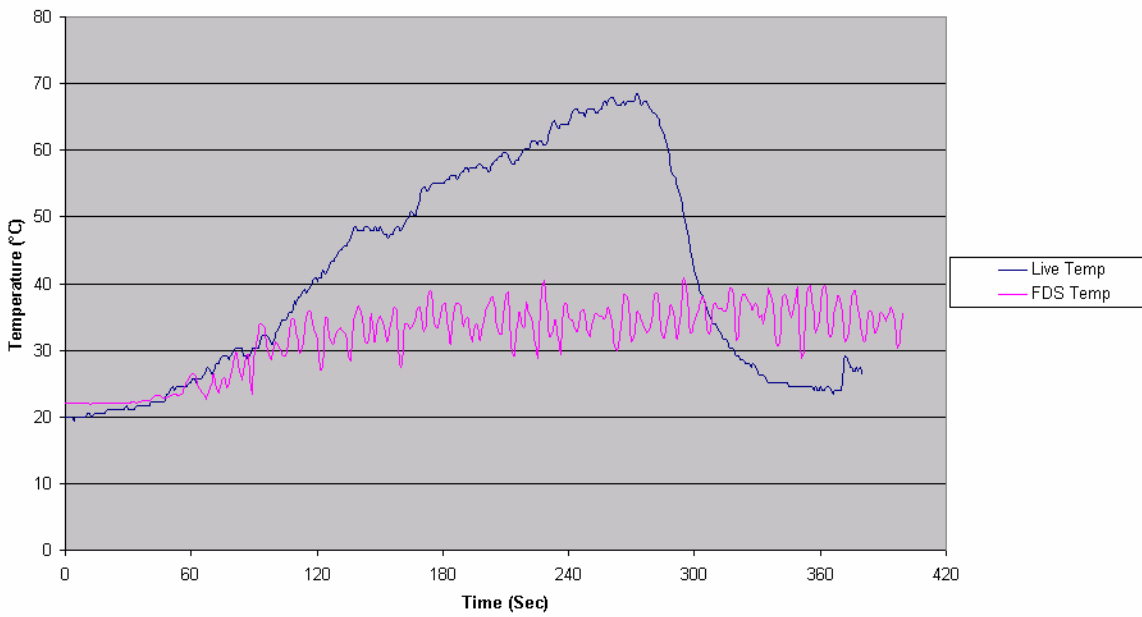
**Centre Fire with High Airflow and No Suppression
Supply Temperature**



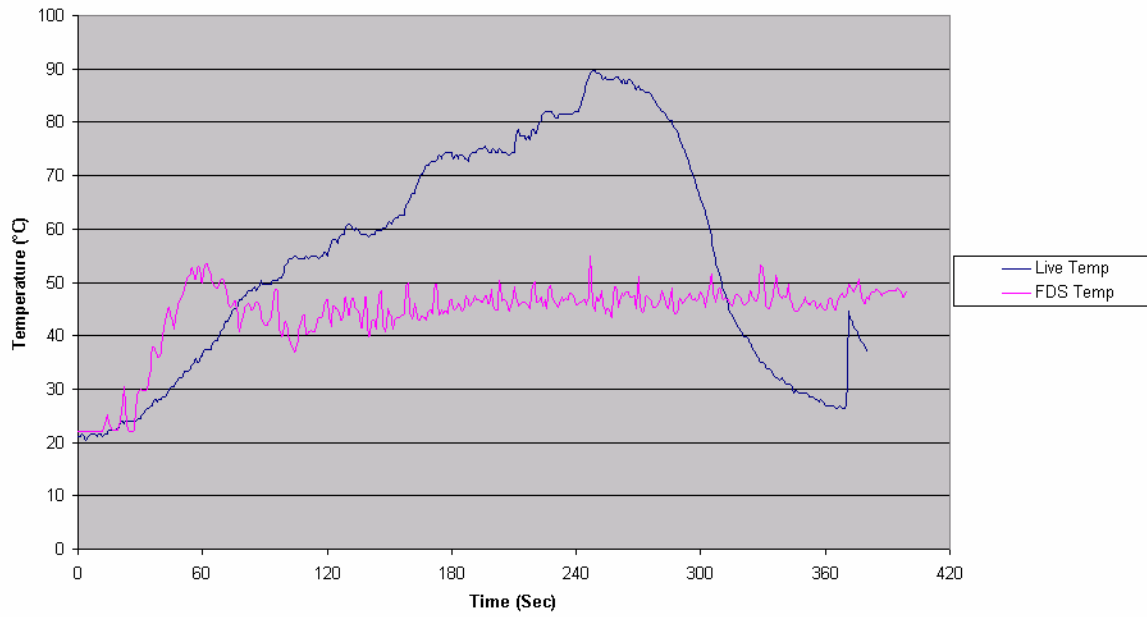
**Centre Fire with High Airflow and No Suppression
Tree 1 (occ) 0.3 m Temperature**



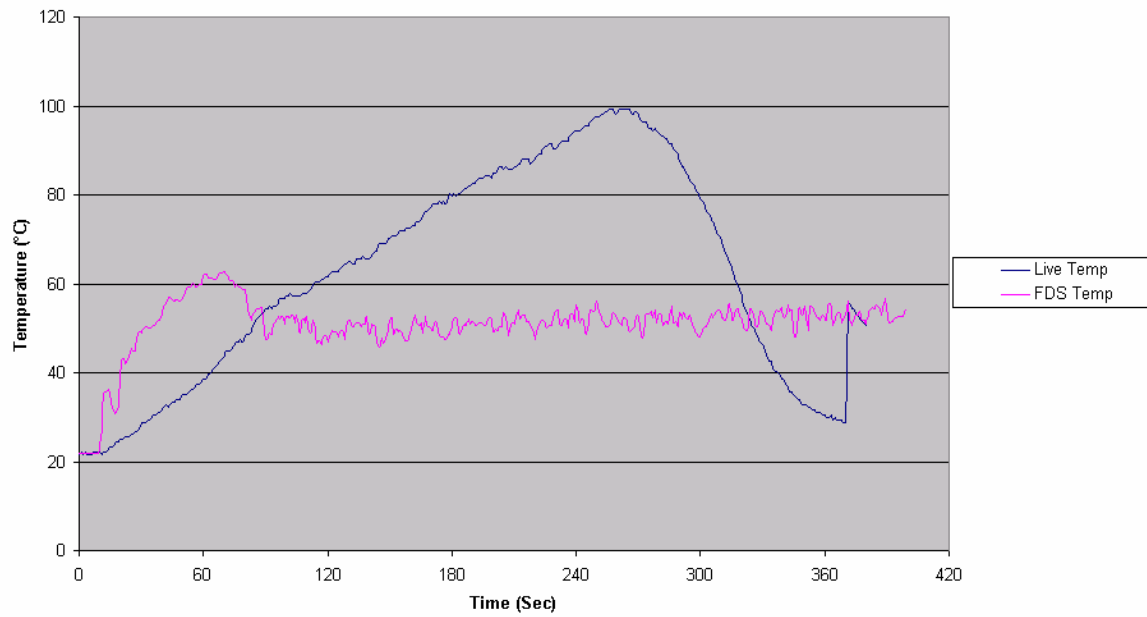
**Centre Fire with High Airflow and No Suppression
Tree 1 (occ) 0.7 m Temperature**



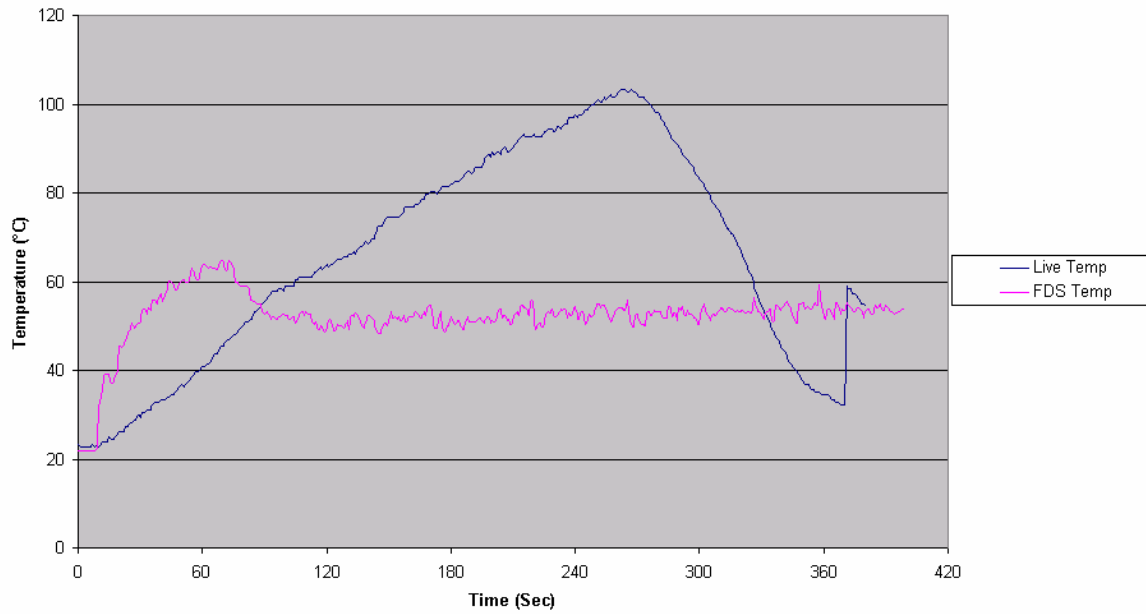
**Centre Fire with High Airflow and No Suppression
Tree 1 (occ) 1.3 m Temperature**



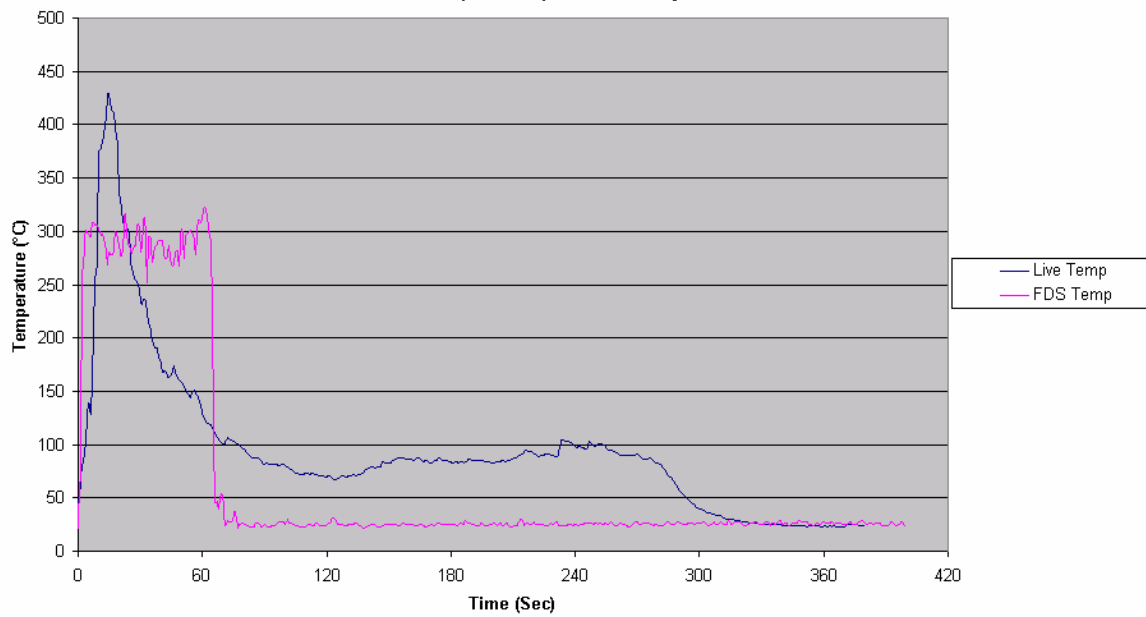
**Centre Fire with High Airflow and No Suppression
Tree 1 (occ) 1.8 m Temperature**



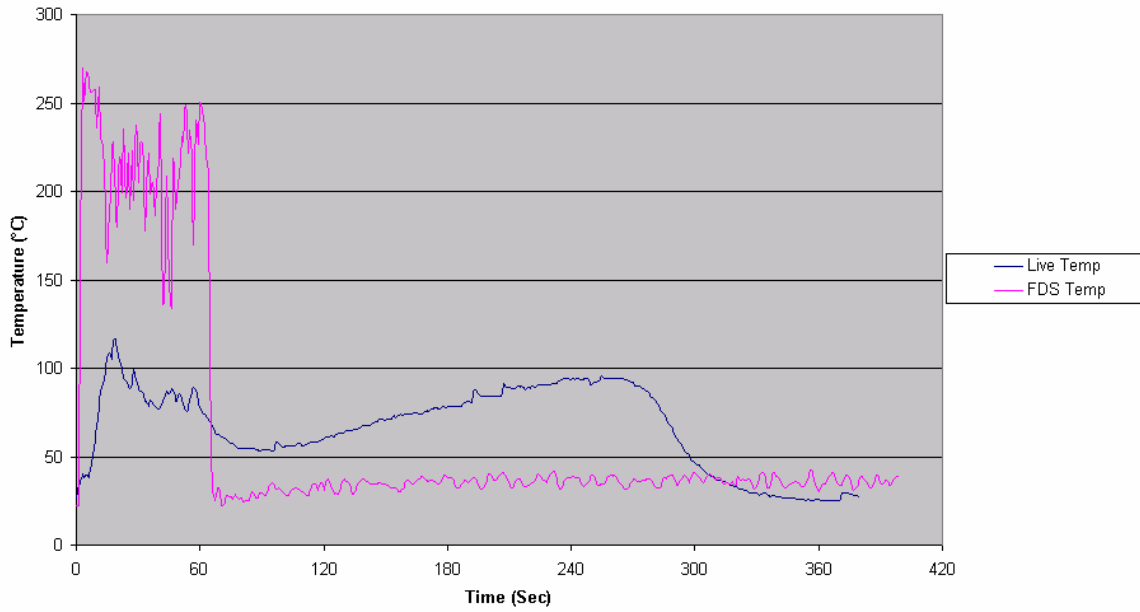
**Centre Fire with High Airflow and No Suppression
Tree 1 (occ) 2.1 m Temperature**



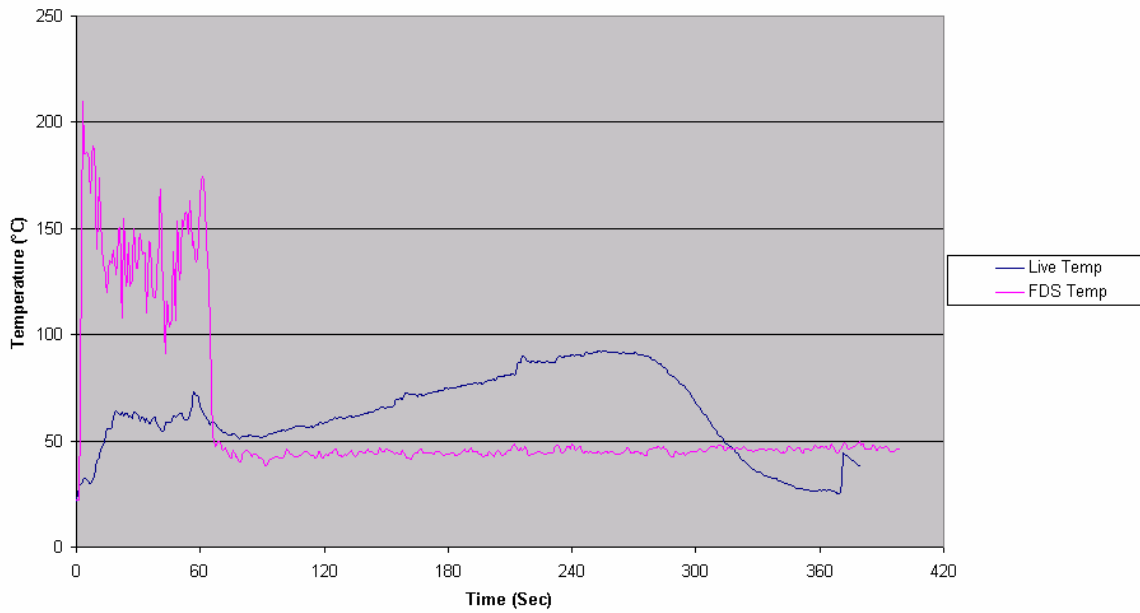
**Centre Fire with High Airflow and No Suppression
Tree 2 (Centre) 0.3 m Temperature**



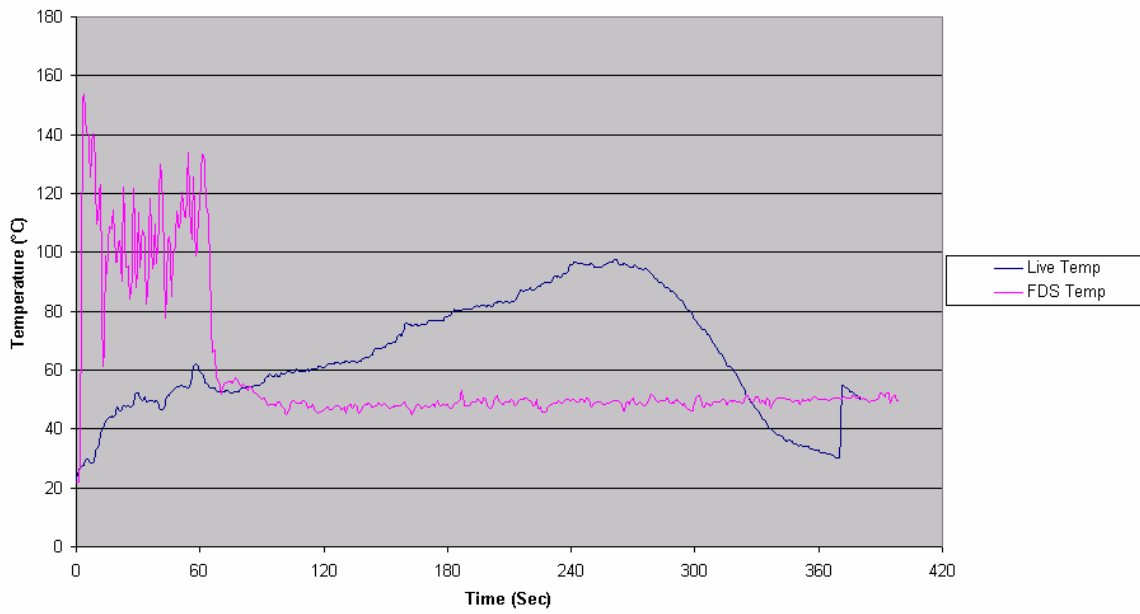
**Centre Fire with High Airflow and No Suppression
Tree 2 (Centre) 0.7 m Temperature**



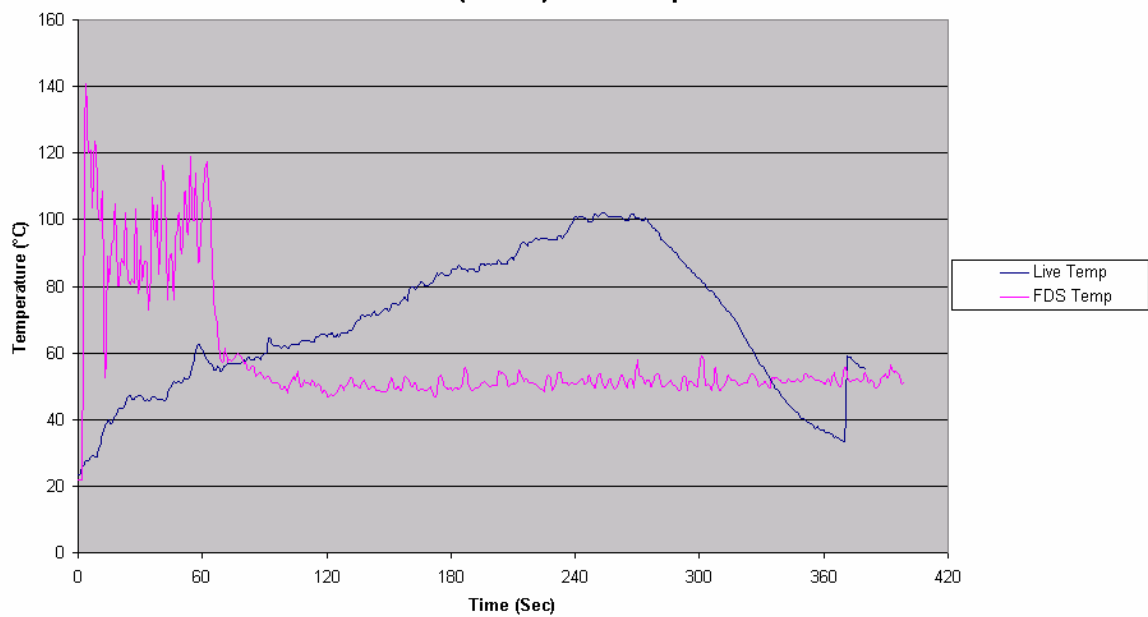
**Centre Fire with High Airflow and No Suppression
Tree 2 (Centre) 1.3 m Temperature**



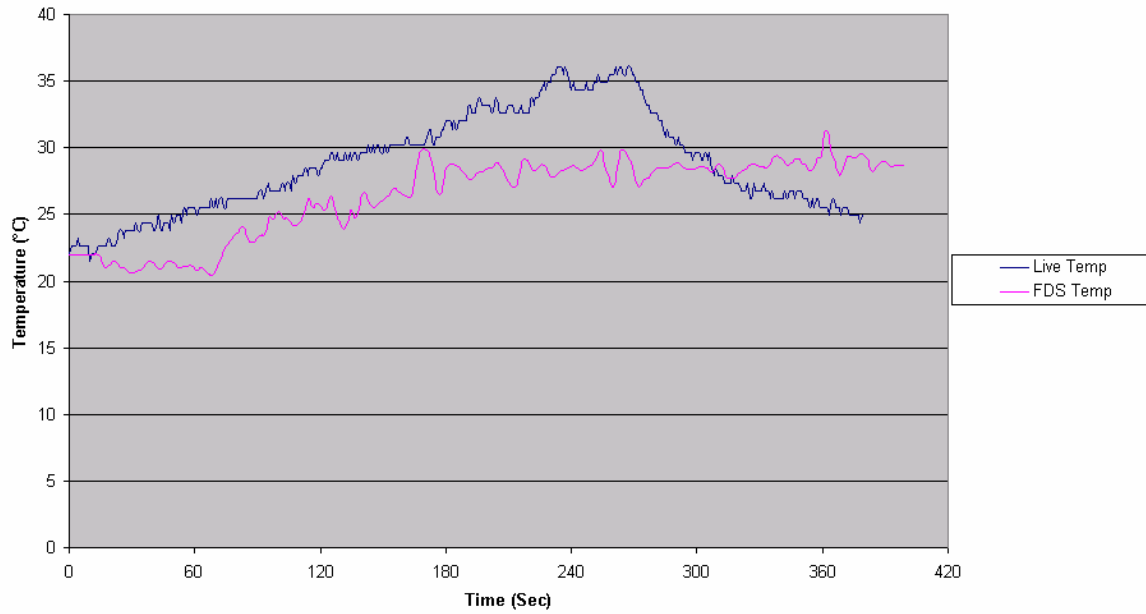
**Centre Fire with High Airflow and No Suppression
Tree 2 (Centre) 1.8 m Temperature**



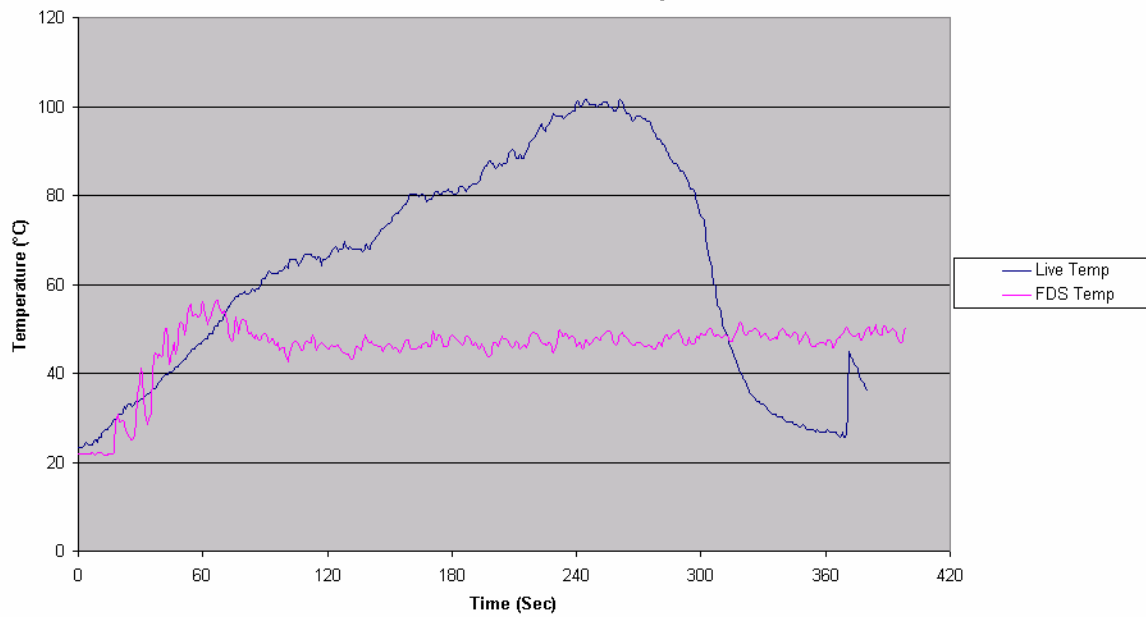
**Centre Fire with High Airflow and No Suppression
Tree 2 (Centre) 2.1 m Temperature**



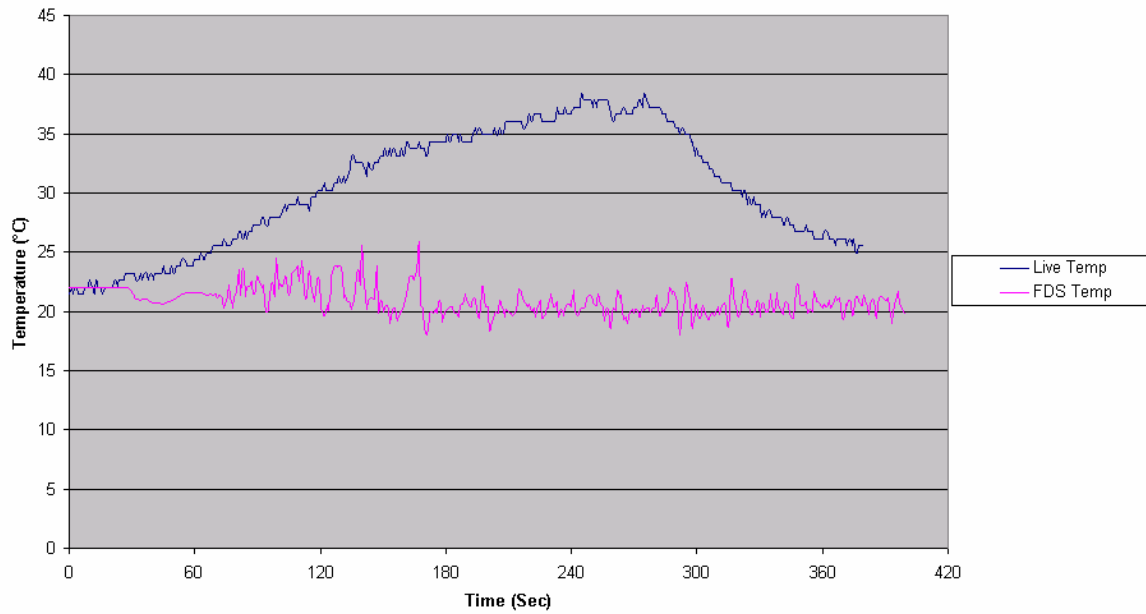
**Centre Fire with High Airflow and No Suppression
Back Corner 0.3 m Temperature**



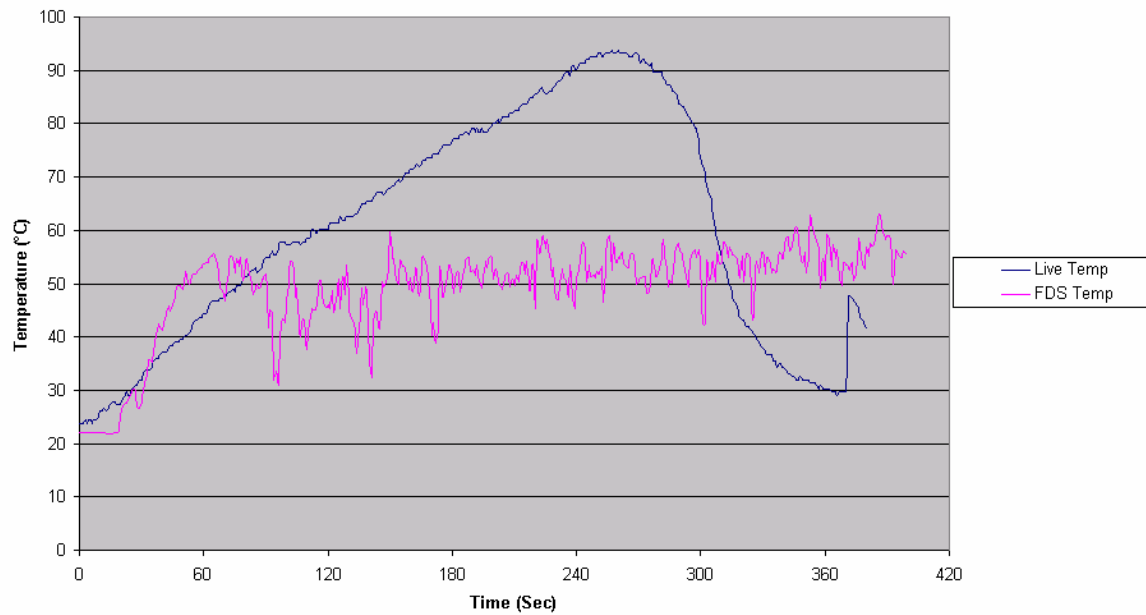
**Centre Fire with High Airflow and No Suppression
Back Corner 1.3 m Temperature**



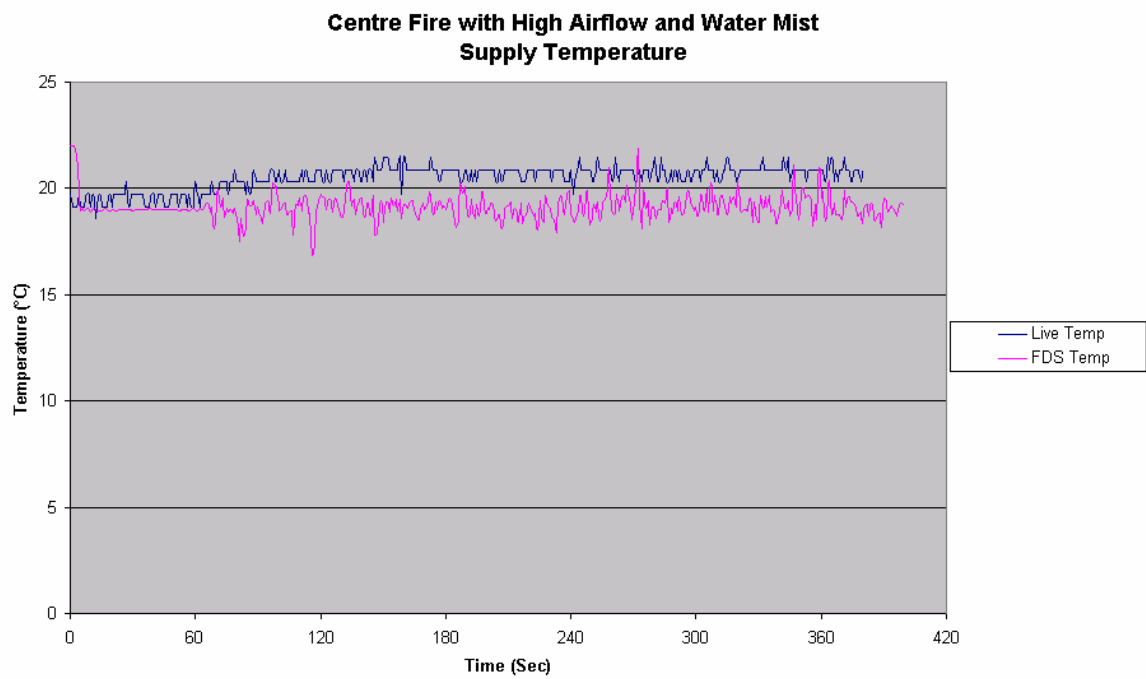
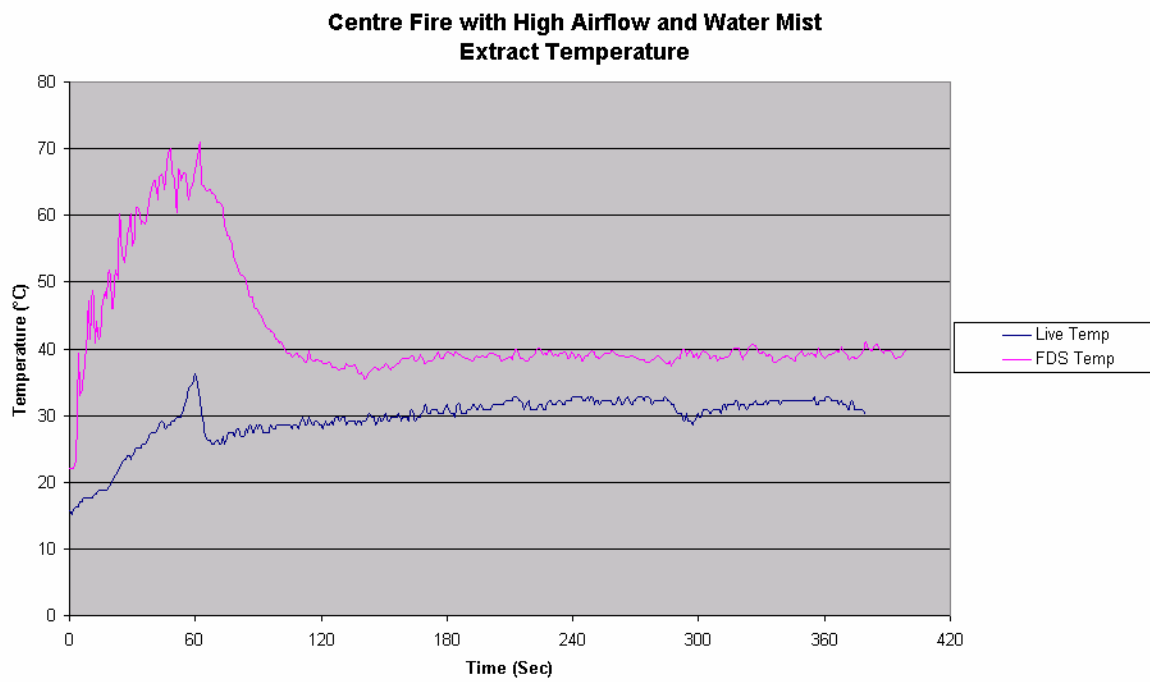
**Centre Fire with High Airflow and No Suppression
Front Corner 0.3 m Temperature**



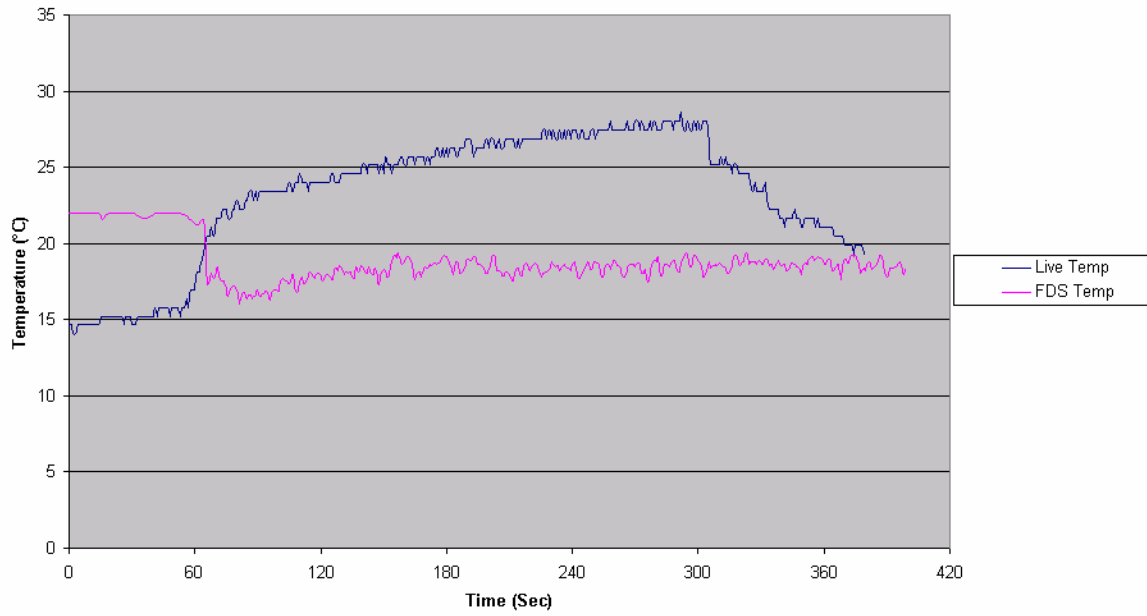
**Centre Fire with High Airflow and No Suppression
Front Corner 1.3 m Temperature**



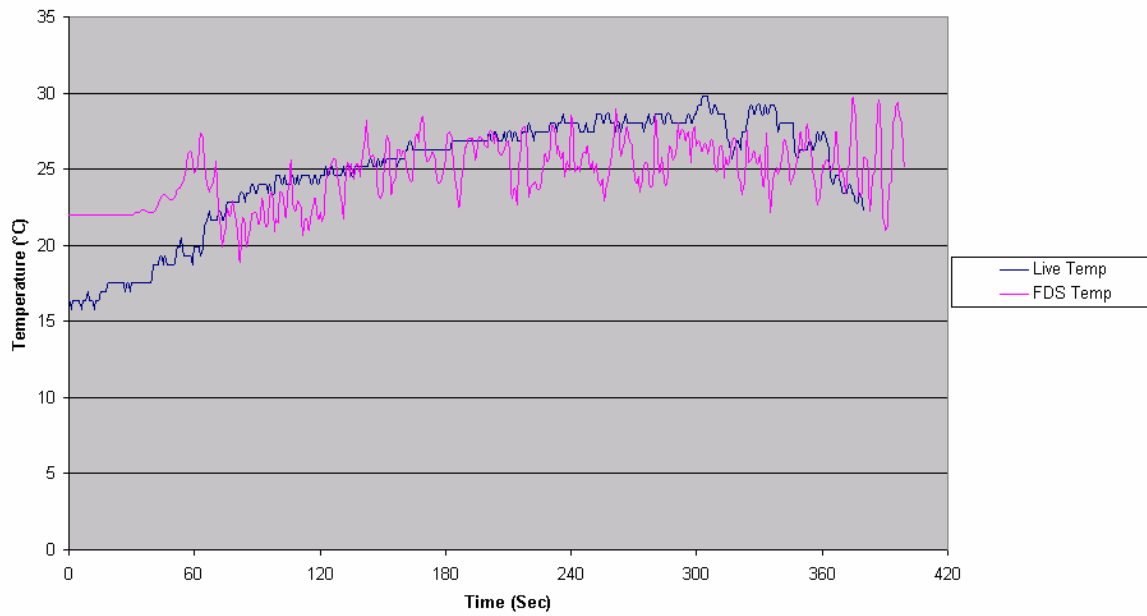
11.8.3 Displacement water mist operation with a central floor fire



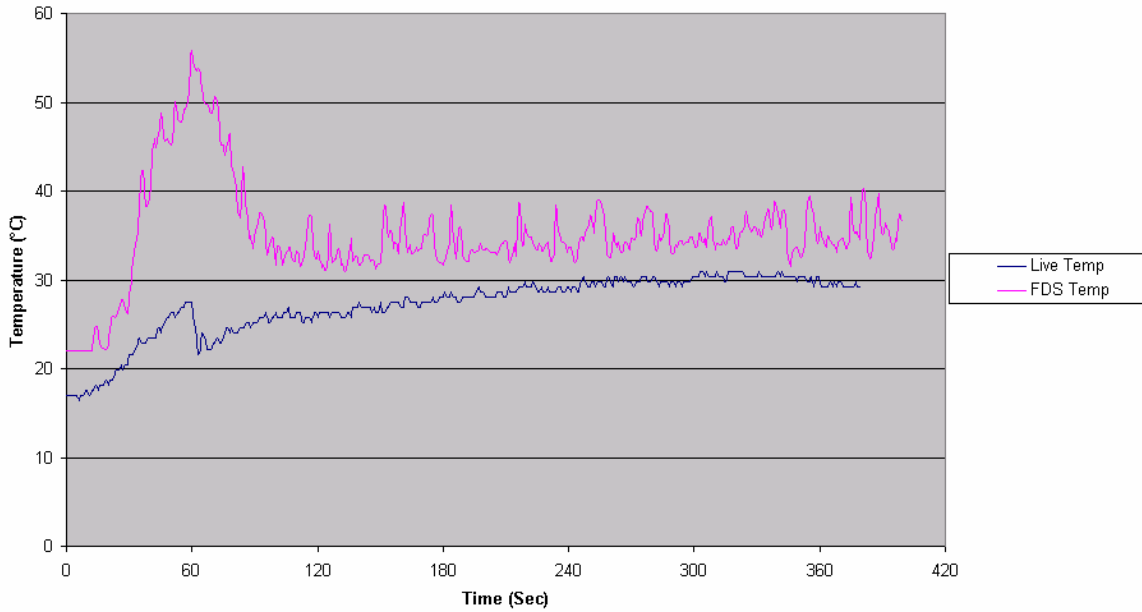
**Centre Fire with High Airflow and Water Mist
Tree 1 (occ) 0.3 m Temperature**



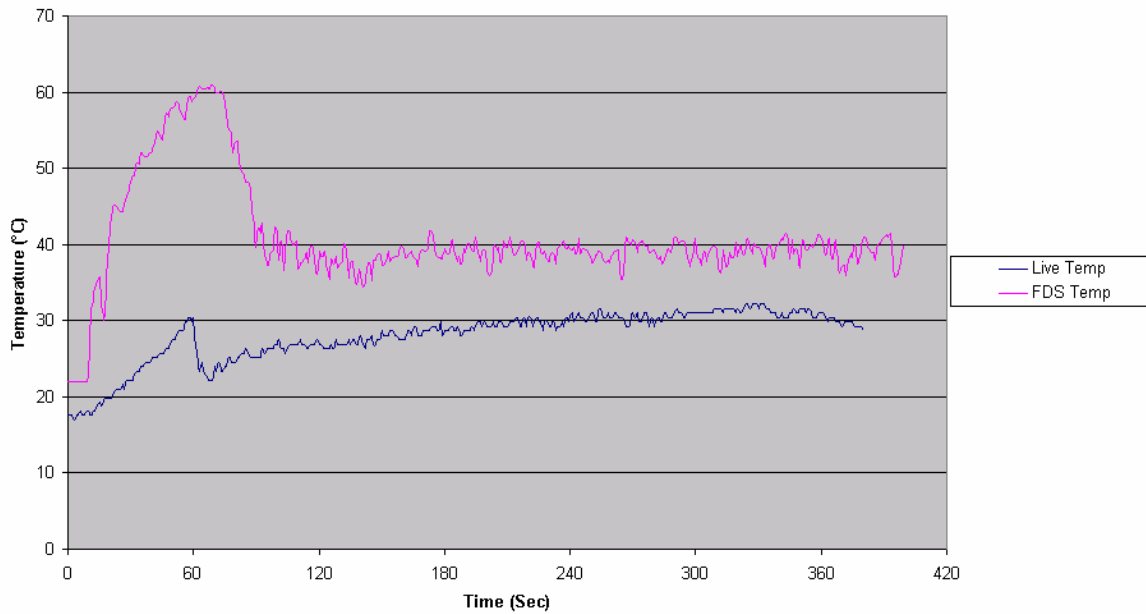
**Centre Fire with High Airflow and Water Mist
Tree 1 (occ) 0.7 m Temperature**



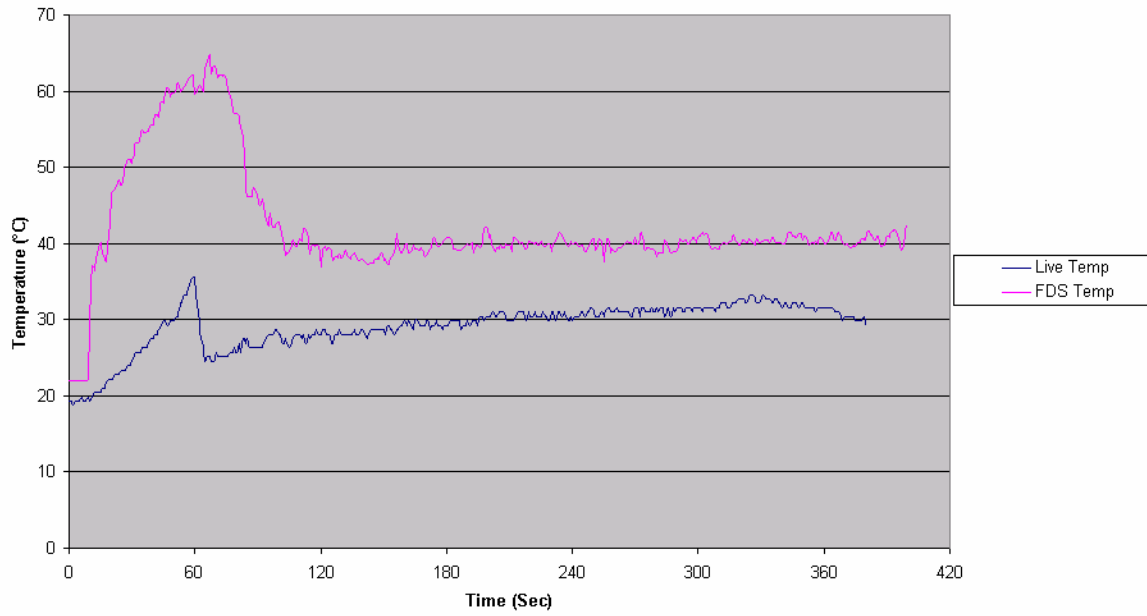
**Centre Fire with High Airflow and Water Mist
Tree 1 (occ) 1.3 m Temperature**



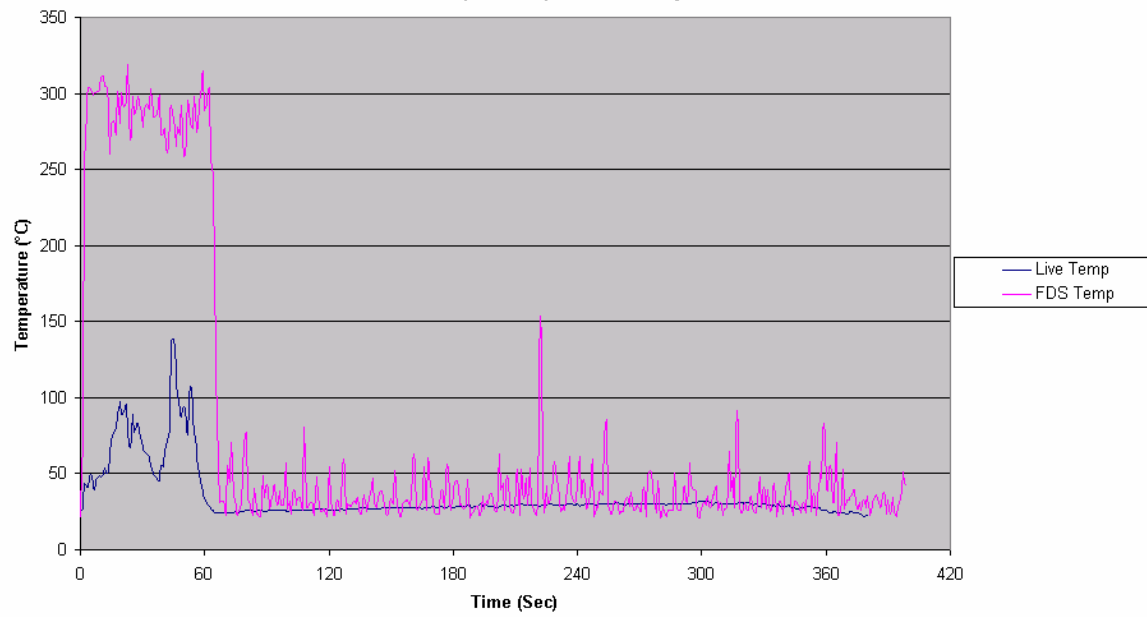
**Centre Fire with High Airflow and Water Mist
Tree 1 (occ) 1.8 m Temperature**



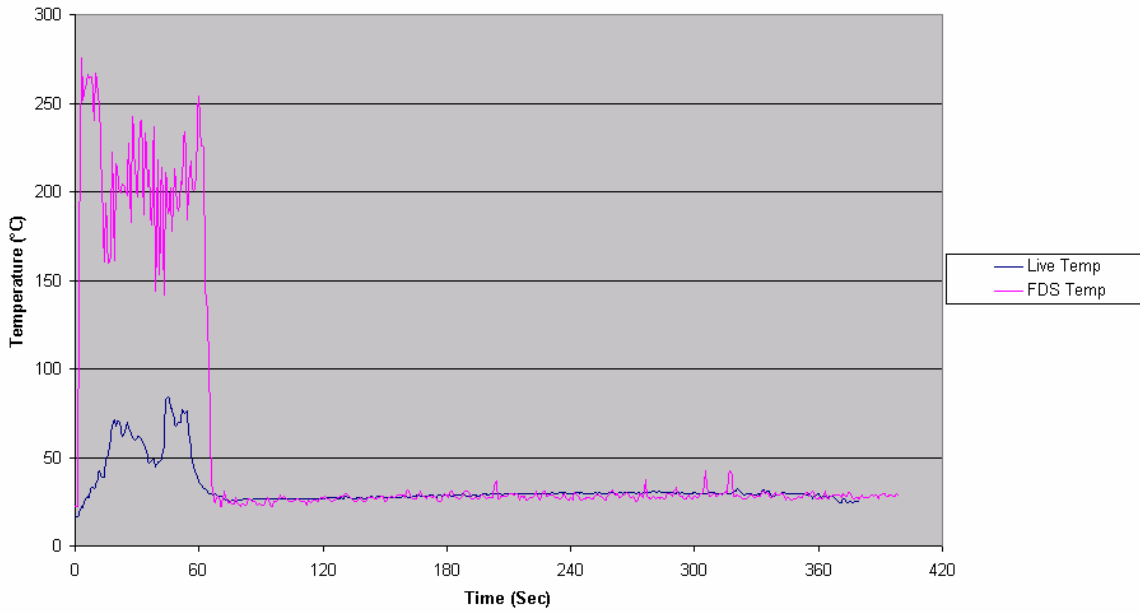
Centre Fire with High Airflow and Water Mist
Tree 1 (occ) 2.1 m Temperature



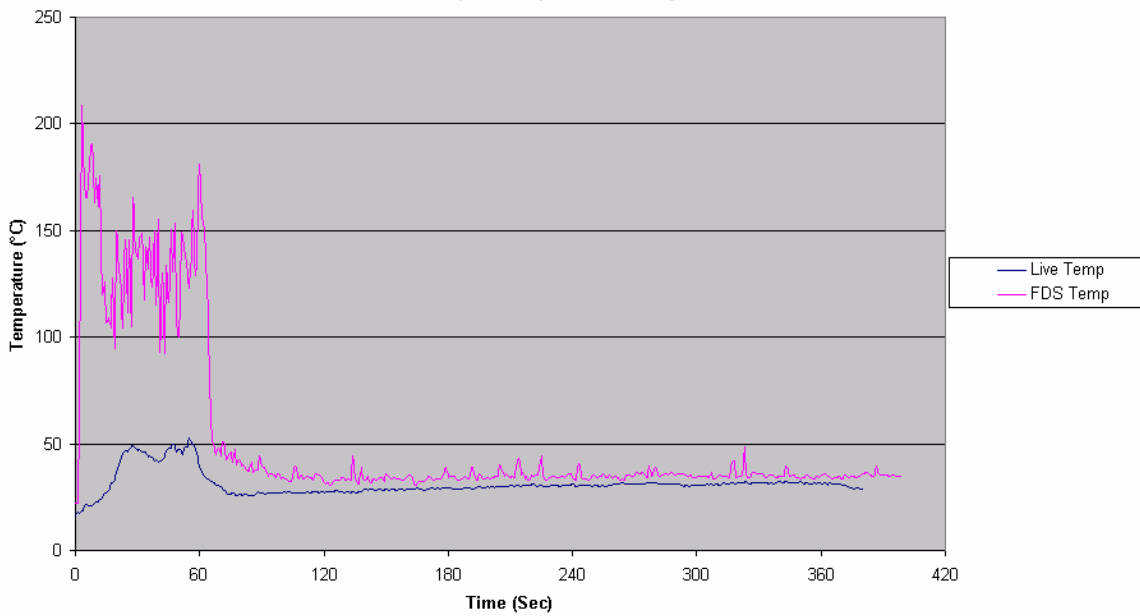
Centre Fire with High Airflow and Water Mist
Tree 2 (Centre) 0.3 m Temperature



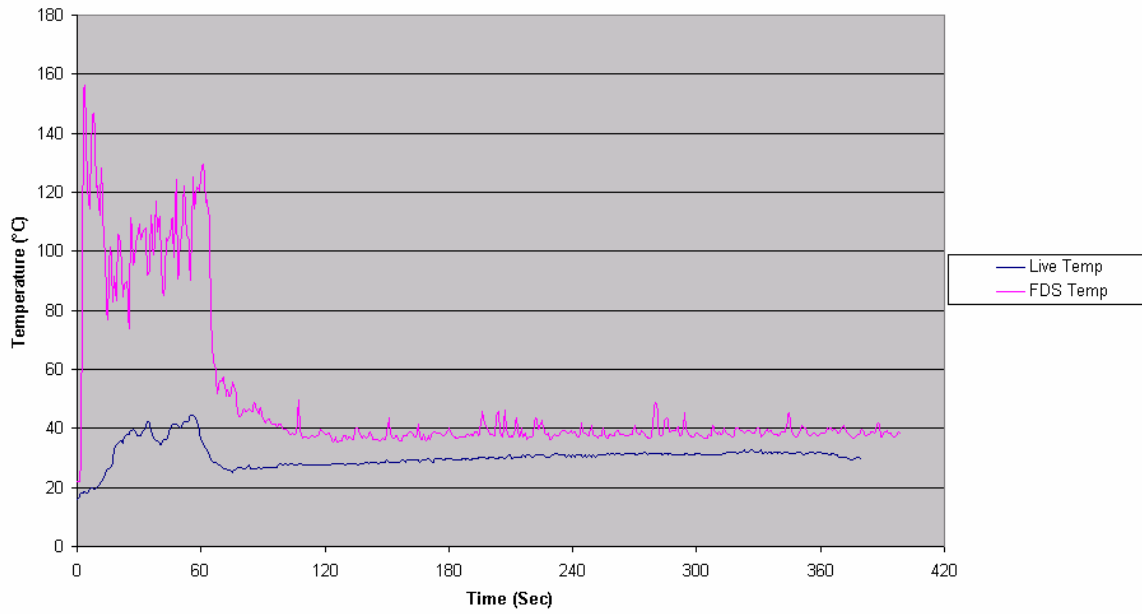
**Centre Fire with High Airflow and Water Mist
Tree 2 (Centre) 0.7 m Temperature**



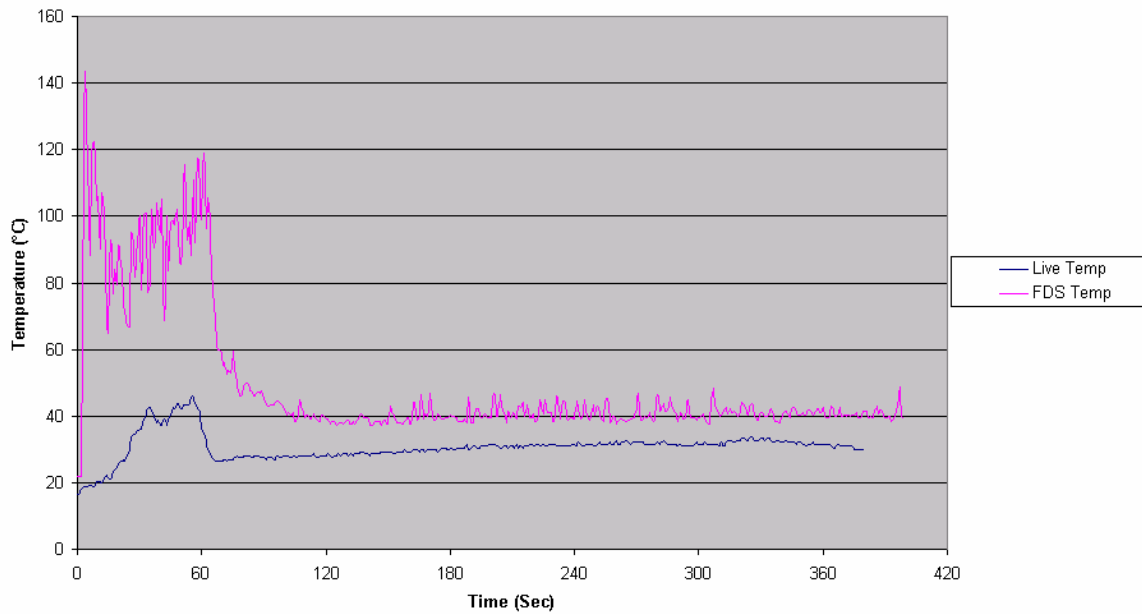
**Centre Fire with High Airflow and Water Mist
Tree 2 (Centre) 1.3 m Temperature**



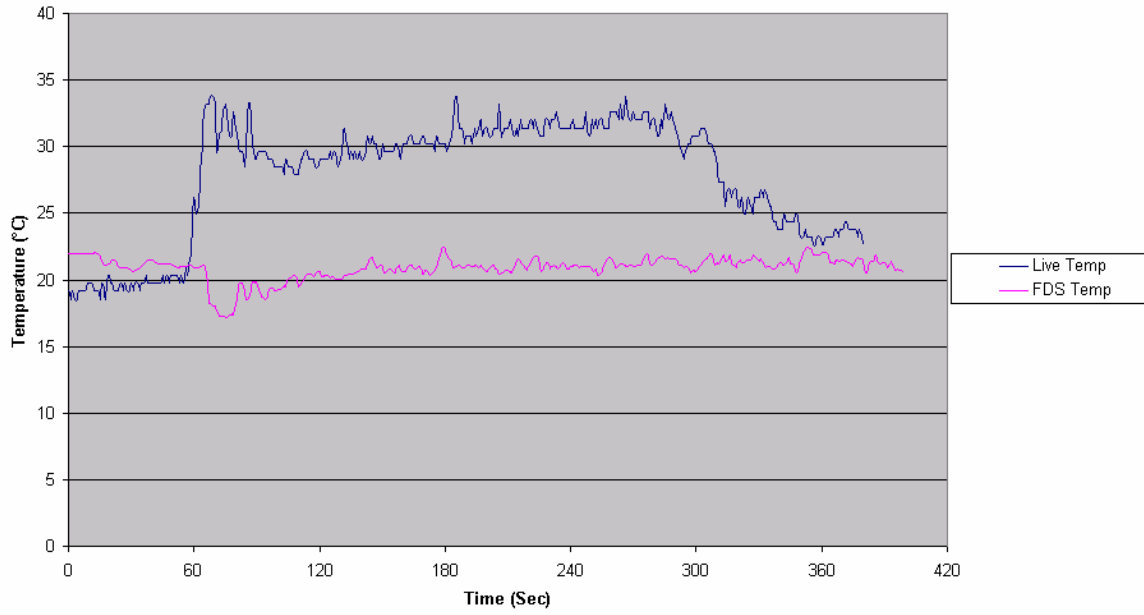
Centre Fire with High Airflow and Water Mist
Tree 2 (Centre) 1.8 m Temperature



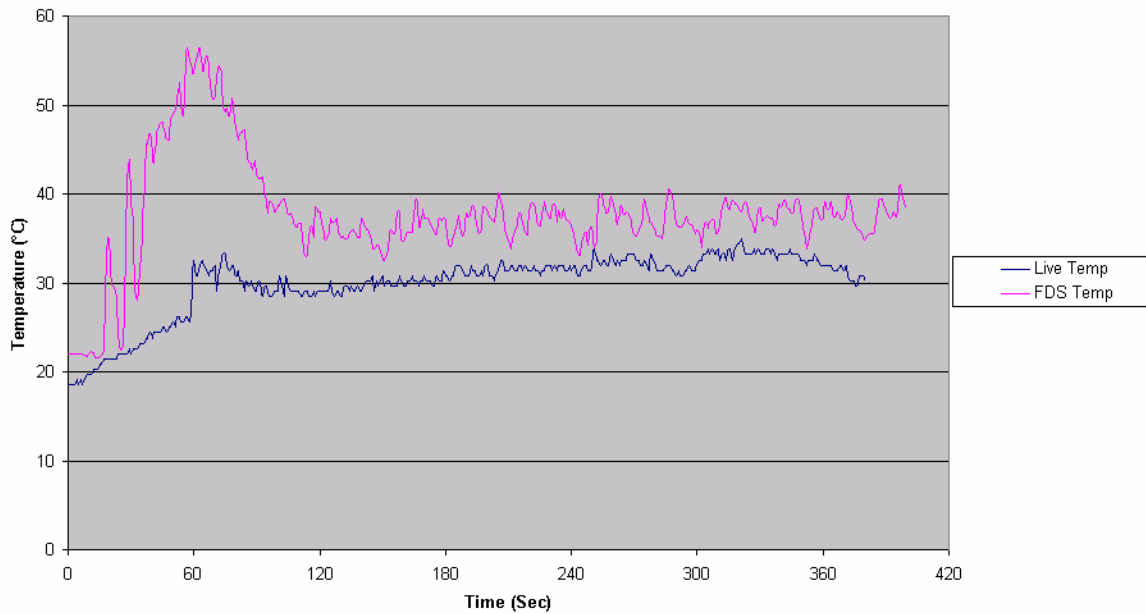
Centre Fire with High Airflow and Water Mist
Tree 2 (Centre) 2.1 m Temperature



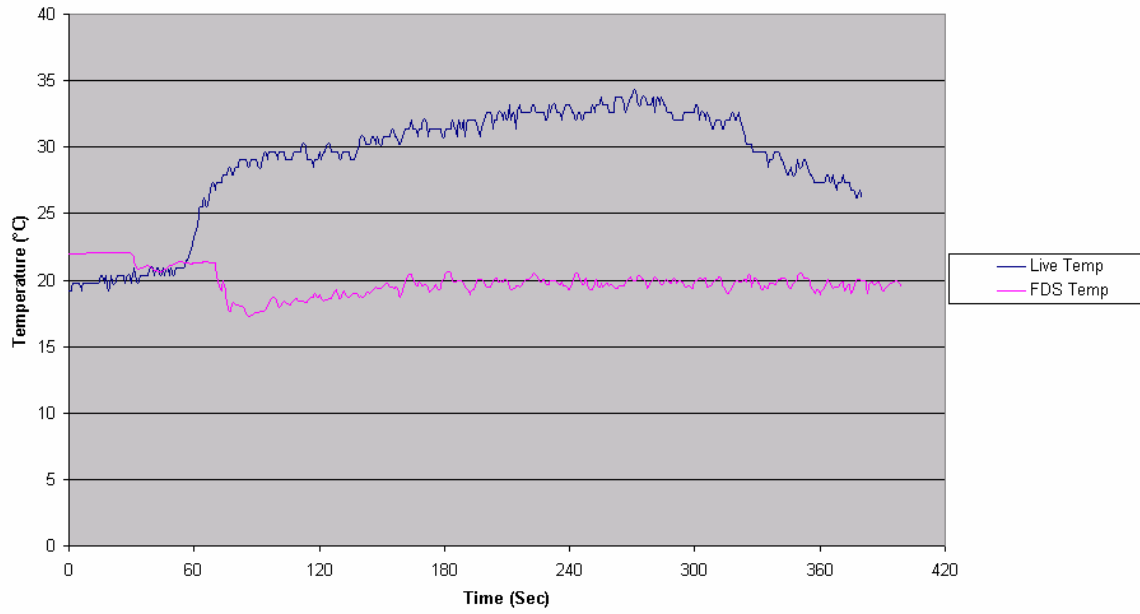
**Centre Fire with High Airflow and Water Mist
Back Corner 0.3 m Temperature**



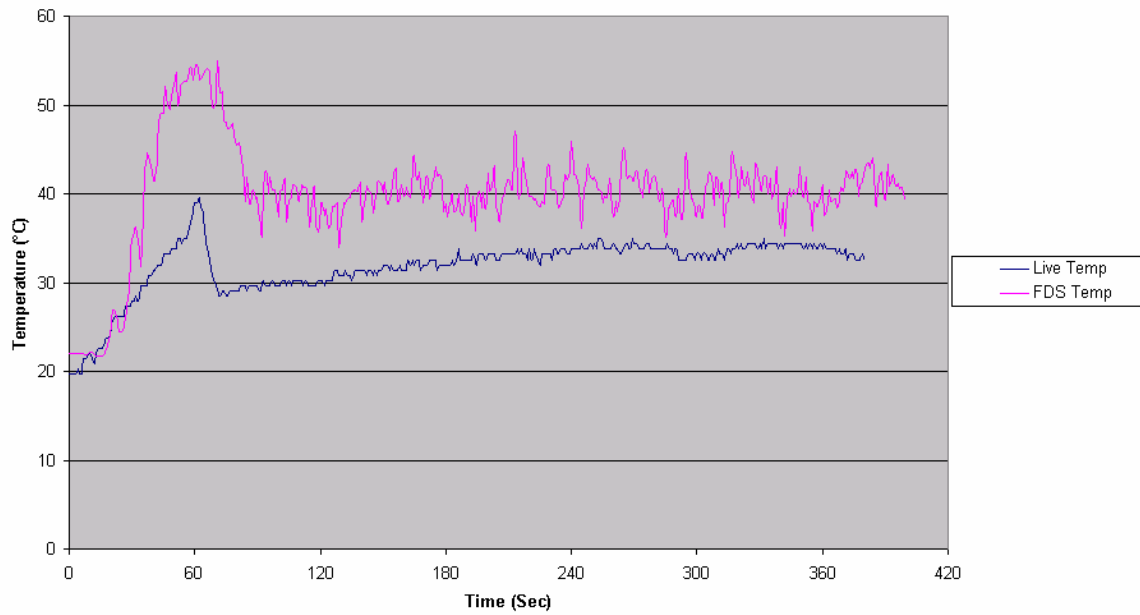
**Centre Fire with High Airflow and Water Mist
Back Corner 1.3 m Temperature**



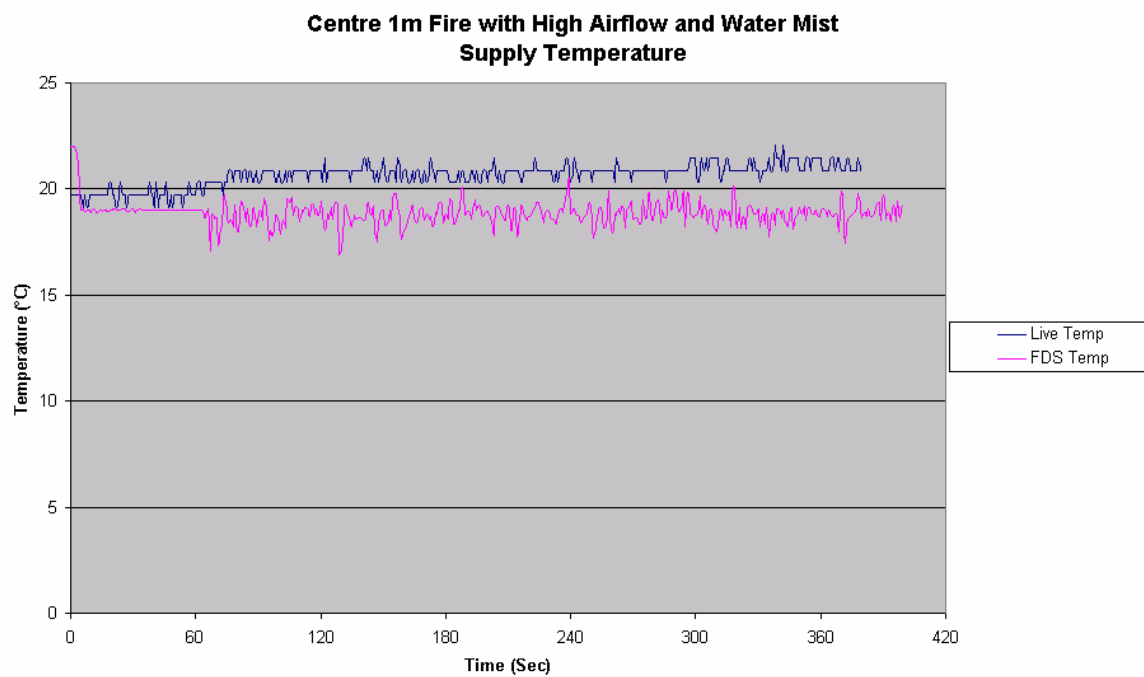
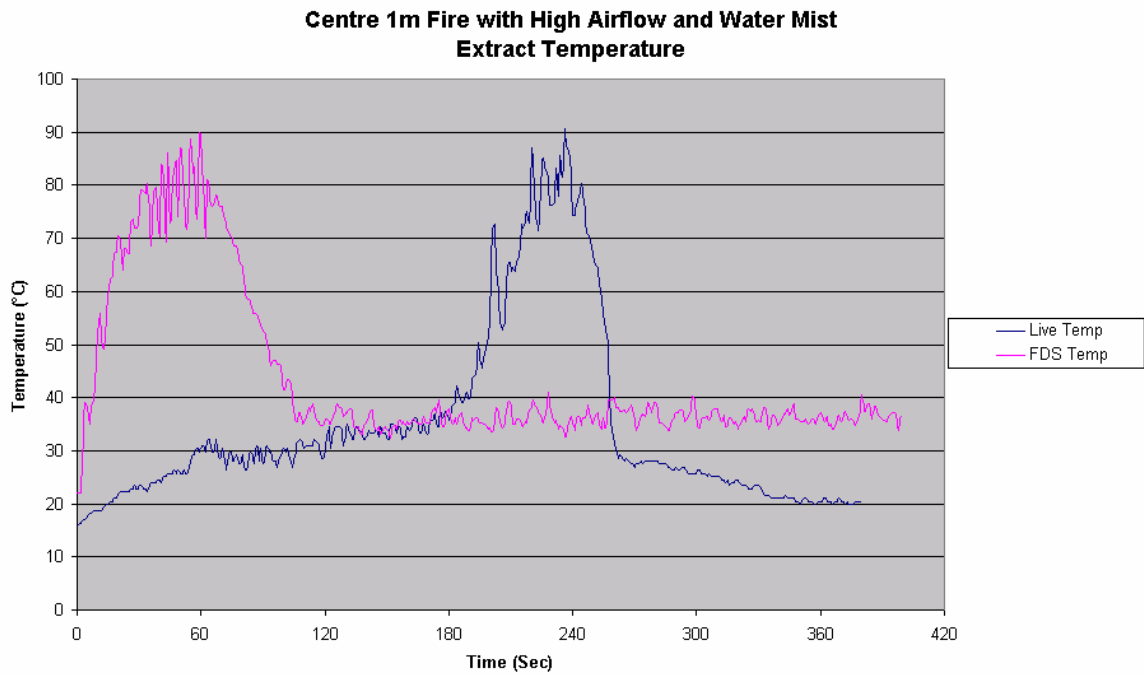
**Centre Fire with High Airflow and Water Mist
Front Corner 0.3 m Temperature**



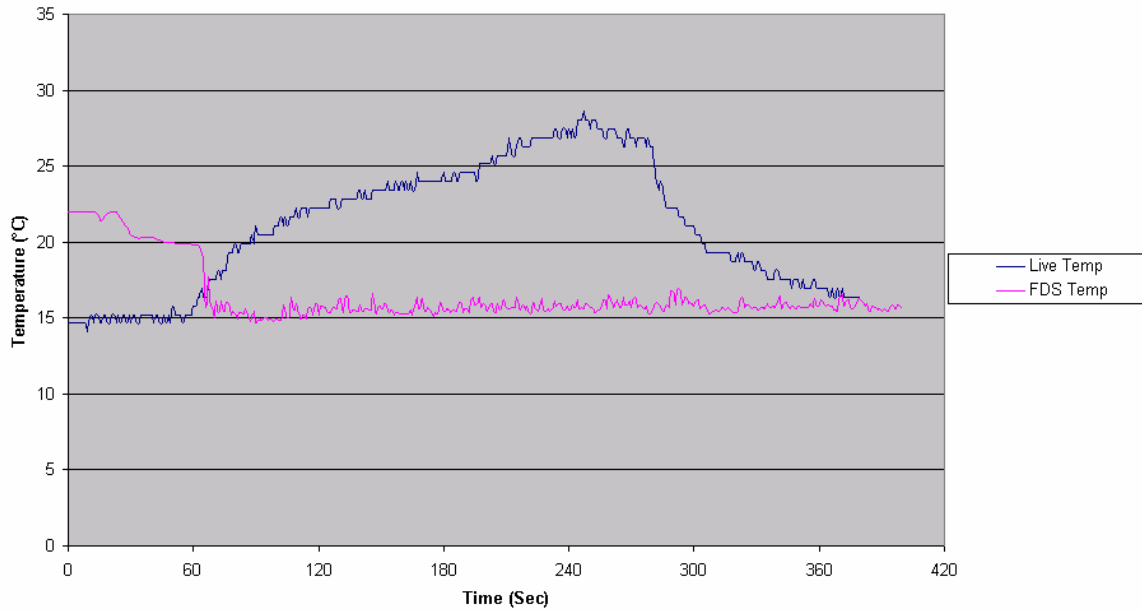
**Centre Fire with High Airflow and Water Mist
Front Corner 1.3 m Temperature**



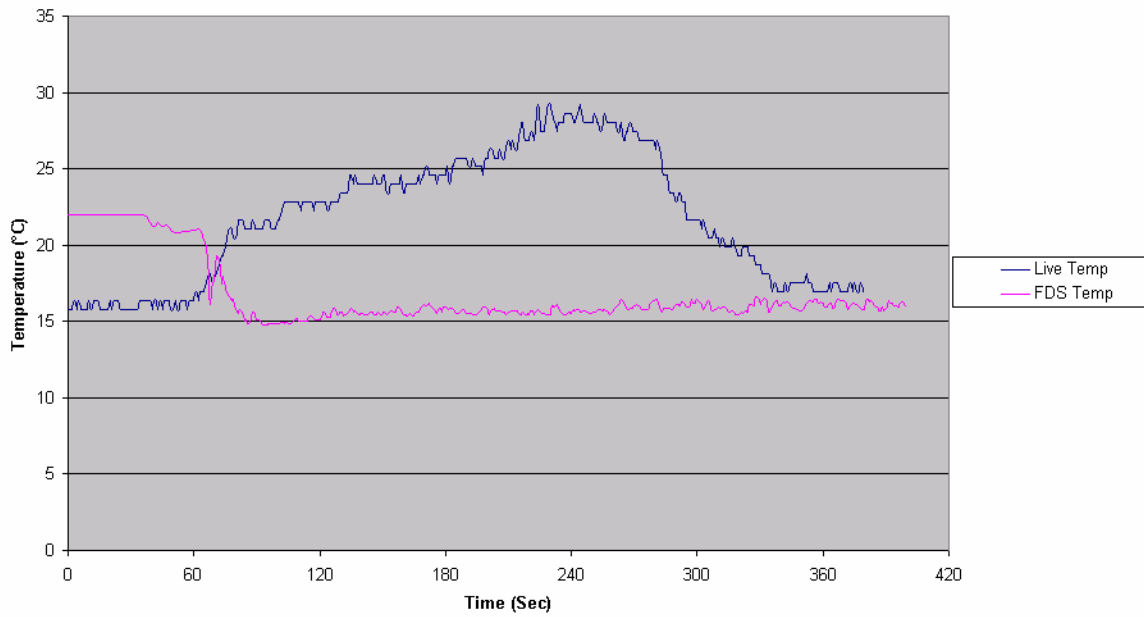
11.8.4 Displacement water mist operation with a central 1m fire



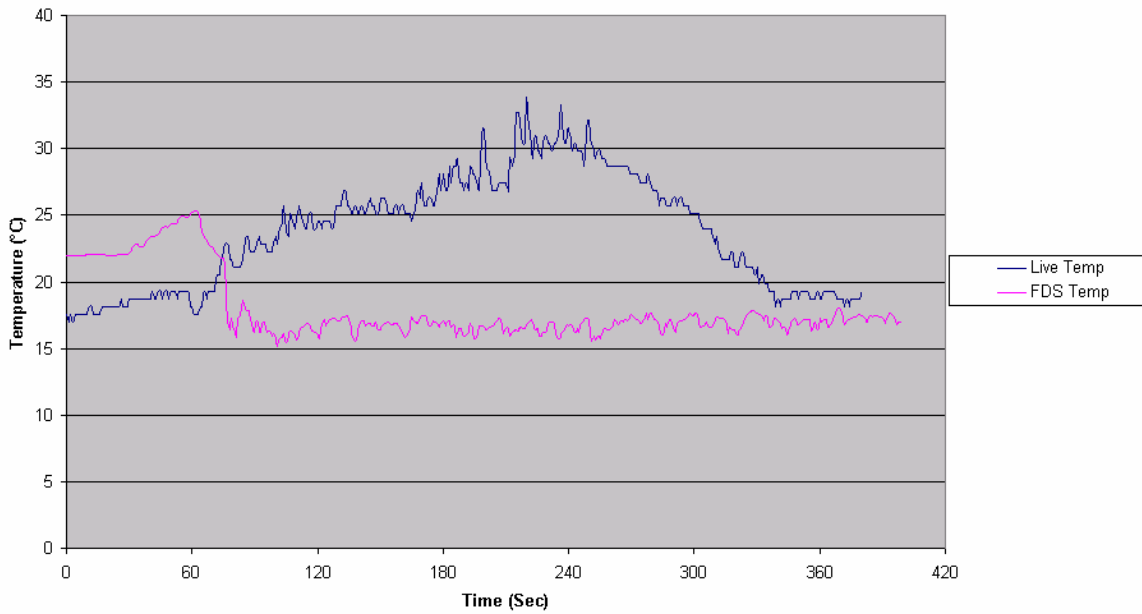
Centre 1m Fire with High Airflow and Water Mist
Tree 1 (occ) 0.3 m Temperature



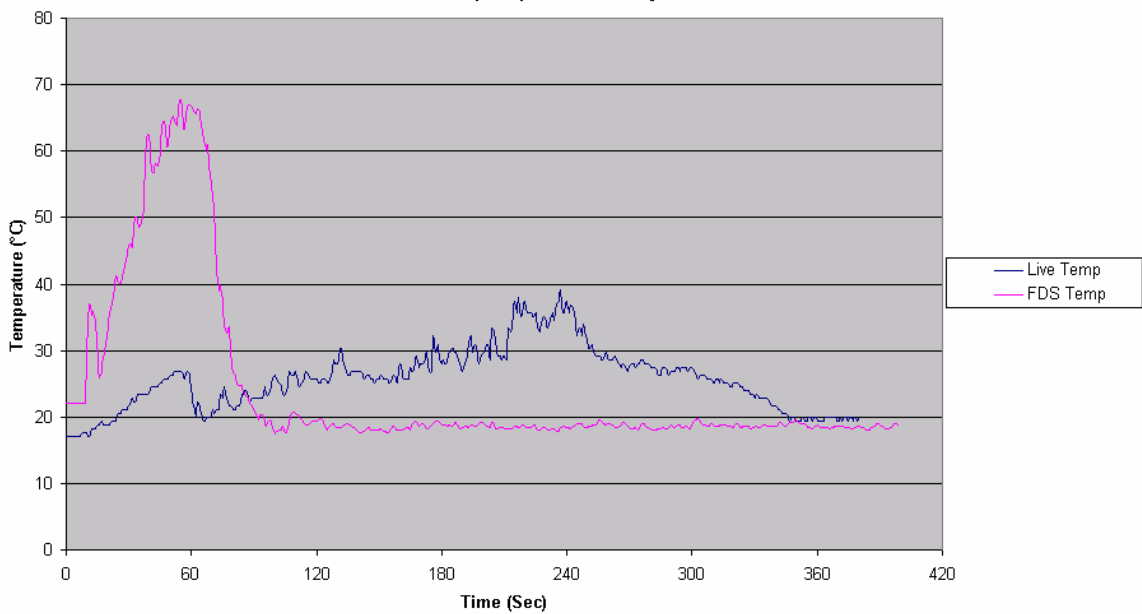
Centre 1m Fire with High Airflow and Water Mist
Tree 1 (occ) 0.7 m Temperature



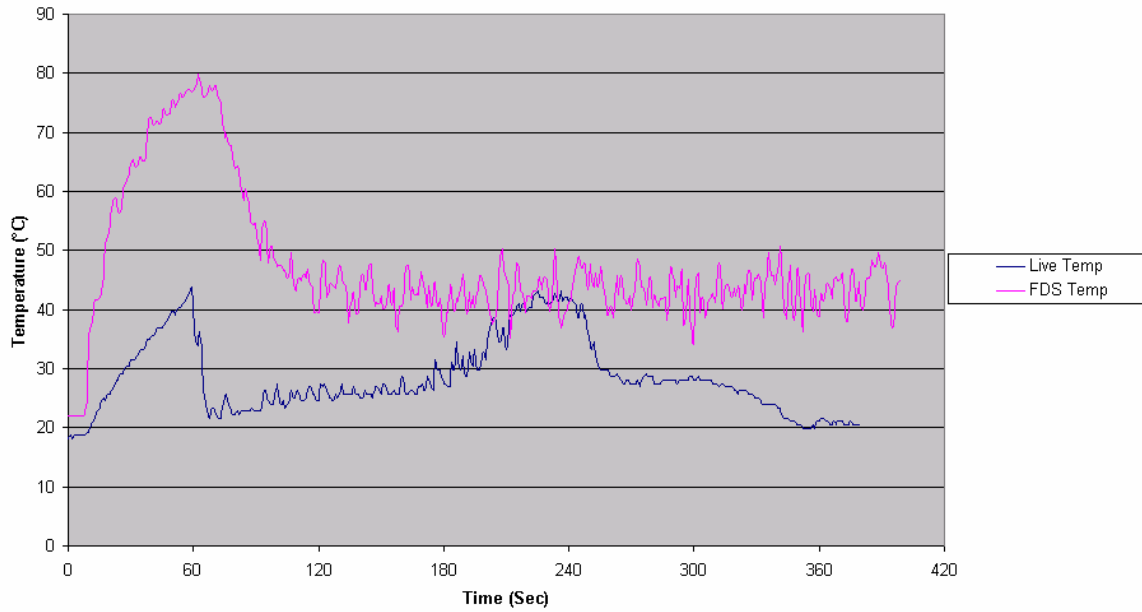
**Centre 1m Fire with High Airflow and Water Mist
Tree 1 (occ) 1.3 m Temperature**



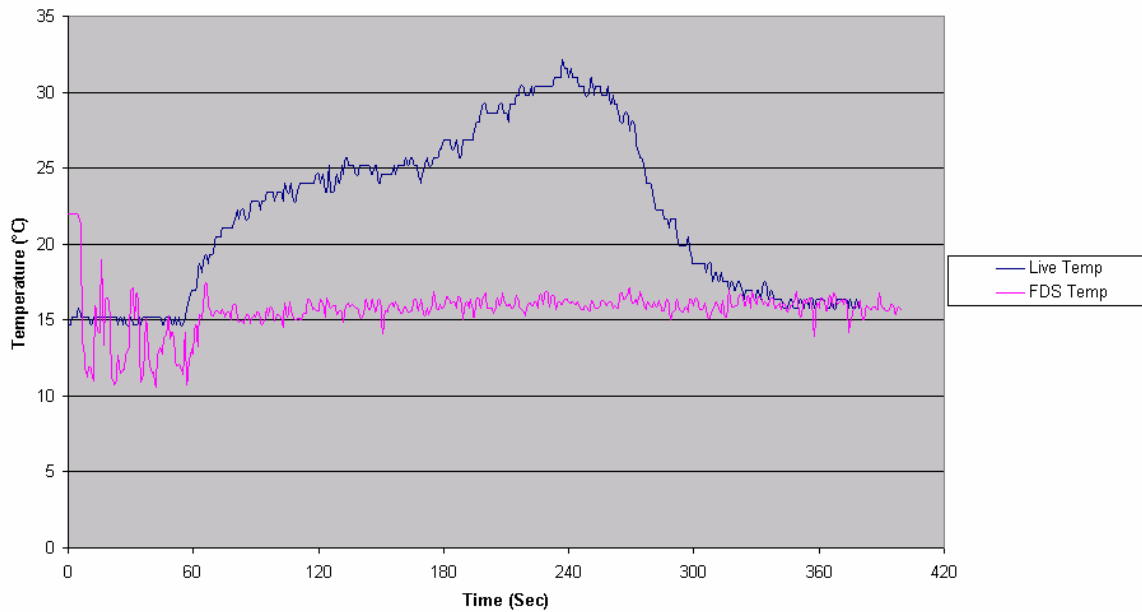
**Centre 1m Fire with High Airflow and Water Mist
Tree 1 (occ) 1.8 m Temperature**



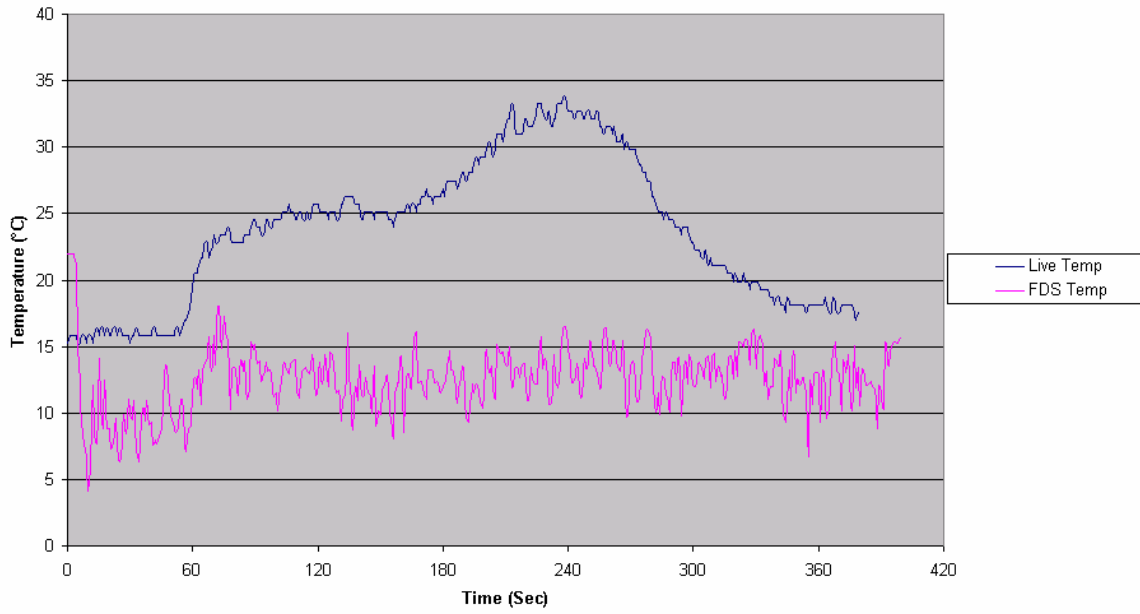
**Centre 1m Fire with High Airflow and Water Mist
Tree 1 (occ) 2.1 m Temperature**



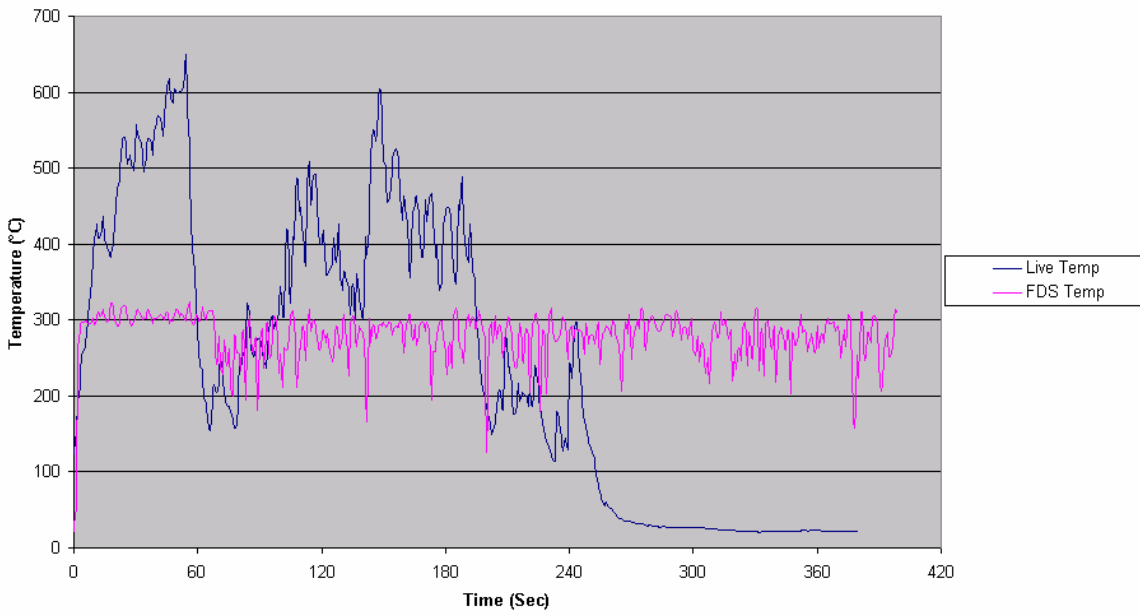
**Centre 1m Fire with High Airflow and Water Mist
Tree 2 (Centre) 0.3 m Temperature**



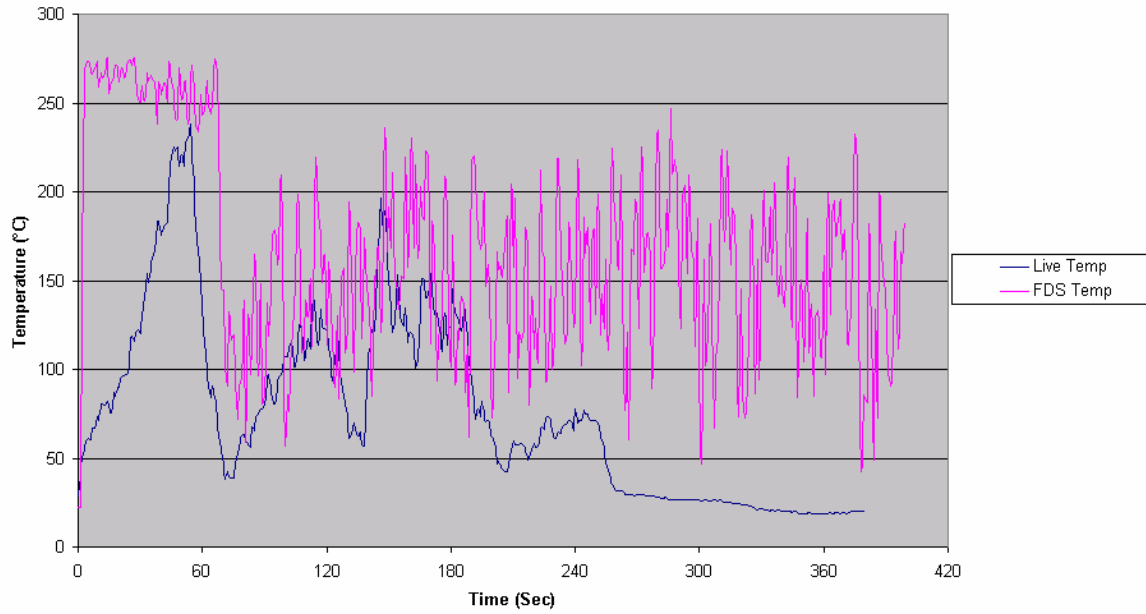
**Centre 1m Fire with High Airflow and Water Mist
Tree 2 (Centre) 0.7 m Temperature**



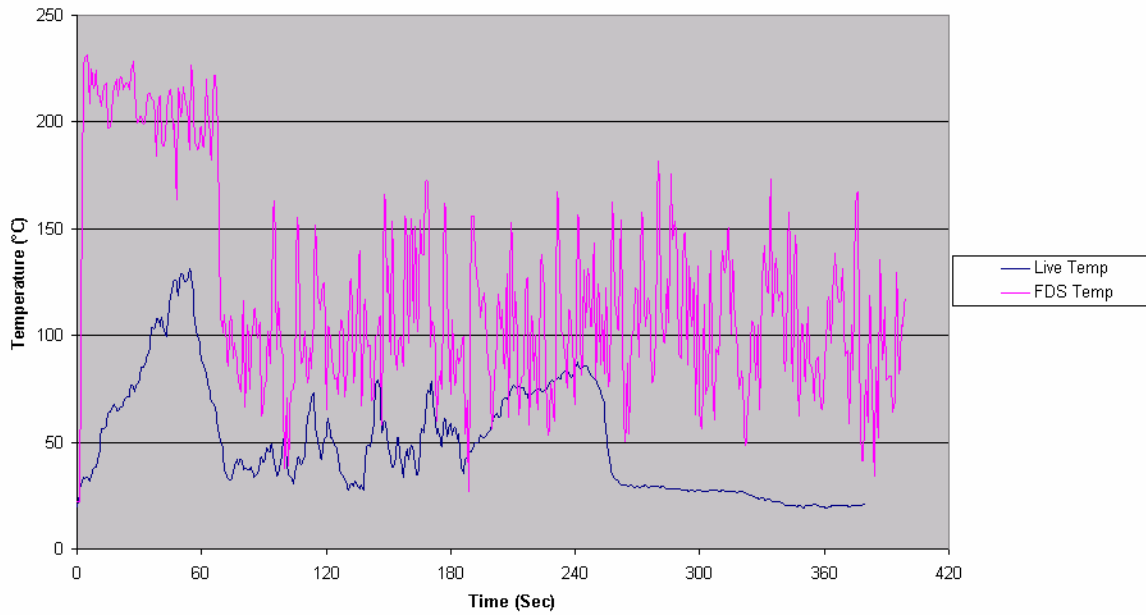
**Centre 1m Fire with High Airflow and Water Mist
Tree 2 (Centre) 1.3 m Temperature**



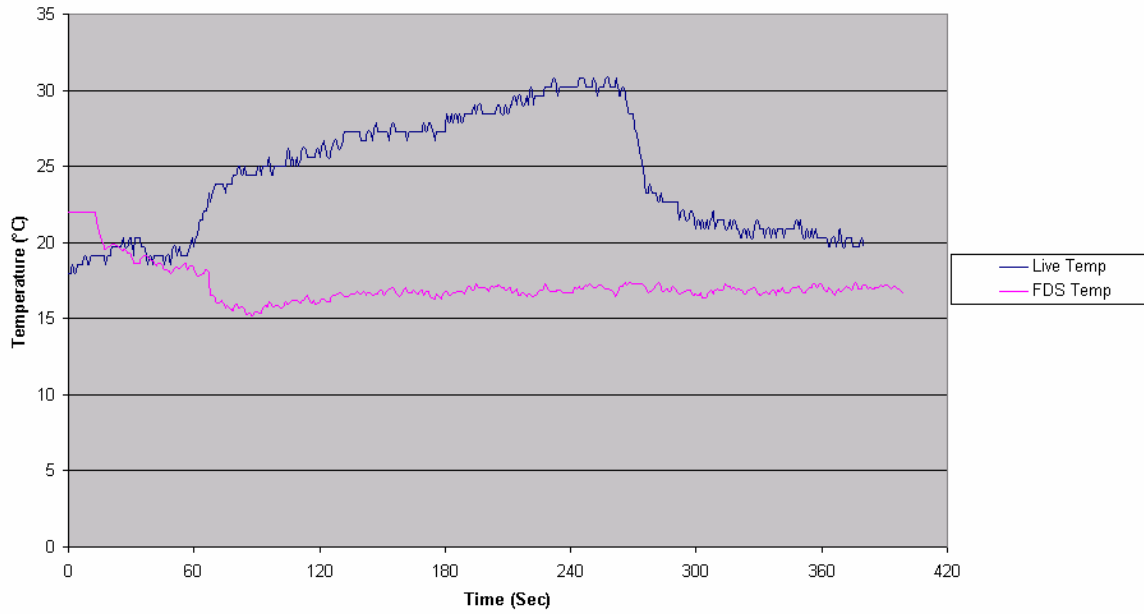
**Centre 1m Fire with High Airflow and Water Mist
Tree 2 (Centre) 1.8 m Temperature**



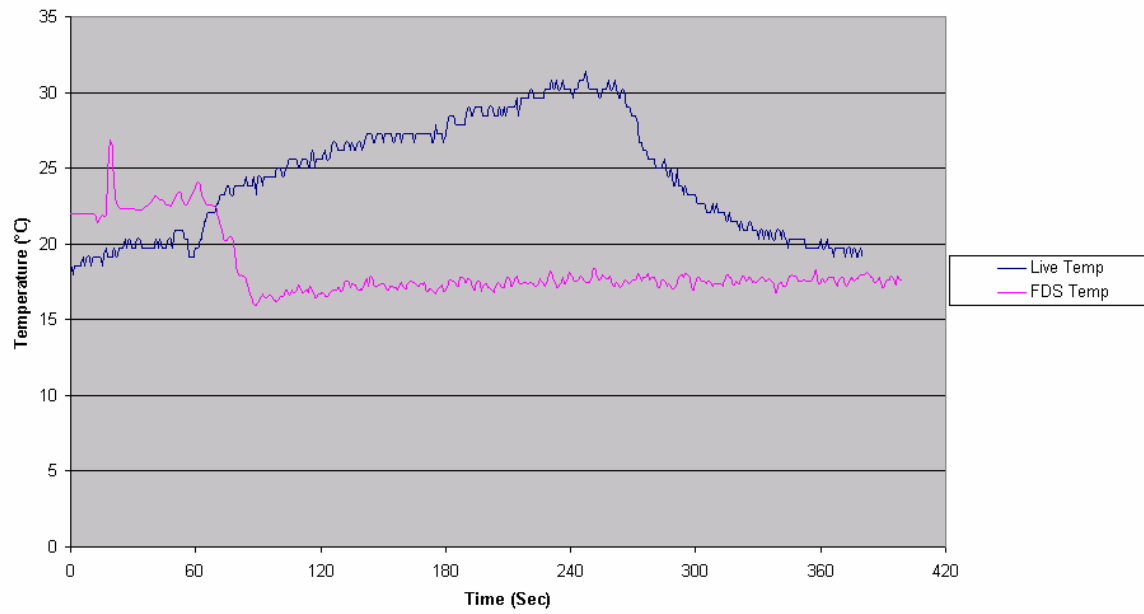
**Centre 1m Fire with High Airflow and Water Mist
Tree 2 (Centre) 2.1 m Temperature**



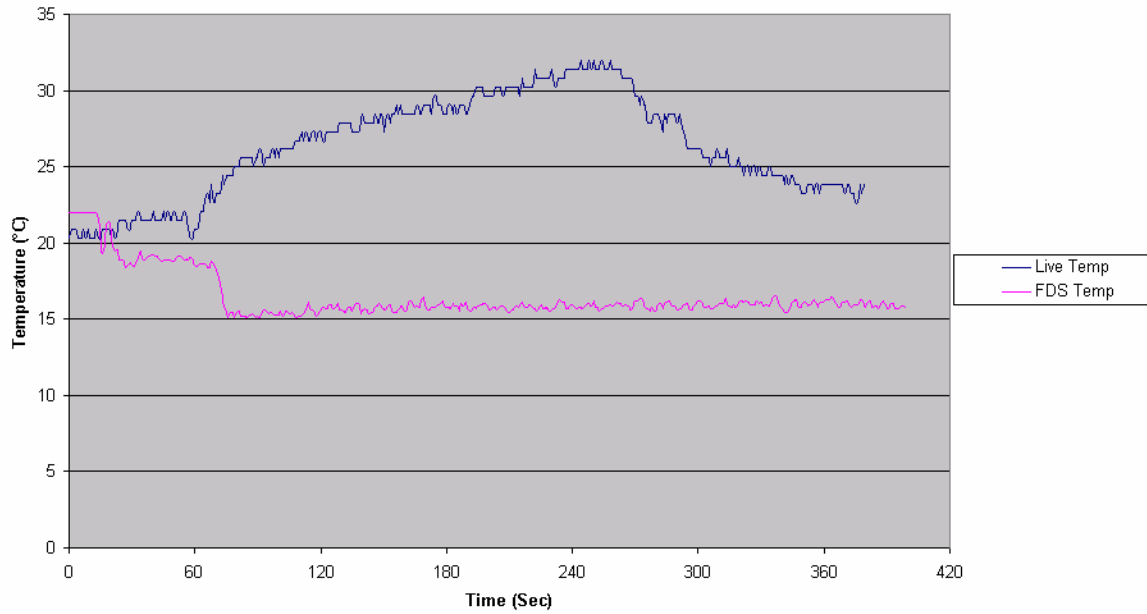
**Centre 1m Fire with High Airflow and Water Mist
Back Corner 0.3 m Temperature**



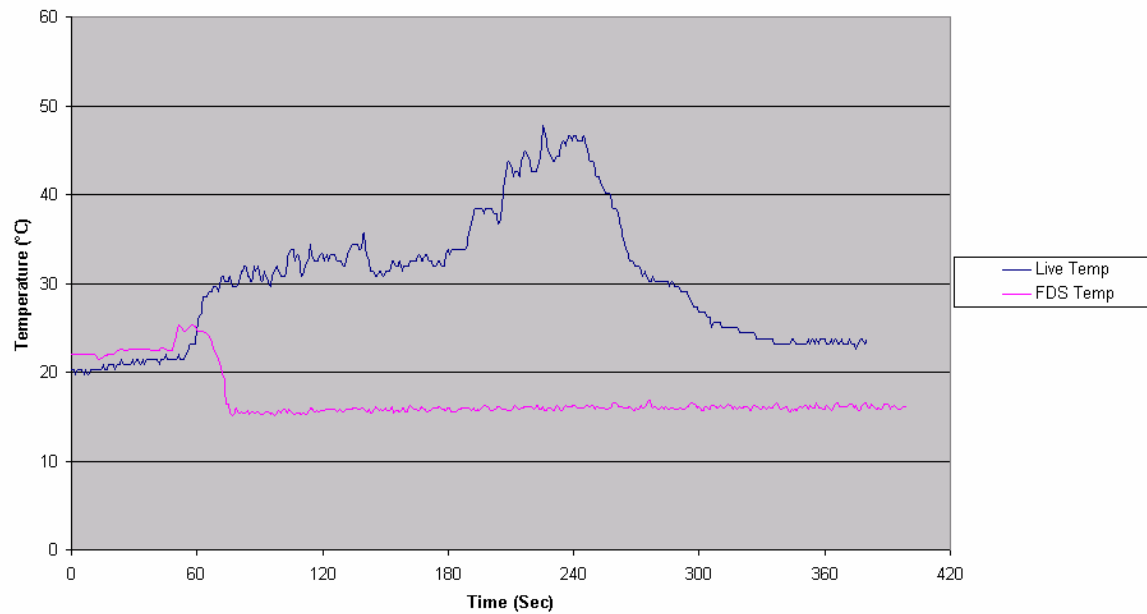
**Centre 1m Fire with High Airflow and Water Mist
Back Corner 1.3 m Temperature**



**Centre 1m Fire with High Airflow and Water Mist
Front Corner 0.3 m Temperature**

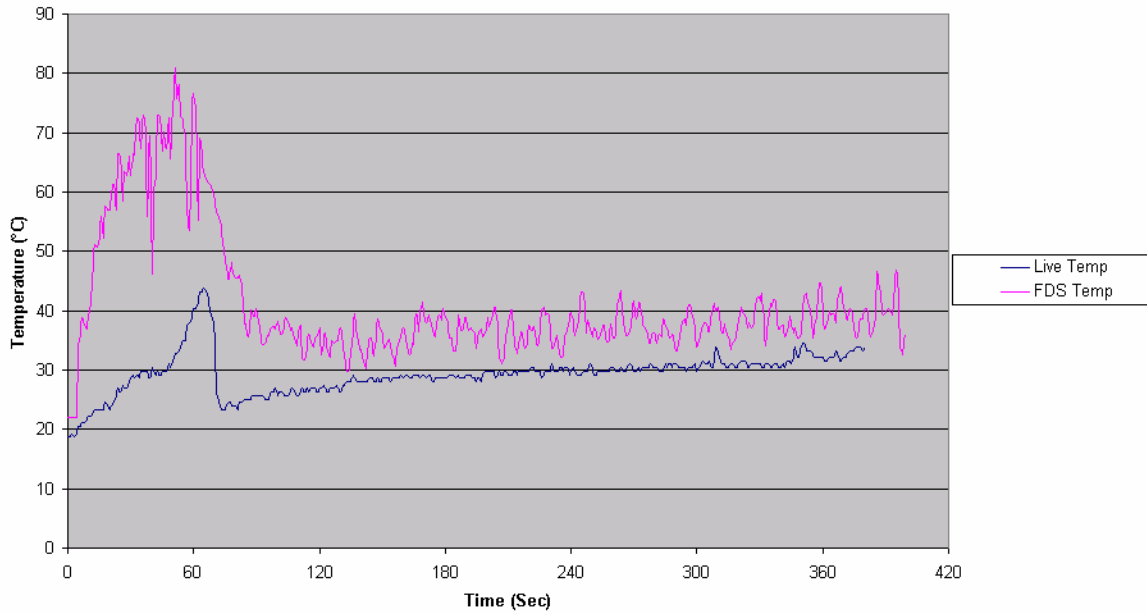


**Centre 1m Fire with High Airflow and Water Mist
Front Corner 1.3 m Temperature**

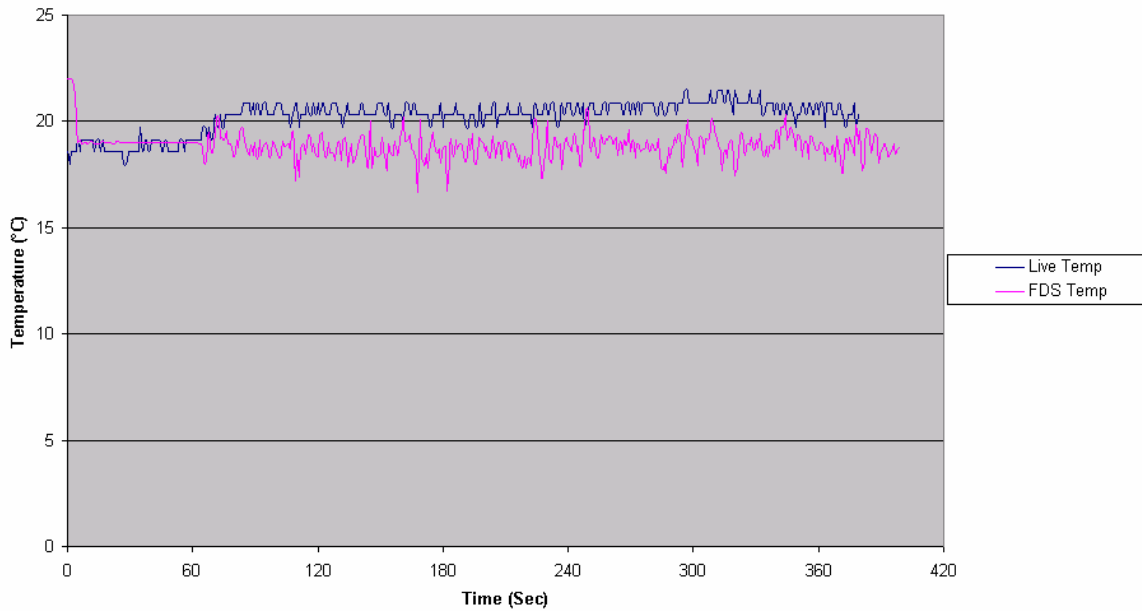


11.8.5 Displacement water mist operation with a front corner floor fire

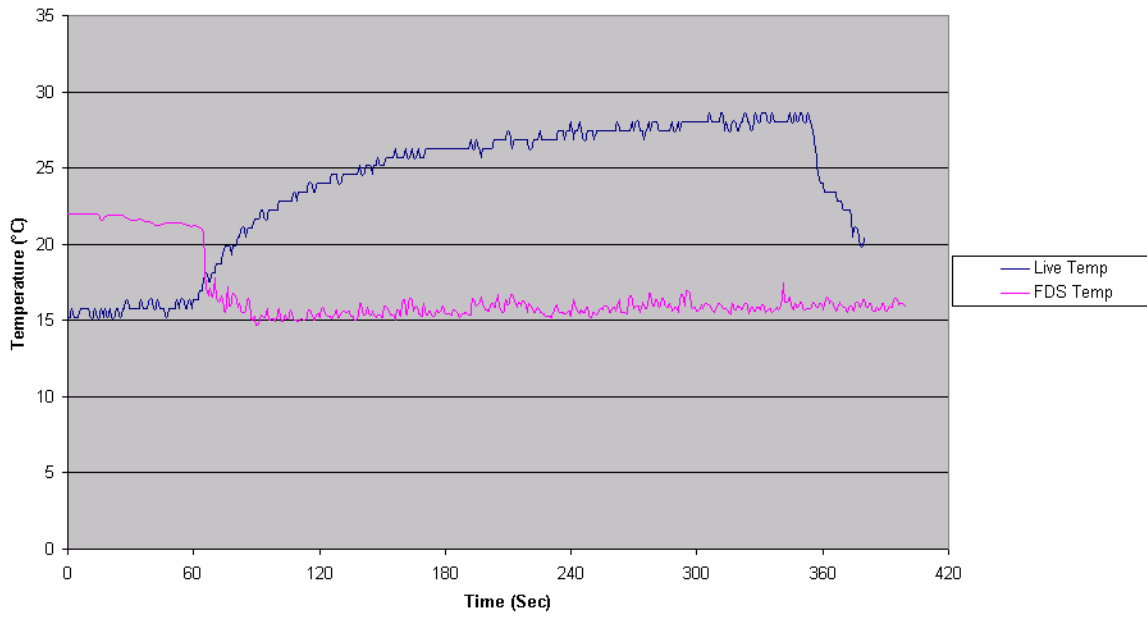
**Front Corner Fire with High Airflow and Water Mist
Extract Temperature**



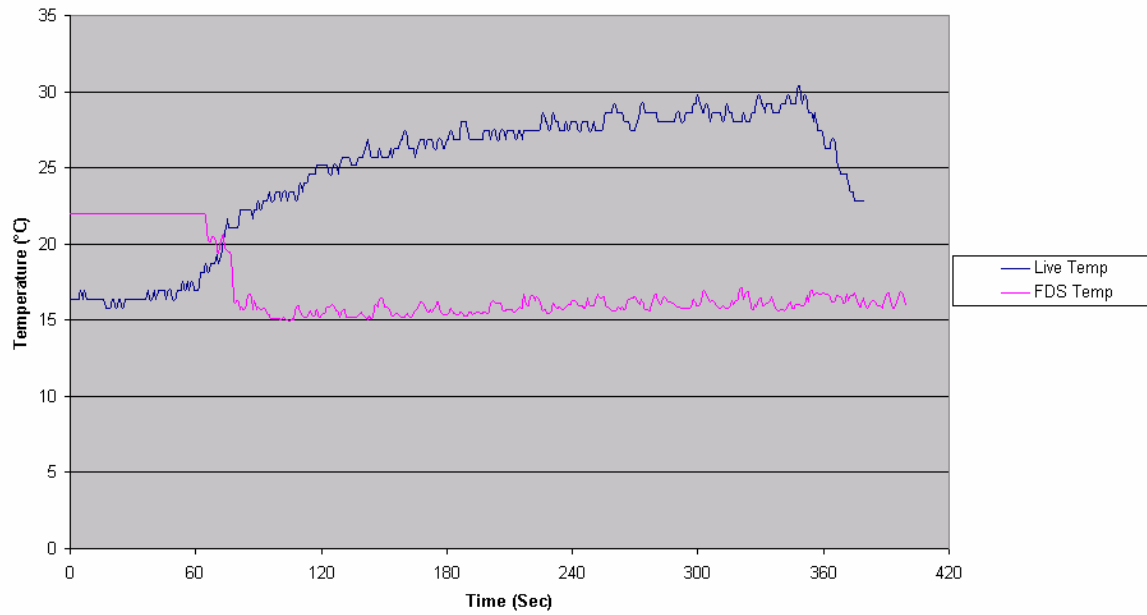
**Front Corner Fire with High Airflow and Water Mist
Supply Temperature**



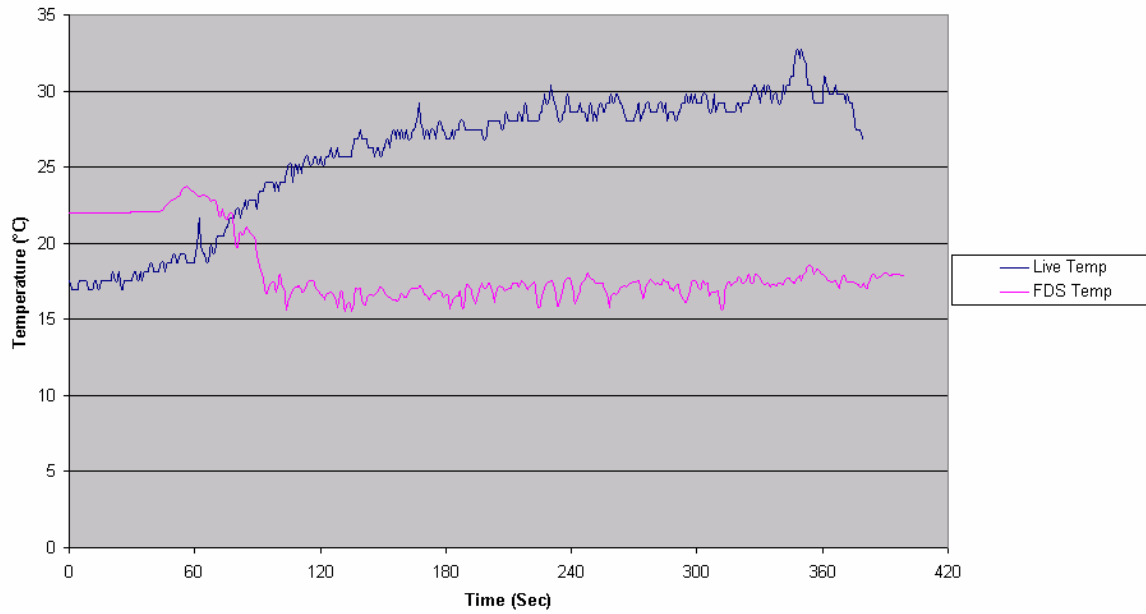
Front Corner Fire with High Airflow and Water Mist
Tree 1 (occ) 0.3 m Temperature



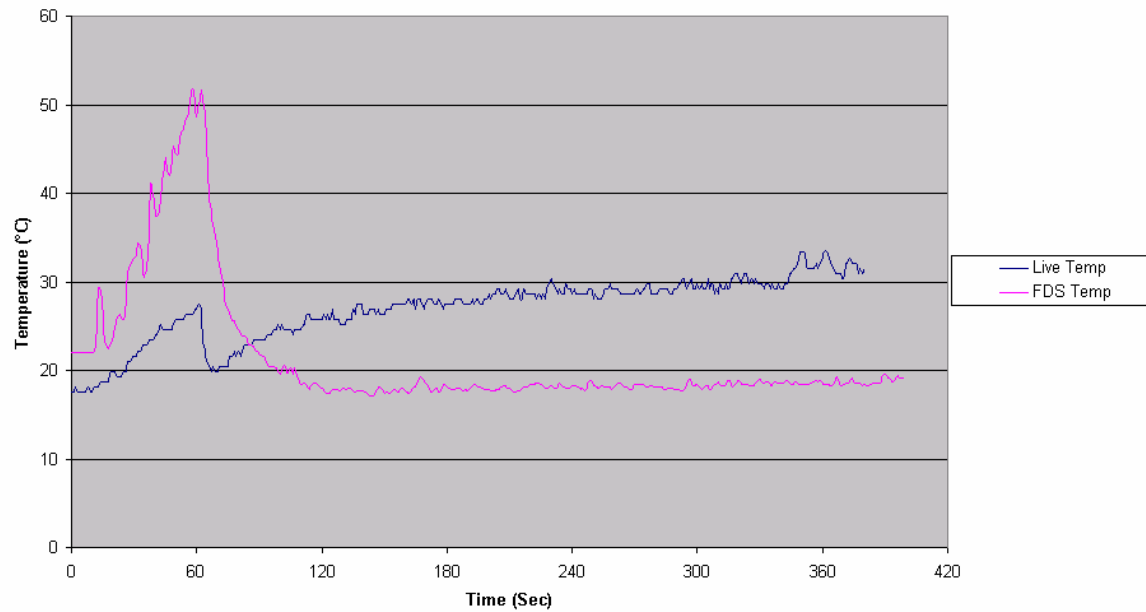
Front Corner Fire with High Airflow and Water Mist
Tree 1 (occ) 0.7 m Temperature



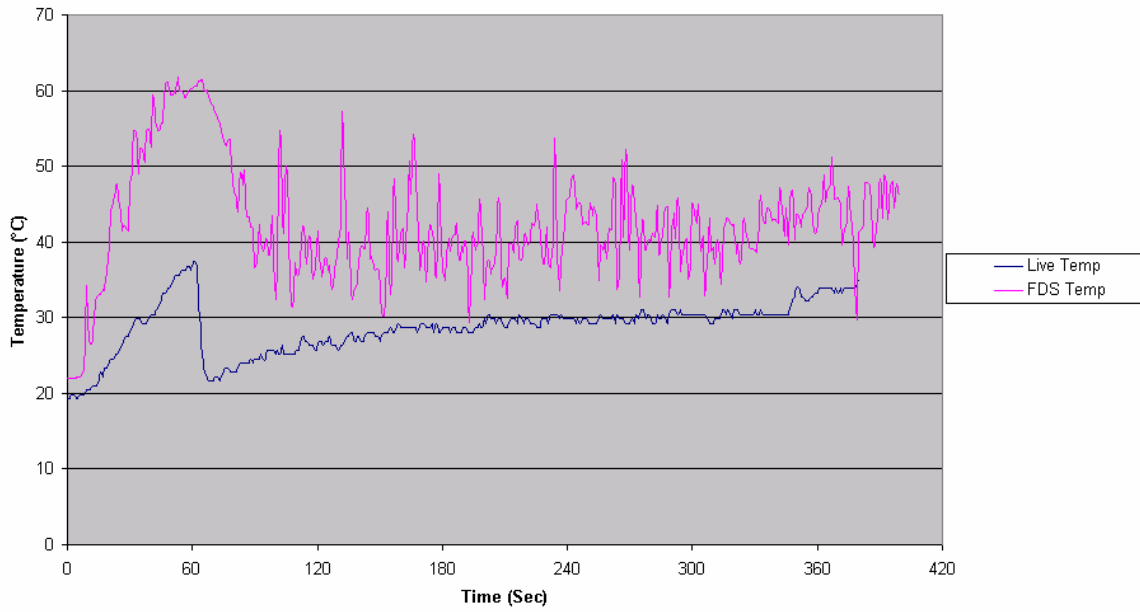
**Front Corner Fire with High Airflow and Water Mist
Tree 1 (occ) 1.3 m Temperature**



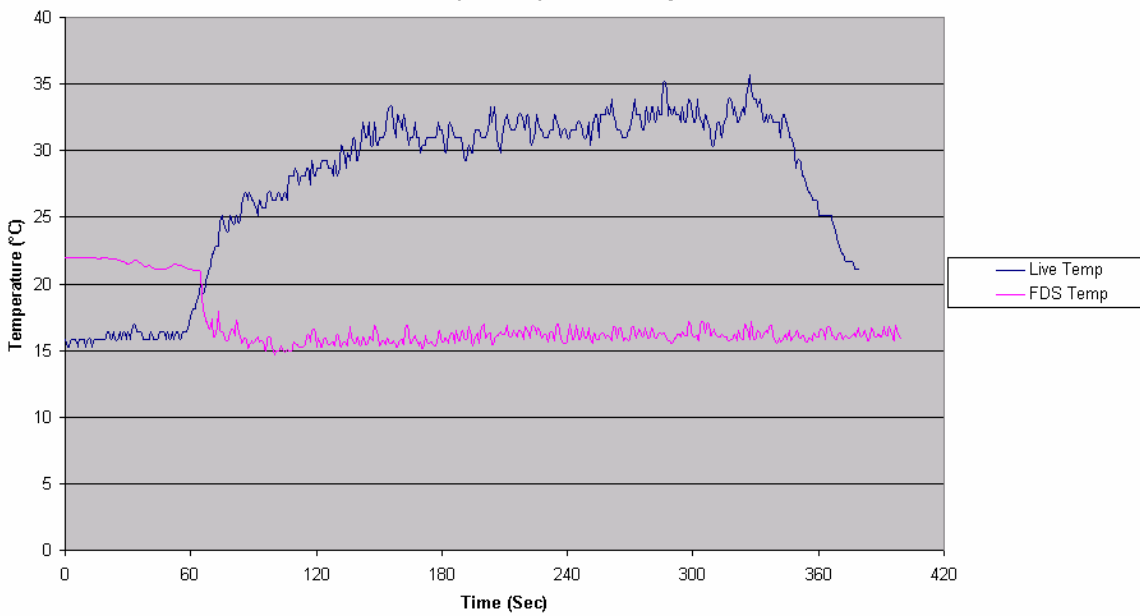
**Front Corner Fire with High Airflow and Water Mist
Tree 1 (occ) 1.8 m Temperature**



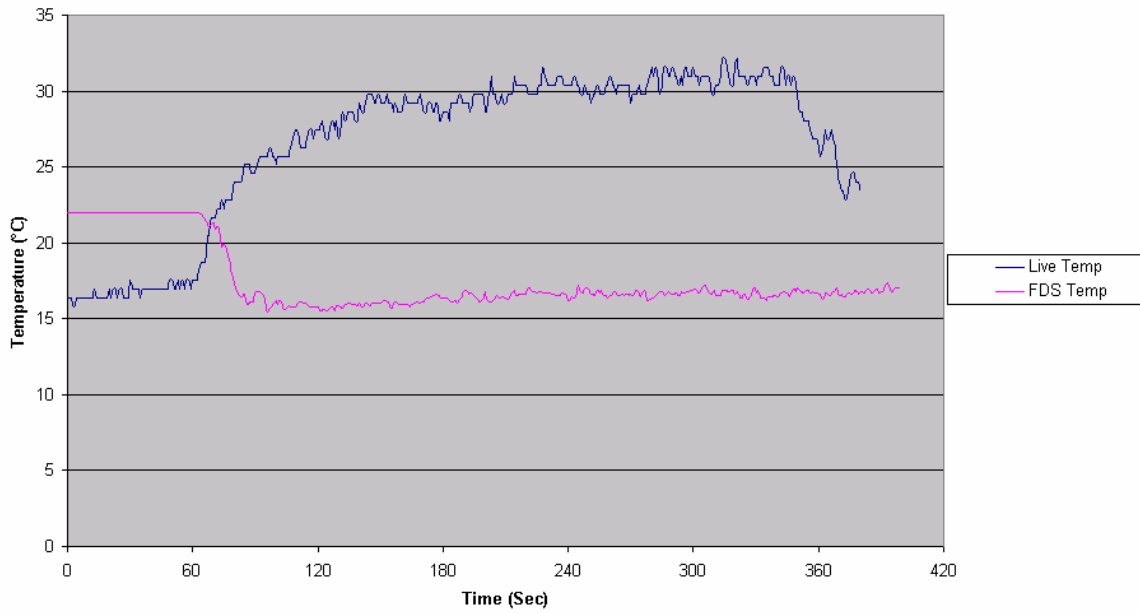
**Front Corner Fire with High Airflow and Water Mist
Tree 1 (occ) 2.1 m Temperature**



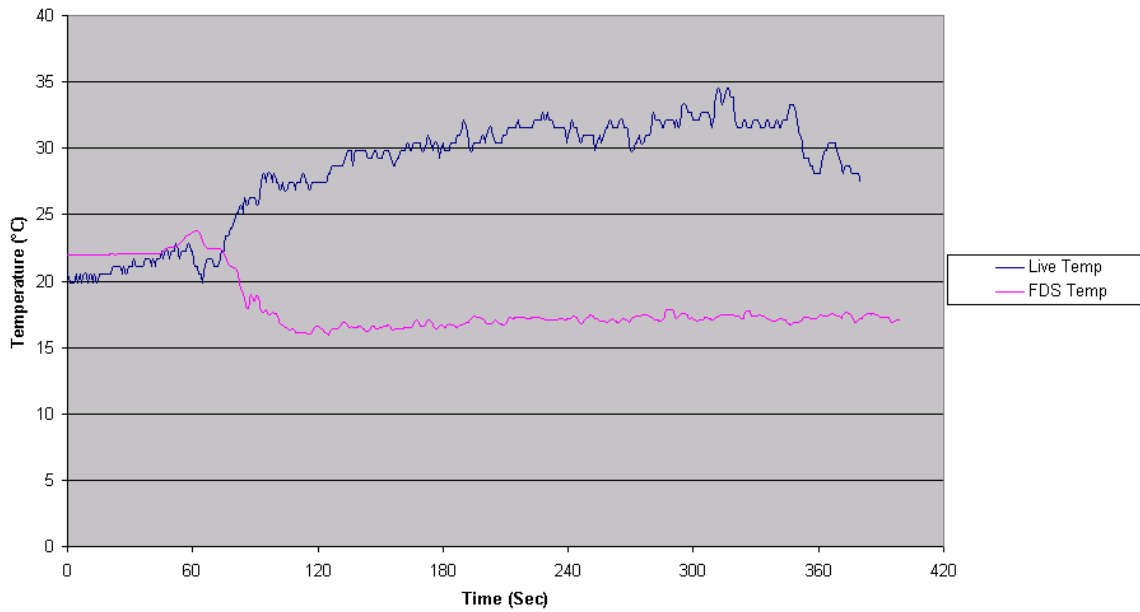
**Front Corner Fire with High Airflow and Water Mist
Tree 2 (Centre) 0.3 m Temperature**



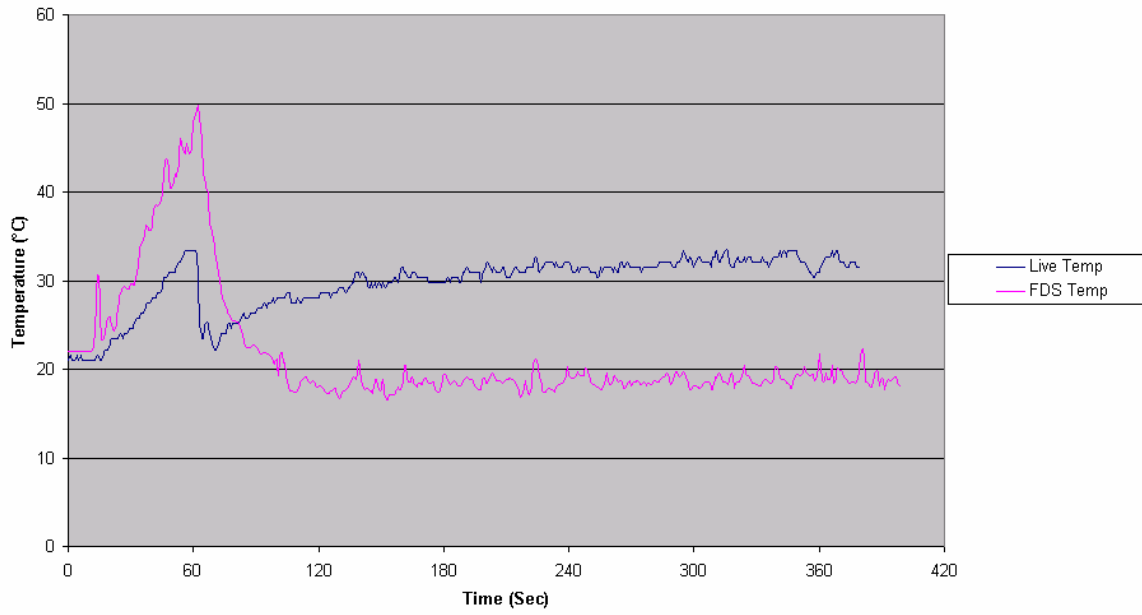
**Front Corner Fire with High Airflow and Water Mist
Tree 2 (Centre) 0.7 m Temperature**



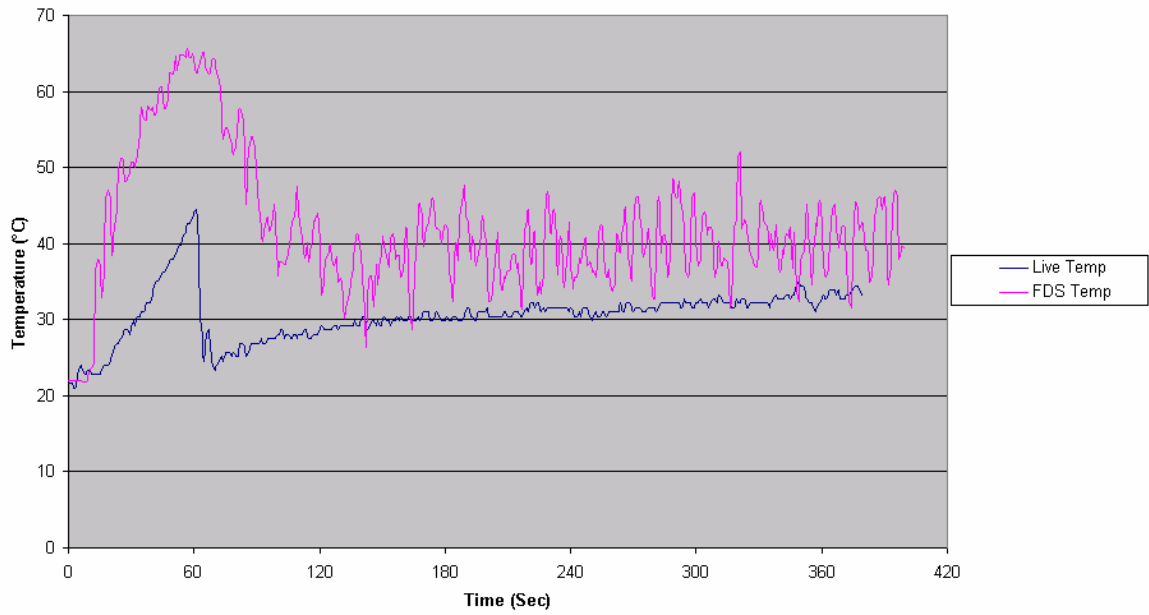
**Front Corner Fire with High Airflow and Water Mist
Tree 2 (Centre) 1.3 m Temperature**



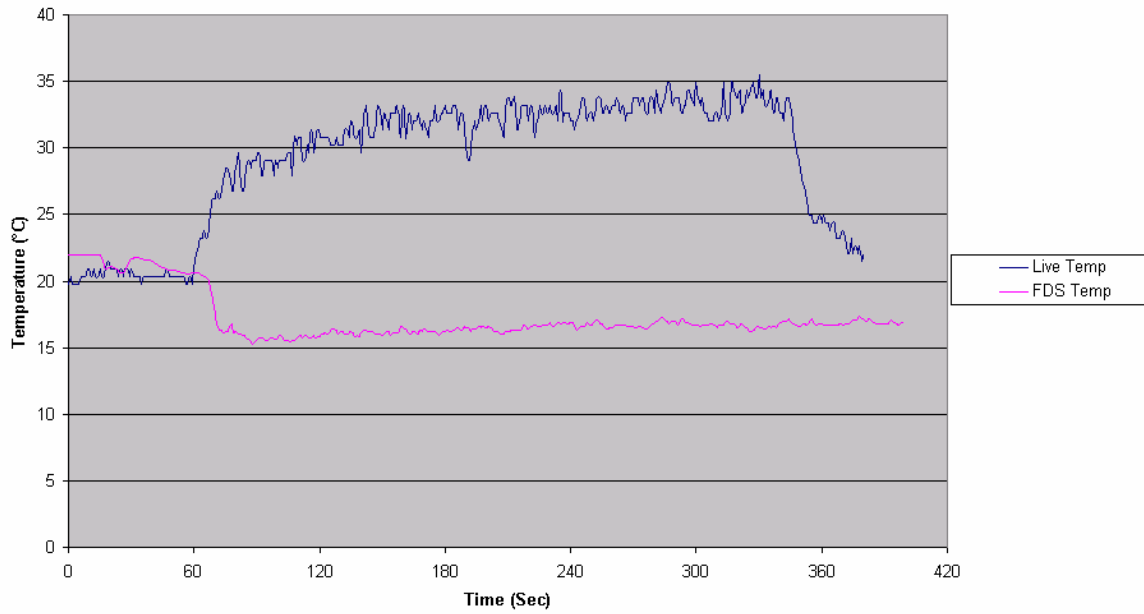
**Front Corner Fire with High Airflow and Water Mist
Tree 2 (Centre) 1.8 m Temperature**



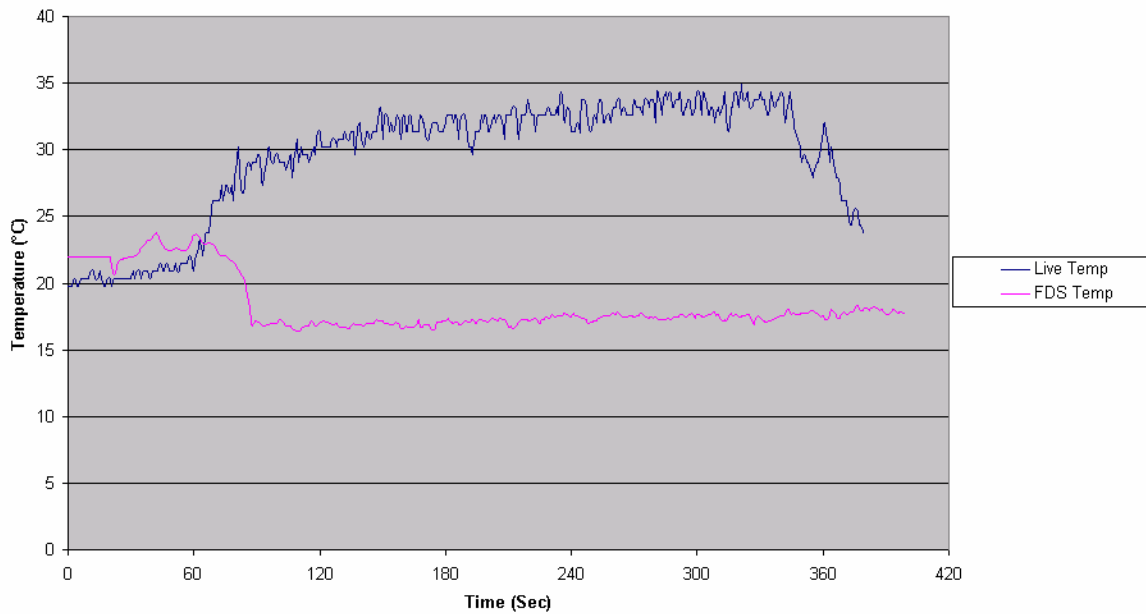
**Front Corner Fire with High Airflow and Water Mist
Tree 2 (Centre) 2.1 m Temperature**



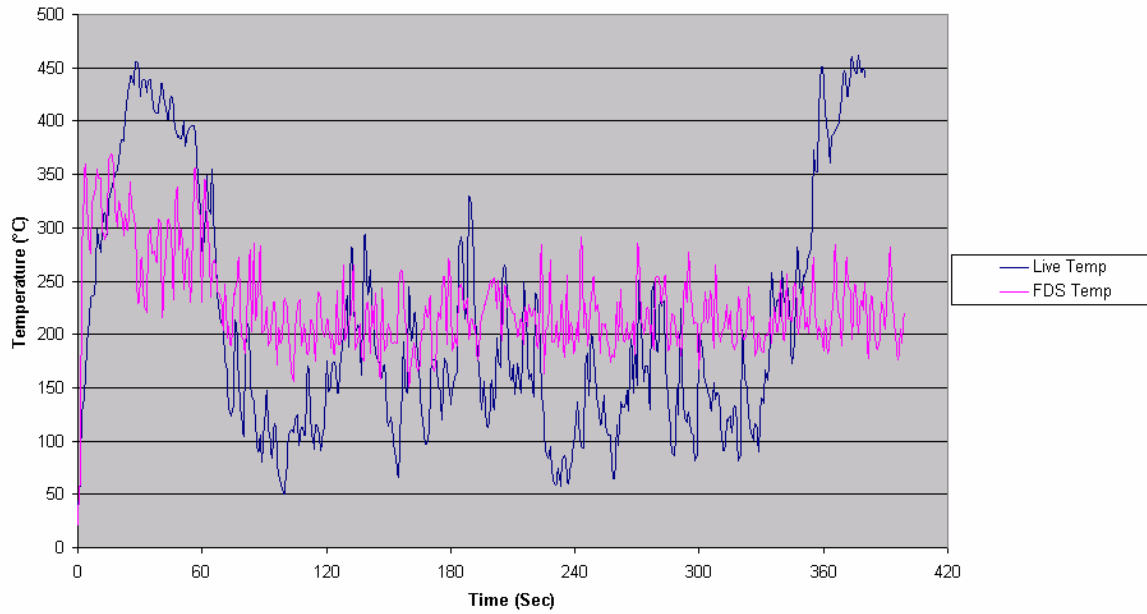
**Front Corner Fire with High Airflow and Water Mist
Back Corner 0.3 m Temperature**



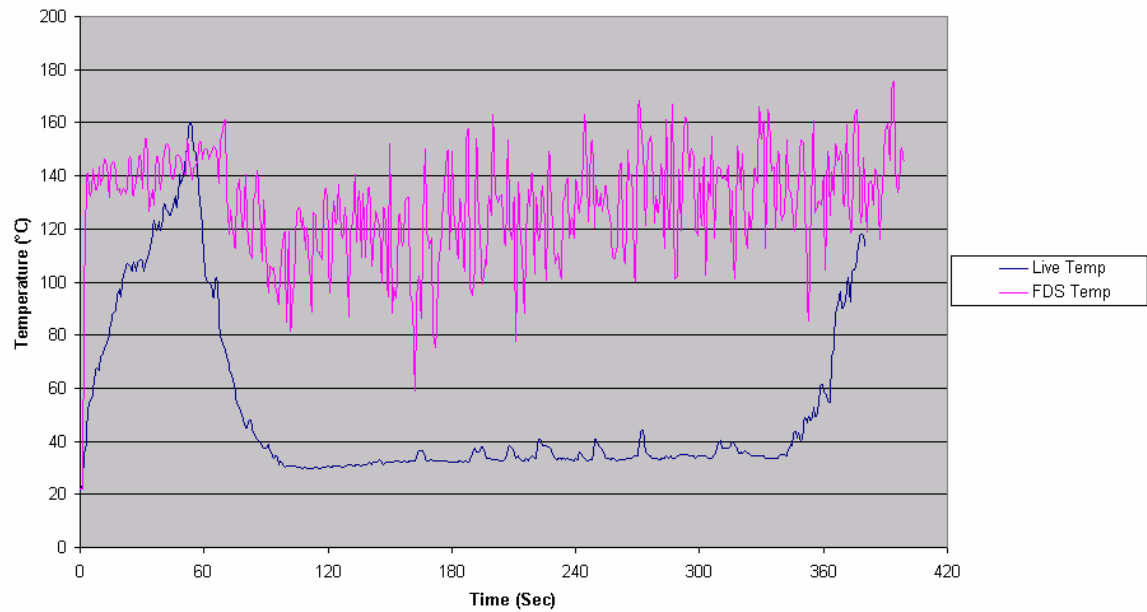
**Front Corner Fire with High Airflow and Water Mist
Back Corner 1.3 m Temperature**



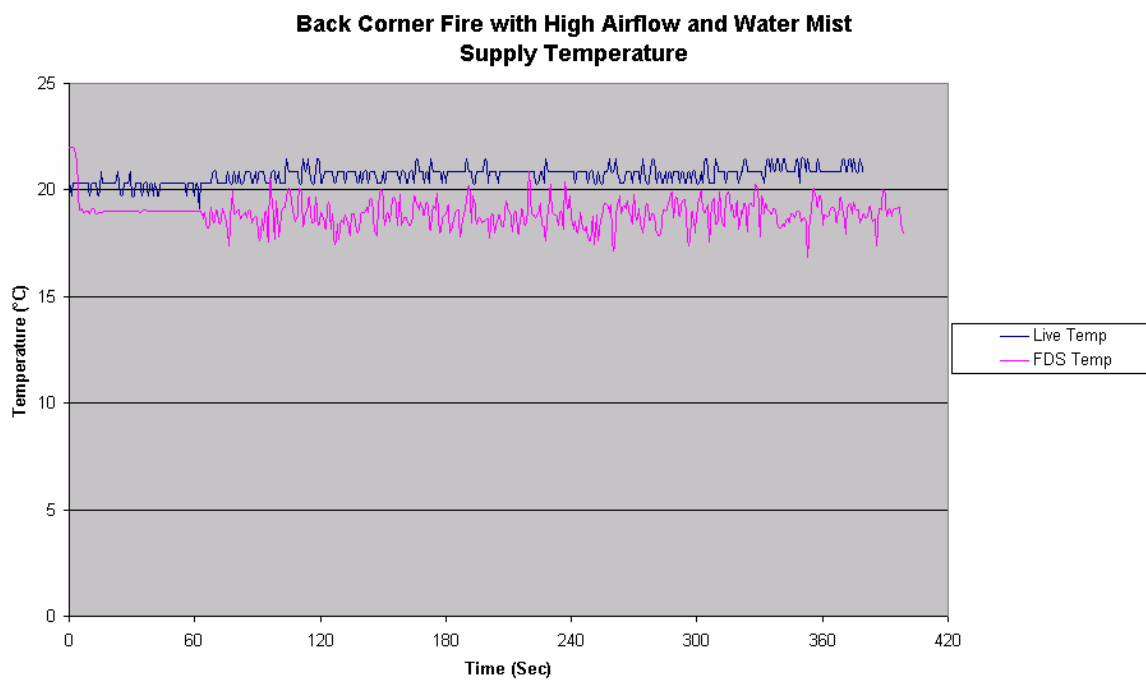
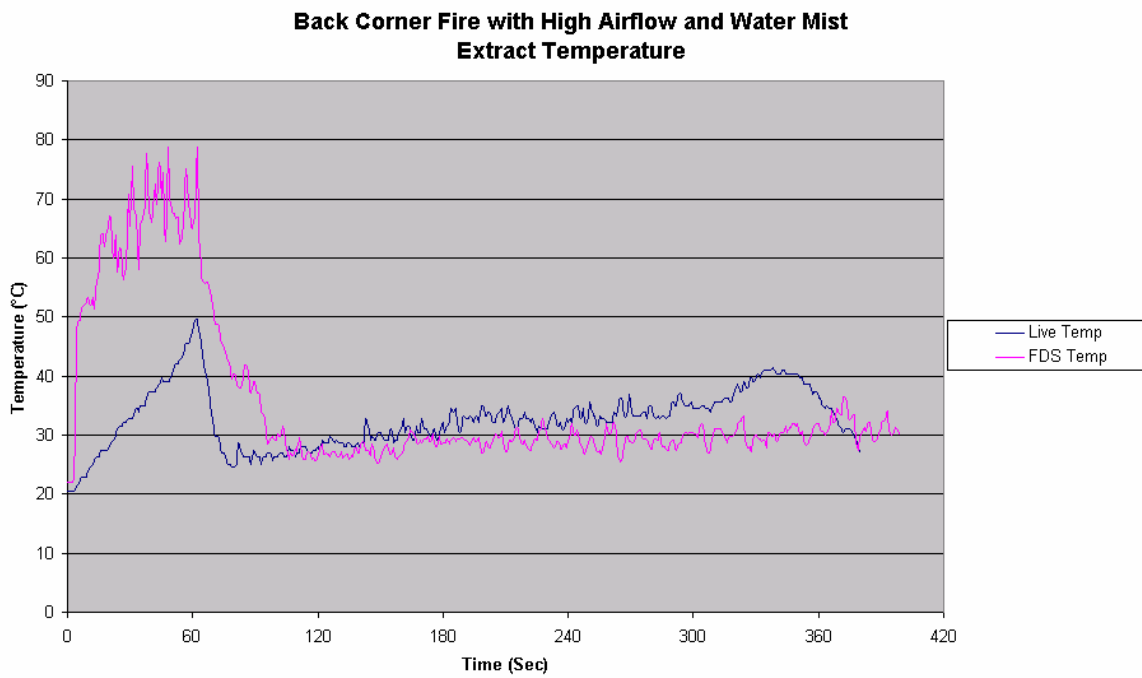
**Front Corner Fire with High Airflow and Water Mist
Front Corner 0.3 m Temperature**



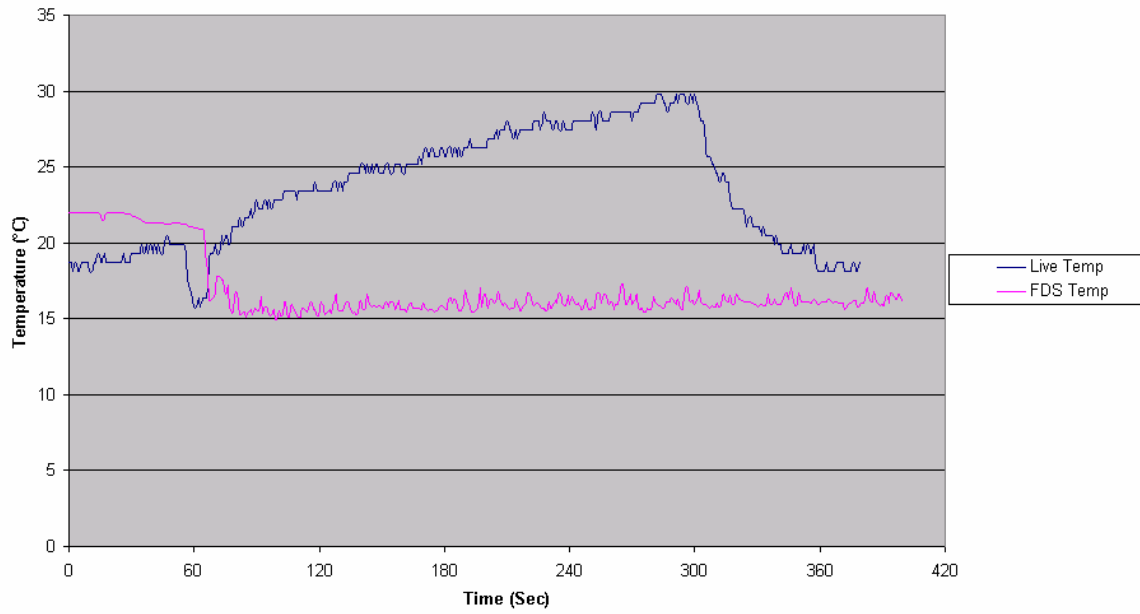
**Front Corner Fire with High Airflow and Water Mist
Front Corner 1.3 m Temperature**



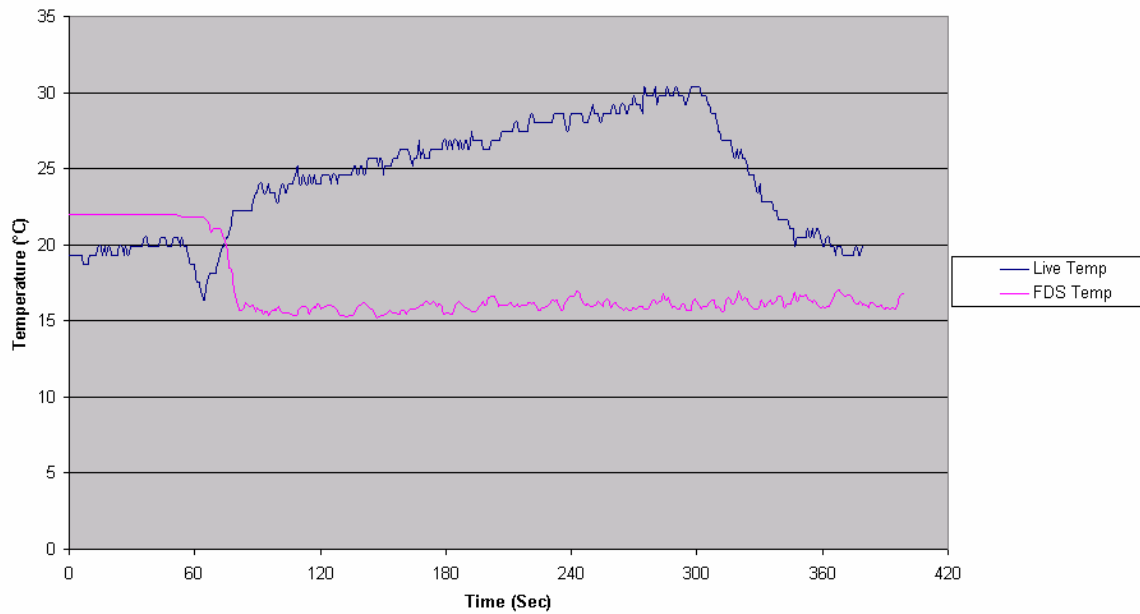
11.8.6 Displacement water mist operation with a back corner floor fire



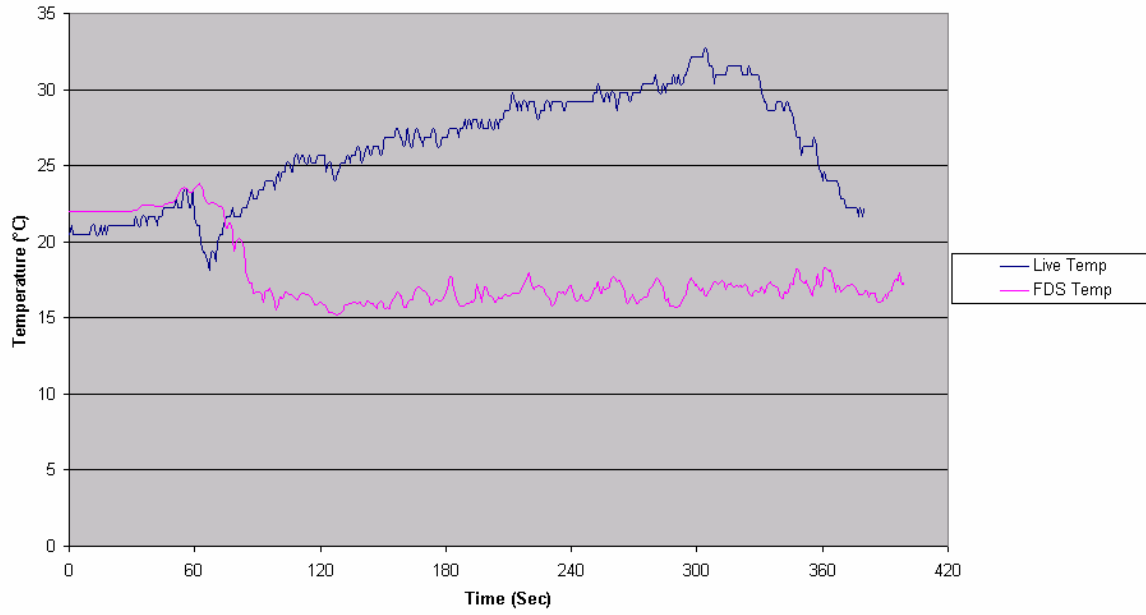
**Back Corner Fire with High Airflow and Water Mist
Tree 1 (occ) 0.3 m Temperature**



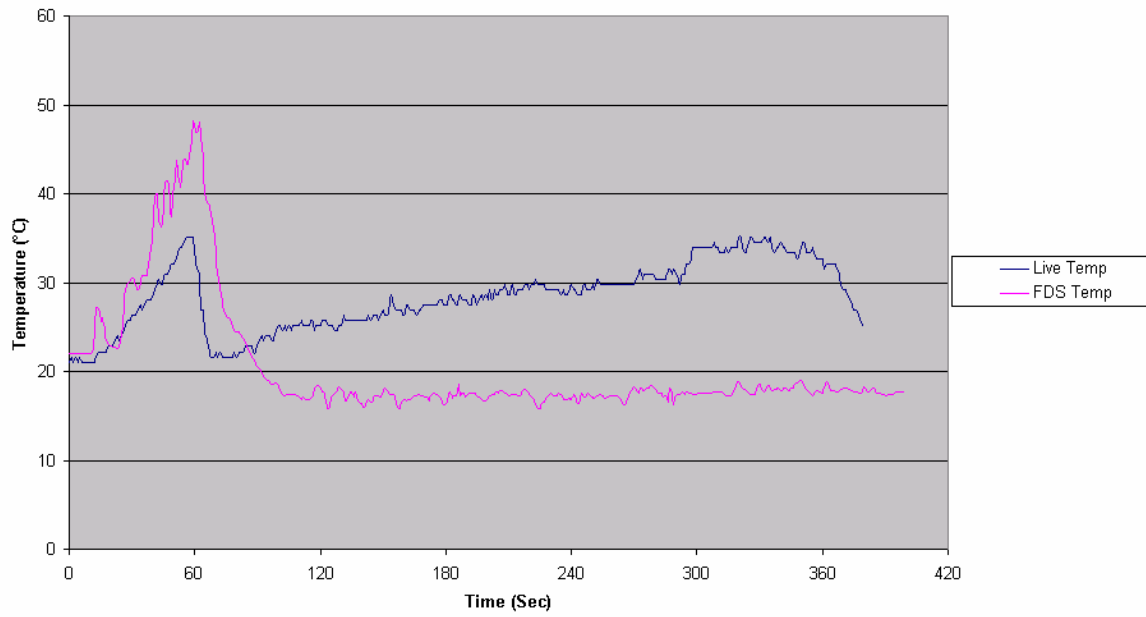
**Back Corner Fire with High Airflow and Water Mist
Tree 1 (occ) 0.7 m Temperature**



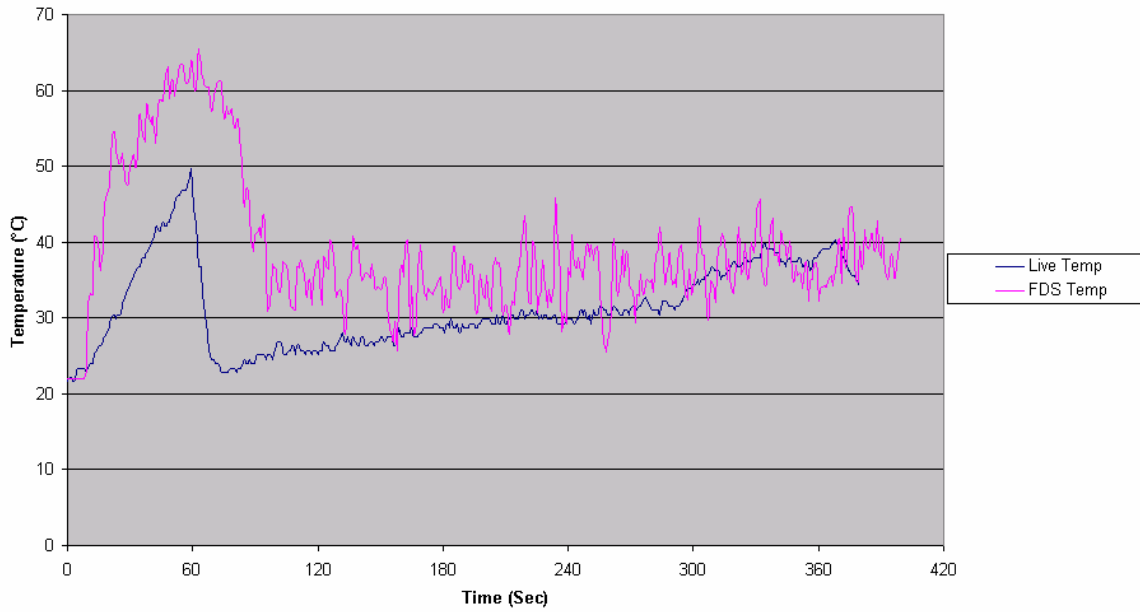
**Back Corner Fire with High Airflow and Water Mist
Tree 1 (occ) 1.3 m Temperature**



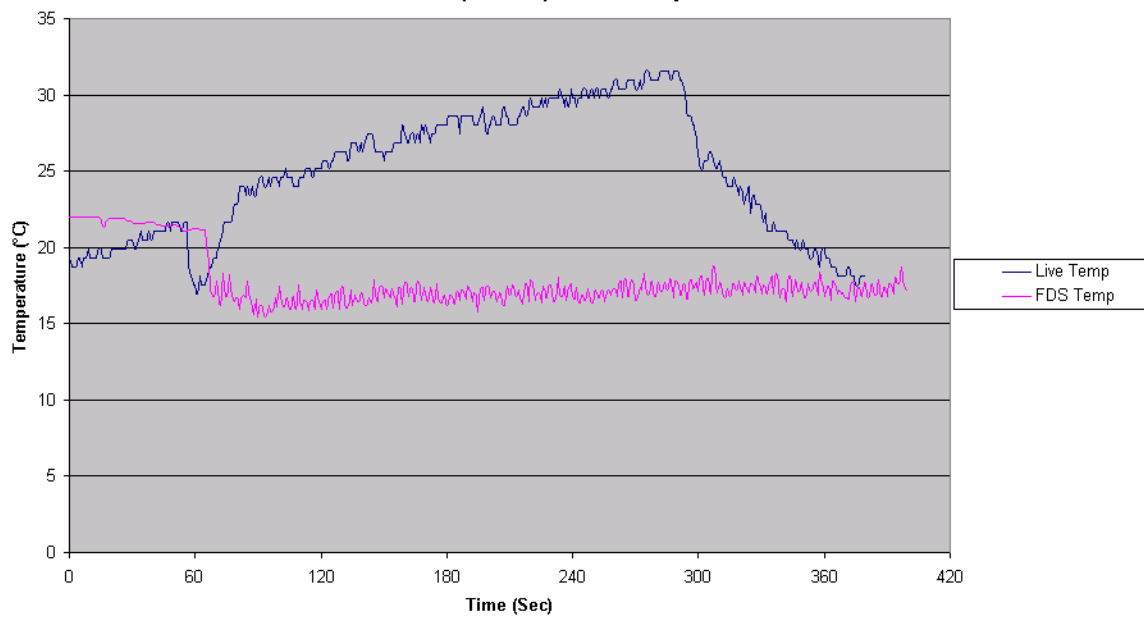
**Back Corner Fire with High Airflow and Water Mist
Tree 1 (occ) 1.8 m Temperature**



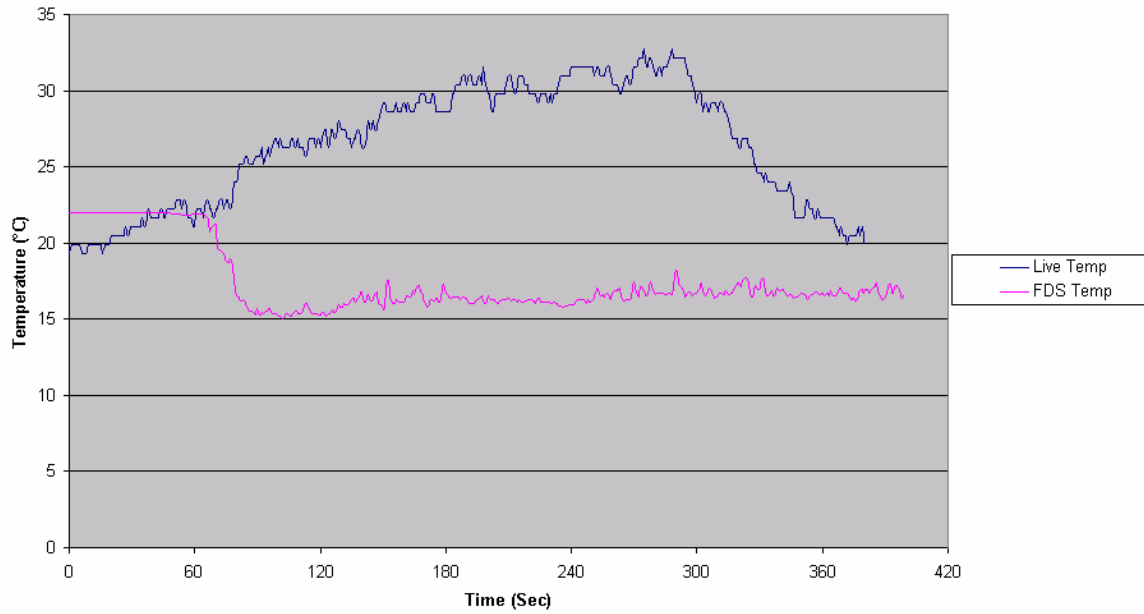
**Back Corner Fire with High Airflow and Water Mist
Tree 1 (occ) 2.1 m Temperature**



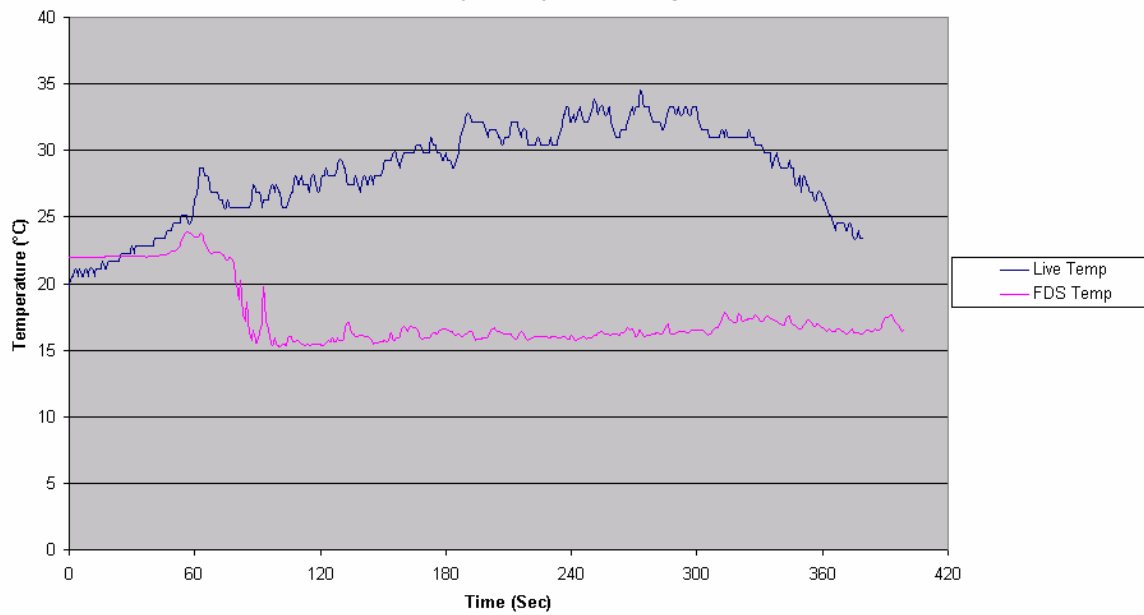
**Back Corner Fire with High Airflow and Water Mist
Tree 2 (Centre) 0.3 m Temperature**



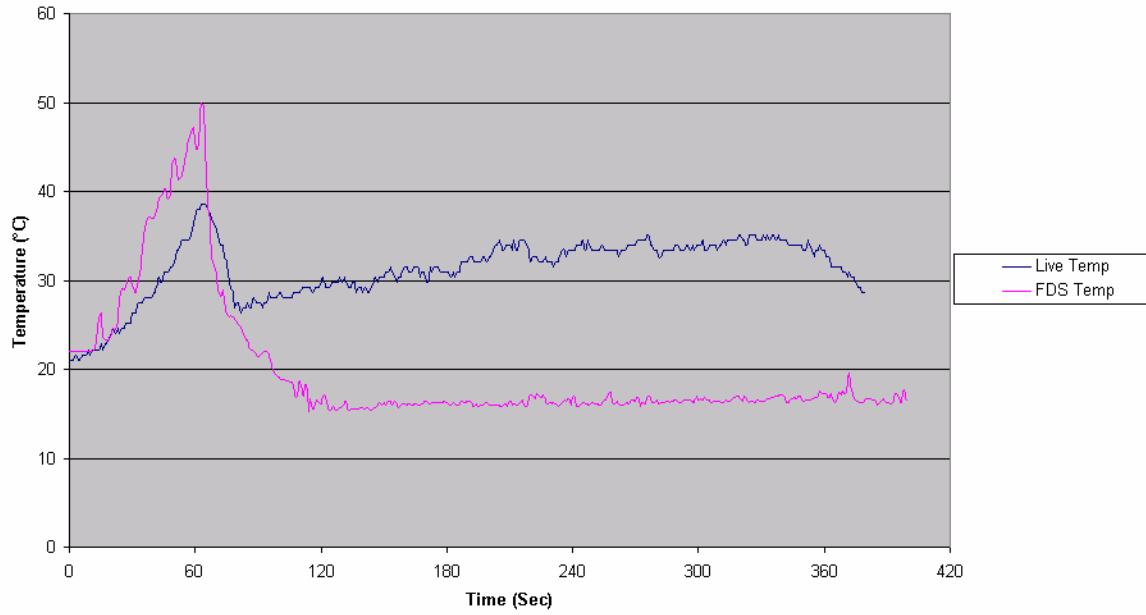
**Back Corner Fire with High Airflow and Water Mist
Tree 2 (Centre) 0.7 m Temperature**



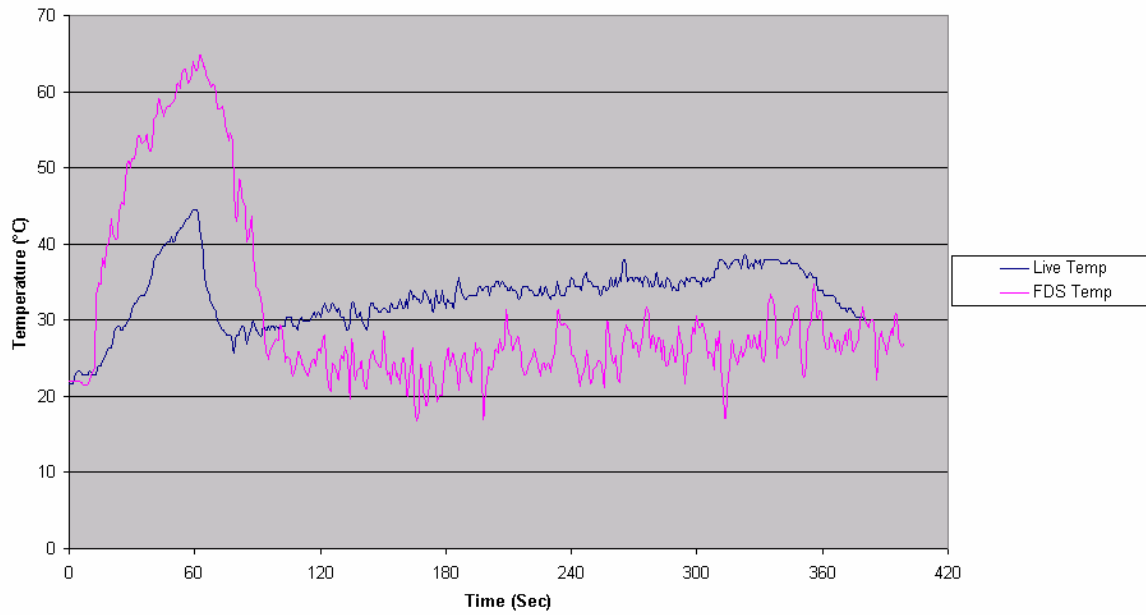
**Back Corner Fire with High Airflow and Water Mist
Tree 2 (Centre) 1.3 m Temperature**



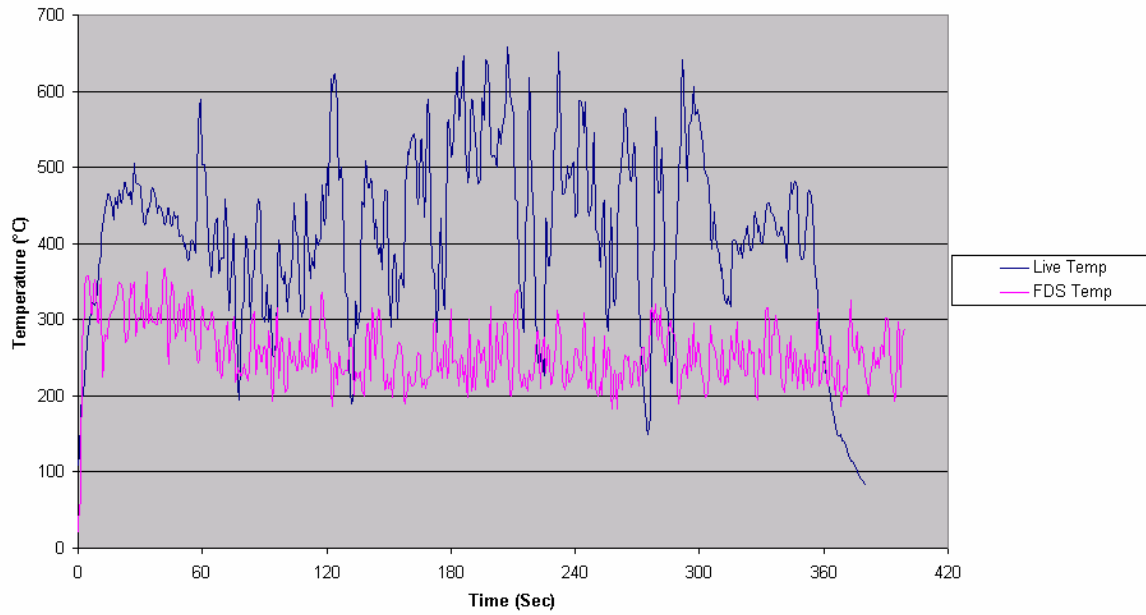
**Back Corner Fire with High Airflow and Water Mist
Tree 2 (Centre) 1.8 m Temperature**



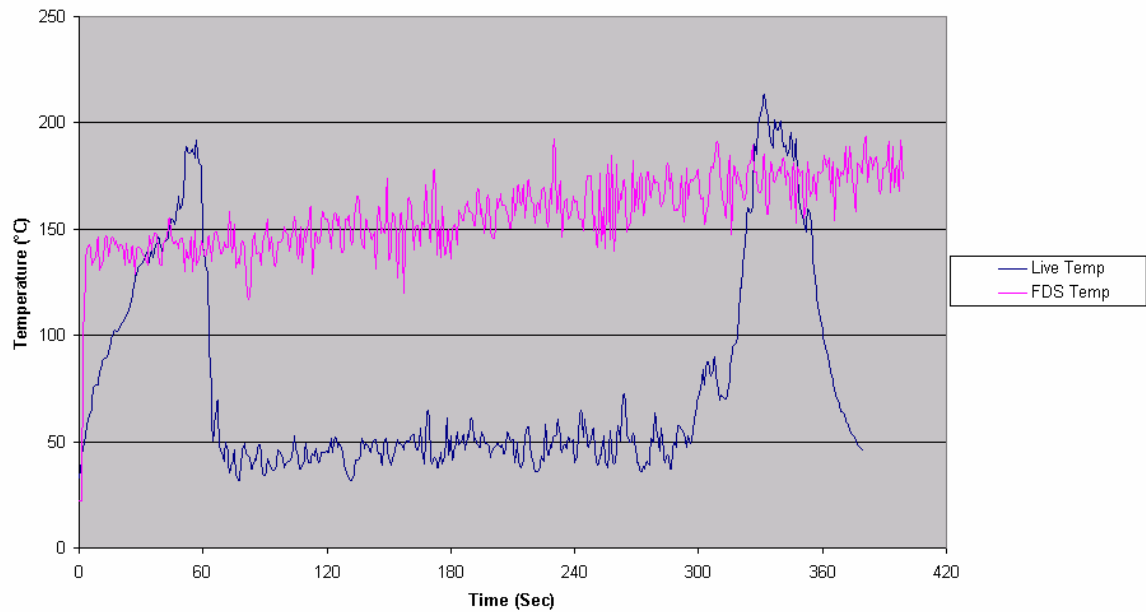
**Back Corner Fire with High Airflow and Water Mist
Tree 2 (Centre) 2.1 m Temperature**



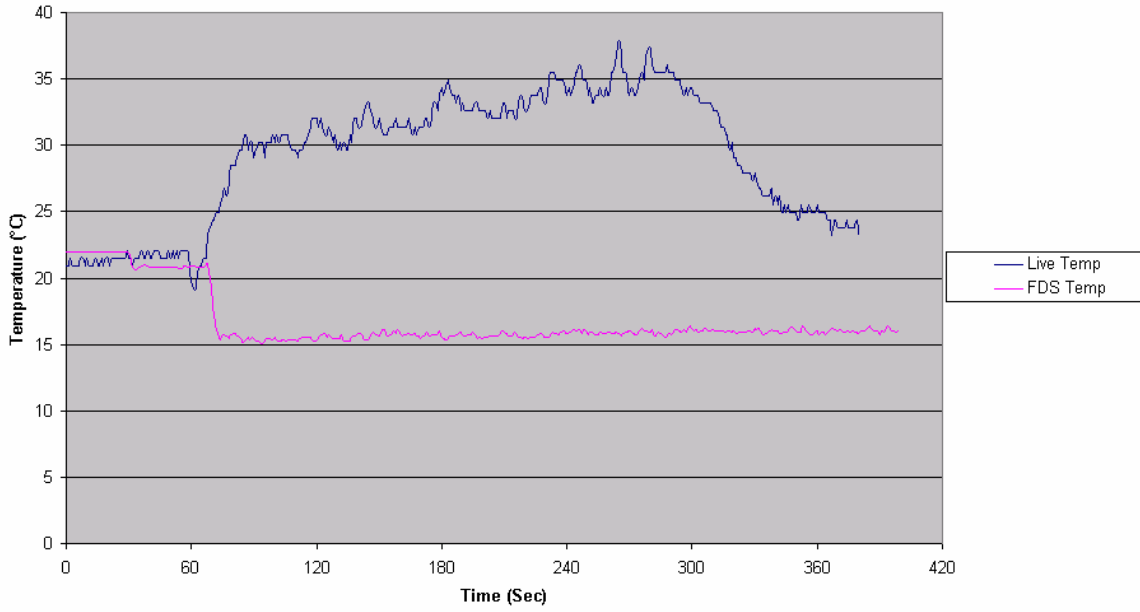
**Back Corner Fire with High Airflow and Water Mist
Back Corner 0.3 m Temperature**



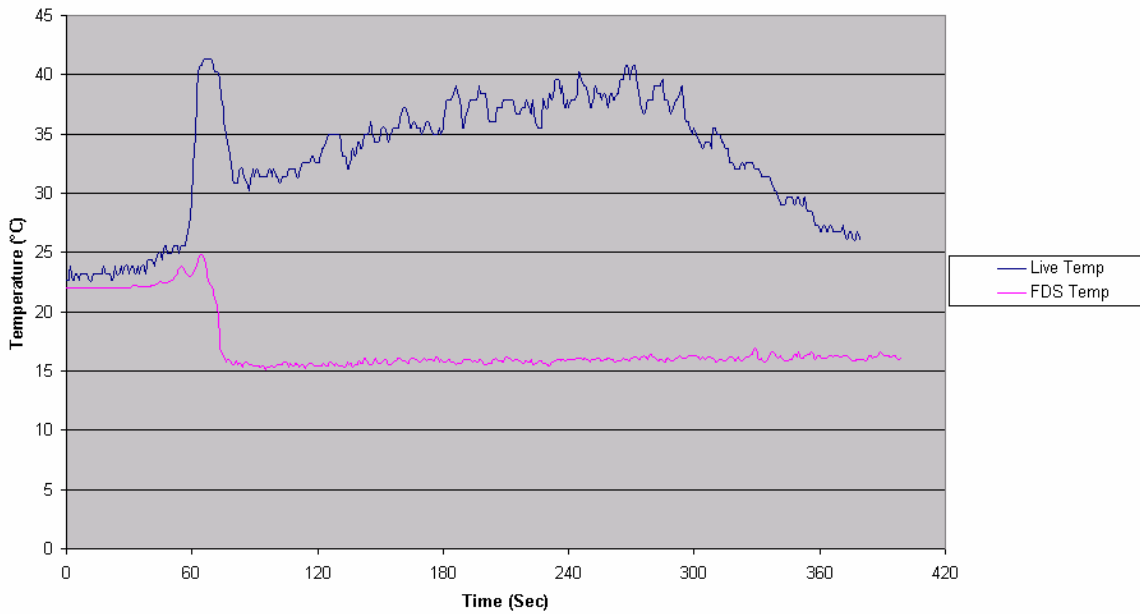
**Back Corner Fire with High Airflow and Water Mist
Back Corner 1.3 m Temperature**



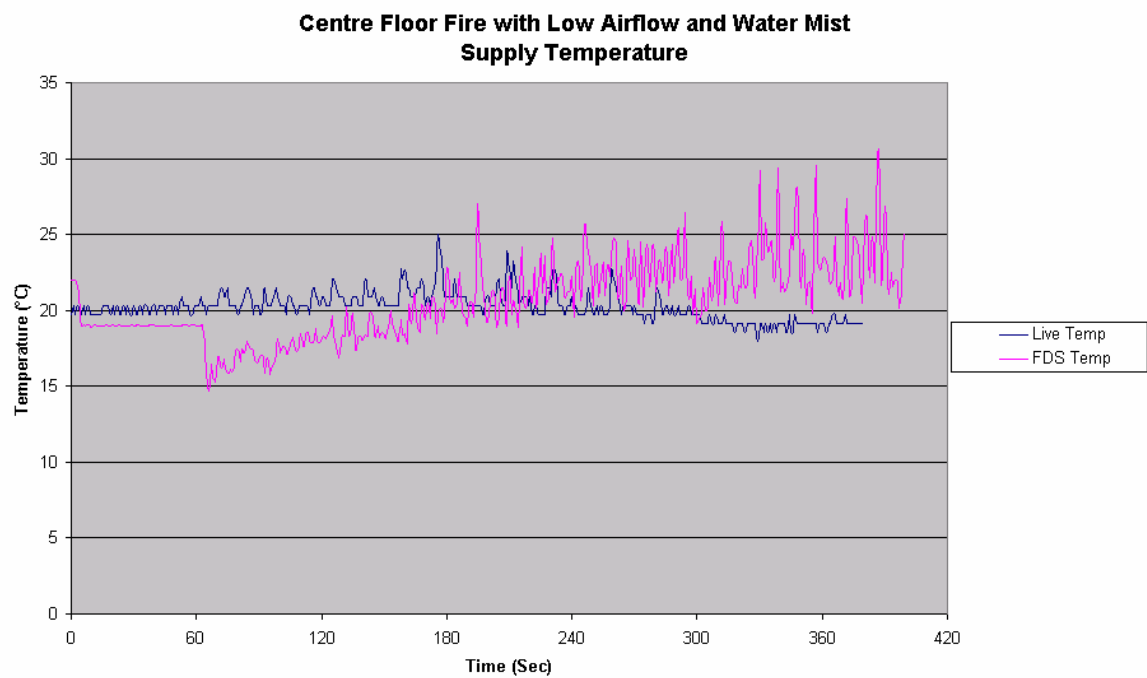
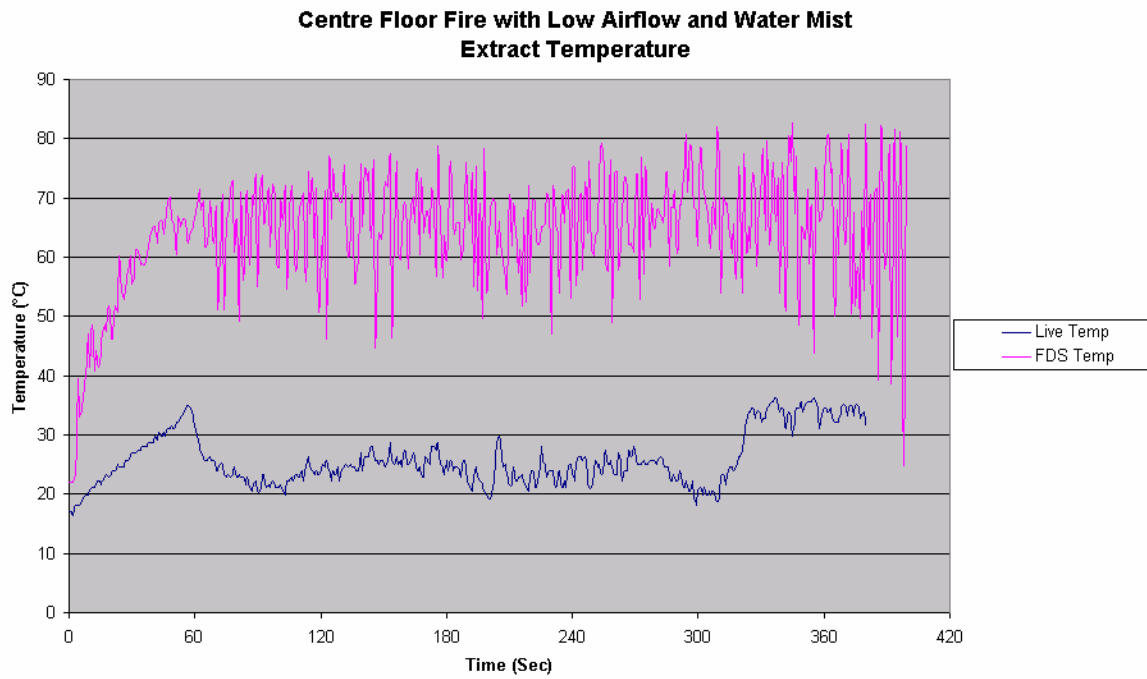
**Back Corner Fire with High Airflow and Water Mist
Front Corner 0.3 m Temperature**



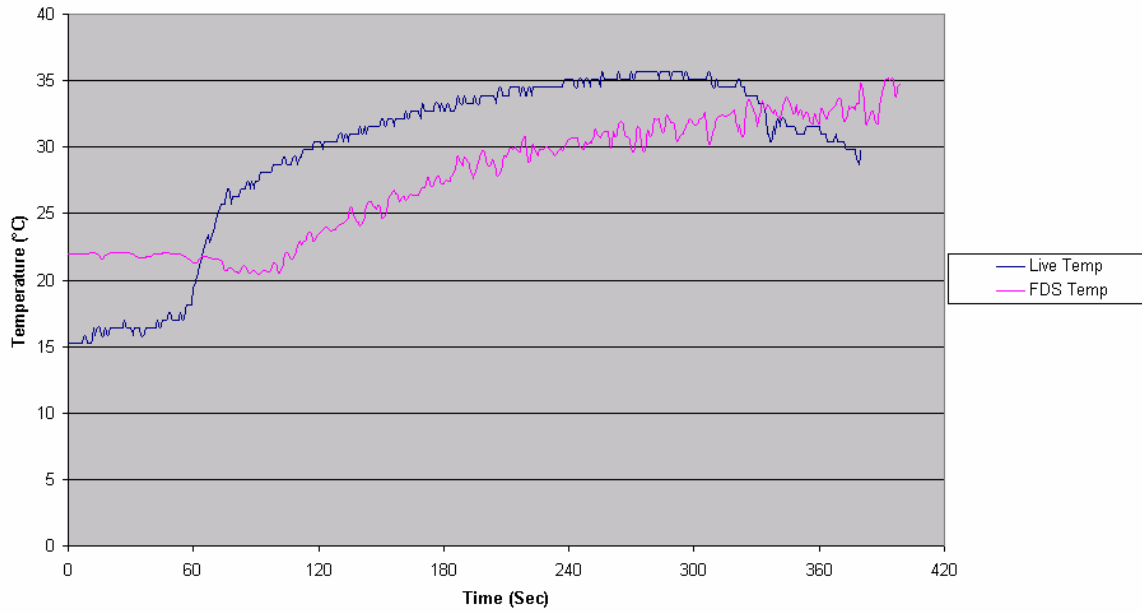
**Back Corner Fire with High Airflow and Water Mist
Front Corner 1.3 m Temperature**



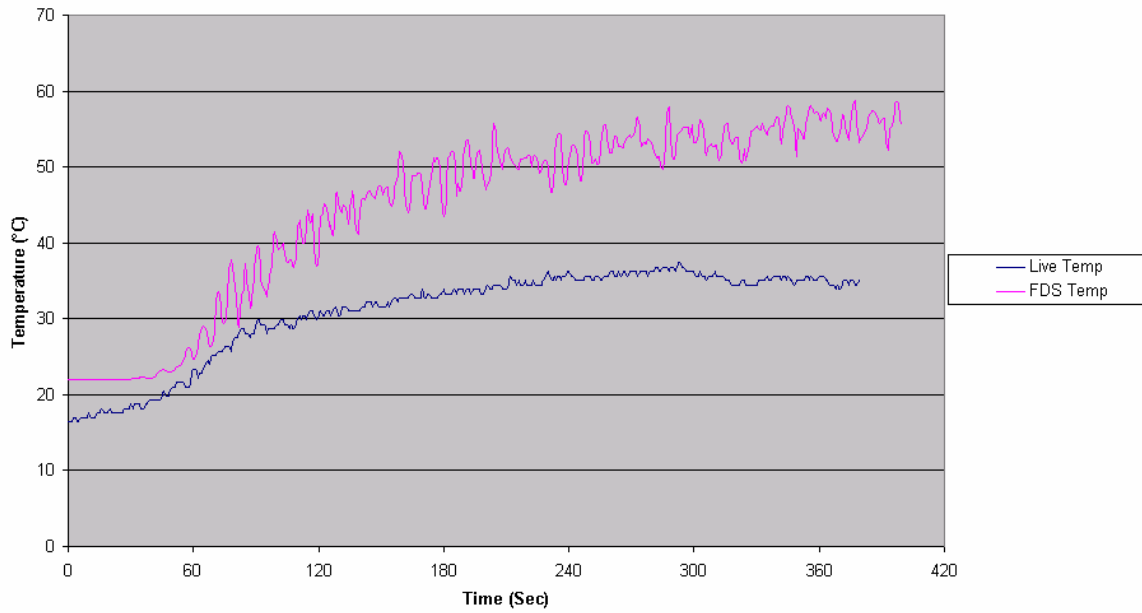
11.8.7 Low airflow and water mist operation with a central floor fire



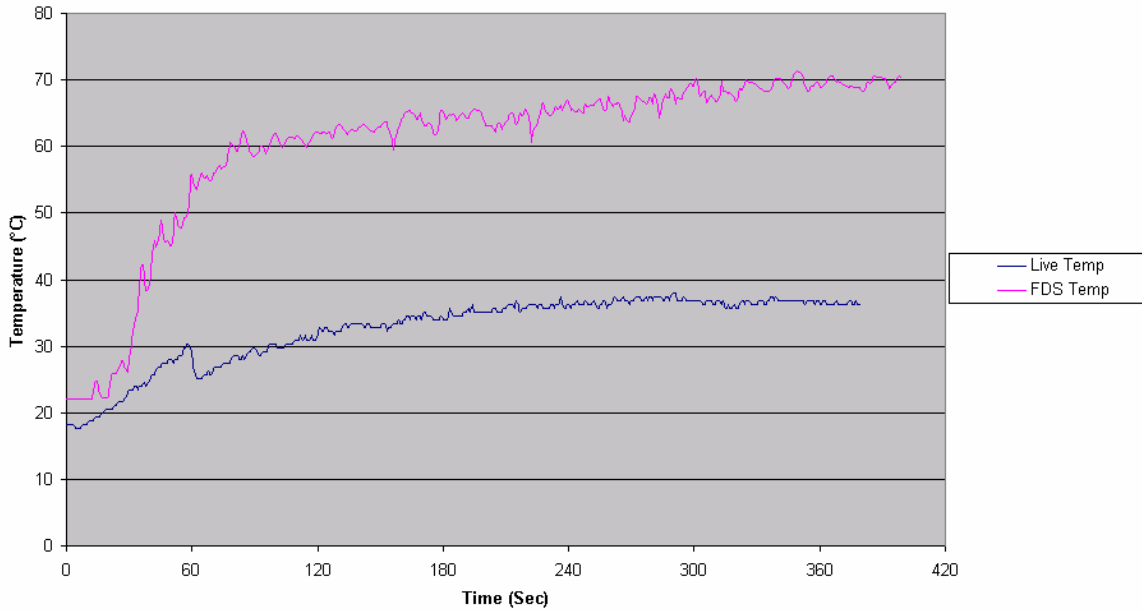
**Centre Floor Fire with Low Airflow and Water Mist
Tree 1 (occ) 0.3 m Temperature**



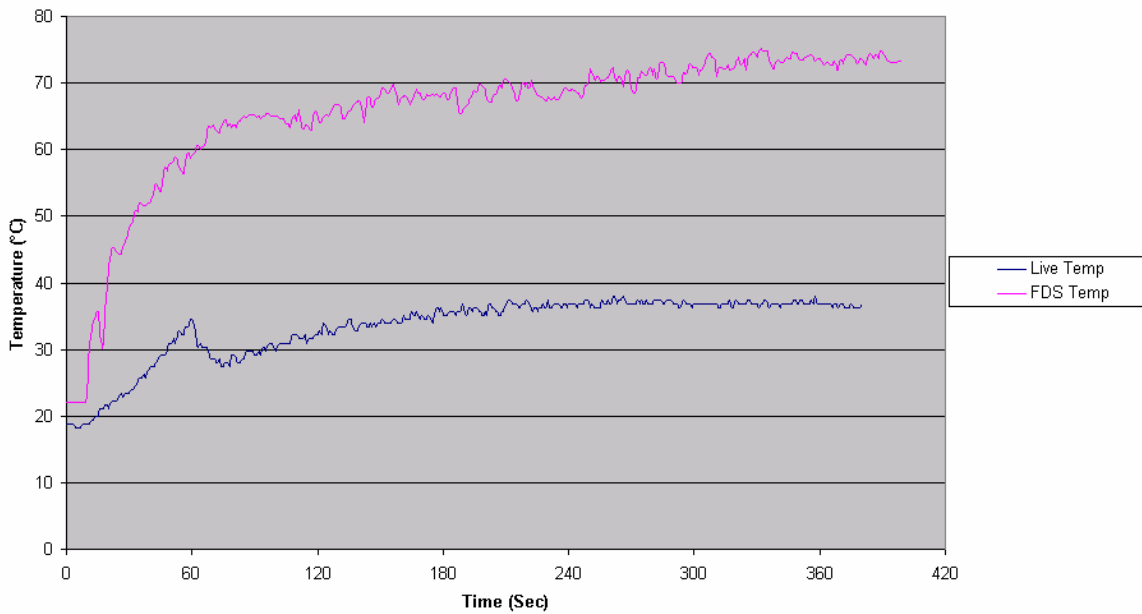
**Centre Floor Fire with Low Airflow and Water Mist
Tree 1 (occ) 0.7 m Temperature**



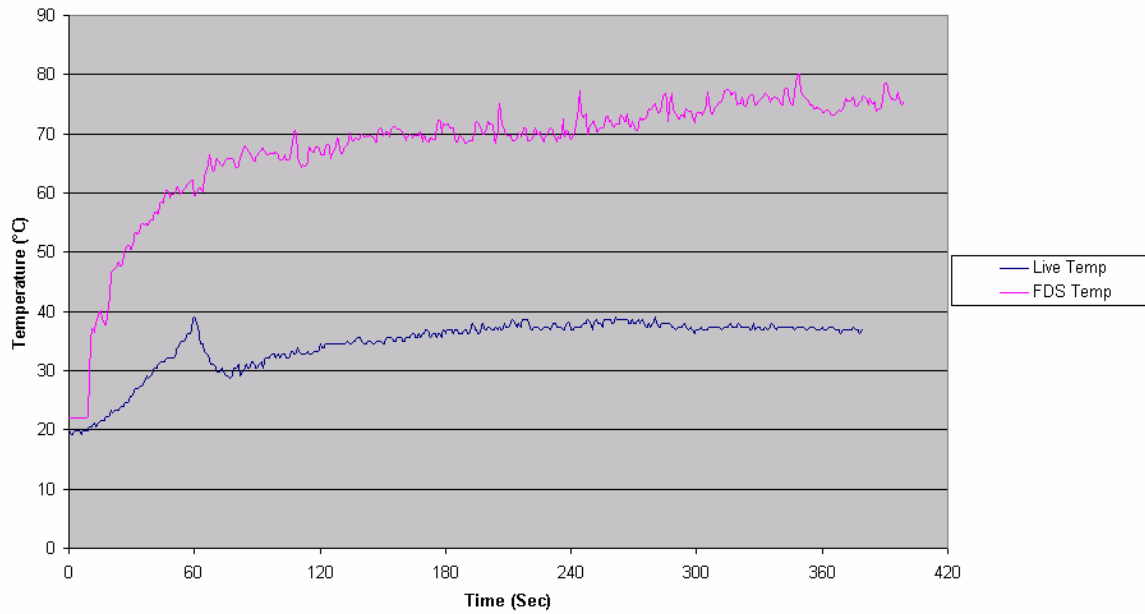
**Centre Floor Fire with Low Airflow and Water Mist
Tree 1 (occ) 1.3 m Temperature**



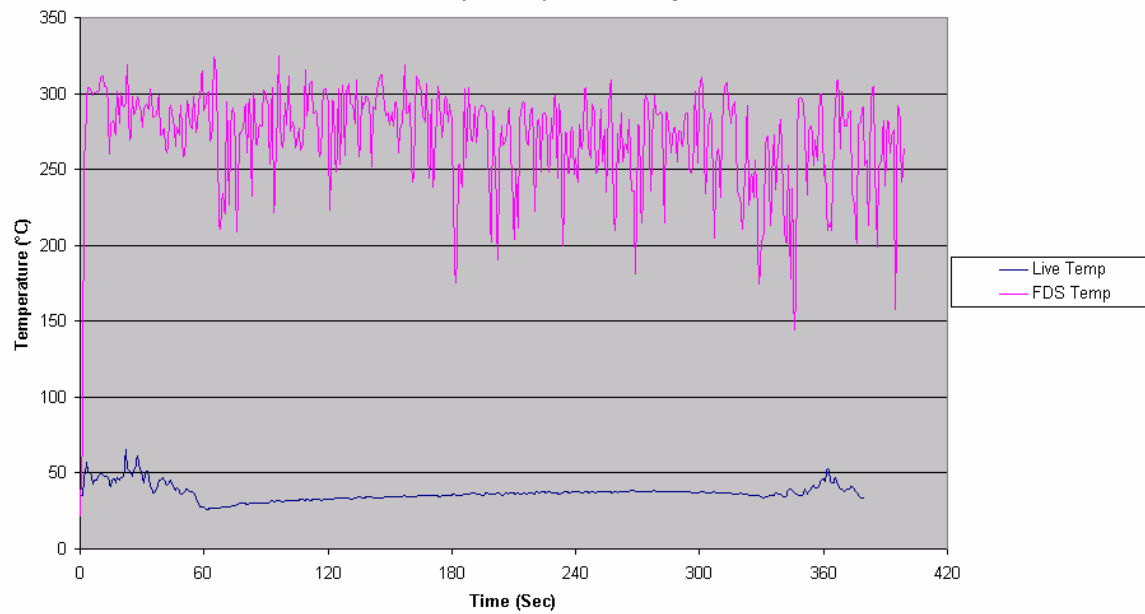
**Centre Floor Fire with Low Airflow and Water Mist
Tree 1 (occ) 1.8 m Temperature**



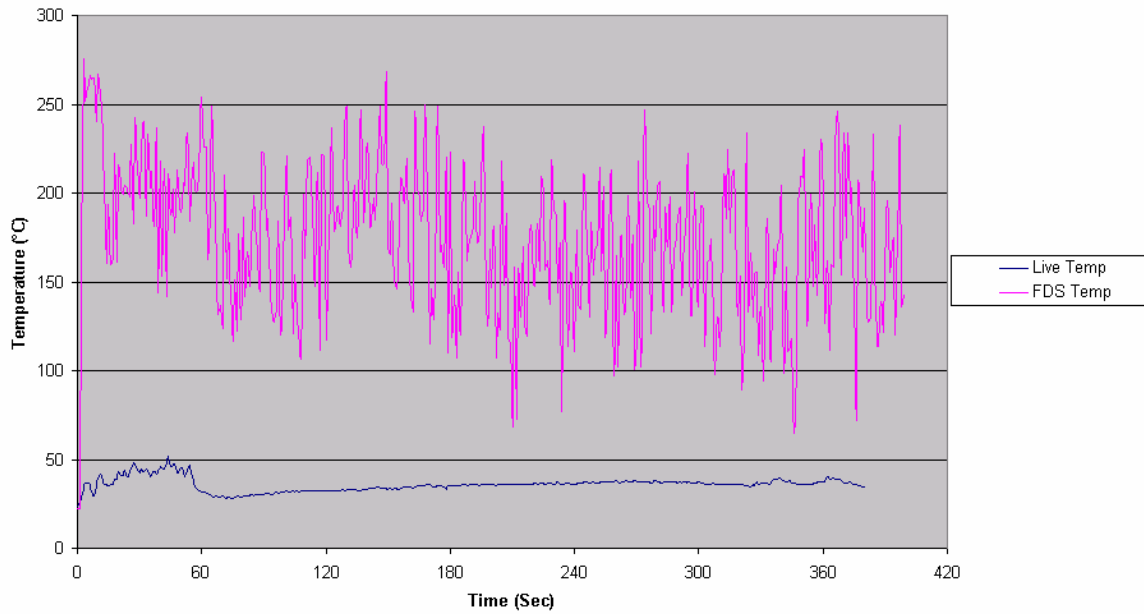
**Centre Floor Fire with Low Airflow and Water Mist
Tree 1 (occ) 2.1 m Temperature**



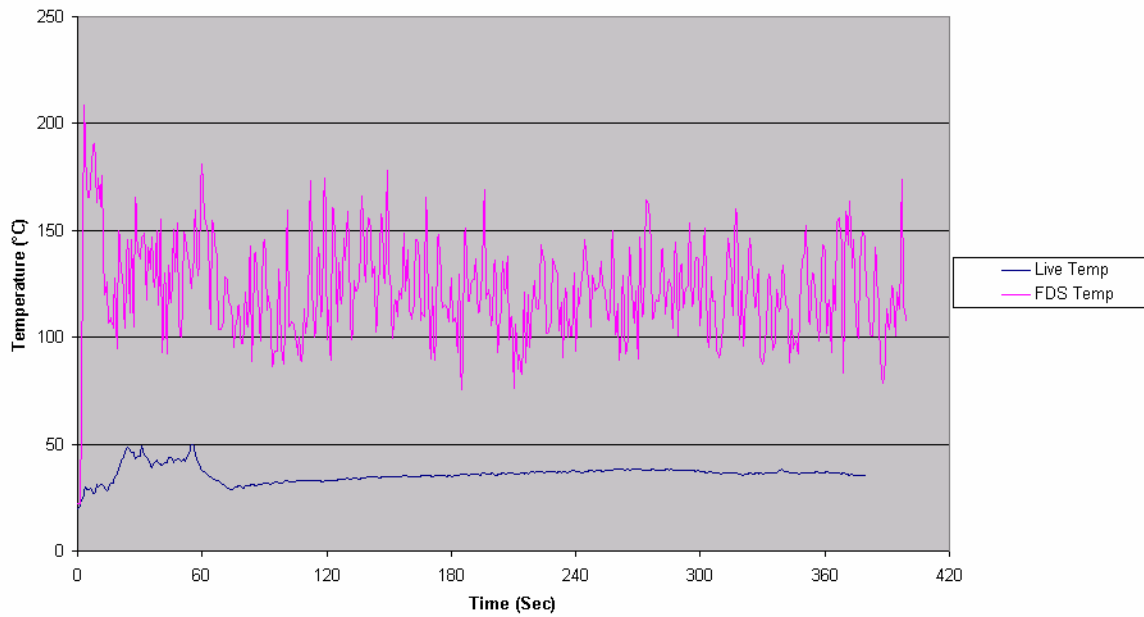
**Centre Floor Fire with Low Airflow and Water Mist
Tree 2 (Centre) 0.3 m Temperature**



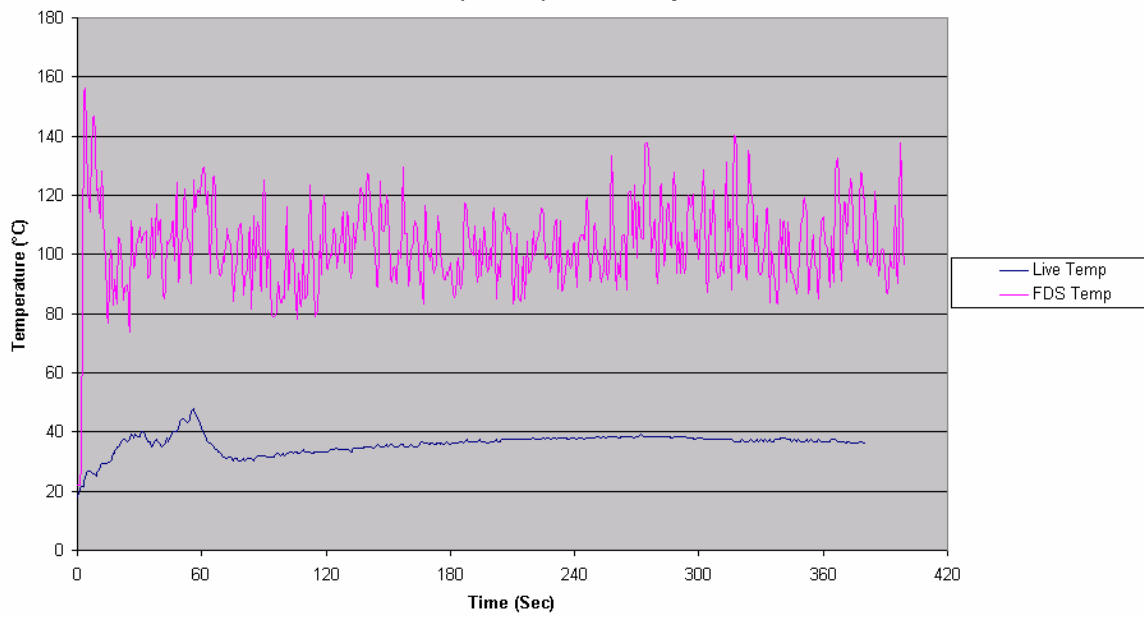
**Centre Floor Fire with Low Airflow and Water Mist
Tree 2 (Centre) 0.7 m Temperature**



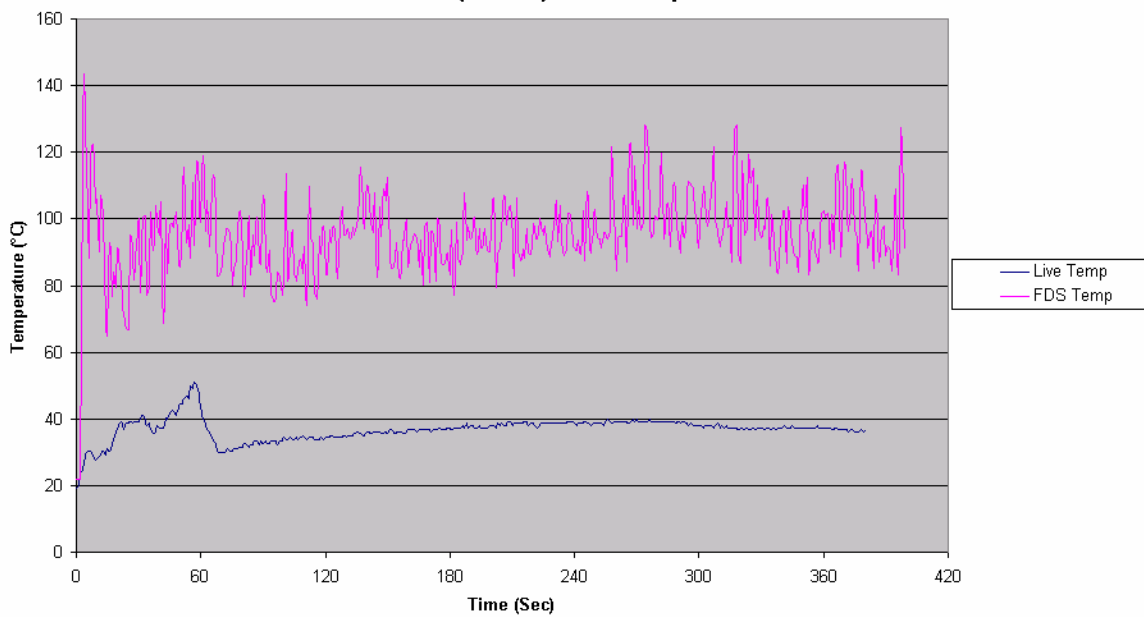
**Centre Floor Fire with Low Airflow and Water Mist
Tree 2 (Centre) 1.3 m Temperature**



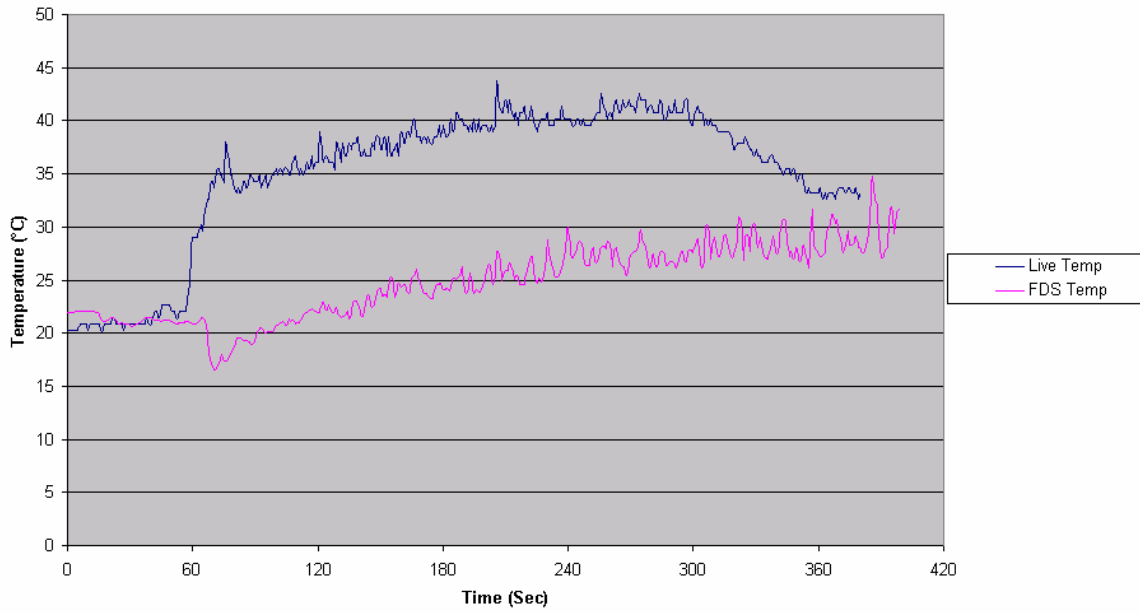
**Centre Floor Fire with Low Airflow and Water Mist
Tree 2 (Centre) 1.8 m Temperature**



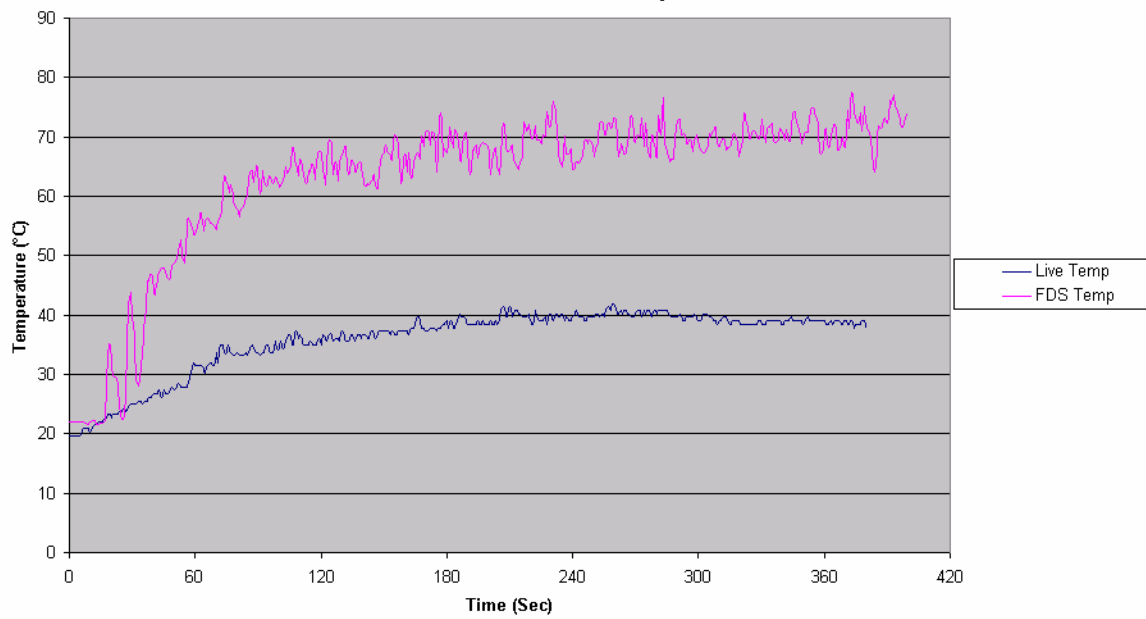
**Centre Floor Fire with Low Airflow and Water Mist
Tree 2 (Centre) 2.1 m Temperature**



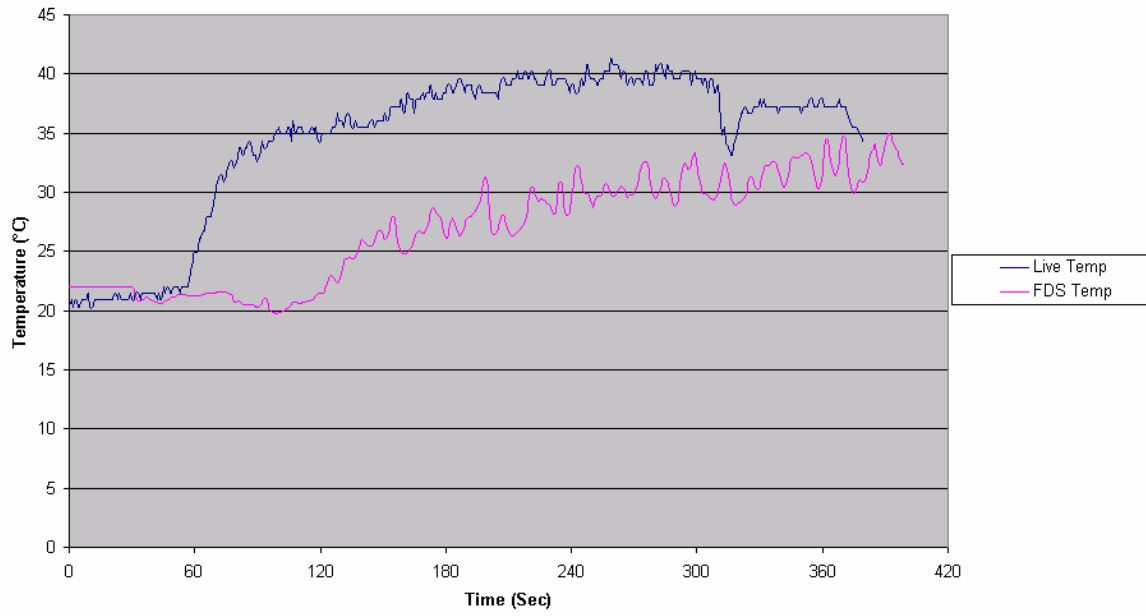
**Centre Floor Fire with Low Airflow and Water Mist
Back Corner 0.3 m Temperature**



**Centre Floor Fire with Low Airflow and Water Mist
Back Corner 1.3 m Temperature**



**Centre Floor Fire with Low Airflow and Water Mist
Front Corner 0.3 m Temperature**



**Centre Floor Fire with Low Airflow and Water Mist
Front Corner 1.3 m Temperature**

